Department of Mechanical Engineering
THE UNIVERSITY OF TEXAS AT AUSTIN
Nuclear Engineering Teaching Laboratory • Austin, Texas 78758
512-232-5370 • FAX 512-471-4589 • http://www.me.utexas.edu/~netl/

March 8, 2018

ATTN: Document Control Desk
Nuclear Regulatory Commission
Washington D.C. 20555-0001

G. A. Wertz, P.E.
Project Manager
Research and Test Reactors
U.S. Nuclear Regulatory Commission

SUBJECT: Docket No. 50-602, Request for Renewal of Facility Operating License R-129

RE: University of Texas at Austin – Request for Additional Information Regarding the License Renewal Request For the Nuclear Engineering Teaching Laboratory TRIGA Mark II Nuclear Research Reactor (TAC NO. ME7694)

Sir:

Attached is a response to Requests for Additional Information including:

1. Summary of RAI numbers and response
2. Report on Neutroinc Analysis for the UT TRIGA Reactor
3. Thermal Hydraulic Analysis for the University of Texas (UT) TRIGA Reactor
4. Modelling a Step Insertion and Continuous Rod Withdrawal Events in a TRIGA
5. Loss of Coolant Analysis for the University of Texas at Austin TRIGA Reactor
6. Analysis of Effluent Argon Production, Release, and Exposure for the University of Texas at Austin TRIGA Reactor
7. UT TRIGA Technical Specifications

Please contact me by phone at 512-232-5373 or email whaley@mail.utexas.edu if you require additional information or if there is a problem with this submittal.

Thank you,

P. M. Whaley
Associate Director, Nuclear Engineering Teaching Laboratory
The University of Texas at Austin

AD35
A020
NRR

I declare under penalty of perjury that the foregoing is true and correct.
Executed on March 8, 2018

William Charlton
NETL Director

7. Please describe the methods used for steady state neutronic (steady-state and kinetics) and thermal-hydraulic analysis and include comparisons with UT TRIGA measurements that demonstrate that those methods are appropriate to analyze the limits imposed by the UT TRIGA TS.

See attached *REPORT ON NEUTRONIC ANALYSIS FOR THE UT TRIGA REACTOR*

8.1 Please provide schematic drawings showing the location of fuel elements, control rods, and other components installed in the lettered-and-numbered lattice positions.

See response to RAI 7, Figure 1

For fuel elements provide a cross reference to fuel element serial numbers and their accumulated burnup.

POSITION	SERIAL	BURNUP (MWD)
B01	2985	5.30
B02	3384	5.01
B03	10878	4.54
B04	3013	6.61
B05	2899	5.44
B06	10809	0.29
C02	2965	4.98
C03	2984	4.80
C04	2944	4.91
C05	2931	4.43
C06	2983	4.91
C07	10146	3.46
C08	2980	4.66
C09	2925	5.42
C10	2941	5.29
C11	2979	4.95
C12	2964	5.05
D01	2910	4.78
D02	2959	4.83
D03	2906	5.06
D04	2992	6.11
D05	2962	4.96
D06	10147	3.22
D07	2928	4.96
D08	2939	4.76
D09	5918	6.20

D10	2977	4.72
D11	2974	4.87
D12	2905	5.30
D13	2943	4.51
D14	10148	3.30
D15	2950	5.03
D16	2929	4.90
D17	2955	5.12
D18	2975	5.00
E01	5845	5.86
E02	6932	5.58
E03	2932	4.87
E04	5915	5.84
E05	6886	5.87
E06	5912	5.85
E07	5846	6.46
E08	5903	6.43
E09	5917	5.30
E10	6929	6.02
E12	6925	5.68
E13	5844	5.89
E14	6923	5.35
E15	5919	5.86
E16	5921	5.91
E17	6927	5.94
E18	5902	6.43
E19	5904	6.46
E20	6930	5.98
E21	6889	5.44
E22	5914	5.64
E23	6142	5.78
E24	6928	5.80
F01	10817	1.61
F02	5911	3.99
F03	3496	4.70
F04	3504	4.68
F05	6931	1.01
F06	10816	1.82
F07	2915	4.37
F08	2946	4.08
F09	6924	5.63
F10	10812	2.03
F11	2958	3.78

F12	5913	5.46
F15	2902	4.25
F16	10813	1.88
F17	2912	4.48
F18	6143	5.12
F19	5916	5.15
F20	2940	4.05
F21	2971	4.10
F22	2969	4.29
F23	6926	5.73
F24	3513	5.34
F25	10811	2.04
F26	2960	4.26
F27	2947	4.10
F28	2911	4.39
F29	5922	5.56
F30	10814	1.88
G02	10704	1.45
G03	2908	4.00
G04	3700	4.48
G05	3703	5.27
G06	5920	4.85
G08	10701	2.09
G09	2957	3.87
G10	2938	3.95
G11	2927	4.27
G12	10702	2.24
G14	2970	3.94
G15	2976	3.95
G16	2952	3.80
G17	10815	1.73
G18	2904	4.23
G20	2968	3.73
G21	2903	4.22
G22	2935	3.96
G23	2930	4.04
G24	2951	3.77
G26	10699	1.73
G27	2948	4.10
G28	2913	4.15
G29	2954	4.16
G30	10700	2.63
G33	2918	4.01

G35	10810	1.75
G36	10703	1.48

Please provide all technical parameters and conclusions supplied for normal operation, accident analysis, and dose estimates using the LCC.

See response to RAI 7and *LOSS OF COOLANT ACCIDENT ANALYSIS FOR THE UNIVERSITY OF TEXAS AT AUSTIN TRIGA REACTOR*

8.2 Please provide analyses that quantify the effects of fuel burnup, plutonium buildup, and the effect of fission products on the UT TRIGA LCC.

See response to RAI 7

8.3 Please provide the technical parameters including analysis of "reactor kinetic behavior, basis reactor criticality, control rod worth, definition of the limiting core configuration (LCC), [etc.]" (NUREG-1537, Section 4.5.1). State whether the comparison of calculated and measured values demonstrates acceptable model development.

See *REACTOR KINETIC BEHAVIOR: PULSE ANALYSIS, ROD WITHDRAWAL ANALYSIS.* Comparison to experimental data is provided in *Verification and Validation*.

For *"Basis reactor criticality, control rod worth, definition of the limiting core configuration (LCC), [etc.]"* see response to RAI 7

9 The GA-4361 unit cell parameters are displayed and compared with UT TRIGA core parameters. Please provide the technical parameters that are applicable to UT TRIGA.

Technical parameters are provided in response to RAI 7

10 Given the difference between the "Reference" and "Current" values of excess reactivity and shutdown margin, which values are being used in the UT TRIGA TS.

Analysis updated; see response to RAI 7.

11.1 Please describe any limits or conditions on the evaluation of excess reactivity contributors, such as those due to temperature variations and poisons (e.g., xenon and samarium).

There are no limits or conditions on the evaluation of excess reactivity from the identified categories.

Please provide calculations of full power reactivity defects for power, xenon, and samarium.

See response to RAI 7

11.2 Please provide calculations for excess reactivity and control rod worths, and evaluate whether they are in agreement with the analytical model and with UT TRIGA performance.

See response to RAI 7.

Provide a discussion that describes the evaluation of these calculations to demonstrate acceptable reactor shutdown and shutdown margin.

See response to RAI 7.

Include consideration of experiment reactivity

Limits on acceptable reactor shutdown and shutdown margin do not differentiate reactivity between fuel and experiments.

11.3 Please provide "a transient analysis assuming that an instrumentation malfunction drives the most reactive control rod out in a continuous ramp mode," (NUREG-1537, Section 4.5.3) of the reactor using a rate of withdrawal consistent with proposed UT TRIGA TS values of the maximum control rod withdrawal speed, reactivity rate, and the control rod scram time including uncertainties.

Attached as *MODELLING A STEP INSERTION AND CONTINUOUS ROD WITHDRAW EVENTS IN A TRIGA*

.

11.4 Please provide all other applicable technical parameters, "excess reactivity, control rod worth, temperature coefficients, [etc.]" (NUREG-1537, Section 4.5.3).

See response to RAI 7

13. Please confirm that the Bernath correlation is used to characterize DNBR for UT TRIGA, or demonstrate the applicability of Biasi correlation to UT TRIGA analysis.

The Bernath correlation is used to calculate the approach to thermal limits.

14.1 Please provide clarification as to the relationship of the reactivity coefficient with the analysis provided in UT SAR Section 4.6.

Superseded by *MODELLING A STEP INSERTION AND CONTINUOUS ROD WITHDRAW EVENTS IN A TRIGA*. Experimentally determined reactivity coefficients and model-calculated values agree, but there assumptions are required to correlate measurements a single point to a core-wide average fuel temperature where temperature and flux both vary across and within fuel elements. In addition, the range of temperatures in operation is very restricted compared to the range to be considered in transient analysis. The 'Prompt Temperature Coefficient for TRIGA fuel vs Temperature' in GA-7882 provides good agreement with the neutronic analysis at 400°K, and is used in the transient calculations that extend to high temperatures.

14.2 The basis for TS 3.2 "Pulsed Mode Operation," states that the reactivity limits are established so as to meet fuel temperature limits. However, this is inconsistent with the statements in UT SAR Section 4.6 as described above. Please revise the discussion in UT SAR Section 4.6 to support the UT TRIGA TS.

The discussion will be revised to describe that reactivity limits are established to meet fuel temperature limits.

14.3 UT SAR, Section 4.6 (p. 4-46) provides a series of statements regarding pulse reactivities and responses that are not supported by analyses. Please provide analysis supporting these statements in sufficient detail so that a confirmatory analysis can be performed.

Section 4.6 will be revised to reflect the information in analysis of *MODELLING A STEP INSERTION AND CONTINUOUS ROD WITHDRAW EVENTS IN A TRIGA*

15.1 Please describe the analytical methods used to determine the DNBR, including the core inlet and exit conditions assumed and other assumptions and correlations employed. This [TRACE DNBR] analysis should describe the parameters determined from the LCC such as peaking factors and limiting coolant inlet temperature and that the inlet temperature used for DNBR is a limiting value by showing how it corresponds to the primary pool water temperature measuring channel value.

The thermal hydraulic analysis is attached *THERMAL HYDRAULIC ANALYSIS OF THE UNIVERSITY OF TEXAS (UT) TRIGA REACTOR*. Nominal and limiting values for pool temperature and hydrostatic pressure associated with pool temperature and barometric pressure are in Table 4.5.

15.2 Please provide a comprehensive description of the calculational methods and the results that demonstrate the acceptability of design assumptions and TS for pulsing at UT TRIGA (e.g., the LCC, the approved power level, the pulse of reactivity inserted by the transient rod as allowed by TS, the value of the fuel temperature coefficient, the effective delayed neutron fraction, the prompt neutron lifetime."

Analysis of pulse and continuous rod withdrawal transient analysis is attached as *MODELLING A STEP INSERTION AND CONTINUOUS ROD WITHDRAW EVENTS IN A TRIGA*

19.1 The licensee cites a correlation that determines effective release height above the building exhaust stack due to effluent momentum from the purged air system or the ventilation system. Please confirm that the correct form of the correlation is $\Delta H = D (Vs/\mu)1.4$ and not as it is stated in the UT SAR.

The correlation is a typographical error in the original analysis; however, new analysis for argon production, release, and exposure has been generated and is attached as *ANALYSIS OF EFFLUENT ARGON PRODUCTION, RELEASE, AND EXPOSURE FOR THE UNIVERSITY OF TEXAS AT AUSTIN TRIGA REACTOR*

19.2 The licensee uses two different stack exit diameter values for the stack (0.4012 m2 on UT SAR, p. 9-6 and 45.72 cm on UT SAR p. 9-2). Please explain this discrepancy.

The inner diameter of the purge flow is 6" (radius of 0.0762 m, cross section of 0.0182 m^2)
Outer diameter of the purge piping is 8" (radius of 0.1016 m, cross section of 0.0323 m^2)
Inner diameter of the HVAC stack is 18" (radius of 0.2286 m, cross section of 0.1642 m^2, with flow partially occluded by the purge piping at 0.1317 m^2)

The SAR will be revised to reflect information in the *ANALYSIS OF EFFLUENT ARGON PRODUCTION, RELEASE, AND EXPOSURE FOR THE UNIVERSITY OF TEXAS AT AUSTIN TRIGA REACTOR*

19.3 Ensure the impact of the above changes on offsite doses for both normal operation and accident conditions are considered and revised accordingly.

See *ANALYSIS OF EFFLUENT ARGON PRODUCTION, RELEASE, AND EXPOSURE FOR THE UNIVERSITY OF TEXAS AT AUSTIN TRIGA REACTOR*

22.2 Please provide the 41Ar occupational exposure including stay times and the effect of ventilation, and how these compare to the limits of 10 CFR Part 20 and the commitments of the UT TRIGA ALARA program.

See *ANALYSIS OF EFFLUENT ARGON PRODUCTION, RELEASE, AND EXPOSURE FOR THE UNIVERSITY OF TEXAS AT AUSTIN TRIGA REACTOR*

Based on information in the analysis (Table IX), during normal operations with HVAC and purge operating stay time is unlimited. When the HVAC system is in isolation with the reactor operating at full power equilibrium conditions (a prohibited condition), stay time is 2.21 hours. If the purge is operating with the HVAC system secured, stay time is unlimited. If the HVAC system is operating with the purge system secured, stay time is 61.38 hours.
The reactor bay is not routinely occupied continuously during operation, and routine personnel monitoring in the UT Radiation Protection Program is adequate to assure radiation worker dose limits are met.

22.4 UT SAR Section 11.1.1.1.2 provides a conservative estimate of offsite 41Ar air concentrations using an equation for ground level concentration at the building center. Please provide a reference for the equation cited, and a discussion of its suitability for providing dose calculations for members of the public and their location.

See *ANALYSIS OF EFFLUENT ARGON PRODUCTION, RELEASE, AND EXPOSURE FOR THE UNIVERSITY OF TEXAS AT AUSTIN TRIGA REACTOR*

The annual dose for the maximally exposed individual for continuous full power operation is calculated to be 77 mR. Operating less than 1,251 MWD in a year will meet the criteria for not exceeding 10 mR in a year. Total current burnup since the inception of the facility is on the order of 300 MWD, and there is no conceivable scenario where the UT reactor could ever operate to provide a 10 mR annual dose to the maximally exposed location.

22.5 Please provide a complete description of the maximally exposed individual calculation, including how the estimates compare to the limits in 10 CFR Part 20 and the commitments of the UT TRIGA ALARA program.

See *ANALYSIS OF EFFLUENT ARGON PRODUCTION, RELEASE, AND EXPOSURE FOR THE UNIVERSITY OF TEXAS AT AUSTIN TRIGA REACTOR*

22.6 UT SAR Section 11.1.1.1.2 provides conservative dose estimates for the maximally exposed individual of 66 mrem per year using the CAP88-PC computer code. UT TRIGA TS 3.5.3(D) indicates that releases of 41Ar from the reactor bay to an unrestricted environment SHALL NOT exceed 100 Ci per year, and provides CAP88-PC model results indicating that 100 Ci per year release of 41Ar would result in a maximally exposed individual dose of 0.142 mrem per year. Please resolve this discrepancy between the maximally exposed individual doses in the UT SAR and those provided in the TS.

Based on *ANALYSIS OF EFFLUENT ARGON PRODUCTION, RELEASE, AND EXPOSURE FOR THE UNIVERSITY OF TEXAS AT AUSTIN TRIGA REACTOR,* the Technical Specifications related to Argon 41 will be removed.

22.7 UT SAR Section 11.1.1.1.2 provides a discussion of the maximally exposed offsite individual, but does not provide doses to members of the public. Please provide a discussion of potential public doses.

See *ANALYSIS OF EFFLUENT ARGON PRODUCTION, RELEASE, AND EXPOSURE FOR THE UNIVERSITY OF TEXAS AT AUSTIN TRIGA REACTOR*

27.1 Please provide an analysis of the MHA for the UT TRIGA including doses to the workers and to the individuals in the non-restricted areas that bounds all other accident analyses. Please describe all assumptions, the operating conditions of the HVAC system, and the sequence of events used in calculating the potential radiological consequences and discuss how those consequences are less than the applicable limits in 10 CFR Part 20. Please provide sufficient detail to allow independent confirmation of these results

MAXIMUM HYPOTHETICAL ACCIDENT ANALYSIS

The maximum hypothetical accident is a release of radioactive noble gas and halogen fission products from a TRGIA fuel elements following discharge. The maximum fission product inventory will occur in a fuel element with the maximum burnup. The maximum burnup is taken to be the burnup that results in a loss of 50% of the initial uranium 235 mass (from 38 grams to 19 grams). This is extremely conservative as the TRIGA fuel temperature reactivity deficit associated with operation at power does not allow support under these conditions.

Depletion calculations using the SCALE T-6 sequence was used to determine burnup and the fission product inventory. A SCALE model of the TRIGA core was configured with a two fuel material composition sets, one representative of a single element to be depleted and the other representing the remaining elements in the core.

A set of SCALE (T-6 depletion) calculations was performed to deplete all elements in the core, generating a fission product inventory for the larger set of elements. A 50% burn interval at 1.5 MW was evaluated, reducing the U-235 mass in the single element from 38 grams to approximately 19 grams. In

determining the 50% burn, the number of fuel elements was adjusted to result in a calculated flux similar to the nominal UT TRIGA full power flux. The uranium, transuranic, and fission product concentration were used to develop a material composition simulating the core average at the end of the interval for the 50% single element burn.

The SCALE model was configured to a single fresh fuel element and the remainder of elements at the core average at the end of the 50% burn interval. Radioactive noble gas and halogen activity was calculated for the 50% burn. A similar calculation was performed except that the constant flux option was used. The maximum value for the activity of the isotopes from the two calculations (constant power and constant flux) was taken as the source term for the radioactive noble gas and halogen inventory for a single fuel element at the maximum burnup.
Using a release fraction of $1X10^{-4}$, and the free volume of the rector bay (4120 m^3), the concentration of the activity of each isotope (A_i, in μCi/ml) in reactor bay atmosphere based on the source term for each isotope (C_i ,in Curies) is calculated as:

$$A_i = \frac{C_i \cdot 10^{-4}}{4.12x10^{-9}}$$

The average activity of isotopic concentration ($A_i(t)$), where λ_i is the isotope decay constant, over some time interval (t) following the release of isotopes from a fuel element into the reactor bay is calculated:

$$A_i(t) = \frac{C_i \cdot 10^{-4}}{4.12x10^{-9}} \cdot \frac{\left(1 - e^{-\lambda_i \cdot t}\right)}{\lambda_i \cdot t}$$

Each isotope has limits (based on continuous activity concentrations over one year) on activity concentration for exposure of workers (Derived Air Concentration, DAC) and the general public (Effluent Limit). For mixtures of isotopes, compliance with the limits is demonstrated if the sum of the ratio of each activity concentration to its individual limit is less than unity. Since the hypothetical accident is not a continuous process, the concentration of each isotope is normalized over a year following the release. The ratio of the average activity ($\langle A_i \rangle$) for the year following release of the source term from a fuel element into the reactor bay for occupational exposure (2000 hours) to the isotopic DAC (DAC_i) is calculated as:

$$\frac{\langle A_i \rangle}{DAC_i} = \frac{C_i \cdot 10^{-4}}{4.12x10^{-9}} \cdot \frac{\left(1 - e^{-\lambda_i \cdot Year_s}\right)}{\lambda_i \cdot Year_s} \cdot \frac{2000}{Year_h}$$

The fraction of average activity over a year to the effluent limit (EL) is calculated:

$$\frac{\langle A_i \rangle}{EL_i} = \frac{C_i \cdot 10^{-4}}{4.12x10^{-9}} \cdot \frac{\left(1 - e^{-\lambda_i \cdot Year_s}\right)}{\lambda_i \cdot Year_s}$$

The sum of the ratios of concentration to limit is $7.52x10^{-5}$ for occupational exposure, and $3.30x10^{-2}$ for effluents. Since a exposure to a DAC for a year results in 5 rem, if the releases is completely contained in the reactor bay and an individual works 2000 hours in the bay then a dose of 0.4 mrem will result. Since exposure to an effluent limit for a year will result in 50 mrem exposure, an individual exposed at the exit of the reactor bay ventilation for a year following the hypothetical release will receive a dose of 1.65 mrem.

Summary of MHA Data

Isotope	Fuel C_i	λ (s^{-1})	DAC	Eff Limit	release from fuel Ci	reactor bay µCi/ml	1 year ave µCi/ml	DAC Fraction	Eff Limit Fraction
br83	1342	8.02E-05	3E-05	9E-08	1.34E-1	3.26E-11	1.29E-14	9.79E-11	1.43E-07
br84m	51	1.93E-03	1E-07	1E-09	5.13E-3	1.24E-12	2.05E-17	4.67E-11	2.05E-08
br84	2344	3.64E-04	2E-05	8E-08	2.34E-1	5.69E-11	4.96E-15	5.66E-11	6.20E-08
br85	3373	3.98E-03	1E-07	1E-09	3.37E-1	8.19E-11	6.51E-16	1.49E-09	6.51E-07
i131	8167	9.99E-07	2E-08	2E-10	8.17E-1	1.98E-10	6.28E-12	7.17E-05	3.14E-02
i132m	56	1.39E-04	4E-06	3E-08	5.57E-3	1.35E-12	3.09E-16	1.76E-11	1.03E-08
i132	12130	8.39E-05	3E-06	2E-08	1.21	2.94E-10	1.11E-13	8.46E-09	5.56E-06
i133	17440	9.24E-06	1E-07	1E-09	1.74	4.23E-10	1.45E-12	3.31E-06	1.45E-03
i134m	1157	3.12E-03	1E-07	1E-09	1.16E-1	2.81E-11	2.85E-16	6.50E-10	2.85E-07
i134	20200	2.20E-04	2E-05	6E-08	2.02	4.90E-10	7.06E-14	8.06E-10	1.18E-06
i135	16420	2.93E-05	7E-07	6E-09	1.64	3.99E-10	4.32E-13	1.41E-07	7.19E-05
i136m	3366	1.47E-02	1E-07	1E-09	3.37E-1	8.17E-11	1.76E-16	4.01E-10	1.76E-07
i136	6740	8.31E-03	1E-07	1E-09	6.74E-1	1.64E-10	6.24E-16	1.42E-09	6.24E-07
kr85m	3254	4.30E-05	2E-05	1E-07	3.25E-1	7.90E-11	5.82E-14	6.64E-10	5.82E-07
kr85	9	2.22E-10	1E-04	7E-07	8.60E-4	2.09E-13	2.08E-13	4.74E-10	2.97E-07
kr87	6275	1.51E-04	5E-06	2E-08	6.28E-1	1.52E-10	3.19E-14	1.45E-09	1.59E-06
kr88	8489	6.78E-05	2E-06	9E-09	8.49E-1	2.06E-10	9.63E-14	1.10E-08	1.07E-05
kr89	10820	3.67E-03	1E-07	1E-09	1.08	2.63E-10	2.27E-15	5.18E-09	2.27E-06
kr90	11580	2.15E-02	1E-07	1E-09	1.16	2.81E-10	4.14E-16	9.45E-10	4.14E-07
kr91	7940	8.09E-02	1E-07	1E-09	7.94E-1	1.93E-10	7.55E-17	1.72E-10	7.55E-08
xe131m	80	6.77E-07	4E-04	2E-06	8.01E-3	1.94E-12	9.09E-14	5.19E-11	4.55E-08
xe133m	184	3.65E-06	1E-04	6E-07	1.84E-2	4.48E-12	3.89E-14	8.87E-11	6.48E-08
xe133	17080	1.53E-06	1E-04	5E-07	1.71	4.15E-10	8.59E-12	1.96E-08	1.72E-05
xe135m	2224	7.55E-04	9E-06	4E-08	2.22E-1	5.40E-11	2.26E-15	5.74E-11	5.66E-08
xe135	375	2.11E-05	1E-05	7E-08	3.75E-2	9.09E-12	1.37E-14	3.12E-10	1.95E-07
xe137	15870	3.03E-03	1E-07	1E-09	1.59	3.85E-10	4.03E-15	9.21E-09	4.03E-06
xe138	16030	8.20E-04	4E-06	2E-08	1.60	3.89E-10	1.50E-14	8.57E-10	7.51E-07
xe139	12560	1.75E-02	1E-07	1E-09	1.26	3.05E-10	5.53E-16	1.26E-09	5.53E-07
xe140	8948	5.10E-02	1E-07	1E-09	8.95E-1	2.17E-10	1.35E-16	3.08E-10	1.35E-07

27.2.1 The [atmospheric dispersion] calculations are then performed for distances from 10 to 100 meters from the building. Because, the reactor building is both tall and wide, any release from the stack could be accumulated in the building wake. Therefore, the applicability of the assumption of elevated release is appears inaccurate. Please justify the use of the elevated release values for dose estimates at nearby distances from the facility.

See *ANALYSIS OF EFFLUENT ARGON PRODUCTION, RELEASE, AND EXPOSURE FOR THE UNIVERSITY OF TEXAS AT AUSTIN TRIGA REACTOR*

27.2.2 if there is an error in the correlation used for the plume rise (see RAI 19.1), the estimated plume rise above the stack height may be inaccurate. Please confirm and revise accordingly.

See *ANALYSIS OF EFFLUENT ARGON PRODUCTION, RELEASE, AND EXPOSURE FOR THE UNIVERSITY OF TEXAS AT AUSTIN TRIGA REACTOR*

27.3 For the determination of effluent leakage around doors and HVAC duct vents the licensee employs complicated discussions and assumptions that are not supported or justified. Please revise the discussion and calculations using applicable assumptions for building overpressure.

The assumptions have been removed from analysis, see *ANALYSIS OF EFFLUENT ARGON PRODUCTION, RELEASE, AND EXPOSURE FOR THE UNIVERSITY OF TEXAS AT AUSTIN TRIGA REACTOR*

27.4 UT SAR page 3-7 states that the reactor bay is about 18.3 m on each side, with a total of 4575 m3 of volume. This leads to a wall cross section area of about 250 m2, which is in-line with the value of 234 m2 given in the original application for licensing safety analysis report in 1991 (1991 SAR). Please confirm the building wall cross section area and revise accordingly.

Blueprint dimensions of the reactor bay are 15.698 m high by 18.288 m wide, with approximately 4 meters below grade. Cross sectional area is therefore 287 m^2, 214 m^2 exposed to the environment.

27.5 For the offsite public dose calculations, in the UT SAR it does not appear consistent with the potential for ground release of the reactor bay air content, similar to that evaluated in the 1991 SAR

See *ANALYSIS OF EFFLUENT ARGON PRODUCTION, RELEASE, AND EXPOSURE FOR THE UNIVERSITY OF TEXAS AT AUSTIN TRIGA REACTOR*

27.6 UT SAR Appendix 13.1, SCALE 6.1 input file, cites an input value 1.6 for the weight fraction of the ZrH1.6U fuel. Is this input value for the weight fraction of hydrogen in the fuel? Please confirm and revise accordingly.

This was a typographical error; analysis used known ratios of H:Zr 1.6 for elements, nominally 1.6.

28.1 It appears that the UT SAR does not provide sufficient information on the peaking factors and other assumptions used to estimate the maximum fuel temperature rise as listed in UT SAR Tables 13.20 and 13.21. Please provide sufficient additional information to allow confirmatory analysis.

Maximum fuel temperature is based on TRACE calculations in parametric variations of power generated in the model element. Power generated in the hot channel is based on the product of power level, the number of fuel elements in the core, and the radial peaking factor. See *REPORT ON NEUTRONIC ANALYSIS FOR THE UT TRIGA REACTOR* and *THERMAL HYDRAULIC ANALYSIS OF THE UNIVERSITY OF TEXAS (UT) TRIGA REACTOR*

29.1 Please provide a LOCA analysis that represents the current licensed power level for the UT TRIGA in sufficient detail to allow confirmatory analysis.

See *LOSS OF COOLANT ACCIDENT ANALYSIS FOR THE UNIVERSITY OF TEXAS AT AUSTIN TRIGA REACTOR*

29.2 Please confirm that the LOCA analysis uses peaking factors that are consistent with the LCC and revise the analysis accordingly.

See *LOSS OF COOLANT ACCIDENT ANALYSIS FOR THE UNIVERSITY OF TEXAS AT AUSTIN TRIGA REACTOR*

29.3 UT SAR Section 13.5.8, "Results and Conclusion," states that the maximum fuel temperature in a LOCA event after "long-term operation at full power of 2000 kW is 750°C." Please provide the analysis that supports this temperature.

The SAR will be revised to incorporate the results of *LOSS OF COOLANT ACCIDENT ANALYSIS FOR THE UNIVERSITY OF TEXAS AT AUSTIN TRIGA REACTOR*

30. Please clarify the source of the activation materials for producing iodine, and identify actions needed if it is not 235U. In addition, please show that the limits for the iodine and strontium are less than the values that could be released in an MHA and the doses to the public from such releases are within the 10 CFR Part 20 limits.

The source as specified is "fueled experiments." See response to RAI-27.1, regarding MHA where exposure to a 100% DAC results in an annual exposure of 5 R and 100% effluent limit concentration results in an annual exposure of 50 mrem, ½ of the annual 10CFR20 public dose limit.

32.1 The proposed UT TRIGA TS definitions section 1.0 does not describe definitions for: core configuration; license; licensee; protective action; reactivity worth of an experiment; reactor operator; reactor operating; responsible authority; safety limit; scram time; senior reactor operator; shall/should/may definitions (only the definition for "shall" is provided); true value; unscheduled shutdown. Please provide definitions for the above or provide justification for not using them

With the exception of 'reactivity worth of an experiment' and 'safety limit' these terms do not appear in the Technical Specifications as an LCO, surveillance requirement, or Design Specification. Given their absence as a Specification there is no need to define. 'Reactivity worth of an experiment' and 'safety limit' are defined by context.

32.2 The following definitions are not consistent with the guidance: channel calibration, excess reactivity; experiment, confinement; movable experiment; secured experiment. Please revise accordingly or provide justification for the deviations.

'channel calibration' is revised; the following are equivalent to the guidance: 'excess reactivity, confinement, movable experiment and secured experiment.'

32.3 Please revise to the following: when IMMEDIATELY is used as a COMPLETION TIME, The REQUIRED ACTION should be pursued without delay and in a controlled manner.

Revised.

32.4 The proposed UT TRIGA TS definition of REACTOR SHUTDOWN only requires the reactor to be subcritical by $0.29. Please explain the discrepancy in using the value of an abnormal condition (shutdown margin) for a normal condition, i.e., the definition of Reactor Shutdown.

Technical Specifications does not specify or differentiate between normal and abnormal conditions, rather provides specification for' functional capability or performance levels of equipment required for safe operation of the facility.' By definition it is safe to operate the facility with the minimum shutdown margin; this is not an 'abnormal condition' but is the lowest functional capability allowed to operate the reactor. Shutdown margin is specified 'to assure that the reactor will remain subcritical without further operator action.' If it is safe to operate the reactor with a minimum shutdown margin it is also safe for

the reactor to be shutdown (i.e., to not operate the reactor) with an actual shutdown margin equal to the minimum shutdown margin.

32.5 The proposed UT TRIGA TS definition of REACTOR SECURED MODE requires that 3 of the 4 control rods be fully inserted. Please either provide analysis demonstrating the acceptability of the insertion of 3 out of 4 rods or revise the definition to require insertion of all 4 control rods in order to satisfy the requirements of this mode

The limiting condition for operation specifies a shutdown margin with the most reactive rod fully withdrawn; by definition the functional capability or performance level for safe operation includes provision for a 'stuck rod.' If it is safe to operate with a control rod that cannot be inserted, it is safe to be shutdown with a control rod fully withdrawn.

In addition, requiring the console be manned for extended intervals in the event that a rod cannot be fully inserted without maintenance and repairs places imposes stress where a measured and planned response is desired, and requires resources that may complicate or inhibit resolution.

33 The basis provided in support of the TS 2.1 references Chapter 4, Section 4.2.1 Z which does not exist. Please discuss this error and/or revise accordingly.

The basis will be revised to identify the correct section.

34.1 The basis provided in support of the UT TRIGA TS 2.2 references Chapter 4 Section 4.6 B which does not exist. Please provide a basis for the LSSS.

The basis will be revised to identify the correct section.

34.2 UT TRIGA TS 2.2.The REQUIRED ACTION, B.1 and B.2, which support condition B seem to be reversed and the completion times are both labeled B.2. Please discuss this error and/or revise accordingly.

B. An INSTRUMENTED FUEL ELEMENT in the B or C ring indicates greater than 550°C	B ENSURE REACTOR SHUTDOWN condition AND EVALUATE whether Safety Limit was exceeded	B.1 IMMEDIATE

34.3 UT TRIGA TS 2.2, B.2 refers to the statement "verify the measurement value is not correct." Please describe how this is verified.

See response to 34.2 above

35.1 Section 3.1 of the guidance describes having specifications for fuel burnup, core configurations, and reactivity coefficients (if such coefficients establish required conditions). Such specifications are not present in the proposed UT TRIGA TS. Please discuss.

These parameters do not establish required conditions.

35.3 Please provide an analysis and evaluation that demonstrates the ability to repeatedly measure core reactivity with sufficient accuracy to justify this small value of the shutdown margin.

This specification was originally approved in 1992 and has been acceptable since.

Reactivity changes are evaluated using a calibration of reactivity worth and position of control rods. Excess reactivity is evaluated prior to each day of reactor operation as well as following changes in experiment configuration. Since UT reactor operations on weekends are extremely rare, the first measurement of each week is essentially a cold, clean critical position at the current burnup. If no experiments are installed in the core, the first measurement of each week reflects the reference core condition less reactivity associated with burnup since the last reference core condition measurement (performed concurrently with control rod reactivity worth calibrations). Reactivity values of sequential first-of-the-week reactivity measurements should be comparable if burnup since the previous measurement is reasonably small, and a reasonable gage of repeatability.

All of the first-of-the-week reactivity measurements with the current core configuration (i.e., since installation of a 3-element facility) were reviewed. Measurements of excess reactivity that did not have experiments installed were tabulated along with core burnup (Table 1, Excess Reactivity Measurement Data, *δk(¢): Excess*, and *ΔMWD: Total*, referenced to the initial reading). The number of days between each measurement and the previous measurement was tabulated (*ΔT: Days*). A graph of the reactivity data (i.e., excess reactivity at first operation of the week, no experiments installed) shows the relationship between excess reactivity and burnup.

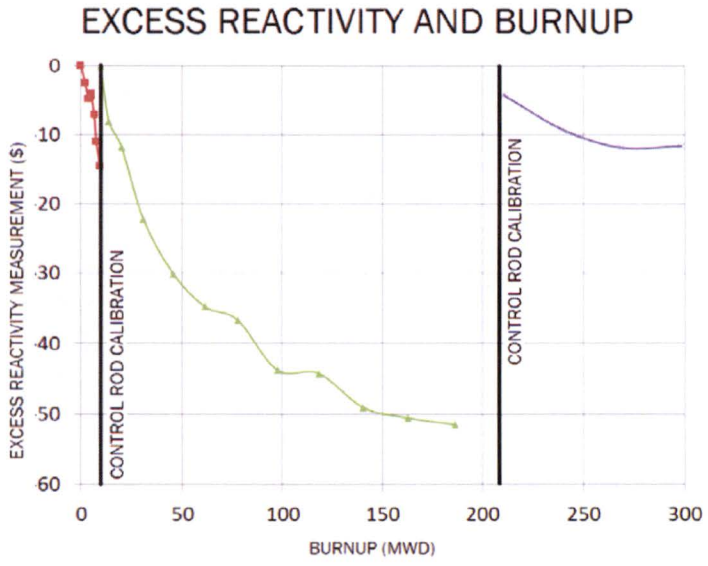

Changes in sequential cold, clean excess reactivity measurements are expected to be minimal if the burnup between measurements in small, and/or if the time between the measurements is small. The 13 measurements with intervals less than 35 days and the 7 measurements for which burnup in the interval is less than 2.12 MWD have reactivity differences less than $0.05.

Table 1, Excess Reactivity Measurement Data

	ΔMWD		ΔT	δk(¢)	
Date	Total	Seq. Interval	Days	Excess	Δ(Seq.)
06/29/10	0.00	0.00	na	0.00	
01/10/11	5.26	0.00	3	-4.55	-0.49
03/21/11	7.56	1.02	28	-10.95	-3.82
06/29/11	9.59	0.24	Rod Cal	0.00	Na
04/02/12	61.37	15.70	7	-34.75	-4.67
04/09/12	77.83	16.46	7	-36.68	-1.93
05/29/12	118.16	20.73	15	-44.27	-0.49
06/11/12	140.06	21.90	13	-48.98	-4.71
06/18/12	162.50	22.43	7	-50.54	-1.56
07/09/12	186.08	23.59	21	-51.45	-0.91
07/13/12	209.69	23.61	Rod Cal	0.00	Na
07/23/12	234.20	24.51	10	-4.26	-4.26
09/17/12	292.36	29.21	7	-11.85	-2.63
09/24/12	321.82	29.47	7	-11.59	0.27
10/01/12	--	--	7	-13.93	-2.35

It is clear that for small burnup intervals and short intervals between measurements, reactivity calculations for sequential measurements are well within a few cents. Reactivity measurements using calibrated control rods at the UT TRIGA reactor are repeatable well within 5 cents.

35.4 "Section 3.2 of the guidance describes that a limit be established for the maximum control rod reactivity insertion rate for non-pulsed operation. The proposed UT TRIGA TS do not provide such a specification. This rate, and the control rod scram times, are typically justified through the analysis of an uncontrolled, control rod withdrawal transient."

See *MODELLING A STEP INSERTION AND CONTINUOUS ROD WITHDRAW EVENTS IN A TRIGA*; the analysis demonstrates an uncontrolled withdrawal at the maximum possible rate does not challenge safety limits.

35.5 "Section 3.2 of the guidance describes a specification for permitted bypassing of channels for checks, calibrations, maintenance, or measurements. Proposed UT TRIGA TS 3.3, "Measuring Channels," does not specify when it is permitted to bypass channels for checks, calibrations, maintenance or measurements"

The facility does not operate under those conditions.

35.6 Proposed UT TRIGA TS 4.3 "Measuring Channels," contain Surveillance Requirements for the Fuel Temperature Channel and the Upper Level Radiation Monitor. However, there are no associated LCO specifications.

There are safety limits on fuel temperature and required measuring channels that require the instruments. Instruments require routine maintenance to assure operability.

35.7 Section 3.3 of the guidance describes specifications for leak or loss of coolant detection and a secondary coolant activity limit. No such specifications are found in the proposed UT TRIGA TS.

The chill water subsystem for the pool cooling system as described in the Safety analysis Report is protected from radioactive contamination by:

1. System design, which maintains chill water pressure greater than pool water pressure so that any potential leakage will be from chill water to pool water, and

2. Automatic closure of a pneumatic valve if differential pressure drops to 2 psid, and

3. Control room alarms if differential pressure falls to 5 psid

The alarm and valve actuation are functionally tested prior to each startup. A pool- to chill- water leak would require multiple failures of the heat exchanger, heat exchanger design, and associated automatic controls as well as personnel failure to respond to an abnormal condition. A primary to secondary leak is not credible for the UT reactor.

35.8 Section 3.8.2 of the regulatory interpretations states that containers for experiments containing known explosive materials shall be designed such that the design pressure of the container is twice the pressure the experiment can potentially produce. The proposed UT TRIGA TS 3.6 "Limitations on Experiments," does not include such a specification, please explain or revise.

This requirement will be added to 5.4, EXPERIMENTS.

36.1 The list of measuring channels presented in Table 1 of proposed UT TRIGA TS 3.3 "Measuring Channels," does not include the data acquisition and control (DAC) and control system computer (CSC) [watchdog] which are [is] listed as [a] SCRAM channels in UT SAR Table 4.6. Please revise or justify

These channels are 'state of health' monitors and do not have a specific criteria as a safety function.

36.2 The setpoint stated for condition B for Specification B in proposed UT TRIGA TS 3.3, "Measuring Channels," is stated as 2mW. However, the neutron count rate should be stated in terms of neutrons per unit time.

The specification provides console indication.

36.3 The basis for propose UT TRIGA TS 3.3 contains a statement "According to General Atomics, detector voltages less than 80% of required operating value do not provide reliable ..." Please explain how this statement applies to UT TRIGA and how the required conditions for safe operation are ensured by your TS. Such information should be discussed in the SAR and then utilized in the TS basis.

The NP1000 and NPP1000 operate in the ion chamber region of the gas detector response curve. Basic principles of gas amplification lead to a constant number of ion pairs collected in the ion chamber region from a minimum voltage (below which ions and electrons recombine, therefore known as the recombination region) to a maximum voltage (above which gas amplification causes a signal increase which varies with voltage). Therefore the signal from the detector is constant over a range of voltages that bound the ion chamber region, providing a reliable signal that does not vary with minor changes in voltage.

The NM1000 is more complex, operating as an ion chamber region at higher power level range but also as a pulse counter in lower ranges. Pulse counting is typically performed in a range of gas detector response curve where pulse height is proportional to voltage. The instrument discriminates for pulses with magnitude greater than pulses from other lower energy sources, such as electronic noise and gamma pulses, to assure the signal is characterizing reactor power as a function of neutron flux. Therefore at low power levels the signal has some sensitivity to detector bias voltage:

- if bias is too low, the pulse height will not exceed the discriminator setting with indicated power artificially constrained, and

- if bias is too high, pulses from non-neutron interactions could be amplified enough to add to the signal with indicated power higher than actual power. This condition would create some non-linearity from gammas created by activated material in comparing actual to indicated power, but safety significance is low.

GA E117-101, Operations and Maintenance Manual for the NP1000 and NPP1000 Percent Power instruments specify calibration of the instruments for a detector bias of 750 VDC with a low voltage trip set point of 600 VDC. The manual for the NM1000 (using a fission chamber) specifies a bias of 800 VDC and a trip set point of 600 VDC for a low voltage trip setting and 850 VDC for a high bias voltage trip (with low safety significance).

36.4 Proposed UT TRIGA TS 3.4 Table 2 does not provided the scram setpoints for the Reactor Power Level, Fuel Temperature, and Pool Water Level SAFETY SYSTEM CHANNELS. Please explain or revise.

Fuel Temperature and power level trip setpoints are in Safety Limits and LSSS. The pool level setpoint is not part of the safety system.

36.5 Proposed UT TRIGA TS 3.5 "Gaseous Effluent Control," Specification A does not establish the conditions that determine HVAC OPERABILITY (e.g., conditions or positions for the fans/louvers/doors); a basis statement is not provided for the stated value of 10,000 cpm; such information should be discussed in the SAR and then utilized in the TS basis. Also, there are more COMPLETION TIMEs for Specification A than there are REQUIRED ACTIONs. Please explain or revise.

The HVAC system is an integrated control with a single switch for all controlled components. It is either operating to support the reactor or it is not.

Specification A has been corrected.

36.6 Proposed UT TRIGA TS 3.5 "Gaseous Effluent Control," Specification B does not provide a basis statement for the stated limit of 10,000 cpm; such information should be discussed in the SAR and then utilized in the TS basis. Also, there is a missing COMPLETION TIME for REQUIRED ACTION B.3.

The basis information from the approved 1992 SAR and Technical Specifications will be incorporated in the proposed SAR and referenced in the Technical Specifications basis.

36.7 Proposed UT TRIGA TS 3.5, "Gaseous Effluent Control," Specification D does not provide a basis statement for the stated limit of 100 Ci/yr; such information should be discussed in the SAR and then utilized in the TS basis.

See response to RAI 22.6.

36.8 The basis for the proposed UT TRIGA TS 3.7 "Fuel Integrity," does not provide an appropriate basis statement to support the limits in Specification C. Specification B is missing the word "not" in the REQUIRED ACTION. The second occurrence of CONDITION B should be CONDITION C.

"A release of fission products indicates cladding challenge" has been added as a basis statement

37.1 Proposed UT TRIGA TS 3.2 "Pulsed Mode Operation," the COMPLETION TIME listed for the REQUIRED ACTION is "immediate." Please consider the COMPLETION TIME to be "prior to commencement of pulsing operation."

Revised

37.2.1 CONDITION A.2 the lumping together of COMPLETION TIME(S) under A.2 is confusing as to which REQUIRED ACTION must be completed first.

Revised

37.2.2 The REQUIRED ACTION(S) A.1.1 and A.1.2 are, "Restore channel to operation OR ENSURE the reactor is SHUTDOWN." The COMPLETION TIME is stated as Immediate for both REQUIRED ACTION(S). Please consider a sequence of events (e.g., either restore the channel to operation within an acceptable COMPLETION TIME, OR shutdown).

A sequence is not required. Steps have been edited.

37.2.3 The COMPLETION TIME(S) for the REQUIRED ACTION(S) A.3.1 through A.3.3 are confusing in that no action is identified to take precedence over another, potentially leaving the operator to make their own assumptions as to the priority of events within one hour of any specified CONDITION.

A sequence is not required; the operator prior has the authority to select the preferred action. Steps have been edited.

37.2.4 CONDITION(S) A.4 through A.7 state a series of REQUIRED ACTION(S) that are not sequentially linked. Use of the same COMPLETION TIME for each action is contradictory.

Steps have been edited.

37.2.5 The REQUIRED ACTION(S) A.4.3 and A.4.4 seem to contradict each other.

Steps have been edited

37.3 Proposed UT TRIGA TS 3.4 "Safety Channel and Control Rod Operability," Specification B has no associated REQUIRED ACTION(S) or COMPLETION TIME(S).

Revised to

B. Fuel elements have visual indication of cladding integrity failure	B. Do not insert or re-insert the fuel element into the upper core grid plate.	B. IMMEDIATE

37.4 Proposed UT TRIGA TS 3.5 "Gaseous Effluent Control," logical "AND/OR" connectors are missing between REQUIRED ACTION(S) C.2.a-C.2.b and C.2.b-C.2.c. COMPLETION TIME(S) are all listed as IMMEDIATE which is contradictory. Please revise providing a clear sequence of the expected steps.

Revised with logical connectors in required action and immediate completion time

37.5 Proposed UT TRIGA TS 3.7 "Fuel Integrity," the COMPLETION TIME listed for all REQUIRED ACTION(S) is IMMEDIATE. Please consider revising the REQUIRED ACTION(S) for Specification A and B to state, "Discharge fuel elements prior to reactor operation."

Required Action and Completion time for B and completion time for C revised

37.6.1 REQUIRED ACTION(S) A.1 through A.3 are in reverse order. The COMPLETION TIME(S) are all IMMEDIATE which is contradictory.

See revised proposed Technical Specifications

37.6.2 REQUIRED ACTION(S) B.1 and B.2 are in reverse order.

The actions are independent, not sequential

37.6.3 REQUIRED ACTION(S) C.1 and C.2 are in reverse order. The COMPLETION TIME(S) are all IMMEDIATE which is contradictory. Also, and the CONDITION seems to be improperly stated.

See revised proposed Technical Specifications

37.6.4 "REQUIRED ACTION(S) D.2 and D.3 are in reverse order. The COMPLETION TIME(S) are all IMMEDIATE which is contradictory. A basis to support the established limits in Specification D is not provided. Such information should be discussed in the SAR and then utilized in the TS basis."

See revised proposed Technical Specifications

38.1 There are no SRs for the DAC or CSC that are listed as SCRAM channels in UT SAR Table 4.6.

The DAC and CSC trips are state of health monitors and not required by or credited in safety analysis.

38.2 There are no SRs for the reactor bay differential pressure for CONDITION A.3 in proposed UT TRIGA TS 3.3 "Measuring Channels."

Removed condition

38.3 Proposed UT TRIGA TS 3.3 "Measuring Channels," contains Surveillance Requirements for the Fuel Temperature Channel and the Upper Level Radiation Monitor but there are no associated LCO specifications

See response to 36.4

38.4 There are no SRs for the Reactor Power Level scram, the Manual scram, or Fuel Temperature scram to support proposed UT TRIGA TS 3.4 "Safety Channel and Control Rod Operability."

Surveillance requirements for instruments are in 4.3

38.5 There are no SRs to support proposed UT TRIGA TS 3.7 "Fuel Integrity," CONDITION C.

4.7.3: The STANDARD FUEL ELEMENTS SHALL be visually inspected for corrosion and mechanical damage

39.1 Proposed UT TRIGA TS 5.1.3(1) allows fuel having a stoichiometry of 1.55 to 1.80 in hydrogen to be used in UT TRIGA.

GA-Report E-117-833 does not specify a range; the range is taken from phase diagrams for the desired phase.

39.2 1) core parameters; 2) conditions for operation of the reactor with damaged or leaking fuel elements; 3) parameters such as maximum core loading, thermal characteristics, physics parameters, etc; and 4) fuel burn-up limits. These design features are not stated in the proposed UT TRIGA TS.

These design features are provided in the SAR analysis.

39.3 Please provide a basis for meeting UT TRIGA TS 5.2 "Reactor Fuel and Fueled Devises in Storage," in recommended by ANS Standard 15.1, Section 5.4.

Storage is either validated subcritical by criticality analysis or bounded by criticality analysis. LOCA analysis demonstrates convection cooling is capable of maintaining fuel integrity for air cooling, which is more severe than water cooling. Thermal hydraulic analysis demonstrates that fuel in the reactor with heat generation levels much greater than decay heat can be cooled by convection in water.

39.4 Proposed UT TRIGA TS 5.4 incorporates considerations for experiments into the design features section. These considerations do not meet the regulations of the definition for design features from 10 CFR 50.36.

§ 50.36 (Technical specifications) states:

(ii) A technical specification limiting condition for operation of a nuclear reactor must be established for each item meeting one or more of the following criteria:

(A) *Criterion 1.* Installed instrumentation that is used to detect, and indicate in the control room, a significant abnormal degradation of the reactor coolant pressure boundary.

(B) *Criterion 2.* A process variable, design feature, or operating restriction that is an initial condition of a design basis accident or transient analysis that either assumes the failure of or presents a challenge to the integrity of a fission product barrier.

(C) *Criterion 3.* A structure, system, or component that is part of the primary success path and which functions or actuates to mitigate a design basis accident or transient that either assumes the failure of or presents a challenge to the integrity of a fission product barrier.

(D) *Criterion 4.* A structure, system, or component which operating experience or probabilistic risk assessment has shown to be significant to public health and safety.

In the absence of a pressure boundary or potential or significant risk to the public health and safety, Criterion 1 and 4 do not apply. In the absence of experiment potential to initiate a design basis accident or challenge the integrity of the fission product barrier (i.e., cladding), Criterion 2 and 3 do not apply. Since the experiment design features specifically limit the impact of failure to prevent significant risk to the heath a safety of the public by preventing potential cladding failure, a limiting condition for operation based on design criteria is inappropriate. In fact, should an experiment introduce the potential to initiate a design basis accident or challenge fuel integrity, it could not be implemented without NRC review. In the event that such an experiment were proposed, specific Limiting Conditions for Operation could be required on specific measurable criteria with specific surveillance requirements to assure the LCOs are met.

(4) *Design features.* Design features to be included are those features of the facility such as materials of construction and geometric arrangements, which, if altered or modified, would have a significant effect on safety and are not covered in categories described in paragraphs (c) (1), (2), and (3) of this section.

The considerations for experiments are features of the experiment such as materials of construction and geometric arrangements, which, if altered or modified, would have a significant effect on safety and are not covered in categories described in paragraphs (c) (1), (2), and (3) of this section

These considerations are neither Safety limits (limits upon important process variables) nor Limiting safety system settings (for automatic protective devices). Limiting conditions for operation are the lowest functional capability or performance levels; these are design criteria for capabilities and performance levels. It may be that some specific experiment feature requires an LCO according to the 10CFR30 criteria, and if so that experiment and the associated LCO will be approved by the USNRC prior to implementation as per 10CFR50.59.

It is notable that placing the experiment design criteria in an LCO leads to a surveillance requirement that simply requires the design criteria is implemented, i.e., the experiment is designed to be acceptable. Therefore a surveillance requirements associated with such an LCO is verification that an administrative control is being exercised. While there are other administrative controls in Technical Specifications, they have not been formatted as LCO/SR. A requirement that the experiment be designed to the criteria would not place limiting condition for operations on the experiment itself, i.e., any parameter associated with the conduct of the experiment.

REPORT ON NEUTRONIC ANALYSIS FOR THE UT TRIGA REACTOR

The UT TRIGA critical mass of the original UT TRIGA reactor core configuration is compared with the critical mass required in prototypical cores. The computer codes used in this analysis is described. The geometry of the UT TRIGA core is identified. The representation of the core geometry and materials in modeling within the program is described. The results of calculations using the model to characterize the UT TRIGA reactor are summarized. Finally, evidence demonstrating validity of the model in characterizing the UT TRIGA reactor is provided.

The UT TRIGA reactor core uses a triangular pitch, composing a hexagonal geometry as shown in Fig. 1. Core positions are indexed as rings (A through G), with index numbers increasing for sequential positions. Neutronic analysis was performed for the UT TRIGA reactor configured with three standard fuel follower control rods located in positions C01, C07, D06, and D14. Position A01 (central thimble) does not contain a standard fuel element. Positions G32 and G34 are reserved for a neutron source and an in-core pneumatic terminal. The A and B rings are within a removable assembly that allows insertion of large experiments; because of the associated reactivity deficit, removing the fuel in these positions severely limits potential operation. Fuel element positions E03, E04, F03, F04, F05, G04 and G05 can similarly be removed with full power operations possible. Two smaller removable "3-element" assemblies are located at the D17/E22/E23 and E11/F12/F14 positions.

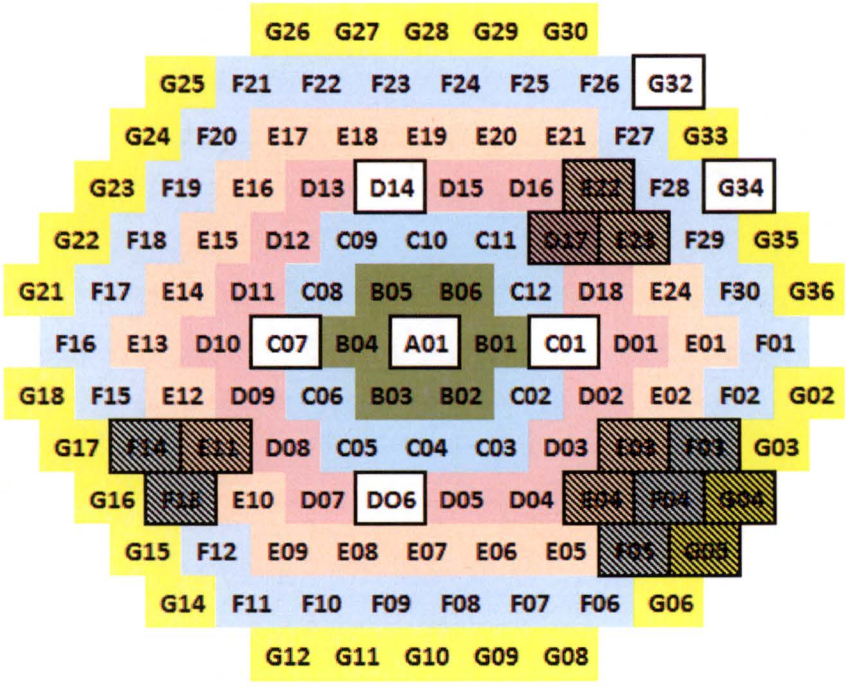

Figure 1, UT TRIGA Reactor Core

1.0 COMPARISON WITH HISTORICAL CRITICAL MASS DATA

The critical mass for the General Atomics prototype reactors is compared to the critical mass of the 1992 UT TRIGA reactor. Critical mass of the UT core was 93% of the GA core.

1.1 CRITICAL MASS OF HISTORICAL GENERAL ATOMICS TRIGA REACTORS

The cylindrical GA TRIGA Mark I reactor achieved critical condition with 54 standard fuel elements (8.5% weight uranium, 20% enriched, 1.94 kg ^{235}U) and four water filled control rod positions. Core positions not occupied by fuel elements used graphite "dummy" rods for reflection; removing the graphite rods increased critical mass about 25%. The GA Advanced TRIGA Prototype reactor achieved critical condition with three fuel follower control rods, 1 transient rod, and 75 standard fuel elements (2.7 kg 235U). The GA TRIGA Mark III reactor achieved critical condition with four fuel follower control rods (including a fuel element in the "A" ring) and 56 standard fuel elements (2.24 kg 235U).

1.2 CRITICAL MASS OF THE 1992 UT TRIGA REACTOR

Initial criticality for the UT TRIGA reactor at the Nuclear Engineering Teaching Laboratory (NETL) was accomplished on 02/13/1992. Criticality was attained with 3 fuel follower control rods (fully withdrawn, i.e., fuel fully inserted) and 56 fuel rods (including two instrumented fuel elements). Total mass of ^{235}U was 2.12 kg in the standard fuel elements and 94.46 g in the three fuel followers.

The UT TRIGA reactor was configured with both water voids and graphite rods in non-fueled positions. With the exception of fuel follower elements (i.e., fuel follower control rods), the 1992 University of Texas (UT) TRIGA reactor core was composed of fuel elements with power history at other facilities (previous UT TRIGA located on main campus in Taylor Hall, Northrup Aircraft, and a General Atomics facility). These lightly-burned fuel elements decayed approximately 1 year prior to use at the current location. The new UT TRIGA core included three new fuel follower elements with fresh fuel. Critical fuel loading is displayed in Fig. 2, with labels:

- CT for the central thimble (water void)
- SFE for standard fuel rods
- TC for instrumented fuel elements
- GR for graphite rods
- S for the neutron source
- WV for water voids
- S2, S1 and RR for the fuel follower control rods (Shim 1 and 2, Regulating Rod)
- TR for the transient rod

Although the pitch is hexagonal, positions are labeled "rings." The B ring is shaded green in Fig. 2, C ring light blue-green, D ring rose, E ring light brown, F ring light blue, and the G ring yellow.

Although the critical masses of the UT reactor and GA Mark III are within 2%, comparison between critical masses of the initial 1992 UT TRIGA core and the historical GA TRIGA cores is complicated by (1) differences in reflection (graphite rod and water void configurations), (2) previous power history for the standard fuel elements at the UT core, and (3) fundamental difference in core geometry.

Power history for the standard fuel elements at UT is based on Special Nuclear Material (SNM) reports. Burnup included 7.91 MWD generated at Taylor Hall in 46 elements, and 41.07 MWD generated at General Atomics or Northrup Aircraft facilities in 56 elements. Fifteen elements had burn from both UT and other facilities. With the exception of the fuel followers and standard fuel elements in positions C11 and D18, fuel in the B ring through the D ring (B01 through D17) SNM reports indicate an average burn of 0.255 MWD per element. With the exception of standard fuel elements in elements in core position F30, the standard fuel elements in the E and F rings and positions C11 and C18 had an average

burnup of 0.710 MWD. The element in position F30 was an outlier, received from GA with almost a gram of ^{235}U depleted.

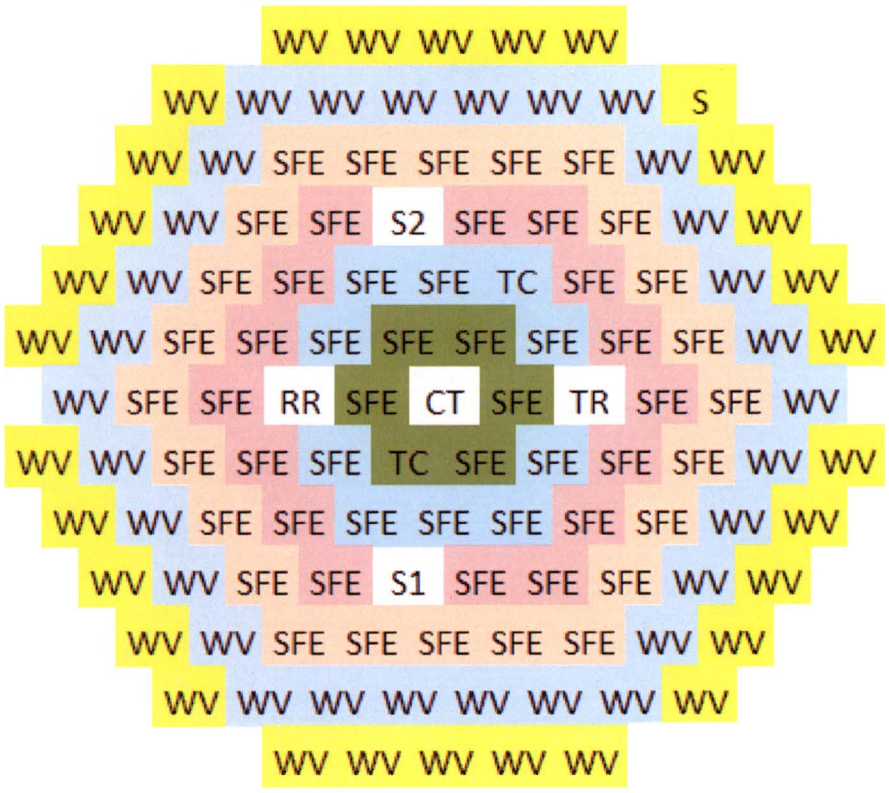

Figure 2, Initial UT TRIGA Core

The total core burnup from the original UT Taylor Hall facility is not in good agreement with the startup report for the 1992 TRIGA installation. SNM reports are designed to account for changes in fissionable material across the core, and not individual elements. Core burnup has historically been distributed to individual elements using very simple correlations that do not account for spatial differences with core physics. Although it is possible that the Taylor Hall facility could be modeled to get a more precise evaluation of burnup for each element, records that identify core position and power generation are not available for the Northrup Aircraft and the General Atomics reactors (and in the case of the GA facilities, the specific prototype in which the fuel was utilized). There a potential issue with other fuel in UT inventory from the University of Illinois that was not loaded the original 1992 core. Therefore SNM records may not have the fidelity to accurately identify burnup for individual elements. Initial calculations demonstrated a bias of approximately +$2 in calculations of excess reactivity. Calculations demonstrate an increase of 0.5 gram in U^{235} for an 80 element core results in $0.80 increase of excess reactivity, suggesting that validating the model against surveillance data is challenging.

1.3 OPERATIONAL LOADING OF THE 1992 UT TRIGA REACTOR

Fuel was loaded in the UT TRIA reactor to support operation at 1.1 MW on 03/16/1992. The core contained 84 standard and 3 fuel follower elements with 3.35 kg ^{235}U. Operational fuel loading is displayed in Fig. 3, using the same labeling as in Fig. 3.

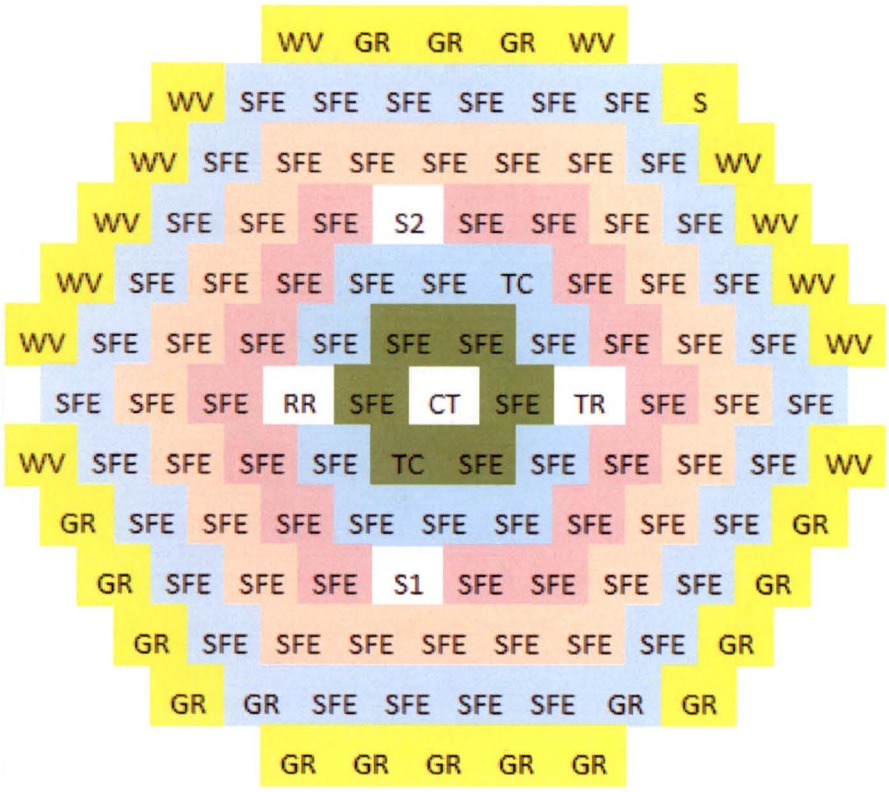

Figure 3, Operational 1992 Core

Control rod calibrations are accomplished under surveillance procedure SURV-6, and excess reactivity determinations are documented with SURV 3. The initial control rod reactivity worth calibration was completed on 03/31/1992, although excess reactivity was not determined until completion of initial testing in July when both SURV-3 and SURV-6 were performed. Surveillance data is provided in Table 1.

Table 1: 1992 UT TRIGA REACTIVITY ($), SURV-6 & SURV 3

PARAMETER	03/25/1992	07/23/1992
EXCESS	NA	6.38
REG ROD	4.59	4.08
TR ROD	3.34	3.26
SHIM 2	3.46	3.30
SHIM 1	3.32	3.17

2.0 NUCLEAR PHYSICS MODELING

Neutronic and gamma transport modeling for the UT TRIGA reactor is based on calculations with SCALE[1] 6.2.2. For the UT TRIGA reactor, the SCALE depletion sequence (T-6) and the criticality sequence (CSAS6) were used to calculate:

- Fuel composition as a function of burnup

[1] ORNL/TM-2005/39 Version 6.2.2, SCALE Code System

- Critical mass
- Core Radial Peaking Factor
- Physics parameters & Flux density
- Fuel Element Axial and Radial Peaking Factors
- Fission Product Poisons
- Transuranic buildup
- Fuel temperature reactivity deficit
- Water temperature reactivity deficit
- Control Rod worth
- Excess reactivity
- Shutdown Margin
- Effects of Experiments
- Effects of Burnup
- Accident source Terms

Scattering data for zirconium hydride is provided in SCALE to more accurately present cross section data. The scattering data was applied to criticality analysis, but is incompatible with ORIGEN in the depletion calculations. This required separating the calculations; material composition was developed for individual fuel elements based on element burnup that does not use the scattering data, and the element burnup distribution was developed from criticality calculations using the scattering data.

2.1 UT CORE AND FUEL GEOMETRY

Principle dimensions used in modeling the UT TRIGA core are taken from General Atomics drawings. Major dimensions of fuel, core shroud, core barrel, and the reflector are incorporated in modeling. Although the models include beam ports and the rotary specimen rack geometry, modeling of these features is not discussed in this section. Fuel end fittings are modeled as conical, stainless steel structures at the ends of the element (not including the fins or end-pins). End fittings for graphite "dummy" elements are not modeled.

2.2 CORE BARREL (REFLECTOR AND GRID PLATES)

The radial reflector is annular, with a cylindrical outer surface (radius of 81.994 cm) and the inner surface conforming to the inner shroud. For convenience the reflector[2] is assumed to extend the full height of the inner shroud; however, the reflector actually ends about 3 in. above the lower grid plate, at an elevation corresponding to about ½ of the fuel element's lower axial reflector (about 1 ⅓ in. below the bottom of the fuel matrix). The reflector annulus (core barrel) and the lower grid plate are composed of aluminum alloy 6061. The core barrel[3] is shaped by two hexagonal prisms, one rotated 30° as illustrated in Fig. 4. One of the hexagonal shapes is 55.625 cm, the other 52.637 cm. The lower grid plate[4] is 1.25 in. thick, with the upper surface 33.249 cm, and the lower surface 36.424 cm below the center of the fuel.

[2] GA Technologies Inc. drawing T2W210J111
[3] GA Technologies Inc. drawing T2W210J111
[4] Drawing NETL BGP001

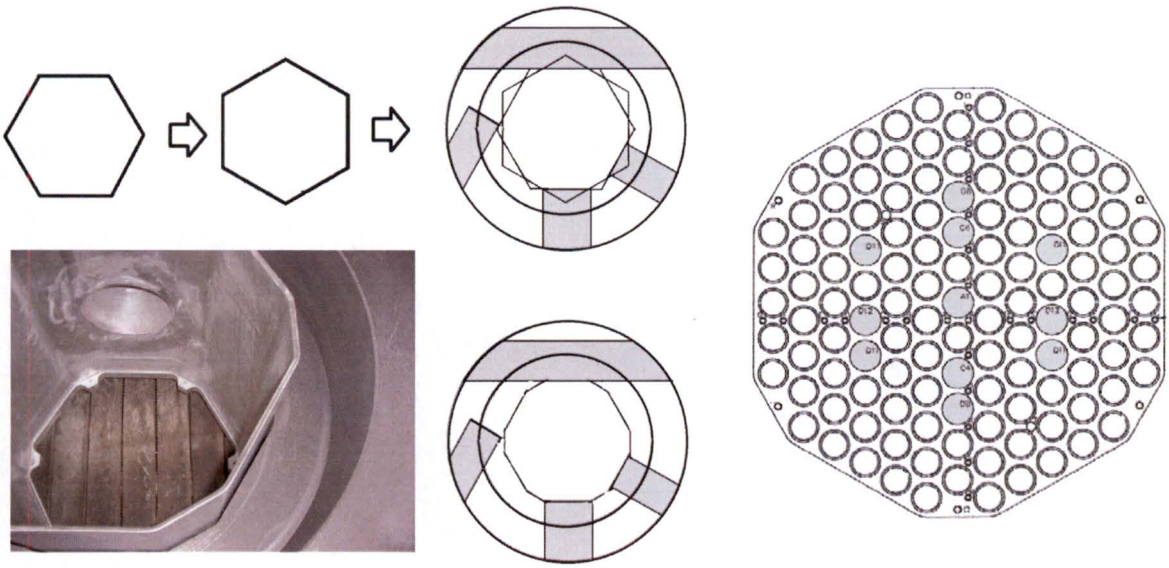

Figure 4, Core Shroud and Lower Gird plate

The annulus at the upper part of the inner reflector surface and the upper grid plate are cylindrical. The upper reflector has a space for a rotary specimen rack[5], displacing the reflector to an outer radius of 35.715 cm. Center to center distance for the fuel element positions[6] (pitch) in the grid plates is 1.714 in. (4.355 cm). Upper grid plate penetrations are nominally 1.505 in. (3.823 cm) in diameter. The bottom grid plate has a set of positions with the same diameter as the top, shaded in Fig. 5, and the remaining positions 1.250 in. in diameter. In addition to the variations in lower grid plate penetration diameters, the upper grid plate has clearance for fuel elements, graphite elements, control rods, control rod guide tubes, and experiments. To simplify modeling, all grid plate penetrations are assumed at the same diameter as the component inserted in the position.

The upper grid plate is 5/8 in. thick, with the lower elevation and the upper elevation referenced to the center of the fuel 42.799 cm and 41.224 respectively. Dimensions of penetrations in the upper grid plate are provided in Table 2.

The reference point selected for physics models is the center of the active fuel, although the core is not actually symmetric about the fuel matrix The distance from the center of the fuel to the top of the lower grid plate is 13.09 in. (33.249 cm) above the top of the lower grid plate (based on dimensions from GA drawings[7]). Modeling of standard fuel elements as based on these dimensions is provided in Table 3.

[5] Rotary Rack Assy. Mark I & II, TO6S14E115

[6] T2W210E108 - Top Grid Plate, NETL BGP0001 - Bottom Grid Plate

[7] TS13S210B217, TS13S210B229, TS13S210C212, TS13S210C214, TS13S210C218, TS13S210C226, TS13S210C227, TS13S210D210, and TS13S210D213, derived by GA

Table 2: Upper Grid Plate Dimensions

Label		
A	Description	In.
B	Fuel Position	1.505
C	6/7 Element Facility diameter	5.140
D	3 Element Facility Y displacement	4.285
E	3 Element Facility X displacement	3.464
F	3 Element Facility Y displacement	5.999
G	3 Element Facility X displacement	3.464
H	Grid Plate Diameter	21.75
I	6/7 Element, Diameter 1	4.002
J	Grid plate thickness	0.62
K	6/7 Element Facility, Diameter 2	4.175
L	3 Element Cutout	2.370
M	Alignment pin hole	5/6

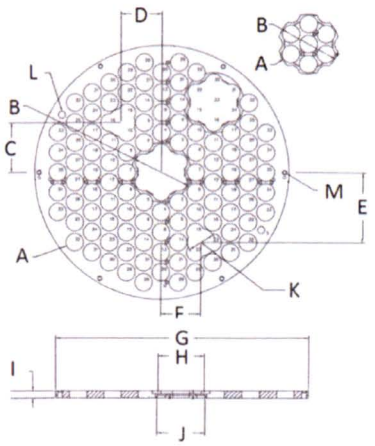

Figure 5, Upper Grid plate

2.3 TRIGA FUEL ASSEMBLIES

Standard TRIGA fuel is identified[8] as

> *8.5 to 12 wt % uranium (20% enriched) as a fine metallic dispersion in a zirconium hydride matrix. The H/Zr ratio is nominally 1.6 (in the face centered cubic delta phase).*

A TRIGA fuel element is fabricated with three 1.435 in. diameter[9] uranium zirconium hydride cylinders with a central hole 0,25 in. as a fuel matrix, each cylinder 5 in. tall,. The fuel is enveloped in 0.2 in. thick stainless steel cladding with a diameter of 1.48 in. Nominal loading is 39 grams U^{235} in the fuel matrix, but the average (unirradiated) value of all the fuel elements received at UT is 38.1 grams U^{235} and the most recent manufactured fuel in inventory has an assay of 38 (38.0 to 38.3) grams; therefore standard loading at UT is assumed to be 38 grams. The fuel matrix inner diameter provides a cavity to enhance hydrogen stoichiometry, and is filled with a 0.225 in. zirconium rod after processing. Axial graphite reflectors are installed above and below the fuel, with a protective molybdenum disk between the lower reflector and the fuel. A gap above the upper axial reflector permits thermal expansion and provides space for outgassing of fission products and hydrogen. End fittings are welded to the cladding above the gas gap and below the lower axial reflector; the completed end fittings are machined to assure clearance in transition through the upper grid plate.

[8] GA Project No. 4314, The U-ZrH_x Alloy: Its Properties and Use in TRIGA Fuel, M. T. Simnad (Feb. 1980) and NUREG 1282, Safety Evaluation Report on High-Uranium Content, Low-Enriched Uranium-Zirconium Hydride Fuels for TRIGA Reactors, Docket No. 50-163 (Aug 1987)

[9] TOS210D210

Table 3: TRIGA Standard Fuel Element (SFE) Dimensions (Referenced to Midplane)

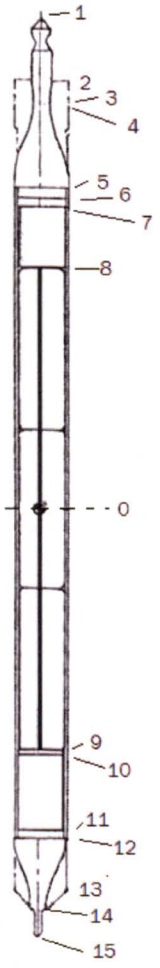

Figure 6, SFE

	NODE	z_2 in.	Cm
1	Top of upper pin	15.50	39.370
2	Top of upper fins	13.94	35.408
3	Top of reinforcment	13.06	33.172
4	Bottom of reinforcment Top of conical shape	12.81	32.537
5	Bottom of conical shape Top of cladding Weldment plug top	10.81	27.457
6	Weldment plug bottom Top of gap	10.56	26.822
7	Bottom of gap Top of axial reflector	10.060	25.552
8	Bottom of axial reflector Top of fuel	7.50	19.050
9	Bottom of fuel Top of Moly disk	-7.5	-19.050
10	Bottom of moly disk Top of axial reflector	-7.531	-19.129
11	Bottom of axial reflector Top of weldment plug	-11.251	-28.578
12	Bottom of welment plug Bottom of cladding Top of conical end-shape Top of lower fins	-11.501	-29.213
13	Top of lower grid plate Start fin taper	-13.09	-33.249
14	Bottom of conical shape Top of lower pin	-13.695	-34.785
15	Bottom of lower pin	-14.441	-36.680

First generation TRIGA fuel was supported in the core by the lower end-pin in a depression in the lower grid plate; later TRIGA fuel is supported by three fins in contact with holes in the lower grid plate. An adapter (Fig. 7) is required to use older fuel in current TRIGA grid plates.

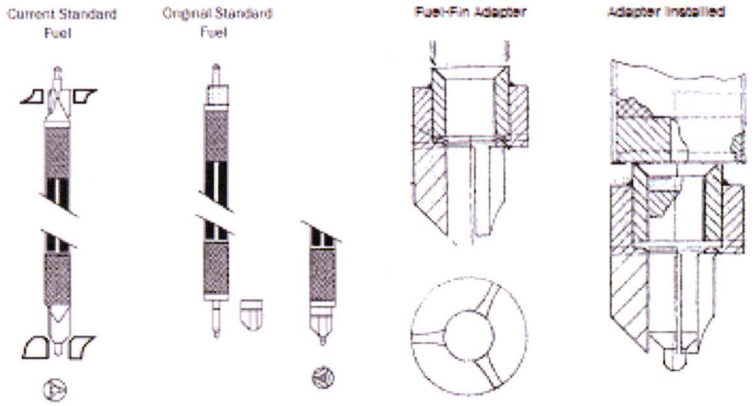

Figure 7, Standard Fuel Element Details

Figure 8, Adapter

Nine grid plate locations are designed to accommodate control rods and the central thimble, with holes at the same diameter in the upper and lower grid plates. Fuel can be used in these locations using an adapter (a hollow cylinder) secured to the aluminum "safety plate" below the lower grid plate. The top of the adapter mimics the top of the lower gird plate, providing support surface for fuel elements fins.

Holes in the surface of the adapter permit cooing flow through the bottom of the fuel element (Fig. 8). These adapters are designed to make the geometry of the lower grid plate in these positions compatible with the geometry of the other penetrations. A photograph of the area under the lower gird plate is provided in Fig. 9.

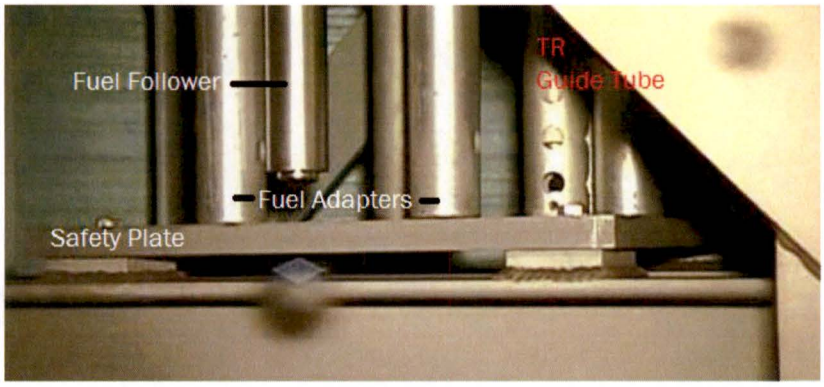

Figure 9, Area Below the Lower Grid Plate

2.4 CONTROL RODS

Two types of control rods are used in the UT TRIGA: fuel follower control rods (FFCR) and a transient control rod, alternately referred to as the pulse rod. The poison sections of control rods are composed of B_4C, heat pressed to a density[10] greater than 2.48 g cm^3 (theoretical density of B_4C is 2.52 g cm^3). As an FFCR is removed, the attached fuel follower is drawn into the core. The transient control rod uses a guide tube and has an air filled follower.

2.4.1 FUEL FOLLOWER CONTROL RODS.

Standard fuel element follower control rods are stainless steel tubes with welded end fittings approximately 45 in. (114 cm) long by 1.35 in. (3.429 cm) in diameter (1991 UT SAR). The upper 6.5 in. (16.51 cm) of the fuel follower control[11] rod is an air void, separated and secured from the poison section by a 0.5 in. (1.27 cm) plug secured with a magneform weld. There is a small (0.12 in, 0.305 cm) air gap at the top of the poison section, between the poison and the plug. The poison is 15 in. (38.1 cm) of B_4C. 1.187 in. (3.015 cm) in diameter. The poison section is separated from the fuel follower section by another 0.5 in. plug and magneform weld. The top of the fuel follower section is a 0.25 in (0.635 cm) air gap, above the fueled. The fuel rests on a double thickness 1 in. (2.54 cm) plug and magneform weld, followed by a 6.5 (16.51) in. air void. The bottom air void has an aluminum insert with wall thickness 0.35 in. (0.089 cm). For convenience, the reference point for the control rod in Table 3 aligns the fuel section with the center of the fuel in standard fuel elements when the rod is withdrawn.

[10] GA Drawing TOS250B226, Poison
[11] GA drawing TOS250D225 (Control Rod – Fuel Follower).

Table 4: Fuel Follower Control Rod Geometry

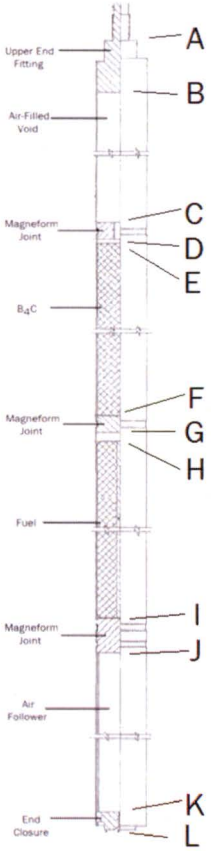

Figure 10, FFCR

KEY	DESCRIPTION	ELEVATION	
		in	cm
A	Top upper end	13.87	35.230
B	Bottom upper end Top of top void	12.37	31.420
C	Bottom of top void Top of top plug	8.87	22.530
D	Bottom of mag plug Top of poison gap	8.37	21.260
E	Bottom of poison gap Top of poison	8.25	20.955
F	Bottom of poison Top of lower poison mag plug	-6.75	-17.145
G	Bottom of lower mag plug top of fuel gap	-7.25	-18.415
H	bottom of fuel gap top of fuel	-7.5	-19.05
H	bottom of fuel top of lower mag plug	-22.5	-57.15
J	bottom of lower mag plug top of lower air follower	-23.5	-59.69
K	bottom of air follower top of lower end fitting	-28.875	-73.343
L	bottom of lower end fitting	-29.375	-74.613

Table 5: FFCR Component Thickness (Z Axis)

Component	in.	cm
Upper End Fitting	1.5	3.81
Upper Air Void	3.5	8.89
Magneform Plug	0.5	1.27
Poison/Air Gap	0.12	0.305
Poison	15	38.1
Magneform Plug	0.5	1.27
Fuel/Air Gap	0.25	0.635
Fuel	15	38.1
Magneform Plug	1	2.54
Lower Air Void	5.375	13.653
Lower End Fitting	0.5	1.27

2.4.2 TRANSIENT CONTROL ROD.

The transient control rod operates within an aluminum guide tube (1.490 in. or 3.7846 cm in diameter machined from 1.5 in./3.81 cm aluminum tubing with a wall thickness 0.065 in. or 0.1651 cm[12]) secured to the upper grid plate and the safety plate (below the lower grid plate). The guide tube is perforated by ½ in. holes at 90° rotations on 1 in. centers at the top and bottom of the core barrel. The guide tube extends 5 feet above the safety plate and below the lower grid plate. Perforations and extensions above the upper- and below the lower-grid plate are not modeled.

Table 6: Transient Rod Dimensions

KEY	DESCRIPTION	ELEVATION[13] in	ELEVATION[13] cm
A	Top of end fitting	9	22.860
B	Bottom of end fitting Top of poison section	7.5	19.050
C	Bottom of poison section Top of magneform weld	-7.5	-19.050
D	Bottom of magneform weld	-8.5	-21.59
	Top of air follower		
E	Bottom of air follower Top of end fitting	-27.75	-70.485
F	Bottom of end fitting	-28.25	-71.755

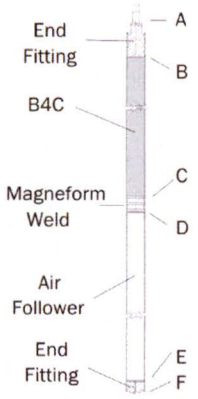

Figure 11, Transient Rod

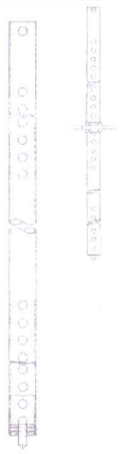

Figure 12, Guide Tube

Transient rod cladding is a 1.25 in. (3.175 cm) diameter aluminum tube with wall thickness 0.028 in. (0.071 cm)[14]. The poison section of the transient rod is 15 in (38.1 cm)[5]. A double (1 in., 2.54 cm) plug with a magneform weld secures the poison section at the top and bottom. The air follower above the poison section is in an assembly 5.94 in., which includes the upper end fitting and the upper magneform weld. The air follower under the plug is 20.88 in. (53.02 cm) long, terminating in a bottom end-fitting.

3.0 LIMITING CORE CONFIGURATION

NUREG 1537 requires a Limiting Core Configuration (LCC) be identified as the configuration that has a fuel element with the highest power density. The highest power density occurs in the fuel element where the ratio of the power in an element to the average power across all elements (power per element) is largest.

NUREG 1537 requires information relative to the operational core. Fuel loading in excess of the limiting core configuration supports compensates for fuel burnup and the negative reactivity that may occur with experiment insertion. Operational core loading is limited by the maximum excess reactivity permitted in the Technical Specifications.

---

[12] T135210D150, Guide Tube – Transient Rod
[13] T0S252D191 & 1991 UT SAR
[14] T0S252D191 – Transient Rod Assembly (ADJ)

3.1 Determining the Limiting Core Configuration

The highest average power per fuel element will occur in a core with the smallest number of fuel elements that will support full power operation. The highest power density will occur in an element closest to the center of the core; the B-ring elements were analyzed discretely within the core to provide an indication of fission rate in each element. The power in each B ring element is determined as the product of the core power and fission rate in an element normalized to the average fission rate across all elements. The use of a reflector reduces the required number of fuel elements by reducing neutron leakage. If non-fuel spaces are filled with graphite rods acting as reflectors, average power generation across the core (i.e., per element) will be more uniform, resulting in a lower the peak-to-average power ratio. For a water voided G ring, the core approaches a water reflected condition where elements further from the core center generate less power and increasing the peaking factor.

Calculations were performed with graphite in non-fuel spaces and a then with water voids in non-fuel spaces to verify that the maximum power in an element occurs with water voids. The calculations were used to determine the minimum number of fuel elements required to achieve criticality and the number of fuel elements that will result in in a calculated excess reactivity of 4.97%. Calculations for limiting core configuration were performed with core configurations from 49 to 115 at 600K (simulating full power operation) with water voids in non-fueled locations.

3.1.1 Zero Power Critical Mass

Minimum fuel loading with graphite rods at 300 K is determined to be 60 elements (57 standard fuel elements and 3 fuel followers). Associated mass is 2.27 kg of ^{235}U (slightly more than the 1.94 kg ^{235}U in the GA TRIGA Mark reactor, slightly less than the 2.7 kg ^{235}U in the GA Advanced TRIGA Prototype reactor, and comparable to 2.24 kg ^{235}U of the GA TRIGA Mark III critical condition, op cit). The water-void configuration requires about 74 fuel element to achieve criticality at room temperature, 23% more fuel elements comparable to the 25% increase noted at GA.

3.1.2 Critical Mass for Power Operation

The UT TRIGA core can be critical at full power operating temperature with 75 fuel elements. Average element power with 75 elements with operation at 1250 kW is 16.67 kW.

3.1.3 Operational Critical Mass

In addition to compensating for operating temperature, fuel is required to provide reactivity to compensate for fission product poisons and burnup. The maximum allowable excess reactivity is established for safe operation at 4.9% $\Delta k/k$. An 82 element core results in a calculated excess reactivity of 5.2% at 300K; an 81 element core with fresh fuel has 4.5% excess reactivity, and an 80 element core 4.3% excess reactivity. The 80 element core has more than 10% margin to the maximum reactivity permissible without exceeding the reactivity limit, and will therefore be considered the operational core.

3.1.4 Fuel Element with Highest Peaking Factor

Elements in the B ring are exposed the highest neutron flux, and therefore generate the most power. The ratio of the power in a fuel element to the average power per element in the core is the "Peaking

Factor. The maximum B ring peaking factor for the core configuration (that can support full power operation) and the core configuration that can approach the limiting reactivity are tabulated in Table 7.

Table 7, B RING PEAKING FACTOR AT CORE LOAD

No. Elements	92	86	85	84	80	76	74
Excess Reactivity	$10.09	$2.68	$8.59	$8.34	$7.44	$6.20	$5.53
B01	1.53	1.49	1.53	1.53	1.51	1.50	1.50
B02	1.53	1.58	1.53	1.52	1.51	1.51	1.50
B03	1.56	1.65	1.56	1.55	1.54	1.53	1.52
B04	1.58	1.67	1.57	1.57	1.55	1.54	1.54
B05	1.56	1.64	1.55	1.56	1.54	1.52	1.52
B06	1.53	1.58	1.53	1.51	1.51	1.50	1.49

3.1.5 B RING ELEMENT POWER

The maximum B ring fuel element power (Table 8) is product of the peaking factor from Table 7 and the power distributed uniformly over all fuel elements, average element power, for each core configuration. The maximum power occurs with 74 elements.

Table 8, FULL CORE POWER, B RING POWER AT CORE LOAD

No. Elements Excess Reactivity	92 $10.09	86 $2.68	85 $8.59	84 $8.34	80 $7.44	76 $6.20	74 $5.53
B01	20.12	20.89	21.78	22.00	22.88	23.85	24.51
B02	20.16	22.16	21.80	21.91	22.85	23.97	24.47
B03	20.55	23.16	22.22	22.29	23.26	24.44	24.91
B04	20.79	23.50	22.37	22.55	23.51	24.59	25.18
B05	20.48	23.04	22.11	22.53	23.31	24.27	24.93
B06	20.13	22.28	21.74	21.71	22.79	23.81	24.42

3.1.6 LIMITING CORE CONFIGURATION

The B ring fuel element with the maximum power across all cores that that will support full power operation generates 25.18 kW.

3.2 Nuclear Characteristics of the Limiting Core Configuration

KENO transport and ORIGEN buildup and decay calculations provide information representative of or useful in determining physics and operational parameters. Control rod positions are adjusted to achieve the desired conditions (critical or rods fully withdrawn, as applicable). The beginning of core life assumes the limiting core configuration with unirradiated fuel. The end of life core assumes a fully fueled core (with water void positions reserved for the neutron source and the pneumatic tube),

operated at full power until criticality cannot be maintained (at full power). Space is reserved in the core lattice for the neutron source and the pneumatic irradiation facility.

3.2.1 Physics Parameters and Flux Density

Physics parameters and flux density are determined from simulation of the critical condition. Control rods were simulated in a banked position (equal translations along the z axis). A series of calculations was performed for the LCC from simulated zero power to full power at fuel temperature of 300 K with the control rods positioned at 18 cm withdrawn.

Table 9: (Critical) Nuclear Physics Parameters

Parameter	300 K 18cm		600 K 18 cm	600 K26 cm
	1E-9 MW	1.1 MW	1.1MW	1.1 MW
Neutron Lifetime	14.32 μs	14.32 μs	14.77 μs	14.62 μs
Neutron Generation time	53.92 μs	53.92 μs	54.83 μs	54.45 μs
Mean free path	1.011 cm	1.011 cm	1.003 cm	0.9964 cm
nu bar	2.439	2.439	2.439	2.4385

Additional simulations were performed at simulated full power operation, first with the same control rod position at temperature of 600 K and then with the control rod position adjusted to compensate for the elevated fuel temperature, approximately critical at control rod position 26.5 cm withdrawn. Table 9 values for "Neutron lifetime," "generation time," "mean free path" are taken from the KENO summary report. Neutron flux from transport calculations at each power level is taken from the (energy) "group" report row totals, tabulated in Table 10.

During reactor operation, ^{235}U is burned and fission products are generated, affecting reactor characteristics. Operation of a fully fueled core load was simulated as representative of changes to the operational core configuration over core life. At the end of core life with a k_{eff} of 1.005, neutron lifetime is 11.25 μs, neutron generation time 52.48 μs, and system mean free path 1.017 cm.

Table 10: Flux Density & Fission, Absorption & Leakage Fractions and Power

POWER	Temp.	Rod Position	keff	thermal flux	total flux	fissions	absorptions	leakage
1.00E-06	300 K	18	1.0037	1.07E+04	3.86E+04	1.00449	0.89233	0.107918
0.01	300 K	18	1.0037	1.07E+08	3.86E+08	1.00449	0.89233	0.107918
0.1	300 K	18	1.0037	1.07E+09	3.86E+09	1.00449	0.89233	0.107918
1	300 K	18	1.0037	1.07E+10	3.86E+10	1.00449	0.89233	0.107918
10	300 K	18	1.0037	1.07E+11	3.86E+11	1.00449	0.89233	0.107918
100	300 K	18	1.0037	1.07E+12	3.86E+12	1.00449	0.89233	0.107918
1000	300 K	18	1.0037	1.07E+13	3.86E+13	1.00449	0.89233	0.107918
1100	300 K	18	1.0037	1.18E+13	4.24E+13	1.00449	0.89233	0.107918
1100	600 K	18	0.9676	1.35E+13	4.53E+13	0.96865	0.890989	0.108998
1100	600 K	26	0.9982	1.35E+13	4.48E+13	0.99950	0.893075	0.107205

Neutron flux density for the LCC core with fuel temperatures of 300 K is shown to be $1.08X10^7$ n/cm^2-s per watt in the thermal range, and $3.91X10^7$ n/cm^2-s per watt above thermal energy range. These

values agree well with calculations reported by General Atomics[15], where 2-D, 24 group calculations indicate average flux values for an 80 element 1 MW TRIGA to have $1.1X10^7$ n/cm^2-s per Watt from 0 to 1 eV and $2.46X10^7$ n/cm^2-s from 1 eV to 10 eV. At the end of core life as described, 1.1 MW power in the operational core requires a thermal neutron flux of $9.16X10^{12}$ n/cm^2-s, and total flux of $3.03X10^{13}$ n/cm^2-s.

3.2.2 Element Peaking Factors

As previously described, data from SCALE calculations to determine critical mass was used to evaluate maximum core peaking factors to support identification of the limiting core configuration, using the base geometry units as identified above. However, power within a fuel element is spatially distributed. Therefore fuel element geometry was segmented first axially (20 segments) then radially (21 segments). The results of calculations B01 are provided in Table 11 and Fig. 13 for axial distribution and Table 12 and Fig. 14 for radial distribution.

Table 11: B01 Axial Peaking Factor

NODE	300 K	600 K
1	5.63E-01	5.64E-01
2	6.48E-01	6.40E-01
3	7.62E-01	7.24E-01
4	8.59E-01	8.86E-01
5	9.33E-01	9.80E-01
6	1.02E+00	1.01E+00
7	1.09E+00	1.12E+00
8	1.12E+00	1.12E+00
9	1.20E+00	1.16E+00
10	1.19E+00	1.20E+00
11	1.18E+00	1.18E+00
12	1.20E+00	1.17E+00
13	1.14E+00	1.16E+00
14	1.15E+00	1.13E+00
15	1.06E+00	1.07E+00
16	1.01E+00	9.66E-01
17	8.63E-01	9.09E-01
18	7.85E-01	7.60E-01
19	6.84E-01	6.65E-01
20	6.11E-01	6.04E-01

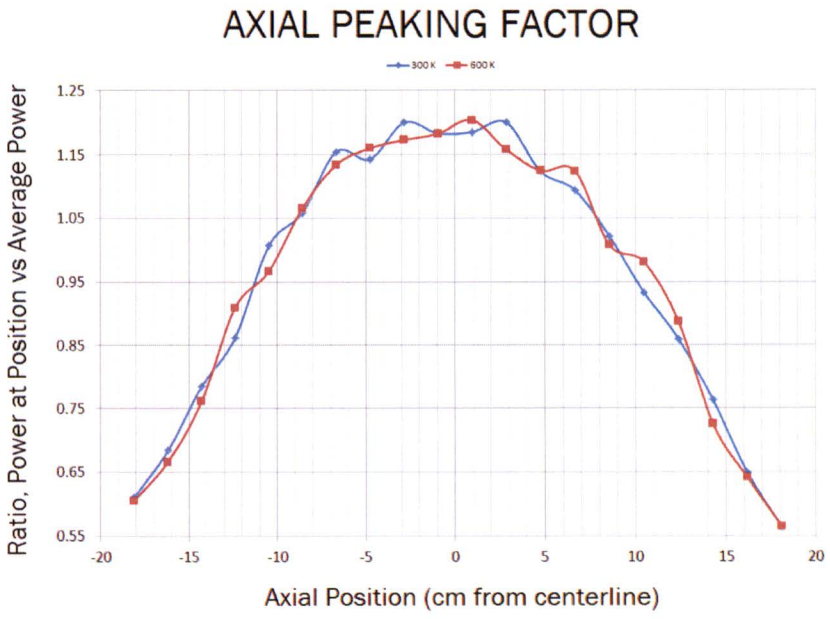

Figure 13, Axial Peaking Factor

[15] GA-4361, Calculated Fluxes and Cross Sections for TRIGA Reactors, G. B. West (August 14, 1963)

Table 12: Fuel Element B01 Radial Peaking Factor

Radial Position			Temperature	
Outer	Inner	Ave.	300	600
1.826	1.753	1.790	1.972	2.088
1.753	1.680	1.716	1.853	1.918
1.680	1.606	1.643	1.718	1.732
1.606	1.533	1.569	1.583	1.599
1.533	1.459	1.496	1.481	1.484
1.459	1.386	1.423	1.380	1.365
1.386	1.313	1.349	1.284	1.271
1.313	1.239	1.276	1.183	1.168
1.239	1.166	1.202	1.096	1.067
1.166	1.092	1.129	1.022	0.989
1.092	1.019	1.056	0.933	0.910
1.019	0.946	0.982	0.849	0.828
0.946	0.872	0.909	0.779	0.763
0.872	0.799	0.835	0.713	0.701
0.799	0.725	0.762	0.649	0.634
0.725	0.652	0.689	0.574	0.570
0.652	0.579	0.615	0.513	0.503
0.579	0.505	0.542	0.441	0.437
0.505	0.432	0.468	0.387	0.383
0.432	0.358	0.395	0.324	0.323
0.358	0.285	0.322	0.267	0.266

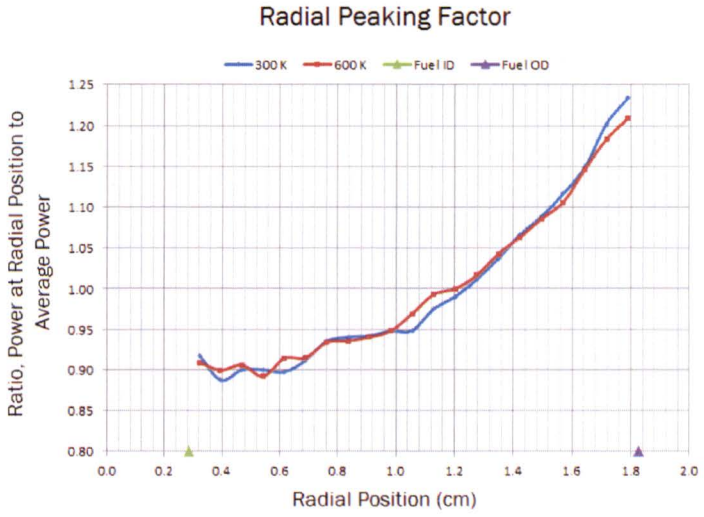

Figure 14, Element Radial Peaking factor

3.2.3 Burnup Effects

Calculations were performed to determine the mass of uranium isotopes (^{235}U and ^{238}U) in a single fuel element (Fig. 15) for two conditions. The uranium burnup for the initial LCC core was determined, and the mass for a core with all locations loaded with fuel to predict the operational core at end of core life. Excess reactivity was calculated from transport k_{eff}, and is shown in Fig. 16.

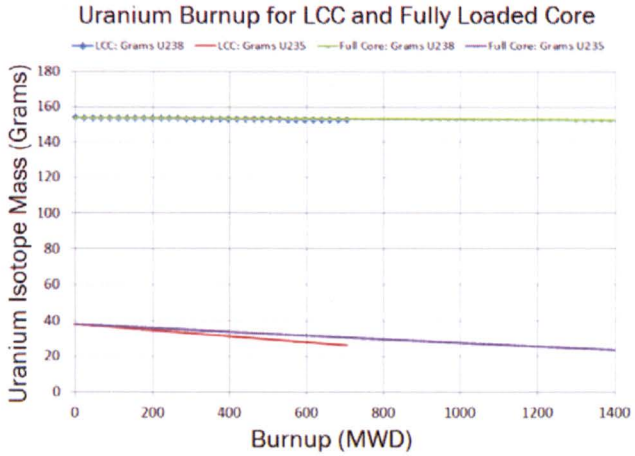

Figure 15: Uranium Burnup

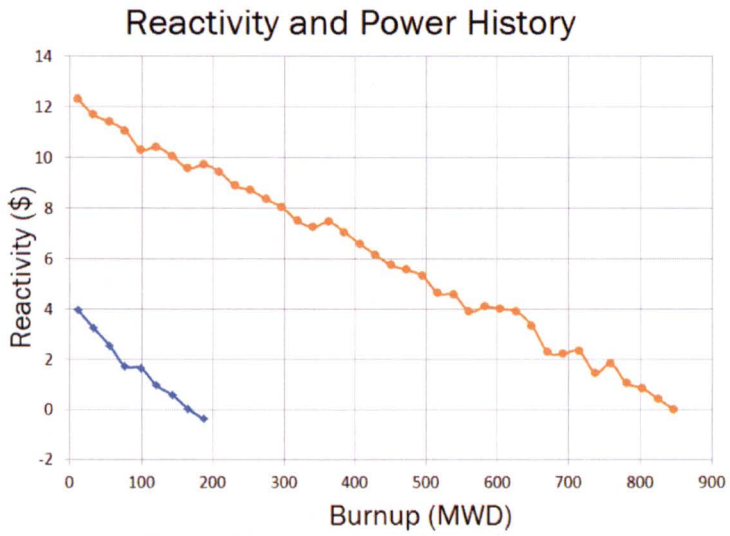

Figure 16: Excess reactivity and Burnup

The change in excess reactivity following startup from a clean core to equilibrium full power operation at 300K was simulated, with excess reactivity determined from KENO criticality calculations. Full power equilibrium excess reactivity decrease attributed principally to fission product poisons is shown in Fig. 17 to result in a reactivity deficit of approximately $3.5. Excess reactivity following shutdown from the operation was simulated, with the results provided in Fig. 18.

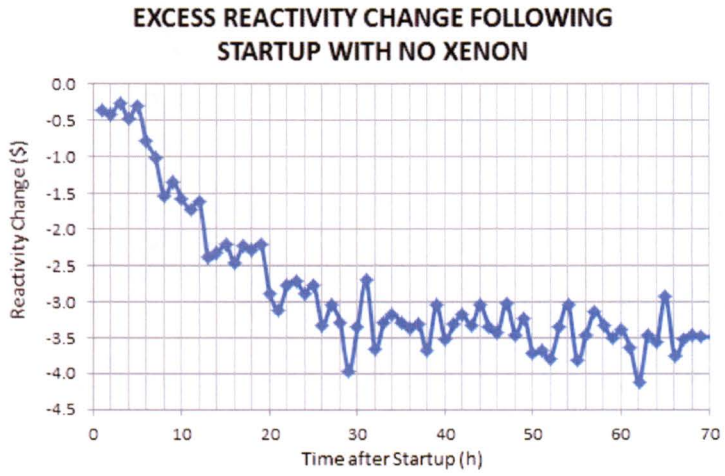

Figure 17, Excess Reactivity from Clean Core

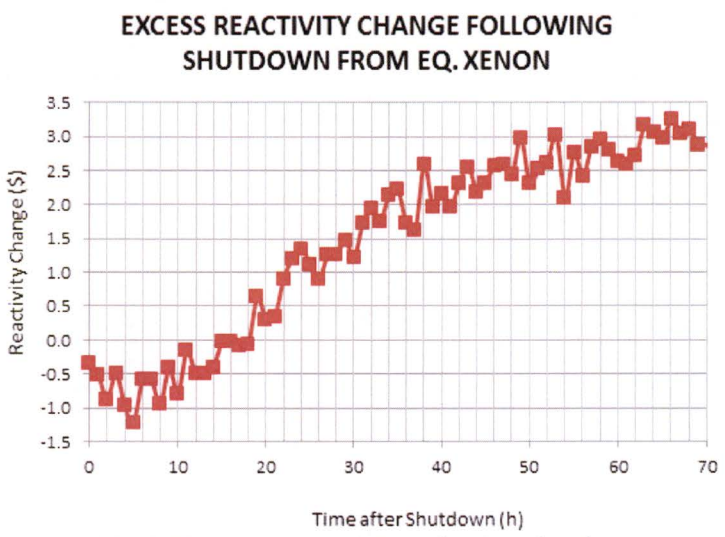

Figure 18: Excess Reactivity Following Shutdown

Simulation of steady state reactor operations at 1.1 MW from initial operation of the LCC to the operational end of core life was performed to predict the behavior of fission product poisons and transuranic isotopes on system performance over time. Absorptions are used in place of reactivity, but ORIGEN calculations are infinite medium, neglecting leakage. Near the beginning of core life, 85.8% of all absorptions occur in the isotopes of interest, as listed in Table 13. A large fraction (on the order of 80-85%) of absorptions in these isotopes occur in 5 isotopes (U235, U238, Pu239, Xe135, and Sm151). The change in absorption for these isotopes over long term, steady state, full power operation is shown in Fig. 23.

Table 13: Isotope Absorption-Fractions

ISOTOPE	0 MWD	66 MWD	198 MWD	264 MWD	396 MWD	462 MWD	550 MWD
U235	8.02E-01	7.67E-01	7.46E-01	7.36E-01	7.14E-01	7.03E-01	6.88E-01
U238	5.93E-02	5.84E-02	6.04E-02	6.15E-02	6.38E-02	6.50E-02	6.68E-02
Pu238	2.46E-17	1.50E-08	3.66E-07	8.60E-07	2.95E-06	4.76E-06	8.25E-06
Pu239	6.79E-17	3.77E-03	1.15E-02	1.53E-02	2.27E-02	2.63E-02	3.09E-02
Pu240	5.46E-17	3.17E-05	2.97E-04	5.29E-04	1.19E-03	1.61E-03	2.28E-03
Pu241	7.54E-17	8.19E-07	2.35E-05	5.55E-05	1.85E-04	2.91E-04	4.86E-04
Pu242	7.03E-18	3.51E-10	3.24E-08	1.05E-07	5.55E-07	1.05E-06	2.16E-06
Xe131	8.24E-18	1.19E-04	4.25E-04	5.86E-04	9.21E-04	1.10E-03	1.34E-03
Xe133	9.14E-18	4.79E-05	4.96E-05	5.05E-05	5.24E-05	5.34E-05	5.49E-05
Xe135	1.49E-13	2.41E-02	2.43E-02	2.43E-02	2.44E-02	2.44E-02	2.45E-02
Sm147	6.33E-18	1.14E-06	1.41E-05	2.60E-05	6.06E-05	8.33E-05	1.19E-04
Sm150	5.97E-18	2.75E-05	1.12E-04	1.57E-04	2.53E-04	3.03E-04	3.74E-04
Sm151	5.75E-16	1.15E-03	2.33E-03	2.60E-03	2.89E-03	2.96E-03	3.02E-03
Sm152	2.30E-17	5.08E-05	2.09E-04	3.06E-04	5.19E-04	6.33E-04	7.92E-04
Sm153	4.27E-17	2.06E-06	2.50E-06	2.76E-06	3.37E-06	3.72E-06	4.21E-06
TOTAL	86.1%	85.5%	84.6%	84.1%	83.1%	82.6%	81.9%

3.2.4 Fuel Temperature Reactivity Coefficient and Excess Reactivity

As previously described, data from SCALE calculations was performed to determine critical mass across a range of temperatures from 300 K to 600 K. The criticality calculation in each configuration and temperature variation was used to calculate net core reactivity, as reported in Table 14.

Table 14: Excess Reactivity at Fuel temperature By Core Configuration:

Fuel Temp (K)	Number of Fuel Elements										
	65	73	74	78	83	87	89	92	97	100	106
	Graphite Configuration										
300	$1.61	$3.24	$4.19	$4.70	$5.64	$6.58	$6.83	$7.46	$8.24	$8.61	$9.55
300	$1.62	$3.29	$4.04	$5.04	$5.73	$6.50	$6.87	$7.36	$8.39	$8.71	$9.47
350	$1.16	$3.05	$3.38	$4.44	$5.32	$5.98	$6.44	$7.18	$8.02	$8.31	$8.97
450	-$0.03	$1.72	$2.32	$3.38	$4.12	$4.99	$5.63	$5.92	$6.80	$7.20	$8.09
550	-$1.65	$0.31	$1.04	$2.08	$2.75	$3.76	$4.04	$4.71	$5.45	$5.98	$6.71
600	-$2.29	-$0.36	$0.11	$1.27	$2.17	$2.88	$3.21	$3.85	$4.86	$5.07	$6.06
	Water Void Configuration										
300	-$2.81	-$0.21	$0.68	$1.94	$2.83	$4.13	$4.72	$5.49	$6.74	$7.47	$8.67
300	-$2.77	-$0.24	$0.77	$1.90	$3.03	$4.24	$4.82	$5.47	$6.92	$7.41	$8.64
350	-$3.53	-$0.83	$0.29	$1.34	$2.37	$4.04	$4.39	$4.95	$6.39	$7.00	$8.23
450	-$4.65	-$2.34	-$0.98	$0.30	$1.37	$2.81	$3.09	$4.11	$5.34	$5.89	$7.15
550	-$6.17	-$3.60	-$2.56	-$1.15	-$0.04	$1.23	$1.86	$2.73	$4.09	$4.43	$5.88
600	-$6.98	-$4.46	-$3.41	-$1.81	-$0.86	$0.60	$1.15	$1.93	$3.38	$3.95	$5.11

The values for the LCC were plotted in Fig. 19 (along with other core configurations near the LCC). The response for all data was remarkably similar, providing confidence that the temperature coefficient of reactivity can reliably be determined by the slope of the linear function relating temperature to reactivity change. The value of $-0.0127/Δ°K is approximately 11% lower than the value reported in the original UT TRIGA SAR for a critical configuration of 64 elements, but agrees with the temperature dependent prompt temperature coefficient of GA-7882. A similar fit for the 65 element core results in agreement with the original UT SAR to within about 6%.

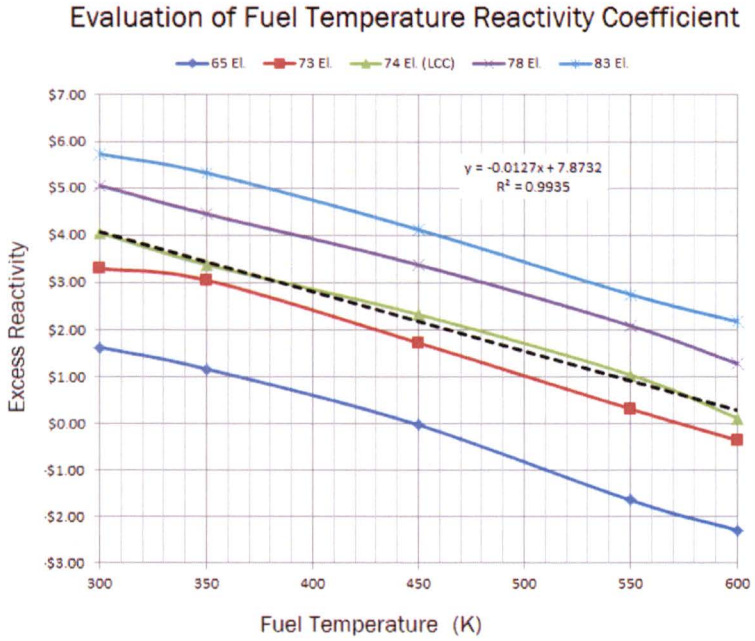

Figure 19: Excess Reactivity and Fuel Temperature

3.2.5 Excess reactivity & Shutdown Margin

Excess reactivity was determined directly from transport k_{eff} for the "all rods out" condition. The worth imposed by control rod insertion was calculated for the remaining conditions using the formula (where insertion is understood to cause negative reactivity worth):

$$\$_{CR} = \frac{k_{eff,ARO} - k_{eff,CRin}}{k_{eff,ARO} \cdot k_{eff,CRin}} \cdot \frac{1}{0.007}$$

The limiting shutdown margin (LSDM) is calculated as the shutdown margin with the most reactive control rod fully withdrawn. In all cases, the regulating rod was determined to be the most reactive control rod.

Table 15: Calculated Reactivity Values

MWD	RR	SH1	SH2	TR	Excess	RW SUM	LSDM
$6.44	$3.74	$2.91	$2.86	$2.63	$5.57	$12.15	$2.84
$8.70	$3.66	$2.97	$2.76	$2.58	$5.56	$11.97	$2.75
$9.65	$3.69	$2.93	$2.82	$2.74	$5.61	$12.18	$2.88
$10.80	$3.64	$2.88	$2.76	$2.59	$5.51	$11.87	$2.71
$11.73	$3.81	$2.99	$2.92	$2.66	$5.62	$12.37	$2.95
$12.79	$3.74	$2.87	$2.79	$2.64	$5.51	$12.04	$2.80
$14.48	$3.71	$2.85	$2.73	$2.72	$5.47	$12.02	$2.84
$17.97	$3.65	$2.85	$2.75	$2.52	$5.35	$11.77	$2.77
$26.00	$3.69	$2.90	$2.73	$2.65	$5.13	$11.97	$3.15
$31.31	$3.59	$3.02	$2.72	$2.61	$5.46	$11.94	$2.89

Table 15: Calculated Reactivity Values

MWD	RR	SH1	SH2	TR	Excess	RW SUM	LSDM
$34.76	$4.56	$4.05	$2.86	$2.64	$4.89	$14.12	$4.66
$34.99	$4.05	$3.52	$2.32	$2.06	$5.39	$11.96	$2.51
$45.81	$3.81	$3.17	$2.27	$1.90	$5.11	$11.14	$2.23
$67.32	$4.18	$3.53	$2.83	$2.69	$4.83	$13.22	$4.22
$81.29	$3.81	$2.97	$2.43	$2.19	$5.73	$11.40	$1.87
$90.33	$3.37	$3.02	$2.17	$2.10	$5.20	$10.67	$2.10
$106.22	$3.24	$2.79	$2.02	$1.80	$5.20	$9.85	$1.41
$121.93	$3.21	$2.94	$2.80	$2.78	$5.26	$11.71	$3.25
$145.21	$3.33	$3.15	$3.02	$3.08	$4.90	$12.57	$4.35
$165.51	$3.40	$3.16	$3.05	$2.94	$4.57	$12.55	$4.58
$186.65	$2.36	$2.11	$2.32	$2.16	$5.05	$8.94	$1.53
$204.99	$3.07	$2.92	$3.06	$2.94	$5.42	$12.00	$3.50
$214.05	$3.78	$2.36	$2.85	$1.68	$5.34	$10.68	$1.55
$226.30	$2.43	$2.02	$2.36	$2.17	$5.68	$8.97	$0.86
$236.82	$3.12	$2.65	$3.10	$2.79	$5.49	$11.67	$3.05
$260.15	$2.71	$2.32	$2.71	$2.48	$5.05	$10.22	$2.46
$281.57	$2.71	$2.33	$2.67	$2.43	$4.74	$10.14	$2.70
$286.66	$2.84	$2.45	$2.75	$2.53	$4.74	$10.56	$2.98

3.2.6 Burnup effects

Over time, the limiting core configuration will require increasing the number of fuel elements to compensate for burnup until all locations reserved for fuel are filled. Therefore, burnup calculations are based on a full core load. A simulation of steady state reactor operations at 1.251 MW from initial operation to end of core life provides data on flux density, changes in uranium mass, and the effects of significant isotopes generated during operation over core life. Average flux values for the fuel matrix are shown in Fig. 20. The total ^{235}U and ^{238}U mass at each burnup interval is calculated by ORIGEN, and reported by OPUS as indicated in Fig. 21. Excess reactivity derived from transport calculations over core life are provided in Fig. 22. Neutron absorption in ^{235}U and ^{238}U (as a fraction of total absorptions) is shown in Fig. 23.

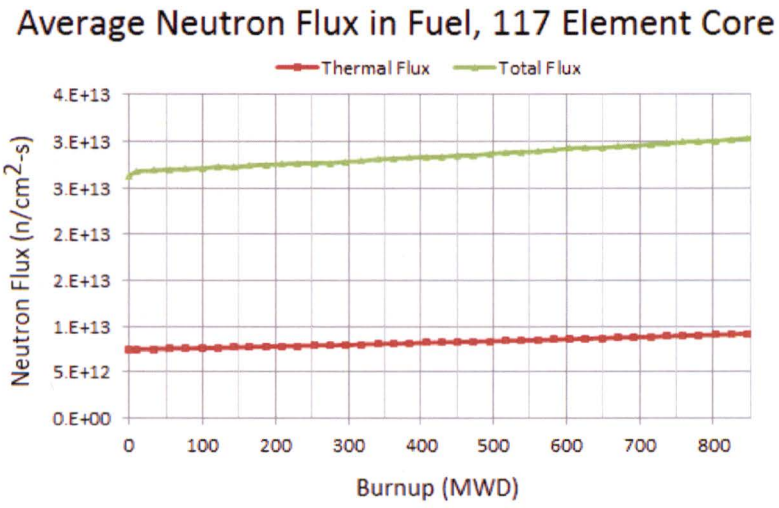

Figure 20: Neutron Flux in Fuel of a 117 Element Core as a Function of Burnup

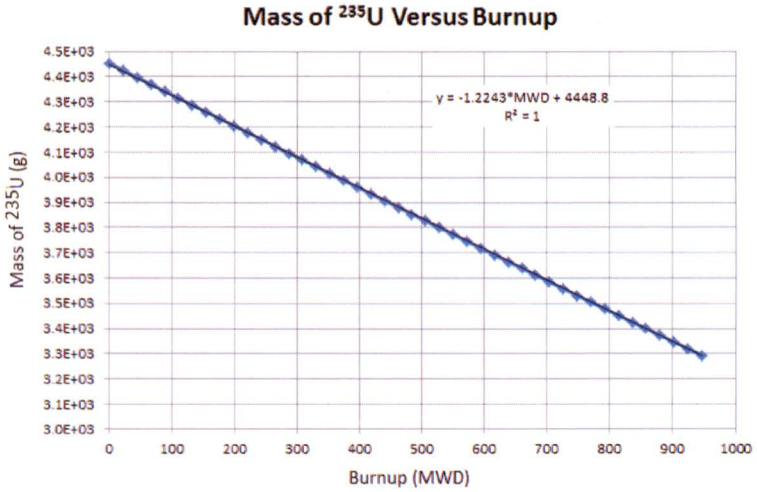

Figure 21: Uranium (235 and 238) Mass in a 117 Element Core as a Function of Burnup

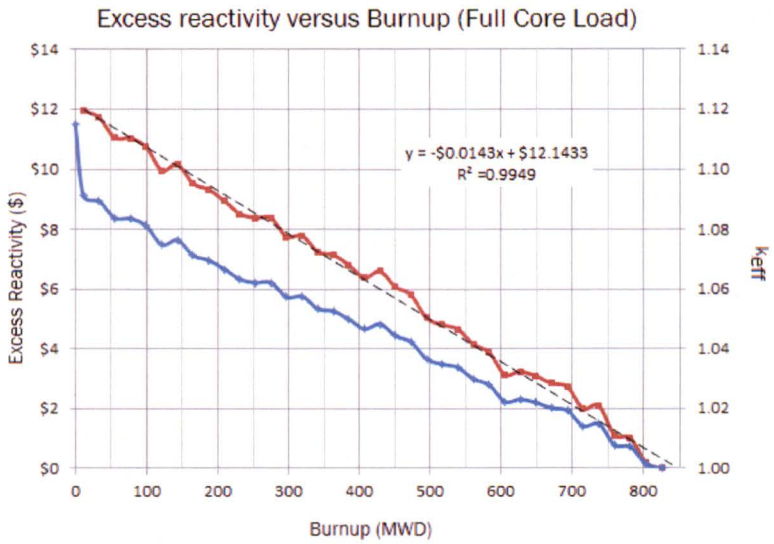

Figure 22: Excess Reactivity in a 117 Element Core as a Function of Burnup

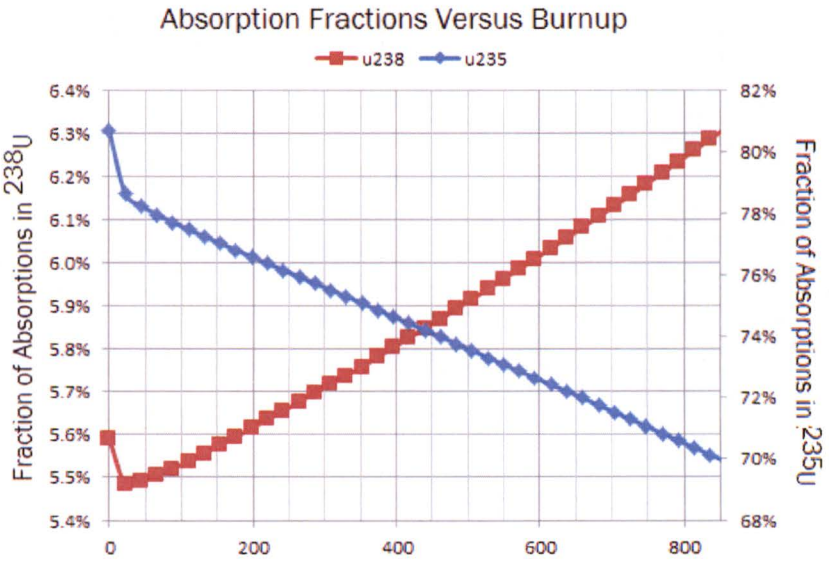

Figure 23: Fraction of Neutrons Absorbed in ^{235}U and ^{238}U (117 Element Core) vs. Burnup

3.2.7 Experiment effects

The limit on experiment worth provides assurance that excess reactivity limits with the most reactive shutdown margin fully withdrawn is met.

3.2.8 Accident Source terms

A simulation was performed with a fully loaded core (all core spaces filled with fresh standard fuel elements) operated at 1.1 MW until k_{excess} was less than unity. The simulation then decayed the core for 20 minutes, simulating the amount of time after shutdown required to remove a fuel element from the core. Activity of the major halogens and iodine isotopes was calculated for strategic time intervals, and is provided in Table 16. Total decay heat was calculated for time intervals after shutdown (Fig. 24).

Table 16: Fission product Inventory, Maximum Single Fuel Element

TIME	20 M	50 M	7.5 H	11.5 H	12 H	1 D	7 D	30 D	180 D	365 D
br82	1.82E-1	1.81E-1	1.80E-1	1.57E-1	1.45E-1	1.14E-1	6.75E-3	1.32E-7	1.64E-11	1.63E-11
br83	6.37E1	6.17E1	5.61E1	7.75	2.44	7.61E-2	5.80E-9	5.80E-9	5.80E-9	5.80E-9
br84m	2.25	2.17E-1	6.67E-3	2.05E-10	2.05E-10	2.05E-10	2.05E-10	2.05E-10	2.05E-10	2.05E-10
br84	1.12E2	7.93E1	4.12E1	4.44E-3	2.35E-5	1.02E-8	1.02E-8	1.02E-8	1.02E-8	1.02E-8
br85	1.61E2	1.51	1.12E-3	1.46E-8	1.47E-8	1.47E-8	1.47E-8	1.47E-8	1.47E-8	1.47E-8
br86	1.98E2	5.78E-5	1.80E-8	1.80E-8	1.80E-8	1.80E-8	1.80E-8	1.80E-8	1.80E-8	1.80E-8
br87	2.39E2	6.58E-5	2.17E-8	2.17E-8	2.17E-8	2.18E-8	2.18E-8	2.18E-8	2.18E-8	2.18E-8
i131	3.56E2	3.56E2	3.55E2	3.48E2	3.43E2	3.30E2	1.98E2	2.72E1	6.38E-5	3.24E-8
i132	5.34E2	5.34E2	5.32E2	5.04E2	4.86E2	4.37E2	1.19E2	8.23E-1	4.82E-8	4.82E-8
i133	8.05E2	8.02E2	7.94E2	6.37E2	5.57E2	3.74E2	3.08	1.05E-7	7.37E-8	7.37E-8
i134	9.40E2	8.85E2	7.44E2	7.12	3.28E-1	2.62E-5	8.57E-8	8.57E-8	8.57E-8	8.57E-8
i135	7.60E2	7.33E2	6.96E2	3.33E2	2.18E2	6.15E1	1.56E-5	6.92E-8	6.92E-8	6.92E-8
i136	3.15E2	1.46E-2	3.31E-8	2.87E-8	2.87E-8	2.87E-8	2.87E-8	2.87E-8	2.87E-8	2.87E-8
kr83m	6.28E1	6.27E1	6.19E1	1.94E1	7.30	2.86E-1	2.67E-7	2.23E-7	7.07E-8	2.04E-8
kr85m	1.55E2	1.49E2	1.38E2	4.69E1	2.52E1	3.94	1.50E-8	1.42E-8	1.42E-8	1.42E-8
kr85	9.59	9.59	9.59	9.59	9.59	9.59	9.58	9.54	9.29	9.00
kr87	3.00E2	2.52E2	1.92E2	4.26	4.79E-1	6.91E-4	2.73E-8	2.73E-8	2.73E-8	2.73E-8
kr88	4.06E2	3.74E2	3.31E2	6.01E1	2.26E1	1.21	3.70E-8	3.70E-8	3.70E-8	3.70E-8
kr89	5.18E2	6.03	7.96E-3	4.72E-8	4.72E-8	4.72E-8	4.72E-8	4.72E-8	4.72E-8	4.73E-8
xe131m	4.25	4.25	4.25	4.25	4.25	4.24	3.87	1.61	3.49E-4	7.23E-9
xe133m	8.93	8.93	8.93	8.79	8.66	8.09	1.57	1.10E-3	8.16E-10	8.16E-10
xe135	3.55E2	3.65E2	3.78E2	4.19E2	3.80E2	2.20E2	6.79E-3	7.26E-8	7.26E-8	7.26E-8
xe137	7.38E2	1.97E1	8.28E-2	6.71E-8	6.71E-8	6.72E-8	6.72E-8	6.72E-8	6.72E-8	6.72E-8
xe138	7.50E2	2.77E2	6.28E1	1.37E-7	6.82E-8	6.83E-8	6.83E-8	6.83E-8	6.83E-8	6.83E-8

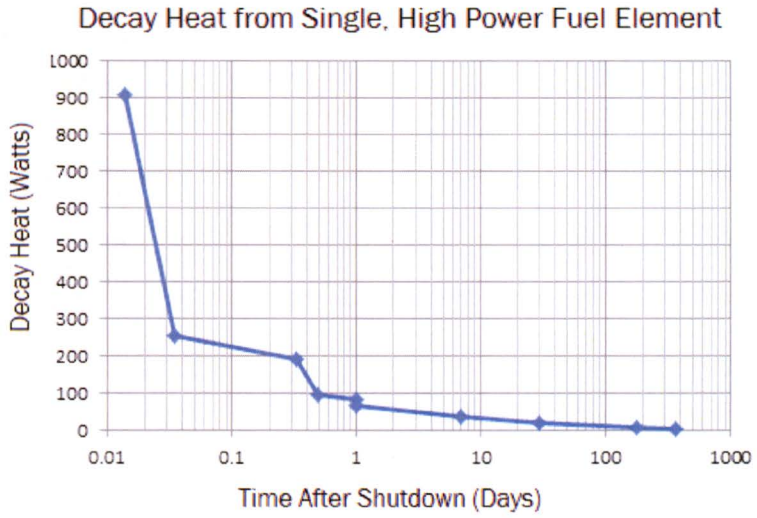

Figure 24, Decay Heat Following Steady State Full Power, End of Life Operations

4.0 Model Validation

Validity of the SCALE model application to the UT TRIGA reactor is verified in two ways. First, the prediction of mass required to support operations is compared to the 1992 operational core loading. Second, data from model calculations is used to evaluate core excess reactivity and the reactivity worth of individual control rods with values compared to measured data for the 1992 operational core.

4.1 Model Comparison with Historical Reactors

The 1992 TRIGA core included 84 lightly burned standard fuel elements and three fresh fuel followers augmented with 18 graphite rods, leaving 13 water voids in the G ring. SCALE predicts excess reactivity (for 87 fuel elements, 84 standard and 3 followers) of approximately $1.00 with fresh fuel and a water-void configured core, $7.00 with a full graphite-configured core. The lightly burned fuel with a measured excess reactivity of approximately $6.4 is within the predicted range for fresh fuel.

4.2 Reactivity Values

Data from calculations using the SCALE model of the UT TRIGA reactor was used to determine excess reactivity and the total reactivity worth of each control rod. Excess reactivity was calculated based on k_{eff} with the control rods in a fully withdrawn position ($k_{eff,ARO}$). The worth of an individual control rod ($\$_{CR}$) was based on the previous calculation and k_{eff} calculation with the control rods in a fully inserted position ($k_{eff,CRin}$) as follows:

$$\$_{CR} = \frac{k_{eff,ARO} - k_{eff,CRin}}{k_{eff,ARO} \cdot k_{eff,CRin}} \cdot \frac{1}{0.007}$$

Reactivity values calculated from SCALE CSAS6 data for control rod worth and excess reactivity measurements are compared to measurements for periodic surveillance.

4.2.1 Core Configurations

There are 52 discrete burnup intervals at which either fuel was reconfigured and/or reactivity surveillances were performed. The configurations are provided in Attachment 1.

4.2.3 Material Composition

A series of calculations was accomplished to determine isotopic concentrations of fuel at various burnup intervals to support criticality calculations for reactivity analysis. The power history for the fuel elements at UT is complex. All of the standard fuel elements used in 1992 had prior power history, lightly burned at the previous UT TRIGA reactor at Taylor Hall, General Atomics, and Northrup Aircraft facilities. Some of the elements had a power history at other facilities followed by operation at the UT Taylor Hall facility. Records are not available to verify the burnup values. Some of the information is inconsistent, with some indication that the distribution of core burnup to elements was not rigorous. All of the fuel elements decayed approximately one year following removal prior to installation at the current UT TRIGA located at the NETL. Assumptions required to accurately model fuel composition based on power history are therefore extremely challenging. Initial calculations had a large ($2) bias.

Weighting factors were assigned to the burnup values to reduce bias and improve model response. Since the power history for 30 elements in the inner rings was approximately 1/3 of the power history for the outer elements and fuel followers were fresh fuel in high reactivity worth positions, three different weighting factors were developed to simulate the core composition for the initial core and the following burnup intervals. Lightly burned fuel from the Illinois reactor received and used until later; a weighting factor was determined to be unnecessary. The weighting factors for the burnup reported from the three facilities were developed from burnup intervals that included only fuel element additions where the burnup occurred at only one facility. The weighting factors were then used to scale the burnups for individual elements in criticality calculations across a range of burnup intervals, and the resultant reactivity changes evaluated to see whether the effect brought calculated values closer or further from the surveillance data. When the weighting factors provided the maximum improvement in comparison to the surveillance data, the adjusted burnups were used to calculate criticality for the 50 burnup intervals where either surveillance data was obtained or a core configuration occurred.

At each burnup interval, an element burnup was calculated (the product of the burnup over the interval and the fraction of total fissions that occurred in each element). The element burnup for the interval was added to the element burnup at the start of the previous interval, and a criticality calculation performed for the start of the next interval using the updated burnup. When adding fresh fuel to start an interval, only the uranium and zirconium hydroxide were included in the input. When lightly burned fuel that had not been utilized in the current core was added, short lived radioactive material was removed from the input. The results are provided in Table 17.

Table 17, Reactivity Surveillance Data

DATE	MWD	RR	SH1	SH2	TR	Excess	RW SUM	TS SDM
10/25/94	6.44	$3.99	$2.93	$3.19	$3.21	$5.56	$13.32	$3.77
08/10/95	8.7	$4.02	$2.98	$3.18	$3.21	$5.46	$13.39	$3.91
03/05/96	9.65	$4.02	$2.98	$3.18	$3.21	$5.48	$13.39	$3.89
07/23/96	10.62	$4.02	$2.98	$3.18	$3.27	$5.50	$13.45	$3.93
01/29/97	11.73	$4.02	$2.98	$3.18	$3.27	$5.49	$13.45	$3.94
09/11/97	12.79	$4.08	$3.00	$3.18	$3.22	$5.44	$13.48	$3.96
01/23/98	14.48	$4.08	$3.00	$3.18	$3.22	$5.40	$13.48	$4.00
07/23/98	17.97	$4.06	$3.06	$3.20	$3.23	$5.40	$13.55	$4.09
07/02/99	26.00	$4.05	$3.01	$3.22	$3.23	$5.00	$13.51	$4.46
04/27/00	31.31	$4.50	$3.48	$2.73	$2.36	$5.53	$13.07	$3.04
06/30/00	34.76	$4.50	$3.48	$2.73	$2.36	$4.56	$13.07	$4.01
09/07/00	34.91	$3.90	$3.02	$3.24	$3.17	$5.50	$13.33	$3.93
07/30/01	45.81	$4.19	$3.24	$2.94	$2.41	$4.59	$12.78	$4.00
07/24/02	67.32	$4.08	$3.16	$2.84	$2.47	$4.09	$12.55	$4.38
11/14/02	81.29	$4.30	$3.34	$2.75	$2.51	$5.69	$12.90	$2.91
07/24/03	90.33	$3.88	$3.31	$2.74	$2.46	$5.20	$12.39	$3.31
07/29/04	106.23	$3.33	$2.78	$3.25	$3.33	$5.77	$12.69	$3.59
07/18/05	121.93	$3.07	$2.94	$3.14	$3.28	$5.55	$12.43	$3.60
07/19/06	145.21	$3.09	$2.89	$3.02	$3.29	$4.97	$12.29	$4.03
01/25/07	165.51	$3.09	$2.89	$3.02	$3.29	$4.47	$12.29	$4.53
07/25/07	186.65	$2.84	$2.75	$3.30	$3.32	$5.04	$12.21	$3.85

06/19/08	205.04	$3.65	$2.35	$3.27	$2.04	$4.45	$11.31	$3.21
06/25/09	214.05	$3.99	$2.45	$3.36	$2.04	$4.75	$11.84	$3.10
06/29/10	226.3	$2.90	$2.54	$3.11	$3.14	$5.79	$11.69	$2.76
06/29/11	236.82	$2.83	$2.52	$3.07	$3.01	$5.56	$11.43	$2.80
07/13/12	260.14	$2.76	$2.47	$3.01	$3.04	$4.83	$11.28	$3.41
07/16/13	281.57	$2.75	$2.45	$2.91	$3.00	$4.20	$11.11	$3.91
07/22/14	286.66	$2.50	$2.74	$3.15	$3.17	$4.70	$11.56	$3.69

There is general agreement for a large set of the data, and the trends from interval to interval are similar, but differences occur after major relocations of fuel or following large fuel additions (although a convergence follows). In addition, surveillance data was accomplished to verify that Technical Specifications requirements are met, and not to provide a resource for validation; the records are fragmented and not well linked to core configuration changes. At interval 205 MWD a large negative change caused by an experiment insertion occurred, active until it was removed at 226 MWD. Surveillance data does not reflect the change, and fuel movement, burnup value, and surveillance data may not be correctly synchronized.

Table 18, Fractional Errors Surveillance and SCALE Calculations

MWD	RR	SH1	SH2	TR	Excess	RW SUM
6.44	-6.3%	-0.6%	-10.3%	-17.9%	0.2%	-8.8%
8.70	-8.9%	-0.3%	-13.2%	-19.7%	1.7%	-10.6%
9.65	-8.1%	-1.7%	-11.4%	-14.5%	2.4%	-9.0%
10.80	-9.4%	-3.3%	-13.3%	-20.8%	0.3%	-11.8%
11.73	-5.3%	0.3%	-8.2%	-18.7%	2.3%	-8.0%
12.79	-8.4%	-4.4%	-12.3%	-17.9%	1.2%	-10.7%
14.48	-9.0%	-4.9%	-14.1%	-15.4%	1.3%	-10.8%
17.97	-10.0%	-6.8%	-14.0%	-22.0%	-1.0%	-13.1%
26.00	-8.9%	-3.7%	-15.2%	-17.8%	2.6%	-11.4%
31.31	-20.3%	-13.1%	-0.2%	10.5%	-1.2%	-8.6%
34.76	1.4%	16.4%	4.8%	11.8%	7.2%	8.0%
34.99	3.9%	16.6%	-28.3%	-35.0%	-1.9%	-10.3%
45.81	-9.2%	-2.2%	-22.8%	-21.2%	11.3%	-12.8%
67.32	2.3%	11.6%	-0.4%	8.8%	18.1%	5.3%
81.29	-11.4%	-11.0%	-11.5%	-12.8%	0.6%	-11.6%
90.33	-13.1%	-8.8%	-20.7%	-14.5%	-0.1%	-13.9%
106.22	-2.7%	0.5%	-37.9%	-46.0%	-9.9%	-22.4%
121.93	4.4%	-0.1%	-11.0%	-15.3%	-5.2%	-5.8%
145.21	7.7%	8.9%	-0.1%	-6.3%	-1.5%	2.3%
165.51	10.1%	9.4%	1.0%	-10.6%	2.2%	2.1%
186.65	-16.9%	-23.5%	-29.7%	-35.0%	0.2%	-26.8%
204.99	-15.8%	24.1%	-6.3%	44.2%	21.8%	6.1%
214.05	-5.2%	-3.8%	-15.1%	-17.5%	12.4%	-9.8%
226.30	-16.3%	-20.6%	-24.2%	-31.0%	-1.9%	-23.3%

Table 18, Fractional Errors Surveillance and SCALE Calculations

MWD	RR	SH1	SH2	TR	Excess	RW SUM
236.82	10.4%	5.2%	1.1%	-7.2%	-1.2%	2.1%
260.15	-1.7%	-6.1%	-9.8%	-18.5%	4.6%	-9.4%
281.57	-1.6%	-4.8%	-8.3%	-19.0%	12.8%	-8.7%

4.3 Conclusion

Core loading for the 1992 fuel using a fraction of non-fuel spaces using graphite rods is consistent with calculations of loading to support full power operation. Flux density calculated for the LCC core agrees with historical calculations performed by General Atomics. There is agreement between measured and calculated reactivity worth values when material specification is adjusted by weighting initial burnup; differences occur between calculations and measurements occur with major configuration changes, and trend towards agreement for operations following the change. Therefore, results of calculations using the SCALE UT TRIGA model provide confidence that the model is capable of adequately predicting reactor performance.

ATTACHMENT 1: UT TRIGA CORE CONFIGURATIONS

Core Burnup, Date, Position, Fuel Elements

DATE	03/16/92	07/01/92	07/23/92	01/19/93	08/10/93	10/25/94	08/10/95	10/13/95	03/05/96	09/23/96	01/29/97
MWD	0	0.173	0.249	1.696	3.983	6.441	8.698	9.201	9.646	10.803	11.731
B01	5921	5921	5921	5921	5921	5921	5921	5921	5921	5921	5921
B02	5922	5922	5922	5922	5922	5922	5922	5922	5922	5922	5922
B03	5981	5981	5981	5981	5981	5981	5981	5982	5982	5982	5982
B04	6143	6143	6143	6143	6143	6143	6143	6143	6143	6143	6143
B05	6886	6886	6886	6886	6886	6886	6886	6886	6886	6886	6886
B06	6889	6889	6889	5283	5283	5283	5283	5283	5283	5283	5283
C01	TR	TR	TR	TR	TR	TR	TR	TR	TR	TR	TR
C02	5916	5916	5916	5916	5916	5916	5916	5916	5916	5916	5916
C03	5917	5917	5917	5917	5917	5917	5917	5917	5917	5917	5917
C04	6924	6924	6924	6924	6924	6924	6924	6924	6924	6924	6924
C05	6926	6926	6926	6926	6926	6926	6926	6926	6926	6926	6926
C06	6927	6927	6927	6927	6927	6927	6927	6927	6927	6927	6927
C07	10146	10146	10146	10146	10146	10146	10146	10146	10146	10146	10146
C08	6928	6928	6928	6928	6928	6928	6928	6928	6928	6928	6928
C09	6929	6929	6929	6929	6929	6929	6929	6929	6929	6929	6929
C10	6930	6930	6930	6930	6930	6930	6930	6930	6930	6930	6930
C11	5283	5283	5283	6889	6889	6889	6889	6889	6889	6889	6889
C12	6932	6932	6932	6932	6932	6932	6932	6932	6932	6932	6932
D01	5844	5844	5844	5844	5844	5844	5844	5844	5844	5844	5844
D02	5845	5845	5845	5845	5845	5845	5845	5845	5845	5845	5845
D03	5846	5846	5846	5846	5846	5846	5846	5846	5846	5846	5846
D04	5902	5902	5902	5902	5902	5902	5902	5902	5902	5902	5902
D05	5903	5903	5903	5903	5903	5903	5903	5903	5903	5903	5903
D06	10147	10147	10147	10147	10147	10147	10147	10147	10147	10147	10147
D07	5904	5904	5904	5904	5904	5904	5904	5904	5904	5904	5904
D08	5912	5912	5912	5912	5912	5912	5912	5912	5912	5912	5912
D09	5913	5913	5913	5913	5913	5913	5913	5913	5913	5913	5913
D10	5914	5914	5914	5914	5914	5914	5914	5914	5914	5914	5914
D11	5915	5915	5915	5915	5915	5915	5915	5915	5915	5915	5915
D12	5918	5918	5918	5918	5918	5918	5918	5918	5918	5918	5918
D13	5919	5919	5919	5919	5919	5919	5919	5919	5919	5919	5919
D14	10148	10148	10148	10148	10148	10148	10148	10148	10148	10148	10148
D15	5920	5920	5920	5920	5920	5920	5920	5920	5920	5920	5920
D16	6142	6142	6142	6142	6142	6142	6142	6142	6142	6142	6142
D17	6923	6923	6923	6923	6923	6923	6923	6923	6923	6923	6923
D18	6925	6925	6925	6925	6925	6925	6925	6925	6925	6925	6925
E01	2899	2899	2899	2899	2899	2899	2899	2899	2899	2899	2899
E02	2902	2902	2902	2902	2902	2902	2902	2902	2902	2902	2902
E03	2903	2903	2903	2903	2903	2903	2903	2903	2903	2903	2903
E04	2904	2904	2904	2904	2904	2904	2904	2904	2904	2904	2904
E05	2905	2905	2905	2905	2905	2905	2905	2905	2905	2905	2905
E06	2906	2906	2906	2906	2906	2906	2906	2906	2906	2906	2906
E07	2908	2908	2908	2908	2908	2908	2908	2908	2908	2908	2908
E08	2910	2910	2910	2910	2910	2910	2910	2910	2910	2910	2910
E09	2911	2911	2911	2911	2911	2911	2911	2911	2911	2911	2911

DATE	03/16/92	07/01/92	07/23/92	01/19/93	08/10/93	10/25/94	08/10/95	10/13/95	03/05/96	09/23/96	01/29/97
MWD	0	0.173	0.249	1.696	3.983	6.441	8.698	9.201	9.646	10.803	11.731
E10	2912	2912	2912	2912	2912	2912	2912	2912	2912	2912	2912
E11	2913	2913	2913	2913	2913	2913	2913	2913	2913	2913	2913
E12	2915	2915	2915	2915	2915	2915	2915	2915	2915	2915	2915
E13	2918	2918	2918	2918	2918	2918	2918	2918	2918	2918	2918
E14	2925	2925	2925	2925	2925	2925	2925	2925	2925	2925	2925
E15	2927	2927	2927	2927	2927	2927	2927	2927	2927	2927	2927
E16	2928	2928	2928	2928	2928	2928	2928	2928	2928	2928	2928
E17	2929	2929	2929	2929	2929	2929	2929	2929	2929	2929	2929
E18	2930	2930	2930	2930	2930	2930	2930	2930	2930	2930	2930
E19	2932	2932	2932	2932	2932	2932	2932	2932	2932	2932	2932
E20	2935	2935	2935	2935	2935	2935	2935	2935	2935	2935	2935
E21	2938	2938	2938	2938	2938	2938	2938	2938	2938	2938	2938
E22	2939	2939	2939	2939	2939	2939	2939	2939	2939	2939	2939
E23	2940	2940	2940	2940	2940	2940	2940	2940	2940	2940	2940
E24	2941	2941	2941	2941	2941	2941	2941	2941	2941	2941	2941
F01	2944	2944	2944	2944	2944	2944	2944	2944	2944	2944	2944
F02	2946	2946	2946	2946	2946	2946	2946	2946	2946	2946	2946
F03	2947	2947	2947	2947	2947	2947	2947	2947	2947	2947	2947
F04	2948	2948	2948	2948	2948	2948	2948	2948	2948	2948	2948
F05	2950	2950	2950	2950	2950	2950	2950	2950	2950	2950	2950
F06											
F07	2952	2952	2952	2952	2952	2952	2952	2952	2952	2952	2952
F08	2954	2954	2954	2954	2954	2954	2954	2954	2954	2954	2954
F09	2955	2955	2955	2955	2955	2955	2955	2955	2955	2955	2955
F10	2957	2957	2957	2957	2957	2957	2957	2957	2957	2957	2957
F11											
F12	2959	2959	2959	2959	2959	2959	2959	2959	2959	2959	2959
F13	2960	2960	2960	2960	2960	2960	2960	2960	2960	2960	2960
F14	2962	2962	2962	2962	2962	2962	2962	2962	2962	2962	2962
F15	2964	2964	2964	2964	2964	2964	2964	2964	2964	2964	2964
F16	2965	2965	2965	2965	2965	2965	2965	2965	2965	2965	2965
F17	2968	2968	2968	2968	2968	2968	2968	2968	2968	2968	2968
F18	2969	2969	2969	2969	2969	2969	2969	2969	2969	2969	2969
F19	2970	2970	2970	2970	2970	2970	2970	2970	2970	2970	2970
F20	2971	2971	2971	2971	2971	2971	2971	2971	2971	2971	2971
F21	2974	2974	2974	2974	2974	2974	2974	2974	2974	2974	2974
F22	2975	2975	2975	2975	2975	2975	2975	2975	2975	2975	2975
F23	2976	2976	2976	2976	2976	2976	2976	2976	2976	2976	2976
F24	2977	2977	2977	2977	2977	2977	2977	2977	2977	2977	2977
F25	2979	2979	2979	2979	2979	2979	2979	2979	2979	2979	2979
F26	2983	2983	2983	2983	2983	2983	2983	2983	2983	2983	2983
F27	2984	2984	2984	2984	2984	2984	2984	2984	2984	2984	2984
F28	2985	2985	2985	2985	2985	2985	2985	2985	2985	2985	2985
F29	5198	5198	5198	5198	5198	5198	5198	5198	5198	5198	5198
F30	3513	3513	3513	3513	3513	3513	3513	3513	3513	3513	3513

DATE	03/16/92	07/01/92	07/23/92	01/19/93	08/10/93	10/25/94	08/10/95	10/13/95	03/05/96	09/23/96	01/29/97
MWD	0	0.173	0.249	1.696	3.983	6.441	8.698	9.201	9.646	10.803	11.731
G02											
G03											
G04											
G05											
G06											
G08											
G09											
G10											
G11											
G12											
G14											
G15											
G16											
G17											
G18											
G20											
G21											
G22											
G23											
G24											
G26											
G27											
G28											
G29											
G30											
G32											
G33											
G34											
G35											
G36											

DATE	09/11/97	01/23/98	05/06/98	06/18/98	07/23/98	03/04/99	04/06/99	05/24/99	07/02/99	04/27/00	06/29/00
MWD	12.791	14.477	17.064	17.266	17.97	23.642	23.818	25.407	25.999	31.313	34.757
B01	5921	5921	5921	5921	5921	5921	5921	5921	5921	5921	5921
B02	5922	5922	5922	5922	5922	5922	5922	5922	5922	5922	5922
B03	5982	5982	5982	5982	5982	5982	5982	5982	5982	5982	5982
B04	6143	6143	6143	6143	6143	6143	6143	6143	6143	6143	6143
B05	6886	6886	6886	6886	6886	6886	6886	6886	6886	6886	6886
B06	5283	5283	10808	10708	10708	10708	10708	10708	10708	10708	10708
C01	TR	TR	TR	TR	TR	TR	TR	TR	TR	TR	TR
C02	5916	5916	5916	5916	5916	5916	5916	5916	5916	5916	5916
C03	5917	5917	5917	5917	5917	5917	5917	5917	5917	5917	5917
C04	6924	6924	6924	6924	6924	6924	6924	6924	6924	6924	6924
C05	6926	6926	6926	6926	6926	6926	6926	6926	6926	6926	6926
C06	6927	6927	6927	6927	6927	6927	6927	6927	6927	6927	6927
C07	10146	10146	10146	10146	10146	10146	10146	10146	10146	10146	10146
C08	6928	6928	6928	6928	6928	6928	6928	6928	6928	6928	6928
C09	6929	6929	6929	6929	6929	6929	6929	6929	6929	6929	6929
C10	6930	6930	6930	6930	6930	6930	6930	6930	6930	6930	6930
C11	6889	6889	6889	6889	6889	6889	6889	6889	6889	6889	6889
C12	6932	6932	6932	6932	6932	6932	6932	6932	6932	6932	6932
D01	5844	5844	5844	5844	5844	5844	5844	5844	5844	5844	5844
D02	5845	5845	5845	5845	5845	5845	5845	5845	5845	5845	5845
D03	5846	5846	5846	5846	5846	5846	5846	5846	5846	5846	5846
D04	5902	5902	5902	5902	5902	5902	5902	5902	5902	5902	5902
D05	5903	5903	5903	5903	5903	5903	5903	5903	5903	5903	5903
D06	10147	10147	10147	10147	10147	10147	10147	10147	10147	10147	10147
D07	5904	5904	5904	5904	5904	5904	5904	5904	5904	5904	5904
D08	5912	5912	5912	5912	5912	5912	5912	5912	5912	5912	5912
D09	5913	5913	5913	5913	5913	5913	5913	5913	5913	5913	5913
D10	5914	5914	5914	5914	5914	5914	5914	5914	5914	5914	5914
D11	5915	5915	5915	5915	5915	5915	5915	5915	5915	5915	5915
D12	5918	5918	5918	5918	5918	5918	5918	5918	5918	5918	5918
D13	5919	5919	5919	5919	5919	5919	5919	5919	5919	5919	5919
D14	10148	10148	10148	10148	10148	10148	10148	10148	10148	10148	10148
D15	5920	5920	5920	5920	5920	5920	5920	5920	5920	5920	5920
D16	6142	6142	6142	6142	6142	6142	6142	6142		6142	6142
D17	6923	6923	6923	6923	6923		6923		6923	6923	
D18	6925	6925	6925	6925	6925	6925	6925	6925	6925	6925	6925
E01	2899	2899	2899	2899	2899	2899	2899	2899	2899	2899	2899
E02	2902	2902	2902	2902	2902	2902	2902	2902	2902	2902	2902
E03	2903	2903	2903	2903	2903	2903	2903	2903	2903	2903	2903
E04	2904	2904	2904	2904	2904	2904	2904	2904	2904	2904	2904
E05	2905	2905	2905	2905	2905	2905	2905	2905	2905	2905	2905
E06	2906	2906	2906	2906	2906	2906	2906	2906	2906	2906	2906
E07	2908	2908	2908	2908	2908	2908	2908	2908	2908	2908	2908
E08	2910	2910	2910	2910	2910	2910	2910	2910	2910	2910	2910
E09	2911	2911	2911	2911	2911	2911	2911	2911	2911	2911	2911

DATE	09/11/97	01/23/98	05/06/98	06/18/98	07/23/98	03/04/99	04/06/99	05/24/99	07/02/99	04/27/00	06/29/00
MWD	12.791	14.477	17.064	17.266	17.97	23.642	23.818	25.407	25.999	31.313	34.757
E10	2912	2912	2912	2912	2912	2912	2912	2912	2912	2912	2912
E11	2913	2913	2913	2913	2913	2913	2913	2913	2913	2913	2913
E12	2915	2915	2915	2915	2915	2915	2915	2915	2915	2915	2915
E13	2918	2918	2918	2918	2918	2918	2918	2918	2918	2918	2918
E14	2925	2925	2925	2925	2925	2925	2925	2925	2925	2925	2925
E15	2927	2927	2927	2927	2927	2927	2927	2927	2927	2927	2927
E16	2928	2928	2928	2928	2928	2928	2928	2928	2928	2928	2928
E17	2929	2929	2929	2929	2929	2929	2929	2929	2929	2929	2929
E18	2930	2930	2930	2930	2930	2930	2930	2930	2930	2930	2930
E19	2932	2932	2932	2932	2932	2932	2932	2932	2932	2932	2932
E20	2935	2935	2935	2935	2935	2935	2935	2935	2935	2935	2935
E21	2938	2951	2951	2951	2951	2951	2951	2951	2951	2938	2938
E22	2939	2939	2939	2939	2939		2939		2939	2939	
E23	2940	2940	2940	2940	2940		2940		2940	2940	
E24	2941	2941	2941	2941	2941	2941	2941	2941	2941	2941	2941
F01	2944	2944	2944	2944	2944	2944	2944	2944	2944	2944	2944
F02	2946	2946	2946	2946	2946	2946	2946	2946	2946	2946	2946
F03	2947	2947	2947	2947	2947	2947	2947	2947	2947	2947	2947
F04	2948	2948	2948	2948	2948	2948	2948	2948	2948	2948	2948
F05	2950	2950	2950	2950	2950	2950	2950	2950	2950	2950	2950
F06						6923		6923		2951	2951
F07	2952	2952	2952	2952	2952	2952	2952	2952	2952	2952	2952
F08	2954	2954	2954	2954	2954	2954	2954	2954	2954	2954	2954
F09	2955	2955	2955	2955	2955	2955	2955	2955	2955	2955	2955
F10	2957	2957	2957	2957	2957	2957	2957	2957	2957	2957	2957
F11						2931		2931	4	2958	2958
F12	2959	2959	2959	2959	2959	2959	2959	2959	2959	2959	2959
F13	2960	2960	2960	2960	2960	2960	2960	2960	2960	2960	2960
F14	2962	2962	2962	2962	2962	2962	2962	2962	2962	2962	2962
F15	2964	2964	2964	2964	2964	2964	2964	2964	2964	2964	2964
F16	2965	2965	2965	2965	2965	2965	2965	2965	2965	2965	2965
F17	2968	2968	2968	2968	2968	2968	2968	2968	2968	2968	2968
F18	2969	2969	2969	2969	2969	2969	2969	2969	2969	2969	2969
F19	2970	2970	2970	2970	2970	2970	2970	2970	2970	2970	2970
F20	2971	2971	2971	2971	2971	2971	2971	2971	2971	2971	2971
F21	2974	2974	2974	2974	2974	2974	2974	2974	2974	2974	2974
F22	2975	2975	2975	2975	2975	2975	2975	2975	2975	2975	2975
F23	2976	2976	2976	2976	2976	2976	2976	2976	2976	2976	2976
F24	2977	2977	2977	2977	2977	2977	2977	2977	2977	2977	2977
F25	2979	2979	2979	2979	2979	2979	2979	2979	2979	2979	2979
F26	2983	2983	2983	2983	2983	2983	2983	2983	2983	2983	2983
F27	2984	2984	2984	2984	2984	2984	2984	2984	2984	2984	2984
F28	2985	2985	2985	2985	2985	2985	2985	2985	2985	2985	2985
F29	5198	5198	5198	5198	5198	5198	5198	5198	5198	5198	5198
F30	3513	3513	3513	3513	3513	3513	3513	3513	3513	3513	3513

DATE	09/11/97	01/23/98	05/06/98	06/18/98	07/23/98	03/04/99	04/06/99	05/24/99	07/02/99	04/27/00	06/29/00
MWD	12.791	14.477	17.064	17.266	17.97	23.642	23.818	25.407	25.999	31.313	34.757
G02											2940
G03											
G04						2939		2939			
G05						2940		2940			
G06											
G08											2980
G09											
G10											
G11											
G12											2992
G14											4
G15						2958		2958			4
G16						2943		2943			4
G17											4
G18											3013
G20											6923
G21											3
G22											3
G23											3
G24											2939
G26											
G27											
G28											
G29											
G30											
G32											
G33											
G34											
G35											
G36											

DATE	07/20/00	09/07/00	09/20/00	01/11/01	02/27/01	03/21/01	04/30/01	07/30/01	07/24/02	11/14/02	07/24/03
MWD	34.849	34.91	34.993	36.593	38.027	38.598	39.084	45.814	67.322	81.288	90.327
B01	5921	5921	5921	5921	5921	5921	5921	5921	2952	2952	2952
B02	5922	5922	5922	5922	5922	5922	5922	5922	5922	5922	5922
B03	5982	5982	5982	5982	10878	10878	10878	10878	10878	10878	10878
B04	6143	6143	6143	6143	6143	6143	6143	6143	6143	6143	6143
B05	6886	6886	6886	6886	6886	6886	6886	6886	6886	6886	6886
B06	10708	10708	10708	10708	10708	10708	10708	10708	10708	10708	10708
C01	TR	TR	TR	TR	TR	TR	TR	TR	TR	TR	TR
C02	5916	5916	5916	5916	5916	5916	5916	5916	2938	2938	2938
C03	5917	5917	5917	5917	5917	5917	5917	5917	5917	5917	5917
C04	6924	6924	6924	6924	6924	6924	6924	6924	6924	6924	6924
C05	6926	6926	6926	6926	6926	6926	6926	6926	6926	6926	6926
C06	6927	6927	6927	6927	6927	6927	6927	6927	6927	6927	6927
C07	10146	10146	10146	10146	10146	10146	10146	10146	10146	10146	10146
C08	6928	6928	6928	6928	6928	6928	6928	6928	6928	6928	6928
C09	6929	6929	6929	6929	6929	6929	6929	6929	6929	6929	6929
C10	6930	6930	6930	6930	6930	6930	6930	6930	6930	6930	6930
C11	6889	6889	6889	6889	6889	6889	6889	6889	2954	2954	2954
C12	6932	6932	6932	6932	6932	6932	6932	6932	2927	2927	2927
D01	5844	5844	5844	5844	5844	5844	5844	5844	2948	2948	2948
D02	5845	5845	5845	5845	5845	5845	5845	5845	2904	2904	2904
D03	5846	5846	5846	5846	5846	5846	5846	5846	5846	5846	5846
D04	5902	5902	5902	5902	5902	5902	5902	5902	5902	5902	5902
D05	5903	5903	5903	5903	5903	5903	5903	5903	5903	5903	5903
D06	10147	10147	10147	10147	10147	10147	10147	10147	10147	10147	10147
D07	5904	5904	5904	5904	5904	5904	5904	5904	5904	5904	5904
D08	5912	5912	5912	5912	5912	5912	5912	5912	5912	5912	5912
D09	5913	5913	5913	5913	5913	5913	5913	5913	5913	5913	5913
D10	5914	5914	5914	5914	5914	5914	5914	5914	5914	5914	5914
D11	5915	5915	5915	5915	5915	5915	5915	5915	5915	5915	5915
D12	5918	5918	5918	5918	5918	5918	5918	5918	5918	5918	5918
D13	5919	5919	5919	5919	5919	5919	5919	5919	5919	5919	5919
D14	10148	10148	10148	10148	10148	10148	10148	10148	10148	10148	10148
D15	5920	5920	5920	5920	5920	5920	5920	5920	5920	5920	5920
D16	6142	6142	6142	6142	6142	6142	6142	6142	2951	2951	2951
D17	6923	6923		6923		6923					
D18	6925	6925	6925	6925	6925	6925	6925	6925	2970	2970	2970
E01	2899	2899	2899	2899	2899	2899	2899	2899	2899	2899	2899
E02	2902	2902	2902	2902	2902	2902	2902	2902	2902	2902	2902
E03	2903	2903	2903	2903	2903	2903	2903	2903	2903	2903	2903
E04	2904	2904	2904	2904	2904	2904	2904	2904	5845	5845	5845
E05	2905	2905	2905	2905	2905	2905	2905	2905	2905	2905	2905
E06	2906	2906	2906	2906	2906	2906	2906	2906	2906	2906	2906
E07	2908	2908	2908	2908	2908	2908	2908	2908	2908	2908	2908
E08	2910	2910	2910	2910	2910	2910	2910	2910	2958	2958	2958
E09	2911	2911	2911	2911	2911	2911	2911	2911	2911	2911	2911

DATE	07/20/00	09/07/00	09/20/00	01/11/01	02/27/01	03/21/01	04/30/01	07/30/01	07/24/02	11/14/02	07/24/03
MWD	34.849	34.91	34.993	36.593	38.027	38.598	39.084	45.814	67.322	81.288	90.327
E10	2912	2912	2912	2912	2912	2912	2912	2912	2912	2912	2912
E11	2913	2913	2913	2913	2913	2913	2913	2913	5198	5198	5198
E12	2915	2915	2915	2915	2915	2915	2915	2915	2915	2915	2915
E13	2918	2918	2918	2918	2918	2918	2918	2918	2918	2918	2918
E14	2925	2925	2925	2925	2925	2925	2925	2925	2925	2925	2925
E15	2927	2927	2927	2927	2927	2927	2927	2927	6932	6932	6932
E16	2928	2928	2928	2928	2928	2928	2928	2928	2928	2928	2928
E17	2929	2929	2929	2929	2929	2929	2929	2929	2929	2929	2929
E18	2930	2930	2930	2930	2930	2930	2930	2930	2930	2930	2930
E19	2932	2932	2932	2932	2932	2932	2932	2932	2932	2932	2932
E20	2935	2935	2935	2935	2935	2935	2935	2935	2935	2935	2935
E21	2938	2938	2938	2938	2938	2938	2938	2938	5916	5916	5916
E22	2939	2939		2939		2939					
E23	2940	2940		2940		2940					
E24	2941	2941	2941	2941	2941	2941	2941	2941	2976	2976	2976
F01	2944	2944	2944	2944	2944	2944	2944	2944	2944	2944	2944
F02	2946	2946	2946	2946	2946	2946	2946	2946	2946	2946	2946
F03	2947	2947	2947	2947	2947	2947	2947	2947	2947	2947	2947
F04	2948	2948	2948	2948	2948	2948	2948	2948	5844	5844	5844
F05	2950	2950	2950	2950	2950	2950	2950	2950	2950	2950	2950
F06	2951	2951	2951	2951	2951	2951	2951	2951	6142	6142	6142
F07	2952	2952	2952	2952	2952	2952	2952	2952	5921	5921	5921
F08	2954	2954	2954	2954	2954	2954	2954	2954	6889	6889	6889
F09	2955	2955	2955	2955	2955	2955	2955	2955	2955	2955	2955
F10	2957	2957	2957	2957	2957	2957	2957	2957	2985	2985	2985
F11	2958	2958	2958	2958	2958	2958	2958	2958	2910	2910	2910
F12	2959	2959	2959	2959	2959	2959	2959	2959	2959	2959	2959
F13	2960	2960	2960	2960	2960	2960	2960	2960	2960	2960	2960
F14	2962	2962	2962	2962	2962	2962	2962	2962	2962	2962	2962
F15	2964	2964	2964	2964	2964	2964	2964	2964	2964	2964	2964
F16	2965	2965	2965	2965	2965	2965	2965	2965	2965	2965	2965
F17	2968	2968	2968	2968	2968	2968	2968	2968	2984	2984	2984
F18	2969	2969	2969	2969	2969	2969	2969	2969	2969	2969	2969
F19	2970	2970	2970	2970	2970	2970	2970	2970	6925	6925	6925
F20	2971	2971	2971	2971	2971	2971	2971	2971	2971	2971	2971
F21	2974	2974	2974	2974	2974	2974	2974	2974	2974	2974	2974
F22	2975	2975	2975	2975	2975	2975	2975	2975	2975	2975	2975
F23	2976	2976	2976	2976	2976	2976	2976	2976	2941	2941	2941
F24	2977	2977	2977	2977	2977	2977	2977	2977	2977	2977	2977
F25	2979	2979	2979	2979	2979	2979	2979	2979	2979	2979	2979
F26	2983	2983	2983	2983	2983	2983	2983	2983	2983	2983	2983
F27	2984	2984	2984	2984	2984	2984	2984	2984	2968	2968	2968
F28	2985	2985	2985	2985	2985	2985	2985	2985	2957	2957	2957
F29	5198	5198	5198	5198	5198	5198	5198	5198	2913	2913	2913
F30	3513	3513	3513	3513	3513	3513	3513	3513	3513	3513	3513

DATE	07/20/00	09/07/00	09/20/00	01/11/01	02/27/01	03/21/01	04/30/01	07/30/01	07/24/02	11/14/02	07/24/03
MWD	34.849	34.91	34.993	36.593	38.027	38.598	39.084	45.814	67.322	81.288	90.327
G02	3	3	2940	3	2940	3	2940	2940	2940	2940	2940
G03										10810	10810
G04											
G05										10811	10811
G06										10812	10812
G08			2980		2980		2980	2980	2980	2980	2980
G09											
G10											
G11											
G12			2992		2992		2992	2992	2992	2992	2992
G14										10813	10813
G15										10814	10814
G16											
G17										10815	10815
G18			3013		3013		3013	3013	3013	3013	3013
G20			6923		6923		6923	6923	6923	6923	6923
G21											
G22											
G23											
G24			2939		2939		2939	2939	2939	2939	2939
G26										10816	10816
G27								2931	2931	2931	2931
G28											
G29								2943	2943	2943	2943
G30										10817	10817
G32											
G33											
G34											
G35											
G36								5911	5911	5911	5911

DATE	03/19/04	07/29/04	07/18/05	07/11/06	07/19/06	01/25/07	07/25/07	06/19/08	06/25/09	06/29/10	06/29/11
MWD	106.221	106.235	121.931	144.914	145.208	165.506	186.647	205.037	214.051	226.297	236.818
B01	2952	2985	2985	2985	2985	2985	2985	2985	2985	2985	2985
B02	5922	5198	5198	5198	5198	5198	5198	3384	3384	3384	3384
B03	10878	10878	10878	10878	10878	10878	10878	10878	10878	10878	10878
B04	6143	3013	3013	3013	3013	3013	3013	3013	3013	3013	3013
B05	6886	2899	2899	2899	2899	2899	2899	2899	2899	2899	2899
B06	10708	10708	10708	10708	10708	10708	10708	10708	10708	10708	10708
C01	TR	TR	TR	TR	TR	TR	TR	TR	TR	TR	TR
C02	2938	2965	2965	2965	2965	2965	2965	2965	2965	2965	2965
C03	5917	2984	2984	2984	2984	2984	2984	2984	2984	2984	2984
C04	6924	2944	2944	2944	2944	2944	2944	2944	2944	2944	2944
C05	6926	2931	2931	2931	2931	2931	2931	2931	2931	2931	2931
C06	6927	2983	2983	2983	2983	2983	2983	2983	2983	2983	2983
C07	10146	10146	10146	10146	10146	10146	10146	10146	10146	10146	10146
C08	6928	2980	2980	2980	2980	2980	2980	2980	2980	2980	2980
C09	6929	2925	2925	2925	2925	2925	2925	2925	2925	2925	2925
C10	6930	2941	2941	2941	2941	2941	2941	2941	2941	2941	2941
C11	2954	2979	2979	2979	2979	2979	2979	2979	2979	2979	2979
C12	2927	2964	2964	2964	2964	2964	2964	2964	2964	2964	2964
D01	2948	2910	2910	2910	2910	2910	2910	2910	2910	2910	2910
D02	2904	2959	2959	2959	2959	2959	2959	2959	2959	2959	2959
D03	5846	2939	2939	2906	2906	2906	2906	2906	2906	2906	2906
D04	5902	2992	2992	2992	2992	2992	2992	2992	2992	2992	2992
D05	5903	2962	2962	2962	2962	2962	2962	2962	2962	2962	2962
D06	10147	10147	10147	10147	10147	10147	10147	10147	10147	10147	10147
D07	5904	2928	2928	2928	2928	2928	2928	2928	2928	2928	2928
D08	5912	2906	2906	2939	2939	2939	2939	2939	2939	2939	2939
D09	5913	2932	2932	5918	5918	5918	5918	5918	5918	5918	5918
D10	5914	2977	2977	2977	2977	2977	2977	2977	2977	2977	2977
D11	5915	2974	2974	2974	2974	2974	2974	2974	2974	2974	2974
D12	5918	2905	2905	2905	2905	2905	2905	2905	2905	2905	2905
D13	5919	2943	2943	2943	2943	2943	2943	2943	2943	2943	2943
D14	10148	10148	10148	10148	10148	10148	10148	10148	10148	10148	10148
D15	5920	2950	2950	2950	2950	2950	2950	2950	2950	2950	2950
D16	2951	2929	2929	2929	2929	2929	2929	2929	2929	2929	2929
D17		2955	2955	2955	2955	2955	2955	2955	2955	2955	2955
D18	2970	2975	2975	2975	2975	2975	2975	2975	2975	2975	2975
E01	2899	5845	5845	5845	5845	5845	5845	5845	5845	5845	5845
E02	2902	6932	6932	6932	6932	6932	6932	6932	6932	6932	6932
E03	2903	5918	5918	2932	2932	2932	2932			2932	2932
E04	5845	5915	5915	5915	5915	5915	5915			5915	5915
E05	2905	6886	6886	6886	6886	6886	6886	6886	6886	6886	6886
E06	2906	6929	6929	5912	5912	5912	5912	5912	5912	5912	5912
E07	2908	5846	5846	5846	5846	5846	5846	5846	5846	5846	5846
E08	2958	5903	5903	5903	5903	5903	5903	5903	5903	5903	5903
E09	2911	5913	5913	5917	5917	5917	5917	5917	5917	5917	5917

DATE	03/19/04	07/29/04	07/18/05	07/11/06	07/19/06	01/25/07	07/25/07	06/19/08	06/25/09	06/29/10	06/29/11
MWD	106.221	106.235	121.931	144.914	145.208	165.506	186.647	205.037	214.051	226.297	236.818
E10	2912	5912	5912	6929	6929	6929	6929	6929	6929	6929	6929
E11	5198							2932	2932		
E12	2915	6923	6923	6925	6925	6925	6925	6925	6925	6925	6925
E13	2918	5844	5844	5844	5844	5844	5844	5844	5844	5844	5844
E14	2925	6925	6925	6923	6923	6923	6923	6923	6923	6923	6923
E15	6932	5919	5919	5919	5919	5919	5919	5919	5919	5919	5919
E16	2928	5921	5921	5921	5921	5921	5921	5921	5921	5921	5921
E17	2929	6927	6927	6927	6927	6927	6927	6927	6927	6927	6927
E18	2930	5902	5902	5902	5902	5902	5902	5902	5902	5902	5902
E19	2932	5904	5904	5904	5904	5904	5904	5904	5904	5904	5904
E20	2935	6930	6930	6930	6930	6930	6930	6930	6930	6930	6930
E21	5916	6889	6889	6889	6889	6889	6889	6889	6889	6889	6889
E22		5914	5914	5914	5914	5914	5914	5914	5914	5914	5914
E23		6142	6142	6142	6142	6142	6142	6142	6142	6142	6142
E24	2976	6928	6928	6928	6928	6928	6928	6928	6928	6928	6928
F01	2944	10817	10817	10817	10817	10817	10817	10817	10817	10817	10817
F02	2946	5911	5911	5911	5911	5911	5911	5911	5911	5911	5911
F03	2947	2918	2918	2918	2918	2918	2918			3496	3496
F04	5844	5920	5920	5920	5920	5920	5920			3504	3504
F05	2950	10810	10810	10810	10810	10810	10810			3703	3703
F06	6142	10816	10816	10816	10816	10816	10816	10816	10816	10816	10816
F07	5921	2915	2915	2915	2915	2915	2915	2915	2915	2915	2915
F08	6889	2946	2946	2946	2946	2946	2946	2946	2946	2946	2946
F09	2955	6924	6924	6924	6924	6924	6924	6924	6924	6924	6924
F10	2985	10812	10812	10812	10812	10812	10812	10812	10812	10812	10812
F11	2910	10815	10815	2958	2958	2958	2958	2958	2958	2958	2958
F12	2959	5917	5917	5913	5913	5913	5913	5913	5913	5913	5913
F13	2960							5915	5915		
F14	2962							6931	6931		
F15	2964	2912	2912	2902	2902	2902	2902	2902	2902	2902	2902
F16	2965	10813	10813	10813	10813	10813	10813	10813	10813	10813	10813
F17	2984	2902	2902	2912	2912	2912	2912	2912	2912	2912	2912
F18	2969	6143	6143	6143	6143	6143	6143	6143	6143	6143	6143
F19	6925	5916	5916	5916	5916	5916	5916	5916	5916	5916	5916
F20	2971	2940	2940	2940	2940	2940	2940	2940	2940	2940	2940
F21	2974	2971	2971	2971	2971	2971	2971	2971	2971	2971	2971
F22	2975	2969	2969	2969	2969	2969	2969	2969	2969	2969	2969
F23	2941	6926	6926	6926	6926	6926	6926	6926	6926	6926	6926
F24	2977	3513	3513	3513	3513	3513	3513	3513	3513	3513	3513
F25	2979	10811	10811	10811	10811	10811	10811	10811	10811	10811	10811
F26	2983	2960	2960	2960	2960	2960	2960	2960	2960	2960	2960
F27	2968	2947	2947	2947	2947	2947	2947	2947	2947	2947	2947
F28	2957	2911	2911	2911	2911	2911	2911	2911	2911	2911	2911
F29	2913	5922	5922	5922	5922	5922	5922	5922	5922	5922	5922
F30	3513	10814	10814	10814	10814	10814	10814	10814	10814	10814	10814

DATE	03/19/04	07/29/04	07/18/05	07/11/06	07/19/06	01/25/07	07/25/07	06/19/08	06/25/09	06/29/10	06/29/11
MWD	106.221	106.235	121.931	144.914	145.208	165.506	186.647	205.037	214.051	226.297	236.818
G02	2940						10704	10704	10704	10704	10704
G03	10810	2908	2908	2908	2908	2908	2908	2908	2908	2908	2908
G04		2968	2968	2968	2968	2968	2968			3700	3700
G05	10811	2951	2951	2951	2951	2951	2951			6931	6931
G06	10812							5920	5920	5920	5920
G08	2980		10701	10701	10701	10701	10701	10701	10701	10701	10701
G09		2957	2957	2957	2957	2957	2957	2957	2957	2957	2957
G10		2976	2976	2938	2938	2938	2938	2938	2938	2938	2938
G11		2927	2927	2927	2927	2927	2927	2927	2927	2927	2927
G12	2992		10702	10702	10702	10702	10702	10702	10702	10702	10702
G14	10813	2970	2970	2970	2970	2970	2970	2970	2970	2970	2970
G15	10814	2938	2938	2976	2976	2976	2976	2976	2976	2976	2976
G16			3	3	3	3	3	2952	2952	2952	2952
G17	10815	2958	2958	10815	10815	10815	10815	10815	10815	10815	10815
G18	3013	2904	2904	2904	2904	2904	2904	2904	2904	2904	2904
G20	6923	3	3	3	3	3	3	2968	2968	2968	2968
G21		2903	2903	2903	2903	2903	2903	2903	2903	2903	2903
G22		2935	2935	2935	2935	2935	2935	2935	2935	2935	2935
G23		2930	2930	2930	2930	2930	2930	2930	2930	2930	2930
G24	2939	3	3	3	3	3	3	2951	2951	2951	2951
G26	10816	3	3	3	3	3	10699	10699	10699	10699	10699
G27	2931	2948	2948	2948	2948	2948	2948	2948	2948	2948	2948
G28		2913	2913	2913	2913	2913	2913	2913	2913	2913	2913
G29	2943	2954	2954	2954	2954	2954	2954	2954	2954	2954	2954
G30	10817						10700	10700	10700	10700	10700
G32											
G33								2918	2918	2918	2918
G34											
G35								10810	10810	10810	10810
G36	5911						10703	10703	10703	10703	10703

DATE	07/13/12	07/16/13	07/21/14	11/20/15	01/22/16	07/26/16
MWD	260.145	281.566	286.658	298.855	299.868	317.809
B01	2985	2985	2985	2985	2985	2985
B02	3384	3384	3384	3384	3384	3384
B03	10878	10878	10878	10878	10878	10878
B04	3013	3013	3013	3013	3013	3013
B05	2899	2899	2899	2899	2899	2899
B06	10708	10708	10708	10809	10809	10809
C01	TR	TR	TR	TR	TR	TR
C02	2965	2965	2965	2965	2965	2965
C03	2984	2984	2984	2984	2984	2984
C04	2944	2944	2944	2944	2944	2944
C05	2931	2931	2931	2931	2931	2931
C06	2983	2983	2983	2983	2983	2983
C07	10146	10146	10146	10146	10146	10146
C08	2980	2980	2980	2980	2980	2980
C09	2925	2925	2925	2925	2925	2925
C10	2941	2941	2941	2941	2941	2941
C11	2979	2979	2979	2979	2979	2979
C12	2964	2964	2964	2964	2964	2964
D01	2910	2910	2910	2910	2910	2910
D02	2959	2959	2959	2959	2959	2959
D03	2906	2906	2906	2906	2906	2906
D04	2992	2992	2992	2992	2992	2992
D05	2962	2962	2962	2962	2962	2962
D06	10147	10147	10147	10147	10147	10147
D07	2928	2928	2928	2928	2928	2928
D08	2939	2939	2939	2939	2939	2939
D09	5918	5918	5918	5918	5918	5918
D10	2977	2977	2977	2977	2977	2977
D11	2974	2974	2974	2974	2974	2974
D12	2905	2905	2905	2905	2905	2905
D13	2943	2943	2943	2943	2943	2943
D14	10148	10148	10148	10148	10148	10148
D15	2950	2950	2950	2950	2950	2950
D16	2929	2929	2929	2929	2929	2929
D17	2955	2955	2955	2955	2955	2955
D18	2975	2975	2975	2975	2975	2975
E01	5845	5845	5845	5845	5845	5845
E02	6932	6932	6932	6932	6932	6932
E03	2932	2932	2932	2932	2932	2932
E04	5915	5915	5915	5915	5915	5915
E05	6886	6886	6886	6886	6886	6886
E06	5912	5912	5912	5912	5912	5912
E07	5846	5846	5846	5846	5846	5846
E08	5903	5903	5903	5903	5903	5903
E09	5917	5917	5917	5917	5917	5917

DATE	07/13/12	07/16/13	07/21/14	11/20/15	01/22/16	07/26/16
MWD	260.145	281.566	286.658	298.855	299.868	317.809
E10	6929	6929	6929	6929	6929	6929
E11						
E12	6925	6925	6925	6925	6925	6925
E13	5844	5844	5844	5844	5844	5844
E14	6923	6923	6923	6923	6923	6923
E15	5919	5919	5919	5919	5919	5919
E16	5921	5921	5921	5921	5921	5921
E17	6927	6927	6927	6927	6927	6927
E18	5902	5902	5902	5902	5902	5902
E19	5904	5904	5904	5904	5904	5904
E20	6930	6930	6930	6930	6930	6930
E21	6889	6889	6889	6889	6889	6889
E22	5914	5914	5914	5914	5914	5914
E23	6142	6142	6142	6142	6142	6142
E24	6928	6928	6928	6928	6928	6928
F01	10817	10817	10817	10817	10817	10817
F02	5911	5911	5911	5911	5911	5911
F03	3496	3496	3496	3496	3496	3496
F04	3504	3504	3504	3504	3504	3504
F05	3703	3703	3703	6931	6931	6931
F06	10816	10816	10816	10816	10816	10816
F07	2915	2915	2915	2915	2915	2915
F08	2946	2946	2946	2946	2946	2946
F09	6924	6924	6924	6924	6924	6924
F10	10812	10812	10812	10812	10812	10812
F11	2958	2958	2958	2958	2958	2958
F12	5913	5913	5913	5913	5913	5913
F13						
F14						
F15	2902	2902	2902	2902	2902	2902
F16	10813	10813	10813	10813	10813	10813
F17	2912	2912	2912	2912	2912	2912
F18	6143	6143	6143	6143	6143	6143
F19	5916	5916	5916	5916	5916	5916
F20	2940	2940	2940	2940	2940	2940
F21	2971	2971	2971	2971	2971	2971
F22	2969	2969	2969	2969	2969	2969
F23	6926	6926	6926	6926	6926	6926
F24	3513	3513	3513	3513	3513	3513
F25	10811	10811	10811	10811	10811	10811
F26	2960	2960	2960	2960	2960	2960
F27	2947	2947	2947	2947	2947	2947
F28	2911	2911	2911	2911	2911	2911
F29	5922	5922	5922	5922	5922	5922
F30	10814	10814	10814	10814	10814	10814

DATE	07/13/12	07/16/13	07/21/14	11/20/15	01/22/16	07/26/16
MWD	260.145	281.566	286.658	298.855	299.868	317.809
G02	10704	10704	10704	10704	10704	10704
G03	2908	2908	2908	2908	2908	2908
G04	3700	3700	3700	3700	3700	3700
G05	6931	6931	6931	3703	3703	3703
G06	5920	5920	5920	5920	5920	5920
G08	10701	10701	10701	10701	10701	10701
G09	2957	2957	2957	2957	2957	2957
G10	2938	2938	2938	2938	2938	2938
G11	2927	2927	2927	2927	2927	2927
G12	10702	10702	10702	10702	10702	10702
G14	2970	2970	2970	2970	2970	2970
G15	2976	2976	2976	2976	2976	2976
G16	2952	2952	2952	2952	2952	2952
G17	10815	10815	10815	10815	10815	10815
G18	2904	2904	2904	2904	2904	2904
G20	2968	2968	2968	2968	2968	2968
G21	2903	2903	2903	2903	2903	2903
G22	2935	2935	2935	2935	2935	2935
G23	2930	2930	2930	2930	2930	2930
G24	2951	2951	2951	2951	2951	2951
G26	10699	10699	10699	10699	10699	10699
G27	2948	2948	2948	2948	2948	2948
G28	2913	2913	2913	2913	2913	2913
G29	2954	2954	2954	2954	2954	2954
G30	10700	10700	10700	10700	10700	10700
G32						
G33	2918	2918	2918	2918	2918	2918
G34						
G35	10810	10810	10810	10810	10810	10810
G36	10703	10703	10703	10703	10703	10703

DATE	03/16/92	07/01/92	07/23/92	01/19/93	08/10/93	10/25/94	08/10/95	10/13/95	03/05/96	09/23/96	01/29/97
MWD	0	0.173	0.249	1.696	3.983	6.441	8.698	9.201	9.646	10.803	11.731
B01	5921	5921	5921	5921	5921	5921	5921	5921	5921	5921	5921
B02	5922	5922	5922	5922	5922	5922	5922	5922	5922	5922	5922
B03	5981	5981	5981	5981	5981	5981	5981	5982	5982	5982	5982
B04	6143	6143	6143	6143	6143	6143	6143	6143	6143	6143	6143
B05	6886	6886	6886	6886	6886	6886	6886	6886	6886	6886	6886
B06	6889	6889	6889	5283	5283	5283	5283	5283	5283	5283	5283
C01	TR	TR	TR	TR	TR	TR	TR	TR	TR	TR	TR
C02	5916	5916	5916	5916	5916	5916	5916	5916	5916	5916	5916
C03	5917	5917	5917	5917	5917	5917	5917	5917	5917	5917	5917
C04	6924	6924	6924	6924	6924	6924	6924	6924	6924	6924	6924
C05	6926	6926	6926	6926	6926	6926	6926	6926	6926	6926	6926
C06	6927	6927	6927	6927	6927	6927	6927	6927	6927	6927	6927
C07	10146	10146	10146	10146	10146	10146	10146	10146	10146	10146	10146
C08	6928	6928	6928	6928	6928	6928	6928	6928	6928	6928	6928
C09	6929	6929	6929	6929	6929	6929	6929	6929	6929	6929	6929
C10	6930	6930	6930	6930	6930	6930	6930	6930	6930	6930	6930
C11	5283	5283	5283	6889	6889	6889	6889	6889	6889	6889	6889
C12	6932	6932	6932	6932	6932	6932	6932	6932	6932	6932	6932
D01	5844	5844	5844	5844	5844	5844	5844	5844	5844	5844	5844
D02	5845	5845	5845	5845	5845	5845	5845	5845	5845	5845	5845
D03	5846	5846	5846	5846	5846	5846	5846	5846	5846	5846	5846
D04	5902	5902	5902	5902	5902	5902	5902	5902	5902	5902	5902
D05	5903	5903	5903	5903	5903	5903	5903	5903	5903	5903	5903
D06	10147	10147	10147	10147	10147	10147	10147	10147	10147	10147	10147
D07	5904	5904	5904	5904	5904	5904	5904	5904	5904	5904	5904
D08	5912	5912	5912	5912	5912	5912	5912	5912	5912	5912	5912
D09	5913	5913	5913	5913	5913	5913	5913	5913	5913	5913	5913
D10	5914	5914	5914	5914	5914	5914	5914	5914	5914	5914	5914
D11	5915	5915	5915	5915	5915	5915	5915	5915	5915	5915	5915
D12	5918	5918	5918	5918	5918	5918	5918	5918	5918	5918	5918
D13	5919	5919	5919	5919	5919	5919	5919	5919	5919	5919	5919
D14	10148	10148	10148	10148	10148	10148	10148	10148	10148	10148	10148
D15	5920	5920	5920	5920	5920	5920	5920	5920	5920	5920	5920
D16	6142	6142	6142	6142	6142	6142	6142	6142	6142	6142	6142
D17	6923	6923	6923	6923	6923	6923	6923	6923	6923	6923	6923
D18	6925	6925	6925	6925	6925	6925	6925	6925	6925	6925	6925
E01	2899	2899	2899	2899	2899	2899	2899	2899	2899	2899	2899
E02	2902	2902	2902	2902	2902	2902	2902	2902	2902	2902	2902
E03	2903	2903	2903	2903	2903	2903	2903	2903	2903	2903	2903
E04	2904	2904	2904	2904	2904	2904	2904	2904	2904	2904	2904
E05	2905	2905	2905	2905	2905	2905	2905	2905	2905	2905	2905
E06	2906	2906	2906	2906	2906	2906	2906	2906	2906	2906	2906
E07	2908	2908	2908	2908	2908	2908	2908	2908	2908	2908	2908
E08	2910	2910	2910	2910	2910	2910	2910	2910	2910	2910	2910
E09	2911	2911	2911	2911	2911	2911	2911	2911	2911	2911	2911

DATE	03/16/92	07/01/92	07/23/92	01/19/93	08/10/93	10/25/94	08/10/95	10/13/95	03/05/96	09/23/96	01/29/97
MWD	0	0.173	0.249	1.696	3.983	6.441	8.698	9.201	9.646	10.803	11.731
E10	2912	2912	2912	2912	2912	2912	2912	2912	2912	2912	2912
E11	2913	2913	2913	2913	2913	2913	2913	2913	2913	2913	2913
E12	2915	2915	2915	2915	2915	2915	2915	2915	2915	2915	2915
E13	2918	2918	2918	2918	2918	2918	2918	2918	2918	2918	2918
E14	2925	2925	2925	2925	2925	2925	2925	2925	2925	2925	2925
E15	2927	2927	2927	2927	2927	2927	2927	2927	2927	2927	2927
E16	2928	2928	2928	2928	2928	2928	2928	2928	2928	2928	2928
E17	2929	2929	2929	2929	2929	2929	2929	2929	2929	2929	2929
E18	2930	2930	2930	2930	2930	2930	2930	2930	2930	2930	2930
E19	2932	2932	2932	2932	2932	2932	2932	2932	2932	2932	2932
E20	2935	2935	2935	2935	2935	2935	2935	2935	2935	2935	2935
E21	2938	2938	2938	2938	2938	2938	2938	2938	2938	2938	2938
E22	2939	2939	2939	2939	2939	2939	2939	2939	2939	2939	2939
E23	2940	2940	2940	2940	2940	2940	2940	2940	2940	2940	2940
E24	2941	2941	2941	2941	2941	2941	2941	2941	2941	2941	2941
F01	2944	2944	2944	2944	2944	2944	2944	2944	2944	2944	2944
F02	2946	2946	2946	2946	2946	2946	2946	2946	2946	2946	2946
F03	2947	2947	2947	2947	2947	2947	2947	2947	2947	2947	2947
F04	2948	2948	2948	2948	2948	2948	2948	2948	2948	2948	2948
F05	2950	2950	2950	2950	2950	2950	2950	2950	2950	2950	2950
F06											
F07	2952	2952	2952	2952	2952	2952	2952	2952	2952	2952	2952
F08	2954	2954	2954	2954	2954	2954	2954	2954	2954	2954	2954
F09	2955	2955	2955	2955	2955	2955	2955	2955	2955	2955	2955
F10	2957	2957	2957	2957	2957	2957	2957	2957	2957	2957	2957
F11											
F12	2959	2959	2959	2959	2959	2959	2959	2959	2959	2959	2959
F13	2960	2960	2960	2960	2960	2960	2960	2960	2960	2960	2960
F14	2962	2962	2962	2962	2962	2962	2962	2962	2962	2962	2962
F15	2964	2964	2964	2964	2964	2964	2964	2964	2964	2964	2964
F16	2965	2965	2965	2965	2965	2965	2965	2965	2965	2965	2965
F17	2968	2968	2968	2968	2968	2968	2968	2968	2968	2968	2968
F18	2969	2969	2969	2969	2969	2969	2969	2969	2969	2969	2969
F19	2970	2970	2970	2970	2970	2970	2970	2970	2970	2970	2970
F20	2971	2971	2971	2971	2971	2971	2971	2971	2971	2971	2971
F21	2974	2974	2974	2974	2974	2974	2974	2974	2974	2974	2974
F22	2975	2975	2975	2975	2975	2975	2975	2975	2975	2975	2975
F23	2976	2976	2976	2976	2976	2976	2976	2976	2976	2976	2976
F24	2977	2977	2977	2977	2977	2977	2977	2977	2977	2977	2977
F25	2979	2979	2979	2979	2979	2979	2979	2979	2979	2979	2979
F26	2983	2983	2983	2983	2983	2983	2983	2983	2983	2983	2983
F27	2984	2984	2984	2984	2984	2984	2984	2984	2984	2984	2984
F28	2985	2985	2985	2985	2985	2985	2985	2985	2985	2985	2985
F29	5198	5198	5198	5198	5198	5198	5198	5198	5198	5198	5198
F30	3513	3513	3513	3513	3513	3513	3513	3513	3513	3513	3513

DATE	03/16/92	07/01/92	07/23/92	01/19/93	08/10/93	10/25/94	08/10/95	10/13/95	03/05/96	09/23/96	01/29/97
MWD	0	0.173	0.249	1.696	3.983	6.441	8.698	9.201	9.646	10.803	11.731
G02											
G03											
G04											
G05											
G06											
G08											
G09											
G10											
G11											
G12											
G14											
G15											
G16											
G17											
G18											
G20											
G21											
G22											
G23											
G24											
G26											
G27											
G28											
G29											
G30											
G32											
G33											
G34											
G35											
G36											

DATE	09/11/97	01/23/98	05/06/98	06/18/98	07/23/98	03/04/99	04/06/99	05/24/99	07/02/99	04/27/00	06/29/00
MWD	12.791	14.477	17.064	17.266	17.97	23.642	23.818	25.407	25.999	31.313	34.757
B01	5921	5921	5921	5921	5921	5921	5921	5921	5921	5921	5921
B02	5922	5922	5922	5922	5922	5922	5922	5922	5922	5922	5922
B03	5982	5982	5982	5982	5982	5982	5982	5982	5982	5982	5982
B04	6143	6143	6143	6143	6143	6143	6143	6143	6143	6143	6143
B05	6886	6886	6886	6886	6886	6886	6886	6886	6886	6886	6886
B06	5283	5283	10808	10708	10708	10708	10708	10708	10708	10708	10708
C01	TR	TR	TR	TR	TR	TR	TR	TR	TR	TR	TR
C02	5916	5916	5916	5916	5916	5916	5916	5916	5916	5916	5916
C03	5917	5917	5917	5917	5917	5917	5917	5917	5917	5917	5917
C04	6924	6924	6924	6924	6924	6924	6924	6924	6924	6924	6924
C05	6926	6926	6926	6926	6926	6926	6926	6926	6926	6926	6926
C06	6927	6927	6927	6927	6927	6927	6927	6927	6927	6927	6927
C07	10146	10146	10146	10146	10146	10146	10146	10146	10146	10146	10146
C08	6928	6928	6928	6928	6928	6928	6928	6928	6928	6928	6928
C09	6929	6929	6929	6929	6929	6929	6929	6929	6929	6929	6929
C10	6930	6930	6930	6930	6930	6930	6930	6930	6930	6930	6930
C11	6889	6889	6889	6889	6889	6889	6889	6889	6889	6889	6889
C12	6932	6932	6932	6932	6932	6932	6932	6932	6932	6932	6932
D01	5844	5844	5844	5844	5844	5844	5844	5844	5844	5844	5844
D02	5845	5845	5845	5845	5845	5845	5845	5845	5845	5845	5845
D03	5846	5846	5846	5846	5846	5846	5846	5846	5846	5846	5846
D04	5902	5902	5902	5902	5902	5902	5902	5902	5902	5902	5902
D05	5903	5903	5903	5903	5903	5903	5903	5903	5903	5903	5903
D06	10147	10147	10147	10147	10147	10147	10147	10147	10147	10147	10147
D07	5904	5904	5904	5904	5904	5904	5904	5904	5904	5904	5904
D08	5912	5912	5912	5912	5912	5912	5912	5912	5912	5912	5912
D09	5913	5913	5913	5913	5913	5913	5913	5913	5913	5913	5913
D10	5914	5914	5914	5914	5914	5914	5914	5914	5914	5914	5914
D11	5915	5915	5915	5915	5915	5915	5915	5915	5915	5915	5915
D12	5918	5918	5918	5918	5918	5918	5918	5918	5918	5918	5918
D13	5919	5919	5919	5919	5919	5919	5919	5919	5919	5919	5919
D14	10148	10148	10148	10148	10148	10148	10148	10148	10148	10148	10148
D15	5920	5920	5920	5920	5920	5920	5920	5920	5920	5920	5920
D16	6142	6142	6142	6142	6142	6142	6142	6142		6142	6142
D17	6923	6923	6923	6923	6923		6923		6923	6923	
D18	6925	6925	6925	6925	6925	6925	6925	6925	6925	6925	6925
E01	2899	2899	2899	2899	2899	2899	2899	2899	2899	2899	2899
E02	2902	2902	2902	2902	2902	2902	2902	2902	2902	2902	2902
E03	2903	2903	2903	2903	2903	2903	2903	2903	2903	2903	2903
E04	2904	2904	2904	2904	2904	2904	2904	2904	2904	2904	2904
E05	2905	2905	2905	2905	2905	2905	2905	2905	2905	2905	2905
E06	2906	2906	2906	2906	2906	2906	2906	2906	2906	2906	2906
E07	2908	2908	2908	2908	2908	2908	2908	2908	2908	2908	2908
E08	2910	2910	2910	2910	2910	2910	2910	2910	2910	2910	2910
E09	2911	2911	2911	2911	2911	2911	2911	2911	2911	2911	2911

DATE	09/11/97	01/23/98	05/06/98	06/18/98	07/23/98	03/04/99	04/06/99	05/24/99	07/02/99	04/27/00	06/29/00
MWD	12.791	14.477	17.064	17.266	17.97	23.642	23.818	25.407	25.999	31.313	34.757
E10	2912	2912	2912	2912	2912	2912	2912	2912	2912	2912	2912
E11	2913	2913	2913	2913	2913	2913	2913	2913	2913	2913	2913
E12	2915	2915	2915	2915	2915	2915	2915	2915	2915	2915	2915
E13	2918	2918	2918	2918	2918	2918	2918	2918	2918	2918	2918
E14	2925	2925	2925	2925	2925	2925	2925	2925	2925	2925	2925
E15	2927	2927	2927	2927	2927	2927	2927	2927	2927	2927	2927
E16	2928	2928	2928	2928	2928	2928	2928	2928	2928	2928	2928
E17	2929	2929	2929	2929	2929	2929	2929	2929	2929	2929	2929
E18	2930	2930	2930	2930	2930	2930	2930	2930	2930	2930	2930
E19	2932	2932	2932	2932	2932	2932	2932	2932	2932	2932	2932
E20	2935	2935	2935	2935	2935	2935	2935	2935	2935	2935	2935
E21	2938	2951	2951	2951	2951	2951	2951	2951	2951	2938	2938
E22	2939	2939	2939	2939	2939		2939		2939	2939	
E23	2940	2940	2940	2940	2940		2940		2940	2940	
E24	2941	2941	2941	2941	2941	2941	2941	2941	2941	2941	2941
F01	2944	2944	2944	2944	2944	2944	2944	2944	2944	2944	2944
F02	2946	2946	2946	2946	2946	2946	2946	2946	2946	2946	2946
F03	2947	2947	2947	2947	2947	2947	2947	2947	2947	2947	2947
F04	2948	2948	2948	2948	2948	2948	2948	2948	2948	2948	2948
F05	2950	2950	2950	2950	2950	2950	2950	2950	2950	2950	2950
F06						6923		6923		2951	2951
F07	2952	2952	2952	2952	2952	2952	2952	2952	2952	2952	2952
F08	2954	2954	2954	2954	2954	2954	2954	2954	2954	2954	2954
F09	2955	2955	2955	2955	2955	2955	2955	2955	2955	2955	2955
F10	2957	2957	2957	2957	2957	2957	2957	2957	2957	2957	2957
F11						2931		2931	4	2958	2958
F12	2959	2959	2959	2959	2959	2959	2959	2959	2959	2959	2959
F13	2960	2960	2960	2960	2960	2960	2960	2960	2960	2960	2960
F14	2962	2962	2962	2962	2962	2962	2962	2962	2962	2962	2962
F15	2964	2964	2964	2964	2964	2964	2964	2964	2964	2964	2964
F16	2965	2965	2965	2965	2965	2965	2965	2965	2965	2965	2965
F17	2968	2968	2968	2968	2968	2968	2968	2968	2968	2968	2968
F18	2969	2969	2969	2969	2969	2969	2969	2969	2969	2969	2969
F19	2970	2970	2970	2970	2970	2970	2970	2970	2970	2970	2970
F20	2971	2971	2971	2971	2971	2971	2971	2971	2971	2971	2971
F21	2974	2974	2974	2974	2974	2974	2974	2974	2974	2974	2974
F22	2975	2975	2975	2975	2975	2975	2975	2975	2975	2975	2975
F23	2976	2976	2976	2976	2976	2976	2976	2976	2976	2976	2976
F24	2977	2977	2977	2977	2977	2977	2977	2977	2977	2977	2977
F25	2979	2979	2979	2979	2979	2979	2979	2979	2979	2979	2979
F26	2983	2983	2983	2983	2983	2983	2983	2983	2983	2983	2983
F27	2984	2984	2984	2984	2984	2984	2984	2984	2984	2984	2984
F28	2985	2985	2985	2985	2985	2985	2985	2985	2985	2985	2985
F29	5198	5198	5198	5198	5198	5198	5198	5198	5198	5198	5198
F30	3513	3513	3513	3513	3513	3513	3513	3513	3513	3513	3513

DATE	09/11/97	01/23/98	05/06/98	06/18/98	07/23/98	03/04/99	04/06/99	05/24/99	07/02/99	04/27/00	06/29/00
MWD	12.791	14.477	17.064	17.266	17.97	23.642	23.818	25.407	25.999	31.313	34.757
G02											2940
G03											
G04						2939		2939			
G05						2940		2940			
G06											
G08											2980
G09											
G10											
G11											
G12											2992
G14											4
G15						2958		2958			4
G16						2943		2943			4
G17											4
G18											3013
G20											6923
G21											3
G22											3
G23											3
G24											2939
G26											
G27											
G28											
G29											
G30											
G32											
G33											
G34											
G35											
G36											

DATE	07/20/00	09/07/00	09/20/00	01/11/01	02/27/01	03/21/01	04/30/01	07/30/01	07/24/02	11/14/02	07/24/03
MWD	34.849	34.91	34.993	36.593	38.027	38.598	39.084	45.814	67.322	81.288	90.327
B01	5921	5921	5921	5921	5921	5921	5921	5921	2952	2952	2952
B02	5922	5922	5922	5922	5922	5922	5922	5922	5922	5922	5922
B03	5982	5982	5982	5982	10878	10878	10878	10878	10878	10878	10878
B04	6143	6143	6143	6143	6143	6143	6143	6143	6143	6143	6143
B05	6886	6886	6886	6886	6886	6886	6886	6886	6886	6886	6886
B06	10708	10708	10708	10708	10708	10708	10708	10708	10708	10708	10708
C01	TR	TR	TR	TR	TR	TR	TR	TR	TR	TR	TR
C02	5916	5916	5916	5916	5916	5916	5916	5916	2938	2938	2938
C03	5917	5917	5917	5917	5917	5917	5917	5917	5917	5917	5917
C04	6924	6924	6924	6924	6924	6924	6924	6924	6924	6924	6924
C05	6926	6926	6926	6926	6926	6926	6926	6926	6926	6926	6926
C06	6927	6927	6927	6927	6927	6927	6927	6927	6927	6927	6927
C07	10146	10146	10146	10146	10146	10146	10146	10146	10146	10146	10146
C08	6928	6928	6928	6928	6928	6928	6928	6928	6928	6928	6928
C09	6929	6929	6929	6929	6929	6929	6929	6929	6929	6929	6929
C10	6930	6930	6930	6930	6930	6930	6930	6930	6930	6930	6930
C11	6889	6889	6889	6889	6889	6889	6889	6889	2954	2954	2954
C12	6932	6932	6932	6932	6932	6932	6932	6932	2927	2927	2927
D01	5844	5844	5844	5844	5844	5844	5844	5844	2948	2948	2948
D02	5845	5845	5845	5845	5845	5845	5845	5845	2904	2904	2904
D03	5846	5846	5846	5846	5846	5846	5846	5846	5846	5846	5846
D04	5902	5902	5902	5902	5902	5902	5902	5902	5902	5902	5902
D05	5903	5903	5903	5903	5903	5903	5903	5903	5903	5903	5903
D06	10147	10147	10147	10147	10147	10147	10147	10147	10147	10147	10147
D07	5904	5904	5904	5904	5904	5904	5904	5904	5904	5904	5904
D08	5912	5912	5912	5912	5912	5912	5912	5912	5912	5912	5912
D09	5913	5913	5913	5913	5913	5913	5913	5913	5913	5913	5913
D10	5914	5914	5914	5914	5914	5914	5914	5914	5914	5914	5914
D11	5915	5915	5915	5915	5915	5915	5915	5915	5915	5915	5915
D12	5918	5918	5918	5918	5918	5918	5918	5918	5918	5918	5918
D13	5919	5919	5919	5919	5919	5919	5919	5919	5919	5919	5919
D14	10148	10148	10148	10148	10148	10148	10148	10148	10148	10148	10148
D15	5920	5920	5920	5920	5920	5920	5920	5920	5920	5920	5920
D16	6142	6142	6142	6142	6142	6142	6142	6142	2951	2951	2951
D17	6923	6923		6923		6923					
D18	6925	6925	6925	6925	6925	6925	6925	6925	2970	2970	2970
E01	2899	2899	2899	2899	2899	2899	2899	2899	2899	2899	2899
E02	2902	2902	2902	2902	2902	2902	2902	2902	2902	2902	2902
E03	2903	2903	2903	2903	2903	2903	2903	2903	2903	2903	2903
E04	2904	2904	2904	2904	2904	2904	2904	2904	5845	5845	5845
E05	2905	2905	2905	2905	2905	2905	2905	2905	2905	2905	2905
E06	2906	2906	2906	2906	2906	2906	2906	2906	2906	2906	2906
E07	2908	2908	2908	2908	2908	2908	2908	2908	2908	2908	2908
E08	2910	2910	2910	2910	2910	2910	2910	2910	2958	2958	2958
E09	2911	2911	2911	2911	2911	2911	2911	2911	2911	2911	2911

DATE	07/20/00	09/07/00	09/20/00	01/11/01	02/27/01	03/21/01	04/30/01	07/30/01	07/24/02	11/14/02	07/24/03
MWD	34.849	34.91	34.993	36.593	38.027	38.598	39.084	45.814	67.322	81.288	90.327
E10	2912	2912	2912	2912	2912	2912	2912	2912	2912	2912	2912
E11	2913	2913	2913	2913	2913	2913	2913	2913	5198	5198	5198
E12	2915	2915	2915	2915	2915	2915	2915	2915	2915	2915	2915
E13	2918	2918	2918	2918	2918	2918	2918	2918	2918	2918	2918
E14	2925	2925	2925	2925	2925	2925	2925	2925	2925	2925	2925
E15	2927	2927	2927	2927	2927	2927	2927	2927	6932	6932	6932
E16	2928	2928	2928	2928	2928	2928	2928	2928	2928	2928	2928
E17	2929	2929	2929	2929	2929	2929	2929	2929	2929	2929	2929
E18	2930	2930	2930	2930	2930	2930	2930	2930	2930	2930	2930
E19	2932	2932	2932	2932	2932	2932	2932	2932	2932	2932	2932
E20	2935	2935	2935	2935	2935	2935	2935	2935	2935	2935	2935
E21	2938	2938	2938	2938	2938	2938	2938	2938	5916	5916	5916
E22	2939	2939		2939		2939					
E23	2940	2940		2940		2940					
E24	2941	2941	2941	2941	2941	2941	2941	2941	2976	2976	2976
F01	2944	2944	2944	2944	2944	2944	2944	2944	2944	2944	2944
F02	2946	2946	2946	2946	2946	2946	2946	2946	2946	2946	2946
F03	2947	2947	2947	2947	2947	2947	2947	2947	2947	2947	2947
F04	2948	2948	2948	2948	2948	2948	2948	2948	5844	5844	5844
F05	2950	2950	2950	2950	2950	2950	2950	2950	2950	2950	2950
F06	2951	2951	2951	2951	2951	2951	2951	2951	6142	6142	6142
F07	2952	2952	2952	2952	2952	2952	2952	2952	5921	5921	5921
F08	2954	2954	2954	2954	2954	2954	2954	2954	6889	6889	6889
F09	2955	2955	2955	2955	2955	2955	2955	2955	2955	2955	2955
F10	2957	2957	2957	2957	2957	2957	2957	2957	2985	2985	2985
F11	2958	2958	2958	2958	2958	2958	2958	2958	2910	2910	2910
F12	2959	2959	2959	2959	2959	2959	2959	2959	2959	2959	2959
F13	2960	2960	2960	2960	2960	2960	2960	2960	2960	2960	2960
F14	2962	2962	2962	2962	2962	2962	2962	2962	2962	2962	2962
F15	2964	2964	2964	2964	2964	2964	2964	2964	2964	2964	2964
F16	2965	2965	2965	2965	2965	2965	2965	2965	2965	2965	2965
F17	2968	2968	2968	2968	2968	2968	2968	2968	2984	2984	2984
F18	2969	2969	2969	2969	2969	2969	2969	2969	2969	2969	2969
F19	2970	2970	2970	2970	2970	2970	2970	2970	6925	6925	6925
F20	2971	2971	2971	2971	2971	2971	2971	2971	2971	2971	2971
F21	2974	2974	2974	2974	2974	2974	2974	2974	2974	2974	2974
F22	2975	2975	2975	2975	2975	2975	2975	2975	2975	2975	2975
F23	2976	2976	2976	2976	2976	2976	2976	2976	2941	2941	2941
F24	2977	2977	2977	2977	2977	2977	2977	2977	2977	2977	2977
F25	2979	2979	2979	2979	2979	2979	2979	2979	2979	2979	2979
F26	2983	2983	2983	2983	2983	2983	2983	2983	2983	2983	2983
F27	2984	2984	2984	2984	2984	2984	2984	2984	2968	2968	2968
F28	2985	2985	2985	2985	2985	2985	2985	2985	2957	2957	2957
F29	5198	5198	5198	5198	5198	5198	5198	5198	2913	2913	2913
F30	3513	3513	3513	3513	3513	3513	3513	3513	3513	3513	3513

DATE	07/20/00	09/07/00	09/20/00	01/11/01	02/27/01	03/21/01	04/30/01	07/30/01	07/24/02	11/14/02	07/24/03
MWD	34.849	34.91	34.993	36.593	38.027	38.598	39.084	45.814	67.322	81.288	90.327
G02	3	3	2940	3	2940	3	2940	2940	2940	2940	2940
G03										10810	10810
G04											
G05										10811	10811
G06										10812	10812
G08			2980		2980		2980	2980	2980	2980	2980
G09											
G10											
G11											
G12			2992		2992		2992	2992	2992	2992	2992
G14										10813	10813
G15										10814	10814
G16											
G17										10815	10815
G18			3013		3013		3013	3013	3013	3013	3013
G20			6923		6923		6923	6923	6923	6923	6923
G21											
G22											
G23											
G24			2939		2939		2939	2939	2939	2939	2939
G26										10816	10816
G27								2931	2931	2931	2931
G28											
G29								2943	2943	2943	2943
G30										10817	10817
G32											
G33											
G34											
G35											
G36								5911	5911	5911	5911

DATE	03/19/04	07/29/04	07/18/05	07/11/06	07/19/06	01/25/07	07/25/07	06/19/08	06/25/09	06/29/10	06/29/11
MWD	106.221	106.235	121.931	144.914	145.208	165.506	186.647	205.037	214.051	226.297	236.818
B01	2952	2985	2985	2985	2985	2985	2985	2985	2985	2985	2985
B02	5922	5198	5198	5198	5198	5198	5198	3384	3384	3384	3384
B03	10878	10878	10878	10878	10878	10878	10878	10878	10878	10878	10878
B04	6143	3013	3013	3013	3013	3013	3013	3013	3013	3013	3013
B05	6886	2899	2899	2899	2899	2899	2899	2899	2899	2899	2899
B06	10708	10708	10708	10708	10708	10708	10708	10708	10708	10708	10708
C01	TR	TR	TR	TR	TR	TR	TR	TR	TR	TR	TR
C02	2938	2965	2965	2965	2965	2965	2965	2965	2965	2965	2965
C03	5917	2984	2984	2984	2984	2984	2984	2984	2984	2984	2984
C04	6924	2944	2944	2944	2944	2944	2944	2944	2944	2944	2944
C05	6926	2931	2931	2931	2931	2931	2931	2931	2931	2931	2931
C06	6927	2983	2983	2983	2983	2983	2983	2983	2983	2983	2983
C07	10146	10146	10146	10146	10146	10146	10146	10146	10146	10146	10146
C08	6928	2980	2980	2980	2980	2980	2980	2980	2980	2980	2980
C09	6929	2925	2925	2925	2925	2925	2925	2925	2925	2925	2925
C10	6930	2941	2941	2941	2941	2941	2941	2941	2941	2941	2941
C11	2954	2979	2979	2979	2979	2979	2979	2979	2979	2979	2979
C12	2927	2964	2964	2964	2964	2964	2964	2964	2964	2964	2964
D01	2948	2910	2910	2910	2910	2910	2910	2910	2910	2910	2910
D02	2904	2959	2959	2959	2959	2959	2959	2959	2959	2959	2959
D03	5846	2939	2939	2906	2906	2906	2906	2906	2906	2906	2906
D04	5902	2992	2992	2992	2992	2992	2992	2992	2992	2992	2992
D05	5903	2962	2962	2962	2962	2962	2962	2962	2962	2962	2962
D06	10147	10147	10147	10147	10147	10147	10147	10147	10147	10147	10147
D07	5904	2928	2928	2928	2928	2928	2928	2928	2928	2928	2928
D08	5912	2906	2906	2939	2939	2939	2939	2939	2939	2939	2939
D09	5913	2932	2932	5918	5918	5918	5918	5918	5918	5918	5918
D10	5914	2977	2977	2977	2977	2977	2977	2977	2977	2977	2977
D11	5915	2974	2974	2974	2974	2974	2974	2974	2974	2974	2974
D12	5918	2905	2905	2905	2905	2905	2905	2905	2905	2905	2905
D13	5919	2943	2943	2943	2943	2943	2943	2943	2943	2943	2943
D14	10148	10148	10148	10148	10148	10148	10148	10148	10148	10148	10148
D15	5920	2950	2950	2950	2950	2950	2950	2950	2950	2950	2950
D16	2951	2929	2929	2929	2929	2929	2929	2929	2929	2929	2929
D17		2955	2955	2955	2955	2955	2955	2955	2955	2955	2955
D18	2970	2975	2975	2975	2975	2975	2975	2975	2975	2975	2975
E01	2899	5845	5845	5845	5845	5845	5845	5845	5845	5845	5845
E02	2902	6932	6932	6932	6932	6932	6932	6932	6932	6932	6932
E03	2903	5918	5918	2932	2932	2932	2932			2932	2932
E04	5845	5915	5915	5915	5915	5915	5915			5915	5915
E05	2905	6886	6886	6886	6886	6886	6886	6886	6886	6886	6886
E06	2906	6929	6929	5912	5912	5912	5912	5912	5912	5912	5912
E07	2908	5846	5846	5846	5846	5846	5846	5846	5846	5846	5846
E08	2958	5903	5903	5903	5903	5903	5903	5903	5903	5903	5903
E09	2911	5913	5913	5917	5917	5917	5917	5917	5917	5917	5917

DATE	03/19/04	07/29/04	07/18/05	07/11/06	07/19/06	01/25/07	07/25/07	06/19/08	06/25/09	06/29/10	06/29/11
MWD	106.221	106.235	121.931	144.914	145.208	165.506	186.647	205.037	214.051	226.297	236.818
E10	2912	5912	5912	6929	6929	6929	6929	6929	6929	6929	6929
E11	5198							2932	2932		
E12	2915	6923	6923	6925	6925	6925	6925	6925	6925	6925	6925
E13	2918	5844	5844	5844	5844	5844	5844	5844	5844	5844	5844
E14	2925	6925	6925	6923	6923	6923	6923	6923	6923	6923	6923
E15	6932	5919	5919	5919	5919	5919	5919	5919	5919	5919	5919
E16	2928	5921	5921	5921	5921	5921	5921	5921	5921	5921	5921
E17	2929	6927	6927	6927	6927	6927	6927	6927	6927	6927	6927
E18	2930	5902	5902	5902	5902	5902	5902	5902	5902	5902	5902
E19	2932	5904	5904	5904	5904	5904	5904	5904	5904	5904	5904
E20	2935	6930	6930	6930	6930	6930	6930	6930	6930	6930	6930
E21	5916	6889	6889	6889	6889	6889	6889	6889	6889	6889	6889
E22		5914	5914	5914	5914	5914	5914	5914	5914	5914	5914
E23		6142	6142	6142	6142	6142	6142	6142	6142	6142	6142
E24	2976	6928	6928	6928	6928	6928	6928	6928	6928	6928	6928
F01	2944	10817	10817	10817	10817	10817	10817	10817	10817	10817	10817
F02	2946	5911	5911	5911	5911	5911	5911	5911	5911	5911	5911
F03	2947	2918	2918	2918	2918	2918	2918			3496	3496
F04	5844	5920	5920	5920	5920	5920	5920			3504	3504
F05	2950	10810	10810	10810	10810	10810	10810			3703	3703
F06	6142	10816	10816	10816	10816	10816	10816	10816	10816	10816	10816
F07	5921	2915	2915	2915	2915	2915	2915	2915	2915	2915	2915
F08	6889	2946	2946	2946	2946	2946	2946	2946	2946	2946	2946
F09	2955	6924	6924	6924	6924	6924	6924	6924	6924	6924	6924
F10	2985	10812	10812	10812	10812	10812	10812	10812	10812	10812	10812
F11	2910	10815	10815	2958	2958	2958	2958	2958	2958	2958	2958
F12	2959	5917	5917	5913	5913	5913	5913	5913	5913	5913	5913
F13	2960							5915	5915		
F14	2962							6931	6931		
F15	2964	2912	2912	2902	2902	2902	2902	2902	2902	2902	2902
F16	2965	10813	10813	10813	10813	10813	10813	10813	10813	10813	10813
F17	2984	2902	2902	2912	2912	2912	2912	2912	2912	2912	2912
F18	2969	6143	6143	6143	6143	6143	6143	6143	6143	6143	6143
F19	6925	5916	5916	5916	5916	5916	5916	5916	5916	5916	5916
F20	2971	2940	2940	2940	2940	2940	2940	2940	2940	2940	2940
F21	2974	2971	2971	2971	2971	2971	2971	2971	2971	2971	2971
F22	2975	2969	2969	2969	2969	2969	2969	2969	2969	2969	2969
F23	2941	6926	6926	6926	6926	6926	6926	6926	6926	6926	6926
F24	2977	3513	3513	3513	3513	3513	3513	3513	3513	3513	3513
F25	2979	10811	10811	10811	10811	10811	10811	10811	10811	10811	10811
F26	2983	2960	2960	2960	2960	2960	2960	2960	2960	2960	2960
F27	2968	2947	2947	2947	2947	2947	2947	2947	2947	2947	2947
F28	2957	2911	2911	2911	2911	2911	2911	2911	2911	2911	2911
F29	2913	5922	5922	5922	5922	5922	5922	5922	5922	5922	5922
F30	3513	10814	10814	10814	10814	10814	10814	10814	10814	10814	10814

DATE	03/19/04	07/29/04	07/18/05	07/11/06	07/19/06	01/25/07	07/25/07	06/19/08	06/25/09	06/29/10	06/29/11
MWD	106.221	106.235	121.931	144.914	145.208	165.506	186.647	205.037	214.051	226.297	236.818
G02	2940						10704	10704	10704	10704	10704
G03	10810	2908	2908	2908	2908	2908	2908	2908	2908	2908	2908
G04		2968	2968	2968	2968	2968	2968			3700	3700
G05	10811	2951	2951	2951	2951	2951	2951			6931	6931
G06	10812							5920	5920	5920	5920
G08	2980		10701	10701	10701	10701	10701	10701	10701	10701	10701
G09		2957	2957	2957	2957	2957	2957	2957	2957	2957	2957
G10		2976	2976	2938	2938	2938	2938	2938	2938	2938	2938
G11		2927	2927	2927	2927	2927	2927	2927	2927	2927	2927
G12	2992		10702	10702	10702	10702	10702	10702	10702	10702	10702
G14	10813	2970	2970	2970	2970	2970	2970	2970	2970	2970	2970
G15	10814	2938	2938	2976	2976	2976	2976	2976	2976	2976	2976
G16			3	3	3	3	3	2952	2952	2952	2952
G17	10815	2958	2958	10815	10815	10815	10815	10815	10815	10815	10815
G18	3013	2904	2904	2904	2904	2904	2904	2904	2904	2904	2904
G20	6923	3	3	3	3	3	3	2968	2968	2968	2968
G21		2903	2903	2903	2903	2903	2903	2903	2903	2903	2903
G22		2935	2935	2935	2935	2935	2935	2935	2935	2935	2935
G23		2930	2930	2930	2930	2930	2930	2930	2930	2930	2930
G24	2939	3	3	3	3	3	3	2951	2951	2951	2951
G26	10816	3	3	3	3	3	10699	10699	10699	10699	10699
G27	2931	2948	2948	2948	2948	2948	2948	2948	2948	2948	2948
G28		2913	2913	2913	2913	2913	2913	2913	2913	2913	2913
G29	2943	2954	2954	2954	2954	2954	2954	2954	2954	2954	2954
G30	10817						10700	10700	10700	10700	10700
G32											
G33								2918	2918	2918	2918
G34											
G35								10810	10810	10810	10810
G36	5911						10703	10703	10703	10703	10703

DATE	07/13/12	07/16/13	07/21/14	11/20/15	01/22/16	07/26/16
MWD	260.145	281.566	286.658	298.855	299.868	317.809
B01	2985	2985	2985	2985	2985	2985
B02	3384	3384	3384	3384	3384	3384
B03	10878	10878	10878	10878	10878	10878
B04	3013	3013	3013	3013	3013	3013
B05	2899	2899	2899	2899	2899	2899
B06	10708	10708	10708	10809	10809	10809
C01	TR	TR	TR	TR	TR	TR
C02	2965	2965	2965	2965	2965	2965
C03	2984	2984	2984	2984	2984	2984
C04	2944	2944	2944	2944	2944	2944
C05	2931	2931	2931	2931	2931	2931
C06	2983	2983	2983	2983	2983	2983
C07	10146	10146	10146	10146	10146	10146
C08	2980	2980	2980	2980	2980	2980
C09	2925	2925	2925	2925	2925	2925
C10	2941	2941	2941	2941	2941	2941
C11	2979	2979	2979	2979	2979	2979
C12	2964	2964	2964	2964	2964	2964
D01	2910	2910	2910	2910	2910	2910
D02	2959	2959	2959	2959	2959	2959
D03	2906	2906	2906	2906	2906	2906
D04	2992	2992	2992	2992	2992	2992
D05	2962	2962	2962	2962	2962	2962
D06	10147	10147	10147	10147	10147	10147
D07	2928	2928	2928	2928	2928	2928
D08	2939	2939	2939	2939	2939	2939
D09	5918	5918	5918	5918	5918	5918
D10	2977	2977	2977	2977	2977	2977
D11	2974	2974	2974	2974	2974	2974
D12	2905	2905	2905	2905	2905	2905
D13	2943	2943	2943	2943	2943	2943
D14	10148	10148	10148	10148	10148	10148
D15	2950	2950	2950	2950	2950	2950
D16	2929	2929	2929	2929	2929	2929
D17	2955	2955	2955	2955	2955	2955
D18	2975	2975	2975	2975	2975	2975
E01	5845	5845	5845	5845	5845	5845
E02	6932	6932	6932	6932	6932	6932
E03	2932	2932	2932	2932	2932	2932
E04	5915	5915	5915	5915	5915	5915
E05	6886	6886	6886	6886	6886	6886
E06	5912	5912	5912	5912	5912	5912
E07	5846	5846	5846	5846	5846	5846
E08	5903	5903	5903	5903	5903	5903
E09	5917	5917	5917	5917	5917	5917

DATE	07/13/12	07/16/13	07/21/14	11/20/15	01/22/16	07/26/16
MWD	260.145	281.566	286.658	298.855	299.868	317.809
E10	6929	6929	6929	6929	6929	6929
E11						
E12	6925	6925	6925	6925	6925	6925
E13	5844	5844	5844	5844	5844	5844
E14	6923	6923	6923	6923	6923	6923
E15	5919	5919	5919	5919	5919	5919
E16	5921	5921	5921	5921	5921	5921
E17	6927	6927	6927	6927	6927	6927
E18	5902	5902	5902	5902	5902	5902
E19	5904	5904	5904	5904	5904	5904
E20	6930	6930	6930	6930	6930	6930
E21	6889	6889	6889	6889	6889	6889
E22	5914	5914	5914	5914	5914	5914
E23	6142	6142	6142	6142	6142	6142
E24	6928	6928	6928	6928	6928	6928
F01	10817	10817	10817	10817	10817	10817
F02	5911	5911	5911	5911	5911	5911
F03	3496	3496	3496	3496	3496	3496
F04	3504	3504	3504	3504	3504	3504
F05	3703	3703	3703	6931	6931	6931
F06	10816	10816	10816	10816	10816	10816
F07	2915	2915	2915	2915	2915	2915
F08	2946	2946	2946	2946	2946	2946
F09	6924	6924	6924	6924	6924	6924
F10	10812	10812	10812	10812	10812	10812
F11	2958	2958	2958	2958	2958	2958
F12	5913	5913	5913	5913	5913	5913
F13						
F14						
F15	2902	2902	2902	2902	2902	2902
F16	10813	10813	10813	10813	10813	10813
F17	2912	2912	2912	2912	2912	2912
F18	6143	6143	6143	6143	6143	6143
F19	5916	5916	5916	5916	5916	5916
F20	2940	2940	2940	2940	2940	2940
F21	2971	2971	2971	2971	2971	2971
F22	2969	2969	2969	2969	2969	2969
F23	6926	6926	6926	6926	6926	6926
F24	3513	3513	3513	3513	3513	3513
F25	10811	10811	10811	10811	10811	10811
F26	2960	2960	2960	2960	2960	2960
F27	2947	2947	2947	2947	2947	2947
F28	2911	2911	2911	2911	2911	2911
F29	5922	5922	5922	5922	5922	5922
F30	10814	10814	10814	10814	10814	10814

DATE	07/13/12	07/16/13	07/21/14	11/20/15	01/22/16	07/26/16
MWD	260.145	281.566	286.658	298.855	299.868	317.809
G02	10704	10704	10704	10704	10704	10704
G03	2908	2908	2908	2908	2908	2908
G04	3700	3700	3700	3700	3700	3700
G05	6931	6931	6931	3703	3703	3703
G06	5920	5920	5920	5920	5920	5920
G08	10701	10701	10701	10701	10701	10701
G09	2957	2957	2957	2957	2957	2957
G10	2938	2938	2938	2938	2938	2938
G11	2927	2927	2927	2927	2927	2927
G12	10702	10702	10702	10702	10702	10702
G14	2970	2970	2970	2970	2970	2970
G15	2976	2976	2976	2976	2976	2976
G16	2952	2952	2952	2952	2952	2952
G17	10815	10815	10815	10815	10815	10815
G18	2904	2904	2904	2904	2904	2904
G20	2968	2968	2968	2968	2968	2968
G21	2903	2903	2903	2903	2903	2903
G22	2935	2935	2935	2935	2935	2935
G23	2930	2930	2930	2930	2930	2930
G24	2951	2951	2951	2951	2951	2951
G26	10699	10699	10699	10699	10699	10699
G27	2948	2948	2948	2948	2948	2948
G28	2913	2913	2913	2913	2913	2913
G29	2954	2954	2954	2954	2954	2954
G30	10700	10700	10700	10700	10700	10700
G32						
G33	2918	2918	2918	2918	2918	2918
G34						
G35	10810	10810	10810	10810	10810	10810
G36	10703	10703	10703	10703	10703	10703

THERMAL HYDRAULIC ANALYSIS OF THE UNIVERSITY OF TEXAS (UT) TRIGA REACTOR

1.0 Introduction

This report documents analysis of the thermal hydraulic characteristics of the UTTRIGA in support of renewal of the U.S. Nuclear Regulatory Commission facility operating license.

The UT Austin TRIGA Research Reactor (UTTRIGA) is a TRIGA Mark-II nuclear research reactor licensed to The University of Texas at Austin for operation up to 1.1 MW thermal power level. The geometry of the UTTRIGA core is based on seven concentric hexagons (designated as rings) that fix locations for fuel elements, graphite filled elements, and various experimental facilities. The core is surrounded by a modified cylindrical annulus in an aluminum container filled with graphite (neutron reflector), a rotary specimen rack (RSR), four beam port penetrations, and void spaces accommodating the RSR and beam port facilities. The core and reflector are located in an aluminum tank (pool) filled with high-purity water. The water acts as a neutron moderator, coolant, and radiation shield.

Thermal hydraulic modeling of the UTTRIGA was performed with TRAC/RELAP Advanced Computational Engine (TRACE) and the RELAP5/MOD3.3 (Patch 04) using the Symbolic Nuclear Analysis Program (SNAP) interface[1]. Thermal hydraulic characteristics were developed from classical methods and corrections for UTTRIGA geometry using the computational fluid dynamics code FLUENT. Distribution of fission activity was developed from transport calculations in SCALE, a comprehensive modeling and simulation suite for nuclear safety analysis and design.

The thermal hydraulic codes TRACE and RELAP are designed to perform best-estimate analyses of operational transients and accident scenarios by modeling physical geometry and thermodynamic conditions. TRACE and RELAP were developed for commercial nuclear reactors applications, and RELAP has been widely used in characterizing research reactor thermal hydraulic performance. TRACE is the NRC's flagship thermal-hydraulics analysis tool consolidating and extending the capabilities of NRC's 3 legacy safety codes - TRAC-P, TRAC-B and RELAP. The Symbolic Nuclear Analysis Package (SNAP) is a graphic user interface that standardizes input and interaction for supported analysis codes.

NRC guidance[2] defines a "limiting core configuration" as the core that would yield the highest power density using the fuel specified for the reactor, with all other core configurations demonstrated to be encompassed by safety analysis for the limiting core configuration.

The guidance references an "operational core." Analytical methods used to define the limiting core configuration are applied to the operational core, providing confidence that the model adequately supports limiting core configuration analysis.

2.0 General Description of Heat transfer at the UTTRIGA

Heat is generated in the fuel by the fission process. Cooling is required to maintain fuel temperature low enough to prevent challenges to cladding integrity. The UT TRIGA reactor operates in a natural convection-cooling mode. Heat transfer from fuel to the coolant in the core area is developed by generation of heat in the fission process, conduction of the heat to external surface of the fuel element, and heat transfer by convection from the fuel element surface to water in the core area.

---

[1] http://www.nrc.gov/about-nrc/regulatory/research/safetycodes.html#th (09/26/2014)

[2] NURGE 1537, Guidelines for Preparing and Reviewing Applications for the Licensing of Non-Power Reactors, Format and Content

Temperature increase of the water in the core area develops buoyancy forces that drive flow. The flow is diminished by momentum changes and friction (across the gird plates, fuel element end fittings, and fuel element cladding surfaces). Above a "critical" heat flux, coolant flow will not be adequate to prevent thermal hydraulic conditions from exceeding limits. This analysis demonstrates that operation at the maximum licensed power level has adequate margin to the critical heat flux.

3.0 Power Distribution

The distribution of heat generation across the fuel element sin the core is affected by the core configuration. The amount of heat generated in a specific fuel element can be characterized as a "peaking factor," the ratio of the power produced in that element to average (total heat distributed equally over all fuel elements). A larger number of fuel elements tends to exacerbate the peaking factor of higher power fuel elements. However, the average power per element is reduced by a larger number of fuel elements so that maximum power produced by a fuel element tends to decease. Determining the maximum power produced by a fuel element requires evaluation of peak to average power ratios for the core configuration. Distribution of heat production within a fuel element also varies spatially, affecting the distribution of fuel temperature in the element as well as localized heat transfer.

3.1 General

"Core power" refers to the total power produced by all fuel elements, and "average power" (per element) is the core power distributed uniformly across all fuel elements. The ratio of a specific fuel element power to the average power per element is referred to as core peaking factor. The hot channel is the fuel element producing the maximum power (the fuel element with the largest peaking factor) and the surrounding cooling flow.

The fuel element and cooling channel geometry is reduced for thermal hydraulic calculations to a "unit cell" (repeatable geometry that can be used to replicate the geometry of the fuel in the core). Acceptable thermal hydraulic performance of the UTTRIGA is based on the heat generated in the hot channel.

Neutron flux has a spatial distribution across the core, causing variations in the rate of fission reactions in fuel elements. The variation is influenced by fuel element location, local geometry, and fuel element materials. SCALE transport codes calculate the fraction of total fissions generated in each element, allowing core peaking factors and the fuel element producing the most power to be identified directly.

Neutron flux also varies within fuel elements, creating spatial variations of heat production within the fuel matrix. More discretized fuel element modeling is used in SCALE to calculate the fraction of fissions occurring in segments of the fuel element. Segmentation allows development of a mesh of radial and axial fuel elements to define the heat-generation structure of the unit cell. SCALE reports the fraction of fission occurring in the segments, used to evaluate spatial variation in power production. These 2-dimensional distributions can be used explicitly in TRACE, while RELAP assumes the distribution can be decomposed into independent axial and radial factors. Analysis is core-specific to the extent that the power distribution specified for a specific fuel element varies with core configuration and burnup.

Fuel element material compositions were calculated for each element in neutronic analysis of the UTTRIGA SCALE model. The SCALE calculations used to develop fuel element material inventories are based on uniform fuel composition. However, burned-material and neutron-flux distribution are not independent; since neutron flux varies spatially, the products of neutron reactions are expected to vary. Modeling material variations within a fuel element based on burnup is considered beyond the scope of this analysis. The effects of this assumption are mitigated in thermal hydraulic analyses since maximum fuel burnup is correlated directly to maximum power production; higher burnup regions are likely to have

lower power and lower local temperature compared to calculations with uniform material composition. Fuel in the center an element that has burnup will consequently generate less power in comparison to SCALE calculations that assume uniform material composition. Consequently the effect on fuel temperature calculations is assumed to be conservative, and small.

Similarly, the initial SCALE calculations assumed a uniform fuel temperature for all fuel elements consistent with full power operation. However, fuel temperature and fission rate have feedbacks as elevated temperatures lower the fission cross section. Higher temperatures near the core midplane during reactor operation are likely to reduce the local fission rate. Consequently, the assumption of uniform temperature in calculations is expected to result in higher element peaking factor compared to actual reactor operations. Therefore, the effect on fuel temperature calculations is assumed to be conservative, and small.

Since the core currently in use is substantially different from the initial operational core, both the original core and the current core configurations are considered. In summary, cases are considered for:

- Fresh fuel and the minimum fuel load for criticality and nominal operating fuel temperature
- A limiting core configuration
- The current core configuration

Limiting pool water level (5 meters above the core) and pool water temperature (49 °C) bound the limiting core configuration, while nominal pool water level (6.25 feet above the core) and pool water temperature (~25 °C) apply to the remainder of the analyses.

3.2 Criticality Calculations

SCALE calculations were performed to determine first the minimum number of close packed fuel elements at ambient temperature (293°K) for criticality, and second the minimum number of close packed fuel elements required for operation at an assumed full power operating temperature (600°K). The minimum number of fuel elements required for criticality at power is the lowest number of fuel elements possible for the limiting core configuration. The actual limiting core configuration is selected by calculating margin to thermal limits for the single fuel element generating the highest power. Three assumptions are used to calculate the minimum number of fuel elements required.

(1) Calculations were performed with graphite dummy rods in all positions which do not contain fuel. The introduction of water voids would reduce neutron reflection and require more fuel to achieve the same core reactivity. The distribution of heat generation over a larger number of fuel elements reduces the heat generated in the hot channel, so this assumption is conservative.

(2) Calculations were performed using material specifications for fresh fuel. Since reactor operation reduces fissionable material and introduces fission product poisons into a fuel element, the number of fuel elements required to support full power operations with fresh fuel is the minimum. As the number of fuel elements increases, the distribution of heat generation over more fuel elements reduces the heat generated in the hot channel.

(3) Fuel material specifications are assumed to be the average initial (unirradiated) values of all TRIGA fuel elements possessed under the UTTRIGA reactor license.

Results of reactivity calculations from 40 to 89 fresh fuel elements at ambient (293°K) and an assumed uniform temperature consistent with full power steady stare operations (600°K) are provided in Fig. 3.1, with excess reactivity calculated as:

$$\$_{EX} = \frac{k_{eff} - 1}{k_{eff}} \cdot \frac{1}{\beta} \qquad 3.1$$

Minimum Number of Fuel Elements for Criticality and Operation

As shown in Fig. 3.1, criticality at ambient temperature requires a minimum of 55 fresh fuel elements. The minimum number required for criticality at full power operating temperature is 69 fuel elements. Although a maximum of 78 fuel elements can be loaded in a close packed core with graphite rods in the remaining core spaces and remain within the maximum excess reactivity limits, replacing graphite rods with water voids reduces excess reactivity and allows more fuel to be loaded. Actual loading that meets reactivity limits is determined and validated experimentally.

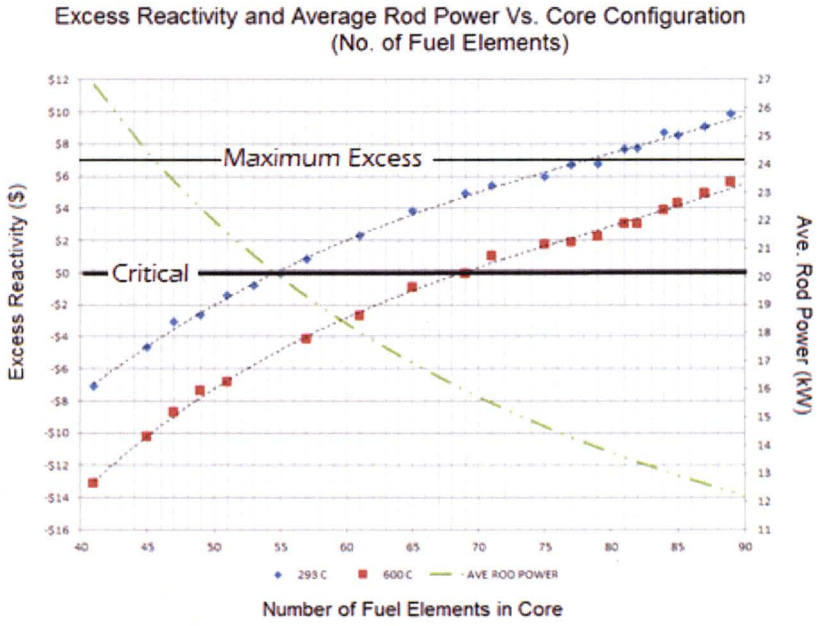

Figure 3.1, Excess Reactivity and Average Rod Power

Hot Channel Selection

Analysis (using SCALE) was performed for core configurations from 69 to 78 to evaluate peaking factors and the heat generated in each B ring element (Table 3.1 and Fig. 3.2) at the nominal core power of 1100 kW. Peaking factors across all the tested configurations varied from 1.41 to 1.53, and power generated in individual B ring elements varied from 20.3 kW to 23.6 kW.

Table 3.1,B Ring Fuel Element Peaking Factors and Power

Position		69	70	71	72	73	74	75	76	77	78
B01	PF	1.467	1.494	1.488	**1.479**	1.506	1.468	1.458	1.474	1.468	1.441
	kW	23.39	23.48	23.05	**22.60**	22.69	21.82	21.38	21.33	20.97	20.32
B02	PF	1.455	**1.499**	1.455	1.462	**1.508**	1.477	1.465	1.484	1.480	1.483
	kW	23.20	**23.56**	22.54	22.34	**22.72**	21.96	21.49	21.48	21.14	20.91
B03	PF	1.458	1.469	1.462	1.462	1.472	1.488	1.490	1.496	1.491	1.512
	kW	23.24	23.08	22.65	22.34	22.18	22.12	21.85	21.65	21.30	21.32
B04	PF	1.465	1.431	1.466	1.481	1.441	**1.518**	**1.510**	**1.516**	**1.515**	**1.532**
	kW	23.36	22.49	22.71	22.63	21.71	**22.56**	**22.15**	**21.94**	**21.64**	**21.61**
B05	PF	1.464	1.413	1.484	1.486	1.420	1.512	1.501	1.505	1.503	1.494
	kW	23.34	22.20	22.99	22.70	21.40	22.48	22.01	21.78	21.47	21.07
B06	PF	**1.473**	1.439	**1.497**	1.494	1.445	1.471	1.464	1.475	1.481	1.453
	kW	**23.48**	22.61	**23.19**	22.83	21.77	21.87	21.47	21.35	21.16	20.49

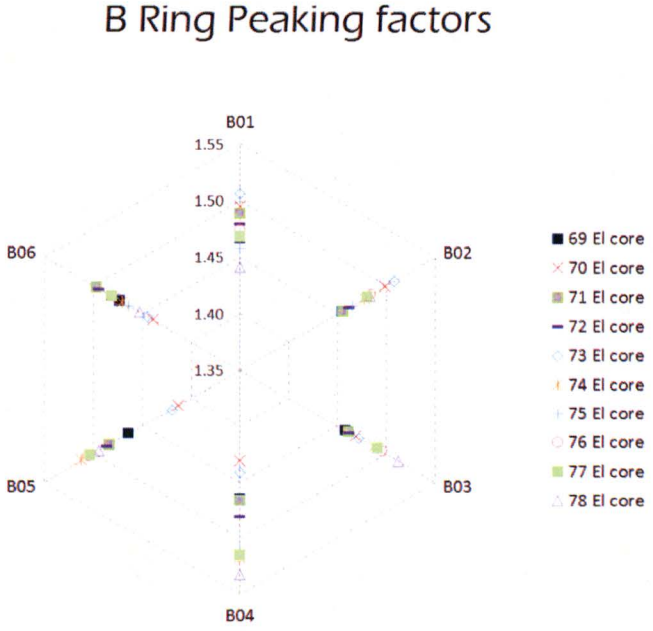

Figure 3.2, B Ring Peaking Factors for Core Configurations

The average fuel element power was calculated distributing 1100 kW over the number of fuel elements in each configuration. The power generated in each B ring element is the product of the applicable peaking factor and the average power (average power, hot channel power, and unit cell power are provided in Fig. 3.3). The 69 and 70 element cores have very similar hot channel characteristics. However, the 69 element core k_{eff} is slightly lower than the average of the 68 and the 70 element cores, and the 70 element core hot channel power (23.55 kW) is slightly higher than the 69 element core hot channel power (23.49 kW). The hot channel power values for the remaining cores demonstrate a definite and decreasing trend in the maximum hot channel power. Therefore the 70 element core is considered the minimum number of elements possible in the limiting core configuration.

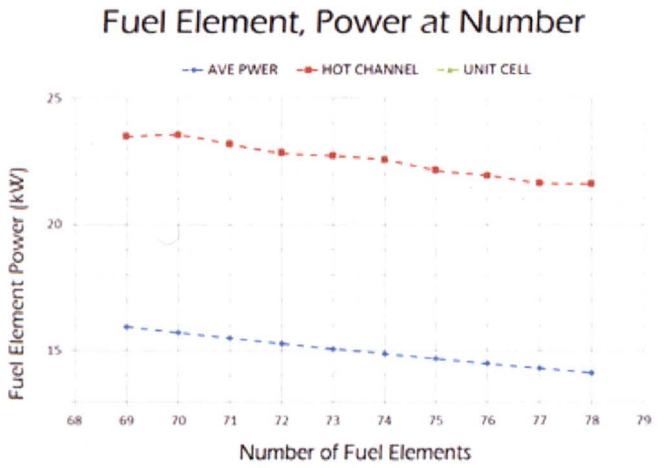

Figure 3.3, Fuel Element Power for Core Configurations

3.3 Power Distribution within Fuel Elements

Interactions in the outer radial segments reduce neutron flux in the inner radial segments of a fuel element, and statistics associated with fission rates near the center of the fuel element are challenging. The Monte Carlo calculations in areas of lower neutron flux in smaller dimensions require a significantly larger number of histories to reduce statistical noise. Consequently the SCALE model modification segmenting the fuel element axially and radially is based on equal volume segments (Table 3.2). Fuel element power distribution is the fraction of power in a specific segment to average fraction of power across 225 equal volume segments. Although fission distributions are calculated for each segment, distributions are provided in this report only for projections (1) near the radial and axial extremes, (2) at the respective centers, and (3) fuel element averages (to reduce complexity).

Table 3.2, Geometry for Fuel Segments

	Axial Segments			Radial Segments		
	z_1	z_2	z_{ave}	r_1	r_2	r_{ave}
1	19.05	16.51	17.78	0.3175	0.5603	0.4389
2	16.51	13.97	15.24	0.5603	0.7260	0.64315
3	13.97	11.43	12.7	0.7260	0.8604	0.7932
4	11.43	8.89	10.16	0.8604	0.9764	0.9184
5	8.89	6.35	7.62	0.9764	1.0801	1.02825
6	6.35	3.81	5.08	1.0801	1.1746	1.12735
7	3.81	1.27	2.54	1.1746	1.2621	1.21835
8	1.27	-1.27	4E-15	1.2621	1.3439	1.303
9	-1.27	-3.81	-2.54	1.3439	1.4210	1.38245
10	-3.81	-6.35	-5.08	1.4210	1.4941	1.45755
11	-6.35	-8.89	-7.62	1.4941	1.5638	1.52895
12	-8.89	-11.43	-10.16	1.5638	1.6306	1.5972
13	-11.43	-13.97	-12.7	1.6306	1.6947	1.66265
14	-13.97	-16.51	-15.24	1.6947	1.7564	1.72555
15	-16.51	-19.05	-17.78	1.7564	1.8161	1.78625

Fission generation data for each segment was used to calculate the fraction of fissions in the fuel element that occurred in each segment. Peaking factors in the axial or radial direction are calculated by normalizing the sum of the fractions on the axis to the average of all summations on the axis.

Fresh Fuel

For the core with the minimum number of fuel elements required for criticality at 293°K (55 elements), the fuel element with the maximum peaking factor occurs in position B03 (Fig. 3.4). Three of the elements in this core required greater precision to differentiate the maximum peaking factor.

		GR	GR	GR	GR	GR				
	GR	GR	GR	GR	GR	GR	GR			
	GR	GR	0.71	0.80	0.86	0.85	0.77	0.66	GR	
	GR	GR	0.77	0.90	0.88	1.04	0.99	0.86	0.70	GR
	GR	GR	0.81	0.97	1.14	1.22	1.20	1.11	0.93	0.73	GR
GR	GR	0.80	0.98	1.19	1.41	1.44	1.31	1.17	0.92	0.72	GR
	GR	GR	0.92	1.00	1.43	CT	1.50	TR	1.12	0.86	GR
GR	GR	0.82	1.02	1.24	1.46	1.49	1.35	1.21	0.96	0.77	GR
	GR	GR	0.86	1.05	1.24	1.33	1.30	1.19	1.00	0.81	GR
	GR	GR	0.87	1.02	1.00	1.19	1.12	0.97	0.81	GR	
	GR	GR	0.80	0.90	0.98	0.95	0.89	0.78	GR		
		GR	GR	0.68	0.74	0.76	0.75	GR	GR		
			GR	GR	GR	GR	GR				

Figure 3.4, Peak to Average Power for 70 Element Core at 293°K

The maximum power in a hot channel occurs in a 70 core, the Limiting Core Configuration. The maximum peaking factor occurs in position B02 (Fig. 3.5).

		GR	H_2O	H_2O	H_2O	GR				
	GR	0.63	0.71	0.75	0.71	0.65	0.58	H_2O		
	GR	0.74	0.82	0.98	0.96	0.94	0.81	0.64	GR	
	GR	0.82	0.93	1.11	1.06	1.17	1.05	0.86	0.68	H_2O
	GR	0.81	1.02	1.19	1.32	1.35	1.27	1.12	0.93	0.74	GR
GR	0.77	0.92	1.22	1.38	1.54	1.49	1.31	1.15	0.84	0.67	GR
0.64	0.87	1.14	1.20	1.57	CT	1.51	TR	1.08	0.75	0.59	
H_2O	0.73	1.00	1.24	1.39	1.55	1.52	1.33	1.17	0.87	0.70	GR
H_2O	0.81	1.07	1.22	1.35	1.37	1.30	1.16	1.00	0.77	H_2O	
H_2O	0.84	1.00	1.14	1.03	1.21	1.11	0.96	0.80	H_2O		
H_2O	0.76	0.89	0.96	1.05	0.94	0.87	0.75	H_2O			
H_2O	H_2O	0.78	0.79	0.80	0.80	H_2O	H_2O				
	H_2O	H_2O	H_2O	H_2O	H_2O						

Figure 3.5, Peak to Average Power for 70 Element Core at 600°K

The SCALE specification for the fuel element in position B02 was modified to determine distribution of power within the fuel element. Selected analysis results for analysis of the 70 element core within B01 are shown in Fig. 3.6 (axial variation) and 3.7 (radial variation).

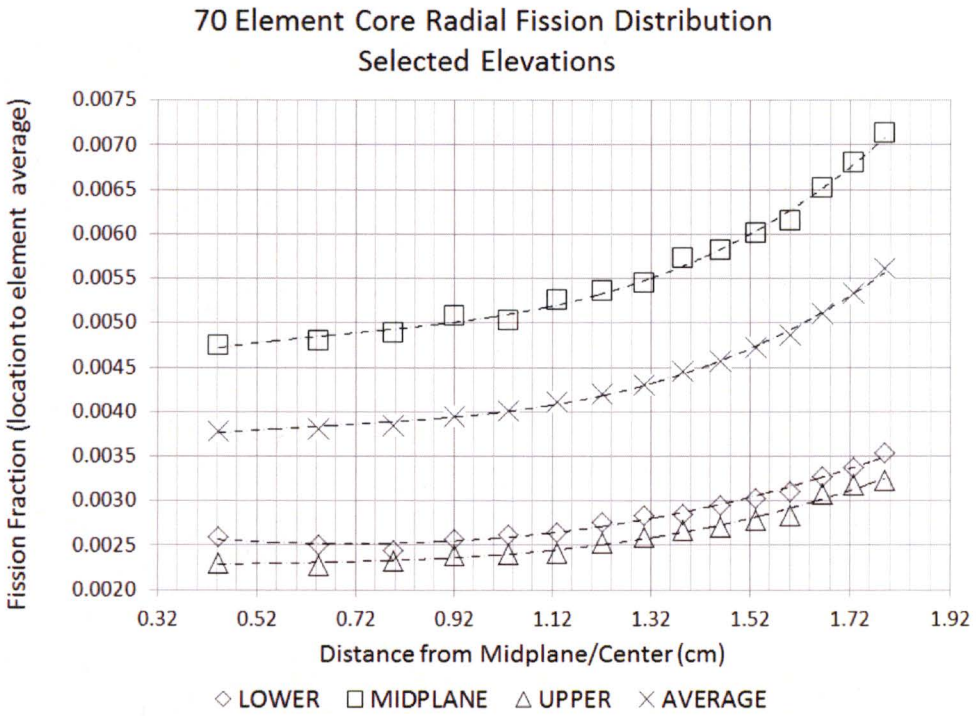

Figure 3.6, 70 Elements 600 °K, B01 Radial Power Distribution (SCALE)

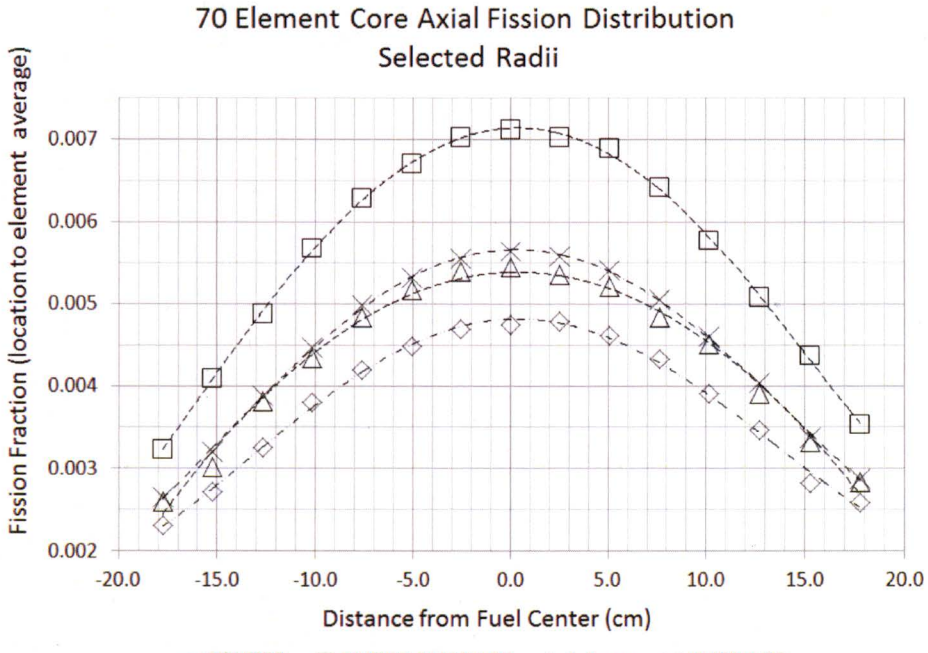

Figure 3.7, 70 Elements 600°K, B01 Axial Power Distribution (SCALE)

Operational Core

The analysis for the core peaking factors of the current 114 element core is provided in in Fig. 3.8. In this analysis, the fuel element in position B02 produces the maximum power. Analyses for axial and radial variations in B04 for the 114 element core are provided in Fig. 3.9 and 3.10.

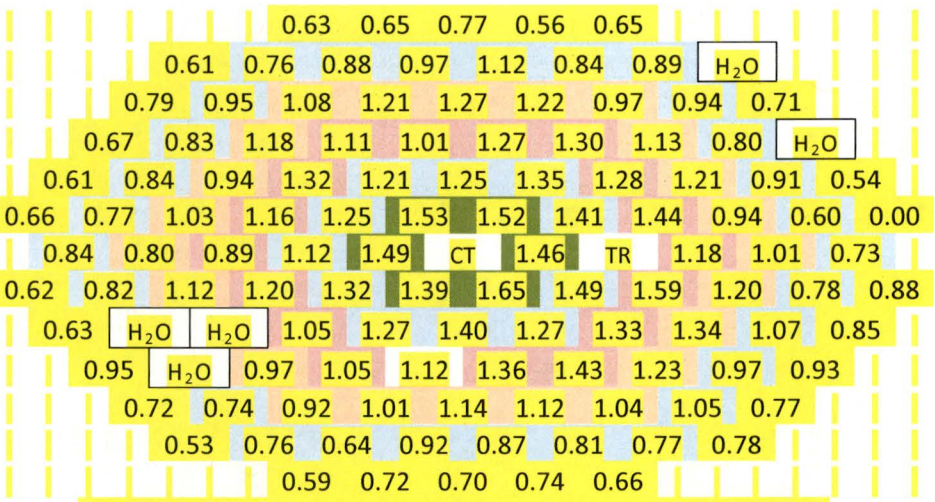

Figure 3.8, Peak to Average Power for 114 Element Core at 600 °K

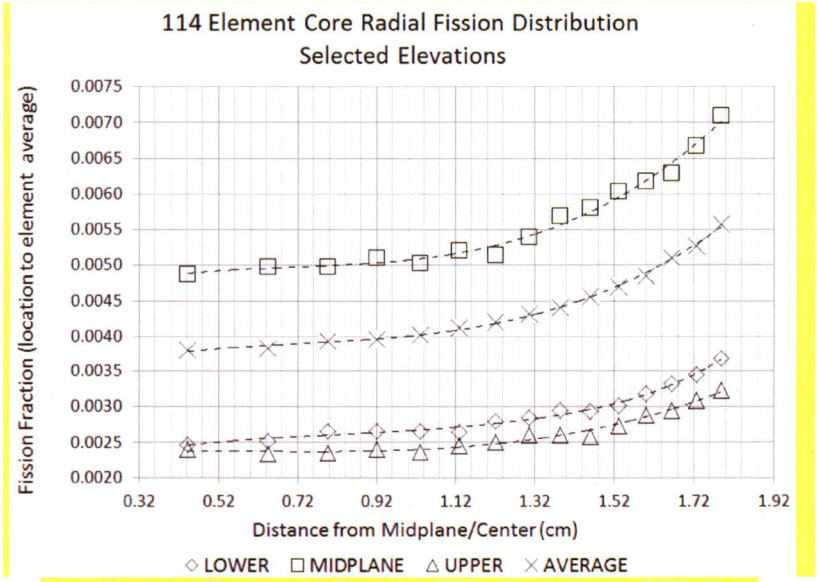

Figure 3.9, 114 Elements 600 °K, B04 Radial Power Distribution

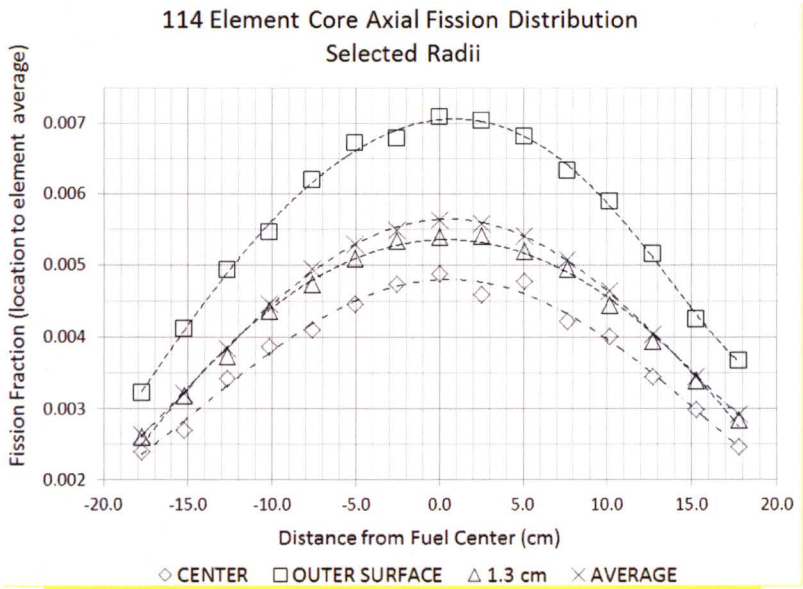

Figure 3.10, 114 Elements 600 °K, B04 Axial Power Distribution

Axial Peaking Factors

Axial peaking factors were developed for cores representing the minimum number of fuel elements required for full power operation, the initial UTTRIGA core, and the current core configuration. While there is some variation in the axial power distribution, the graphical analyses in Figs. 3.7 and 3.9 suggest that axial power distribution for the specified locations is similar regardless of the core configuration. The calculations show that normalized axial power distribution is relatively stable over varying core configurations. Although specific power distributions were used to develop input for thermal hydraulic analysis, it is evident that the effect on axial distribution, and any associated errors, should be insignificant. The major effect on variations in power distribution is on core-wide, fuel-element peaking factors.

Table 3.3, Fuel Element Axial Peaking Factors

Segment	No. of Fuel Elements in Core			AVE	DEV
	70	87	114		
1	0.65	0.63	0.66	0.64	1.83%
2	0.76	0.76	0.78	0.76	1.28%
3	0.91	0.90	0.91	0.91	0.52%
4	1.04	1.04	1.04	1.04	0.27%
5	1.14	1.14	1.14	1.14	0.26%
6	1.22	1.22	1.22	1.22	0.28%
7	1.26	1.27	1.26	1.26	0.40%
8	1.27	1.28	1.27	1.27	0.39%
9	1.25	1.25	1.24	1.25	0.65%
10	1.20	1.20	1.19	1.20	0.30%
11	1.12	1.12	1.11	1.12	0.47%
12	1.01	1.02	1.00	1.01	0.52%
13	0.87	0.87	0.87	0.87	0.36%
14	0.72	0.71	0.72	0.72	0.45%
15	0.60	0.59	0.59	0.59	0.76%

A summary of some important data derived from SCALE calculations is provided in Table 3.4.

Table 3.4, Summary of Significant Parameters

CORE CONFIG.	LCC	Current Core		
No. ELEMENTS	70	114		
k_{eff}	1.00601	1.02048		
Excess ($)	$0.853	$2.867		
PEAKING FACTOR	1.499	1.654	1.387	1.523
POSITION	B02	B02	B03[3]	B06[2]

4.0 Thermal Hydraulic Modeling, Unit Cell Geometry and Thermal Hydraulic Characteristics

The flow channel unit cell cross section is based on the fuel element geometry, as illustrated in Fig. 4.1 (unit cell and the surrounding fuel elements). As illustrated, the unit cell is a fuel element and the surrounding flow area (end fittings have more complex geometry) circumscribed by a hexagon with an inner radius of ½ of the pitch. The cooling flow channel is modeled as a heated pipe with thermodynamic characteristics based on physical dimensions and properties of the coolant around the fuel elements. A large fraction of the unit cell is occupied by the fuel element, leaving a relatively small flow area. The complex geometry of the fuel element end fittings are approximated as hydrodynamic characteristics.

Since a regular hexagon can be decomposed into six equilateral triangles, a triangular unit cell is the smallest possible unit cell. However, RELAP and TRACE heat structures (described in a following section) have limited options for temperature analysis of sold structures; a cylinder can be used to develop a heat source, but a half-cylinder is not possible. This does not limit fluid analysis in thermal hydraulic calculations with a triangular unit cell, but limits the ability to calculate temperatures in the fuel element since the geometry of a triangular unit is ½ of the heat contribution from a single fuel element. Intrinsic properties used to calculate thermal hydraulic conditions are fully represented, but total heat for the cylindrical fuel element (used in material temperature calculations) in a triangular unit cell is not.

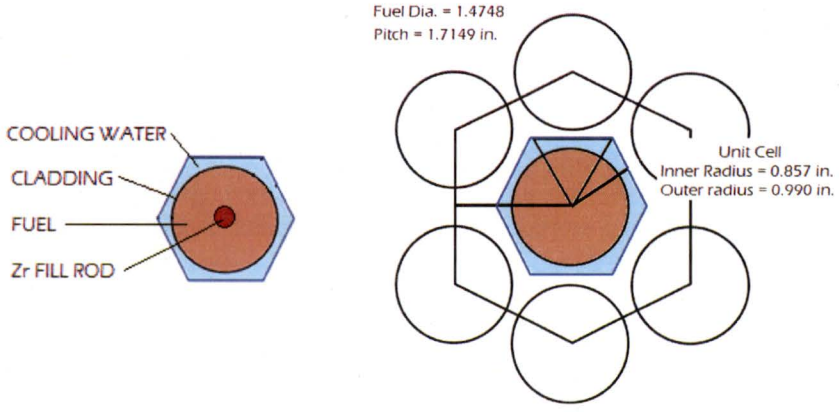

Figure 4.1, Flow Channel for UT TRIGA

The volume of the flow channel is calculated as the product of the flow area and length. The length of the TRIGA flow channel is defined for the heated (adjacent to fuel) and unheated surfaces of fuel element cladding. The heated length is divided into smaller sections for analysis, consistent with the axial segmenting indicated in Table 3.3. The geometries and thermal hydraulic parameters of the upper and

[3] The fuel elements in B03 and B06 are instrumented with thermocouples

lower gird plate/fuel element are calculated through equations 4.1-4.6, with results summarized in Table 4.1.

4.1.1 Unit Cell Geometric Parameters

The area of a regular polygon is calculated using the interior radius (r_i) and perimeter (P) as:

$$A = \frac{1}{2} \cdot r_i \cdot P \qquad 4.1$$

The unit cell is a hexagon (i.e., 6-sided perimeter) with each side one leg of an equilateral triangle; the height of the triangle is the hexagon's interior radius. The hexagon/triangle dimension (a) in terms of the internal radius is calculated:

$$a = \frac{2}{\sqrt{3}} \cdot r_i \qquad 4.2$$

Substituting 4.1 into 4.2, the cross sectional area of the hexagonal unit cell (A_{UC}) using the interior radius is therefore:

$$A_{UC} = \frac{1}{2} \cdot r_i \cdot \left(6 \cdot \frac{2}{\sqrt{3}} \cdot r_i \right) = 2 \cdot \sqrt{3} \cdot r_i^2 \qquad 4.3$$

The inner radius of the unit cell is ½ the distance between two fuel elements or ½ of the fuel element pitch (p_e) so that:

$$A_{UC} = \frac{\sqrt{3}}{2} \cdot p_e^2 \qquad 4.4$$

The cross sectional area of a fuel element (A_F) is calculated:

$$A_F = \pi \cdot \left(\frac{D_F}{2} \right)^2 \qquad 4.5$$

The area of the flow channel in the unit cell (A_{FC}) is the difference between the unit cell area (eq. 4.1) and the area occupied by fuel (eq. 4.2). Since the interior radius is ½ of the pitch, the area of the flow channel is calculated by:

$$A_{FC} = \frac{\sqrt{3}}{2} \cdot p_e^2 - \pi \cdot \left(\frac{D_F}{2} \right)^2 \qquad 4.3$$

Non-circular pipes are approximated as a pipe with an equivalent hydraulic diameter (D_h) with a wetted perimeter (P_W), where the hydraulic diameter is calculated as:

$$D_h = \frac{4 \cdot A_{FC}}{P_W} \qquad 4.5$$

The wetted perimeter is the length of the flow channel in contact with channel wall surfaces (i.e., the perimeter of the fuel element):

$$P_W = \pi \cdot D_F \qquad 4.4$$

Substituting equations 4.3 and 4.4 for flow area and perimeter into equation 4.5, hydraulic diameter is:

$$D_h = \frac{4}{\pi \cdot D_F} \cdot \left[\frac{\sqrt{3}}{2} \cdot p_e^2 - \pi \cdot \left(\frac{D_F}{2} \right)^2 \right] = \frac{2 \cdot \sqrt{3}}{\pi} \cdot \frac{p_e^2}{D_F} - D_F = D_F \cdot \left[\frac{\sqrt{3}}{2} \cdot \frac{p_e^2}{D_F^2} - 1 \right] \qquad 4.5a$$

A summary of primary and calculated parameters is provided in Table 4.1.

Table 4.1, Summary of Principle Thermal Hydraulic Values

Description	Var.	Value							
Fuel Element Pitch	P	1.714	in	0.142833	ft.	4.35356	cm	0.043536	m
Fuel Element Diameter	$Dfuel$	1.4784	in	0.123200	ft.	3.755136	cm	0.037551	m
Wetted Perimeter	P_W	4.64453058	in	0.387044	ft.	11.79711	cm	0.117971	m
Fuel Cross Section/Area	A_{FC}	1.7166185	in^2	0.011921	ft^2	11.07494	cm^2	0.001107	m^2
Unit Cell Area	A_{Cell}	2.54420597	in^2	0.017668	ft^2	16.4142	cm^2	0.001641	m^2
Flow Channel Area	A_{FC}	0.82758747	in^2	0.005747	ft^2	5.339263	cm^2	0.000534	m^2
Hydraulic Diameter	D_h	0.71274154	in.	0.059395	ft.	1.810364	cm	0.018106	m

4.1.2 Unit Cell Thermo Dynamic Loss Factors

Pressure drops (head loss) across hydraulic components are the product of the fluid flow and factors such as the coefficient of friction between the fluid and the pipe wall, changes in flow area and diameter, flow channel surface roughness, and/or flow channel length. Within limits, the factors (K factors) are constant, the sum of the pressure drops in linear flow is additive. This analysis provides a traditional approach to evaluating the loss factors and loss factors reported by analysis and experiments conducted at the UT reactor, followed by the results of analysis and experiments conducted for the UTTRIGA facility.

Traditional Loss Factor Calculations

The impact of sudden expansion or contraction is principally in velocity changes. Bernoulli's equation applied to non-compressible fluids relates area and velocity. The K factors for sudden expansions or contractions are based on the ratio of the flow areas (Equation 7).

$$K_e = \left[1 - \frac{d_1^2}{d_2^2} \right] = \left[1 - \frac{A_1}{A_2} \right] \qquad 4.7$$

Other K factors are based on the magnitude of the direction change, the pipe surface roughness, and flow mode (turbulent, laminar, etc.). Calculations are simplified by using the Darcy-Weisbach friction factor (f) as a multiplier on applicable aspects of system geometry. The friction factor is a function of the Reynolds number, wall surface roughness, and flow channel. The relationship is described in the Colebrook formula:

$$\frac{1}{\sqrt{f}} = -2.0 \cdot \log_{10} \cdot \left(\frac{\varepsilon}{3.7 \cdot D} + \frac{2.51}{\mathrm{Re} \cdot \sqrt{f}} \right) \qquad 4.8$$

In practice, the Moody chart (Fig. 4.2, a parametric representation of the friction factors) is frequently used to determine the friction factor. For reasonable and expected flow rates at the TRIGA reactor, the Reynolds number is between $1X10^4$ and $3X10^5$. Over this range, convergence exists for wall surface roughness values between $5X10^{-7}$ to $1X10^{-3}$. The broad range of surface roughness values indicates a very low sensitivity for roughness, and that any surface roughness within this range can be used without affecting the friction factor significantly. For comparison RELAP analysis conducted for DOW Chemical[4] reactor used surface roughness of 2.13E-6.

For losses in a straight pipe:

$$K = f \cdot \frac{L}{D} \qquad 4.9$$

For a 45° turn:

$$K_{45} = f \cdot 16 \qquad 4.10$$

For a 90° turn:

$$K_{90} = f \cdot 30 \qquad 4.11$$

Table 4.2:

Location	Component	Eff. Area
Bottom Entrance	Lower grid plate	1.2 cm^2
Bottom Exit	Lower End fitting/Channel	3.9 cm^2
Top Entrance	Upper End Fitting/ Channel	3.9 cm^2
Top Exit	Upper Grid Plate	1.2 cm^2

The K factor for elevations above the flow channel is based on a 45° turn out of the main channel (0.344) and sudden contraction at the upper grid plate (0.43). The K factor below the flow channel is based on a sudden expansion exiting the grid plate (0.9) and a 45° turn (0.344) into the main channel. Therefore the K factors are 1.244 at the inlet and 0.844 at the outlet. The results of calculations for K factors associated with the hydraulic parameters in Tables 4.1 and 4.2 and are provided in Table 4.3.

Table 4.3: K factors

Location	Characteristic	K Factor
Inlet	45° Turn[5]	0.344
	Expansion	0.9
	TOTAL lower	1.244
Outlet	45° Turn	0.344
	Contraction	0.43
	TOTAL Upper	0.774

[4] ANALYSIS OF THE THERMAL HYDRAULIC AND REACTIVITY INSERTION BEHAVIOR OF THE DOW TRIGA RESEARCH REACTOR, Submitted to the NRC in support of the DTRR License Renewal (M. H. Hartman, 03/12/2011).

[5] Friction factor times 16

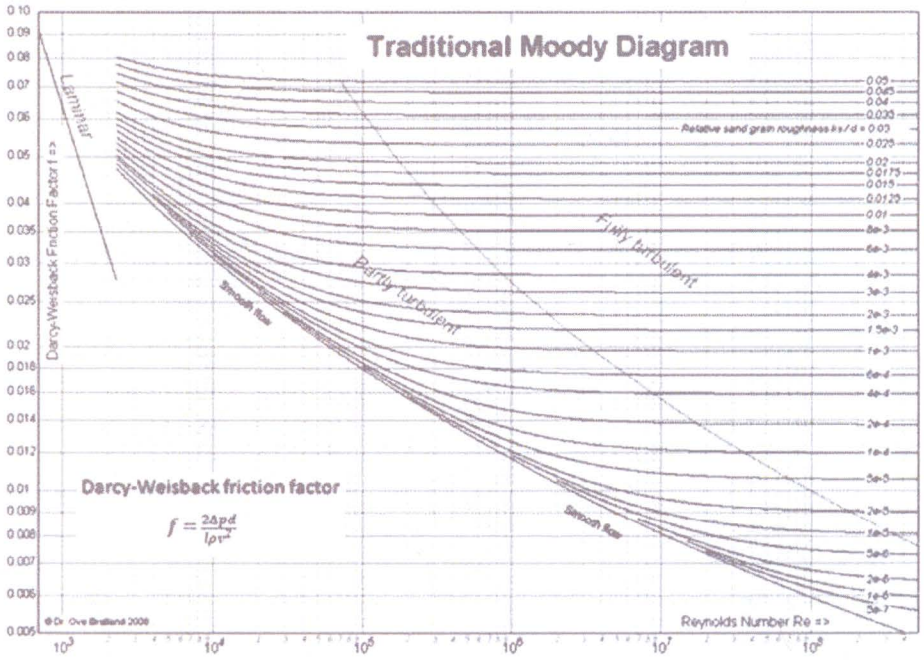

Figure 4.2, Moody Diagram

Correlation of K factors and flow are based on historical, experimental measurements with cylindrical pipes. Additional work validated this approach for rectangular ducts. In practice, non-circular cross sections are reduced to a flow area and hydraulic diameter with the length as measured for the pipe. However, the complexity of the TRIGA inlet and exit flow channel geometry is challenging. As fluid interacts with non-circular structures (or components), non-uniform surfaces can result in forces leading to secondary and/or internal flow paths that affect head loss/pressure drops. This suggests two potential issues using K factors calculated classically in analyzing thermal hydraulic response of the TRIGA reactor.

- The actual entrance and exit to the flow channel between the grid plates is directed by fins mounted on a conical shape that terminates in cylindrical alignment (bottom end fitting) and handling (upper end fitting) structures. The wetted perimeters and flow areas vary continuously from entrance and exit for each end fitting.

- The interface between adjacent fuel channels is not separated by a physical boundary. Differential pressure between adjacent flow channels at interfaces can support cross-channel flow.

Therefore thermal hydraulic analysis to support relicensing was developed[6] to:

(1) Model the UT TRIGA reactor using TRACE

(2) Develop an independent solution tool using MATLAB to calculate thermal hydraulic performance based on mass and energy balance and K factors,

(3) Develop a computational fluid dynamics model using FLUENT, and

(4) Conduct experiments to develop a UT TRIGA specific heat transfer correlation

[6] Development of Thermal Hydraulic Correlations for the University of Texas at Austin TRIGA Reactor Using Computational Fluid Dynamics and In-Core Measurements, A. D. Brand

These methodologies were used to independently model thermal hydraulic performance from (1) first principles, (2) TRACE thermal hydraulics code, and (3) FLUENT computational fluid dynamics code. The results of experiments in the TRIGA core were used to evaluate UTTRIGA-specific K factors based on actual fuel element geometry. A summary of K values determined from both the traditional/classical method and the UT analysis is provided in Table 4.4 with a fractional deviation between factors provided. For comparison, RELAP work[7] performed for DOW Chemical facility used K factors of 2.26 and 0.63 for the lower and upper channels.

Table 4.4, K Factors

APPLICATION	CLASSICAL	FLUENT[8]	DEVIATION
Lower Channel	1.244	1.63	23.7%
Upper Channel	0.844	1.12	33.6%

The values determined from the UT research program were used in modeling for TRACE calculations.

4.2 Physical UTTRIGA Thermal Hydraulic Model

Standard TRACE and RELAP components are structured to simulate physical characteristics of flow loop components. Descriptions of the TRACE and RELAP components required to characterize the UTTRIGA hot channel are provided below, followed by the specific facility application. There are slight differences between some component specifications in TRACE and RELAP, reflected in the descriptions.

4.2.1 Fluid System Component Modeling

TRACE and RELAP analysis is based on modeling a set of representative, defined components where component characteristics are specified by the user to model the system. The UTTRIGA model uses Break (TRACE only), Time-Dependent Volume Components (RELAP only), Pipe, Heat Structure, Power Component (TRACE only), and a Control System/Function (RELAP only). Heat structure material properties are used to calculate temperature distribution for fuel element components (zirconium fill rod, U-ZrH matrix, gas gap, and cladding).

a. Break (TRACE only): A break component is a boundary component normally used to provide a sink for liquid flows exiting the system. TRACE also uses a "Fill" as a similar component for inlet flows, but the fill flow rate is specified by the user while flow rate in a break is developed in calculations, and therefore not constrained. Since flow rates in the UTTRIGA model are developed by convection during reactor operation, the flow rate is not specified as an input. Therefore the use of a fill is precluded and breaks are used to specify both the entrance and exit conditions.

b. Time-Dependent Volume Component (RELAP only): A Time Dependent Volume Component is used in RELAP to model pressure boundaries. For steady state analysis, constant pressure and temperature are simulated by specifying constant values across time intervals.

c. Pipe: The pipe component is a cylindrical volume containing water flow with various geometric and hydrodynamic properties. Analysis of the flow loop requires the flow across changes in elevation balance. Analysis requires limits on the magnitude of changes in adjacent flow areas.

---

[7] ANALYSIS OF THE THERMAL HYDRAULIC AND REACTIVITY INSERTION BEHAVIOR OF THE DOW TRIGA RESEARCH REACTOR, Submitted to the NRC in support of the DTRR License Renewal (M. H. Hartman, 03/12/2011).

d. Heat Structure: TRACE and RELAP define heat structures as rigid components that absorb, transfer, or radiate heat. A heat structure is specified by geometry, inner and outer radial boundary conditions, and material information. These attributes are specified in the "general" section. Power distribution is specified in RELAP within the heat structure, but in the "Power Component" section of TRACE. The power distribution in RELAP is accomplished by independent axial and radial distributions. In RELAP, the control specifying power levels for analysis are provided in the axial cells/boundary conditions section of the heat structure.

   Heat structure cells are axially uniform. Geometry is specified in the "Radial Geometry" section. Geometry includes both radial data which is constant along the axial length of the structure, and axial data that identifies surface areas for heat transfer. Initial conditions for the surfaces at each axial location are specified in "Initial Temperature." The gas gap heat transfer coefficient is explicitly specified the TRACE in the "Gas Gap HTC." Boundary conditions for heat transfer are specified for axial nodes/surfaces, linking the heat source to the heated lengths of the pipe to represent the active (fueled) part of the fuel element.

e. Power Component (TRACE only): The power component specifies how power is provided to the heat structure.

   The shape of power distribution in TRACE is managed by specifying the fraction of power supplied between the inner and outer radial boundaries at each axial node. The "power shape" section of the power component is used to specify a 2 dimensional distribution. The power distribution fractions are specified based on axial and radial locations that segment the fuel element.

   The Numerical solutions to the heat transfer equations are determined iteratively in TRACE. Iterative calculations with large step changes may lead to instability in solutions. A Power Table in the "general" section of the power component allows time based changes to simulate steps in calculation leading to a final power level.

f. Control Systems/General Tables: In RELAP the power levels for analysis are specified as a control in a table, and lined to the table in the heat source section.

g. Materials: TRACE and RELAP have a limited set of material characteristics applicable to nuclear power plants. The default set of materials can be augmented by the user.

   User defined materials are defined either in a data table or a functional fit table. The functional fit is a 5^{th} order polynomial in temperature, although setting the coefficients to 0 can reduce the order of the polynomial. Properties are specified over a range of temperature, and include (1) density, (2) specific heat for TRACE, (3) volumetric heat capacity for RELAP, (3) thermal conductivity, and (4) emissivity.

4.2.2 UTTRIGA Application

TRACE and RELAP components were assembled to model the thermal hydraulic performance of the unit cell flow channel as shown in Fig. 4.3. User supplied values for the source, downcomer, connecting pipe, fuel element, and sink simulate the thermal hydraulic characteristics of the components.

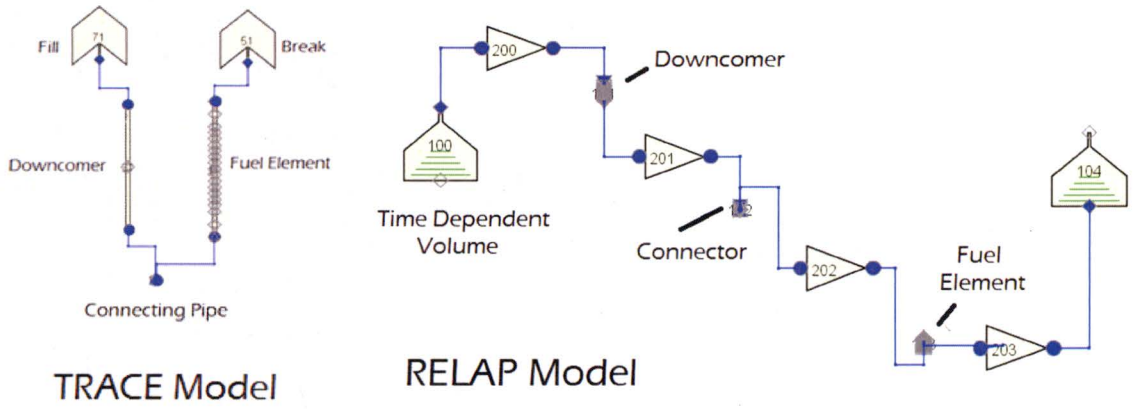

Figure 4.3, TRACE and RELAP Models

a. Break/Time-Dependent Volume (TDV) Components applications:

The TRIGA hot channel pressure and temperature specifications are based on local environmental conditions (barometric pressure, confinement pressure regulation) and the pool (level and water temperature), specified as in the TRACE break component.

The NETL building is approximately 240 m above sea level, corresponding to 96 kPa at standard atmospheric conditions. The reactor bay confinement system is designed to control differential pressure to 0.06 in. (14.9 Pa) below atmospheric (minimal compared to atmospheric pressure). Total pressure at the top of the core is therefore:

$$p_T = 96\{KPa\} + p_{H_2O} \qquad 4.13$$

Pool water is a minimum of 5.25 m above the core, nominally 7.25 m. Constant pressure is established by setting the "rate of change" variable to zero in the break, and with a single value for pressure over RELAP time intervals. Pool water temperature is limited to less than 49 °C, nominally 25-27 °C. Where g denotes the gravitational constant (9.8 m·s^{-2}), the pressure (p_{H2O}) exerted by a column of water (at density ρ in kg·m^{-2}and height h in m) is given by:

$$p_{H_2O} = \rho \cdot g \cdot h \qquad 4.12$$

A second break (TRACE) or TDV (RELAP) is connected to the exit of the core, simulating exit from the flow channel. Parameters associated with the exit are the same as the entrance. Pressure boundary conditions for the limiting and nominal cases are provided in Table 4.5.

Table 4.5, Pressure Boundary Condition

Condition	Temp	Density	Height	Hydrostatic Pressure	Pressure	Pressure
	°C	kg·m^{-2}	m	kPa	kPa	psia
Limiting	49	988.4881	5.25	50.9	146.9	21.3
Nominal	25	997.0479	7.25	70.8	166.8	24.2
	27	996.5162	7.25	70.8	166.8	24.2

b. Pipe applications:

Three pipes are used in modeling. One pipe represents movement of cooling flow from the top to the bottom of the flow channel. A second pipe moves flow to the entrance of the flow channel, connecting the down comer to the third pipe, the flow channel.

Down Comer/Cold Leg

Conservation requirements for calculations require balanced elevation changes, with a "downcomer" at the same length and area as the fuel element region. Instabilities can occur in TRACE calculations if adjacent volumes are sufficiently different, and the downcomer is segmented to meet the ratio criteria (for convenience, segmenting has equal lengths). Dimensions for the down-comer pipe are provided in Table 4.6.

Table 4.6, Down-comer Pipe

Length (segments)	0.09985 m
Length (total)	0.5991 m
Flow area	5.39E-4 m^2
Volume (segments)	5.38E-5 m^3
Volume (total)	3.23E-4 m^3
Hydraulic diameter	0.0183 m
Height Change (segments)	-0.09985 m
Height Change (total)	-0.5991 m

Connector

A pipe with two elbows (Fig. 4.4) connects flow from the downcomer to the unit cell flow channel. Dimensions of the connecting pipe are provided in Table 4.8.

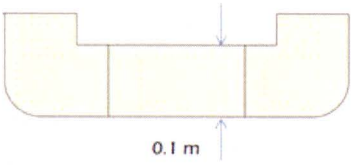

Figure 4.4, Cold Leg to Flow Channel Connector

Table 4.7, Connecting Pipe

SEGMENT	VOLUME	LENGTH	FLOW AREA	HEIGHT CHANGE
	m^3	m	m^2	m
1	5.38E-05	0.01	5.39E-04	-5.0E-3
2	5.38E-05	0.01	5.39E-04	0.0
3	5.38E-05	0.01	5.39E-04	5.0E-3

Unit Cell Flow Channel/Fuel Element Region

The flow channel for the fuel element region in the unit cell is modeled as a pipe. Specifications for the simulated fuel element cooling channel are provided in Table 4.8. Inlet and outlet geometry are reduced to loss factors (previously discussed K). The K factors as previously described are applied to the 2nd and the 19th segments.

Table 4.8, Specifications for Unit Cell Flow Channel

	VOL m^3	LENGTH m	FLOW AREA m^2	Δz m
1	5.14E-06	0.01905	2.70E-04	0.01905
2	2.43E-05	0.09	2.70E-04	0.09
3	6.86E-06	0.0254	2.70E-04	0.0254
4	6.86E-06	0.0254	2.70E-04	0.0254
5	6.86E-06	0.0254	2.70E-04	0.0254
6	6.86E-06	0.0254	2.70E-04	0.0254
7	6.86E-06	0.0254	2.70E-04	0.0254
8	6.86E-06	0.0254	2.70E-04	0.0254
9	6.86E-06	0.0254	2.70E-04	0.0254
10	6.86E-06	0.0254	2.70E-04	0.0254
11	6.86E-06	0.0254	2.70E-04	0.0254
12	6.86E-06	0.0254	2.70E-04	0.0254
13	6.86E-06	0.0254	2.70E-04	0.0254
14	6.86E-06	0.0254	2.70E-04	0.0254
15	6.86E-06	0.0254	2.70E-04	0.0254
16	6.86E-06	0.0254	2.70E-04	0.0254
17	6.86E-06	0.0254	2.70E-04	0.0254
18	2.43E-05	0.09	2.70E-04	0.09
19	5.14E-06	0.01905	2.70E-04	0.01905
Total	1.62E-04	0.5991	5.13E-03	0.5991

c. Heat Structure Application

The heat structure consists of 15 axial cells connected to the heated section of the flow channel (cells 3 through 17 of the unit cell flow channel pipe). "Outer surface boundary" conditions are connected to the unit cell pipe segments, with "Inner Surface Boundary Conditions" of 0.

Heat structure cells simulate the zirc fill rod at the center of the fuel element, ZrH-U fuel, the gap between the fuel and cladding, and the cladding. The UTTRIGA model includes:

- zirconium from a radius of 0 cm to 0.3175 cm (3.175E-3 m)
- zirconium-hydride from a radius of 0.3175 cm to 1.74117 cm (0.0174117 m), subdivided into 15 equal volume segments
- gap gases from a radius of 1.74117 cm to 1.8161 cm (0.018161 m)
- stainless steel 304 cladding from a radius of 1.8161 cm to 1.8263 cm (0.018263 m)

The gas gap heat transfer coefficient[9] of 2840 W m^{-2} K^{-1} is specified in TRACE as "Gas Gap HTC."

Power distribution is accomplished in the heat source geometry. The axial segments are divided radially to provide equal volume segments. As previously discussed, heat generation is distributed in the heat structure based on SCALE transport calculations, based on the fission rate in each segment. Although the SCALE model provides data for each of the 225 segments of the radial and axial boundaries, RELAP uses only a single distribution along each axis. Therefore, the complete distribution is used in TRACE (Power Component section) and the axial and radial averages used in

[9] Reference for the gas gap heat transfer coefficient

RELAP.

d. Power component (TRACE only): Two sections of the power component module are used in the UTTRIGA model, "General," and "Power Shape."

General

Large changes in power can cause instability in calculation; the "Power Table" allows incremental steps at user specified times form a minimum to maximum power, allowing the calculation to stabilize. This function is accomplished in RELAP through a data table in the Control Systems section.

Power Shape

The 2-dimensional fission density profile as described previously is used in the TRACE power shape.

e. Materials: Material data is specified in the Thermal section of TRACE and the RELAP Materials section. A library of reactor material characteristics are provided, but only "gap gases" and "Stainless 304" apply to TRIGA fuel; characterization of ZrH-U fuel and zirconium is required.

The thermal conductivity of TRIGA fuel is noted to be 0.042 $cal \cdot s^{-1} cm^{-1} \cdot °C^{-1}$ (17.573 $W \cdot m^{-1} \cdot °K^{-1}$) [10], insensitive to temperature. The volumetric heat capacity calculated ($C_{,p}$, referenced to temperature T in °C) as:

$$C_{p(U-ZrH,1.6)} = 2.04 + 4.17x10^{-3} \cdot T \left\{ \frac{W \cdot s}{cm^3 \cdot °C} \right\} \qquad 4.14$$

Specific heat capacity is calculated by normalizing the volumetric heat capacity by the density (ρ), with the density of the fuel in the matrix ($\rho_{U\text{-}ZrH1.6}$) calculated as:

$$\rho_{U-ZrH,1.6} \left\{ \frac{g}{cm^3} \right\} = \frac{1}{\frac{w_U}{\rho_U} + \frac{w_{ZrH}}{\rho_{ZrH}}} \qquad 4.15$$

With subscripts indicating Uranium and Zirconium-Hydride, the weight-percent of the components represented as w, the density of $ZrH_{1.6}$ ($\rho_{ZrH1.6}$) is reported as:

$$\rho_{ZrH,1.6} \left\{ \frac{g}{cm^3} \right\} = 0.1706 + 0.0042 \cdot 1.6 = 5.6395 \qquad 4.16$$

Calculations of U-ZrH density and heat capacity (volumetric, $C_{p,v}$ used in RELAP, and specific C_p - as determined by $C_{p,v}$ normalized to the density - used in TRACE) at a wide range of temperatures were performed (Table 4.9).

Thermal conductivity for the zirconium fill rod at the center of the fuel element was taken (even 100 temperature values) from the *Journal of Physical and Chemical reference Data (Volume 3, 1974, Supplement 1, Table 184)*, with intermittent values interpolated. Volumetric heat capacity data was

[10] Simnad, *The U-ZrHx Alloy: Its Properties and Use in TRIGA Fuel* (August 1980)

taken from a compilation[11], with data interpolated by a curve fit. Mass-specific heat capacity used in TRACE is calculated as the ratio of the volumetric heat capacity to the density. Zirconium data is provided in Table 4.9.

Table 4.9, TRIGA Fuel and Zirconium Material Properties

TRIGA Fuel ($ZrH_{1.6}$-U)				Zirconium (Fill Rod)				
T	$C_{p,v}$	ρ	C_p	$C_{p,v}$	ρ	C_p	Conductivity	Emiss.
°K	$J \cdot m^{-3} \cdot K^{-1}$	$kg \cdot m^{-3}$	$W \cdot s \cdot kg^{-1} \cdot K^{-1}$	$J \cdot m^{-3} \cdot K^{-1}$	$kg \cdot m^{-3}$	$W \cdot s \cdot kg^{-1} \cdot K^{-1}$	$W \cdot m^{-1} \cdot K^{-1}$	
200	1.73E+06	6000.507	2.89E+02	1.71E+06	6520	261.7	25.2	0.8
300	2.15E+06	6000.507	3.59E+02	1.76E+06	6520	269.62	22.7	0.8
350	2.36E+06	6000.507	3.93E+02	1.81E+06	6520	276.91	22.1	0.8
400	2.57E+06	6000.507	4.28E+02	1.83E+06	6520	280.56	21.6	0.8
450	2.78E+06	6000.507	4.63E+02	1.85E+06	6520	284.21	21.3	0.8
500	2.99E+06	6000.507	4.98E+02	1.88E+06	6520	287.86	21	0.8
550	3.19E+06	6000.507	5.32E+02	1.90E+06	6520	291.51	20.85	0.8
600	3.40E+06	6000.507	5.67E+02	1.92E+06	6520	295.16	20.7	0.8
650	3.61E+06	6000.507	6.02E+02	1.95E+06	6520	298.81	20.8	0.8
700	3.82E+06	6000.507	6.37E+02	1.97E+06	6520	302.46	20.9	0.8
750	4.03E+06	6000.507	6.71E+02	2.00E+06	6520	306.11	21.25	0.8
800	4.24E+06	6000.507	7.06E+02	2.02E+06	6520	309.76	21.6	0.8
850	4.45E+06	6000.507	7.41E+02	2.04E+06	6520	313.41	22.1	0.8
900	4.65E+06	6000.507	7.76E+02	2.07E+06	6520	317.06	22.6	0.8
950	4.86E+06	6000.507	8.10E+02	2.09E+06	6520	320.7	23.15	0.8
1000	5.07E+06	6000.507	8.45E+02	2.10E+06	6520	322.53	23.43	0.8
1050	5.28E+06	6000.507	8.80E+02	2.11E+06	6520	324.35	23.7	0.8
1100	5.49E+06	6000.507	9.15E+02	2.14E+06	6520	328	24.3	0.8

5.0 Model Validation

Measured fuel temperature channel indications at varying power level are compared to thermocouple location temperatures calculated by RELAP and TRACE. Assumptions used in calculating peaking factors are evaluated. There is no actual measurement of heat fluxes available for comparison with calculations of critical heat flux ratio, CHFR (the ratio of fuel element local heat flux to the heat flux that could result in departure form nucleate boiling). Model validation is supported by comparing results to data associated with accepted reference work.

Instrumented fuel elements (IFEs) are located in the B ring (currently B03 and B06). Three thermocouples are installed in each IFE, although only one thermocouple in each IFE is normally instrumented. The thermocouples are nominally located 0.762 cm from the center of the fuel element, with one installed an inch above the mid-plane, a second at the mid-plane, and a third an inch below the mid-plane. The B03 IFE active thermocouple is labeled as the center position. The B06 IFE active thermocouple is labeled "A", and has been tentatively identified as the upper position.

5.1 Operating Data

Power level, fuel temperature, and control rod position data are routinely recorded in nuclear

[11] http://www.efunda.com

engineering laboratory classes at 20 kW, 60 kW, 100 kW, 500 kW, 750 kW and 950 kW. Data from a 2013 lab class is provided in Table 5.1. Since the pool temperature varies slightly between data points, pool temperature was subtracted from the thermocouple reading for comparisons between observed and calculated temperatures. The values to be compared therefore represent the temperature rise only across the fuel element from the cladding to the thermocouple position. Data obtained confirmatory measurements during the summer of 2014 showed deviation of less than 1% for all values except 100 kW. The deviation at 100 kW was 2% for FT1 and 1.5% for FT2. Based on historical values and confirmatory measurements, temperature response to the heat generated during reactor operation is well characterized by the values in Table 5.1 and Fig. 5.1.

Table 5.1, Operating Data

Core Pwr (kW)	FT1 °C	FT2 °C	Pool °C	B03 ΔT[12] °C	B02 ΔT[1] °C
20	27	32	19	8	13
60	47	60	19	28	41
100	68	86	19	49	67
250	136	171	19.4	117	152
500	221	264	20.7	200	243
750	278	331	23	255	308
950	319	370	23.4	296	347

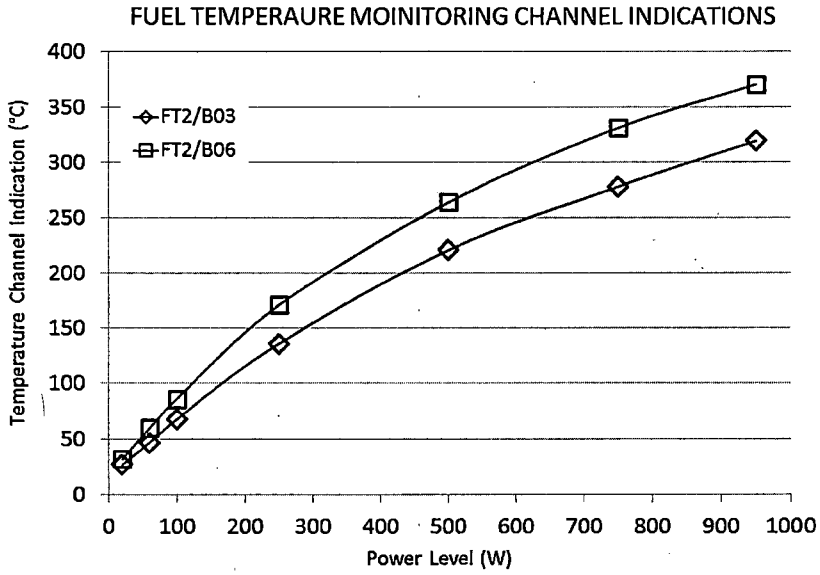

Figure 5.1, Observed Fuel Temperatures During power Operation

Uniform Temperature Assumption

Transport calculations in SCALE calculate the fraction of fissions occurring in each fuel element; this is the basis for core peaking factors used in thermal hydraulic calculations. TRACE and RELAP heat structure temperatures are calculated from material properties, heat generation rate and distribution based on peaking factors, and heat transfer calculations. Initial SCALE calculations assumed a uniform, core-wide fuel temperature.

[12] Difference between thermocouple readings for fuel channel and bulk pool

As previously noted, fuel element temperature affects cross sections used in the transport calculations. Since interaction-rates are reduced at higher temperatures and higher temperatures (such as expected in inner ring elements) initial calculations were assumed to overestimate the power in the B ring elements and inflate peaking factors. Consequently, this assumption is expected to have a conservative effect in fuel temperature and critical heat flux calculations. The conservatism impedes comparison of model results with observed data. It was therefore necessary to develop a more representative fuel element temperature assumption for transport calculations.

Multi-group neutron cross section calculations allow compensation for resonance self-shielding, including temperature effects. (Calculations using continuous energy libraries select cross sections from the library which has a temperature closest to the user specified material temperature.) The cross section processing requires complete definition of the fuel and surrounding environment, including the zirconium fill rod, fuel, gas gap, cladding and the water moderator.

As previously discussed, geometry used in nuclear analysis was specified to provide equal volume segments to mitigate the impact of self-shielding on statistical errors. The geometry of the heat structure in thermal hydraulic analysis was established consistently with the nuclear analysis. The average of the all temperatures in a fuel element (heat structure component) is therefore the volume average temperature of the component. A relationship between fuel element power and temperature was determined from TRACE and RELAP temperature data (Fig. 5.2) at varying power levels. The TRACE calculations indicate slightly higher average temperatures. Power distribution specifications in TRACE are based on a 2-D mesh, while power distribution in RELAP assumes independent radial and axial distributions (which may be a cause for the difference). Since the TRACE mesh is a more precise representation of the power produced in the fuel element, the TRACE fit was used to determine volume average fuel temperatures as a function of fuel element power (Fig. 5.2).

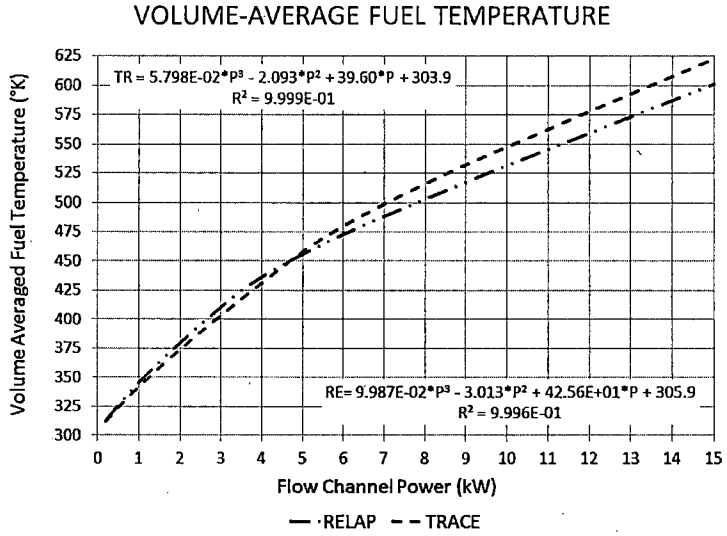

Figure 5.2, Volume-Average Fuel Temperature as a Function of Element Power

Since self-shielding calculations require material compositions from the center of the fuel element to the cooling water boundary, the temperature of each component is also required. However, the temperature calculations are somewhat simplified by comparing the average fuel element temperature to the average component temperature based on the thermal hydraulic calculations.

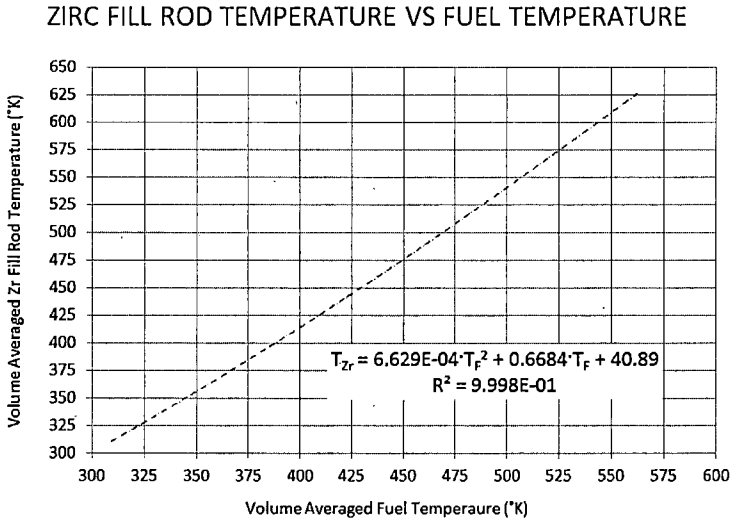

Figure 5.3, Zirconium Fill Rod Volume Average Temperature

Peaking factors were used to determine the power generated in each fuel element for each core power level in Table 5.2. The power generated in each fuel element was used to calculate the average fuel temperatures for each element (Fig. 5.2, TRACE data). The element average temperatures were used to calculate the average temperatures of the zirconium fill rod, gas gap, cladding, and water (Figs. 5.3 and 5.4). The SCALE material statements were modified with temperature data applicable to each fuel element. Calculations in SCALE using the modified temperatures were used to generate new peaking factors. The updated peaking factors were used to re-calculate the power level in each fuel element.

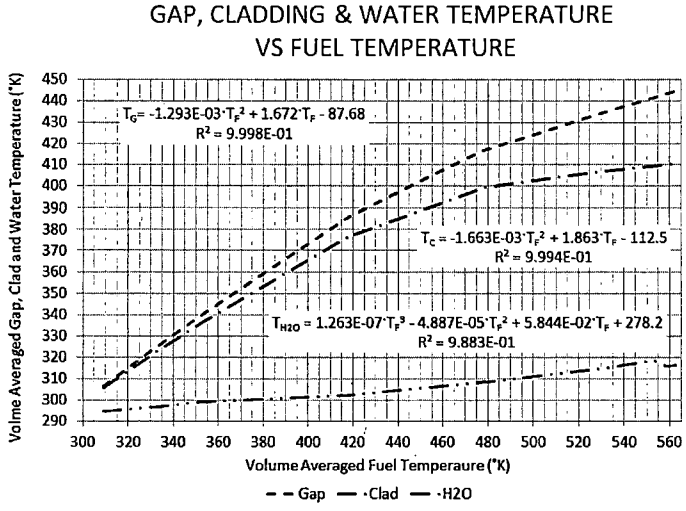

Figure 5.4, Volume Average Fuel Temperatures for Gas Gap, Cladding, and Coolant

The difference (fractional deviation) between successive calculations for each element power was calculated. The standard deviation between all fraction deviations was calculated. This process was iterated until the standard deviation between successive iterations converged, taken as all standard deviations for all power levels less than 1%. An additional iteration was conducted to assure stability.

Peaking factor data associated with the initial calculation and the calculation that approaches stability are provided in Table 5.2 for the instrumented fuel elements (B03 and B06). Core average fuel element and IFE power levels associate with the power levels are provide in Fig. 5.5. Temperature data (minimum, maximum, average and standard deviation across all fuel elements) is provided in Table 5.3.

Table 5.2, Peaking Factors for Hot Channel and Instrumented Fuel Elements

	Power Level:	20 kW	60 kW	100 kW	250 kW	500 kW	750 kW	900 kW	950 kW
B03	Initial	1.480	1.481	1.468	1.471	1.457	1.454	1.454	1.480
	6th Iteration	1.475	1.477	1.473	1.459	1.447	1.437	1.437	1.435
B06	Initial	1.503	1.507	1.490	1.493	1.488	1.475	1.482	1.503
	6th Iteration	1.500	1.510	1.499	1.480	1.473	1.466	1.469	1.456

There is a significant difference between the initial peaking factors based on uniform core fuel temperatures and peaking factors assuming (volume average) fuel temperatures correlated to power level (Table 5.2), even at 20 kW where the element fuel temperature range is small (311 ± 4 °C, with a standard deviation of 2°C). There is a significant difference in peaking factors for each fuel element positon as power increases.

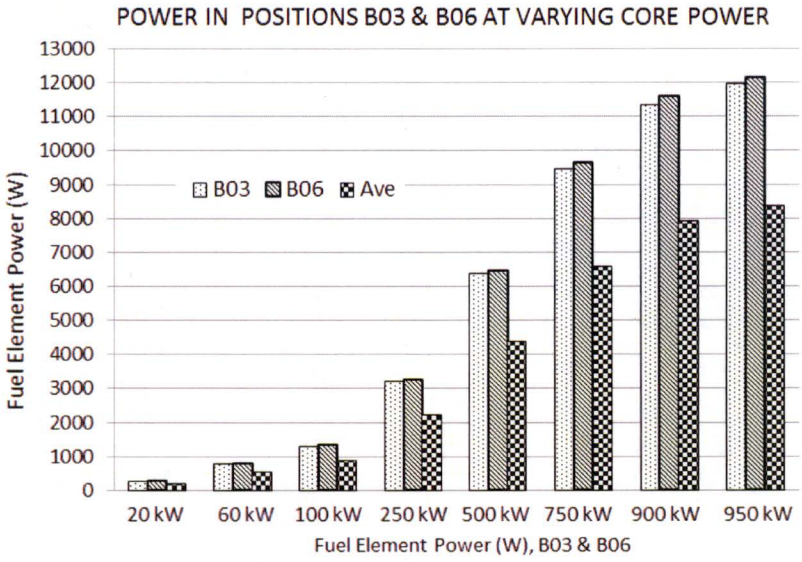

Figure 5.5, Fuel Element Power Generation for Core Average, B03, and B06

Table 5.3, Volume Averaged Fuel Element Temperature Data

Power Level (kW)	20	60	100	250	500	750	900	950
Max Fuel Temp	315	335	354	414	487	538	564	573
Min Fuel Temp	308	316	324	351	393	429	446	452
Core Ave Temp	311	323	336	378	434	478	500	507
Std. Dev.	2	5	8	16	24	28	30	30

Comparison of Observed and Calculated Fuel Temperatures

Observations

Observed temperatures occurred with different pool water temperatures at each power level; therefore observed temperatures were modified by subtracting pool temperature to be comparable to thermal hydraulic calculations.

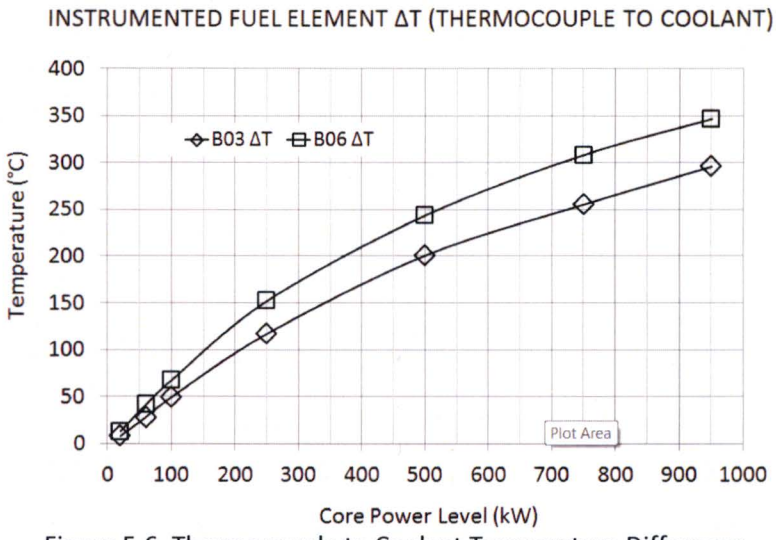

Figure 5.6, Thermocouple to Coolant Temperature Difference

FT-1 and FT-2 Comparisons

The FT-1 fuel element is functioning at some fraction of the power of the FT-2 element based on the peaking factors.

Simplistically, heat transfer (Q) is based on temperature difference (T_{CL} as maximum fuel temperature, T_b as bulk cooling temperature, A as the heat transfer area) driving heat transfer though a system with an overall heat transfer coefficient (h):

$$Q = h \cdot A \cdot (T_{CL} - T_b) \qquad 5.1$$

Factors implicit in the overall heat transfer coefficient are not independent of the magnitude of heat generated; however considering the small differences power between B03 and B06, the overall heat transfer coefficients should be comparable. Where average core power remains constant and the overall heat transfer coefficient is similar, the ratio of the power produced in the two fuel elements with peaking factors PF_{B03} and PF_{B06} is:

$$\frac{PF_{B06}}{PF3} = \frac{(T_{CL} - T_b)_{B03}}{(T_{CL} - T_b)_{B06}} \approx 1.014 \qquad 5.2$$

When the fuel temperature channel data were compared, the ratio of the temperature differences was found to be on the order 1.172 (well above 1.014). The measuring channel behavior response to power was qualitatively similar, indicating the thermocouple was responding, but the FT1/B03 measuring channel indicated much lower than the expected temperature.

Portable thermocouple instrumentation was used during 950 kW operations to measure the temperature of the spare (i.e., not currently monitored by reactor instrumentation) thermocouples. Portable meter indication was less stable than installed console instrumentation, but showed the two functional thermocouples in B06 to agree with a few degrees, consistent with RELAP calculations. The portable instrument indication for the unmonitored thermocouple in the instrumented fuel element of B03 was significantly higher than the installed FT1 channel.

The spare thermocouple was connected to the FT1 fuel temperature channel. The FT1 indication at a 950 kW test operation was 327°C with the original thermocouple, and 343°C with the alternate installed in the

measuring channel.

Since the characteristic response to changes in power level indicated on FT1 and FT2 were qualitatively similar, neither the instrument nor the thermocouple was considered the likely source of the disagreement. If the radial position of the thermocouple previously in the FT1 channel is different than the nominal value, the channel response would be qualitatively similar but biased to the temperature associated with the different positon.

Fuel Temperature Calculations

Thermal hydraulic calculations were performed at fuel element power levels based on the peaking factors in Table5.2. Power generated in the instrumented fuel elements (P_{IFE}) is calculated as the product of the core-wide average generated by all elements ($P_{CORE}/114$) and the peaking factors associated with the instrumented fuel element positions (PF_{IFE}).

$$p_{IFE} = \frac{P_{CORE}}{114} \cdot PF_{IFE} \qquad 5.3$$

The power levels in Table 5.1 were scaled to the peaking factor in table 5.2 to identify power level in table 5.3. RELAP calculations were performed at each of the power levels identified in Table 5.4.

Table 5.4, Power Levels for Calculations

Core Power kW	B03 Power kW	B06 Power kW
20	0.259	0.263
60	0.777	0.795
100	1.292	1.315
250	3.200	3.246
500	6.346	6.461
750	9.454	9.645
900	11.345	11.597
950	11.958	12.133

Calculated temperatures using at 0.726 cm and 0.860 cm from RELAP and TRACE, bracketing the nominal thermocouple position (core midplane, 0.762 cm radially), are provided for B03 and B06 in Tables 5.5 and Table 5.6. A comparison of the results from the two codes is provided in Table 5.7.

Additional data was provided for B03 at locations with calculated temperatures approaching the observed data. As shown in Tables 5.5/5.6 and Fig. 5.7/5.9, the FT1 data is consistent with temperatures displaced from the nominal position. While it is not possible to definitively prove the source of the anomalous thermocouple data, Fig. 5.7/5.9 suggests a reasonable correlation for data farther from the centerline than the nominal thermocouple position.

Figs. 5.8/5.10 show clearly that calculated temperatures for B06 in locations adjacent to the FT2 thermocouple are in close agreement with observed data, with some deviation at higher power levels. Polynomial interpolation of all calculated fuel temperatures from the inner surface to the outer surface was used to generate temperature data at 0.762 cm (the nominal thermocouple position), with the data compared to observed data in Table 5.6/5.7.

Table 5.5, Observed and Calculated (RELAP) Temperature Data

CORE POWER kW	FT1 °C	B03 0.726 °C	0.860 °C	1.175 °C	1.262 °C	1.344 °C	FT2 °C	B06 0.726 °C	0.860 °C	0.762 °C	ΔT °C
20	8	20	20	19	19	18	13	20	20	20	-7
60	28	49	48	46	45	44	41	50	49	50	-9
100	49	75	73	69	68	66	67	76	74	75	-8
250	117	159	156	146	142	138	152	160	157	160	-8
500	200	239	233	213	206	198	243	242	235	240	3
750	255	312	303	273	262	251	308	316	307	314	-6
950	296	355	344	308	296	283	347	374	362	371	-24

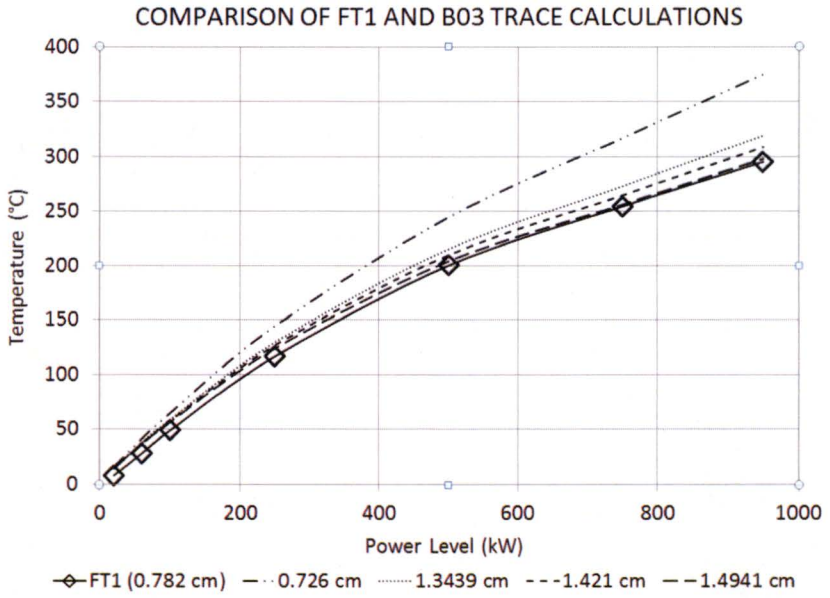

Figure 5.7, Comparison of FT1 Response and B03 RELAP Calculations at Applicable Locations

The FT-2 data is remarkably consistent with calculated temperatures, with some divergence at higher power (Fig. 5.8 and 5.10). There is strong correlation between observed and calculated fuel temperatures for FT-2 (B03) up to about 750 kW, with only minor deviation at lower power. At power levels above 750 kW the divergence between calculation and observation become more significant, although calculations give conservative values (i.e., higher temperatures).

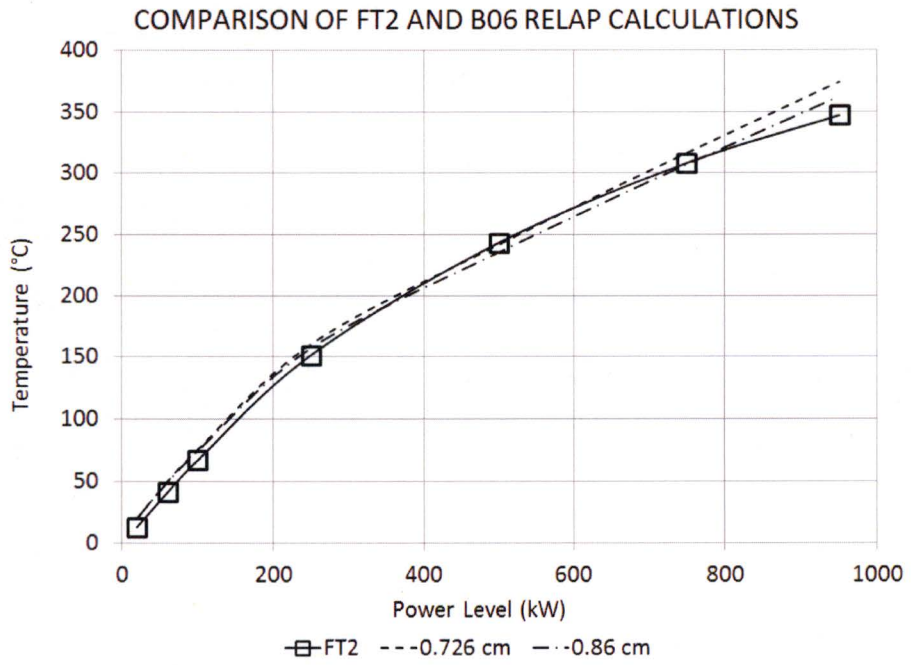

Figure 5.8, Comparison of FT2 Response and B06 RELAP Calculations at Applicable Locations

As previously noted, flow channels are not well isolated from adjacent flow channels. Significantly different hydrostatic or hydrodynamic conditions at the boundary could interact to affect flow rates in modes not characterized by this analysis. Flow and local pressures calculated by RELAP and TRACE at power levels associated with adjacent fuel elements are not significantly different from values for B03 and B06.

The onset of nucleate boiling occurs in circular TRIGA cores as low as 210 kW[13]. Subcooled nucleate boiling effects are extremely short range and do not survive distance required to exit the flow channel. During full power operations, there is frequently a vigorous stream of bubbles entrained in coolant flow from the core to the pool surface, not nucleate boiling.

Nitrogen solubility decreases as depth and temperature increase[14]. The change in depth as water passes through the core causes a decrease of approximately 6% in nitrogen gas solubility. At 750 kW, maximum water temperature is calculated to increase from ambient to 15 °C, resulting in an additional 41% decrease in solubility as cooling water passes through the hot channel. With a nearly 50% decrease in nitrogen gas solubility occurring over 38.1 cm of heated water, some nitrogen degassing is expected. Nucleate boiling from the fuel element surfaces could provide nucleation sites for evolution of nitrogen bubbles.

These effects are not modeled, but could contribute to a complex flow with additional mixing action. Potential for these mixing effects is minimized at the low water temperature changes associated with low power levels. Higher flow associated with better mixing would cause lower fuel temperatures in

---

[13] *Thermohydraulics Analysis of the University of Utah TRIGA Reactor of Higher Power Designs,* P.M. Babitz, University of Utah, December 2012

[14] EIFAC. 1986. Report of the working group on terminology, format and units of measurement as related to flow-through and recirculation system. European Inland Fisheries Advisory commission. Tech. Pap., 49. 100 pp. & Multiphase Flow Dynamics. http://dx.doi.org/10.1007/978-3-642-20749-5_11 Springer Berlin Heidelberg 2012-01-01 A Kolev, Nikolaylvanov P 209-239

the B ring fuel elements as local water temperatures increase and affect nitrogen solubility. This mechanism is consistent with the observed deviation between fuel temperature measuring channels and thermal hydraulic calculations that occurs at power levels greater than about 750 kW.

Table 5.6, Observed and Calculated (TRACE) Temperature Data

CORE	FT1	B03					FT2	B06			
POWER	°C	0.726	0.860	1.175	1.262	1.344	°C	0.726	0.860	0.762	ΔT
kW		°C	°C	°C	°C	°C		°C	°C	°C	°C
20	8	20	20	15	15	15	13	16	16	20	-7
60	28	49	48	39	39	38	41	42	42	50	-9
100	49	75	73	61	60	59	67	66	65	75	-8
250	117	159	156	135	132	130	152	146	144	160	-8
500	200	239	233	226	221	215	243	248	243	240	3
750	255	312	303	289	281	273	308	322	315	314	-6
950	296	370	358	340	330	319	347	379	371	371	-24

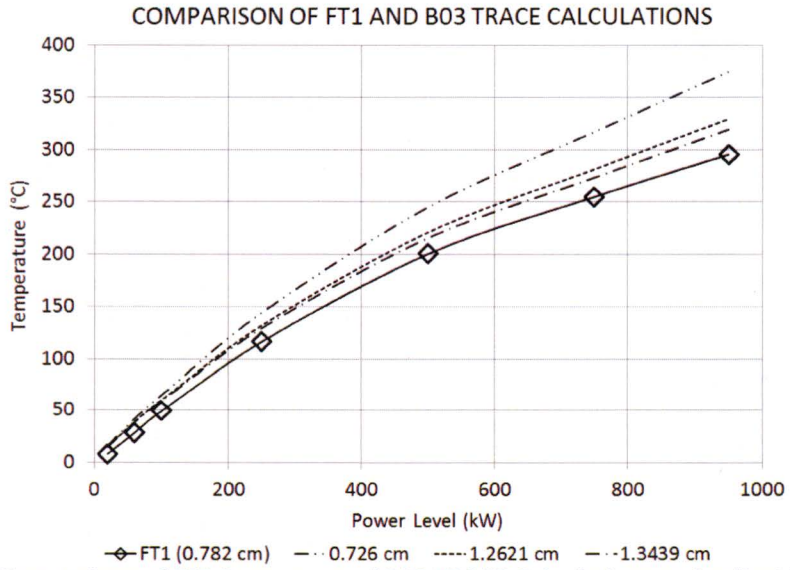

Figure 5.9, Comparison of FT1 Response and B03 TRACE Calculations at Applicable Locations

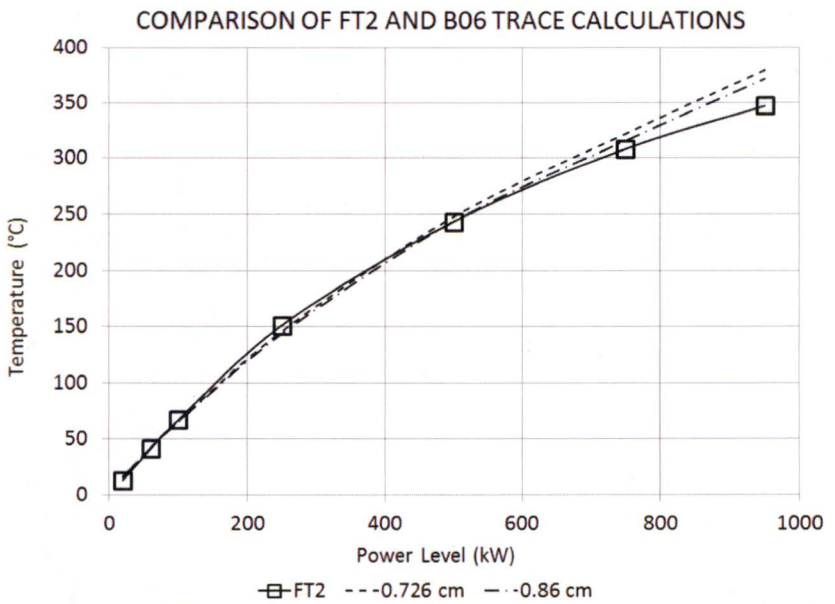

Figure 5.10, Comparison of FT2 Response and B06 TRACE Calculations at Applicable Locations

The temperature values calculated by TRACE and RELAP are in good agreement near the center of the fuel element, with difference increasing at increased radial positons. Although the calculated results corresponding for FT2 are nearly identical for both TRACE and RELAP, agreement with FT1 at possible altered thermocouple locations is not as good. Using RELAP data, the thermocouple may be close to 1.344 cm radial position; using TRACE data, the thermocouple may be 1.49 cm radial positon.

However, there is also axial variation in fuel temperatures and considering only the radial displacement neglects the angle of the thermocouple penetration in the fuel meat. The correlation of radial positon based on temperature is not rigorous. Given variations in RELAP and TRACE temperature calculations and the angle, it is difficult to infer thermocouple location with any certainty.

Table 5.7, Comparison B03 RELAP and TRACE Calculations (ΔT, °C)

Core Power (kW)	B03							B03	
	0.726 cm	0.860 cm	1.1746 cm	1.2621 cm	1.3439 cm	1.421 cm	1.4941 cm	0.726 cm	0.860 cm
20	-4	-4	-4	-4	-4	-4	-3	-4	-4
60	-8	-7	-7	-6	-6	-6	-6	-8	-7
100	-10	-9	-8	-8	-7	-7	-7	-10	-9
250	-14	-13	-11	-10	-9	-8	-7	-14	-13
500	6	8	14	15	17	19	21	6	8
750	5	8	17	19	22	25	27	5	8
950	5	9	20	23	26	30	33	5	9

Summary

The comparison of TRACE and RELAP temperature calculations to installed fuel temperature measuring channels gives confidence that the models predict reasonably accurate values for fuel temperature

calculations. The calculations are less accurate but conservative at power levels exceeding about 750 kW. Fuel temperature calculations simplified by assuming a single uniform core wide temperature are less accurate, but conservative as the use of peaking factors that incorporate individual average fuel element temperatures reduce differences between observed and calculated temperature.

5.2 Comparison to Comparable Thermal Hydraulic Analysis

Benchmark data is not available to validate the use of RELAP and TRACE for thermal hydraulic analysis, except to the extent that the model is capable of predicting fuel temperature where the fuel element is cooled by water flow. Nevertheless, RELAP has a long history in analysis of TRIGA systems, and TRACE is the current platform endorsed by NRC (incorporating RELAP and TRAC codes). A comprehensive review of methods for predicting power at which critical heat flux occurs in TRIGA fuel is documented in ANL/RERTR/TM-07-01[15]; the report provides thermal hydraulic data for comparing the UTTRIGA to a generic hexagonal TRIGA core. The ANL report did not use TRACE:

- Mass flow rates calculated by the UTTRIGA model using RELAP and TRACE are compared to the reference document values.

- Axial distribution of critical heat flux ratios from the UTRRIGA model using RELAP is compared to the reference document values; the reference document uses a total heat generation of 30 kW and the TRACE model will not execute successfully at 30 kW.

TRACE calculations greater than 25 kW exhibited some vapor generation indicating localized boiling at the upper elevations of the fuel channel; the vapor was condensed prior to channel exit, with residual vapor in the 29000 W case surviving the heated length. The 30 kW case failed execution.

RELAP calculations indicate vapor generation at power levels at 19 kW and above. Vapor was principally reduced prior to channel exit, with some residual. The void fractions were substantially smaller than those calculated by TRACE.

Coolant Flow Rates/Outlet Coolant Temperatures

Data from ANL/RERTR/TM-07-01 (Fig. 4 and 5) for mass flow rate and outlet cooling water temperature is used as reference for comparison of values calculated with the UTTRIGA RELAP and TRACE models. The UTTRIGA cooling water inlet was assumed to be 30 °C for consistent with reference-data inlet cooling water temperature for comparison. Power levels considered in the reference extend considerably higher than the benchmark data used in temperature comparisons.

Calculated TRACE UTTRIGA model flow rates were higher than both UTTRIGA RELAP and reference RELAP calculations (Fig. 5.11). The difference in flows has a direct impact on temperatures, but as previously noted, the mass flow and coolant outlet temperatures for the UTTRIGA models results in values reasonably close to the reference.

[15] ANL/RERTR/TM-07-01, Fundamental Approach to TRIGA Steady-State Thermal-Hydraulic CHF Analysis (E.E. Feldman, Nuclear Engineering Division, Argonne National Laboratory) 2007

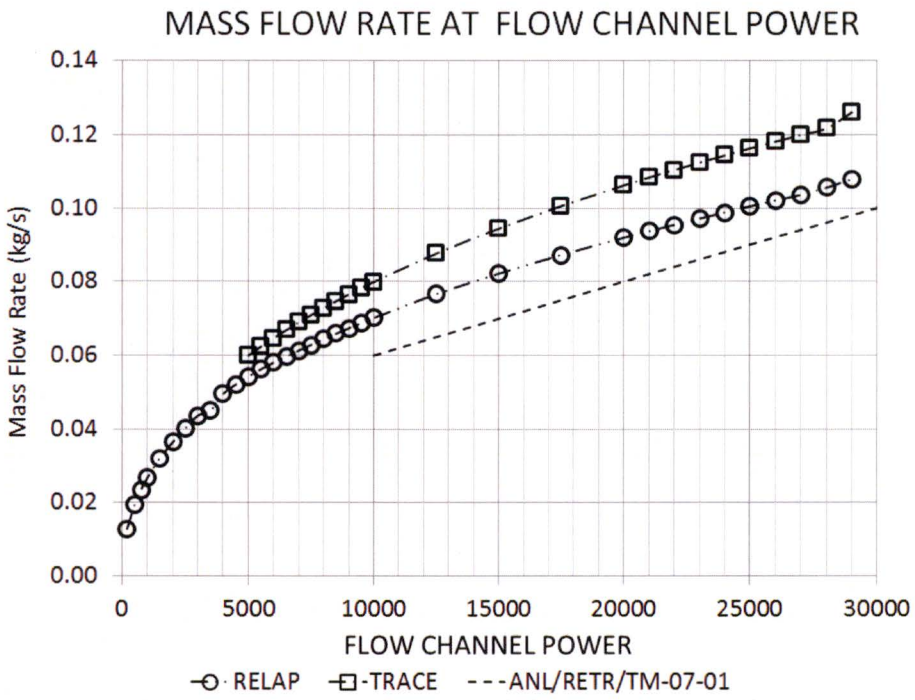

Figure 5.11, Comparison of Calculated Flow Rates for UTTRIGA and Reference Calculation

Critical Heat Flux Ratio

Critical heat flux ratio (CHFR) is the ratio of the critical heat flux (CHF) to the actual heat flux. The ANL/RERTR/TM-07-01 reference provides a series of calculations with different correlations for critical heat flux, including the Bernath correlation. The correlation for critical heat flux developed by Bernath is recommended by the reference in evaluating TRIGA fuel performance. The Bernath correlation (where CHF_{BO} is the heat flux that results in burnout h_{BO} is the convection heat transfer correlation at burnout, $T_{W,BO}$ is the temperature of the cladding surface at burnout, and V is the fluid velocity, T_b is the cooling water bulk temperature, and dimensional variables as described in Table 4.2) determines the critical heat flux that results in burnout as:

$$CHF_{BO} = h_{BO} \cdot \left(T_{W,BO} - T_b\right) \tag{5.4}$$

Where the heat transfer coefficient for burnout conditions is calculated:

$$h_{BO} = 10890 \cdot \frac{D_e}{D_e + D_i} + V \cdot \frac{48}{D_e^{0.6}} \tag{5.5}$$

The formula predicting wall temperature at burnout is:

$$T_{W,BO} = 57 \cdot \ln P - 54 \cdot \frac{P}{P+15} - \frac{V}{4} \tag{5.6}$$

Substituting equations 14 and 15 into equation 13 results in:

$$CHF_{BO} = \left[10890 \cdot \frac{D_e}{D_e + D_i} + V \cdot \frac{48}{D_e^{0.6}}\right] \cdot \left(\left[57 \cdot \ln P - 54 \cdot \frac{P}{P+15} - \frac{V}{4}\right] - T_b\right) \qquad 5.7$$

The Bernath formulation is in "pound centigrade units," converted to BTU h^{-1} ft^{-2} by a factor of 1.8.

$$W_{CHF} = 1.8 \cdot \left[10890 \cdot \frac{D_e}{D_e + D_i} + V \cdot \frac{48}{D_e^{0.6}}\right] \cdot \left(\left[57 \cdot \ln P - 54 \cdot \frac{P}{P+15} - \frac{V}{4}\right] - T_b\right) \qquad 5.8$$

The results of calculations of CHFR from the reference document at 30 kW and as determined by RELAP for 28 and 29 kW shows reasonable agreement, with a shift in the location of the minimum CHFR possibly because of the higher flow rates calculated for the UTTRIGA model.

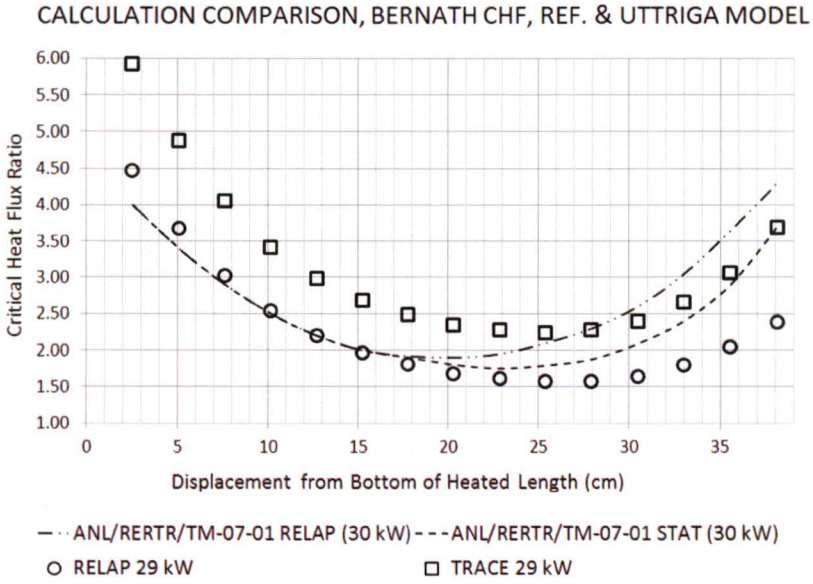

Figure 5.12, Comparison CHFR for Reference and UTTRIGA Model

CHFR values were calculated at a range of power levels for the UTTRIGA model using RELAP and TRACE. Although the values show some difference at low power levels, there is convergence at high power levels (Fig. 5.13).

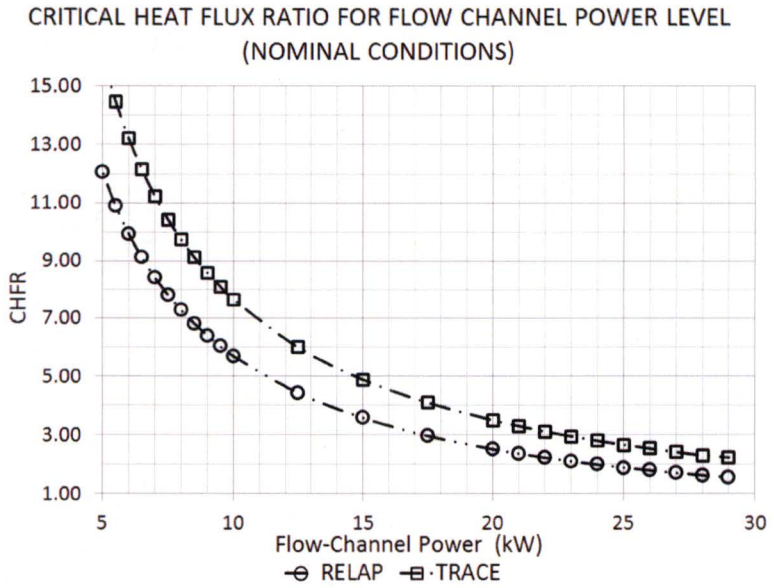

Figure 5.13, CHFR Response to Flow-Channel Power

Summary

The UTTRIGA model shows results similar to the reference in the comparison of the reference values to the UTTRIGA model, providing confidence that the UTTRIGA model provides reasonable results in thermal hydraulic calculations.

6.0 Results

A limiting case and a nominal case were defined for analysis of the fuel element producing the maximum power in the core, based on Technical Specifications and normal operating conditions in Table 6.1. The maximum peaking factor was calculated as a function of the number of fuel elements for the licensed power limit with the maximum power level measuring channel error.

Calculations of temperature across the fuel element were performed by TRACE and RELAP using hot channel analysis. The results of temperature calculations are used to demonstrate that the fuel temperature measuring channels with protective action at 550 °C are capable of limiting the maximum hot channel fuel temperature less than 830 °C. The results of thermodynamic analysis for the hot channel were used in the Bernath correlation to demonstrate that the heat flux for the limiting and nominal cases will not result in departure from nucleate boiling for the hot channel.

UTTRIGA Core Analysis

Maximum Fuel Element Peaking Factor

Independent calculations were performed with the UTTRIGA SCALE and MCNP models using close packed core configurations ranging from 75 to 119 fuel elements with an assumed uniform 600°K core temperature. The MCNP library cross section data was at 587°K, comparable to the 600°K data in the SCALE library. The SCALE/KENO fission density and an MCNP fission tally provided data used to calculate core peaking factors. The maximum B ring peaking factor was calculated for each core (Table 6.1).

The calculations agree reasonably well, although peaking factors based on the MCNP model are slightly

higher; since the fission rate is temperature sensitive and the MCNP library is based on cross sections at a higher temperature, some difference is expected. Water filled voids result in a higher peaking factor than cores using graphite rods in non-fuel spaces, as expected.

Table 6.1, Peaking Factors from MCP and TRACE for Graphite or Water Void Spacers

No. Elements	75	77	83	86	89	95	111	117	119
MCNP									
H2O	1.648	1.654	1.670	1.673	1.690	1.701	1.761	1.773	1.773
Graphite	1.605	1.611	1.638	1.634	1.657	1.676	1.743	1.768	1.773
SCALE									
H2O	1.607	1.607	1.618	1.626	1.631	1.649	1.667	1.661	1.656
Graphite	1.531	1.545	1.559	1.568	1.575	1.597	1.657	1.635	1.656

The active core has a water filled boundary until fuel is introduced into the outer ring. Since the outer ring is bounded by the graphite reflector which does not have the water component of a fuel channel filled with a graphite rod, peaking factors begin to converge cores as the outer ring is filled. The SCALE and MCNP data indicates convergence, but less pronounced in the MCNP data. The convergence reduces peaking factors slightly for cores exceeding 111 elements from general trends for cores with water voids.

Since the MCNP data generates the highest peaking factors (compared to SACLE), the MCNP for CNP data was used to develop a relationship for the hot channel peaking factor (PF) as a function of the number of fuel elements (N) in the core. The maximum core peaking factors as a linear equation is represented by:

$$PF = N \cdot 0.0031 + 1.415 \qquad 6.1$$

6.1 Fuel Temperature

The maximum fuel temperature is limited to prevent long term fuel degradation and short term cladding failure. The limiting values for TRIGA reactors are 950 °C for cladding temperature greater than 500 °C, and 1150 °C for cladding temperature below 500 °C. Recent operating experience resulted in a modification of a maximum 830°C for pulsing operations. Temperature monitoring by instrumented fuel elements provides assurance that temperature limits are met. The trip setpoint for fuel temperature measuring channels will automatically terminate reactor operations if fuel temperature exceeds the maximum permitted fuel temperature.

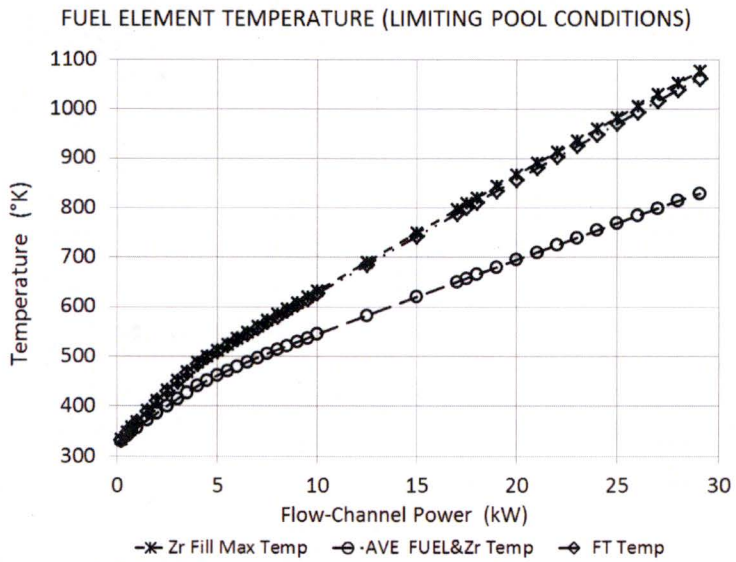

Figure 6.1, Fuel Temperature Response to Flow-Channel Power

At fuel element power levels greater than about 5 kW the change in temperature with respect to power is essentially linear. Equations above about 5 kW describing the maximum fuel temperature ((in the zirconium fill rod), the average temperature across the fuel element (including the zirconium fill rod), and the temperature expected from the fuel temperature measuring channel (FT) are:

$$T_{max} = 23.423 \cdot P_{HC} + 397.3 \qquad 6.1a$$

$$T_{FT} = 22.922 \cdot P_{HC} + 397.43 \qquad 6.1b$$

$$T_{AVE} = 14.9913 \cdot P_{HC} + 394.16 \qquad 6.1c$$

The power level at which the maximum fuel temperature achieves 950°C is calculated as

$$P_{HC} = \frac{T_{max} - 397.3}{23.423} \qquad 6.2$$

For a maximum temperature of 950°C, the corresponding fuel temperature channel indication is 938°C and the average fuel temperature is 748°C at a hot channel power of 23.60 kW.

Number of Fuel Elements

The peaking factor (PF) is defined as average power is the core power (P_{core}) divided by the number of fuel elements (N) while maximum power in a single element (P_{HC}) is the average power times the peaking factor:

$$P_{HC} = \frac{P_{core}}{N} \cdot PF \qquad 6.2$$

Substituting equation 6.2 as the peaking factor:

$$P_{HC} = \frac{P_{core}}{N} \cdot (0.0031 \cdot N + 1.415) \qquad 6.3$$

Which leads to:

$$N = \frac{1.415}{\frac{P_{HC}}{P_{core}} - 0.0031} \qquad 6.4$$

For a hot channel power of 23.60 kW, the numbers of elements at specific core powers are calculated in Table 6.2, illustrated in Fig. 6.2

Table 6.2, Core Power & Elements

P_{core} kW	N
950	65.1
1000	69.0
1050	73.0
1100	77.1
1130	79.6
1135	80.0
1210	86.3
1500	112.0
2000	162.6

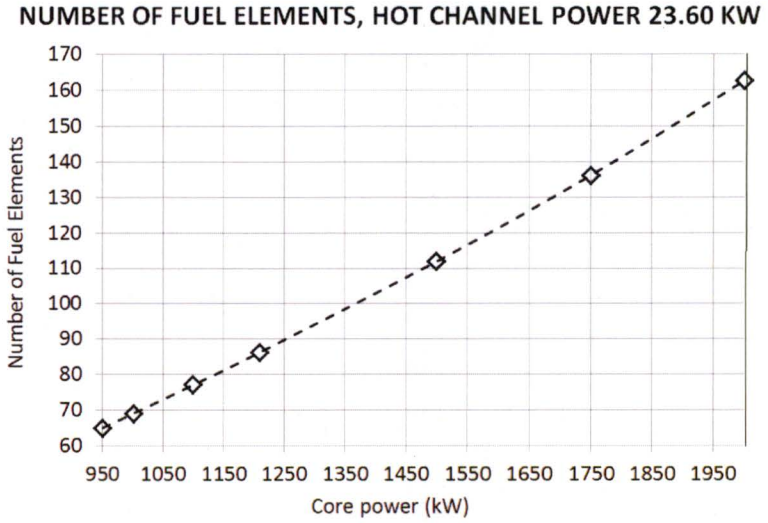

Figure 6.2, Number of Fuel Elements and Core power for 23.60 kW Hot Channel

Fuel Temperature Measuring Channel Protective Action

As previously described, fuel elements are installed with embedded thermocouples to monitor representative fuel temperatures. The instrumented fuel elements are fabricated with the thermocouples approximately 0.762 cm from the center of the element (with some possible difference for FT1 as previously discussed). The center of the fuel element is a fill rod (i.e., not loaded with fuel) and therefore does not generate fission heat; the temperature profile across the fill rod is flat.

Radial variation in fuel temperature taken from the RELAP and TRACE heat structure analysis at various power levels from 20 kW to 950 kW characterizes fuel temperatures. RELAP and TRAC calculations at greater than ab0ut 750 kW have been demonstrated to be higher than actual temperatures, and therefore conservative with respect to limiting temperatures. Fig. 6.3 provides graphical representation for the centerline temperature of B02, a positon approximately at the nominal thermocouple location for B03 and B06, and the location in B03 that represents a close approximation of the FT1 measuring channel response at the maximum permissible pool temperature.

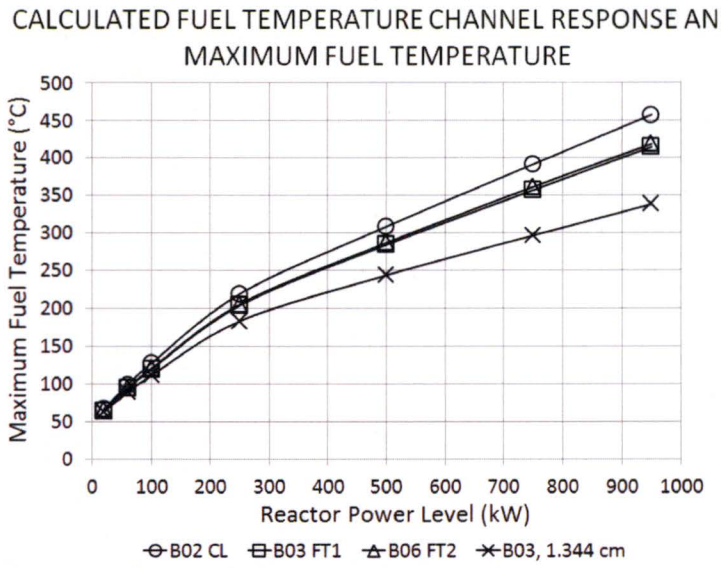

Figure 6.3, Fuel Temperature at power

Since the monitored temperatures are a fraction of the maximum core fuel temperature, limiting safety system set-points on fuel temperature are set to a fraction of the maximum allowed fuel temperature. Fig. 6.4 shows the ratio of the fuel temperature in the instrumented fuel elements at power (nominal locations for B03 and B06) to the maximum core fuel temperature (located in B02). In the case of B03, the fuel temperature is in a position that closely corresponds to the actual measuring channel response. Therefore with a maximum allowed fuel temperature of 830 °C, a trip setting of approximately 750 °C (830 °C /1.1) assures that the reactor will not operate if fuel temperature reaches the limit. For FT1, a setting of approximately 615 °C assures the reactor will not operate if fuel temperature reaches the limit. Therefore, temperature monitoring by instrumented fuel elements provides adequate assurance that temperature limits are met.

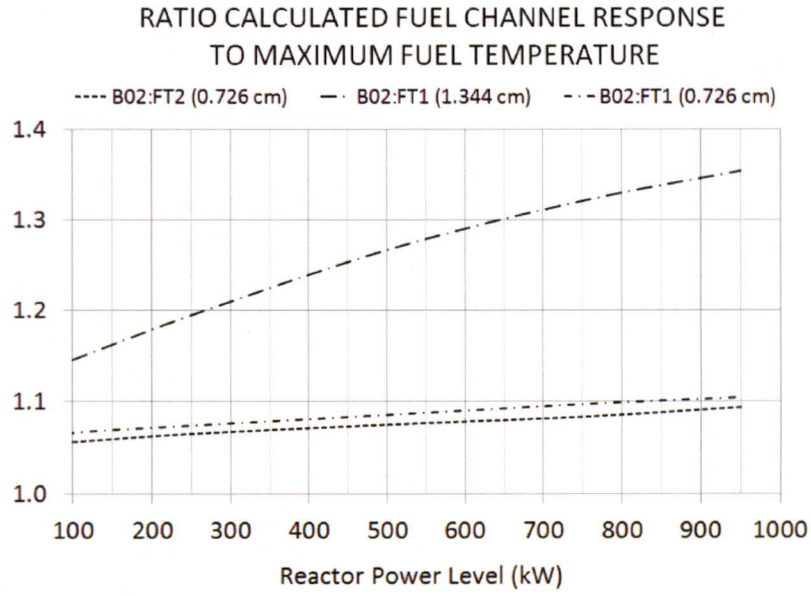

Figure 6.4, Ratio of measuring Channel Response to Maximum Fuel Temperature

6.2 Critical Heat Flux

Limiting the critical heat flux ratio (CHFR) in the hot channel assures that departure from nucleate boiling will not occur. Since RELAP provides the minimum CHFR, calculations using RELAP were performed using (1) the limiting and (2) the nominal values for pressure and water temperature over a range of fuel element heat generation/power levels. Water temperature, pressure, and mass flow rate at each elevation were used to calculate critical heat flux using the Bernath correlation (eqn. 5.8).

Hot Channel Response Function (HCFR vs Fuel Element Power)

The minimum ratio of heat flux to critical heat flux as a function of power level is provided in Fig. 6.5, The position of the minimum CHFR (usually elevation 10) is affected by volume flow rates at specific nodes in TRACE and RELAPS calculations; increased flows cause critical heat fluxes to increase and improve CHFR. A power function was developed to provide a relationship between channel power and the minimum CHFR for the thermal hydraulic conditions limiting core configuration (eqns. 6.1 and 6.2).

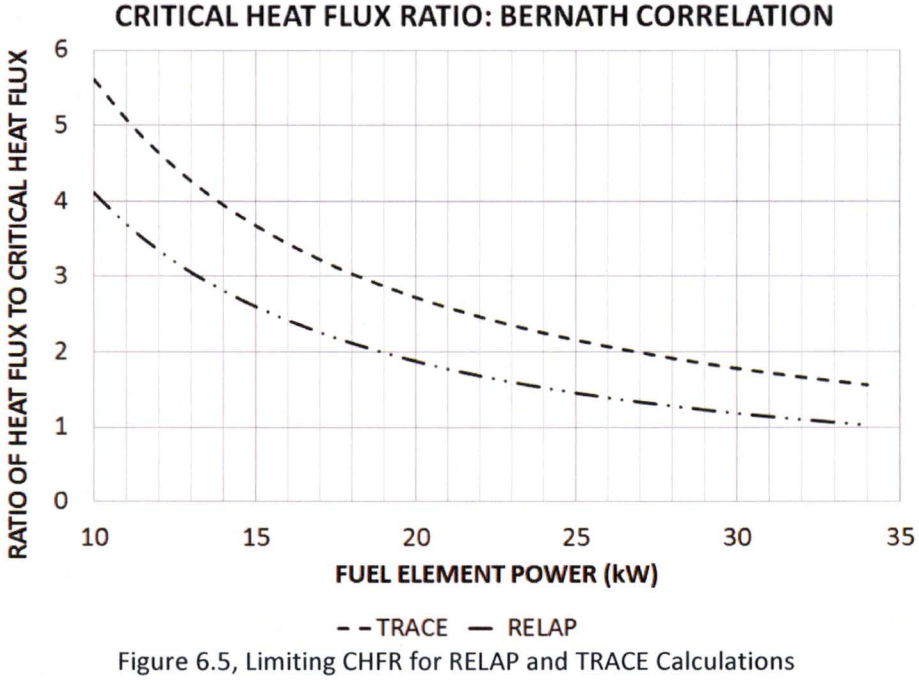

Figure 6.5, Limiting CHFR for RELAP and TRACE Calculations

Power functions were used to approximate both (nominal and the limiting condition) curves with an R^2 value greater than 0.99 (eq. 6.1 and 6.2).

$$CHFR_{TRACE} = 62.24 \cdot P^{-1.045} \qquad 6.1$$
$$R^2=0.9973$$

$$CHFR_{RELAP} = 55.866 \cdot P^{-1.133} \qquad 6.2$$
$$CRIR^2=0.9994$$

A critical heat flux ratio limit of 2.0 requires power in the hot channel to be less than approximately 30 kW based on TRACE calculations under limiting conditions of pool water and temperature. Conservative factors in UTTRIGA analysis:

(1) Peaking factors were calculated based on a uniform average fuel temperature; the uniform average fuel temperature assumption was shown to result in higher peaking factors than a more realistic description of fuel temperature distribution.

(2) The conservative MCNP model for peaking factor was used.

(3) Calculated temperatures are higher than observed temperatures above approximately 750 kW, so that actual thermal hydraulic conditions are not as severe as calculated.

(4) Modeling a flow channel does not account for mixing with adjacent flow channels; mixing flow from adjacent channels reduces hot channel cooling temperatures.

Summary

The minimum core configuration is selected to be 87 elements. For steady state operations at 1210 kW (the licensed limit with maximum measuring channel error), slightly more than 86 fuel elements will support steady state operations with the hot channel remaining at or below the maximum fuel temperature limit.

TRACE calculations at power levels up to 1210 kW demonstrate that a minimum CHFR of 2.0 is assured in the limiting core configuration (minimum pool water level, maximum pool temperature) for all cores from 75 elements to the maximum number of fuel element locations in the core. Cores with greater than 83 elements maintain CHFR greater than 2.0 up to 1500 kW.

The instrumented fuel elements are capable of initiating a reactor trip prior to exceeding maximum permitted fuel temperatures in the hot channel. A trip setpoint of 500 °C accounts for differences between the sensor location and the maximum temperature of the hot channel.

Modelling of Continuous Rod Withdraw and Pulse Transients in a TRIGA MK II Reactor at The University of Texas at Austin using a Coupled Neutronics Thermal-Hydraulics Model

G. Kline

Table of Contents

List of Figures

List of Tables

Introduction

The following outlines the model and the analysis of two specific events: a pulse and a continuous rod withdraw. Both simulations use a zero-dimensional neutronics model based on the In-hour equation found in an Idaho National Laboratory paper[1] and Akcasu's dynamics[2]. and equations from the 2015 UT LOCA model. Simnad provides the fuel specific properties such as material and geometric, while the UT TRIGA was used for the site-specific quantities including fuel loading, burnup, and rod worth; Weaver provides the neutronics data.

The neutronics portion takes into account the three major fissile isotopes' effects, as well as decay heat fractions and the current UT poison loading. MATLAB was chosen as the programming language for its ease, user input accessibility, and effective ODE solution methods for stiff and non-stiff equation sets. Consideration is taken to incorporate as many state dependent variables as possible to improve accuracy; however, the program is currently designed for events on the order of hours or less, where fuel loading and fission product poison concentration can be considered constant.

The verification process involved historical records for the pulse, and actual reactor operations for the rod withdraw portion. The whole program revolves around an accurate and easy user interface.

Prior Work

General Atomics

General Atomics (GA) did a number of studies around the early 1960's on the feasibility and behavior of a research reactor.[3] [4] The codes General Atomics used to develop the kinetic behavior (GAM-II, GATHER-II,GAZE-II,GAMBLE, and DTF-IV) are unavailable for use. The kinetics presented in these papers are well defined for two specific TRIGA configurations, neither of which are physically exacting enough to conditions at The University of Texas at Austin (UT) to determine valid local criteria.

Simnad and Hawley provide the basis for the 1150°C safety Limit for high Zr:H ratio fuels. This stems from the phase change occurring at ~2000°C.[5], [6] It is also established that the limiting factor in reactivity insertions is the cladding itself.[5] In order to limit this cladding temperature, which is difficult to measure, the fuel temperature, which is already being measured, is limited to 940°C in Hawley's paper[5].

Argonne National Laboratory performed pulsing analysis for GA and found a number of temperatures relative to added energy levels for various fuels.[7] This newer report, from 2008, also recommends a temperature limit of 830°C for 20% LEU fuel. This is based on the pressure of Hydrogen in the fuel matrix above 874°C causing microscopic expansion of cracks in the fuel.[7]

Argonne also performed a thermal-hydraulic analysis of the TRIGA coolant channel.[8] Here another proprietary code, STAT, was used to analyze a limiting channel. The nature of the TRIGA fuel geometry and core configuration shows independence of a channel on the neighboring channels and a need only to analyze the limiting channel. Additionally, a number of codes and correlations are compared for critical heat flux calculations that are not considered directly here, but through a site-specific peaking factor from UT SCALE.

UT TRIGA

Previous to the creation of the reactivity event modelling, a loss of coolant accident model (LOCA) was created for the limiting site-specific core.[9], [10] This model incorporated a one-dimensional, radial, finite element analysis. A sub-model involved a one-dimensional fluid flow analysis of the fuel element coolant space. From this, a number of items were gained including: a thermal hydraulic geometric model, code configuration, buoyancy driven flow analysis, solution control for large system linear ODE solvers. Aspects from this model were taken, and improved upon in the thermal-hydraulic portion discussed below.

The Model

The basis of the model is to take zero-dimensional point neutronics combined with a simplified form of a two-dimensional energy balance and solve for limiting values using site specific configurations in a *state-determined system* model[11]. This will be referred to subsequently as the $\{\mathbb{R}^0, \mathbb{R}^2\}$ model, implying the vector spaces of the neutronics and thermal-hydraulics respectively. The theoretical basis is split between neutronics and thermal-hydraulics. The site-specific criteria define components necessary for accurate verification and validation (VnV), while the programming section outlines the code structure and ease of use.

List of Symbols

Table 1. List of Symbols

$n(t)$	*Total Neutron Density (n^0/m^3)*	$\mathbb{R}^n$	*Real Number Vector Space of Dimension, n*
$C_i(t)$	*Delayed Neutron Precursor Density of the i^{th} Group (n^0/m^3)*	$S(t)$	*Neutronics Independent Sources (n/s)*
λ_i	*Decay Constant for the i^{th} Group (s^{-1})*	Λ	*Neutron Generation Time (s)*
$\rho(t)$	*Event Reactivity* $(\frac{\Delta k}{k})$	β_i^{mix}	*Delayed Neutron Fraction of the Fuel Mixture for the i^{th} Group* $(\frac{\Delta k}{k})$
$\alpha_{F,M}$	*Temperature Feedback for the Fuel and Moderator* $(\frac{\Delta k/k}{C})$	υ	*Neutron Velocity (m/s)*
$T_{F,M}(t)$	*Time Dependent Temperature of Fuel or Moderator (C)*	$\phi(t)$	*Core Flux (n^0/m^2s)*
$T_{F,M,0}(t)$	*Initial Temperature of Fuel of Moderator (C)*	k	*Boltzmann Constant (J/K)*
β_{eff}^{mix}	*Total Core Effective Delayed Neutron Fraction for the Current Fuel Mixture* $(\frac{\Delta k}{k})$	m_n	*Mass of a Neutron (kg)*

K_{Beta}	*Delayed Neutron Fraction Proportionality Constant*	$\sigma_{f,a,s}$	*Microscopic cross section for fission, absorption, and scattering. (m^2)*
$K_{sp,j}$	*Spontaneous Fission Factor (n^0/s)*	N_j	*Number Density of the j^{th} Item ($atoms/m^3$)*
V_{core}	*Volume of the Core (m^3)*	m_j	*Mass of Material (kg)*
$s(t)$	*Installed Neutron Source Neutron Density (n^0/m^3s)*	$S(t)$	*Total Source Density (n^0/m^3s)*
$\rho_{State}(t)$	*Current Reactivity Including Feedback* $(\frac{\Delta k}{k})$	$\bar{s}(t)$	*Calibration Sheet Neutron Production (n^0/s)*
$k_{eff}(t)$	*Effective Multiplication Factor*	$\rho_{M,F}(t)$	*Feedback Reactivity* $(\frac{\Delta k}{k})$
l	*Mean Neutron Lifetime (s)*	$\Lambda(t)$	*Neutron Generation Time (s)*
H_{ij}	*Delayed Power of Group j of Isotope i (W)*	E_{ij}	*Delayed Power Fraction (MeV/fission-s)*
P_i	*Total Power of Isotope i (W)*	$\tilde{\lambda}_{ij}$	*Decay Constant of Group j of Isotope i (s)*
Q	*Energy per Fission (MeV)*	$P_{eff}(t)$	*Effective Power (W)*
$P_{inst}(t)$	*Instantaneous Power (W)*	$P_d^i(t)$	*Delayed Power (W)*
E_f	*Recoverable Energy from Fission (W)*	$\rho_{trans}(t)$	*Event Reactivity as a Result of State* $(\frac{\Delta k}{k})$
RR	*Reactivity Addition Rate* $(\frac{\Delta k/_k}{s})$	CRW	*Maximum Event Reactivity* $(\frac{\Delta k}{k})$
$\dot{m}$	*Mass Flow Rate (kg/s)*	$\tilde{\rho}_i$	*Density (kg/m^3)*
A_i	*Flow Area (m^2)*	w_i	*Fluid Velocity (m/s)*
R_i	*Radius of i (m)*	$\check{A} - \check{D}$	*Density Correlation Constants*
dR_i	*Width of Pin Radial Element (m)*	dz_i	*Conductive Path Distance of i (m)*
h_i	*Height of Component i (m)*	dz_cond_i	*Conductive Path Radially of i (m)*
c_p	*Specific Heat Capacity (J/ kg K)*	$\tilde{\alpha}$	*Thermal Diffusivity (m^2/s)*
k_i	*Thermal Conductivity of i (W/ m K)*	g, g'	*Gravity and Density Compensated Reduced Gravity (m/s^2)*
$\dot{E}_{st}, \dot{E}_{in}, \dot{E}_{out}, \dot{E}_{gen}$	*Change in Energy: Stored, In, Out, Generated (W)*	q_{cond}	*Heat Transfer Rate (W)*
$\hat{h}_k$	*Specific Enthalpy of k (J/kg)*	z_k	*Height of k (m)*
$U_{wt\%}$	*Weight Percent of Uranium (kg/kg)*	$\hat{h}_0$	*Reference Enthalpy (j/kg)*

$\tilde{\beta}$	*Thermal Expansion Coefficient (1/K)*	μ	*Dynamic Viscosity (N s/m²)*
D	*Diameter (m)*	ν	*Kinematic Viscosity (m²/s)*
F_{Drag}	*Drag Force (N)*	F_g	*Gravity Resistive Force (N)*
C_D	*Coefficient of Drag (unit less)*	Δp	*Pressure Loss from Friction (Pa)*
f_D	*Darcy Friction Factor (unit less)*	D_H	*Hydraulic Diameter (m)*
ϵ	*Surface Roughness (m)*	P_{wet}	*Wetted Parameter (m)*
h_{cone}	*Cone Height (m)*	η_{fin}	*Fin Efficiency (unit less)*
I_i	*Modified Bessel Function of the i^{th} Kind*	L_{fin}	*Fin Height (m)*

Theory

Neutronics

The neutronics portion uses a zero-dimensional, single neutron velocity solution to the in-hour equation set presented by Johnson, et al. of Idaho National Laboratory.[1] The coupled ordinary linear ODE set presented by Johnson presents itself as a usable representation of Akcasu's point kinetic solution to the integrodifferential forms.[2] Namely, it provides a form free of a shape function and energy distribution, and the layout allows ease of transition to numerical solutions. The generic terms in this set are then made TRIGA specific using GA papers and UT specific using local parameters from UT SCALE, UT TRACE analyses and UT SAR.[12][13][9]

In-Hour Equations

The In-hour equation lies at the heart of the $\{\mathbb{R}^0, \mathbb{R}^2\}$ model. The choice of point kinetics reduces the order of the geometric vector space. The use of the single neutron velocity removes the velocity vector space and need to track lethargy.[2] The overall breakdown can be found below.

Neutron Density and Six DNP Group

The model is designed to simulate transients occurring over a very short time frame. These transients involve reactivity addition from rod withdraw only. Given the time frame, items such as burnup and fission product poison buildup are not considered. Additionally, the time dependence of β from change in isotope concentration is ignored. Values are dependent only on current UT core conditions. Thus, the equations of state for neutron population can be based on reactivity balance, feedback effects, sources, and DNP population only.[1] While Johnson and Akcasu both provide methodologies to track fuel burnup and poisons, this is considered beyond the scope for the model's initial phase. The $\{\mathbb{R}^0, \mathbb{R}^2\}$ model's basis equation is[1]:

$$\frac{dn(t)}{dt} = \frac{\rho(t) + \alpha_F\left(T_F(t) - T_{F,0}\right) + \alpha_M\left(T_M(t) - T_{M,0}\right) - \beta_{eff}^{mix}}{\Lambda(t)} n(t) + \sum_{i=1}^{6} \lambda_i C_i(t) + S(t) \qquad 1$$

$$\frac{dC_i(t)}{dt} = \frac{\beta_i^{mix}}{\Lambda(t)} n(t) - \lambda_i C_i(t) \ , \qquad i = 1 \ldots 6 \qquad 2$$

The governing equation for neutron population is relative to the prompt effects, delayed precursor concentration and external sources. While the use of a single velocity model would allow for a flux term instead of a neutron density, it would make the solution technique more difficult for future work. A single velocity model was chosen because it simplifies calculations involving flux by removing the need to track velocity and diffusion vector spaces in $\mathbb{R}^3$ or lethargy vector space in $\mathbb{R}^2$.[2] Any terms involving flux have the velocities accounted for with:

$$\phi(t) = vn(t) \quad 3$$

$$v = \sqrt{\frac{2kT_F\{K\}}{m_n}} \quad 4$$

Here, the fuel temperature, in Kelvin, is used to determine the velocity of the neutrons using the Maxwellian distribution assumption and equation for neutron mean temperature. While the neutron temperature is better represented by the bound hydrogen energy levels, due to their Einstein oscillator tendency[3], this was thought to impinge too much on the kinetic effects covered under the prompt temperature coefficient of the fuel. The dynamics are tracked using neutron density, the velocity term only comes into play in the density initial condition and the output calculation of peak power, so this assumption is considered appropriate.

The DNP concentrations are accounted for in (2) while the external sources, discussed below, include the core's external AmBe source and spontaneous fission effects of the fuel materials. The prompt neutron reactivity balance includes the event reactivity, feedback effects and the effective delayed neutron fraction.

The Delayed Neutron Fraction (β) and Effective Delayed Neutron Fraction (β_{eff})

The mixture delayed neutron fraction of a core is dependent upon the fuel materials used and their relative concentrations. In this model, the effects of ^{235}U, ^{238}U, and ^{239}Pu are all accounted for. Their concentrations are determined from SCALE. Here, the energy levels and decay constants of each fuel's 6 groups is combined using a weighted average.[1], [2], [14] The model accounts for the ith group's mixture delayed neutron fractions and decay constants using:

$$\beta_i^{mix} = \frac{\sum_{j=1}^{3} v_j \sigma_f^j N_j(t) \beta_j^i}{\sum_{j=1}^{3} v_j \sigma_f^j N_j(t)} \quad 5$$

$$\lambda_i^{mix} = \frac{\sum_{j=1}^{3} v_j \sigma_f^j N_j(t) \lambda_j^i}{\sum_{j=1}^{3} v_j \sigma_f^j N_j(t)} \quad 6$$

The effective delayed neutron fraction is dependent on a number of factors including birth energy distributions, core buckling, diffusion constants and neutron age.[2], [15] These values are not readily available for most cores as they are geometrically specific and thus site-specific and difficult to measure and verify. This lead to an alternative method for calculating the effective delayed neutron fraction. According to GA-7882, the TRIGA core with ^{235}U has an effective delayed neutron fraction of *.007*.[12] Taking into account the delayed neutron fraction of ^{235}U, a proportionality constant can be found:

$$K_{Beta} = \frac{\beta_{eff}^{235}}{\beta^{235}} \quad (7)$$

The total delayed neutron fraction for the mixture is given by:[14]

$$\beta^{mix} = \sum_{i=1}^{6} \beta_i^{mix} \quad (8)$$

This yields the mixture effective delayed neutron fraction using:

$$\beta_{eff}^{mix} = K_{Beta}\beta^{mix} \quad (9)$$

Both Weaver and Akcasu imply an effective delayed neutron fraction gain of 20-30%. This method slightly under estimates that at ~7% gain; however, this is considered an acceptable approximation. The basis for the current equation is: accepted research, and the real value's computational complexity does not fit the premise of the initial model.

Feedback

A majority of the prompt feedback in the $\{\mathbb{R}^0, \mathbb{R}^2\}$ model is accounted for in the fuel and water temperature coefficient terms.

α_F of Fuel

The fuel prompt temperature coefficient is a weighted average of multiple effects including: Einstein oscillator effect, Doppler broadening, Cell effect, and leakage.[3], [12] With a reactivity based point source model, it is desirable to lump these effects into a temperature coefficient term. GA-7882 provides a temperature dependent temperature coefficient for TRIGA fuel.[12]. Experimentally

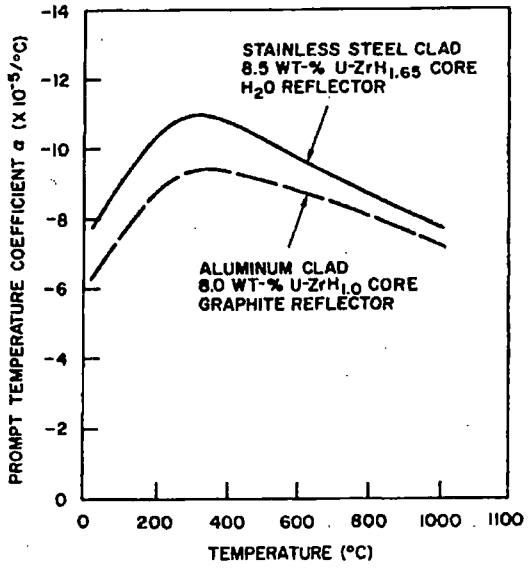

determined data is in good agreement with the temperature coefficient data at approximately 400°C.

1. Prompt Temperature Coefficient for TRIGA fuel vs Temperature from GA-7882

From this curve, a temperature dependent polynomial fitted curve was made.

$$\alpha_F(T,t) = 1.4990e^{-16}T_F(t)^4 - 5.3734e^{-13}T_F(t)^3 + 6.5947e^{-10}T_F(t)^2 - 2.8159e^{-7}T_F(t) + 6.9571e^{-5} \quad (10)$$

The value is temperature and time dependent; the equation is time dependent based on the time dependency of the fuel temperature. This time dependence is only notational; in reality the coefficient is based only on fuel temperature alone. Each time iteration, the value is recalculated based on the current state. The reactivity effects of the fuel are accounted for using the current temperature relative to the initial temperature:

$$\rho_F(t) = \alpha_F(T,t)\left[T_F(t) - T_{F,0}\right] \quad (11)$$

α_M of Water

The dominant feedback in a TRIGA reactor is fuel temperature feedback. Local modelling analysis can confirm this.[16] The effect of the water from a neutronics standpoint is only a minor consideration using the locally found temperature coefficient, and using a constant value for it. The reactivity effects are then similar to the fuel, but without state dependency of the coefficient:

$$\rho_M(t) = \alpha_M\left(T_M(t) - T_{M,0}\right) \quad (12)$$

The water tends to have a slightly positive effect.[16]

Xenon and poisons

While poison buildup, especially Xenon, would have an effect on the dynamics, the core is considered cold clean critical initially. With a timescale of seconds and minutes, this effect is considered negligible given the half-lives of Xenon and Iodine being on the order of hours.

Burnup

Burnup would account for a long term feedback effect. However, the intent is to model events on the order of seconds and minutes, so these effects are neglected. Core age does play a role in the initial condition vector and fissile material concentrations, but not the dynamic model.

Neutron Generation Time

According to Weaver,[14] the neutron lifetime is related to the current effective neutron multiplication factor and the mean energy lifetime[14]. The mean neutron lifetime is taken directly from the UT SAR.[13] The effective multiplication factor is found from the current state of event reactivity and feedback.[14]

$$\rho_{State}(t) = \rho(t) + \rho_F(t) + \rho_M(t) \quad (13)$$

$$k_{eff}(t) = \frac{1}{1 - \rho_{State}(t)} \quad (14)$$

$$\Lambda(t) = \frac{l}{k_{eff}(t)} \quad (15)$$

This dependency on the feedback state ensures the generation time is changing relative to current core conditions.[14]

External Sources

The external sources considered are the added AmBe source and the spontaneous fission of ^{235}U, ^{238}U, and ^{239}Pu.

$$S(t) = s(t) + \sum_{j=1}^{3} \frac{K_{sp,j} m_j}{V_{core}} \quad 16$$

The source density is determined from its calibration sheet neutron production rate and the volume of the core:

$$s(t) = \frac{\bar{s}(t)}{V_{core}} \quad 17$$

While source neutrons are not evenly distributed in higher dimensional models, the $\mathbb{R}^0$ assumption negates that geometric effect. While the spontaneous fission neutron production is from the factors found in [1] and the local material properties of mass and volume.

ANSI Decay Heat and Effective Power

Decay Heat

Decay heat in the core comes from radioactive decay of nuclides born at unstable energies.[1] ANS standards provide the information for the decay heat fractions of ^{235}U, ^{238}U, and ^{239}Pu.[17] This allows a state dependent calculation of the heat (power) associated with the radioactive decay of fission products. This heat has a role in the energy generation term of the fuel, but is not normally accounted for in the neutronics equations of state (1), (2). This requires "delayed power 'concentrations'"[1] and tracking their changes with state changes:

$$\frac{dH_{ij}}{dt} = \frac{E_{ij} P_i}{Q} - \tilde{\lambda}_{ij} H_{ij} \ , \qquad i = 1 \dots 3 \; j = 1 \dots 23 \quad 18$$

This leads to a term tracking the power of each nuclide fraction of each of the isotopes in the core. This lends to calculating the 'effective power' of the core.[1], [17]

Effective Power, Instantaneous Power, and Delayed Power

Three different forms of energy need to be tracked for each cycle. Instantaneous power is the recoverable energy from fission at the current state, mostly due to kinetic energy of the fission products.[1] Delayed power is the fraction of energy produced from each isotope that is delayed from the current state. Effective power takes into account the instantaneous power, the state's current power from the delayed power concentrations and compensating for this state's power produced delayed:

$$P_{eff}(t) = P_{inst}(t) - \sum_{i=1}^{3} P_d^i(t) + \sum_{i=1}^{3} \sum_{j=1}^{23} H_{ij}(t) \quad 19$$

$$P_{inst}(t) = \sum_{i=1}^{3} \phi(t) E_f N_i \sigma_f^i V_{core} \quad 20$$

$$P_d^i(t) = \frac{{P_{inst}}^i(t)}{Q} \sum_{j=1}^{23} \frac{E_{ij}}{\tilde{\lambda}_{ij}} \quad 21$$

The effective power plays an important role in the thermal hydraulic model. The instantaneous power equation is used during the output phase to determine the peak power from the stored neutron density.

Input Reactivity

The input reactivity term is relative to the chosen model.

$$\rho(t) = \rho(t_0) + \rho_{trans}(t) \quad 22$$

$$\frac{d\rho_{trans}(t)}{dt} = 0 \{Pulse, Rod\ Withdraw\ \rho_{trans}(t) \geq CRW\}; \quad 23$$

$$\frac{d\rho_{trans}(t)}{dt} = RR \{Rod\ Withdraw, \rho_{trans}(t) < CRW\} \quad 24$$

The reactivity addition rate is considered constant with the current version. Realistically, this value would vary along the differential rod worth curve. Additionally, rod withdraw events are limited to the maximum allowed reactivity, as chosen by the user. A pulse is considered an instantaneous addition of reactivity, and thus the event reactivity is constant. Thus, pulses use a step insertion and rod withdraws use ramp insertion, whose slope is based on the reactivity addition rate.

Time Dependence and State Considerations

The model lends itself to time dependence on items such as source strength, poison effects, and delayed neutron fraction. These items are driven by fissile material concentrations and are neglected. Tracking of the neutron density stems from the point kinetics model.[1], [2] The decision to use a single velocity neutron spectrum is a result of initial model phasing and computational access.

Thermal Hydraulics

The $\{\mathbb{R}^0, \mathbb{R}^2\}$ model uses simplified two-dimensional thermal hydraulic interactions. The generic regions of fuel, graphite, gas, cladding and coolant channels are discretized. The state dependent mass, momentum, and energy balances are solved to find the temperatures of these regions. The coolant and fuel temperatures then feed directly into the neutronics equations.

The geometry is based on the UT TRIGA hexagonally arranged core with simplified entry and exit criteria. The fuel pin used accounts for the inner Zirconium pin, fuel meat, gas gap, cladding and coolant channel. The edges of the hexagonal coolant channel bisect the distance between the related pin, and create a single pin representative unit. This is based on the assumption the flow between pins is symmetric.

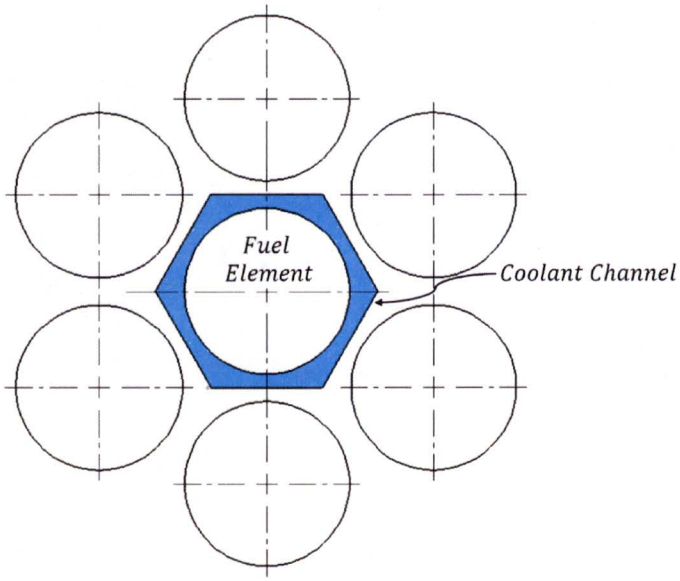

2. Coolant Channel Geometrics

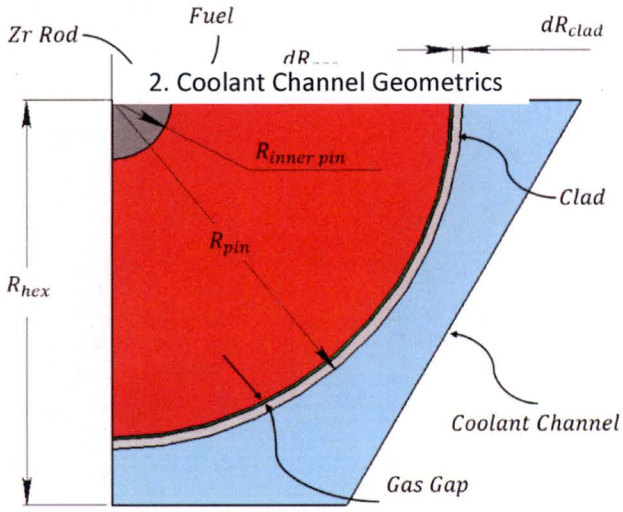

3. Radial Section View of Fuel Element and Coolant Channel

The axial portion of the pin model, shown below, accounts for fuel and graphite regions.

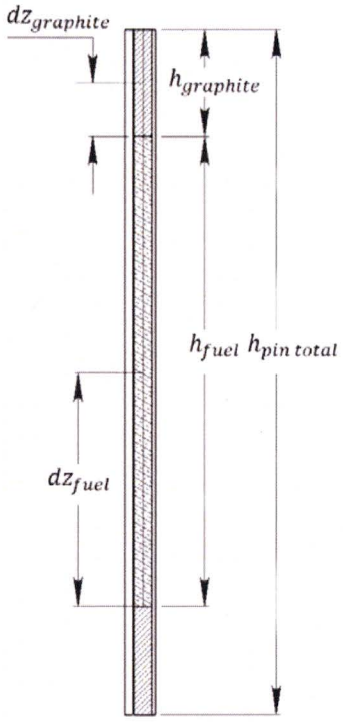

4. Axial Fuel Pin Heights

Mass Balance and Buoyancy Driven Flow

The mass balance assumption allows simplification in the solution technique of the energy balance. Mass flow rate is considered constant:[18]–[22]

$$\dot{m} = \tilde{\rho}_i A_i w_i = \tilde{\rho}_{i+1} A_{i+1} w_{i+1} \tag{25}$$

This allows the known or limiting region mass flow rate to be found and used for the entire channel. This simplification is necessary to maintain the linearity of the system of equations and to optimize them to non-super computer solution methods.

Geometry

The mass flow rate area is based on the surface normal to the surface of the fuel pin. The core configuration is hexagonal, leaving a hexagonal shaped coolant channel with a circular portion occupied by the pin. The area of the coolant hexagon is given by:

$$A_{hex} = \frac{\sqrt{3}}{2}(2R_{hex})^2 - \pi R_{pin}^2 \tag{26}$$

This gives the area for a single pin along the axial region of constant diameter. With the constant mass flow assumption, this is the only required area for coolant fluid flux.

Density

The TRIGA reactor uses buoyancy driven flow causing coolant density to become a state dependent function. A temperature based water density correlation was found to be:[23]

$$\tilde{\rho}(T,t) = \frac{\check{A}}{\check{B}\left(1+\left(1-\frac{T_M(t)}{\check{C}}\right)^{\check{D}}\right)} \quad (27)$$

Its time dependency stems from the need to calculate it each iteration.

Specific Heat Capacity

Specific Heat capacity is also a temperature dependent function, making is a state dependent function. A curve fit was created from a table of specific heat values:[24]

$$c_p(T,t) = 3.16744e^{-10}{T_M}^4 - 1.05772e^{-7}{T_M}^3 + 2.3533e^{-5}{T_M}^2 - 1.4767e^{-3}T_M + 4.20617 \quad (28)$$

This function return needs to be multiplied by 1000 to give the proper units of (J/kg K).

Thermal Diffusivity

Thermal diffusivity relates the ability of a material to conduct thermal energy versus store thermal energy. It contains the state dependent variables of density, specific heat capacity, and thermal conductivity. This makes it state dependent.

$$\tilde{\alpha}(T,t) = \frac{k(T,t)}{\tilde{\rho}(T,t)c_p(T,t)} \quad (29)$$

The temperature dependence of the thermal conductivity is found with the state dependent equation:

$$k(T,t) = -1.488445 + 4.12292\frac{T_w}{298.15} - 1.63866\left(\frac{T_w}{298.15}\right)^2 \quad (30)$$

Mass Flow Rate

Buoyancy driven flow adds a number of complexities to a finite element, constant volume model greater than $\mathbb{R}^0$ as the equations are coupled and elliptic partial differential equations.[19], [25], [26] The flow itself is driven by density changes, which in this case, occur from heat transfer from the fuel pin. This density change is found by comparing element inlet and outlet temperatures. The temperature rise is associated with the total energy transferred into the volume from the fuel element. To find the total energy transferred, either a coolant velocity or volume residence time needs to be known. Both of which are related to the density change itself.

Channel Characteristics

In an effort to simplify these equations and find a velocity relationship, a number of assumptions are made. The first of which relates to the coolant channel characteristics. It is assumed that the space between the pins results in a symmetrical flow of constant radial velocity, allowing only half the gap between pins to be considered. This leads to the hexagonal channel shape. Additionally, the velocity in the radial direction, $\vec{u}_{Radial}$, is considered to be 0. Also, the flow is considered to be fully developed with a uniform radial velocity profile.

Plume Model

The next simplification was to find a model outlining a buoyant driven velocity relationship that is solvable. The velocity profile of buoyant plumes is a topic of study in the geological field.[27], [28]

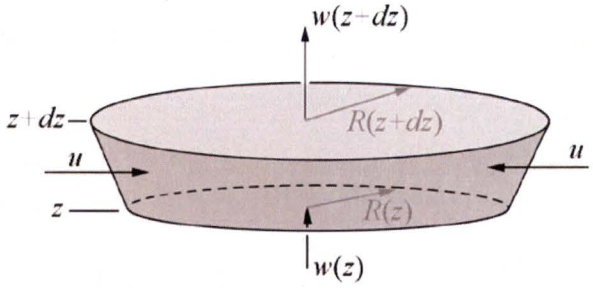

5. Momentum Balance in a Thermal Plume[27]

Above shows the momentum balance of a thermal plume. It takes into account height, axial and radial velocities and momentum flux. Derivation of the momentum equations leads to the velocity differential:

$$\frac{d}{dz}(R^2w^2) = R^2g' \tag{31}$$

However, in the case of the pin coolant channel with the $\vec{u}_{Radial} = 0$ assumption, the radius is constant not dependent on the height. This leads to:

$$dw = \sqrt{g'dz} \tag{32}$$

The reduced gravity term in (31) is a state dependent variable defined by:[29]

$$g'(t) = g\frac{\rho_i(t) - \rho_{i+1}(t)}{\rho_i(t)} \tag{33}$$

Boussinesq Assumption

The next assumption is the Boussinesq assumption, used to find a relationship for outlet density. Here the density differences are neglected, except those related to gravity, [19] and changes in density are due to temperature alone.[25] This makes the equation for outlet density:

$$\tilde{\rho}_{i+1}(T,t) = \tilde{\rho}_i(T,t)[1 - \tilde{\alpha}(T,t)(T_{i+1} - T_i)] \tag{34}$$

Substituting (31) and (30) into (29) gives a differential velocity term related to a temperature difference:

$$\frac{dw}{dt} \cong \sqrt{\tilde{\alpha}(T,t)[T_{i+1} - T_i]dz} \tag{35}$$

Using the constant mass flow rate assumption, solving for one mass flow in a known region leads to the required mass flow in the energy balance for all axial, convective regions. The coolant channel is segmented axially into three regions, correlated with the fuel and graphite regions on the pin.

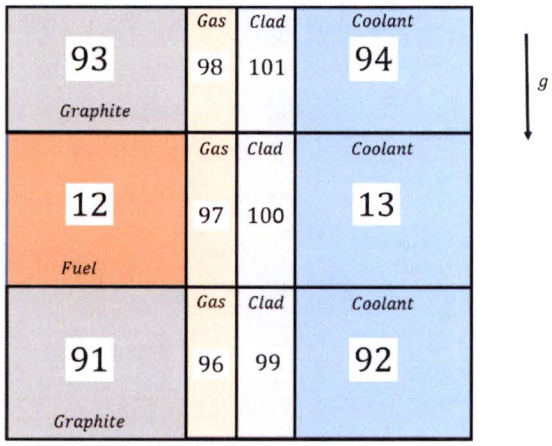

6. Region Distribution in Thermal Hydraulics[9], [62]

Velocity is calculated using the densities of regions 13 and 94. The area is taken from the boundary between these two regions and the density used is from region 13. The assumption is that region 94 will tend to be less dense than region 13. This leads to the mass flow rate equation:

$$\dot{m}(t) = \rho_{13} A_{13-94} w_{13-94}(t) \tag{36}$$

The final assumption revolves around the solution technique. Fully transient conditions would tend to satisfy a momentum balance, but not necessarily a mass balance. The computational instability of the momentum balance equation led to using a pseudo steady state solution at each iteration. This is the same method used in RELAP5 and is considered acceptable.[8]

Momentum Balance Expansion of Thermal Hydraulics

The momentum balance expansion takes the simplified geometries and assumptions of the mass balance and develops them further. The regions are expanded to incorporate the effects of the fuel pin components above and below the graphite; a one-dimensional flow vector, vice a constant value, represents fluid velocity. On the fuel element ends, the fins are taken into consideration both in flow development and heat transfer, and the effects of drag are accounted for. Conservation of momentum is obtained using the following equation:

$$\rho_{out} A_{out} w_{out}^2 - \rho_{in} A_{in} w_{in}^2 = F_{Drag} + F_g \tag{37}$$

Where resistive forces of gravity and drag offset the change in inlet and outlet conditions.[20], [21] Much like the mass balance, a pseudo steady state condition is assumed, to allow removal of the transient term. This equation represents a better characterization of the flow, but contributes to the extreme stiffness of the ODE set.

Regional Expansion

The regions being tracked are expanded to compensate for the new equations and relationships. The fuel element had two added regions of all stainless steel, while the coolant channel has two additional volumes added.

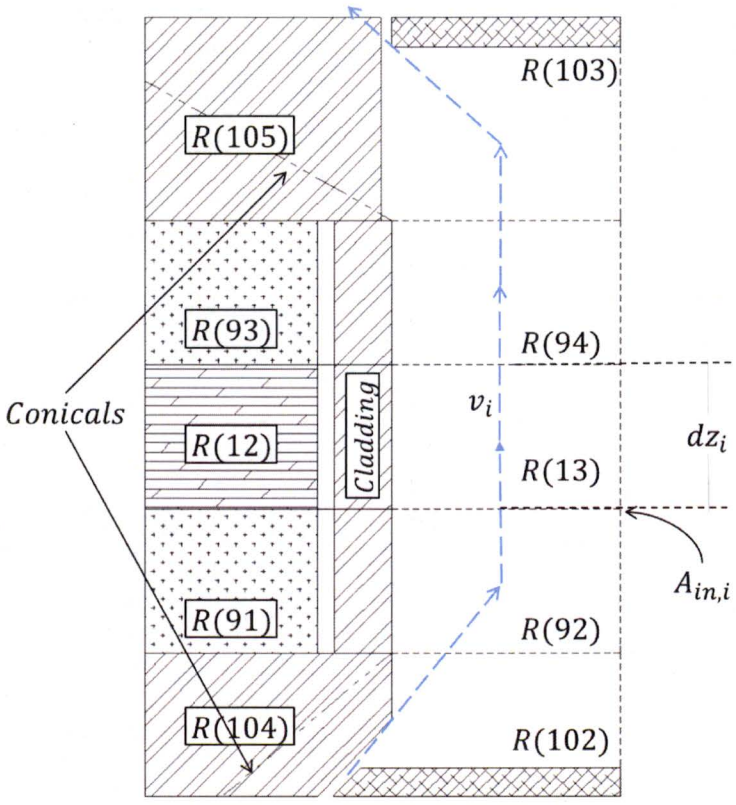

Each region has an inlet and outlet areas, as well as relative differential height for the drag calculations. There are five distinct velocities to be considered as well as five different density regions.

The areas of regions 92, 13, and 94 are constant along the constant radius cylinder. The inlet and outlet area are calculated from solid models based on fuel element drawings.

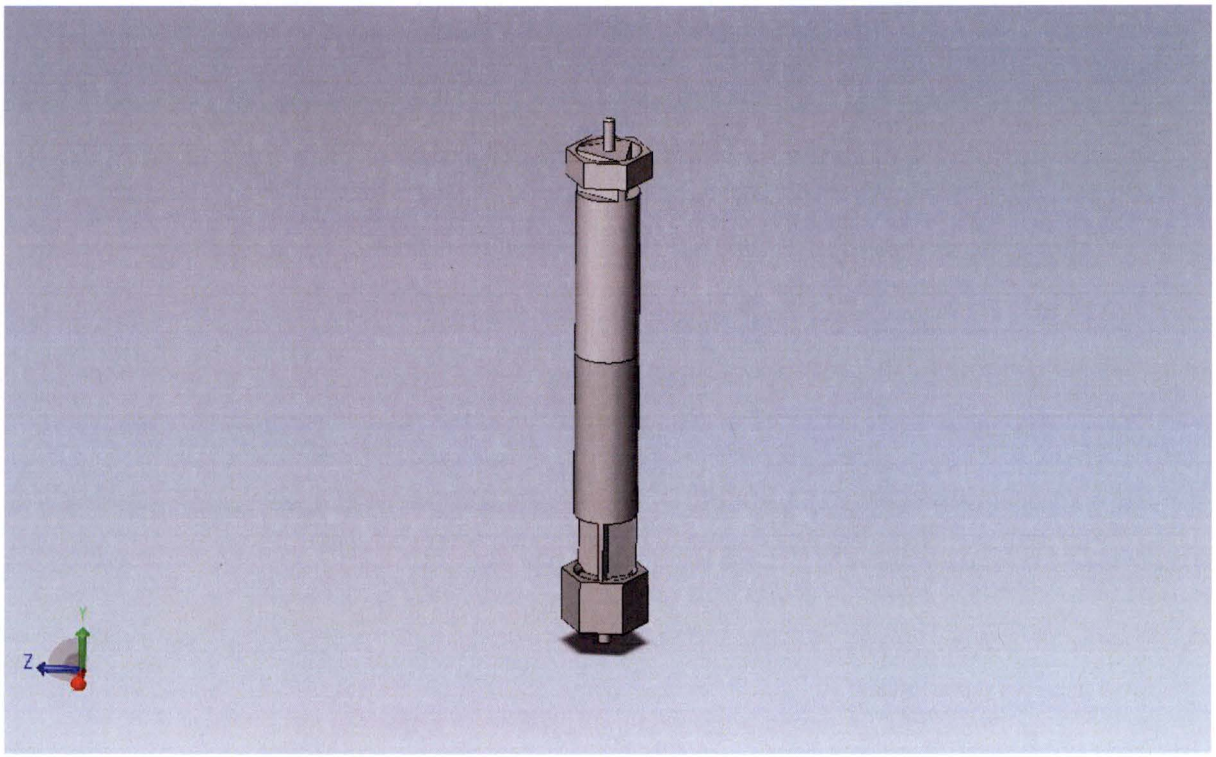

7. Fuel Pin Solid Model from 10000 Series Used for Inlet and Outlet Flow Area Characteristics (Note: this top represents the simpler 2000 Series for Initial Geometric Design. The Model Uses the Geometry in Figure 10 for Actual Values.)

Using the solid part and creating a part from the void, the area and parameter values are measured and used in the iterative mass flow calculator.

Flow Development

With the expansion into the momentum balance, the flow is considered differently than the mass balance. In the mass balance, the plume model provides a differential velocity between the fuel area coolant and the upper graphite coolant. Flow, and thus mass flow, is then considered constant. In the momentum balance, the flow between these two regions, 13 and 94, is developed in the same way; however, each region's specific velocity and mass flow rate are calculated using a sub-function. This provides better representation in the energy balance.

The major defining factor is the drag force, defined by:

$$F_{Drag} = \frac{1}{2}\rho w^2 C_D A_S \qquad 38$$

The drag force is divided into the effects of the cylinder walls and the cone features. The fins are considered triangular extended surfaces, whose heat transfer effects are considered, but not drag features.[30]–[39] They were modeled in Solidworks and used to find surface area for heat transfer.[32] Models were made for both the top and bottom fin assemblies.

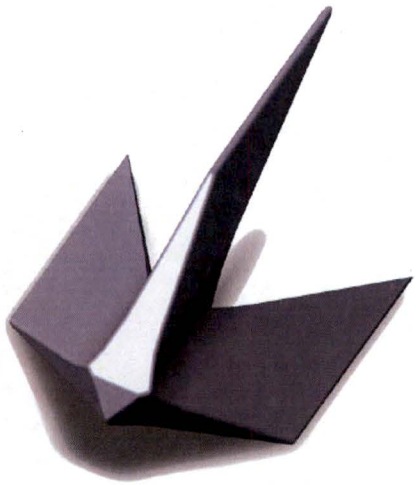

8. Lower Fuel Element Fin Geometry

Cylindrical Drag Force

The drag force along the cylindrical portions of the fuel pin is calculated from the Darcy friction equation. The effects of flow axial along a rough cylinder are not well categorized directly from a drag coefficient. Most analyses revolve around cross-flow.[18], [20], [21], [40], [41] However, the drag coefficient can also be found from a pressure loss using:[40]

$$C_D = \frac{\Delta p}{\frac{1}{2}\rho w^2} \tag{39}$$

Where the differential pressure can be found with:[40]

$$\Delta p = \frac{1}{2} f_D \frac{dz}{D_H} \rho w^2 \tag{40}$$

And the friction factor is found using the Swamee–Jain equation with:

$$f_D = \left[-2 \log\left(\frac{\epsilon}{3.7 D_H} + \frac{5.74}{\left(\frac{w\rho}{\nu}\right)^{.9}} \right) \right]^{-2} \tag{41}$$

For the state dependence, the friction factor's Reynolds number is found using the coolant regions temperature dependent density, viscosity and velocity. The roughness for stainless steel is based on values from White, while the hydraulic diameters are found with 42.[40]

The Darcy drag force is found for each region's cylindrical sections. The conical portions are considered to have a higher geometric effect and the change in pressure from the walls can be neglected.

Characterization of Fuel Element Extremities

The fuel element ends are characterized by considering the effects of: the heat transfer from the fin, the drag on the conical sections and cylindrical sections, and the heat transfer from the region (considered one unit for mass and temperature) to the coolant.

Each loop the ODE solver recalculates the velocity distribution using a sub-function. First, the area and parameter values from the solid models are used to find the hydraulic diameters:

$$D_H = \frac{4A_{flow}}{P_{wet}} \tag{42}$$

This plays a role in both the momentum balance and the Darcy friction factor.[20], [31]

Cone Section

The conical section plays two roles: it has a drag factor for the resistive force and provides a surface area for heat transfer to the coolant.

The surface area of a cone is found with:

$$A_{s,cone} = \pi r_{pin}\left(h_{cone}^2 + r_{pin}^2\right) \tag{43}$$

Since the lateral portion is the only portion exposed to the water, the flat portion is ignored. Additionally, for simplicity, the portions occupied by the thin fins are not neglected.

The coefficient of drag for a cone was found using rocketry correlations, and White[40] specifically:

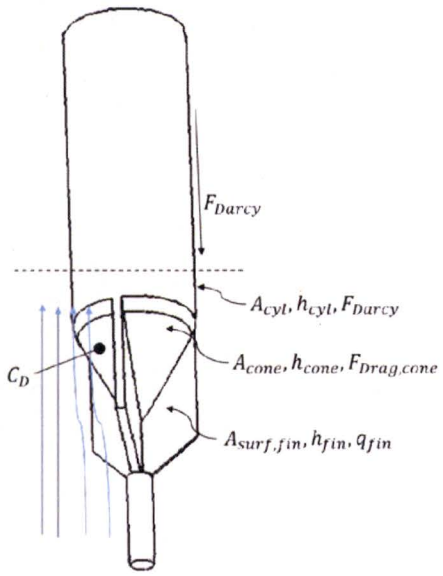

9. Lower Fuel Element Geometry

$C_{D,cone} = .8$ [42]–[44] Where the drag coefficient is based on the angle of attack of the cone.

The heat transfer coefficient from the cone is found using the Rayleigh number from the fin calculations and finding the Nusselt number using:[35], [45]

$$Nu_{cone} = 2.0963 + .669 Gr_{fin} Pr_i \quad 44$$

The heat transfer from the cone uses Newton's law of cooling 61.

Fin Sections

The fin sections are considered triangular extended surfaces. Their heat transfer effect on the region of the cone and cylinder are considered; and they are used to develop that region's flow properties, such as the Rayleigh number. Their energy contribution to the region is found with:[30], [36], [39], [46]

$$q_{fin} = \eta_{fin} h_{fin} A_{S,fin} (T_{SS,i} - T_{coolant,i}) \quad 45$$

To find the heat transfer coefficient first Rayleigh number must be found from the Grashof and Prandtl numbers. The Prandtl number is found with 63 and the Grashof number is found with 62 where, D in this case is replaced with the height of the fin in the radial direction. 45 contains an efficiency factor whose derivation is below.

Geometry

The fin geometry was developed using solid modelling software in Solidworks. A replica fuel element of the 10,000 series type and a micrometer was used to develop the upper and lower fins. This allowed for a surface area and parameter values using grid plate interfaces built from the UT TRIGA original drawings.

The lower fuel element extension below the fins sits below the lower grid plate and is neglected. The upper fin geometry was simplified to be solely an array triangular section and it disregards the radially flat portions of the fins.

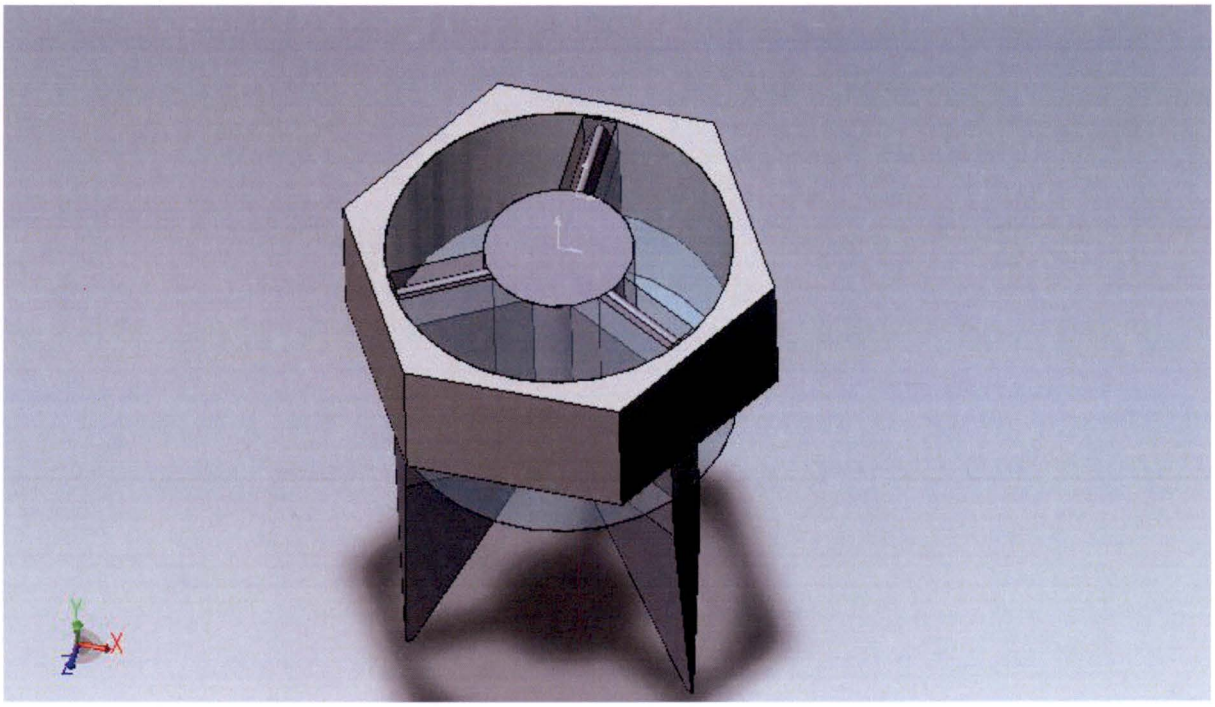

10. Fuel Element Upper Portion for Flow Analysis and Fin Properties

The portion used to grasp the fuel with the tool is also ignored, as its effects are considered negligible.

Efficiency

The efficiency of the fin plays a key role in the effect it has on the transient temperature of the extended fuel element regions. It is found based on the flow conditions in the surrounding area.[21], [31]

While the efficiency factor varies, the computational demands were excessive enough to validate a static analysis and calculation of an effective constant value. A temperature of 30°C was used for the coolant and a value of 450°C was used for the fuel temperature. These represent median values for the respective regions based off of the mass balance analysis.

The Rayleigh number was calculated with both a 1°C and 800°C ΔT. It was seen that the flow remains near laminar Rayleigh numbers up to ~650°C ΔT so the laminar flow correlation was used:

$$Nu_{fin} = .59 * Ra_{fin}^{.25} \quad 46$$

Where the Rayleigh number is found using equation 64, but with the Grashof and Prandtl numbers for water at 30°C.

The fin efficiency was found using the equation from Bergman that ratios modified Bessel functions of the first and zero order:[21]

$$\eta_{fin} = \frac{1}{mL_{fin}} \frac{I_1(2mL_{fin})}{I_0(2mL_{fin})} \quad 47$$

Here, *m*, is a factor found using:

$$m = \sqrt{\frac{2h_{fin}}{k_{SS}t}} \quad 48$$

The heat transfer coefficient is found using 46, but the length L representing the fin extension from base surface varies over the length of the fin. An array in MATLAB was created with 1000 points from the minimum to maximum heights as measured from the Solidworks models. This gave an

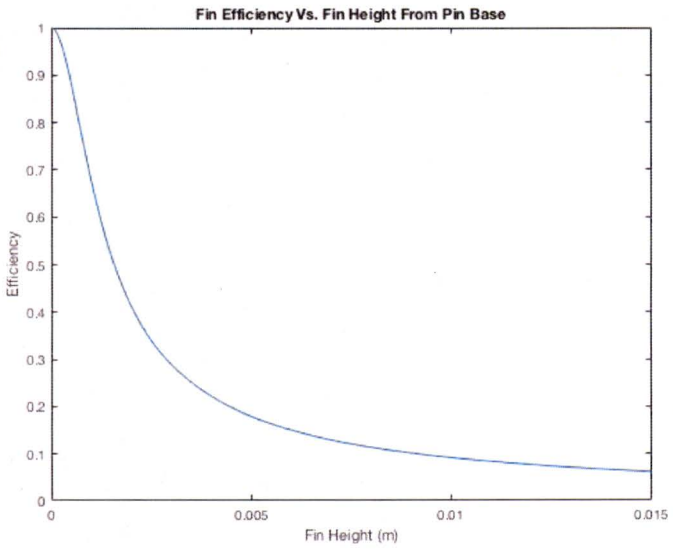

output efficiency curve:

It is evident from the shape of the curve that for a majority of the heights the efficiency is between 10% and 20%. Since the fin shape tends toward mostly heights greater than .0075m, the median efficiencies were used for the upper and lower fins. 45 can now be used to find the energy lost from the stainless region by the extended surface.

Flow calculations

With the development of velocity based on the 13-94, the momentum equation is solved to find the unknown velocity for each region.

$$w_{in} = \sqrt{\frac{\rho_{out} A_{out} w_{out}^2 - F_{Drag,cyl} - F_{Drag,cone} - F_g}{\rho_{in} A_{in}}} \quad 49$$

Which leads to that surface's mass flow rate using equation 36. The sub-function outputs each of the control volume's boundary mass flow in to the energy equation using (36).

Energy Balance

The energy balance is a fundamental aspect of the $\{\mathbb{R}^0, \mathbb{R}^2\}$ model. The basis lies in a constant volume, finite element analysis (FEA) method using nano-scale time steps. The UT LOCA showed using nanosecond time steps leads to acceptable Fourier numbers.[9] While the mass flow rates involved are the pseudo steady-state values found from (36), the temperatures are considered purely transient. The effects of radiation are neglected due to the water filled channel.[20], [21] The energy balance is the transient version of the first law of thermodynamics:

$$\dot{E}_{st} = \dot{E}_{in} - \dot{E}_{out} + \dot{E}_{gen} \rightarrow \quad 50$$

$$\rho \forall c_p \frac{dT}{dt} = q_{cond} + q_{conv} + q_{gen} + \dot{m} \sum_k (\hat{h}_k + g z_k) \rightarrow \quad 51$$

$$\frac{dT}{dt} = \frac{1}{m(t) c_p(t)} \left[q_{cond} + q_{conv} + q_{gen} + \dot{m} \sum_k (\hat{h}_k + g z_k) \right] \quad 52$$

In the above balance, considerations are made for state dependent mass (based on temperature dependent density), specific heat and energy transfer. The water is considered to be entirely in the liquid phase at near STP with a small temperature change across the liquid region, allowing changes in specific energy to be approximated by changes in specific enthalpy.

Conductive Pathways

Geometry

The conduction equations used are standard mixed material conduction for square geometry. The differential radii of the gas and cladding regions are considered small enough to allow this.

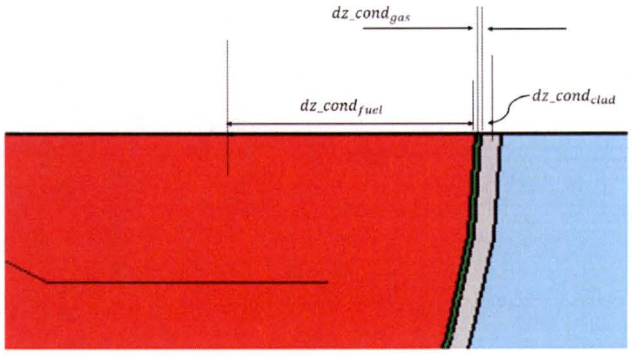

11. Radial Conduction Terms

Thus the conduction path between material A and B is defined as:

$$q_{cond,A}(t) = \frac{(T_B - T_A)A_{AB}}{\frac{dz_A}{k_A} + \frac{dz_B}{k_B}} \quad (53)$$

Here the differential heights are the distance from the geometric center to the boundary along the dimension of conduction. In FEA, all the conductive energies are considered inward so changes in

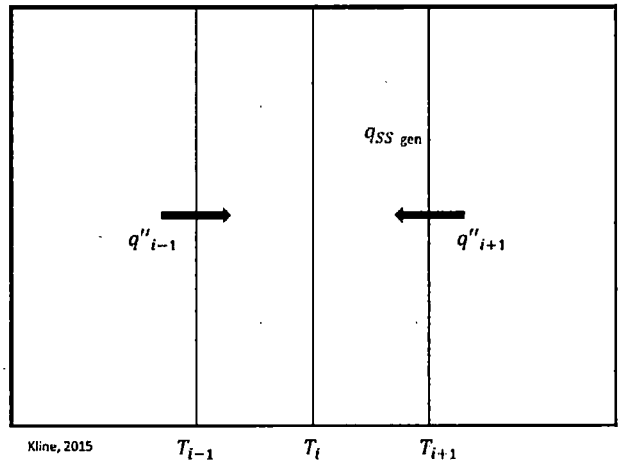

12. Conductive Layout for Finite Element Analysis

temperatures of the regions will naturally work out the proper energy transfer.[9], [21]

Heat Capacity

The specific heat capacity of the fuel element materials is considered to have a transient temperature dependence as well. The graphite specific heat is taken from a material properties chart and curve fit:[24]

$$c_{p,graph}(T,t) = .10795e^{8}T_G^{-3} - .61257e^{5}T_G^{-2} + .30795e^{-4}T_G + .44391 \quad (54)$$

This value has to be adjusted for (J/ kg K) by multiplying by 4183.995. The heat capacity of the fuel, like all values used for TRIGA fuel is taken from Simnad.[6]

$$c_{p,vol}\left\{\frac{J}{m^3K}\right\} = 2.04 + 4.17e - 3 \cdot T_F(t) \quad (55)$$

This gives the volumetric heat capacity but, the specific mass based version is required. Simnad again provides the equation for density:[6]

$$\rho_{Fuel} = \frac{1}{\left(\frac{U_{wt\%}}{\rho_U}\right) + \frac{(1 - U_{wt\%})}{\rho_{Zr}}} \quad (56)$$

This allows conversion to mass based using:

$$c_{p,fuel}\left\{\frac{J}{kg * K}\right\} = \frac{\rho_{Fuel}}{c_{p,vol}} \quad (57)$$

The specific heat capacities of the gas and clad were taken from Pacific Northwest National Laboratory and Makeitfrom materials websites.[47], [48]

Gas

The fundamentals of the gas film layer between the fuel and the cladding are taken mostly from Fenech.[49] The heat transfer coefficient is taken from the Kansas State SAR.[50] Using Fenech's correlation, the thermal conductivity can be found:

$$k_{gas} = \frac{\hat{h}_{gas}}{dR_{gas}} \tag{58}$$

The extreme complexities of the gas gap are simplified by assuming a constant consistency of Hydrogen, and a conductive behavior vice internal circulatory flow.

Work Terms

The work terms arise in the energy balance in the regions containing coolant flow. Constant volume, pseudo steady-state analysis involves both an enthalpy balance and potential energy change.

$$\dot{m}\sum_{k}\left(\hat{h}_k(T,t) + gz_k\right) \tag{59}$$

The enthalpy is dependent on both specific heat capacity and deviation in temperature from a reference temperature. The reference enthalpy is calculated at a reference temperature of 0°C with a value of 9007 (J/kg).

$$\hat{h}_k(T,t) = c_{p,k}(T,t)T_k(t) + \hat{h}_0 \tag{60}$$

The potential energy term is calculated using the differential pin axial height.

Heat Transfer Coefficient

The convection effects of the energy balance are considered using Newton's Law of Cooling[20] and the heat transfer coefficient relationship:

$$q_{conv,k}(T,t) = \tilde{h}_k A_{surf}\left(T_{clad,k} - T_k\right) \tag{61}$$

This requires finding an appropriate heat transfer coefficient. The heat transfer coefficient is considered constant over the length of each axial region.

Rayleigh Number

The Rayleigh number is a product of the Grashof and Prandtl numbers. The Grashof relates buoyancy and viscosity within a fluid:[20], [21]

$$Gr_{L,k} = \frac{g \cdot \tilde{\beta} \cdot \left(T_{clad,k} - T_k\right) \cdot {D_{pin}}^3}{\mu^2} \tag{62}$$

While the Prandtl number relates momentum and thermal diffusivities:[21]

$$Pr = \frac{\nu}{\alpha} \quad (63)$$

This leads to the Rayleigh number:[20]

$$Ra_{L,k} = Gr_{L,k}Pr = \frac{g\tilde{\beta}\left(T_{clad,k} - T_k\right)dz_k{}^3}{\alpha\nu}Pr \quad (64)$$

This number applies to each vertical coolant section individually, as the temperature of the channel and cladding varies axially.

Nusselt Number

The Nusselt number is the essential correlation in the convective phase. It relates convective and conductive heat transfer and is used to find the heat transfer coefficient. This model uses a vertical cylinder correlation relating the Prandtl and Rayleigh numbers for external free convection.[41]

$$\overline{Nu_{L,k}} = \left\{ .825 + \frac{.387Ra_{L,k}^{1/6}}{\left[1 + \left(\frac{.492}{Pr}\right)^{9/16}\right]^{8/27}} \right\}^2 \quad (65)$$

This correlation was chosen as it best represents the physical situation.

Heat Transfer Coefficient

The heat transfer coefficient can now be calculated using the Nusselt number correlation:[20]

$$\overline{Nu_{L,k}} = \frac{\tilde{h}_k dz_k}{k_{water}} \rightarrow \tilde{h}_k = \frac{\overline{Nu_{L,k}}k_{water}}{dz_k} \quad (66)$$

With the convective relationship found, the region specific energy balances can be built

Fuel Energy Balance

The fuel energy balance is the only region with heat generation. The other terms are conductive, as the cladding is the only convective boundary:

$$\frac{dT_F}{dt} = \frac{1}{m_F(t)c_{p,F}(t)}\left[P_{eff}(t) + \frac{\left(T_{graph,1}(t) - T_F(t)\right)A_{F,G}}{\left(\frac{dz_{graphite}}{k_{graphite}} + \frac{dz_{fuel}}{k_{fuel}}\right)} + \frac{\left(T_{graph,2}(t) - T_F(t)\right)A_{F,G}}{\left(\frac{dz_{graphite}}{k_{graphite}} + \frac{dz_{fuel}}{k_{fuel}}\right)} + \frac{\left(T_{gas,2}(t) - T_F(t)\right)A_{S-F,G}}{\left(\frac{dz\_cond_{gas}}{k_{gas}} + \frac{dz\_cond_{fuel}}{k_{fuel}}\right)}\right] \quad 67$$

The effective power is the value discussed in the neutronics decay heat calculations. The areas represent the surface areas along the conduction vector. The mass is calculated from the Simnad density equation (56). The remaining values are state variables.

Graphite Energy Balance

The graphite sections have similar energy balances. No energy is created internally and the border along the grid plate areas is considered insulated. This leaves conduction between the fuel and gas only:

$$\frac{dT_{graphite}}{dt} = \frac{1}{m_{graph}(t)c_{p,graph}(t)}\left[\frac{\left(T_F(t) - T_{graph,1}(t)\right)A_{F,G}}{\left(\frac{dz_{graphite}}{k_{graphite}} + \frac{dz_{fuel}}{k_{fuel}}\right)} + \frac{\left(T_{gas}(t) - T_{graph,1}(t)\right)A_{S-Graph,G}}{\left(\frac{dz\_cond_{gas}}{k_{gas}} + \frac{dz\_cond_{fuel}}{k_{graphite}}\right)}\right] \quad 68$$

Gas energy Balance

The gas is considered to interact via conduction and not convection. Its energy balance is:

$$\frac{dT_{gas,2}}{dt} = \frac{1}{m_{gas}(t)c_{p,gas}(t)}\left[\frac{(T_{gas,1}(t) - T_{gas,2}(t))A_{G-G}}{\left(\frac{dz_{graphite}}{k_{graphite}} + \frac{dz_{fuel}}{k_{graphite}}\right)} + \frac{(T_{gas,3}(t) - T_{gas,2}(t))A_{G-G}}{\left(\frac{dz_{graphite}}{k_{graphite}} + \frac{dz_{fuel}}{k_{graphite}}\right)}\right.$$
$$\left. + \frac{(T_{clad,2}(t) - T_{gas,2}(t))A_{S-Graph,C}}{\left(\frac{dz\_cond_{gas}}{k_{gas}} + \frac{dz\_cond_{clad}}{k_{clad}}\right)} + \frac{(T_{gas,2}(t) - T_F(t))A_{S-F,G}}{\left(\frac{dz\_cond_{gas}}{k_{gas}} + \frac{dz\_cond_{fuel}}{k_{fuel}}\right)}\right] \quad (69)$$

The axial region will determine either fuel or graphite interaction.

Clad Energy Balance

The cladding interacts conductively with the gas and clad, and convectively with the coolant channel. The energy balance is:

$$\frac{dT_{clad,2}}{dt} = \frac{1}{m_{clad}(t)c_{p,cald}(t)}\left[\frac{(T_{clad,1}(t) - T_{clad,2}(t))A_{C-C}}{\left(\frac{dz_{graphite}}{k_{clad}} + \frac{dz_{fuel}}{k_{clad}}\right)} + \frac{(T_{clad,3}(t) - T_{clad,2}(t))A_{C-C}}{\left(\frac{dz_{graphite}}{k_{clad}} + \frac{dz_{fuel}}{k_{clad}}\right)}\right.$$
$$\left. + \frac{(T_{gas,2}(t) - T_{clad,2}(t))A_{S-Graph,C}}{\left(\frac{dz\_cond_{gas}}{k_{gas}} + \frac{dz\_cond_{clad}}{k_{clad}}\right)} - \tilde{h}_2(t)A_{s-C,w}(T_{clad,2}(t) - T_{13}(t))\right] \quad (70)$$

This relationship is for the mid cladding; the other regions will have graphite interaction.

Water Channel Energy Balance

The water control volume balances the energy from the cladding surface temperatures and the mass balance. The mass of the water is found with the state's density and the volume of the coolant channel in that region.

$$\frac{dT_{coolant,2}}{dt} = \frac{1}{m_{coolant}(t)c_{p,coolant}(t)}\left[\tilde{h}_2(t)A_{s-C,w}\left(T_{clad,2}(t) - T_{13}(t)\right) + \dot{m}(\hat{h}_{in}(t) + gz_{in})\right.$$
$$\left. - \dot{m}(\hat{h}_{out}(t) + gz_{out})\right] \quad (71)$$

The inlet and outlet enthalpies are state dependent variables calculated using the previous time step's regional temperatures.

The energy balance considers the effects of heat generation through the effective power calculation, from neutronics. Mass flow rate model leads to the fluid energy transport, while conduction completes the surface interaction of heat transfer around the control volume. The transient equations of the energy balance are added to the linear system of neutronics to complete the $\{\mathbb{R}^0, \mathbb{R}^2\}$ model.

Output

The reactor instantaneous power is not recorded during the solution process, it is found afterwards from the neutron population vector using (20) and (3). This array is used to find the maximum power and time of occurrence.

The fuel temperature vector represents a core average temperature. To find a limiting temperature, a peaking factor formula must be used. This formula is power dependent:

$$PF(P_{inst}) = 2.433e^{-19}{P_{inst}}^3 - 5.3307e^{-13}{P_{inst}}^2 + 4.1352e^{-7}P_{inst} + 1.0094 \quad 72$$

This creates a vector the same length as the power and temperature vectors. The peaking factor and temperature vectors are multiplied elementally to find the transient peak temperature:

$$\vec{T}_{peak,n} = \vec{T}_{Fuel,m} PF_m \quad 73$$

The peak temperature vector is then searched for a maximum value and associated time.

UT TRIGA Specifics

The $\{\mathbb{R}^0, \mathbb{R}^2\}$ input values are made specific for the University of Texas at Austin TRIGA reactor. Below are lists of the variables, their values, and the source.

Fuel Specifications

The fuel burnup was calculated using ORIGIN and SCALE to find the burnup factor from the original inventory and the number density of ^{239}Pu and other trace elements. The gas layer is considered to be Hydrogen and the cladding is 304 stainless steel. UT uses 8.5wt%, 19.7% enriched Uranium with a Zr:H ratio of 1.6.

Table 2. University of Texas Fuel Specific Model Parameters

Parameter	Value	Source
Outer Pin Radius	.018771 (m)	UT SAR[13]
Inner Zr Rod Radius	.003175 (m)	UT SAR[13]
Cladding Thickness	.000508 (m)	UT SAR[13]
Gas Thickness	1.3105e^{-4} (m)	Fenech[49]
Active Fuel Region	.381 (m)	UT SAR[13]
Graphite Height	.087376 (m)	UT SAR[13]
Total Pin Height	.73152 (m)	UT SAR[13]
Burn Factor ^{235}U	.922896237	ORIGIN
Burn Factor ^{238}U	.863175801	ORIGIN
$U_{wt\%}$	8.5 (%kg/kg)	UT SAR[13]
Enrichment	19.7 (%)	UT SAR[13]
Mass of ^{239}Pu	.406333 (kg)	ORIGIN
K_{Beta}	1.077	GA Paper, UT SAR[12], [13]
l^*	51.9e^{-6} (s)	ORIGIN, SCALE
AmBe Source Strength	7.4e^{10} (n^0/s)	Calibration Certificate
k_{fuel}	17.573 (W/m K)	Simnad[6]
$k_{graphite}$	112.4 (W/m K)	Engineering Toolbox[24]

$c_{p,gas}$	14.53e^3 (J/kg K)	PNNL[51]
$c_{p,clad}$	500 (J/kg K)	Makeitfrom[48]
h_{gas}	2.84e^3 (W/m^2 K)	KSU SAR[50]

Core Geometrics

The parameters below are related to the core configuration at The University of Texas at Austin.

Table 3. University of Texas Core Geometry Model Specifics

Parameter	Value	Source
Number of Pins*	113.7 (#)	UT SAR[13]
Inner Coolant Hex Radius	.0217678 (m)	UT Core Drawing
α_M	3.8952e^{-6} $(\frac{\Delta k/k}{C})$	Lab Report[16]
Gravity	9.8066 (m/s^2)	UT SAR[13]
Kinematic Viscosity of Water	.279e^{-6} (m^2/s)	Engineering Toolbox[24]
Expansion Coefficient	.207e^{-3} (1/K)	Engineering Toolbox[24]

* The number of pins is a non-integer to account for the diameter variation between the fuel pins and the fuel followed control rods (FFCRs)

Programming

The $\{\mathbb{R}^0, \mathbb{R}^2\}$ model creates a set of 101 coupled linear ordinary differential equations and a number of state variables, requiring recalculation at each time step. These equations tend to be stiff due to rapid neutronics change relative to slower temperature changes, and require attention in solving.[2] It was decided that MATLAB would provide an appropriate environment due to its performance in handling linear systems.

The program is a set of triple nested code. A governing program is used to allow parallel computing of multiple events. This program calls the main function. The main function accounts for user input, site-

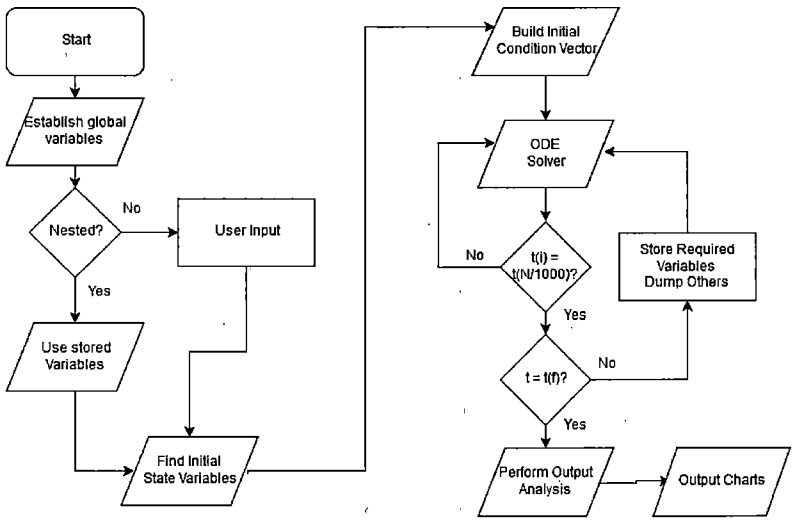

13. Block Diagram of UT TRIGA Solver

specific variables, calls the ODE, and creates outputs. The large ODE set and small time scale creates a memory burden. This is handled through creative use of a 'for' loop and ODE solver call. A basic flow diagram is below.

The program can be used in two ways, one as a called function from a governing program, the other prompts the user in the MATLAB command line. The program takes the initial conditions given and calculates the neutronics and thermal hydraulics based on a cold clean critical core for the input power.

During the ODE solution process a large amount of memory is used due to the system size and small time step. To increase performance, the ODE solver is nested. Beginning from time 0, it runs through a temporary final time dictated by the subdivision of the event final time. The column vectors of interest are stored in memory, the final row vector of time t(i) is stored as the initial condition of t(i+1) in the next loop, and the rest of the information, such as decay heat fractions, is deleted. This information is unnecessary for post run analysis but vital to an accurate solution. This method reduces the size of the read/write array the ode uses. Increases in performance include a $1/32^{nd}$ reduction in memory usage and $1/5^{th}$ reduction in solution time, while still tracking power and temperature for each time step.

ODE solver

ODE113 was the chosen ode solver. Mathworks recommends usage of ODE113 based on increased accuracy and performance.[52] The only issue of concern is the stiffness of the equations. ODE113 is a variable order method that uses information from previous iterations in calculation of the current. This makes it efficient and accurate. It uses a variable time step to ensure these meet the error requirements.[53] It also has the highest accuracy according to Mathworks. This method is used to

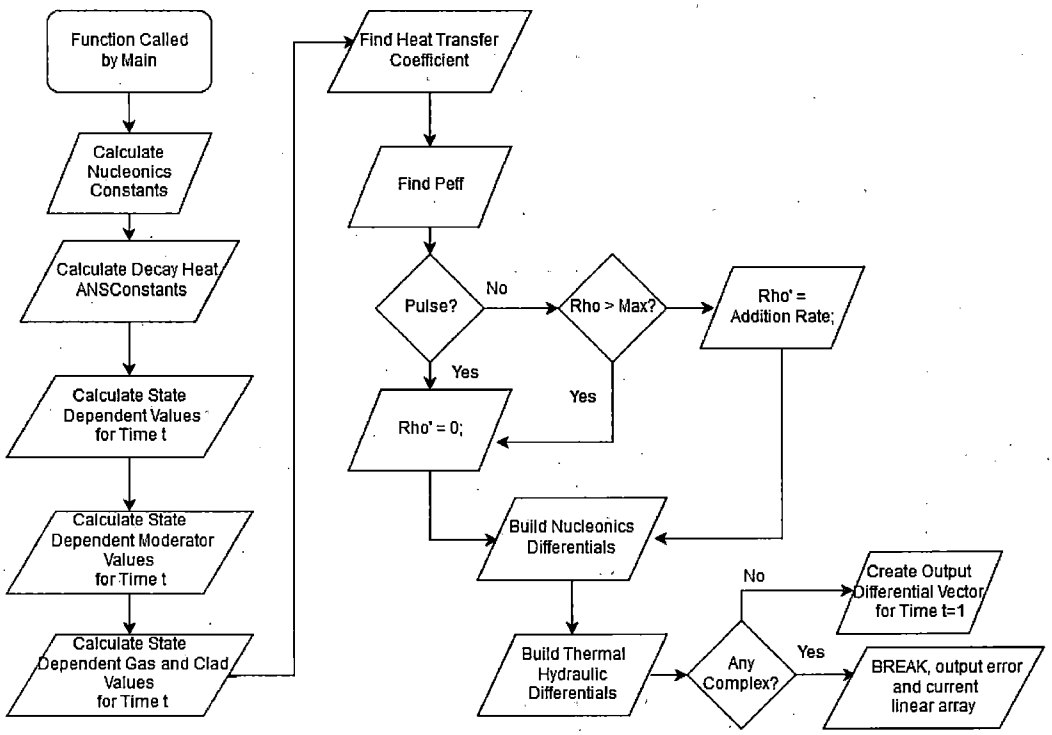

14. ODE Functional Block Diagram

solve the ODE function called by the main program:

The function begins by finding the current constants based on the global variables and neutronics constants. The previous loops temperature data is used to find the state of moderator based parameters. The current heat transfer coefficient is found followed by the current powers from (19-21).

If the event is a pulse, the change in reactivity is 0, as a pulse adds all of the reactivity instantaneously. If the event is a rod withdraw, the current event reactivity is compared to the maximum reactivity limit set by user input. If it is equal or above this, the change Is 0, otherwise the change is based on a reactivity addition rate.

The differential vector is built from the differential equations. It is then checked for complex values. The elements being solved for are real and physical values and should not contain complex numbers.[2] This is a method of checking for calculation execution errors in code and physical representation. If there are no errors in the array it is passed to the next time step.

Output Variable Tracking and Handling

Upon completion of the solver, the code finds the maximum power and temperature as discussed above. It then creates a reduced array for output to plots. The solution arrays are on the order of $5e^8$ in length. To reduce the size but keep fidelity, a subset of the arrays is chosen using 10,000 points each. The program outputs: Power, Temperature, Reactivity, maximum times for power and temperature, and the reduced arrays.

If the main function is nested in a solver script, as is the case for VnV, the output values are stored in a cell structure and the next event is processed.

Verification and Validation

Verification and validation of the model involves a number of steps including: verification of equations, ODE stability analysis, ODE drift analysis, comparison with pulse maintenance, reactor operation rod withdraw validation.

Event Validation

The University of Texas at Austin has an annual pulse comparison maintenance, SURV-7, that makes pulse output comparison very easy. The inherent 'reactivity added' value from the QNX pulse record window is not calculated using 8.5wt% Uranium of Zr:H of 1.6. In order to find a better approximation of the added reactivity, the Fuchs-Hansen model was solved based on the QNX recorded peak powers.[54]

Rod withdraw validation is based on the UT TRIGA reactor and set reactivity additions. The transient rod was brought to a height nearing the flatter portion of the differential rod worth curve (~370 units). This creates the most constant reactivity addition rate possible, as the rod drive speed is constant and the rod worth is at its flattest. The reactor was left for at least 20min at 50W. The rod was withdrawn to add the desired amount of total reactivity: $.20, $.30, $.40, $.50. It was the left to sit for a minimum of 10 min without any external interaction. All of the values were recorded using a local UT ICS program.[55]

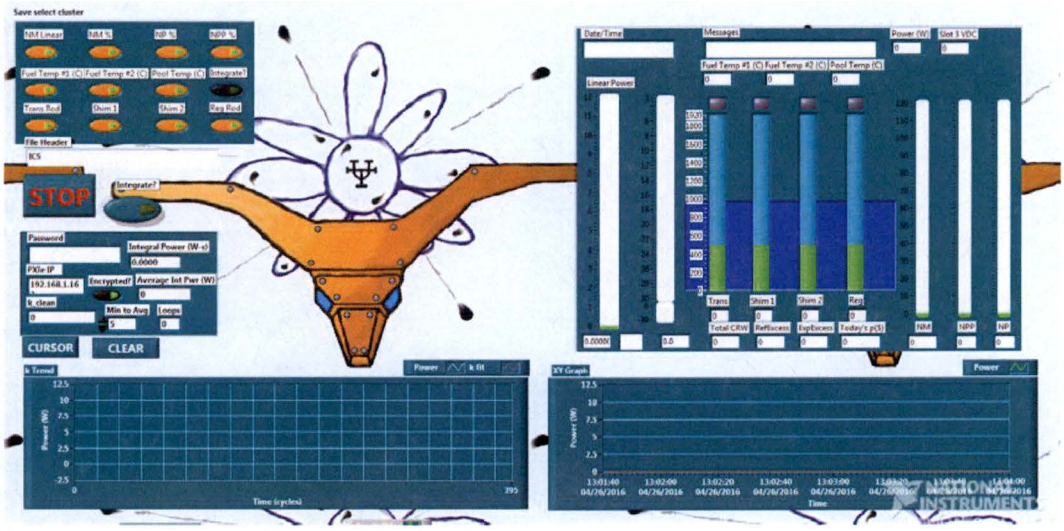

15. ICS Logging Program with LabVIEW and PXIe

The program continuously predicts, k_{eff}, allowing DNP equilibrium to be ensured. Additionally, it logs all outputs of the QNX screen at the same frequency the QNX program itself updates, allowing very little data loss and increased fidelity.

The data was analyzed using MATLAB's curve fitting tool to find the maximum powers and

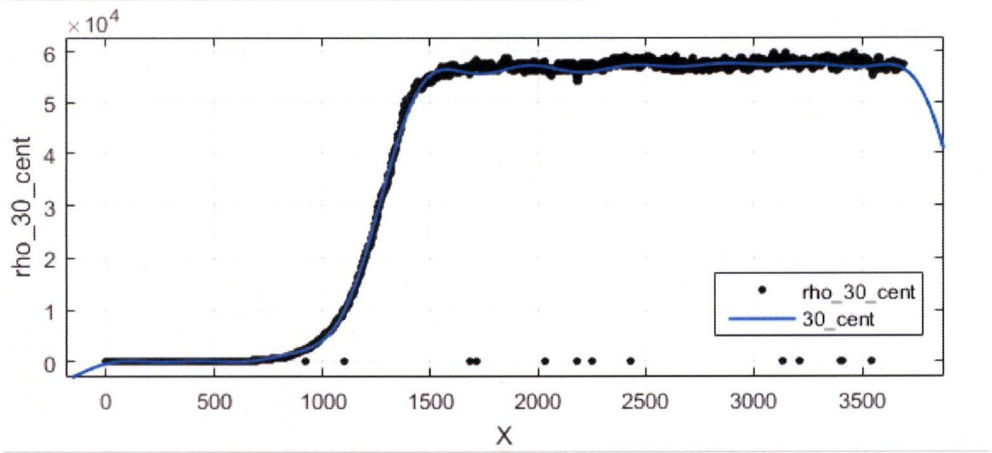

16. Curve Fitting $.30 Reactivty Addition Recorded Data

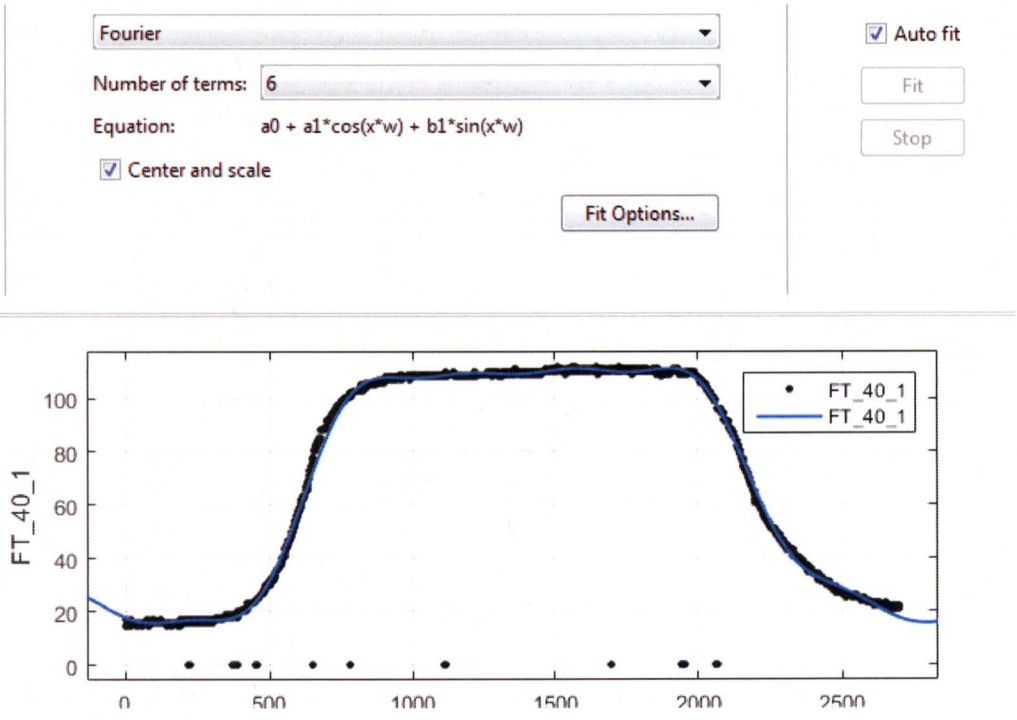

17. Curve Fitting Thermocouple Data

temperatures.

ODE Validation

ODE Solver Drift

The ODE equation set's size and relationships led to mild stiffness and solver drift possibilities. The initial few seconds of the incident are some of the worst, as a prompt jump event is combined with a sluggish thermal system, as the reactor is below the point of adding heat. The rod withdraw event has a linear reactivity addition. If the ODE solver is drifting considerably, the first initial seconds' reactivity

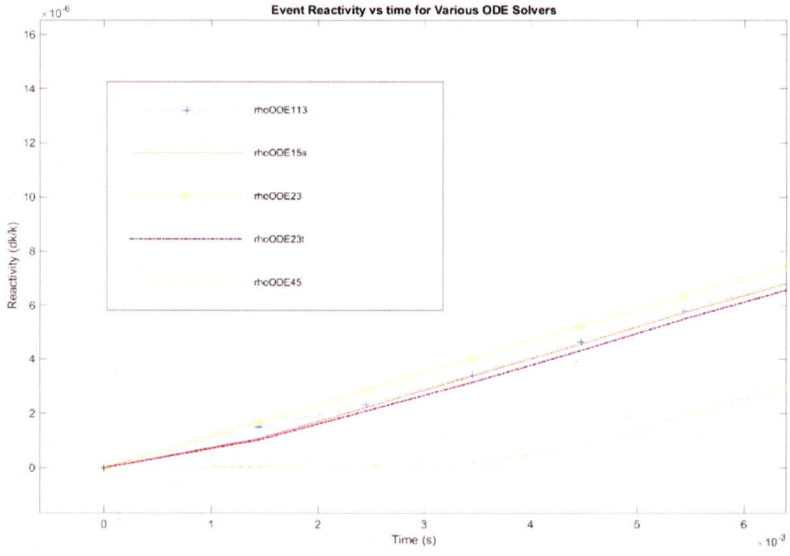

18. ODE Solver Drift in the Initial Model Time

curve will be nonlinear, as shown below.

This was the basis for choosing ODE 113, as the other options led to very nonlinear initial seconds. ODE45 was initially chosen, until initial drift, above, was noticed. The reactivity added from a rod withdraw should be linear in this case, since the reactivity addition rate is constant. ODE23 and 15 provided excessive deviation in the previous $\{\mathbb{R}^0, \mathbb{R}^0\}$ model.

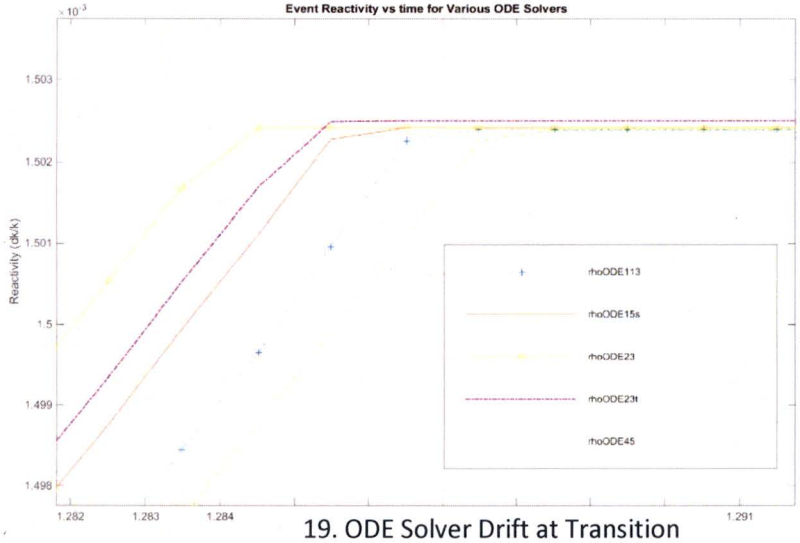

19. ODE Solver Drift at Transition

The additional benefit of ODE113 is the efficiency with high error tolerances. The default settings for ODE solvers is $1e^{-3}$ (~.1%) of the local and absolute values. This means the higher decimal places are neglected. With an even like a prompt jump or neutronics right at the point of deviation from criticality, this can be very error prone. The settings were increased to a local and absolute error of $1e^{-9}$, which decreases step size and increases solution time. This makes the choice of ODE113 even more justifiable.

ODE Perturbation Analysis

In addition to the ODE selections, the model was verified using uncertainty analysis. The factors affecting differential temperature were varied based on partial derivative error analysis:

$$y = f(\boldsymbol{x}, \boldsymbol{\theta}, t)\ where: \boldsymbol{x} \rightarrow variables, \boldsymbol{\theta} \rightarrow constants \tag{74}$$

$$\delta y = \sqrt{\sum \left(\frac{\partial y}{\partial x_i}\delta x_i\right)^2 + \sum \left(\frac{\partial y}{\partial \theta_j}\delta \theta_j\right)^2} \tag{75}$$

In this method, the partial derivatives of the main function with respect to all variables and constants are found. In the model, constants are values like geometric dimensions. These have a fixed error that is state-independent. Variables are items that are state-dependent, such as Rayleigh number, or thermal conductivity. This leads to a maximum and minimum equation for the time step's change. The ODE set was rerun with this new value set and error bars on the model based on perturbations were found. This is expressed below by the use of error bars.

Results

Pulses

The $\{\mathbb{R}^0, \mathbb{R}^2\}$ model was run in pulse mode for all of the reactivities of the last 18 pulses. Comparisons were made between both peak power and peak temperature. The input reactivity was taken from the

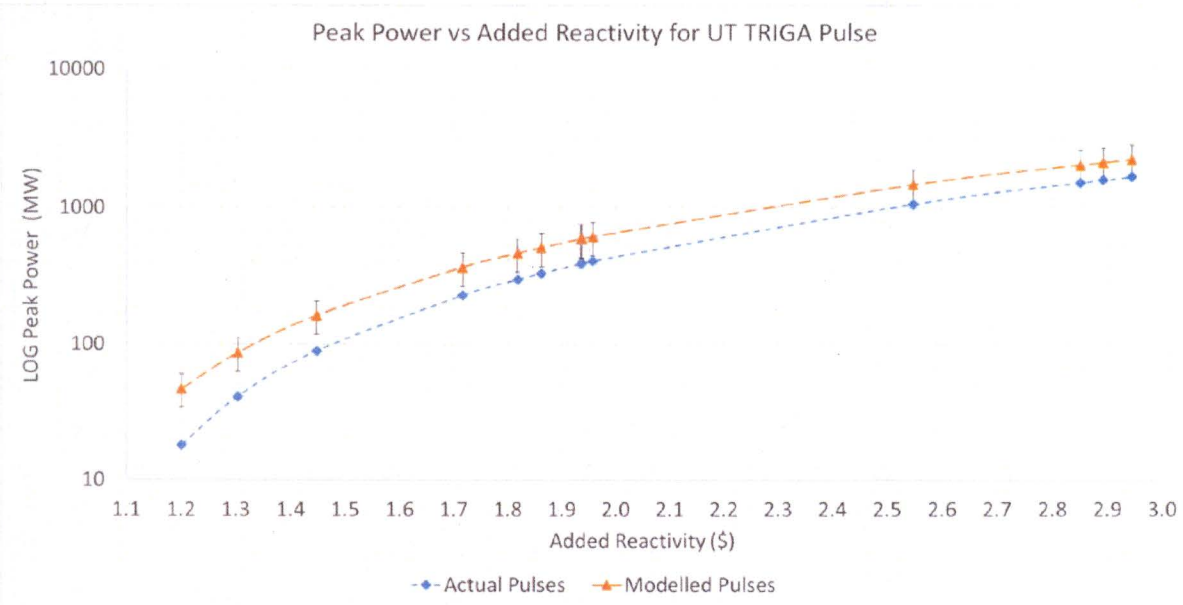

21. Peak Power Vs. Added Reactivity for Modelled and Actual Pulses at UT TRIGA

actual peak powers of the pulses and solved using the Fuchs-Hansen Model

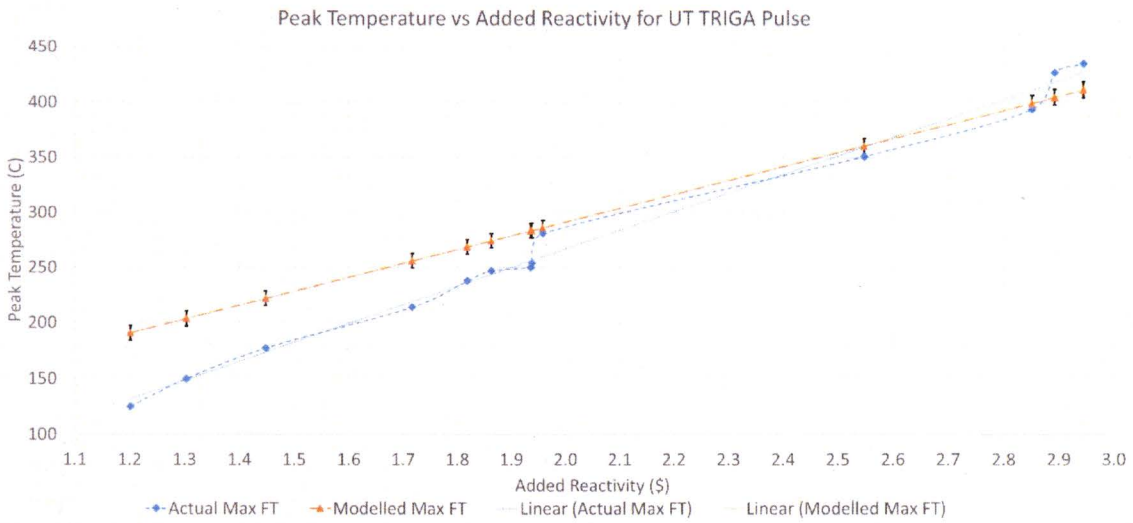

20. Peak Temperature Vs. Added Reactivity of Modelled and Actual Pulses at UT TRIGA

$$P_{max} = \frac{(\rho')^2}{2l\gamma} \tag{76}$$

The error between the model and reality tends to decrease as the added reactivity increases. This can be seen by the convergence of the two curves on a log scale.

Errors in actual measured temperature include a new IFE installed on 2016, which has a higher peaking factor due to lower fission product poison inventory and minimal burnup.

Rod Withdraw

Four rod withdraw events were run in addition to the pulses. Reactivity additions above $.50 were avoided as the continuous withdraw causes periods beyond the measurability of the NM-1000 and this

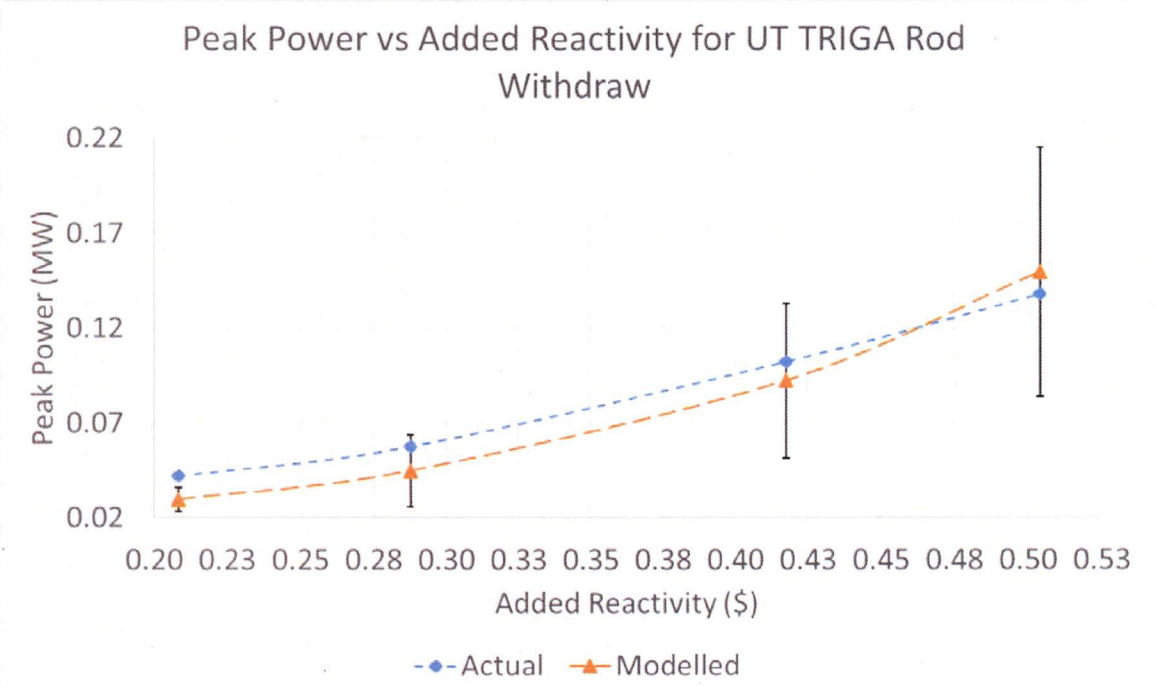

22. Peak Power Vs. Added Reactivity for Modelled and Actual Rod Withdraw Events at UT TRIGA

is considered undesirable.

Much like the pulse event, the error decreases with reactivity. It is also worth noting the underestimation of temperature below $.35 and the overestimation above it, additionally the power follows the same trend but at $.47. This effect will be analyzed during the momentum model.

Both temperature and peak power errors decrease in absolute value with reactivity within the event. Further investigation is required for events with low reactivity additions and those in the area of prompt criticality.

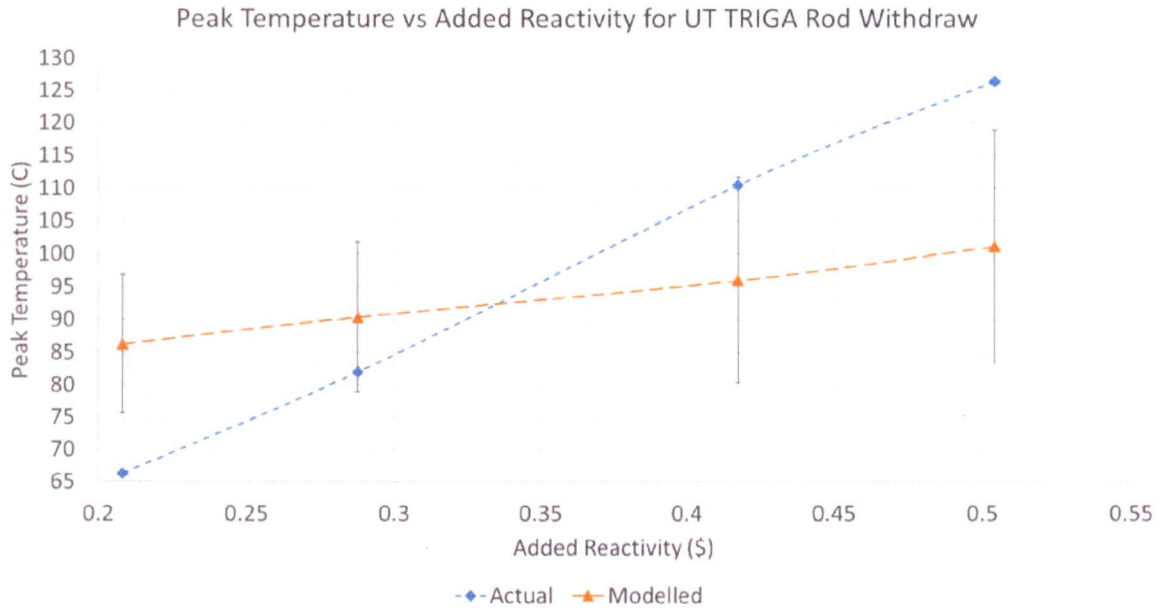

24. Peak Temperature Vs Added Reactivity for Modelled and Actual Rod Withdraw Events

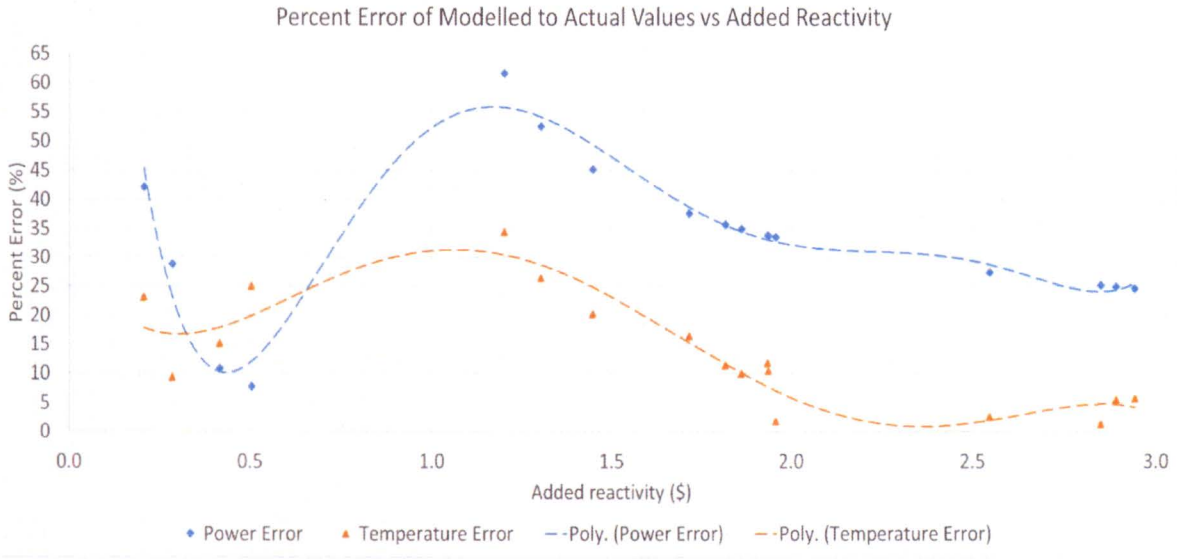

23. Percent Error of Modelled to Actual Values Vs. Event Reactivity

It is worth noting that the slopes of the temperature error trends for both pulse and rod withdraw are in the same relative direction. This implies a global trend error, possibly corrected in the momentum version.

The median errors and standard deviations can be found in the table below. The error is split by region for the pulses since the behavior of higher reactivity additions tends to have lower overall error between model and reality.

Table 4. Error Percentages in Model VnV

	Median Error (%)	Standard Deviation (%)
Pulse Peak Power	33.9	10.6
Pulse Peak Temperature	10.4	9.6
Pulse Peak Power ($1-1.5)	52.5	8.2
Pulse Peak Temperature ($1-1.5)	3.5	7.1
Pulse Peak Power ($1.5-2)	35.0	1.6
Pulse Peak Temperature ($1.5-2)	11.4	2.6
Pulse Peak Power (>$2.5)	25.2	3.8
Pulse Peak Temperature (>$2.5)	2.6	2.1
Rod Withdraw Peak Power	19.8	13.9
Rod Withdraw Peak Temperature	19.1	6.3

Sources of Error

The greatest source of error in the $\{\mathbb{R}^0, \mathbb{R}^2\}$ model is the lack of dimensions. Point kinetics using a reactivity balance is much less representative than an $\{\mathbb{R}^3, \mathbb{R}^3\}$ kinetic model would be.[2] However, the complexity increases by the power of n for each additional dimension in the calculations alone.[2] Adding to the point kinetics error is the use of a single energy neutron speed. Lethargy and core geometrics play key roles that are estimated, vice accounted for, in the reactivity balance.[2], [14] Additionally, an $\{\mathbb{R}^3, \mathbb{R}^3\}$ model would solve locally for each pin and its interactions with the surrounding pins, as well as control rod effects. This would remove the need for a peaking factor correction, as it would be part of the solution.

The constant mass flow rate assumption is better represented by a constant momentum balance over an increased amount of regions. This would incorporate the Darcy friction factor and flow processes occurring at the endpoints of the fuel pin.

The use of GA-7882 temperature coefficient of reactivity takes complex nuclear processes and lumps them into a temperature dependence. It is worth noting, the fuel temperature accuracy increased markedly in the model when switching from a constant value to this curve. This shows good correlation between actual UT TRIGA kinetics and those predicted in GA-7882.

The material properties' temperature dependence is curve fit to engineering tables. These tables and the measurements to make them carry inherent error. Alongside this, most fluids correlations are best fit data assumptions. The complexity of fluid flow goes well beyond that which can be correlated with a simple equation.

The ODE solver error was large at first but then reduced, however, the equation set has not been perturbed in an effort to find the bookend error values.

The site-specific values carry measurement error, both the values from UT SAR and drawings for the model as well as the measured values used in model VnV as the actual. For example, peak power measured by the QNX software.

When performing VnV, the input reactivity for the actual pulses is calculated using the Fuchs-Northeim model.[54], [56] This error pays into the final outcome but would have little to no bearing on the error

within the system. It acts almost as a mild perturbation on the ODE input, which is accounted for in ODE113.[57]–[61]

Unanticipated Transient Analyses

The model can be used to predict the outcome of events such as unanticipated reactivity addition events. This allows reactivity insertion limits to be analyzed. Using the criteria in previous work,[5], [7], [8], [13] and the model outputs, the limiting pulse reactivity additions are found below:

Table 5. Reactivity Addition Limits for Limiting Fuel Temperatures for TRIGA LEU

Limit	Reactivity Added ($)	Peak Temperature (C)	Percentage of Technical Specifications Limit (%)
Safety Limit[13]	6.21	950	213
Hawley Limit[5]	6.16	940	211
Argonne Pulse Limit[7]	5.60	830	187
Transient Rod Worth (2016)	3.36	475	107
UT Technical Specification	3.14	445	100

Pulse Event

The maximum reactivity added due to an unanticipated pulse event is limited by the total rod worth of the transient rod. The rack and pinion design of the standard control rods prevents any rod ejection event on the order of a pulse. Thus for the current core configuration the limiting pulse causes a peak

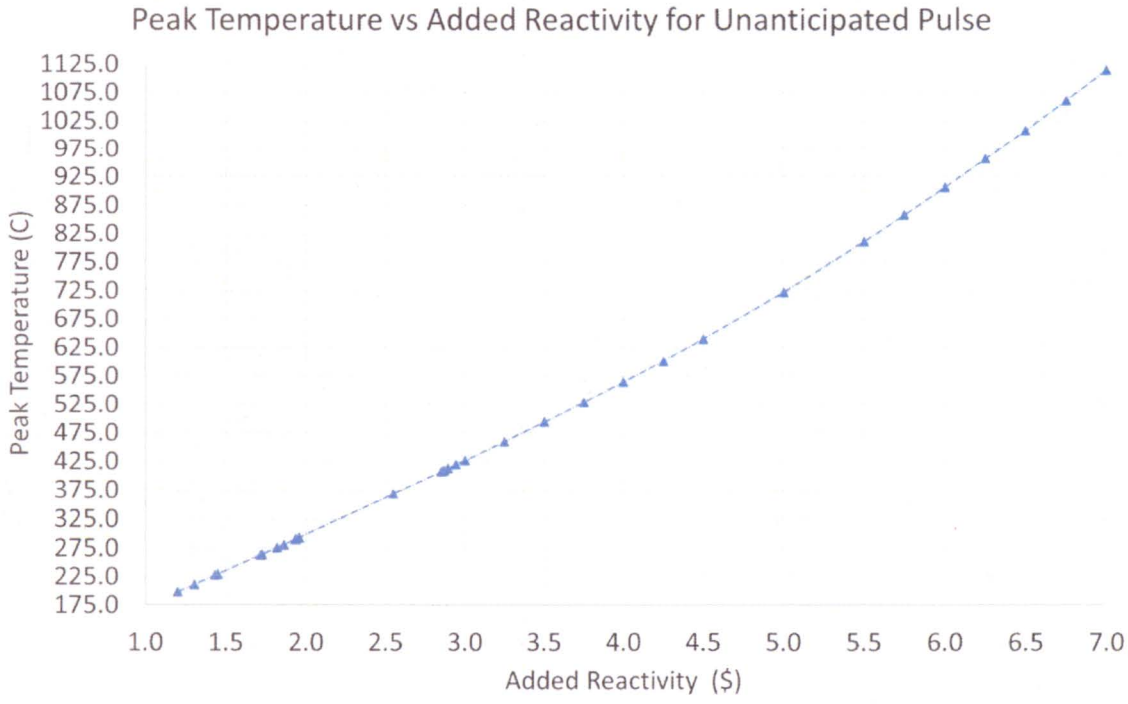

25. Predicted Peak Fuel Element Temperature Vs Added Reactivity

temperature of only 475°C.

Given the extreme rate of rod ejection of the pulse under normal circumstances, the event is considered a step insertion and variations in transient rod pressure are ignored.

Rod Withdraw Event

An unanticipated rod withdraw event can be caused by multiple sources including: grounded armature magnets, failed relay inputs, or control circuitry; however, any failure results in the same general outcome so only the reactivity addition event is analyzed. The maximum reactivity value used is the UT SAR's excess reactivity limit of $7.[13] This considers the worst possible case: a critical reactor with maximum possible excess reactivity.

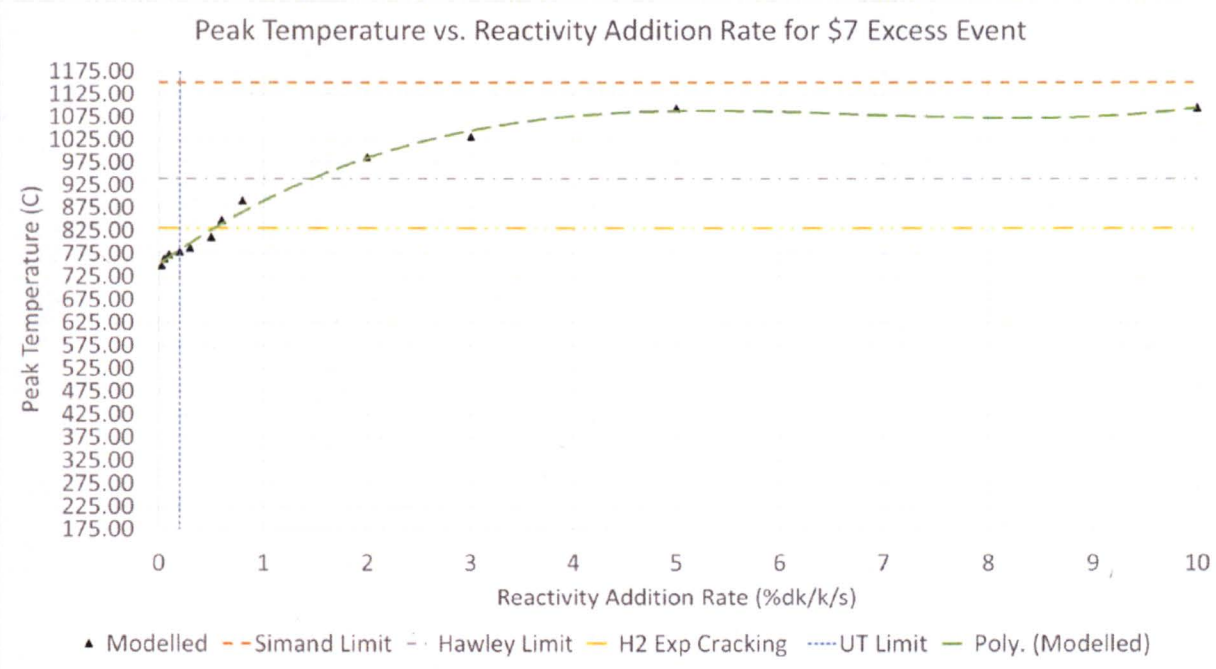

26. Peak Temperature Vs. Reactivity Addition Rate for an Unanticipated Rod Withdraw Event

The figure above shows the peak temperatures modelled as a result of an unanticipated $7 insertion from a rod withdraw. The vertical blue line represents the UT reactivity addition limit, which shows that the if the event were to take place at UT with the maximum allowable reactivity, the Argonne suggested limit to prevent hydrogen cracking would not be exceeded.

It is also worth noting that above ~2%dk/k the peak temperature flattens and approaches, but does not exceed the Simnad limit.

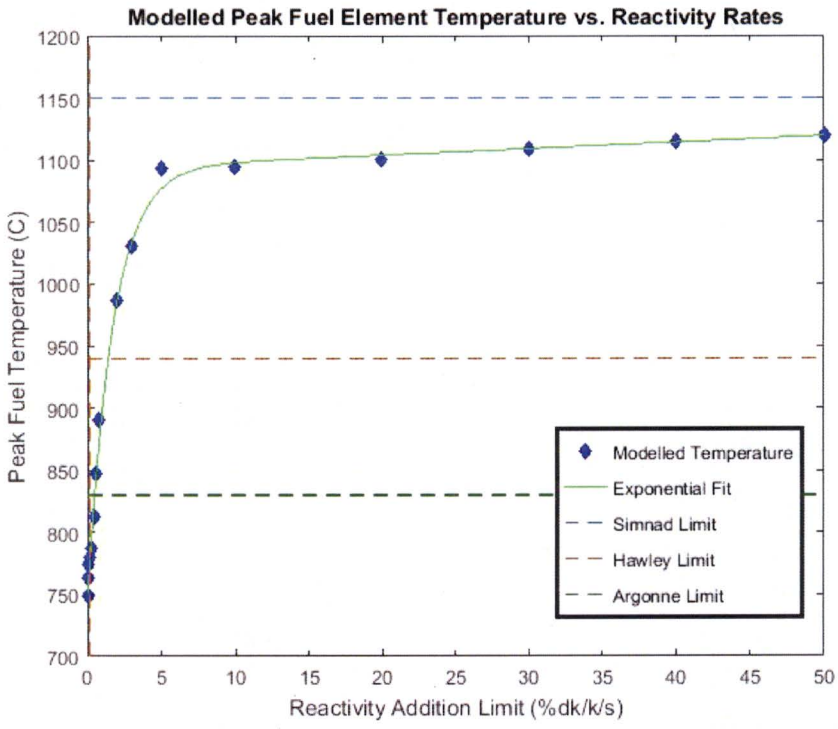

28. Extended Analysis of Reactivity Addition Rate

Reactivity Addition Rate (%dk/k)	Added Energy (MWs)
0.025	26.78
0.05	26.81
0.10	27.93
0.20	28.81
0.30	29.98
0.50	31.52
0.60	33.71
0.70	37.02
0.80	42.53
0.90	44.60
2.00	45.02
3.00	58.53
5.00	92.07
10.00	129.57
Pulse	130.58

27. Energy added for a $7 reactivity addition

It is worth noting that above ~2%dk/k the peak temperature flattens and approaches, but does not exceed the Simnad limit.

Conclusions

The methods used in modeling these transients provide transient power and temperature performance in good agreement with experimental data.

From the modeling and data above, it can be seen that the peak fuel temperature is related both to the total reactivity added and the rate at which it is added.

Pulsing to $7 does not exceeds the Simnad limit during transient and non-pulsing operations; pulsing to approximately $5.5 does not exceed 825°C.

Because the peak temperature levels off when adding approximately 2%δk or more, the Simnad limit is not exceeded.

References

[1] M. Johnson and M. Johnson, "Modeling of Reactor Kinetics and Dynamics Modeling of Reactor Kinetics and Dynamics," Idaho Falls, 2010.

[2] L. M. S. Ziya Akcasu, Gerald S. Lellouche, *Mathematical Methods in Nuclear Reactor Dynamics*. New York, NY: Academic Press, 1971.

[3] G. Atomics, "Technical Foundation of TRIGA," San Diego, CA, 1958.

[4] D. R. Tobergte and S. Curtis, "Kinetic Behavior of TRIGA Reactors," in *Conference on Utilization of Research Reactors*, 1967.

[5] R. L. K. S. C. Hawley, "NUREG/CR-2387: Credible Accident Analyses for TRIGA and TRIGA-Fueled Reactors," 1982.

[6] M. T. Simnad, "The U-ZrHx Alloy: Its Properties and Use in TRIGA Fuel," *Nucl. Eng. Des.*, vol. 64, pp. 403–422, 1981.

[7] Argonne National Laboratory, "Pulsing Temperature Limit for TRIGA LEU Fuel.pdf," San Diego , CA, 2008.

[8] Argonne National Laboratory, "Fundamental Approach to TRIGA Steady-State Thermal-Hydraulic CHF Analysis," San Diego, CA, 2007.

[9] G. Kline, "UT LOCA 2016," 2016.

[10] G. Kline, "LOSS OF COOLANT ACCIDENT ANALYSIS FOR THE UNIVERSITY OF TEXAS AT AUSTIN," 2016.

[11] D. Karnopp, R. Rosenberg, and A. S. Perelson, "System Dynamics: A Unified Approach," *IEEE Trans. Syst. Man. Cybern.*, vol. 6, no. 10, 1976.

[12] D. R. Tobergte and S. Curtis, "GA-7882 Kinetic Behavior of TRIGA Reactors," in *Conference on Utilization of Research Reactors*, 1967, p. 39.

[13] M.Krause, "The University of Texas at Austin TRIGA Safety and Analysis Report," Austin, TX, 1991.

[14] L. E. Weaver, *Reactor Dynamics and Control*. New York, NY: American Elsevier Publishing Company, 1968.

[15] P. N. Haubenreich, "Prediction of Effective Yields of Delayed Neutrons in MSRE," 1962.

[16] K. Dayman, "Laboratory 5 : Temperature Feedbacks on Reactivity," 2013.

[17] V. E. Schrock, "A Revised ANS Standard for Decay Heat from Fission Products," 1973.

[18] R. G. R. G. Rehm, R. Howard, and H. R. Baum, "The equations of motion for thermally driven, buoyant flows," *J. Res. Natl. Bur. Stand. (1934).*, vol. 8, no. 3, p. 297, 1978.

[19] A. Wirth, "A Guided Tour Through Buoyancy Driven Flows and Mixing," p. 66, 2015.

[20] F. P. Incropera, D. P. DeWitt, T. L. Bergman, and A. S. Lavine, *Fundamentals of Heat and Mass Transfer*, vol. 6th. 2007.

[21] T. L. Bergman, A. S. Lavine, F. P. Incropera, and D. P. DeWitt, *Fundamentals of Heat and Mass*

Transfer. 2011.

[22] J. Cleveland, N. Aksan, P. Vijayan, and A. Nayak, "Natural circulation in water cooled nuclear power plants," *Ewp.Rpi.Edu*, no. November, 2005.

[23] D. GmBH, "Liquid Density Calculaiton," 2016. [Online]. Available: http://ddbonline.ddbst.de/DIPPR105DensityCalculation/DIPPR105CalculationCGI.exe?component=Water.

[24] Engineeringtoolbox.com, "Property Tables," *Engineeringtoolbox.com*, 2016. [Online]. Available: http://www.engineeringtoolbox.com/water-thermal-properties-d_162.html.

[25] N. Convection, "Natural Convection," vol. 1, pp. 735–777, 2003.

[26] P. Talukdar, "Natural/Free Convection."

[27] D. Coast, "Plumes and Thermals," pp. 163–180.

[28] D. T. Allen and C. J. Durrenberger, "Gaussian Plume Modeling." 2014.

[29] R. Huang, "Lecture 7: Reduced Gravity models of the wind-driven circulation," pp. 1–19, 2006.

[30] A. Example and G. C. Equation, "Extended Surface Heat Transfer," no. 2, pp. 1–10.

[31] D. Roncati, "Iterative calculation of the heat transfer coefficient," no. 2.

[32] N. G. Narve, N. K. Sane, and R. T. Jadhav, "Natural Convection Heat Transfer from Symmetrical Triangular Fin Arrays on Vertical Surface," vol. 4, no. 5, pp. 775–780, 2013.

[33] S. Edition, "10–6 ■ heat transfer from finned surfaces," pp. 432–447, 2008.

[34] D. W. Mackowski, "Conduction Heat Transfer Notes for MECH 7210."

[35] L. F. Crabtree, R. L. Dommett, and J. G. Woodley, "Estimation of Heat Transfer to Flat Plates , Cones and Blunt Bodies : Estimation of Heat Transfer to Flat Plates , Cones and Blunt Bodies," no. 3637, 1970.

[36] P. Talukdar, "HEAT CONDUCTION THROUGH."

[37] X. He, D. P. M. Van Gils, E. Bodenschatz, and G. Ahlers, "Prandtl- and Rayleigh-number dependence of Reynolds numbers in turbulent enard convection at high Rayleigh and small Prandtl numbers," pp. 1–5.

[38] R. S. Subramanian, "Natural or Free Convection," pp. 1–7.

[39] S. Mirapalli and P. S. Kishore, "Heat Transfer Analysis on a Triangular Fin," vol. 19, no. 5, pp. 279–284, 2015.

[40] F. M. White, *Fluid Mechanics*. 2003.

[41] P. State, "External Flow Correlations (Average , Isothermal Surface) Internal Flow Correlations (Local , Fully Developed Flow)," 2016.

[42] B. R. S. Bartlett and B. R. S. Bartlett, "Tables of Supersonic Symmetrica ! Flow around Right Circular Cones , with and without the Addition of Heat at the Wave Tables of Supersonic Symmetrical Flow around Right Circular Cones , with and without the Addition of Heat at the

Wave," 1968.

[43] "G5A0V." .

[44] J. F. Wendt and P. Fn, "AIR FORCE SYSTEMS COMMAND," 1972.

[45] K. J. Yaser Hadad, "Laminar Forced Convection Heat Transfer from Isothermal Bodies with Unit Aspect Ratio," pp. 443–451, 2008.

[46] M. OCW, "fin-design." .

[47] W. G. Luscher and K. J. Geelhood, "Material Property Correlations : Comparisons between FRAPCON, FRAPTRAN and MATPRO," no. August, 2010.

[48] "Material Properties of Metals," 2016. [Online]. Available: makeitfrom.com.

[49] Henri Fenech, *Heat Transfer and Fluid Flow in Nuclear Systems*. Pergamon Press, 1981.

[50] Kansas State, "Kansas State University Safety and Analysis Report '06." KSU, Manhatten, 2006.

[51] "Hydrogen properties." .

[52] "Mathworks," *Mathworks.com*, 2016. [Online]. Available: http://www.mathworks.com/help/matlab/ref/ode45.html?s_tid=gn_loc_drop#References.

[53] "Mathworks," *Mathworks.com*, 2016. .

[54] C. Johnson, "Lab 6 – Reactor Pulse," 2013.

[55] G. Kline, "PXIe_ICS_Power_Cal_Etc_2015." Greg Kline, Austin, TX, p. 100, 2015.

[56] N. I. S. D. of the IAEA, "IAEA TRIGA," 2004. [Online]. Available: https://ansn.iaea.org/Common/documents/Training/TRIGA Reactors (Safety and Technology)/chapter1/characteristics33.htm. [Accessed: 01-Jan-2016].

[57] P. Howard, *Analysis of ODE Models*. 2009.

[58] L. F. Shampine, "Error Estimation and Control for ODEs," *J. Sci. Comput.*, vol. 25, no. 1, pp. 3–16, 2005.

[59] O. A. Chkrebtii and A. Science, "Probabilistic solution of differential equations for Bayesian uncertainty quantification and inference," 2013.

[60] H. Report, T. Mark, and I. I. Pulsing, "General. dynamics," 1998.

[61] H. Banks and S. Hu, "Propagation of Uncertainty in Dynamical Systems," *Ncsu.Edu*, 2011.

[62] G. Kline, "UT {R^0,R^2 } Model." 2016.

Appendix

Mass Balance Program

Main Function File Version 4.6.2

```
function [ P_out, T_out, t_out, rho_out, max_P, max_T, max_P_t, max_T_t ] =
in_hour_EQN_4_6_2_FUNC( R_in, t_in, RR_in, type)
%% HEADER
% In-hour EQN solver
% Author: Greg Kline
% Date: 08 Jan 2016
% Revision Date 15 Jun 2016
% Revision: 4.6.2
%
% Modelling of a pulse insertion as well as a rod withdraw event.
%
%
% The purpose of this code is to simulate both a pulse event and a continuous
% rod withdraw event.
%
% The parameters are modelled using the University of Texas parameters
% Revisions
% 4.1.0
%     - Added Plutonium 239 to mixture
%     - Accounted for core fuel burnup
% 4.6.0
%     - Expanded temperature regions to 6 from 2 ( 1 fuel 1 mod, to 3 fuel 3 mod)
%
% P_out is the vector of power vs time (MW)
% T_out is the vector of temperature vs time (C)
% t_out is time (s)
% rho_out is the event reactivity vs time (dk/k)
% max_P is max Power (MW)
% max_T is max temperature (C)
% max_P_t is the time of peak power (s)
% max_T_t is the time of peak temperature (s)
% R_in is the reactivity limit ($)
% t_in is the max time (s)
% RR_in is the reactivity addition rate in (dk/k/s)
% type is model type: 'Rod Withdraw' or 'Pulse'
%
% Example:
% [ P_out, T_out, t_out, rho_out, max_P, max_T, max_P_t, max_T_t ] =
in_hour_EQN_4_6_2_FUNC( 3, 10, .001170, 'Rod Withdraw')
%
% Pseudo Code
% Global Variables
%     - Define the global variables that talk to the ODE solving function
%
% User Input
%     - When not in function mode, the user input pings the MATLAB command
%         line for the same function inputs
%
% Fuel Constants
%     - Define the geometric constants IAW local values
%     - Define material properties IAW Simnad and local values
%
% Neutronics Constants
%     - Define isotope fractions
%     - Find the mixture delayed neutron fraction and decay constant
%     - Account for spontaneous fission
%
% Decay Heat Constants
%     - Define the ANS Standard decay heat constants
%
% Define State Dependent Functions using the initial conditions as the state
%     - Find material state properties
%     - Find initial flux
%     - Find instantaneous power
%
```

```
% Find Total Power
%
% Build Initial Condition Vector
%     - Neutronics ICs
%     - Thermal-hydraulic ICs
%     - Event Reactivity IC
%
% Output
%     - Find the instantaneous power from neutron population
%     - Find maximum
%     - Calculate peaking factor vector
%     - Apply to temperature vector
%     - Downsize output vectors
%

tic

%% Global Constants
global Tinit_fuel Tinit_mod  Max_reactivity Reactivity_add_rate
global  N_238 N_235 surface_area_fuel volume_core pin_height
global mass_U_235 mass_U_238 mass_fuel_mix  Event_type density_fuel
global N_Pu_239 mass_Pu_239 l_star  alpha_mod volume_cooling_core
global Area_pin_internal dz_cond_fuel mass_graphite_half_core
global surface_area_graphite area_cooling_pin graphite_height number_pins
global volume_cooling_graphite_core dz_cond_grap radius_pin inner_radius

%% User Input
% Default values are shown in []

% Model Type
% Constants for use in function method
Initial_Power = 50;
Tinit_fuel = 16;
Tinit_mod = 20;

% From user input
Max_reactivity = R_in;
t_f = t_in;
Reactivity_add_rate = RR_in;
Model_type = type;
Event_type = type;

% Make a nice display for the output
display(sprintf(['Your model is: \n' ...
    '   Model Type: %s \n' ...
    '   Reactivity addition rate(dk/k): %2.2d dk/k \n' ...
    '   Maximum Reactivity($): $%d \n' ...
    '   Initial Power(W): %dW \n' ...
    '   Initial Fuel Temperature(C): %dC \n' ...
    '   Initial Moderator Temperature(C): %dC \n' ...
    '   Duration (s): %ds \n'], Model_type, Reactivity_add_rate, ...
    Max_reactivity, Initial_Power, Tinit_fuel, Tinit_mod, t_f));

display(' Beginning Calculations  ... ');

 %% User Input Non-Function Version
% % Default values are shown in []
%
% % Model Type
%
% MT = input( 'Which model are you going to use? Pulse, Rod Withdraw, Both. [Both]',
's');
%
% if isempty(MT)
%     Model_type = 'Both';
%     Event_type = 'Pulse';
%
% elseif strcmp(MT, 'Rod Withdraw')
%     Model_type = 'Rod Withdraw';
%     Event_type = 'Rod Withdraw';
%
```

```
% elseif strcmp(MT, 'Pulse')
%     Model_type = 'Pulse';
%     Event_type = 'Pulse';
%
% elseif strcmp(MT, 'Both')
%     % This will run function file twice once with each model so select
%     % pulse first
%     Model_type = 'Both';
%     Event_type = 'Pulse';
%
% else
%     Model_type = 'Pulse';
%     Event_type = 'Pulse';
% end
%
% % Reactivity Limit/Insertion(Pulse)
% MR = input( 'What is the maximum reactivity for the event? ($) [$2.94]');
%
% if MR <= 0
%     display ('   Reactivity must be a positive value, using default');
%     Max_reactivity = 2.944447748;
%
% elseif MR >= 13
%     display (sprintf(['   This reactivity exceeds the total rod worth of the '...
%     'UT TRIGA core, results may not be accurate']));
%     Max_reactivity = MR;
%
% elseif isnan(MR)
%     display ('   Reactivity must be a numeric value, using default');
%     Max_reactivity = 2.944447748;
%
% elseif isempty(MR)
%     display ('   Reactivity must be a numeric value, using default');
%     Max_reactivity = 2.944447748;
%
% elseif MR > 3.1429 && MR < 13
%     display ('   Reactivity exceeds UT TechSpec limits ');
%     Max_reactivity = MR;
%
% else
%     Max_reactivity = MR;
% end
%
% % Initial Power (W)
% IP = input('What is the initial power? (W) [50W]');
%
% if IP <= 0
%     display ('   Initial Power must be a positive value, using default');
%     Initial_Power = 50;
%
% elseif isnan(IP)
%     display ('   Initial Power must be a numeric value, using default');
%     Initial_Power = 50;
%
% elseif isempty(IP)
%     display ('   Initial Power must be a numeric value, using default');
%     Initial_Power = 50;
%
% elseif IP > 1.1e6
%     display ('   Initial Power exceeds UT TechSpec limits ');
%     Initial_Power = IP;
%
% else
%     Initial_Power = IP;
% end
%
% % Initial Fuel Temperature (C)
% iFT = input('What is the initial fuel temperature? (C) [20C]');
%
% if iFT <= 0
%     display ('   Initial Fuel Temperature must be a positive value, using default');
```

```
%     Tinit_fuel = 20;
%
% elseif isnan(iFT)
%     display ('   Initial Fuel Temperature must be a numeric value, using default');
%     Tinit_fuel = 20;
%
% elseif isempty(iFT)
%     display ('   Initial Fuel Temperature must be a numeric value, using default');
%     Tinit_fuel = 20;
%
% elseif iFT > 950
%     display ('   Initial Fuel Temperature exceeds UT TechSpec limits ');
%     Tinit_fuel = iFT;
%
% else
%     Tinit_fuel = iFT;
% end
%
% % Initial Moderator Temperature (C)
% iMT = input('What is the initial moderator temperature? (C) [20C]');
%
% if iMT <= 0
%     display ('   Initial Moderator Temperature must be a positive value, using
default');
%     Tinit_mod = 20;
%
% elseif isnan(iMT)
%     display ('   Initial Moderator Temperature must be a numeric value, using
default');
%     Tinit_mod = 20;
%
% elseif isempty(iMT)
%     display ('   Initial Moderator Temperature must be a numeric value, using
default');
%     Tinit_mod = 20;
%
% elseif iMT > 48
%     display ('   Initial Moderator Temperature exceeds UT TechSpec limits ');
%     Tinit_mod = iMT;
%
% else
%     Tinit_mod = iMT;
% end
%
% % time length
% ft = input('How long of a run? (s)');
% % check values
% if ft <= -0
%     t_f = 100;
%     display('Time cannot be negative, using 100s');
%
% elseif isnan(ft)
%     t_f = 100;
%     display('Time must be a number, using 100s');
%
% elseif isempty(ft)
%     t_f = 100;
%     display('Time must be a number, using 100s');
%
% else
%     t_f = ft;
%
% end
%
% if sum(strcmp(Model_type, {'Both','Rod Withdraw'}))
%     RR = input('What is the reactivity addition rate?(dk/k) [.002dk/k]');
%
%     if RR <= 0
%         display ('   Reactivity must be a positive value, using default');
%         Reactivity_add_rate = .002;
%
```

```
%     elseif isnan(RR)
%         display ('   Reactivity must be a numeric value, using default');
%         Reactivity_add_rate = .002;
%
%     elseif isempty(RR)
%         display ('   Reactivity must be a numeric value, using default');
%         Reactivity_add_rate = .002;
%
%     elseif RR > .2
%         display ('   Reactivity exceeds UT TechSpec limits ');
%         Reactivity_add_rate = RR;
%
%     else
%         Reactivity_add_rate = RR;
%     end
%
%     % Make a  nice display for the output
%     display(sprintf(['Your model is: \n' ...
%         '   Model Type: %s \n' ...
%         '   Reactivity addition rate(dk/k): %2.2d dk/k \n' ...
%         '   Maximum Reactivity($): $%d \n' ...
%         '   Initial Power(W): %dW \n' ...
%         '   Initial Fuel Temperature(C): %dC \n' ...
%         '   Initial Moderator Temperature(C): %dC \n' ...
%         '   Duration (s): %ds \n'], Model_type, Reactivity_add_rate, ...
%         Max_reactivity, Initial_Power, Tinit_fuel, Tinit_mod, t_f));
%
% elseif ~sum(strcmp(Model_type, {'Both','Rod Withdraw'}))
%
%     Reactivity_add_rate = 0;
%
%     % Make a  nice display for the output
%     display(sprintf(['Your model is: \n' ...
%     '   Model Type: %s \n' ...
%     '   Maximum Reactivity($): $%d \n' ...
%     '   Initial Power(W): %dW \n' ...
%     '   Initial Fuel Temperature(C): %dC \n' ...
%     '   Initial Moderator Temperature(C): %dC \n' ...
%     '   Duration(s): %d \n'], Model_type, Max_reactivity, ...
%     Initial_Power, Tinit_fuel, Tinit_mod, t_f));
%
% else
%     display(' There is a model error');
%
% end
%
% display(' Beginning Calculations  ... ');

%% fuel constants %%%

%%% Geometry %%%
% Pin radius (m)
radius_pin = 0.018771; % .735in
inner_radius = 0.003175; %.125in

% clad width (m)
dl_clad = 0.000508;

% Active region (m)
pin_height = .381;
graphite_height = 0.087376;
dz_cond_fuel = .5 * pin_height;
dz_cond_grap = .5 * graphite_height;
Graphite_offset_from_tip = .087884;

% pin fuel volume (m^3)
volume_pin = pi * pin_height * ((radius_pin-dl_clad)^2 - inner_radius^2);

% pin graphite volume (m^3)
volume_graphite_pin = pi * radius_pin^2 * graphite_height;
```

```
% surface area graphite (m^2)
surface_area_graphite = 2 * pi * radius_pin * graphite_height;

% surface area of pin (m^2)
surface_area_fuel = 2 * pi * radius_pin * pin_height;

%%% Reactor Constants %%%
% Number of pins (#)
number_pins = 113.7; % account for FFCR smaller diameter

% Volume of the core (m^3)
volume_core = volume_pin * number_pins;

% Volume of graphite in one half of core (m^3)
volume_graphite_half_core = volume_graphite_pin * number_pins;

% Surface area core (m^2)
surface_area_fuel = surface_area_fuel * number_pins;

% Radius of cooling hexagon (m)
inner_hex = 0.0217678;
outer_hex = 0.025146;

% Total spatial area of cooling hex and pin (m^2)
total_space = sqrt(3)/2 * (2 * inner_hex)^2;

% Area of pin radially (m^2)
Area_pin_internal = pi * radius_pin^2;

% Area of cooling hexagon around pin (m^2)
area_cooling_pin = total_space - Area_pin_internal;

% Volume of cooling (m^3)
% total pin height (m)
total_pin_height = 0.73152;

% the water mass uses the entire height of pin, not just heated length
volume_cooling_pin = area_cooling_pin * pin_height;
volume_cooling_graphite_pin = area_cooling_pin * graphite_height;

volume_cooling_core = volume_cooling_pin * number_pins;
volume_cooling_graphite_core = volume_cooling_graphite_pin * number_pins;

% Flow inlet area (m^2)
% pin top (m^2)
area_top_pin = .00063789;

% area of grid plate hole (m^2)
area_grid_hole = pi * (0.038227/2)^2;

% flow area of a pin (m^2)
flow_area_pin_upper = area_grid_hole - area_top_pin;

flow_outlet_core = flow_area_pin_upper * number_pins;

flow_area_pin_lower = 0.00063885; %m^2

flow_inlet_core = flow_area_pin_lower * number_pins;

% Channel width (m)
width_channel = 0.0061976;

% Percent Burn (Fraction)
burn_factor_238 = 0.922896237;
burn_factor_235 = 0.863175801;

%%% Fuel meat constants %%%
% wt% U_238
U_wt = .085;

% enrichment percentage (fraction) [UT SAR]
```

```
Enrich = .197; % 19.7%

% density (kg/m^3) [Simnad]
density_U = 19070;

% density of ZrH based on ratio (kg/m^3)[Simnad]
density_Zr = 1 / (.1706 + .0042 * 1.6) * 1000;

% Material Densities (kg/m^3)
density_fuel = 1 / ( U_wt / density_U + (1 - U_wt) / density_Zr ); %[Simnad]

% density of Pu 239 based on burnup equations (kg/m^3)
density_Pu239 = 19618;

% density of graphite (kg/m3)
density_graphite = 2500;

% Avogadro's number (atoms/mol)
N_A = 6.022e23;

% Molar mass (kg/mol) [Burns]
M_U = .23807;

% Molar mass Pu239 (kg/mol)
M_Pu = .2390521634;

% Molar mass Sm (kg/mol)
M_Sm = .15036;

% Molar mass Zr (kg/mol)
M_Zr = .091224;

%%% Masses %%%
% Mass Uranium (kg)
mass_U_pin = density_fuel * volume_pin * U_wt;

% Mass U235 (kg)
mass_U_235_pin = mass_U_pin * Enrich;

% Mass U238 (kg)
mass_U_238_pin = mass_U_pin - mass_U_235_pin;

% Mass Pu239 (kg)
mass_Pu239_pin = density_Pu239 * volume_pin;

% Mass Zr per pin (kg)
mass_ZrH_pin = density_fuel * volume_pin * ( 1- U_wt );

% Total U238 mass (kg)
mass_U_238 = mass_U_238_pin * number_pins;

% Total U235 mass (kg)
mass_U_235 = mass_U_235_pin * number_pins;

% Total Pu239 mass (kg)
mass_Pu_239 = mass_Pu239_pin * number_pins;

% Total Fuel Mass (kg)
mass_fuel_mix = density_fuel * volume_pin * number_pins;

% Total mass of one half of graphite (kg)
mass_graphite_half_core = density_graphite * volume_graphite_half_core * number_pins;

%%% Number Densities %%%
% Number density of U238 per pin (atoms/m^3)
N_238_pin = ( mass_U_238_pin / M_U * N_A ) / volume_pin  * burn_factor_238;

% Number density of U235 per pin (atoms/m^3)
N_235_pin = ( mass_U_235_pin / M_U * N_A ) / volume_pin  * burn_factor_235;

% Number density Pu239 per pin (atoms/m^3)
```

```
% N_Pu_239_pin = ( mass_Pu_239 / M_Pu * N_A ) / volume_pin;
N_Pu_239_pin = 0.406333333 / M_Pu * N_A;

% Number density of Sm per pin (atoms )
% constants for Sm and Pu are found from neutronics burnup data and
% are in units of kg/m^3
N_Sm_pin = 0.077307608 / M_Sm * N_A * volume_pin;

% Number density of ZR per pin (atoms)
N_Zr_pin = ( mass_ZrH_pin / M_Zr * N_A ) / 2.6;

% Number density U238 per core (atoms/m^3)
N_238 = N_238_pin * number_pins;

% Number density U235 per core (atoms/m^3)
N_235 = N_235_pin * number_pins;

% Number Density Pu239 per core (atoms/m^3)
% This value is taken from burn data so it does not need corrected
N_Pu_239 = N_Pu_239_pin * number_pins;

% Number of Sm (atoms)
N_Sm = N_Sm_pin * number_pins;

% Number of Zr (atoms)
N_Zr = N_Zr_pin * number_pins;

% fuel negative coefficient of reactivity in del_k/k/C [UT SAR]
alpha_fuel = -1e-4;

% Moderator temperature coefficient (del_k/k/C)
 alpha_mod = 3.8952e-6;

%% neutronics constants
% Group Lambdas
% U235
U235_L_1 = .0127;
U235_L_2 = .0317;
U235_L_3 = .115;
U235_L_4 = .311;
U235_L_5 = 1.40;
U235_L_6 = 3.87;

% U238
U238_L_1 = .0132;
U238_L_2 = .0321;
U238_L_3 = .139;
U238_L_4 = .358;
U238_L_5 = 1.41;
U238_L_6 = 4.02;

% Pu239
Pu239_L_1 = .0129;
Pu239_L_2 = .0313;
Pu239_L_3 = .135;
Pu239_L_4 = .333;
Pu239_L_5 = 1.36;
Pu239_L_6 = 4.04;

% total delayed neutron fraction U238 [Weaver, 1968]
B_238 = .0157;
% group i fraction is B * relative abundance
B_1_238 = B_238 * .013; %group 1
B_2_238 = B_238 * .137;
B_3_238 = B_238 * .162;
B_4_238 = B_238 * .388;
B_5_238 = B_238 * .225;
B_6_238 = B_238 * .075;

% total delayed neutron fraction U235 [Weaver, 1968]
B_235 = .0065;
```

```
B_1_235 = B_235 * .038;
B_2_235 = B_235 * .213;
B_3_235 = B_235 * .188;
B_4_235 = B_235 * .407;
B_5_235 = B_235 * .128;
B_6_235 = B_235 * .026;

% total delayed neutron fraction Pu239
B_Pu_239 = .0026;
B_1_Pu_239 = B_Pu_239 * .038;
B_2_Pu_239 = B_Pu_239 * .280;
B_3_Pu_239 = B_Pu_239 * .216;
B_4_Pu_239 = B_Pu_239 * .328;
B_5_Pu_239 = B_Pu_239 * .103;
B_6_Pu_239 = B_Pu_239 * .035;

% define fission cross sections for precursor ratios
%fission cross section (m^2)
sig_f_238 = 3.3e-28;

%fission cross section (m^2)
sig_f_235 = 584.4e-28;

% fission cross section (m^2)
sig_f_Pu_239 = 747.4e-28;

% Absorption cross sections for poisons (m^2)
% Zr, Zirconium has 5 stable isotopes, NIST provides cross sections for each
% so a weighted average is taken Zr 90, 91, 92, 94, 95
sig_a_Zr = .5145 * .011e-28 + .1132 * 1.17e-28 + .1719 * .22e-28 ...
    + .1728 * .0499e-28 + .0276 * .0229e-28;

% Samarium has 7 stable states (m^2)
sig_a_Sm = .031 * .7e-28 + .151 * 57e-28 + .113 * 2.4e-28 ...
    + .139 * 42080e-28 + .074 * 104e-28 + .266 * 206e-28 ...
    + .226 * 8.4e-28;

% neutron velocity (m/s)

% Boltzmann constant (m2 kg s-2 K-1)
k_b = 1.38064852e-23;

% Mass of neutron (kg)
m_nu = 1.674927471e-27;

% velocity neutron = 2197;
velocity_neutron = sqrt( 2 * k_b * (Tinit_fuel + 273.15) / m_nu );

% U235 Beta factor (atoms/s)
Beta_factor_U235 = velocity_neutron * sig_f_235 * N_235;

% U238 Beta factor (atoms/s)
Beta_factor_U238 = velocity_neutron * sig_f_238 * N_238;

% Pu239 Beta factor (atoms/s)
Beta_factor_Pu239 = velocity_neutron * sig_f_Pu_239 * N_Pu_239;

% Beta of the DNP mix
B_1_mix = ( Beta_factor_U238 * B_1_238 + Beta_factor_U235 * B_1_235 ...
    + Beta_factor_Pu239 * B_1_Pu_239) ...
    / ( Beta_factor_U238 + Beta_factor_U235 + Beta_factor_Pu239);
B_2_mix = ( Beta_factor_U238 * B_2_238 + Beta_factor_U235 * B_2_235 ...
    + Beta_factor_Pu239 * B_2_Pu_239) ...
    / ( Beta_factor_U238 + Beta_factor_U235 + Beta_factor_Pu239);
B_3_mix = ( Beta_factor_U238 * B_3_238 + Beta_factor_U235 * B_3_235 ...
    + Beta_factor_Pu239 * B_3_Pu_239) ...
    / ( Beta_factor_U238 + Beta_factor_U235 + Beta_factor_Pu239);
B_4_mix = ( Beta_factor_U238 * B_4_238 + Beta_factor_U235 * B_4_235 ...
    + Beta_factor_Pu239 * B_4_Pu_239) ...
    / ( Beta_factor_U238 + Beta_factor_U235 + Beta_factor_Pu239);
B_5_mix = ( Beta_factor_U238 * B_5_238 + Beta_factor_U235 * B_5_235 ...
```

```
    + Beta_factor_Pu239 * B_5_Pu_239) ...
    / ( Beta_factor_U238 + Beta_factor_U235 + Beta_factor_Pu239);
B_6_mix = ( Beta_factor_U238 * B_6_238 + Beta_factor_U235 * B_6_235 ...
    + Beta_factor_Pu239 * B_6_Pu_239) ...
    / ( Beta_factor_U238 + Beta_factor_U235 + Beta_factor_Pu239);

% Lambda of the DNP mix
lambda_1 = ( Beta_factor_U238 * U238_L_1 + Beta_factor_U235 * U235_L_1 ...
    + Beta_factor_Pu239 * Pu239_L_1) ...
    / ( Beta_factor_U238 + Beta_factor_U235 + Beta_factor_Pu239);
lambda_2 = ( Beta_factor_U238 * U238_L_2 + Beta_factor_U235 * U235_L_2 ...
    + Beta_factor_Pu239 * Pu239_L_2) ...
    / ( Beta_factor_U238 + Beta_factor_U235 + Beta_factor_Pu239);
lambda_3 = ( Beta_factor_U238 * U238_L_3 + Beta_factor_U235 * U235_L_3 ...
    + Beta_factor_Pu239 * Pu239_L_3) ...
    / ( Beta_factor_U238 + Beta_factor_U235 + Beta_factor_Pu239);
lambda_4 = ( Beta_factor_U238 * U238_L_4 + Beta_factor_U235 * U235_L_4 ...
    + Beta_factor_Pu239 * Pu239_L_4) ...
    / ( Beta_factor_U238 + Beta_factor_U235 + Beta_factor_Pu239);
lambda_5 = ( Beta_factor_U238 * U238_L_5 + Beta_factor_U235 * U235_L_5 ...
    + Beta_factor_Pu239 * Pu239_L_5) ...
    / ( Beta_factor_U238 + Beta_factor_U235 + Beta_factor_Pu239);
lambda_6 = ( Beta_factor_U238 * U238_L_6 + Beta_factor_U235 * U235_L_6 ...
    + Beta_factor_Pu239 * Pu239_L_6) ...
    / ( Beta_factor_U238 + Beta_factor_U235 + Beta_factor_Pu239);

% Beta mix
% Beff correction factor based on Beff/B ratio for U235 (.007/.0065)
% Weaver and Hetrick show up to 30% difference between B and Beff
Beta_correction = 1.076923076923077;

% Beta mix
Beta_mix = B_1_mix + B_2_mix + B_3_mix + B_4_mix + B_5_mix + B_6_mix;

% Beff mix
Beff_mix = Beta_mix * Beta_correction;

%prompt neutron lifetime (s) [UT SAR]
l_star = 51.9e-6;
% l_star = 41e-6;

% 2 Ci AmBe source (atoms/s)
AmBe_source = 7.4e10;

% U238 spontaneous fission (atoms/s)
U238_spontaneous = 1.80e-2 * mass_U_238 * 1000; % factor in (n/g-s)

% U235 spontaneous fission (atoms/s)
U235_spontaneous = 7.43e-4 * mass_U_235 * 1000; % factor in (n/g-s)

% Pu239 spontaneous fission (atoms/s)
Pu_239_spontaneuos = 2.30e-2 * mass_Pu_239 * 1000;

%% Decay Heat Constants %%%
% Decay (1/s)
% U235
H_lambda_235(1) = 2.2138e1;
H_lambda_235(2) = 5.1587e-1;
H_lambda_235(3) = 1.9594e-1;
H_lambda_235(4) = 1.0314e-1;
H_lambda_235(5) = 3.3656e-2;
H_lambda_235(6) = 1.1681e-2;
H_lambda_235(7) = 3.5870e-3;
H_lambda_235(8) = 1.3930e-3;
H_lambda_235(9) = 6.2630e-4;
H_lambda_235(10) = 1.8906e-4;
H_lambda_235(11) = 5.4988e-5;
H_lambda_235(12) = 2.0958e-5;
H_lambda_235(13) = 1.0010e-5;
H_lambda_235(14) = 2.5438e-6;
H_lambda_235(15) = 6.6361e-7;
```

```
H_lambda_235(16) = 1.2290e-7;
H_lambda_235(17) = 2.7213e-8;
H_lambda_235(18) = 4.3714e-9;
H_lambda_235(19) = 7.5780e-10;
H_lambda_235(20) = 2.4786e-10;
H_lambda_235(21) = 2.2384e-13;
H_lambda_235(22) = 2.4600e-14;
H_lambda_235(23) = 1.5699e-14;

% U238
H_lambda_238(1) = 3.2881e00;
H_lambda_238(2) = 9.3805e-1;
H_lambda_238(3) = 3.7073e-1;
H_lambda_238(4) = 1.1118e-1;
H_lambda_238(5) = 3.6143e-2;
H_lambda_238(6) = 1.3272e-2;
H_lambda_238(7) = 5.0133e-3;
H_lambda_238(8) = 1.3655e-3;
H_lambda_238(9) = 5.5158e-4;
H_lambda_238(10) = 1.7873e-4;
H_lambda_238(11) = 4.9032e-5;
H_lambda_238(12) = 1.7058e-5;
H_lambda_238(13) = 7.0465e-6;
H_lambda_238(14) = 2.3190e-6;
H_lambda_238(15) = 6.4480e-7;
H_lambda_238(16) = 1.2649e-7;
H_lambda_238(17) = 2.5548e-8;
H_lambda_238(18) = 8.4782e-9;
H_lambda_238(19) = 7.5130e-10;
H_lambda_238(20) = 2.4188e-10;
H_lambda_238(21) = 2.2739e-13;
H_lambda_238(22) = 9.0536e-14;
H_lambda_238(23) = 5.6098e-15;

% Pu239
H_lambda_Pu239(1) = 1.0020e1;
H_lambda_Pu239(2) = 6.4330e-1;
H_lambda_Pu239(3) = 2.1860e-1;
H_lambda_Pu239(4) = 1.0040e-1;
H_lambda_Pu239(5) = 3.7280e-2;
H_lambda_Pu239(6) = 1.4350e-2;
H_lambda_Pu239(7) = 4.5490e-3;
H_lambda_Pu239(8) = 1.3280e-3;
H_lambda_Pu239(9) = 5.3560e-4;
H_lambda_Pu239(10) = 1.7300e-4;
H_lambda_Pu239(11) = 4.8810e-5;
H_lambda_Pu239(12) = 2.0060e-5;
H_lambda_Pu239(13) = 8.3190e-6;
H_lambda_Pu239(14) = 2.3580e-6;
H_lambda_Pu239(15) = 6.4500e-7;
H_lambda_Pu239(16) = 1.2780e-7;
H_lambda_Pu239(17) = 2.4660e-8;
H_lambda_Pu239(18) = 9.3780e-9;
H_lambda_Pu239(19) = 7.4500e-10;
H_lambda_Pu239(20) = 2.4260e-10;
H_lambda_Pu239(21) = 2.2100e-13;
H_lambda_Pu239(22) = 2.6400e-14;
H_lambda_Pu239(23) = 1.3800e-14;

% Power fraction
% U235
H_fraction_235(1) = 6.5057e-1;
H_fraction_235(2) = 5.1264e-1;
H_fraction_235(3) = 2.4384e-1;
H_fraction_235(4) = 1.3850e-1;
H_fraction_235(5) = 5.5440e-2;
H_fraction_235(6) = 2.2225e-2;
H_fraction_235(7) = 3.3088e-3;
H_fraction_235(8) = 9.3015e-4;
H_fraction_235(9) = 8.0943e-4;
H_fraction_235(10) = 1.9567e-4;
```

```
H_fraction_235(11) = 3.2535e-5;
H_fraction_235(12) = 7.5595e-6;
H_fraction_235(13) = 2.5232e-6;
H_fraction_235(14) = 4.9948e-7;
H_fraction_235(15) = 1.8531e-7;
H_fraction_235(16) = 2.6608e-8;
H_fraction_235(17) = 2.2398e-9;
H_fraction_235(18) = 8.1641e-12;
H_fraction_235(19) = 8.7797e-11;
H_fraction_235(20) = 2.5131e-14;
H_fraction_235(21) = 3.2176e-16;
H_fraction_235(22) = 4.5038e-17;
H_fraction_235(23) = 7.4791e-17;

% U238
H_fraction_238(1) = 1.2311e00;
H_fraction_238(2) = 1.1486e00;
H_fraction_238(3) = 7.0701e-1;
H_fraction_238(4) = 2.5209e-1;
H_fraction_238(5) = 7.1870e-2;
H_fraction_238(6) = 2.8291e-2;
H_fraction_238(7) = 6.8382e-3;
H_fraction_238(8) = 1.2322e-3;
H_fraction_238(9) = 6.8409e-4;
H_fraction_238(10) = 1.6975e-4;
H_fraction_238(11) = 2.4182e-5;
H_fraction_238(12) = 6.6356e-6;
H_fraction_238(13) = 1.0075e-6;
H_fraction_238(14) = 4.9894e-7;
H_fraction_238(15) = 1.6352e-7;
H_fraction_238(16) = 2.3355e-8;
H_fraction_238(17) = 2.8094e-9;
H_fraction_238(18) = 3.6236e-11;
H_fraction_238(19) = 6.4577e-11;
H_fraction_238(20) = 4.4963e-14;
H_fraction_238(21) = 3.6654e-16;
H_fraction_238(22) = 5.6293e-17;
H_fraction_238(23) = 7.1602e-17;

% Pu239
H_fraction_Pu239(1) = 2.0830e-1;
H_fraction_Pu239(2) = 3.8530e-1;
H_fraction_Pu239(3) = 2.2130e-1;
H_fraction_Pu239(4) = 9.4600e-2;
H_fraction_Pu239(5) = 3.5310e-2;
H_fraction_Pu239(6) = 2.2920e-2;
H_fraction_Pu239(7) = 3.9460e-3;
H_fraction_Pu239(8) = 1.3170e-3;
H_fraction_Pu239(9) = 7.0520e-4;
H_fraction_Pu239(10) = 1.4320e-4;
H_fraction_Pu239(11) = 1.7650e-5;
H_fraction_Pu239(12) = 7.3470e-6;
H_fraction_Pu239(13) = 1.7470e-6;
H_fraction_Pu239(14) = 5.4810e-7;
H_fraction_Pu239(15) = 1.6710e-7;
H_fraction_Pu239(16) = 2.1120e-8;
H_fraction_Pu239(17) = 2.9960e-9;
H_fraction_Pu239(18) = 5.1070e-11;
H_fraction_Pu239(19) = 5.7300e-11;
H_fraction_Pu239(20) = 4.1380e-14;
H_fraction_Pu239(21) = 1.0880e-15;
H_fraction_Pu239(22) = 2.4540e-17;
H_fraction_Pu239(23) = 7.5570e-17;

%% State dependent functions
display(' Calculating State Dependent Functions ...');

% place holder for delta t
t_last = 0;

% volumetric heat capacity from Simnad (J/ m3 K)
```

```
cp_fuel_vol = (2.04 + 4.17e-3 * Tinit_fuel ) * 1e6;

% Convert to specific heat ( J / kg K )
cp_fuel = cp_fuel_vol / density_fuel;

% find keff
current_keff = 1;

% keff adjusted neutron lifetime (s)
A = l_star / current_keff;

% Heat transfer coefficient (W/m^2K) UT LOCA
h = 3200;  %3200 default

% Instantaneous Power (W)
% Find the initial flux and neutron population from user input
% Flux ( n / m^2 s)
initial_flux = Initial_Power / ( ...
    (200e6 * 1.602677e-19) * N_235 * sig_f_235 * volume_core ...
    + (200e6 * 1.602677e-19) * N_238 * sig_f_238 * volume_core ...
    + (200e6 * 1.602677e-19) * N_Pu_239 * sig_f_Pu_239 * volume_core );

% neutron density (n/m^3)
initial_neutron_density = initial_flux / velocity_neutron;

% U235 contribution
P_inst_235 = initial_flux * (200e6 * 1.602677e-19) * N_235 ...
    * sig_f_235 * volume_core;

% U238 contribution
P_inst_238 = initial_flux * (200e6 * 1.602677e-19) * N_238 ...
    * sig_f_238 * volume_core;

% Pu239 contribution (W)
P_inst_Pu239 = initial_flux * velocity_neutron * (200e6 * 1.602677e-19) * N_Pu_239 ...
    * sig_f_Pu_239 * volume_core;

% Total instantaneous (W)
P_inst = P_inst_235 + P_inst_238 + P_inst_Pu239;

% Temperature Dependent Density (kg/m^3) [ddbst.de, 273K-648K]
A_cp = .14395;
B_cp = .0112;
C_cp = 649.727;
D_cp = .05107;

density_init_water = A_cp / ( B_cp^(1 + (1 - (Tinit_mod + 273.15)/C_cp)^D_cp));

% Mass of water (kg)
mass_cooling_water = volume_cooling_core * density_init_water;

% Temperature dependent Specific heat (KJ/kg) [steam tables]
cp_H2O_KJ = 3.16744e-10 * Tinit_mod^4 - 1.05772e-7 * Tinit_mod^3 ...
    + 2.35330e-5 * Tinit_mod^2 - 1.47670e-3 * Tinit_mod + 4.20617e0;

% Convert to J/kg
cp_H2O = cp_H2O_KJ * 1000;

% specific heat capacity of graphite (cal / g C) [Entegris, inc.]
cp_graphite_cal = .10795e8 * Tinit_fuel^-3 - .61257e5 * Tinit_fuel^-2 ...
    + .30795e-4 * Tinit_fuel + .44391;
cp_graphite = 4183.995381 * cp_graphite_cal;

% Temperature dependent alpha_t
alpha_fuel_T = -1.62895e-7 * Tinit_fuel - 2.53543e-5;

%% Delayed Power State Function (W)
display(' Calculating Delayed Power Initial Condition... ');

% U235 delayed
P_d_235 =  ( P_inst_235 / 200 ) * sum( H_fraction_235 ./ H_lambda_235 );
```

```
% U238 delayed
P_d_238 =  ( P_inst_238 / 200 ) * sum( H_fraction_238 ./ H_lambda_238 );

% Pu239 delayed (W)
P_d_Pu_239 = ( P_inst_Pu239 / 200 ) * sum( H_fraction_Pu239 ./ H_lambda_Pu239 );

%% Total power by isotope (W)
% U235
P_i_235 = P_inst_235 + P_d_235;

% U238
P_i_238 = P_inst_238 + P_d_238;

% Pu239
P_i_Pu239 = P_inst_Pu239 + P_d_Pu_239;

%% Initial Condition Vector
display(' Building Initial Condition Vector... ');

% Build initial condition vector based on inputs
% In hour items
IC(1) = initial_neutron_density;
IC(2) =  (B_1_mix * initial_neutron_density / A ) / lambda_1;
IC(3) =  (B_2_mix * initial_neutron_density / A ) / lambda_2;
IC(4) =  (B_3_mix * initial_neutron_density / A ) / lambda_3;
IC(5) =  (B_4_mix * initial_neutron_density / A ) / lambda_4;
IC(6) =  (B_5_mix * initial_neutron_density / A ) / lambda_5;
IC(7) =  (B_6_mix * initial_neutron_density / A ) / lambda_6;

% Sources
% AmBe (n/s/m^3)
IC(8) = AmBe_source;
IC(9) = U238_spontaneous;
IC(10) = U235_spontaneous;

% Reactivity (assuming keff = 1, this IC is too balance the moderator and fuel
IC(12) = Tinit_fuel;
IC(13) = Tinit_mod;

% Betas
IC(14) = Beff_mix;
IC(15) = B_1_mix;
IC(16) = B_2_mix;
IC(17) = B_3_mix;
IC(18) = B_4_mix;
IC(19) = B_5_mix;
IC(20) = B_6_mix;

display(' Building Decay Heat Matrix Initial Condition... ');

% Decay heat matrix
% U235 Fraction
IC(21) = (H_fraction_235(1) * P_i_235) / (200 * H_lambda_235(1));
IC(22) = (H_fraction_235(2) * P_i_235) / (200 * H_lambda_235(2));
IC(23) = (H_fraction_235(3) * P_i_235) / (200 * H_lambda_235(3));
IC(24) = (H_fraction_235(4) * P_i_235) / (200 * H_lambda_235(4));
IC(25) = (H_fraction_235(5) * P_i_235) / (200 * H_lambda_235(5));
IC(26) = (H_fraction_235(6) * P_i_235) / (200 * H_lambda_235(6));
IC(27) = (H_fraction_235(7) * P_i_235) / (200 * H_lambda_235(7));
IC(28) = (H_fraction_235(8) * P_i_235) / (200 * H_lambda_235(8));
IC(29) = (H_fraction_235(9) * P_i_235) / (200 * H_lambda_235(9));
IC(30) = (H_fraction_235(10) * P_i_235) / (200 * H_lambda_235(10));
IC(31) = (H_fraction_235(11) * P_i_235) / (200 * H_lambda_235(11));
IC(32) = (H_fraction_235(12) * P_i_235) / (200 * H_lambda_235(12));
IC(33) = (H_fraction_235(13) * P_i_235) / (200 * H_lambda_235(13));
IC(34) = (H_fraction_235(14) * P_i_235) / (200 * H_lambda_235(14));
IC(35) = (H_fraction_235(15) * P_i_235) / (200 * H_lambda_235(15));
IC(36) = (H_fraction_235(16) * P_i_235) / (200 * H_lambda_235(16));
IC(37) = (H_fraction_235(17) * P_i_235) / (200 * H_lambda_235(17));
IC(38) = (H_fraction_235(18) * P_i_235) / (200 * H_lambda_235(18));
```

```
IC(39) = (H_fraction_235(19) * P_i_235) / (200 * H_lambda_235(19));
IC(40) = (H_fraction_235(20) * P_i_235) / (200 * H_lambda_235(20));
IC(41) = (H_fraction_235(21) * P_i_235) / (200 * H_lambda_235(21));
IC(42) = (H_fraction_235(22) * P_i_235) / (200 * H_lambda_235(22));
IC(43) = (H_fraction_235(23) * P_i_235) / (200 * H_lambda_235(23));

% U238 Fraction
IC(44) = (H_fraction_238(1) * P_i_238) / (200 * H_lambda_238(1));
IC(45) = (H_fraction_238(2) * P_i_238) / (200 * H_lambda_238(2));
IC(46) = (H_fraction_238(3) * P_i_238) / (200 * H_lambda_238(3));
IC(47) = (H_fraction_238(4) * P_i_238) / (200 * H_lambda_238(4));
IC(48) = (H_fraction_238(5) * P_i_238) / (200 * H_lambda_238(5));
IC(49) = (H_fraction_238(6) * P_i_238) / (200 * H_lambda_238(6));
IC(50) = (H_fraction_238(7) * P_i_238) / (200 * H_lambda_238(7));
IC(51) = (H_fraction_238(8) * P_i_238) / (200 * H_lambda_238(8));
IC(52) = (H_fraction_238(9) * P_i_238) / (200 * H_lambda_238(9));
IC(53) = (H_fraction_238(10) * P_i_238) / (200 * H_lambda_238(10));
IC(54) = (H_fraction_238(11) * P_i_238) / (200 * H_lambda_238(11));
IC(55) = (H_fraction_238(12) * P_i_238) / (200 * H_lambda_238(12));
IC(56) = (H_fraction_238(13) * P_i_238) / (200 * H_lambda_238(13));
IC(57) = (H_fraction_238(14) * P_i_238) / (200 * H_lambda_238(14));
IC(58) = (H_fraction_238(15) * P_i_238) / (200 * H_lambda_238(15));
IC(59) = (H_fraction_238(16) * P_i_238) / (200 * H_lambda_238(16));
IC(60) = (H_fraction_238(17) * P_i_238) / (200 * H_lambda_238(17));
IC(61) = (H_fraction_238(18) * P_i_238) / (200 * H_lambda_238(18));
IC(62) = (H_fraction_238(19) * P_i_238) / (200 * H_lambda_238(19));
IC(63) = (H_fraction_238(20) * P_i_238) / (200 * H_lambda_238(20));
IC(64) = (H_fraction_238(21) * P_i_238) / (200 * H_lambda_238(21));
IC(65) = (H_fraction_238(22) * P_i_238) / (200 * H_lambda_238(22));
IC(66) = (H_fraction_238(23) * P_i_238) / (200 * H_lambda_238(23));

IC(68) = (H_fraction_Pu239(1) * P_i_Pu239) / (200 * H_lambda_Pu239(1));
IC(69) = (H_fraction_Pu239(2) * P_i_Pu239) / (200 * H_lambda_Pu239(2));
IC(70) = (H_fraction_Pu239(3) * P_i_Pu239) / (200 * H_lambda_Pu239(3));
IC(71) = (H_fraction_Pu239(4) * P_i_Pu239) / (200 * H_lambda_Pu239(4));
IC(72) = (H_fraction_Pu239(5) * P_i_Pu239) / (200 * H_lambda_Pu239(5));
IC(73) = (H_fraction_Pu239(6) * P_i_Pu239) / (200 * H_lambda_Pu239(6));
IC(74) = (H_fraction_Pu239(7) * P_i_Pu239) / (200 * H_lambda_Pu239(7));
IC(75) = (H_fraction_Pu239(8) * P_i_Pu239) / (200 * H_lambda_Pu239(8));
IC(76) = (H_fraction_Pu239(9) * P_i_Pu239) / (200 * H_lambda_Pu239(9));
IC(77) = (H_fraction_Pu239(10) * P_i_Pu239) / (200 * H_lambda_Pu239(10));
IC(78) = (H_fraction_Pu239(11) * P_i_Pu239) / (200 * H_lambda_Pu239(11));
IC(79) = (H_fraction_Pu239(12) * P_i_Pu239) / (200 * H_lambda_Pu239(12));
IC(80) = (H_fraction_Pu239(13) * P_i_Pu239) / (200 * H_lambda_Pu239(13));
IC(81) = (H_fraction_Pu239(14) * P_i_Pu239) / (200 * H_lambda_Pu239(14));
IC(82) = (H_fraction_Pu239(15) * P_i_Pu239) / (200 * H_lambda_Pu239(15));
IC(83) = (H_fraction_Pu239(16) * P_i_Pu239) / (200 * H_lambda_Pu239(16));
IC(84) = (H_fraction_Pu239(17) * P_i_Pu239) / (200 * H_lambda_Pu239(17));
IC(85) = (H_fraction_Pu239(18) * P_i_Pu239) / (200 * H_lambda_Pu239(18));
IC(86) = (H_fraction_Pu239(19) * P_i_Pu239) / (200 * H_lambda_Pu239(19));
IC(87) = (H_fraction_Pu239(20) * P_i_Pu239) / (200 * H_lambda_Pu239(20));
IC(88) = (H_fraction_Pu239(21) * P_i_Pu239) / (200 * H_lambda_Pu239(21));
IC(89) = (H_fraction_Pu239(22) * P_i_Pu239) / (200 * H_lambda_Pu239(22));
IC(90) = (H_fraction_Pu239(23) * P_i_Pu239) / (200 * H_lambda_Pu239(23));

display(' Building Model Specific Reactivity IC... ');

% Rod reactivity
if sum(strcmp(Model_type, {'Rod Withdraw'}))
    % Start
    IC(67) = 0;
    IC(11) = -(alpha_fuel_T * Tinit_fuel + alpha_mod * Tinit_mod );

elseif ~sum(strcmp(Model_type, {'Rod Withdraw'}))
    IC(67) = Max_reactivity * Beff_mix;
    IC(11) = -(alpha_fuel_T * Tinit_fuel + alpha_mod * Tinit_mod ) ...
        + Max_reactivity * Beff_mix;

else
    IC(67) = 0;
    IC(11) = -(alpha_fuel_T * Tinit_fuel + alpha_mod * Tinit_mod );
```

```
end

% Temperature expansion
IC(91) = Tinit_fuel;
IC(92) = Tinit_mod;
IC(93) = Tinit_fuel;
IC(94) = Tinit_mod;

% Initial coolant velocity (m/s) [<POAH]
IC(95) = 0;

% Gas / SS expansion
IC(95) = Tinit_mod;
IC(96) = Tinit_mod;
IC(97) = Tinit_mod;
IC(98) = Tinit_mod;
IC(99) = Tinit_mod;
IC(100) = Tinit_mod;
IC(101) = Tinit_mod;

%% Solve for time dependent ODE
% Always run at least one
display(' Beginning ODE calculations... ');

% Establish arrays for saving
Y_out_L = [];
T_out_L = [];
t_out_calc = [];
IC_loop(1,:) = IC;
rho_event = [];
Tm_out_L = [];

% Divide into time for display output
N = 10000;

% Build the option set for the ODE
options = odeset('RelTol', 1e-9,'AbsTol',1e-9);

% Loop the solution of the ODE top allow dumping of array values needed for
% solution but not the output
for i = 1:N
    display(sprintf(' \nBeginning Run %d of %d', i, N));

    IC_loop(i,:);
    [t_out_loop, Y_out_loop] = ode113(@in_hour_FUN_6_2_0, [(i-1)*t_f/N i*t_f/N],
IC_loop(i,:), options);

    Y_out_L = [ Y_out_L Y_out_loop(:,1)' ];
    T_out_L = [ T_out_L Y_out_loop(:,12)' ];
    t_out_calc = [ t_out_calc t_out_loop' ];
    rho_event = [rho_event Y_out_loop(:,67)' ];
    Tm_out_L = [ Tm_out_L Y_out_loop(:,13)' ];

    IC_loop(i+1,:) = Y_out_loop(end,:);

    if ~isreal(Y_out_loop)
        Y_out_loop
        return;
    end

    clear Y_out_loop t_out_loop;

end

%% Output
display(' Building Output Displays... ');

% Find output items of concern
% Find the power out in MW
P_out_temp = 1e-6 * Y_out_L * velocity_neutron * (200e6 * 1.602677e-19) * volume_core ...
```

```
    * ( N_235 * sig_f_235 + N_238 * sig_f_238 + N_Pu_239 * sig_f_Pu_239 );

% Find the maximum power (MW) and time it occurs (s)
[ max_P, max_P_t_i] = max(P_out_temp);

% peaking factors based on power, this accounts for a higher pin temperature in the B
ring
% vs the average core temperature from the calculations (unit less)
% y = 2.4338E-19x3 - 5.3307E-13x2 + 4.1352E-07x + 1.0094E+00
peaking_factor_12_1 = 2.433e-19 .* P_out_temp.^3 - 5.3307e-13 .* P_out_temp.^2 ...
    + 4.1352e-7 .* P_out_temp + 1.0094;

% Peak core temperatures corrected (C)
T_out_temp = peaking_factor_12_1 .* T_out_L;

% Maximum core average temperature (C) and time it occurs (s)
[ max_T, max_T_t_i ] = max(T_out_temp);

max_P_t = t_out_calc(max_P_t_i);

max_T_t = t_out_calc(max_T_t_i);

% In order to save memory, make subsets of the gigantic arrays.  This shows a trend
% but saves space in the calling function of this function
Np = floor(linspace(1,length(t_out_calc), 10000));

P_out = P_out_temp(Np);

T_out = T_out_temp(Np);

t_out = t_out_calc(Np);

rho_out = rho_event(Np);

Tm_out = Tm_out_L(Np);

toc
```

ODE Function File 6.2.0

```
function [ R_dot ] = in_hour_FUN_6_2_0(t, R)
%% In hour equation function file
% The University of Texas at Austin (UT)
% Author: Greg Kline
% Date: 7/3/2015
% Revision: 6.2.0
%
% Modelling of a pulse insertion as well as a rod withdraw event using the
% information in Simnad, 1980 and Johnson, Lucas Tsvetkov, 2010
%
% The purpose of this code is to simulate both a pulse event and a continuous
% rod withdraw event.
%
% The parameters are modelled using the University of Texas parameters
%
% Revisions
% 5.1.0
%     - Added Plutonium 239 to mixture
%     - Accounted for core fuel burnup
%
% 5.2.0
%     - Added changes in moderator temperature based on temperature dependent
%       properties
%
% 5.3.0
%     - Added changing h based on channel properties
%
% 6.0.0
%    - Segmented fuel pin temperature regions and moderator regions
%
```

```
% 6.1.0
%    - Added gas and SS interactions
%
% 6.2.0
%    - Finalized state dependencies
%
%ODE Variables
% R(1) - neutron density
% R(2) - group 1 concentration
% R(3) - group 2 concentration
% R(4) - group 3 concentration
% R(5) - group 4 concentration
% R(6) - group 5 concentration
% R(7) - group 6 concentration
% R(8) - AmBe source concentration
% R(9) - spontaneous U238 concentration
% R(10) - spontaneous U235 concentration
% R(11) - reactivity at t
% R(12) - temperature of the fuel at t
% R(13) - temperature of the moderator at t
% R(14) - B_eff_mix at t
% R(15) - B_mix_1 at t
% R(16) - B_mix_2 at t
% R(17) - B_mix_3 at t
% R(18) - B_mix_4 at t
% R(19) - B_mix_5 at t
% R(20) - B_mix_6 at t
% R(21) - H_U2325_group_1 decay heat matrix
% R(22) - H_U2325_group_2
% R(23) - H_U2325_group_3
% R(24) - H_U2325_group_4
% R(25) - H_U2325_group_5
% R(26) - H_U2325_group_6
% R(27) - H_U2325_group_7
% R(28) - H_U2325_group_8
% R(29) - H_U2325_group_9
% R(30) - H_U2325_group_10
% R(31) - H_U2325_group_11
% R(32) - H_U2325_group_12
% R(33) - H_U2325_group_13
% R(34) - H_U2325_group_14
% R(35) - H_U2325_group_15
% R(36) - H_U2325_group_16
% R(37) - H_U2325_group_17
% R(38) - H_U2325_group_18
% R(39) - H_U2325_group_19
% R(40) - H_U2325_group_20
% R(41) - H_U2325_group_21
% R(42) - H_U2325_group_22
% R(43) - H_U2325_group_23
% R(44) - H_U2328_group_1
% R(45) - H_U2328_group_2
% R(46) - H_U2328_group_3
% R(47) - H_U2328_group_4
% R(48) - H_U2328_group_5
% R(49) - H_U2328_group_6
% R(50) - H_U2328_group_7
% R(51) - H_U2328_group_8
% R(52) - H_U2328_group_9
% R(53) - H_U2328_group_10
% R(54) - H_U2328_group_11
% R(55) - H_U2328_group_12
% R(56) - H_U2328_group_13
% R(57) - H_U2328_group_14
% R(58) - H_U2328_group_15
% R(59) - H_U2328_group_16
% R(60) - H_U2328_group_17
% R(61) - H_U2328_group_18
% R(62) - H_U2328_group_19
% R(63) - H_U2328_group_20
% R(64) - H_U2328_group_21
```

```
% R(65) - H_U2328_group_22
% R(66) - H_U2328_group_23
% R(67) - control rod reactivity at t
% R(68-90) - Pu239
% R(91) - Lower graphite temp
% R(92) - Lower moderator temp
% R(93) - Upper graphite temp
% R(94) - Upper mod temp
% R(95) - velocity
% R(96) - Lower Gas region
% R(97) - Mid Gas region
% R(98) - Upper Gas region
% R(99) - Lower SS Region
% R(100) - Mid SS region
% R(101) - Upper SS region

%% Constants
%%% global variables %%
global Tinit_fuel Tinit_mod  Max_reactivity Reactivity_add_rate
global  N_238 N_235 surface_area_fuel volume_core pin_height
global mass_U_235 mass_U_238 mass_fuel_mix  Event_type density_fuel
global N_Pu_239 mass_Pu_239 l_star  alpha_mod volume_cooling_core
global Area_pin_internal dz_cond_fuel mass_graphite_half_core
global surface_area_graphite area_cooling_pin graphite_height number_pins
global volume_cooling_graphite_core dz_cond_grap radius_pin inner_radius

%% neutronics constants %%%

% Group Lambdas
% U235
U235_L_1 = .0127;
U235_L_2 = .0317;
U235_L_3 = .115;
U235_L_4 = .311;
U235_L_5 = 1.40;
U235_L_6 = 3.87;

% U238
U238_L_1 = .0132;
U238_L_2 = .0321;
U238_L_3 = .139;
U238_L_4 = .358;
U238_L_5 = 1.41;
U238_L_6 = 4.02;

% Pu239
Pu239_L_1 = .0129;
Pu239_L_2 = .0313;
Pu239_L_3 = .135;
Pu239_L_4 = .333;
Pu239_L_5 = 1.36;
Pu239_L_6 = 4.04;

% total delayed neutron fraction U238 [Weaver, 1968]
B_238 = .0157;
% group i fraction is B * relative abundance
B_1_238 = B_238 * .013; %group 1
B_2_238 = B_238 * .137;
B_3_238 = B_238 * .162;
B_4_238 = B_238 * .388;
B_5_238 = B_238 * .225;
B_6_238 = B_238 * .075;

% total delayed neutron fraction U235 [Weaver, 1968]
B_235 = .0065;
B_1_235 = B_235 * .038;
B_2_235 = B_235 * .213;
B_3_235 = B_235 * .188;
B_4_235 = B_235 * .407;
B_5_235 = B_235 * .128;
B_6_235 = B_235 * .026;
```

```
% total delayed neutron fraction Pu239
B_Pu_239 = .0026;
B_1_Pu_239 = B_Pu_239 * .038;
B_2_Pu_239 = B_Pu_239 * .280;
B_3_Pu_239 = B_Pu_239 * .216;
B_4_Pu_239 = B_Pu_239 * .328;
B_5_Pu_239 = B_Pu_239 * .103;
B_6_Pu_239 = B_Pu_239 * .035;

% define fission cross sections for precursor ratios
%fission cross section (m^2) [NIST]
sig_f_238 = 3.3e-28;

%fission cross section (m^2)
sig_f_235 = 584.4e-28;

% fission cross section (m^2)
sig_f_Pu_239 = 747.4e-28;

% Boltzmann constant (m2 kg s-2 K-1)
k_b = 1.38064852e-23;

% Mass of neutron (kg)
m_nu = 1.674927471e-27;

% neutron velocity (m/s)
 velocity_neutron = sqrt( 2 * k_b * (R(12) + 273.15) / m_nu );
% velocity_neutron = 2197;

% U235 Beta factor (atoms/s)
Beta_factor_U235 = velocity_neutron * sig_f_235 * N_235;

% U238 Beta factor (atoms/s)
Beta_factor_U238 = velocity_neutron * sig_f_238 * N_238;

% Pu239 Beta factor (atoms/s)
Beta_factor_Pu239 = velocity_neutron * sig_f_Pu_239 * N_Pu_239;

% Beta of the DNP mix
B_1_mix = ( Beta_factor_U238 * B_1_238 + Beta_factor_U235 * B_1_235 ...
    + Beta_factor_Pu239 * B_1_Pu_239) ...
    / ( Beta_factor_U238 + Beta_factor_U235 + Beta_factor_Pu239);
B_2_mix = ( Beta_factor_U238 * B_2_238 + Beta_factor_U235 * B_2_235 ...
    + Beta_factor_Pu239 * B_2_Pu_239) ...
    / ( Beta_factor_U238 + Beta_factor_U235 + Beta_factor_Pu239);
B_3_mix = ( Beta_factor_U238 * B_3_238 + Beta_factor_U235 * B_3_235 ...
    + Beta_factor_Pu239 * B_3_Pu_239) ...
    / ( Beta_factor_U238 + Beta_factor_U235 + Beta_factor_Pu239);
B_4_mix = ( Beta_factor_U238 * B_4_238 + Beta_factor_U235 * B_4_235 ...
    + Beta_factor_Pu239 * B_4_Pu_239) ...
    / ( Beta_factor_U238 + Beta_factor_U235 + Beta_factor_Pu239);
B_5_mix = ( Beta_factor_U238 * B_5_238 + Beta_factor_U235 * B_5_235 ...
    + Beta_factor_Pu239 * B_5_Pu_239) ...
    / ( Beta_factor_U238 + Beta_factor_U235 + Beta_factor_Pu239);
B_6_mix = ( Beta_factor_U238 * B_6_238 + Beta_factor_U235 * B_6_235 ...
    + Beta_factor_Pu239 * B_6_Pu_239) ...
    / ( Beta_factor_U238 + Beta_factor_U235 + Beta_factor_Pu239);

% Lambda of the DNP mix
lambda_1 = ( Beta_factor_U238 * U238_L_1 + Beta_factor_U235 * U235_L_1 ...
    + Beta_factor_Pu239 * Pu239_L_1) ...
    / ( Beta_factor_U238 + Beta_factor_U235 + Beta_factor_Pu239);
lambda_2 = ( Beta_factor_U238 * U238_L_2 + Beta_factor_U235 * U235_L_2 ...
    + Beta_factor_Pu239 * Pu239_L_2) ...
    / ( Beta_factor_U238 + Beta_factor_U235 + Beta_factor_Pu239);
lambda_3 = ( Beta_factor_U238 * U238_L_3 + Beta_factor_U235 * U235_L_3 ...
    + Beta_factor_Pu239 * Pu239_L_3) ...
    / ( Beta_factor_U238 + Beta_factor_U235 + Beta_factor_Pu239);
lambda_4 = ( Beta_factor_U238 * U238_L_4 + Beta_factor_U235 * U235_L_4 ...
    + Beta_factor_Pu239 * Pu239_L_4) ...
```

```
    / ( Beta_factor_U238 + Beta_factor_U235 + Beta_factor_Pu239);
lambda_5 = ( Beta_factor_U238 * U238_L_5 + Beta_factor_U235 * U235_L_5 ...
    + Beta_factor_Pu239 * Pu239_L_5) ...
    / ( Beta_factor_U238 + Beta_factor_U235 + Beta_factor_Pu239);
lambda_6 = ( Beta_factor_U238 * U238_L_6 + Beta_factor_U235 * U235_L_6 ...
    + Beta_factor_Pu239 * Pu239_L_6) ...
    / ( Beta_factor_U238 + Beta_factor_U235 + Beta_factor_Pu239);

% Beta mix
% Beff correction factor based on Beff/B ratio for U235 .007/,0065
Beta_correction = 1.076923076923077;

% Beta mix
Beta_mix = B_1_mix + B_2_mix + B_3_mix + B_4_mix + B_5_mix + B_6_mix;

% Beff mix
Beff_mix = Beta_mix * Beta_correction;

%prompt neutron lifetime (s) [UT SAR]
% l_star = 51.9e-6;

% 2 Ci AmBe source (atoms/s/m^3)
AmBe_source = 7.4e10;

% U238 spontaneous fission (atoms/s/m^3)
U238_spontaneous = 1.80e-2 * mass_U_238 * 1000; % factor in (n/g-s)

% U235 spontaneous fission (atoms/s/m^3)
U235_spontaneous = 7.43e-4 * mass_U_235 * 1000; % factor in (n/g-s)

% Pu239 spontaneous fission (atoms/s/m^3)
Pu_239_spontaneuos = 2.30e-2 * mass_Pu_239 * 1000;

%% Decay Heat Constants %%%
% Decay (1/s)
% U235
H_lambda_235(1) = 2.2138e1;
H_lambda_235(2) = 5.1587e-1;
H_lambda_235(3) = 1.9594e-1;
H_lambda_235(4) = 1.0314e-1;
H_lambda_235(5) = 3.3656e-2;
H_lambda_235(6) = 1.1681e-2;
H_lambda_235(7) = 3.5870e-3;
H_lambda_235(8) = 1.3930e-3;
H_lambda_235(9) = 6.2630e-4;
H_lambda_235(10) = 1.8906e-4;
H_lambda_235(11) = 5.4988e-5;
H_lambda_235(12) = 2.0958e-5;
H_lambda_235(13) = 1.0010e-5;
H_lambda_235(14) = 2.5438e-6;
H_lambda_235(15) = 6.6361e-7;
H_lambda_235(16) = 1.2290e-7;
H_lambda_235(17) = 2.7213e-8;
H_lambda_235(18) = 4.3714e-9;
H_lambda_235(19) = 7.5780e-10;
H_lambda_235(20) = 2.4786e-10;
H_lambda_235(21) = 2.2384e-13;
H_lambda_235(22) = 2.4600e-14;
H_lambda_235(23) = 1.5699e-14;

% U238
H_lambda_238(1) = 3.2881e00;
H_lambda_238(2) = 9.3805e-1;
H_lambda_238(3) = 3.7073e-1;
H_lambda_238(4) = 1.1118e-1;
H_lambda_238(5) = 3.6143e-2;
H_lambda_238(6) = 1.3272e-2;
H_lambda_238(7) = 5.0133e-3;
H_lambda_238(8) = 1.3655e-3;
H_lambda_238(9) = 5.5158e-4;
H_lambda_238(10) = 1.7873e-4;
```

```
H_lambda_238(11) = 4.9032e-5;
H_lambda_238(12) = 1.7058e-5;
H_lambda_238(13) = 7.0465e-6;
H_lambda_238(14) = 2.3190e-6;
H_lambda_238(15) = 6.4480e-7;
H_lambda_238(16) = 1.2649e-7;
H_lambda_238(17) = 2.5548e-8;
H_lambda_238(18) = 8.4782e-9;
H_lambda_238(19) = 7.5130e-10;
H_lambda_238(20) = 2.4188e-10;
H_lambda_238(21) = 2.2739e-13;
H_lambda_238(22) = 9.0536e-14;
H_lambda_238(23) = 5.6098e-15;

% Pu239
H_lambda_Pu239(1) = 1.0020e1;
H_lambda_Pu239(2) = 6.4330e-1;
H_lambda_Pu239(3) = 2.1860e-1;
H_lambda_Pu239(4) = 1.0040e-1;
H_lambda_Pu239(5) = 3.7280e-2;
H_lambda_Pu239(6) = 1.4350e-2;
H_lambda_Pu239(7) = 4.5490e-3;
H_lambda_Pu239(8) = 1.3280e-3;
H_lambda_Pu239(9) = 5.3560e-4;
H_lambda_Pu239(10) = 1.7300e-4;
H_lambda_Pu239(11) = 4.8810e-5;
H_lambda_Pu239(12) = 2.0060e-5;
H_lambda_Pu239(13) = 8.3190e-6;
H_lambda_Pu239(14) = 2.3580e-6;
H_lambda_Pu239(15) = 6.4500e-7;
H_lambda_Pu239(16) = 1.2780e-7;
H_lambda_Pu239(17) = 2.4660e-8;
H_lambda_Pu239(18) = 9.3780e-9;
H_lambda_Pu239(19) = 7.4500e-10;
H_lambda_Pu239(20) = 2.4260e-10;
H_lambda_Pu239(21) = 2.2100e-13;
H_lambda_Pu239(22) = 2.6400e-14;
H_lambda_Pu239(23) = 1.3800e-14;

% Power fraction
% U235
H_fraction_235(1) = 6.5057e-1;
H_fraction_235(2) = 5.1264e-1;
H_fraction_235(3) = 2.4384e-1;
H_fraction_235(4) = 1.3850e-1;
H_fraction_235(5) = 5.5440e-2;
H_fraction_235(6) = 2.2225e-2;
H_fraction_235(7) = 3.3088e-3;
H_fraction_235(8) = 9.3015e-4;
H_fraction_235(9) = 8.0943e-4;
H_fraction_235(10) = 1.9567e-4;
H_fraction_235(11) = 3.2535e-5;
H_fraction_235(12) = 7.5595e-6;
H_fraction_235(13) = 2.5232e-6;
H_fraction_235(14) = 4.9948e-7;
H_fraction_235(15) = 1.8531e-7;
H_fraction_235(16) = 2.6608e-8;
H_fraction_235(17) = 2.2398e-9;
H_fraction_235(18) = 8.1641e-12;
H_fraction_235(19) = 8.7797e-11;
H_fraction_235(20) = 2.5131e-14;
H_fraction_235(21) = 3.2176e-16;
H_fraction_235(22) = 4.5038e-17;
H_fraction_235(23) = 7.4791e-17;

% U238
H_fraction_238(1) = 1.2311e00;
H_fraction_238(2) = 1.1486e00;
H_fraction_238(3) = 7.0701e-1;
H_fraction_238(4) = 2.5209e-1;
H_fraction_238(5) = 7.1870e-2;
```

```
H_fraction_238(6) = 2.8291e-2;
H_fraction_238(7) = 6.8382e-3;
H_fraction_238(8) = 1.2322e-3;
H_fraction_238(9) = 6.8409e-4;
H_fraction_238(10) = 1.6975e-4;
H_fraction_238(11) = 2.4182e-5;
H_fraction_238(12) = 6.6356e-6;
H_fraction_238(13) = 1.0075e-6;
H_fraction_238(14) = 4.9894e-7;
H_fraction_238(15) = 1.6352e-7;
H_fraction_238(16) = 2.3355e-8;
H_fraction_238(17) = 2.8094e-9;
H_fraction_238(18) = 3.6236e-11;
H_fraction_238(19) = 6.4577e-11;
H_fraction_238(20) = 4.4963e-14;
H_fraction_238(21) = 3.6654e-16;
H_fraction_238(22) = 5.6293e-17;
H_fraction_238(23) = 7.1602e-17;

% Pu239
H_fraction_Pu239(1) = 2.0830e-1;
H_fraction_Pu239(2) = 3.8530e-1;
H_fraction_Pu239(3) = 2.2130e-1;
H_fraction_Pu239(4) = 9.4600e-2;
H_fraction_Pu239(5) = 3.5310e-2;
H_fraction_Pu239(6) = 2.2920e-2;
H_fraction_Pu239(7) = 3.9460e-3;
H_fraction_Pu239(8) = 1.3170e-3;
H_fraction_Pu239(9) = 7.0520e-4;
H_fraction_Pu239(10) = 1.4320e-4;
H_fraction_Pu239(11) = 1.7650e-5;
H_fraction_Pu239(12) = 7.3470e-6;
H_fraction_Pu239(13) = 1.7470e-6;
H_fraction_Pu239(14) = 5.4810e-7;
H_fraction_Pu239(15) = 1.6710e-7;
H_fraction_Pu239(16) = 2.1120e-8;
H_fraction_Pu239(17) = 2.9960e-9;
H_fraction_Pu239(18) = 5.1070e-11;
H_fraction_Pu239(19) = 5.7300e-11;
H_fraction_Pu239(20) = 4.1380e-14;
H_fraction_Pu239(21) = 1.0880e-15;
H_fraction_Pu239(22) = 2.4540e-17;
H_fraction_Pu239(23) = 7.5570e-17;

%% State dependent functions
% ALPHA T
% Temperature dependent alpha T of fuel from UT TRIGA Lab experiment
% dp/dT = -8.14475e-8 * T^2 - 2.53543e-5 * T - 1.56396e-4 ->
% alpha_t_T = -1.62895e-7 * T - 2.53543e-5
% alpha_fuel_T = -1.62895e-7 * R(12) - 2.53543e-5
% alpha_fuel_T = -1.65149e-7 * R(12) - 2.5056e-5;
% alpha_fuel_T = -6.9235e-5;
% alpha_fuel_T = -5.6196e-5;

% constant Alpha_T from SAR
% alpha_fuel_T = -1e-4;

% Curve fits to GA chart from SAR
% 6th order poly
% alpha_fuel_T = -1.9631e-21*R(12)^6 + 6.5610e-18*R(12)^5 - 8.210e-15*R(12)^4 ...
%    + 4.5051e-12*R(12)^3 - 7.8572e-10*R(12)^2 - 1.1061e-7*R(12) - 7.4965e-5;
% 4th order poly
  alpha_fuel_T = 1.4990e-16*R(12)^4 - 5.3734e-13*R(12)^3 + 6.5947e-10*R(12)^2 ...
    - 2.8159e-7*R(12) - 6.9571e-5;
% 2nd order poly
% alpha_fuel_T = 3.1802e-10*R(12)^2 - 2.1800e-7*R(12) - 7.2126e-5;

% volumetric heat capacity from Simnad (J/ m3 K)
cp_fuel_vol = (2.04 + 4.17e-3 * R(12) ) * 1e6;

% Convert to specific heat ( J / kg K )
```

```
cp_fuel = cp_fuel_vol / density_fuel;

% find keff
current_keff = 1 / ( 1 - ( R(11) + (alpha_fuel_T * R(12) + alpha_mod * R(13) ) ) );

% keff adjusted neutron lifetime (s)
 A = l_star / current_keff;
% A = l_star;

% Instantaneous Power (W)
% U235 contribution
P_inst_235 = R(1) * velocity_neutron * (200e6 * 1.602677e-19) * N_235 ...
    * sig_f_235 * volume_core;

% U238 contribution (W)
P_inst_238 = R(1) * velocity_neutron * (200e6 * 1.602677e-19) * N_238 ...
    * sig_f_238 * volume_core;

% Pu239 contribution (W)
P_inst_Pu239 = R(1) * velocity_neutron * (200e6 * 1.602677e-19) * N_Pu_239 ...
    * sig_f_Pu_239 * volume_core;

% Total instantaneous (W)
P_inst = P_inst_235 + P_inst_238 + P_inst_Pu239;

% specific heat capacity of graphite (cal / g C) [Entegris, inc.]
cp_graphite_cal_91 = .10795e8 * R(91)^-3 - .61257e5 * R(91)^-2 ...
    + .30795e-4 * R(91) + .44391;
cp_graphite_91 = 4183.995381 * cp_graphite_cal_91; %Conversion to J / kg K

cp_graphite_cal_93 = .10795e8 * R(93)^-3 - .61257e5 * R(93)^-2 ...
    + .30795e-4 * R(93) + .44391;
cp_graphite_93 = 4183.995381 * cp_graphite_cal_93;

%% Moderator state equations

% Temperature Dependent Density (kg/m^3) [ddbst.de, 273K-648K]
A_cp = .14395;
B_cp = .0112;
C_cp = 649.727;
D_cp = .05107;
low_temp = R(94);
c_temp = R(101);
f_temp = R(12);

% density of outlet water/core area water (kg/m^3)
density_water_13 = A_cp / ( B_cp^(1 + (1 - (R(13) + 273.15)/C_cp)^D_cp));
density_water_92 = A_cp / ( B_cp^(1 + (1 - (R(92) + 273.15)/C_cp)^D_cp));
density_water_94 = A_cp / ( B_cp^(1 + (1 - (R(94) + 273.15)/C_cp)^D_cp));

% density of inlet water, bulk tank (kg/m^3)
density_water_0 =  A_cp / ( B_cp^(1 + (1 - (Tinit_mod + 273.15)/C_cp)^D_cp));

% Mass of water (kg)
mass_cooling_water_fuel = volume_cooling_core * density_water_13;
mass_cooling_water_graphite_92 = volume_cooling_graphite_core * density_water_92;
mass_cooling_water_graphite_94 = volume_cooling_graphite_core * density_water_94;

% specific heat of inlet water (KJ/kg K)
cp_H2O_KJ_0 = 3.16744e-10 * Tinit_mod^4 - 1.05772e-7 * Tinit_mod^3 ...
    + 2.35330e-5 * Tinit_mod^2 - 1.47670e-3 * Tinit_mod + 4.20617e0;

% Convert to J/kg
cp_H2O_0 = cp_H2O_KJ_0 * 1000;

% Temperature dependent Specific heat (J/kgK) [steam tables]
cp_H2O_1 = ( 3.16744e-10 * R(92)^4 - 1.05772e-7 * R(92)^3 ...
    + 2.35330e-5 * R(92)^2 - 1.47670e-3 * R(92) + 4.20617e0 ) * 1000;

cp_H2O_2 = ( 3.16744e-10 * R(13)^4 - 1.05772e-7 * R(13)^3 ...
    + 2.35330e-5 * R(13)^2 - 1.47670e-3 * R(13) + 4.20617e0 ) * 1000;
```

```
cp_H2O_3 = ( 3.16744e-10 * R(94)^4 - 1.05772e-7 * R(94)^3 ...
    + 2.35330e-5 * R(94)^2 - 1.47670e-3 * R(94) + 4.20617e0 ) * 1000;

% Use the Plume formulas from Dartmouth Paper/UT LOCA to find current mass flow
% gravity (m/s^2)
gravity = 9.8066;

% Prandtl Number (Pr)
Pr_water = 1.76;

% Kinetic Viscosity (m^2/s)
kinetic_viscosity_water = .279e-6;

% Expansion Coefficient (1/K)
B_water = .207e-3;

% Thermal conductivity [NIST](W/mK)
k_water = -1.48445 + 4.12292 * ((R(13) + 273.15)/298.15) ...
    - 1.63866 * ((R(13) + 273.15)/298.15)^2;
k_fuel = 17.5730;  % [Simnad]
k_graphite = 112.4;

% Gradient Prandtl (gPr)
gPr_water = (.75 * Pr_water)^.5 / (.609 + 1.221 * Pr_water^.5 + 1.238 * Pr_water)^.25;

% Thermal diffusivity (m^2/s)
% therm_diff_water = 0.143e-6;
therm_diff_water_13 = k_water / ( density_water_13 * cp_H2O_2 );
therm_diff_water_92 = k_water / ( density_water_92 * cp_H2O_1 );
therm_diff_water_94 = k_water / ( density_water_94 * cp_H2O_3 );

% find this loops transient factor (m(T) * cp(T)) [J/K, J/C]
trans_factor_13 = mass_cooling_water_fuel * cp_H2O_2;
trans_factor_92 = mass_cooling_water_graphite_92 * cp_H2O_1;
trans_factor_94 = mass_cooling_water_graphite_94 * cp_H2O_3;

% find the mass flow rate of inlet (kg/s) rho(T) * A_opening * velocity
m_dot = R(95) * density_water_13 * area_cooling_pin * number_pins;

% Enthalpy (J/kgK)
% find saturation temperature for depth of 7.5m (C)
T_sat_water = 114.79;

% find current specific enthalpy h = cp * (T(t) - T_ref) + h_ref;
enthalpy_ref = 9007; % J/kg @ 0C saturated

h_0 = cp_H2O_0 * Tinit_mod + enthalpy_ref;

h_1 = cp_H2O_1 * R(92) + enthalpy_ref;

h_2 = cp_H2O_2 * R(13) + enthalpy_ref;

h_3 = cp_H2O_3 * R(94) + enthalpy_ref;

%% Gas and SS expansion coefficients [ UT LOCA]
% Mass (kg)
mass_gas_fuel = .08375 * pi * ( (radius_pin - .000508)^2 - (radius_pin - .000508 -
1.310588235294116e-04)^2 ) * pin_height;
mass_gas_gr = .08375 * pi * ( (radius_pin - .000508)^2 - (radius_pin - .000508 -
1.310588235294116e-04)^2 ) * graphite_height;
mass_clad_fuel = 7740 * pi * ( radius_pin^2 - (radius_pin - .000508)^2 ) * pin_height;
mass_clad_gr = 7740 * pi * ( radius_pin^2 - (radius_pin - .000508)^2 ) * graphite_height;

% cp (J/kg K)
cp_gas = 14.53e3;
cp_clad = 500;

% dz for conduction (m)
inner_radius = 0.003175;
dz_gas = 1.310588235294116e-04/2;
```

```
dz_clad = 0.000508/2;
dz_fuel_unit = ( radius_pin - .000508 - 1.310588235294116e-04 - inner_radius ) /2;

% Gas heat transfer from KSU SAR (W/m^2 K) [Whaley]
h_gas = 2.84e3;

% Thermal conductivity (W/m K)
k_gas = h_gas * 1.310588235294116e-04; % k ~ h/dx
k_clad = 16.2;

% Area (m^2)
A_gas = pi * ( (radius_pin - .000508)^2 - (radius_pin - .000508 - 1.310588235294116e-
04)^2 );
A_clad = pi * ( (radius_pin )^2 - (radius_pin - .000508)^2 );

% Surface areas (m^2)
surface_gas_out_grap = 2 * pi * (radius_pin - .000508) * graphite_height;
surface_gas_out_fuel = 2 * pi * (radius_pin - .000508) * pin_height;
surface_gas_in_grap = 2 * pi * (radius_pin - .000508 - 1.310588235294116e-04) *
graphite_height;
surface_gas_in_fuel = 2 * pi * (radius_pin - .000508 - 1.310588235294116e-04) *
pin_height;

%% heat transfer coefficient
% Grashof Number [Clarkson.edu]
% Gr_s = reduced_gravity * pin_height^3 / kinetic_viscosity_water^2

% Find the Ra_s [ Kaminski ]
% Ra_s = Gr_s * Pr_water;
Ra_L_1 =  ( gravity * B_water ) / ( kinetic_viscosity_water * therm_diff_water_13 ) ...
    * abs( R(99) - R(92) ) * graphite_height^3;
Ra_L_2 =  ( gravity * B_water ) / ( kinetic_viscosity_water * therm_diff_water_92 ) ...
    * abs( R(100) - R(13) ) * pin_height^3;
Ra_L_3 =  ( gravity * B_water ) / ( kinetic_viscosity_water * therm_diff_water_94 ) ...
    * abs( R(101) - R(94) ) * graphite_height^3;

% Nusselt number
% external free convection vertical cylinder
Nu_L_1 = ( .825 + ( .387 * Ra_L_1^(1/6) ) / ( 1 + ( .492/Pr_water)^(9/16) )^(8/27))^2;
%penn.edu
Nu_L_2 = ( .825 + ( .387 * Ra_L_2^(1/6) ) / ( 1 + ( .492/Pr_water)^(9/16) )^(8/27))^2;
%penn.edu
Nu_L_3 = ( .825 + ( .387 * Ra_L_3^(1/6) ) / ( 1 + ( .492/Pr_water)^(9/16) )^(8/27))^2;
%penn.edu

% Heat transfer coefficient ( W/ m^2 K )
h_bar_1 = Nu_L_1 * k_water / graphite_height;
h_bar_2 = Nu_L_2 * k_water / pin_height;
h_bar_3 = Nu_L_3 * k_water / graphite_height;

%% Delayed Power State Function (W)
% U235 delayed (W)
P_d_235 =  ( P_inst_235 / 200 ) * sum( H_fraction_235 ./ H_lambda_235 );

% U238 delayed (W)
P_d_238 =  ( P_inst_238 / 200 ) * sum( H_fraction_238 ./ H_lambda_238 );

% Pu239 delayed (W)
P_d_Pu_239 = ( P_inst_Pu239 / 200 ) * sum( H_fraction_Pu239 ./ H_lambda_Pu239 );

P_delay = P_d_235 + P_d_238 + P_d_Pu_239;

%% Total power by isotope (W)
% U235
P_i_235 = P_inst_235 + P_d_235;

% U238
P_i_238 = P_inst_238 + P_d_238;

% Pu239
P_i_Pu239 = P_inst_Pu239 + P_d_Pu_239;
```

```
P_eff = P_inst - P_delay + sum(R(21:66));

%% Differentials
% Reactor Kinetics
% overall in hour
R_dot(1) = ( R(11) + alpha_fuel_T * ( R(12) - Tinit_fuel ) ...
    + alpha_mod * ( R(13) - Tinit_mod ) - Beff_mix ) / A * R(1) ...
    + lambda_1 * R(2) ...
    + lambda_2 * R(3) ...
    + lambda_3 * R(4) ...
    + lambda_4 * R(5) ...
    + lambda_5 * R(6) ...
    + lambda_6 * R(7) ...
    + AmBe_source ...
    + U238_spontaneous + U235_spontaneous + Pu_239_spontaneuos; % ...
    % - R(1) * velocity_neutron * N_Sm * sig_a_Sm;
    % - R(1) * velocity_neutron * N_Zr * sig_a_Zr;

% DNP groups
R_dot(2) = (B_1_mix / A) * R(1) - lambda_1 * R(2);
R_dot(3) = (B_2_mix / A) * R(1) - lambda_2 * R(3);
R_dot(4) = (B_3_mix / A) * R(1) - lambda_3 * R(4);
R_dot(5) = (B_4_mix / A) * R(1) - lambda_4 * R(5);
R_dot(6) = (B_5_mix / A) * R(1) - lambda_5 * R(6);
R_dot(7) = (B_6_mix / A) * R(1) - lambda_6 * R(7);

% Source strength
R_dot(8) = 0;
R_dot(9) = 0;
R_dot(10) = 0;

% Reactivities
% event reactivity
switch Event_type
    case 'Pulse'
        R_dot(11) = 0;

    case 'Rod Withdraw'
        if R(11) < Max_reactivity * Beff_mix
            R_dot(11) = Reactivity_add_rate;

        elseif R(11) >= Max_reactivity * Beff_mix
            R_dot(11) = 0;

        else
            display (' Error in Reactivity Addition ');
        end

    otherwise
        R_dot(11) = 0;
end

% Fuel Temperature
R_dot(12) = ( 1 / ( mass_fuel_mix * cp_fuel ) ) * ( P_eff ...
    + ( R(91) - R(12) ) / ( dz_cond_fuel/k_fuel + dz_cond_grap/k_graphite ) *
Area_pin_internal ...
    + ( R(93) - R(12) ) / ( dz_cond_fuel/k_fuel + dz_cond_grap/k_graphite ) *
Area_pin_internal ...
    + ( R(97) - R(12) ) / ( dz_fuel_unit/k_fuel + dz_gas/k_gas ) *  surface_gas_in_fuel
);

% Moderator Temperature
R_dot(13) = 1/trans_factor_13 * ( h_bar_2 * surface_area_fuel * (R(100) - R(13)) ...
        + m_dot * ( h_1 + gravity * graphite_height) ...
        - m_dot * ( h_2 + gravity * (graphite_height + pin_height) ) );

% Changes in Beta effective
% [ current model will be 0 ]
R_dot(14) = 0;
R_dot(15) = 0;
```

```
R_dot(16) = 0;
R_dot(17) = 0;
R_dot(18) = 0;
R_dot(19) = 0;
R_dot(20) = 0;

%% Decay Heat calculations
% Delayed heat from U235 antecedes
R_dot(21) = H_fraction_235(1) * P_i_235 / 200 - H_lambda_235(1) * R(21);
R_dot(22) = H_fraction_235(2) * P_i_235 / 200 - H_lambda_235(2) * R(22);
R_dot(23) = H_fraction_235(3) * P_i_235 / 200 - H_lambda_235(3) * R(23);
R_dot(24) = H_fraction_235(4) * P_i_235 / 200 - H_lambda_235(4) * R(24);
R_dot(25) = H_fraction_235(5) * P_i_235 / 200 - H_lambda_235(5) * R(25);
R_dot(26) = H_fraction_235(6) * P_i_235 / 200 - H_lambda_235(6) * R(26);
R_dot(27) = H_fraction_235(7) * P_i_235 / 200 - H_lambda_235(7) * R(27);
R_dot(28) = H_fraction_235(8) * P_i_235 / 200 - H_lambda_235(8) * R(28);
R_dot(29) = H_fraction_235(9) * P_i_235 / 200 - H_lambda_235(9) * R(29);
R_dot(30) = H_fraction_235(10) * P_i_235 / 200 - H_lambda_235(10) * R(30);
R_dot(31) = H_fraction_235(11) * P_i_235 / 200 - H_lambda_235(11) * R(31);
R_dot(32) = H_fraction_235(12) * P_i_235 / 200 - H_lambda_235(12) * R(32);
R_dot(33) = H_fraction_235(13) * P_i_235 / 200 - H_lambda_235(13) * R(33);
R_dot(34) = H_fraction_235(14) * P_i_235 / 200 - H_lambda_235(14) * R(34);
R_dot(35) = H_fraction_235(15) * P_i_235 / 200 - H_lambda_235(15) * R(35);
R_dot(36) = H_fraction_235(16) * P_i_235 / 200 - H_lambda_235(16) * R(36);
R_dot(37) = H_fraction_235(17) * P_i_235 / 200 - H_lambda_235(17) * R(37);
R_dot(38) = H_fraction_235(18) * P_i_235 / 200 - H_lambda_235(18) * R(38);
R_dot(39) = H_fraction_235(19) * P_i_235 / 200 - H_lambda_235(19) * R(39);
R_dot(40) = H_fraction_235(20) * P_i_235 / 200 - H_lambda_235(20) * R(40);
R_dot(41) = H_fraction_235(21) * P_i_235 / 200 - H_lambda_235(21) * R(41);
R_dot(42) = H_fraction_235(22) * P_i_235 / 200 - H_lambda_235(22) * R(42);
R_dot(43) = H_fraction_235(23) * P_i_235 / 200 - H_lambda_235(23) * R(43);

% Delayed heat from U238 antecedes
R_dot(44) = H_fraction_238(1) * P_i_238 / 200 - H_lambda_238(1) * R(44);
R_dot(45) = H_fraction_238(2) * P_i_238 / 200 - H_lambda_238(2) * R(45);
R_dot(46) = H_fraction_238(3) * P_i_238 / 200 - H_lambda_238(3) * R(46);
R_dot(47) = H_fraction_238(4) * P_i_238 / 200 - H_lambda_238(4) * R(47);
R_dot(48) = H_fraction_238(5) * P_i_238 / 200 - H_lambda_238(5) * R(48);
R_dot(49) = H_fraction_238(6) * P_i_238 / 200 - H_lambda_238(6) * R(49);
R_dot(50) = H_fraction_238(7) * P_i_238 / 200 - H_lambda_238(7) * R(50);
R_dot(51) = H_fraction_238(8) * P_i_238 / 200 - H_lambda_238(8) * R(51);
R_dot(52) = H_fraction_238(9) * P_i_238 / 200 - H_lambda_238(9) * R(52);
R_dot(53) = H_fraction_238(10) * P_i_238 / 200 - H_lambda_238(10) * R(53);
R_dot(54) = H_fraction_238(11) * P_i_238 / 200 - H_lambda_238(11) * R(54);
R_dot(55) = H_fraction_238(12) * P_i_238 / 200 - H_lambda_238(12) * R(55);
R_dot(56) = H_fraction_238(13) * P_i_238 / 200 - H_lambda_238(13) * R(56);
R_dot(57) = H_fraction_238(14) * P_i_238 / 200 - H_lambda_238(14) * R(57);
R_dot(58) = H_fraction_238(15) * P_i_238 / 200 - H_lambda_238(15) * R(58);
R_dot(59) = H_fraction_238(16) * P_i_238 / 200 - H_lambda_238(16) * R(59);
R_dot(60) = H_fraction_238(17) * P_i_238 / 200 - H_lambda_238(17) * R(60);
R_dot(61) = H_fraction_238(18) * P_i_238 / 200 - H_lambda_238(18) * R(61);
R_dot(62) = H_fraction_238(19) * P_i_238 / 200 - H_lambda_238(19) * R(62);
R_dot(63) = H_fraction_238(20) * P_i_238 / 200 - H_lambda_238(20) * R(63);
R_dot(64) = H_fraction_238(21) * P_i_238 / 200 - H_lambda_238(21) * R(64);
R_dot(65) = H_fraction_238(22) * P_i_238 / 200 - H_lambda_238(22) * R(65);
R_dot(66) = H_fraction_238(23) * P_i_238 / 200 - H_lambda_238(23) * R(66);

R_dot(68) = H_fraction_Pu239(1) * P_i_Pu239 / 200 - H_lambda_Pu239(1) * R(68);
R_dot(69) = H_fraction_Pu239(2) * P_i_Pu239 / 200 - H_lambda_Pu239(2) * R(69);
R_dot(70) = H_fraction_Pu239(3) * P_i_Pu239 / 200 - H_lambda_Pu239(3) * R(70);
R_dot(71) = H_fraction_Pu239(4) * P_i_Pu239 / 200 - H_lambda_Pu239(4) * R(71);
R_dot(72) = H_fraction_Pu239(5) * P_i_Pu239 / 200 - H_lambda_Pu239(5) * R(72);
R_dot(73) = H_fraction_Pu239(6) * P_i_Pu239 / 200 - H_lambda_Pu239(6) * R(73);
R_dot(74) = H_fraction_Pu239(7) * P_i_Pu239 / 200 - H_lambda_Pu239(7) * R(74);
R_dot(75) = H_fraction_Pu239(8) * P_i_Pu239 / 200 - H_lambda_Pu239(8) * R(75);
R_dot(76) = H_fraction_Pu239(9) * P_i_Pu239 / 200 - H_lambda_Pu239(9) * R(76);
R_dot(77) = H_fraction_Pu239(10) * P_i_Pu239 / 200 - H_lambda_Pu239(10) * R(77);
R_dot(78) = H_fraction_Pu239(11) * P_i_Pu239 / 200 - H_lambda_Pu239(11) * R(78);
R_dot(79) = H_fraction_Pu239(12) * P_i_Pu239 / 200 - H_lambda_Pu239(12) * R(79);
R_dot(80) = H_fraction_Pu239(13) * P_i_Pu239 / 200 - H_lambda_Pu239(13) * R(80);
R_dot(81) = H_fraction_Pu239(14) * P_i_Pu239 / 200 - H_lambda_Pu239(14) * R(81);
```

```
R_dot(82) = H_fraction_Pu239(15) * P_i_Pu239 / 200 - H_lambda_Pu239(15) * R(82);
R_dot(83) = H_fraction_Pu239(16) * P_i_Pu239 / 200 - H_lambda_Pu239(16) * R(83);
R_dot(84) = H_fraction_Pu239(17) * P_i_Pu239 / 200 - H_lambda_Pu239(17) * R(85);
R_dot(85) = H_fraction_Pu239(18) * P_i_Pu239 / 200 - H_lambda_Pu239(18) * R(85);
R_dot(86) = H_fraction_Pu239(19) * P_i_Pu239 / 200 - H_lambda_Pu239(19) * R(86);
R_dot(87) = H_fraction_Pu239(20) * P_i_Pu239 / 200 - H_lambda_Pu239(20) * R(87);
R_dot(88) = H_fraction_Pu239(21) * P_i_Pu239 / 200 - H_lambda_Pu239(21) * R(88);
R_dot(89) = H_fraction_Pu239(22) * P_i_Pu239 / 200 - H_lambda_Pu239(22) * R(89);
R_dot(90) = H_fraction_Pu239(23) * P_i_Pu239 / 200 - H_lambda_Pu239(23) * R(90);

%% Input reactivity
switch Event_type
    case 'Pulse'
        R_dot(67) = 0;

    case 'Rod Withdraw'
        if R(67) < Max_reactivity * Beff_mix
            R_dot(67) = Reactivity_add_rate;

        elseif R(67) >= Max_reactivity * Beff_mix
            R_dot(67) = 0;
        else
            display (' Error in Reactivity Addition ');
        end

    otherwise
        R_dot(67) = 0;
end

%% Temperature expansion
% Lower Graphite
R_dot(91) = ( 1 / ( mass_graphite_half_core * cp_graphite_91 ) ) ...
    * ( ( R(91) - R(12) ) / ( dz_cond_fuel/k_fuel + dz_cond_grap/k_graphite ) *
Area_pin_internal ...
        + ( R(96) - R(91) ) / ( dz_fuel_unit/k_fuel + dz_gas/k_gas ) *
surface_gas_in_grap );

% upper graphite
R_dot(93) = ( 1 / ( mass_graphite_half_core * cp_graphite_93 ) ) ...
    * ( ( R(93) - R(12) ) / ( dz_cond_fuel/k_fuel + dz_cond_grap/k_graphite ) *
Area_pin_internal ...
        + ( R(98) - R(93) ) / ( dz_fuel_unit/k_fuel + dz_gas/k_gas ) *
surface_gas_in_grap );

% Lower water channel
R_dot(92) = 1/trans_factor_92 * ( h_bar_1 * surface_area_graphite * (R(99) - R(92)) ...
        + m_dot * ( h_0 + gravity * ( 0 ) )...
        - m_dot * ( h_1 + gravity * (graphite_height) ) );

% Upper water channel
R_dot(94) = 1/trans_factor_94 * ( h_bar_3 * surface_area_graphite * (R(101) - R(94)) ...
        + m_dot * ( h_2 + gravity * (graphite_height + pin_height) )...
        - m_dot * ( h_3 + gravity * ( 2 * graphite_height + pin_height) ) );

% Velocity
R_dot(95) = sqrt( therm_diff_water_13 * abs( R(13) - R(94) ) * ( dz_cond_fuel +
dz_cond_grap)  );

%% Gas/ SS expansion
% Lower gas
R_dot(96) = 1/(mass_gas_gr * cp_gas) * ( ( R(97) - R(96) )* k_gas * A_gas / (
dz_cond_fuel + dz_cond_grap) ...
        + (  R(91) - R(96) ) / ( dz_fuel_unit/k_graphite + dz_gas/k_gas ) *
surface_gas_in_grap ...
        + (  R(99) - R(96) ) / ( dz_clad/k_clad + dz_gas/k_gas ) * surface_gas_out_grap
);

% Mid gas
R_dot(97) = 1/(mass_gas_fuel * cp_gas) * ( ( R(96) - R(97) )* k_gas * A_gas / (
dz_cond_fuel + dz_cond_grap) ...
```

```
        + (  R(12) - R(97) ) / ( dz_fuel_unit/k_fuel + dz_gas/k_gas ) *
surface_gas_in_fuel ...
        + (  R(100) - R(97) ) / ( dz_clad/k_clad + dz_gas/k_gas ) * surface_gas_out_fuel
...
        + (  R(98) - R(97) ) * k_gas * A_gas / ( dz_cond_fuel + dz_cond_grap) );

% Upper gas
R_dot(98) = 1/(mass_gas_gr * cp_gas) * ( ( R(97) - R(98) ) * k_gas * A_gas / (
dz_cond_fuel + dz_cond_grap) ...
        + (  R(93) - R(98) ) / ( dz_fuel_unit/k_graphite + dz_gas/k_gas ) *
surface_gas_in_grap ...
        + (  R(101) - R(98) ) / ( dz_clad/k_clad + dz_gas/k_gas ) * surface_gas_out_grap
);

% Lower Clad (SS304)
R_dot(99) = 1/(mass_clad_gr * cp_clad) * ( ( R(100) - R(99) )* k_clad * A_clad / (
dz_cond_fuel + dz_cond_grap) ...
    + (  R(96) - R(99) ) / ( dz_clad/k_clad + dz_gas/k_gas ) * surface_gas_out_grap  ...
    - h_bar_1 * surface_area_graphite * (R(99) - R(92)) );

% Mid Clad (SS304)
R_dot(100) = 1/(mass_clad_fuel * cp_clad) * ( ( R(99) - R(100) )* k_clad * A_clad / (
dz_cond_fuel + dz_cond_grap) ...
    + ( R(101) - R(100) )* k_clad * A_clad / ( dz_cond_fuel + dz_cond_grap) ...
    + (  R(97) - R(100) ) / ( dz_clad/k_clad + dz_gas/k_gas ) * surface_gas_out_fuel ...
    - h_bar_2 * surface_area_graphite * (R(100) - R(13)) );

% Upper Clad (SS304)
R_dot(101) = 1/(mass_clad_gr * cp_clad) * ( ( R(100) - R(101) )* k_clad * A_clad / (
dz_cond_fuel + dz_cond_grap) ...
    + (  R(98) - R(101) ) / ( dz_clad/k_clad + dz_gas/k_gas ) * surface_gas_out_grap ...
    - h_bar_3 * surface_area_graphite * (R(101) - R(94)) );

%% Output
R_dot = R_dot';

if ~isreal(R)
    low_temp
    c_temp
    f_temp
    R94_1
    R94_2
    R94_3
    cp_H2O_3
    return;
end
```

Momentum Balance Program

Main Function

```
function [ P_out, T_out, t_out, rho_out, max_P, max_T, max_P_t, max_T_t ] = in_hour_EQN_4_7_0_FUNC( R_in, t_in, RR_in, type)
%% HEADER
% In_hour EQN solver
% Author: Greg Kline
% Date: 08 Jan 2016
% Revision Date 15 Jun 2016
% Revision: 4.6.2
%
% Modelling of a pulse insertion as well as a rod withdraw event.
%
%
% The purpose of this code is to simulate both a pulse event and a continuous
% rod withdraw event.
%
% The parameters are modelled using the University of Texas parameters
% Revisions
% 4.1.0
%    - Added Plutonium 239 to mixture
%    - Accounted for core fuel burnup
```

```
% 4.6.0
%    - Expanded temperature regions to 6 from 2 ( 1 fuel 1 mod, to 3 fuel 3 mod)
%
% P_out is the vector of power vs time (MW)
% T_out is the vector of temperature vs time (C)
% t_out is time (s)
% rho_out is the event reactivity vs time (dk/k)
% max_P is max Power (MW)
% max_T is max temperature (C)
% max_P_t is the time of peak power (s)
% max_T_t is the time of peak temperature (s)
% R_in is the reactivity limit ($)
% t_in is the max time (s)
% RR_in is the reactivity addition rate in (dk/k/s)
% type is model type: 'Rod Withdraw' or 'Pulse'
%
% Example:
% [ P_out, T_out, t_out, rho_out, max_P, max_T, max_P_t, max_T_t ] = in_hour_EQN_4_6_2_FUNC( 3, 10, .001170, 'Rod Withdraw')
%
% Pseudo Code
% Global Variables
%    - Define the global variables that talk to the ODE solving function
%
% User Input
%    - When not in function mode, the user input pings the MATLAB command
%      line for the same function inputs
%
% Fuel Constants
%    - Define the geometric constants IAW local values
%    - Define material properties IAW Simnad and local values
%
% Neutronics Constants
%    - Define isotope fractions
%    - Find the mixture delayed neutron fraction and decay constant
%    - Account for spontaneous fission
%
% Decay Heat Constants
%    - Define the ANS Standard decay heat constants
%
% Define State Dependent Functions using the initial conditions as the state
%    - Find material state properties
%    - Find initial flux
%    - Find instantaneous power
%
% Find Total Power
%
% Build Initial Condition Vector
%    - Neutronics ICs
%    - Thermal-hydraulic ICs
%    - Event Reactivity IC
%
% Output
%    - Find the instantaneous power from neutron population
%    - Find maximum
%    - Calculate peaking factor vector
%    - Apply to temperature vector
%    - Downsize output vectors
%

tic

%% Global Constants
% global Tinit_fuel Tinit_mod  Max_reactivity Reactivity_add_rate
% global  N_238 N_235 surface_area_fuel volume_core pin_height inner_hex
% global mass_U_235 mass_U_238 mass_fuel_mix  Event_type density_fuel
% global N_Pu_239 mass_Pu_239 l_star  alpha_mod volume_cooling_core
```

```
% global Area_pin_internal dz_cond_fuel mass_graphite_half_core
% global surface_area_graphite area_cooling_pin graphite_height number_pins
% global volume_cooling_graphite_core dz_cond_grap radius_pin inner_radius
% global Area_pin_internal_cond flow_outlet_core flow_inlet_core
% global low_fin_height upper_fin_height A_flow_outlet_grid P_flow_outlet_grid
% global lower_cone_height upper_cone_height A_flow_inlet_grid P_flow_inlet_grid
% global volume_cooling_lower_conical volume_cooling_upper_conical

%% User Input
% Default values are shown in []

% Model Type
% Constants for use in function method
Initial_Power = 50;
Tinit_fuel = 16;
Tinit_mod = 16;

% From user input
Max_reactivity = R_in;
t_f = t_in;
Reactivity_add_rate = RR_in;
Model_type = type;
Event_type = type;

% Make a  nice display for the output
display(sprintf(['Your model is: \n' ...
   ' Model Type: %s \n' ...
   ' Reactivity addition rate(dk/k): %2.2d dk/k \n' ...
   ' Maximum Reactivity($): $%d \n' ...
   ' Initial Power(W): %dW \n' ...
   ' Initial Fuel Temperature(C): %dC \n' ...
   ' Initial Moderator Temperature(C): %dC \n' ...
   ' Duration (s): %ds \n'], Model_type, Reactivity_add_rate, ...
  Max_reactivity, Initial_Power, Tinit_fuel, Tinit_mod, t_f));

display(' Beginning Calculations  ... ');

 %% User Input Non-Function Version
% % Default values are shown in []
%
% % Model Type
%
% MT = input( 'Which model are you going to use? Pulse, Rod Withdraw, Both. [Both]', 's');
%
% if isempty(MT)
%    Model_type = 'Both';
%    Event_type = 'Pulse';
%
% elseif strcmp(MT, 'Rod Withdraw')
%    Model_type = 'Rod Withdraw';
%    Event_type = 'Rod Withdraw';
%
% elseif strcmp(MT, 'Pulse')
%    Model_type = 'Pulse';
%    Event_type = 'Pulse';
%
% elseif strcmp(MT, 'Both')
%    % This will run function file twice once with each model so select
%    % pulse first
%    Model_type = 'Both';
%    Event_type = 'Pulse';
%
% else
%    Model_type = 'Pulse';
%    Event_type = 'Pulse';
% end
```

```
%
% % Reactivity Limit/Insertion(Pulse)
% MR = input( 'What is the maximum reactivity for the event? ($) [$2.94]');
%
% if MR <= 0
%    display ('  Reactivity must be a positive value, using default');
%    Max_reactivity = 2.944447748;
%
% elseif MR >= 13
%    display (sprintf(['  This reactivity exceeds the total rod worth of the '...
%    'UT TRIGA core, results may not be accurate']));
%    Max_reactivity = MR;
%
% elseif isnan(MR)
%    display ('  Reactivity must be a numeric value, using default');
%    Max_reactivity = 2.944447748;
%
% elseif isempty(MR)
%    display ('  Reactivity must be a numeric value, using default');
%    Max_reactivity = 2.944447748;
%
% elseif MR > 3.1429 && MR < 13
%    display ('  Reactivity exceeds UT TechSpec limits ');
%    Max_reactivity = MR;
%
% else
%    Max_reactivity = MR;
% end
%
% % Initial Power (W)
% IP = input('What is the initial power? (W) [50W]');
%
% if IP <= 0
%    display ('  Initial Power must be a positive value, using default');
%    Initial_Power = 50;
%
% elseif isnan(IP)
%    display ('  Initial Power must be a numeric value, using default');
%    Initial_Power = 50;
%
% elseif isempty(IP)
%    display ('  Initial Power must be a numeric value, using default');
%    Initial_Power = 50;
%
% elseif IP > 1.1e6
%    display ('  Initial Power exceeds UT TechSpec limits ');
%    Initial_Power = IP;
%
% else
%    Initial_Power = IP;
% end
%
% % Initial Fuel Temperature (C)
% iFT = input('What is the initial fuel temperature? (C) [20C]');
%
% if iFT <= 0
%    display ('  Initial Fuel Temperature must be a positive value, using default');
%    Tinit_fuel = 20;
%
% elseif isnan(iFT)
%    display ('  Initial Fuel Temperature must be a numeric value, using default');
%    Tinit_fuel = 20;
%
% elseif isempty(iFT)
%    display ('  Initial Fuel Temperature must be a numeric value, using default');
%    Tinit_fuel = 20;
```

```
%
% elseif iFT > 950
%    display ('  Initial Fuel Temperature exceeds UT TechSpec limits ');
%    Tinit_fuel = iFT;
%
% else
%    Tinit_fuel = iFT;
% end
%
% % Initial Moderator Temperature (C)
% iMT = input('What is the initial moderator temperature? (C) [20C]');
%
% if iMT <= 0
%    display ('  Initial Moderator Temperature must be a positive value, using default');
%    Tinit_mod = 20;
%
% elseif isnan(iMT)
%    display ('  Initial Moderator Temperature must be a numeric value, using default');
%    Tinit_mod = 20;
%
% elseif isempty(iMT)
%    display ('  Initial Moderator Temperature must be a numeric value, using default');
%    Tinit_mod = 20;
%
% elseif iMT > 48
%    display ('  Initial Moderator Temperature exceeds UT TechSpec limits ');
%    Tinit_mod = iMT;
%
% else
%    Tinit_mod = iMT;
% end
%
% % time length
% ft = input('How long of a run? (s)');
% % check values
% if ft <= -0
%    t_f = 100;
%    display('Time cannot be negative, using 100s');
%
% elseif isnan(ft)
%    t_f = 100;
%    display('Time must be a number, using 100s');
%
% elseif isempty(ft)
%    t_f = 100;
%    display('Time must be a number, using 100s');
%
% else
%    t_f = ft;
%
% end
%
% if sum(strcmp(Model_type, {'Both','Rod Withdraw'}))
%    RR = input('What is the reactivity addition rate?(dk/k) [.002dk/k]');
%
%    if RR <= 0
%       display ('  Reactivity must be a positive value, using default');
%       Reactivity_add_rate = .002;
%
%    elseif isnan(RR)
%       display ('  Reactivity must be a numeric value, using default');
%       Reactivity_add_rate = .002;
%
%    elseif isempty(RR)
%       display ('  Reactivity must be a numeric value, using default');
%       Reactivity_add_rate = .002;
```

```
%
%   elseif RR > .2
%      display ('  Reactivity exceeds UT TechSpec limits ');
%      Reactivity_add_rate = RR;
%
%   else
%      Reactivity_add_rate = RR;
%   end
%
%   % Make a  nice display for the output
%   display(sprintf(['Your model is: \n' ...
%      '  Model Type: %s \n' ...
%      '  Reactivity addition rate(dk/k): %2.2d dk/k \n' ...
%      '  Maximum Reactivity($): $%d \n' ...
%      '  Initial Power(W): %dW \n' ...
%      '  Initial Fuel Temperature(C): %dC \n' ...
%      '  Initial Moderator Temperature(C): %dC \n' ...
%      '  Duration (s): %ds \n'], Model_type, Reactivity_add_rate, ...
%      Max_reactivity, Initial_Power, Tinit_fuel, Tinit_mod, t_f));
%
% elseif ~sum(strcmp(Model_type, {'Both','Rod Withdraw'}))
%
%   Reactivity_add_rate = 0;
%
%   % Make a  nice display for the output
%   display(sprintf(['Your model is: \n' ...
%   '  Model Type: %s \n' ...
%   '  Maximum Reactivity($): $%d \n' ...
%   '  Initial Power(W): %dW \n' ...
%   '  Initial Fuel Temperature(C): %dC \n' ...
%   '  Initial Moderator Temperature(C): %dC \n' ...
%   '  Duration(s): %d \n'], Model_type, Max_reactivity, ...
%   Initial_Power, Tinit_fuel, Tinit_mod, t_f));
%
% else
%   display(' There is a model error');
%
% end
%
% display(' Beginning Calculations  ... ');

%% fuel constants %%%

%%% Geometry %%%
% Pin radius (m)
radius_pin = 0.018771; % .735in
inner_radius = 0.003175; %.125in

% clad width (m)
dl_clad = 0.000508;
dl_gas = - 1.310588235294116e-04;

% Active region (m)
pin_height = .381;
graphite_height = 0.08763;
dz_cond_fuel = .5 * pin_height;
dz_cond_grap = .5 * graphite_height;
Graphite_offset_from_tip = .087884;

%% momentum expansion
% Heights (m)
lower_cone_height = .035;
upper_cone_height = .03;
lower_pin_below_gr = .041;
upper_pin_above_gr = 0.072;
lower_fin_height = lower_cone_height; % long direction
```

```
upper_fin_height = .0625; %(m)
lower_cyl_height = lower_pin_below_gr - lower_fin_height;
upper_cyl_height = upper_pin_above_gr - upper_fin_height;
dz_lower_ss_cond = lower_cyl_height + lower_cone_height / 4;
dz_upper_ss_cond = upper_cyl_height + upper_cone_height / 4;

% Areas and parameters (m^2 , m)
A_grid = pi * (.038227/2)^2;
P_grid = 2 * pi * (.038227/2);
P_pin_top = .12335;
A_pin_top = .00061;
A_flow_outlet_grid = 8.0742e-4;
P_flow_outlet_grid = .2358; %P_grid + P_pin_top;
A_flow_inlet_grid = 5.3771e-4;
P_flow_inlet_grid = P_grid + P_pin_top;
A_s_lower_fin = 2.28336e-3; %lower fin surface area
A_s_upper_fin = 4.63457e-3; % upper fin surface area
A_s_lower_cyl = 2 * pi * radius_pin * lower_cyl_height;
A_s_upper_cyl = 2 * pi * radius_pin * upper_cyl_height;
A_s_lower_cone = pi * radius_pin * sqrt( lower_cyl_height^2 + radius_pin^2);
A_s_upper_cone = pi * radius_pin * sqrt( upper_cyl_height^2 + radius_pin^2);

% Volumes (m^3)
volume_lower_cyl = pi * radius_pin^2 * lower_cyl_height;
volume_lower_cone = pi * radius_pin^2 * lower_cone_height / 3;
volume_upper_cyl = pi * radius_pin^2 * upper_cyl_height;
volume_upper_cone = pi * radius_pin^2 * upper_cone_height / 3;

% Mass and density (kg, kg/m^3)
density_304SS = 7800;
mass_lower_cyl = volume_lower_cyl * density_304SS;
mass_lower_cone = volume_lower_cone * density_304SS;
mass_upper_cyl = volume_upper_cyl * density_304SS;
mass_upper_cone = volume_upper_cone * density_304SS;
mass_104 = mass_lower_cyl + mass_lower_cone;
mass_105 = mass_upper_cyl + mass_upper_cone;

%% Volumes and areas
% pin fuel volume (m^3)
volume_pin = pi * pin_height * ((radius_pin - dl_clad - dl_gas)^2 - inner_radius^2);

% pin graphite volume (m^3)
volume_graphite_pin = pi * radius_pin^2 * graphite_height;

% surface area graphite (m^2)
surface_area_graphite = 2 * pi * radius_pin * graphite_height;

% surface area of pin (m^2)
surface_area_fuel = 2 * pi * radius_pin * pin_height;

%%% Reactor Constants %%%
% Number of pins (#)
number_pins = 113.7; % account for FFCR smaller diameter

% Volume of the core (m^3)
volume_core = volume_pin * number_pins;

% Volume of graphite in one half of core (m^3)
volume_graphite_half_core = volume_graphite_pin * number_pins;

% Surface area core (m^2)
surface_area_fuel = surface_area_fuel * number_pins;

% Radius of cooling hexagon (m)
inner_hex = 0.0217678;
outer_hex = 0.025146;
```

```
% Total spatial area of cooling hex and pin (m^2)
total_space = sqrt(3)/2 * (2 * inner_hex)^2;

% Area of pin radially (m^2)
Area_pin_internal = pi * radius_pin^2;
Area_pin_internal_cond = pi * ( (radius_pin - dl_clad - dl_gas)^2 - inner_radius^2);

% Area of cooling hexagon around pin (m^2)
area_cooling_pin = total_space - Area_pin_internal;

% Volume of cooling (m^3)
% total pin height (m)
total_pin_height = 0.73152;

% the water mass uses the entire height of pin, not just heated length
volume_cooling_pin = area_cooling_pin * pin_height;
volume_cooling_graphite_pin = area_cooling_pin * graphite_height;

volume_cooling_core = volume_cooling_pin * number_pins;
volume_cooling_graphite_core = volume_cooling_graphite_pin * number_pins;
volume_cooling_lower_conical = total_space * 0.059055 - pi * radius_pin^2 * lower_cone_height / 3;
volume_cooling_upper_conical = total_space * 0.059055 - pi * radius_pin^2 * upper_cone_height / 3;

% Flow inlet area (m^2)
% pin top (m^2)
area_top_pin = .00063789;

% area of grid plate hole (m^2)
area_grid_hole = pi * (0.038227/2)^2;

% flow area of a pin (m^2)
flow_area_pin_upper = area_grid_hole - area_top_pin;

flow_outlet_core = flow_area_pin_upper * number_pins;

flow_area_pin_lower = 0.00063885; %m^2

flow_inlet_core = flow_area_pin_lower * number_pins;

% Channel width (m)
width_channel = 0.0061976;

% Percent Burn (Fraction)
burn_factor_238 = 0.922896237;
burn_factor_235 = 0.863175801;

%%% Fuel meat constants %%%
% wt% U_238
U_wt = .085;

% enrichment percentage (fraction) [UT SAR]
Enrich = .197; % 19.7%

% density (kg/m^3) [Simnad]
density_U = 19070;

% density of ZrH based on ratio (kg/m^3)[Simnad]
density_Zr = 1 / (.1706 + .0042 * 1.6) * 1000;

% Material Densities (kg/m^3)
density_fuel = 1 / ( U_wt / density_U + (1 - U_wt) / density_Zr ); %[Simnad]

% density of Pu 239 based on burnup equations (kg/m^3)
density_Pu239 = 19618;
```

```
% density of graphite (kg/m3)
density_graphite = 2500;

% Avogadro's number (atoms/mol)
N_A = 6.022e23;

% Molar mass (kg/mol) [Burns]
M_U = .23807;

% Molar mass Pu239 (kg/mol)
M_Pu = .2390521634;

% Molar mass Sm (kg/mol)
M_Sm = .15036;

% Molar mass Zr (kg/mol)
M_Zr = .091224;

%%% Masses %%%
% Mass Uranium (kg)
mass_U_pin = density_fuel * volume_pin * U_wt;

% Mass U235 (kg)
mass_U_235_pin = mass_U_pin * Enrich;

% Mass U238 (kg)
mass_U_238_pin = mass_U_pin - mass_U_235_pin;

% Mass Pu239 (kg)
mass_Pu239_pin = density_Pu239 * volume_pin;

% Mass Zr per pin (kg)
mass_ZrH_pin = density_fuel * volume_pin * ( 1- U_wt );

% Total U238 mass (kg)
mass_U_238 = mass_U_238_pin * number_pins;

% Total U235 mass (kg)
mass_U_235 = mass_U_235_pin * number_pins;

% Total Pu239 mass (kg)
mass_Pu_239 = mass_Pu239_pin * number_pins;

% Total Fuel Mass (kg)
mass_fuel_mix = density_fuel * volume_pin * number_pins;

% Total mass of one half of graphite (kg)
mass_graphite_half_core = density_graphite * volume_graphite_half_core * number_pins;

%%% Number Densities %%%
% Number density of U238 per pin (atoms/m^3)
N_238_pin = ( mass_U_238_pin / M_U * N_A ) / volume_pin  * burn_factor_238;

% Number density of U235 per pin (atoms/m^3)
N_235_pin = ( mass_U_235_pin / M_U * N_A ) / volume_pin  * burn_factor_235;

% Number density Pu239 per pin (atoms/m^3)
% N_Pu_239_pin = ( mass_Pu_239 / M_Pu * N_A ) / volume_pin;
N_Pu_239_pin = 0.406333333 / M_Pu * N_A;

% Number density of Sm per pin (atoms )
% constants for Sm and Pu are found from nucleonics burnup data and
% are in units of kg/m^3
N_Sm_pin = 0.077307608 / M_Sm * N_A * volume_pin;

% Number density of ZR per pin (atoms)
```

```
N_Zr_pin = ( mass_ZrH_pin / M_Zr * N_A ) / 2.6;

% Number density U238 per core (atoms/m^3)
N_238 = N_238_pin * number_pins;

% Number density U235 per core (atoms/m^3)
N_235 = N_235_pin * number_pins;

% Number Density Pu239 per core (atoms/m^3)
% This value is taken from burn data so it does not need corrected
N_Pu_239 = N_Pu_239_pin * number_pins;

% Number of Sm (atoms)
N_Sm = N_Sm_pin * number_pins;

% Number of Zr (atoms)
N_Zr = N_Zr_pin * number_pins;

% fuel negative coefficient of reactivity in del_k/k/C [UT SAR]
alpha_fuel = -1e-4;

% Moderator temperature coefficient (del_k/k/C)
 alpha_mod = 3.8952e-6;

%% neutronics constants
% Group Lambdas
% U235
U235_L_1 = .0127;
U235_L_2 = .0317;
U235_L_3 = .115;
U235_L_4 = .311;
U235_L_5 = 1.40;
U235_L_6 = 3.87;

% U238
U238_L_1 = .0132;
U238_L_2 = .0321;
U238_L_3 = .139;
U238_L_4 = .358;
U238_L_5 = 1.41;
U238_L_6 = 4.02;

% Pu239
Pu239_L_1 = .0129;
Pu239_L_2 = .0313;
Pu239_L_3 = .135;
Pu239_L_4 = .333;
Pu239_L_5 = 1.36;
Pu239_L_6 = 4.04;

% total delayed neutron fraction U238 [Weaver, 1968]
B_238 = .0157;
% group i fraction is B * relative abundance
B_1_238 = B_238 * .013; %group 1
B_2_238 = B_238 * .137;
B_3_238 = B_238 * .162;
B_4_238 = B_238 * .388;
B_5_238 = B_238 * .225;
B_6_238 = B_238 * .075;

% total delayed neutron fraction U235 [Weaver, 1968]
B_235 = .0065;
B_1_235 = B_235 * .038;
B_2_235 = B_235 * .213;
B_3_235 = B_235 * .188;
B_4_235 = B_235 * .407;
```

```
B_5_235 = B_235 * .128;
B_6_235 = B_235 * .026;

% total delayed neutron fraction Pu239
B_Pu_239 = .0026;
B_1_Pu_239 = B_Pu_239 * .038;
B_2_Pu_239 = B_Pu_239 * .280;
B_3_Pu_239 = B_Pu_239 * .216;
B_4_Pu_239 = B_Pu_239 * .328;
B_5_Pu_239 = B_Pu_239 * .103;
B_6_Pu_239 = B_Pu_239 * .035;

% define fission cross sections for precursor ratios
%fission cross section (m^2)
sig_f_238 = 3.3e-28;

%fission cross section (m^2)
sig_f_235 = 584.4e-28;

% fission cross section (m^2)
sig_f_Pu_239 = 747.4e-28;

% Absorption cross sections for poisons (m^2)
% Zr, Zirconium has 5 stable isotopes, NIST provides cross sections for each
% so a weighted average is taken Zr 90, 91, 92, 94, 95
sig_a_Zr = .5145 * .011e-28 + .1132 * 1.17e-28 + .1719 * .22e-28 ...
  + .1728 * .0499e-28 + .0276 * .0229e-28;

% Samarium has 7 stable states (m^2)
sig_a_Sm = .031 * .7e-28 + .151 * 57e-28 + .113 * 2.4e-28 ...
  + .139 * 42080e-28 + .074 * 104e-28 + .266 * 206e-28 ...
  + .226 * 8.4e-28;

% neutron velocity (m/s)

% Boltzmann constant (m2 kg s-2 K-1)
k_b = 1.38064852e-23;

% Mass of neutron (kg)
m_nu = 1.674927471e-27;

% velocity neutron = 2197;
velocity_neutron = sqrt( 2 * k_b * (Tinit_fuel + 273.15) / m_nu );

% U235 Beta factor (atoms/s)
Beta_factor_U235 = velocity_neutron * sig_f_235 * N_235;

% U238 Beta factor (atoms/s)
Beta_factor_U238 = velocity_neutron * sig_f_238 * N_238;

% Pu239 Beta factor (atoms/s)
Beta_factor_Pu239 = velocity_neutron * sig_f_Pu_239 * N_Pu_239;

% Beta of the DNP mix
B_1_mix = ( Beta_factor_U238 * B_1_238 + Beta_factor_U235 * B_1_235 ...
  + Beta_factor_Pu239 * B_1_Pu_239) ...
  / ( Beta_factor_U238 + Beta_factor_U235 + Beta_factor_Pu239);
B_2_mix = ( Beta_factor_U238 * B_2_238 + Beta_factor_U235 * B_2_235 ...
  + Beta_factor_Pu239 * B_2_Pu_239) ...
  / ( Beta_factor_U238 + Beta_factor_U235 + Beta_factor_Pu239);
B_3_mix = ( Beta_factor_U238 * B_3_238 + Beta_factor_U235 * B_3_235 ...
  + Beta_factor_Pu239 * B_3_Pu_239) ...
  / ( Beta_factor_U238 + Beta_factor_U235 + Beta_factor_Pu239);
B_4_mix = ( Beta_factor_U238 * B_4_238 + Beta_factor_U235 * B_4_235 ...
  + Beta_factor_Pu239 * B_4_Pu_239) ...
  / ( Beta_factor_U238 + Beta_factor_U235 + Beta_factor_Pu239);
```

```
B_5_mix = ( Beta_factor_U238 * B_5_238 + Beta_factor_U235 * B_5_235 ...
  + Beta_factor_Pu239 * B_5_Pu_239) ...
  / ( Beta_factor_U238 + Beta_factor_U235 + Beta_factor_Pu239);
B_6_mix = ( Beta_factor_U238 * B_6_238 + Beta_factor_U235 * B_6_235 ...
  + Beta_factor_Pu239 * B_6_Pu_239) ...
  / ( Beta_factor_U238 + Beta_factor_U235 + Beta_factor_Pu239);

% Lambda of the DNP mix
lambda_1 = ( Beta_factor_U238 * U238_L_1 + Beta_factor_U235 * U235_L_1 ...
  + Beta_factor_Pu239 * Pu239_L_1) ...
  / ( Beta_factor_U238 + Beta_factor_U235 + Beta_factor_Pu239);
lambda_2 = ( Beta_factor_U238 * U238_L_2 + Beta_factor_U235 * U235_L_2 ...
  + Beta_factor_Pu239 * Pu239_L_2) ...
  / ( Beta_factor_U238 + Beta_factor_U235 + Beta_factor_Pu239);
lambda_3 = ( Beta_factor_U238 * U238_L_3 + Beta_factor_U235 * U235_L_3 ...
  + Beta_factor_Pu239 * Pu239_L_3) ...
  / ( Beta_factor_U238 + Beta_factor_U235 + Beta_factor_Pu239);
lambda_4 = ( Beta_factor_U238 * U238_L_4 + Beta_factor_U235 * U235_L_4 ...
  + Beta_factor_Pu239 * Pu239_L_4) ...
  / ( Beta_factor_U238 + Beta_factor_U235 + Beta_factor_Pu239);
lambda_5 = ( Beta_factor_U238 * U238_L_5 + Beta_factor_U235 * U235_L_5 ...
  + Beta_factor_Pu239 * Pu239_L_5) ...
  / ( Beta_factor_U238 + Beta_factor_U235 + Beta_factor_Pu239);
lambda_6 = ( Beta_factor_U238 * U238_L_6 + Beta_factor_U235 * U235_L_6 ...
  + Beta_factor_Pu239 * Pu239_L_6) ...
  / ( Beta_factor_U238 + Beta_factor_U235 + Beta_factor_Pu239);

% Beta mix
% Beff correction factor based on Beff/B ratio for U235 (.007/.0065)
% Weaver and Hetrick show up to 30% difference between B and Beff
Beta_correction = 1.076923076923077;

% Beta mix
Beta_mix = B_1_mix + B_2_mix + B_3_mix + B_4_mix + B_5_mix + B_6_mix;

% Beff mix
Beff_mix = Beta_mix * Beta_correction;

%prompt neutron lifetime (s) [UT SAR]
l_star = 51.9e-6;
% l_star = 41e-6;

% 2 Ci AmBe source (atoms/s)
AmBe_source = 7.4e10;

% U238 spontaneous fission (atoms/s)
U238_spontaneous = 1.80e-2 * mass_U_238 * 1000; % factor in (n/g-s)

% U235 spontaneous fission (atoms/s)
U235_spontaneous = 7.43e-4 * mass_U_235 * 1000; % factor in (n/g-s)

% Pu239 spontaneous fission (atoms/s)
Pu_239_spontaneuos = 2.30e-2 * mass_Pu_239 * 1000;

%% Decay Heat Constants %%%
% Decay (1/s)
% U235
H_lambda_235(1) = 2.2138e1;
H_lambda_235(2) = 5.1587e-1;
H_lambda_235(3) = 1.9594e-1;
H_lambda_235(4) = 1.0314e-1;
H_lambda_235(5) = 3.3656e-2;
H_lambda_235(6) = 1.1681e-2;
H_lambda_235(7) = 3.5870e-3;
H_lambda_235(8) = 1.3930e-3;
H_lambda_235(9) = 6.2630e-4;
```

```
H_lambda_235(10) = 1.8906e-4;
H_lambda_235(11) = 5.4988e-5;
H_lambda_235(12) = 2.0958e-5;
H_lambda_235(13) = 1.0010e-5;
H_lambda_235(14) = 2.5438e-6;
H_lambda_235(15) = 6.6361e-7;
H_lambda_235(16) = 1.2290e-7;
H_lambda_235(17) = 2.7213e-8;
H_lambda_235(18) = 4.3714e-9;
H_lambda_235(19) = 7.5780e-10;
H_lambda_235(20) = 2.4786e-10;
H_lambda_235(21) = 2.2384e-13;
H_lambda_235(22) = 2.4600e-14;
H_lambda_235(23) = 1.5699e-14;

% U238
H_lambda_238(1) = 3.2881e00;
H_lambda_238(2) = 9.3805e-1;
H_lambda_238(3) = 3.7073e-1;
H_lambda_238(4) = 1.1118e-1;
H_lambda_238(5) = 3.6143e-2;
H_lambda_238(6) = 1.3272e-2;
H_lambda_238(7) = 5.0133e-3;
H_lambda_238(8) = 1.3655e-3;
H_lambda_238(9) = 5.5158e-4;
H_lambda_238(10) = 1.7873e-4;
H_lambda_238(11) = 4.9032e-5;
H_lambda_238(12) = 1.7058e-5;
H_lambda_238(13) = 7.0465e-6;
H_lambda_238(14) = 2.3190e-6;
H_lambda_238(15) = 6.4480e-7;
H_lambda_238(16) = 1.2649e-7;
H_lambda_238(17) = 2.5548e-8;
H_lambda_238(18) = 8.4782e-9;
H_lambda_238(19) = 7.5130e-10;
H_lambda_238(20) = 2.4188e-10;
H_lambda_238(21) = 2.2739e-13;
H_lambda_238(22) = 9.0536e-14;
H_lambda_238(23) = 5.6098e-15;

% Pu239
H_lambda_Pu239(1) = 1.0020e1;
H_lambda_Pu239(2) = 6.4330e-1;
H_lambda_Pu239(3) = 2.1860e-1;
H_lambda_Pu239(4) = 1.0040e-1;
H_lambda_Pu239(5) = 3.7280e-2;
H_lambda_Pu239(6) = 1.4350e-2;
H_lambda_Pu239(7) = 4.5490e-3;
H_lambda_Pu239(8) = 1.3280e-3;
H_lambda_Pu239(9) = 5.3560e-4;
H_lambda_Pu239(10) = 1.7300e-4;
H_lambda_Pu239(11) = 4.8810e-5;
H_lambda_Pu239(12) = 2.0060e-5;
H_lambda_Pu239(13) = 8.3190e-6;
H_lambda_Pu239(14) = 2.3580e-6;
H_lambda_Pu239(15) = 6.4500e-7;
H_lambda_Pu239(16) = 1.2780e-7;
H_lambda_Pu239(17) = 2.4660e-8;
H_lambda_Pu239(18) = 9.3780e-9;
H_lambda_Pu239(19) = 7.4500e-10;
H_lambda_Pu239(20) = 2.4260e-10;
H_lambda_Pu239(21) = 2.2100e-13;
H_lambda_Pu239(22) = 2.6400e-14;
H_lambda_Pu239(23) = 1.3800e-14;

% Power fraction
```

```
% U235
H_fraction_235(1) = 6.5057e-1;
H_fraction_235(2) = 5.1264e-1;
H_fraction_235(3) = 2.4384e-1;
H_fraction_235(4) = 1.3850e-1;
H_fraction_235(5) = 5.5440e-2;
H_fraction_235(6) = 2.2225e-2;
H_fraction_235(7) = 3.3088e-3;
H_fraction_235(8) = 9.3015e-4;
H_fraction_235(9) = 8.0943e-4;
H_fraction_235(10) = 1.9567e-4;
H_fraction_235(11) = 3.2535e-5;
H_fraction_235(12) = 7.5595e-6;
H_fraction_235(13) = 2.5232e-6;
H_fraction_235(14) = 4.9948e-7;
H_fraction_235(15) = 1.8531e-7;
H_fraction_235(16) = 2.6608e-8;
H_fraction_235(17) = 2.2398e-9;
H_fraction_235(18) = 8.1641e-12;
H_fraction_235(19) = 8.7797e-11;
H_fraction_235(20) = 2.5131e-14;
H_fraction_235(21) = 3.2176e-16;
H_fraction_235(22) = 4.5038e-17;
H_fraction_235(23) = 7.4791e-17;

% U238
H_fraction_238(1) = 1.2311e00;
H_fraction_238(2) = 1.1486e00;
H_fraction_238(3) = 7.0701e-1;
H_fraction_238(4) = 2.5209e-1;
H_fraction_238(5) = 7.1870e-2;
H_fraction_238(6) = 2.8291e-2;
H_fraction_238(7) = 6.8382e-3;
H_fraction_238(8) = 1.2322e-3;
H_fraction_238(9) = 6.8409e-4;
H_fraction_238(10) = 1.6975e-4;
H_fraction_238(11) = 2.4182e-5;
H_fraction_238(12) = 6.6356e-6;
H_fraction_238(13) = 1.0075e-6;
H_fraction_238(14) = 4.9894e-7;
H_fraction_238(15) = 1.6352e-7;
H_fraction_238(16) = 2.3355e-8;
H_fraction_238(17) = 2.8094e-9;
H_fraction_238(18) = 3.6236e-11;
H_fraction_238(19) = 6.4577e-11;
H_fraction_238(20) = 4.4963e-14;
H_fraction_238(21) = 3.6654e-16;
H_fraction_238(22) = 5.6293e-17;
H_fraction_238(23) = 7.1602e-17;

% Pu239
H_fraction_Pu239(1) = 2.0830e-1;
H_fraction_Pu239(2) = 3.8530e-1;
H_fraction_Pu239(3) = 2.2130e-1;
H_fraction_Pu239(4) = 9.4600e-2;
H_fraction_Pu239(5) = 3.5310e-2;
H_fraction_Pu239(6) = 2.2920e-2;
H_fraction_Pu239(7) = 3.9460e-3;
H_fraction_Pu239(8) = 1.3170e-3;
H_fraction_Pu239(9) = 7.0520e-4;
H_fraction_Pu239(10) = 1.4320e-4;
H_fraction_Pu239(11) = 1.7650e-5;
H_fraction_Pu239(12) = 7.3470e-6;
H_fraction_Pu239(13) = 1.7470e-6;
H_fraction_Pu239(14) = 5.4810e-7;
H_fraction_Pu239(15) = 1.6710e-7;
```

```
H_fraction_Pu239(16) = 2.1120e-8;
H_fraction_Pu239(17) = 2.9960e-9;
H_fraction_Pu239(18) = 5.1070e-11;
H_fraction_Pu239(19) = 5.7300e-11;
H_fraction_Pu239(20) = 4.1380e-14;
H_fraction_Pu239(21) = 1.0880e-15;
H_fraction_Pu239(22) = 2.4540e-17;
H_fraction_Pu239(23) = 7.5570e-17;

%% State dependent functions
display(' Calculating State Dependent Functions ...');

% place holder for delta t
t_last = 0;

% volumetric heat capacity from Simnad (J/ m3 K)
cp_fuel_vol = (2.04 + 4.17e-3 * Tinit_fuel ) * 1e6;

% Convert to specific heat ( J / kg K )
cp_fuel = cp_fuel_vol / density_fuel;

% find keff
current_keff = 1;

% keff adjusted neutron lifetime (s)
A = l_star / current_keff;

% Heat transfer coefficient (W/m^2K) UT LOCA
h = 3200;  %3200 default

% Instantaneous Power (W)
% Find the initial flux and neutron population from user input
% Flux ( n / m^2 s)
initial_flux = Initial_Power / ( ...
   (200e6 * 1.602677e-19) * N_235 * sig_f_235 * volume_core ...
   + (200e6 * 1.602677e-19) * N_238 * sig_f_238 * volume_core ...
   + (200e6 * 1.602677e-19) * N_Pu_239 * sig_f_Pu_239 * volume_core );

% neutron density (n/m^3)
initial_neutron_density = initial_flux / velocity_neutron;

% U235 contribution
P_inst_235 = initial_flux * (200e6 * 1.602677e-19) * N_235 ...
   * sig_f_235 * volume_core;

% U238 contribution
P_inst_238 = initial_flux * (200e6 * 1.602677e-19) * N_238 ...
   * sig_f_238 * volume_core;

% Pu239 contribution (W)
P_inst_Pu239 = initial_flux * velocity_neutron * (200e6 * 1.602677e-19) * N_Pu_239 ...
   * sig_f_Pu_239 * volume_core;

% Total instantaneous (W)
P_inst = P_inst_235 + P_inst_238 + P_inst_Pu239;

% Temperature Dependent Density (kg/m^3) [ddbst.de, 273K-648K]
A_cp = .14395;
B_cp = .0112;
C_cp = 649.727;
D_cp = .05107;

density_init_water = A_cp / ( B_cp^(1 + (1 - (Tinit_mod + 273.15)/C_cp)^D_cp));

% Mass of water (kg)
mass_cooling_water = volume_cooling_core * density_init_water;
```

```
% Temperature dependent Specific heat (KJ/kg) [steam tables]
cp_H2O_KJ = 3.16744e-10 * Tinit_mod^4 - 1.05772e-7 * Tinit_mod^3 ...
  + 2.35330e-5 * Tinit_mod^2 - 1.47670e-3 * Tinit_mod + 4.20617e0;

% Convert to J/kg
cp_H2O = cp_H2O_KJ * 1000;

% specific heat capacity of graphite (cal / g C) [Entegris, inc.]
cp_graphite_cal = .10795e8 * Tinit_fuel^-3 - .61257e5 * Tinit_fuel^-2 ...
  + .30795e-4 * Tinit_fuel + .44391;
cp_graphite = 4183.995381 * cp_graphite_cal;

% Temperature dependent alpha_t
alpha_fuel_T = -1.62895e-7 * Tinit_fuel - 2.53543e-5;

%% Delayed Power State Function (W)
display(' Calculating Delayed Power Initial Condition... ');

% U235 delayed
P_d_235 =  ( P_inst_235 / 200 ) * sum( H_fraction_235 ./ H_lambda_235 );

% U238 delayed
P_d_238 =  ( P_inst_238 / 200 ) * sum( H_fraction_238 ./ H_lambda_238 );

% Pu239 delayed (W)
P_d_Pu_239 = ( P_inst_Pu239 / 200 ) * sum( H_fraction_Pu239 ./ H_lambda_Pu239 );

%% Total power by isotope (W)
% U235
P_i_235 = P_inst_235 + P_d_235;

% U238
P_i_238 = P_inst_238 + P_d_238;

% Pu239
P_i_Pu239 = P_inst_Pu239 + P_d_Pu_239;

%% Initial Condition Vector
display(' Building Initial Condition Vector... ');

% Build initial condition vector based on inputs
% In hour items
IC(1) = initial_neutron_density;
IC(2) =  (B_1_mix * initial_neutron_density / A ) / lambda_1;
IC(3) =  (B_2_mix * initial_neutron_density / A ) / lambda_2;
IC(4) =  (B_3_mix * initial_neutron_density / A ) / lambda_3;
IC(5) =  (B_4_mix * initial_neutron_density / A ) / lambda_4;
IC(6) =  (B_5_mix * initial_neutron_density / A ) / lambda_5;
IC(7) =  (B_6_mix * initial_neutron_density / A ) / lambda_6;

% Sources
% AmBe (n/s/m^3)
IC(8) = AmBe_source;
IC(9) = U238_spontaneous;
IC(10) = U235_spontaneous;

% Reactivity (assuming keff = 1, this IC is too balance the moderator and fuel
IC(12) = Tinit_fuel;
IC(13) = Tinit_mod;

% Betas
IC(14) = Beff_mix;
IC(15) = B_1_mix;
IC(16) = B_2_mix;
IC(17) = B_3_mix;
```

```
IC(18) = B_4_mix;
IC(19) = B_5_mix;
IC(20) = B_6_mix;

display(' Building Decay Heat Matrix Initial Condition... ');

% Decay heat matrix
% U235 Fraction
IC(21) = (H_fraction_235(1) * P_i_235) / (200 * H_lambda_235(1));
IC(22) = (H_fraction_235(2) * P_i_235) / (200 * H_lambda_235(2));
IC(23) = (H_fraction_235(3) * P_i_235) / (200 * H_lambda_235(3));
IC(24) = (H_fraction_235(4) * P_i_235) / (200 * H_lambda_235(4));
IC(25) = (H_fraction_235(5) * P_i_235) / (200 * H_lambda_235(5));
IC(26) = (H_fraction_235(6) * P_i_235) / (200 * H_lambda_235(6));
IC(27) = (H_fraction_235(7) * P_i_235) / (200 * H_lambda_235(7));
IC(28) = (H_fraction_235(8) * P_i_235) / (200 * H_lambda_235(8));
IC(29) = (H_fraction_235(9) * P_i_235) / (200 * H_lambda_235(9));
IC(30) = (H_fraction_235(10) * P_i_235) / (200 * H_lambda_235(10));
IC(31) = (H_fraction_235(11) * P_i_235) / (200 * H_lambda_235(11));
IC(32) = (H_fraction_235(12) * P_i_235) / (200 * H_lambda_235(12));
IC(33) = (H_fraction_235(13) * P_i_235) / (200 * H_lambda_235(13));
IC(34) = (H_fraction_235(14) * P_i_235) / (200 * H_lambda_235(14));
IC(35) = (H_fraction_235(15) * P_i_235) / (200 * H_lambda_235(15));
IC(36) = (H_fraction_235(16) * P_i_235) / (200 * H_lambda_235(16));
IC(37) = (H_fraction_235(17) * P_i_235) / (200 * H_lambda_235(17));
IC(38) = (H_fraction_235(18) * P_i_235) / (200 * H_lambda_235(18));
IC(39) = (H_fraction_235(19) * P_i_235) / (200 * H_lambda_235(19));
IC(40) = (H_fraction_235(20) * P_i_235) / (200 * H_lambda_235(20));
IC(41) = (H_fraction_235(21) * P_i_235) / (200 * H_lambda_235(21));
IC(42) = (H_fraction_235(22) * P_i_235) / (200 * H_lambda_235(22));
IC(43) = (H_fraction_235(23) * P_i_235) / (200 * H_lambda_235(23));

% U238 Fraction
IC(44) = (H_fraction_238(1) * P_i_238) / (200 * H_lambda_238(1));
IC(45) = (H_fraction_238(2) * P_i_238) / (200 * H_lambda_238(2));
IC(46) = (H_fraction_238(3) * P_i_238) / (200 * H_lambda_238(3));
IC(47) = (H_fraction_238(4) * P_i_238) / (200 * H_lambda_238(4));
IC(48) = (H_fraction_238(5) * P_i_238) / (200 * H_lambda_238(5));
IC(49) = (H_fraction_238(6) * P_i_238) / (200 * H_lambda_238(6));
IC(50) = (H_fraction_238(7) * P_i_238) / (200 * H_lambda_238(7));
IC(51) = (H_fraction_238(8) * P_i_238) / (200 * H_lambda_238(8));
IC(52) = (H_fraction_238(9) * P_i_238) / (200 * H_lambda_238(9));
IC(53) = (H_fraction_238(10) * P_i_238) / (200 * H_lambda_238(10));
IC(54) = (H_fraction_238(11) * P_i_238) / (200 * H_lambda_238(11));
IC(55) = (H_fraction_238(12) * P_i_238) / (200 * H_lambda_238(12));
IC(56) = (H_fraction_238(13) * P_i_238) / (200 * H_lambda_238(13));
IC(57) = (H_fraction_238(14) * P_i_238) / (200 * H_lambda_238(14));
IC(58) = (H_fraction_238(15) * P_i_238) / (200 * H_lambda_238(15));
IC(59) = (H_fraction_238(16) * P_i_238) / (200 * H_lambda_238(16));
IC(60) = (H_fraction_238(17) * P_i_238) / (200 * H_lambda_238(17));
IC(61) = (H_fraction_238(18) * P_i_238) / (200 * H_lambda_238(18));
IC(62) = (H_fraction_238(19) * P_i_238) / (200 * H_lambda_238(19));
IC(63) = (H_fraction_238(20) * P_i_238) / (200 * H_lambda_238(20));
IC(64) = (H_fraction_238(21) * P_i_238) / (200 * H_lambda_238(21));
IC(65) = (H_fraction_238(22) * P_i_238) / (200 * H_lambda_238(22));
IC(66) = (H_fraction_238(23) * P_i_238) / (200 * H_lambda_238(23));

IC(68) = (H_fraction_Pu239(1) * P_i_Pu239) / (200 * H_lambda_Pu239(1));
IC(69) = (H_fraction_Pu239(2) * P_i_Pu239) / (200 * H_lambda_Pu239(2));
IC(70) = (H_fraction_Pu239(3) * P_i_Pu239) / (200 * H_lambda_Pu239(3));
IC(71) = (H_fraction_Pu239(4) * P_i_Pu239) / (200 * H_lambda_Pu239(4));
IC(72) = (H_fraction_Pu239(5) * P_i_Pu239) / (200 * H_lambda_Pu239(5));
IC(73) = (H_fraction_Pu239(6) * P_i_Pu239) / (200 * H_lambda_Pu239(6));
IC(74) = (H_fraction_Pu239(7) * P_i_Pu239) / (200 * H_lambda_Pu239(7));
IC(75) = (H_fraction_Pu239(8) * P_i_Pu239) / (200 * H_lambda_Pu239(8));
IC(76) = (H_fraction_Pu239(9) * P_i_Pu239) / (200 * H_lambda_Pu239(9));
```

```
IC(77) = (H_fraction_Pu239(10) * P_i_Pu239) / (200 * H_lambda_Pu239(10));
IC(78) = (H_fraction_Pu239(11) * P_i_Pu239) / (200 * H_lambda_Pu239(11));
IC(79) = (H_fraction_Pu239(12) * P_i_Pu239) / (200 * H_lambda_Pu239(12));
IC(80) = (H_fraction_Pu239(13) * P_i_Pu239) / (200 * H_lambda_Pu239(13));
IC(81) = (H_fraction_Pu239(14) * P_i_Pu239) / (200 * H_lambda_Pu239(14));
IC(82) = (H_fraction_Pu239(15) * P_i_Pu239) / (200 * H_lambda_Pu239(15));
IC(83) = (H_fraction_Pu239(16) * P_i_Pu239) / (200 * H_lambda_Pu239(16));
IC(84) = (H_fraction_Pu239(17) * P_i_Pu239) / (200 * H_lambda_Pu239(17));
IC(85) = (H_fraction_Pu239(18) * P_i_Pu239) / (200 * H_lambda_Pu239(18));
IC(86) = (H_fraction_Pu239(19) * P_i_Pu239) / (200 * H_lambda_Pu239(19));
IC(87) = (H_fraction_Pu239(20) * P_i_Pu239) / (200 * H_lambda_Pu239(20));
IC(88) = (H_fraction_Pu239(21) * P_i_Pu239) / (200 * H_lambda_Pu239(21));
IC(89) = (H_fraction_Pu239(22) * P_i_Pu239) / (200 * H_lambda_Pu239(22));
IC(90) = (H_fraction_Pu239(23) * P_i_Pu239) / (200 * H_lambda_Pu239(23));

display(' Building Model Specific Reactivity IC... ');

% Rod reactivity
if sum(strcmp(Model_type, {'Rod Withdraw'}))
  % Start
  IC(67) = 0;
  IC(11) = -(alpha_fuel_T * Tinit_fuel + alpha_mod * Tinit_mod );

elseif ~sum(strcmp(Model_type, {'Rod Withdraw'}))
  IC(67) = Max_reactivity * Beff_mix;
  IC(11) = -(alpha_fuel_T * Tinit_fuel + alpha_mod * Tinit_mod ) ...
    + Max_reactivity * Beff_mix;

else
  IC(67) = 0;
  IC(11) = -(alpha_fuel_T * Tinit_fuel + alpha_mod * Tinit_mod );

end

% Temperature expansion
IC(91) = Tinit_fuel;
IC(92) = Tinit_mod;
IC(93) = Tinit_fuel;
IC(94) = Tinit_mod;

% Initial coolant velocity (m/s) [<POAH]
IC(95) = 0;

% Gas / SS expansion
IC(96) = Tinit_mod;
IC(97) = Tinit_mod;
IC(98) = Tinit_mod;
IC(99) = Tinit_mod;
IC(100) = Tinit_mod;
IC(101) = Tinit_mod;

% Momentum expansion
IC(102) = Tinit_mod;
IC(103) = Tinit_mod;
IC(104) = Tinit_fuel;
IC(105) = Tinit_fuel;

%% Build parameter vector to pass to ode function

GV = [Tinit_fuel Tinit_mod Max_reactivity Reactivity_add_rate N_238 N_235 ...
  surface_area_fuel volume_core pin_height inner_hex mass_U_235 mass_U_238 ...
  mass_fuel_mix 0 density_fuel N_Pu_239 mass_Pu_239 l_star alpha_mod ...
  volume_cooling_core Area_pin_internal dz_cond_fuel mass_graphite_half_core ...
  surface_area_graphite area_cooling_pin graphite_height number_pins ...
  volume_cooling_graphite_core dz_cond_grap radius_pin inner_radius ...
  Area_pin_internal_cond flow_outlet_core flow_inlet_core lower_fin_height ...
```

```
  upper_fin_height A_flow_outlet_grid P_flow_outlet_grid lower_cone_height ...
  upper_cone_height A_flow_inlet_grid P_flow_inlet_grid ...
  volume_cooling_lower_conical volume_cooling_upper_conical ...
  lower_pin_below_gr upper_pin_above_gr lower_fin_height ...
  lower_cyl_height upper_cyl_height mass_104 mass_105 ...
  dz_lower_ss_cond dz_upper_ss_cond A_s_lower_fin A_s_upper_fin ...
  A_s_lower_cyl A_s_upper_cyl A_s_lower_cone A_s_upper_cone ];

SV = [ Event_type ];
%% Solve for time dependent ODE
% Always run at least one
display(' Beginning ODE calculations... ');

% Establish arrays for saving
Y_out_L = [];
T_out_L = [];
t_out_calc = [];
IC_loop(1,:) = IC;
rho_event = [];
Tm_out_L = [];

% Divide into time for display output
N = 1000000000;

% Build the option set for the ODE
% Is there a peak in the power curve
peak_found = false;

% has the derivative fallen off enough to be past the power peak
dpdt_e = false;
e = 1;

% account for telling the user error switched
switch_error = false;

option = odeset('RelTol', 1e-5,'AbsTol',1e-5,'Vectorized','on');

% Loop the solution of the ODE to allow dumping of array values needed for
% solution but not the output
for i = 1:N
  if ~mod(i,10000)
    display(sprintf(' \nBeginning Run %d of %d', i, N));
  end

  IC_loop(i,:);

  % Establish error tolerances based on the curves
  if peak_found && dpdt_e && switch_error
    option = odeset('RelTol', 1e-4,'AbsTol',1e-4,'Vectorized','on');
  elseif peak_found && dpdt_e && ~switch_error
    option = odeset('RelTol', 1e-4,'AbsTol',1e-4,'Vectorized','on');
    display(' Switching error tolerances ');
    switch_error = true;
  else
    option = odeset('RelTol', 1e-5,'AbsTol',1e-5,'Vectorized','on');
  end

  % Calculate the subsections ODE
  [t_out_loop, Y_out_loop] = ode113(@(t,y)in_hour_FUN_7_0_0(t,y,GV,SV), [(i-1)*t_f/N i*t_f/N], IC_loop(i,:), option);

  % Update the output vectors
  Y_out_L = [ Y_out_L Y_out_loop(:,1)' ];
  T_out_L = [ T_out_L Y_out_loop(:,12)' ];
  t_out_calc = [ t_out_calc t_out_loop' ];
  rho_event = [rho_event Y_out_loop(:,67)' ];
```

```
    Tm_out_L = [ Tm_out_L Y_out_loop(:,13)' ];

    % Build the next loop's initial condition
    IC_loop(i+1,:) = Y_out_loop(end,:);

    % Check for error tolerance conditions
    if ~peak_found
      peak_found = ~isempty(findpeaks(Y_out_loop(:,1)));
    end

    dpdt_e = max(abs(diff(Y_out_loop(:,1)))) < e;

    if ~isreal(Y_out_loop)
      Y_out_loop
      return;
    end

    clear Y_out_loop t_out_loop;

end

%% Output
display(' Building Output Displays... ');

% Find output items of concern
% Find the power out in MW
P_out_temp = 1e-6 * Y_out_L * velocity_neutron * (200e6 * 1.602677e-19) * volume_core ...
    * ( N_235 * sig_f_235 + N_238 * sig_f_238 + N_Pu_239 * sig_f_Pu_239 );

% Find the maximum power (MW) and time it occurs (s)
[ max_P, max_P_t_i] = max(P_out_temp);

% peaking factors based on power, this accounts for a higher pin temperature in the B ring
% vs the average core temperature from the calculations (unit less)
% y = 2.4338E-19x3 - 5.3307E-13x2 + 4.1352E-07x + 1.0094E+00
peaking_factor_12_1 = 2.433e-19 .* P_out_temp.^3 - 5.3307e-13 .* P_out_temp.^2 ...
    + 4.1352e-7 .* P_out_temp + 1.0094;

% Peak core temperatures corrected (C)
T_out_temp = peaking_factor_12_1 .* T_out_L;

% Maximum core average temperature (C) and time it occurs (s)
[ max_T, max_T_t_i ] = max(T_out_temp);

max_P_t = t_out_calc(max_P_t_i);

max_T_t = t_out_calc(max_T_t_i);

% In order to save memory, make subsets of the gigantic arrays.  This shows a trend
% but saves space in the calling function of this function
Np = floor(linspace(1,length(t_out_calc), 10000));

P_out = P_out_temp(Np);

T_out = T_out_temp(Np);

t_out = t_out_calc(Np);

rho_out = rho_event(Np);

Tm_out = Tm_out_L(Np);

toc
```

ODE Solver

```
function [ R_dot ] = in_hour_FUN_7_0_0(t, R, GV, SV )
%% In hour equation function file
% The University of Texas at Austin (UT)
% Author: Greg Kline
% Date: 7/3/2015
% Revision: 6.2.0
%
% Modelling of a pulse insertion as well as a rod withdraw event using the
% information in Simnad, 1980 and Johnson, Lucas Tsvetkov, 2010
%
% The purpose of this code is to simulate both a pulse event and a continuous
% rod withdraw event.
%
% The parameters are modelled using the University of Texas parameters
%
% Revisions
% 5.1.0
%     - Added Plutonium 239 to mixture
%     - Accounted for core fuel burnup
%
% 5.2.0
%     - Added changes in moderator temperature based on temperature dependent
%         properties
%
% 5.3.0
%     - Added changing h based on channel properties
%
% 6.0.0
%    - Segmented fuel pin temperature regions and moderator regions
%
% 6.1.0
%    - Added gas and SS interactions
%
% 6.2.0
%    - Finalized state dependencies
% 7.0.0
%    - Momentum balance, functionalization of water properties
%
%ODE Variables
% R(1) - neutron density
% R(2) - group 1 concentration
% R(3) - group 2 concentration
% R(4) - group 3 concentration
% R(5) - group 4 concentration
% R(6) - group 5 concentration
% R(7) - group 6 concentration
% R(8) - AmBe source concentration
% R(9) - spontaneous U238 concentration
% R(10) - spontaneous U235 concentration
% R(11) - reactivity at t
% R(12) - temperature of the fuel at t
% R(13) - temperature of the moderator at t
% R(14) - B_eff_mix at t
% R(15) - B_mix_1 at t
% R(16) - B_mix_2 at t
% R(17) - B_mix_3 at t
% R(18) - B_mix_4 at t
% R(19) - B_mix_5 at t
% R(20) - B_mix_6 at t
% R(21) - H_U2325_group_1 decay heat matrix
% R(22) - H_U2325_group_2
% R(23) - H_U2325_group_3
% R(24) - H_U2325_group_4
% R(25) - H_U2325_group_5
% R(26) - H_U2325_group_6
% R(27) - H_U2325_group_7
% R(28) - H_U2325_group_8
% R(29) - H_U2325_group_9
% R(30) - H_U2325_group_10
```

```
% R(31) - H_U2325_group_11
% R(32) - H_U2325_group_12
% R(33) - H_U2325_group_13
% R(34) - H_U2325_group_14
% R(35) - H_U2325_group_15
% R(36) - H_U2325_group_16
% R(37) - H_U2325_group_17
% R(38) - H_U2325_group_18
% R(39) - H_U2325_group_19
% R(40) - H_U2325_group_20
% R(41) - H_U2325_group_21
% R(42) - H_U2325_group_22
% R(43) - H_U2325_group_23
% R(44) - H_U2328_group_1
% R(45) - H_U2328_group_2
% R(46) - H_U2328_group_3
% R(47) - H_U2328_group_4
% R(48) - H_U2328_group_5
% R(49) - H_U2328_group_6
% R(50) - H_U2328_group_7
% R(51) - H_U2328_group_8
% R(52) - H_U2328_group_9
% R(53) - H_U2328_group_10
% R(54) - H_U2328_group_11
% R(55) - H_U2328_group_12
% R(56) - H_U2328_group_13
% R(57) - H_U2328_group_14
% R(58) - H_U2328_group_15
% R(59) - H_U2328_group_16
% R(60) - H_U2328_group_17
% R(61) - H_U2328_group_18
% R(62) - H_U2328_group_19
% R(63) - H_U2328_group_20
% R(64) - H_U2328_group_21
% R(65) - H_U2328_group_22
% R(66) - H_U2328_group_23
% R(67) - control rod reactivity at t
% R(68-90) - Pu239
% R(91) - Lower graphite temp
% R(92) - Lower moderator temp
% R(93) - Upper graphite temp
% R(94) - Upper mod temp
% R(95) - velocity
% R(96) - Lower Gas region
% R(97) - Mid Gas region
% R(98) - Upper Gas region
% R(99) - Lower SS Region
% R(100) - Mid SS region
% R(101) - Upper SS region
% R(102) - Lower pin grid plate coolant region
% R(103) - Upper pin grid plate coolant region
% R(104) - Pin lower fins and region
% R(105) - Pin upper fins and region

%% Constants
%%% global variables %%
% global Tinit_fuel Tinit_mod  Max_reactivity Reactivity_add_rate
% global N_238 N_235 surface_area_fuel volume_core pin_height inner_hex
% global mass_U_235 mass_U_238 mass_fuel_mix  Event_type density_fuel
% global N_Pu_239 mass_Pu_239 l_star  alpha_mod volume_cooling_core
% global Area_pin_internal dz_cond_fuel mass_graphite_half_core
% global surface_area_graphite area_cooling_pin graphite_height number_pins
% global volume_cooling_graphite_core dz_cond_grap radius_pin inner_radius
% global Area_pin_internal_cond flow_outlet_core flow_inlet_core
% global low_fin_height upper_fin_height A_flow_outlet_grid P_flow_outlet_grid
% global lower_cone_height upper_cone_height A_flow_inlet_grid P_flow_inlet_grid
% global volume_cooling_lower_conical volume_cooling_upper_conical

%% Parameter arguments passed
% Tinit_fuel = GV(1);
% Tinit_mod = GV(2);
```

```
% Max_reactivity = GV(3);
% Reactivity_add_rate = GV(4);
% N_238 = GV(5);
% N_235 = GV(6);
% surface_area_fuel = GV(7);
% volume_core = GV(8);
% pin_height = GV(9);
% inner_hex = GV(10);
% mass_U_235 = GV(11);
% mass_U_238 = GV(12);
% mass_fuel_mix = GV(13);
% Event_type = GV(14);
% density_fuel = GV(15);
% N_Pu_239 = GV(16);
% mass_Pu_239 = GV(17);
% l_star = GV(18);
% alpha_mod = GV(19);
% volume_cooling_core = GV(20);
% Area_pin_internal = GV(21);
% dz_cond_fuel = GV(22);
% mass_graphite_half_core = GV(23);
% surface_area_graphite = GV(24);
% area_cooling_pin = GV(25);
% graphite_height = GV(26);
% number_pins = GV(27);
% volume_cooling_graphite_core = GV(28);
% dz_cond_grap = GV(29);
% radius_pin = GV(30);
% inner_radius = GV(31);
% Area_pin_internal_cond = GV(32);
% flow_outlet_core = GV(33);
% flow_inlet_core = GV(34);
% lower_fin_height = GV(35);
% upper_fin_height = GV(36);
% A_flow_outlet_grid = GV(37);
% P_flow_outlet_grid = GV(38);
% lower_cone_height = GV(39);
% upper_cone_height = GV(40);
% A_flow_inlet_grid = GV(41);
% P_flow_inlet_grid = GV(42);
% volume_cooling_lower_conical = GV(43);
% volume_cooling_upper_conical = GV(44);
% lower_pin_below_gr GV(45)
% upper_pin_above_gr
% lower_fin_height ...
% lower_cyl_height
% upper_cyl_height
% mass 104 ss region GV(50)
% mass 105 ss region
% dz_lower_ss_cond
% dz_upper_ss_cond
% A_s_lower_fin
% A_s_upper_fin GV(55)
% A_s_lower_cyl
% A_s_upper_cyl
% A_s_lower_cone
% A_s_upper_cone

%% neutronics constants %%%

% Group Lambdas
% U235
U235_L_1 = .0127;
U235_L_2 = .0317;
U235_L_3 = .115;
U235_L_4 = .311;
U235_L_5 = 1.40;
U235_L_6 = 3.87;

% U238
U238_L_1 = .0132;
```

```
U238_L_2 = .0321;
U238_L_3 = .139;
U238_L_4 = .358;
U238_L_5 = 1.41;
U238_L_6 = 4.02;

% Pu239
Pu239_L_1 = .0129;
Pu239_L_2 = .0313;
Pu239_L_3 = .135;
Pu239_L_4 = .333;
Pu239_L_5 = 1.36;
Pu239_L_6 = 4.04;

% total delayed neutron fraction U238 [Weaver, 1968]
B_238 = .0157;
% group i fraction is B * relative abundance
B_1_238 = B_238 * .013; %group 1
B_2_238 = B_238 * .137;
B_3_238 = B_238 * .162;
B_4_238 = B_238 * .388;
B_5_238 = B_238 * .225;
B_6_238 = B_238 * .075;

% total delayed neutron fraction U235 [Weaver, 1968]
B_235 = .0065;
B_1_235 = B_235 * .038;
B_2_235 = B_235 * .213;
B_3_235 = B_235 * .188;
B_4_235 = B_235 * .407;
B_5_235 = B_235 * .128;
B_6_235 = B_235 * .026;

% total delayed neutron fraction Pu239
B_Pu_239 = .0026;
B_1_Pu_239 = B_Pu_239 * .038;
B_2_Pu_239 = B_Pu_239 * .280;
B_3_Pu_239 = B_Pu_239 * .216;
B_4_Pu_239 = B_Pu_239 * .328;
B_5_Pu_239 = B_Pu_239 * .103;
B_6_Pu_239 = B_Pu_239 * .035;

% define fission cross sections for precursor ratios
%fission cross section (m^2) [NIST]
sig_f_238 = 3.3e-28;

%fission cross section (m^2)
sig_f_235 = 584.4e-28;

% fission cross section (m^2)
sig_f_Pu_239 = 747.4e-28;

% Boltzmann constant (m2 kg s-2 K-1)
k_b = 1.38064852e-23;

% Mass of neutron (kg)
m_nu = 1.674927471e-27;

% neutron velocity (m/s)
 velocity_neutron = sqrt( 2 * k_b * (R(12) + 273.15) / m_nu );
% velocity_neutron = 2197;

% U235 Beta factor (atoms/s)
Beta_factor_U235 = velocity_neutron * sig_f_235 * GV(6);

% U238 Beta factor (atoms/s)
Beta_factor_U238 = velocity_neutron * sig_f_238 * GV(5);

% Pu239 Beta factor (atoms/s)
Beta_factor_Pu239 = velocity_neutron * sig_f_Pu_239 * GV(16);
```

```
% Beta of the DNP mix
B_1_mix = ( Beta_factor_U238 * B_1_238 + Beta_factor_U235 * B_1_235 ...
    + Beta_factor_Pu239 * B_1_Pu_239) ...
    / ( Beta_factor_U238 + Beta_factor_U235 + Beta_factor_Pu239);
B_2_mix = ( Beta_factor_U238 * B_2_238 + Beta_factor_U235 * B_2_235 ...
    + Beta_factor_Pu239 * B_2_Pu_239) ...
    / ( Beta_factor_U238 + Beta_factor_U235 + Beta_factor_Pu239);
B_3_mix = ( Beta_factor_U238 * B_3_238 + Beta_factor_U235 * B_3_235 ...
    + Beta_factor_Pu239 * B_3_Pu_239) ...
    / ( Beta_factor_U238 + Beta_factor_U235 + Beta_factor_Pu239);
B_4_mix = ( Beta_factor_U238 * B_4_238 + Beta_factor_U235 * B_4_235 ...
    + Beta_factor_Pu239 * B_4_Pu_239) ...
    / ( Beta_factor_U238 + Beta_factor_U235 + Beta_factor_Pu239);
B_5_mix = ( Beta_factor_U238 * B_5_238 + Beta_factor_U235 * B_5_235 ...
    + Beta_factor_Pu239 * B_5_Pu_239) ...
    / ( Beta_factor_U238 + Beta_factor_U235 + Beta_factor_Pu239);
B_6_mix = ( Beta_factor_U238 * B_6_238 + Beta_factor_U235 * B_6_235 ...
    + Beta_factor_Pu239 * B_6_Pu_239) ...
    / ( Beta_factor_U238 + Beta_factor_U235 + Beta_factor_Pu239);

% Lambda of the DNP mix
lambda_1 = ( Beta_factor_U238 * U238_L_1 + Beta_factor_U235 * U235_L_1 ...
    + Beta_factor_Pu239 * Pu239_L_1) ...
    / ( Beta_factor_U238 + Beta_factor_U235 + Beta_factor_Pu239);
lambda_2 = ( Beta_factor_U238 * U238_L_2 + Beta_factor_U235 * U235_L_2 ...
    + Beta_factor_Pu239 * Pu239_L_2) ...
    / ( Beta_factor_U238 + Beta_factor_U235 + Beta_factor_Pu239);
lambda_3 = ( Beta_factor_U238 * U238_L_3 + Beta_factor_U235 * U235_L_3 ...
    + Beta_factor_Pu239 * Pu239_L_3) ...
    / ( Beta_factor_U238 + Beta_factor_U235 + Beta_factor_Pu239);
lambda_4 = ( Beta_factor_U238 * U238_L_4 + Beta_factor_U235 * U235_L_4 ...
    + Beta_factor_Pu239 * Pu239_L_4) ...
    / ( Beta_factor_U238 + Beta_factor_U235 + Beta_factor_Pu239);
lambda_5 = ( Beta_factor_U238 * U238_L_5 + Beta_factor_U235 * U235_L_5 ...
    + Beta_factor_Pu239 * Pu239_L_5) ...
    / ( Beta_factor_U238 + Beta_factor_U235 + Beta_factor_Pu239);
lambda_6 = ( Beta_factor_U238 * U238_L_6 + Beta_factor_U235 * U235_L_6 ...
    + Beta_factor_Pu239 * Pu239_L_6) ...
    / ( Beta_factor_U238 + Beta_factor_U235 + Beta_factor_Pu239);

% Beta mix
% Beff correction factor based on Beff/B ratio for U235 .007/,0065
Beta_correction = 1.076923076923077;

% Beta mix
Beta_mix = B_1_mix + B_2_mix + B_3_mix + B_4_mix + B_5_mix + B_6_mix;

% Beff mix
Beff_mix = Beta_mix * Beta_correction;

%prompt neutron lifetime (s) [UT SAR]
% l_star = 51.9e-6;

% 2 Ci AmBe source (atoms/s/m^3)
AmBe_source = 7.4e10;

% U238 spontaneous fission (atoms/s/m^3)
U238_spontaneous = 1.80e-2 * GV(12) * 1000; % factor in (n/g-s)

% U235 spontaneous fission (atoms/s/m^3)
U235_spontaneous = 7.43e-4 * GV(11) * 1000; % factor in (n/g-s)

% Pu239 spontaneous fission (atoms/s/m^3)
Pu_239_spontaneuos = 2.30e-2 * GV(17) * 1000;

%% Decay Heat Constants %%%
% Decay (1/s)
% U235
H_lambda_235(1) = 2.2138e1;
H_lambda_235(2) = 5.1587e-1;
H_lambda_235(3) = 1.9594e-1;
```

```
H_lambda_235(4) = 1.0314e-1;
H_lambda_235(5) = 3.3656e-2;
H_lambda_235(6) = 1.1681e-2;
H_lambda_235(7) = 3.5870e-3;
H_lambda_235(8) = 1.3930e-3;
H_lambda_235(9) = 6.2630e-4;
H_lambda_235(10) = 1.8906e-4;
H_lambda_235(11) = 5.4988e-5;
H_lambda_235(12) = 2.0958e-5;
H_lambda_235(13) = 1.0010e-5;
H_lambda_235(14) = 2.5438e-6;
H_lambda_235(15) = 6.6361e-7;
H_lambda_235(16) = 1.2290e-7;
H_lambda_235(17) = 2.7213e-8;
H_lambda_235(18) = 4.3714e-9;
H_lambda_235(19) = 7.5780e-10;
H_lambda_235(20) = 2.4786e-10;
H_lambda_235(21) = 2.2384e-13;
H_lambda_235(22) = 2.4600e-14;
H_lambda_235(23) = 1.5699e-14;

% U238
H_lambda_238(1) = 3.2881e00;
H_lambda_238(2) = 9.3805e-1;
H_lambda_238(3) = 3.7073e-1;
H_lambda_238(4) = 1.1118e-1;
H_lambda_238(5) = 3.6143e-2;
H_lambda_238(6) = 1.3272e-2;
H_lambda_238(7) = 5.0133e-3;
H_lambda_238(8) = 1.3655e-3;
H_lambda_238(9) = 5.5158e-4;
H_lambda_238(10) = 1.7873e-4;
H_lambda_238(11) = 4.9032e-5;
H_lambda_238(12) = 1.7058e-5;
H_lambda_238(13) = 7.0465e-6;
H_lambda_238(14) = 2.3190e-6;
H_lambda_238(15) = 6.4480e-7;
H_lambda_238(16) = 1.2649e-7;
H_lambda_238(17) = 2.5548e-8;
H_lambda_238(18) = 8.4782e-9;
H_lambda_238(19) = 7.5130e-10;
H_lambda_238(20) = 2.4188e-10;
H_lambda_238(21) = 2.2739e-13;
H_lambda_238(22) = 9.0536e-14;
H_lambda_238(23) = 5.6098e-15;

% Pu239
H_lambda_Pu239(1) = 1.0020e1;
H_lambda_Pu239(2) = 6.4330e-1;
H_lambda_Pu239(3) = 2.1860e-1;
H_lambda_Pu239(4) = 1.0040e-1;
H_lambda_Pu239(5) = 3.7280e-2;
H_lambda_Pu239(6) = 1.4350e-2;
H_lambda_Pu239(7) = 4.5490e-3;
H_lambda_Pu239(8) = 1.3280e-3;
H_lambda_Pu239(9) = 5.3560e-4;
H_lambda_Pu239(10) = 1.7300e-4;
H_lambda_Pu239(11) = 4.8810e-5;
H_lambda_Pu239(12) = 2.0060e-5;
H_lambda_Pu239(13) = 8.3190e-6;
H_lambda_Pu239(14) = 2.3580e-6;
H_lambda_Pu239(15) = 6.4500e-7;
H_lambda_Pu239(16) = 1.2780e-7;
H_lambda_Pu239(17) = 2.4660e-8;
H_lambda_Pu239(18) = 9.3780e-9;
H_lambda_Pu239(19) = 7.4500e-10;
H_lambda_Pu239(20) = 2.4260e-10;
H_lambda_Pu239(21) = 2.2100e-13;
H_lambda_Pu239(22) = 2.6400e-14;
H_lambda_Pu239(23) = 1.3800e-14;
```

```
% Power fraction
% U235
H_fraction_235(1) = 6.5057e-1;
H_fraction_235(2) = 5.1264e-1;
H_fraction_235(3) = 2.4384e-1;
H_fraction_235(4) = 1.3850e-1;
H_fraction_235(5) = 5.5440e-2;
H_fraction_235(6) = 2.2225e-2;
H_fraction_235(7) = 3.3088e-3;
H_fraction_235(8) = 9.3015e-4;
H_fraction_235(9) = 8.0943e-4;
H_fraction_235(10) = 1.9567e-4;
H_fraction_235(11) = 3.2535e-5;
H_fraction_235(12) = 7.5595e-6;
H_fraction_235(13) = 2.5232e-6;
H_fraction_235(14) = 4.9948e-7;
H_fraction_235(15) = 1.8531e-7;
H_fraction_235(16) = 2.6608e-8;
H_fraction_235(17) = 2.2398e-9;
H_fraction_235(18) = 8.1641e-12;
H_fraction_235(19) = 8.7797e-11;
H_fraction_235(20) = 2.5131e-14;
H_fraction_235(21) = 3.2176e-16;
H_fraction_235(22) = 4.5038e-17;
H_fraction_235(23) = 7.4791e-17;

% U238
H_fraction_238(1) = 1.2311e00;
H_fraction_238(2) = 1.1486e00;
H_fraction_238(3) = 7.0701e-1;
H_fraction_238(4) = 2.5209e-1;
H_fraction_238(5) = 7.1870e-2;
H_fraction_238(6) = 2.8291e-2;
H_fraction_238(7) = 6.8382e-3;
H_fraction_238(8) = 1.2322e-3;
H_fraction_238(9) = 6.8409e-4;
H_fraction_238(10) = 1.6975e-4;
H_fraction_238(11) = 2.4182e-5;
H_fraction_238(12) = 6.6356e-6;
H_fraction_238(13) = 1.0075e-6;
H_fraction_238(14) = 4.9894e-7;
H_fraction_238(15) = 1.6352e-7;
H_fraction_238(16) = 2.3355e-8;
H_fraction_238(17) = 2.8094e-9;
H_fraction_238(18) = 3.6236e-11;
H_fraction_238(19) = 6.4577e-11;
H_fraction_238(20) = 4.4963e-14;
H_fraction_238(21) = 3.6654e-16;
H_fraction_238(22) = 5.6293e-17;
H_fraction_238(23) = 7.1602e-17;

% Pu239
H_fraction_Pu239(1) = 2.0830e-1;
H_fraction_Pu239(2) = 3.8530e-1;
H_fraction_Pu239(3) = 2.2130e-1;
H_fraction_Pu239(4) = 9.4600e-2;
H_fraction_Pu239(5) = 3.5310e-2;
H_fraction_Pu239(6) = 2.2920e-2;
H_fraction_Pu239(7) = 3.9460e-3;
H_fraction_Pu239(8) = 1.3170e-3;
H_fraction_Pu239(9) = 7.0520e-4;
H_fraction_Pu239(10) = 1.4320e-4;
H_fraction_Pu239(11) = 1.7650e-5;
H_fraction_Pu239(12) = 7.3470e-6;
H_fraction_Pu239(13) = 1.7470e-6;
H_fraction_Pu239(14) = 5.4810e-7;
H_fraction_Pu239(15) = 1.6710e-7;
H_fraction_Pu239(16) = 2.1120e-8;
H_fraction_Pu239(17) = 2.9960e-9;
H_fraction_Pu239(18) = 5.1070e-11;
H_fraction_Pu239(19) = 5.7300e-11;
```

```
H_fraction_Pu239(20) = 4.1380e-14;
H_fraction_Pu239(21) = 1.0880e-15;
H_fraction_Pu239(22) = 2.4540e-17;
H_fraction_Pu239(23) = 7.5570e-17;

%% State dependent functions
% ALPHA T
% Temperature dependent alpha T of fuel from UT TRIGA Lab experiment
% dp/dT = -8.14475e-8 * T^2 - 2.53543e-5 * T - 1.56396e-4 ->
% alpha_t_T = -1.62895e-7 * T - 2.53543e-5
% alpha_fuel_T = -1.62895e-7 * R(12) - 2.53543e-5
% alpha_fuel_T = -1.65149e-7 * R(12) - 2.5056e-5;
% alpha_fuel_T = -6.9235e-5;
% alpha_fuel_T = -5.6196e-5;

% constant Alpha_T from SAR
% alpha_fuel_T = -1e-4;

% Curve fits to GA chart from SAR
% 6th order poly
% alpha_fuel_T = -1.9631e-21*R(12)^6 + 6.5610e-18*R(12)^5 - 8.210e-15*R(12)^4 ...
%     + 4.5051e-12*R(12)^3 - 7.8572e-10*R(12)^2 - 1.1061e-7*R(12) - 7.4965e-5;
% 4th order poly
  alpha_fuel_T = 1.4990e-16*R(12)^4 - 5.3734e-13*R(12)^3 + 6.5947e-10*R(12)^2 ...
    - 2.8159e-7*R(12) - 6.9571e-5;
% 2nd order poly
% alpha_fuel_T = 3.1802e-10*R(12)^2 - 2.1800e-7*R(12) - 7.2126e-5;

% volumetric heat capacity from Simnad (J/ m3 K)
cp_fuel_vol = (2.04 + 4.17e-3 * R(12) ) * 1e6;

% Convert to specific heat ( J / kg K )
cp_fuel = cp_fuel_vol / GV(15);

% find keff
current_keff = 1 / ( 1 - ( R(11) + (alpha_fuel_T * R(12) + GV(19) * R(13) ) ) );

% keff adjusted neutron lifetime (s)
 A = GV(18) / current_keff;
% A = l_star;

% Instantaneous Power (W)
% U235 contribution
P_inst_235 = R(1) * velocity_neutron * (200e6 * 1.602677e-19) * GV(6) ...
    * sig_f_235 * GV(8);

% U238 contribution (W)
P_inst_238 = R(1) * velocity_neutron * (200e6 * 1.602677e-19) * GV(5) ...
    * sig_f_238 * GV(8);

% Pu239 contribution (W)
P_inst_Pu239 = R(1) * velocity_neutron * (200e6 * 1.602677e-19) * GV(16) ...
    * sig_f_Pu_239 * GV(8);

% Total instantaneous (W)
P_inst = P_inst_235 + P_inst_238 + P_inst_Pu239;

% specific heat capacity of graphite (cal / g C) [Entegris, inc.]
cp_graphite_cal_91 = .10795e8 * R(91)^-3 - .61257e5 * R(91)^-2 ...
    + .30795e-4 * R(91) + .44391;
cp_graphite_91 = 4183.995381 * cp_graphite_cal_91; %Conversion to J / kg K

cp_graphite_cal_93 = .10795e8 * R(93)^-3 - .61257e5 * R(93)^-2 ...
    + .30795e-4 * R(93) + .44391;
cp_graphite_93 = 4183.995381 * cp_graphite_cal_93;

%% Moderator state equations

% Temperature Dependent Density (kg/m^3) [ddbst.de, 273K-648K]
A_cp = .14395;
B_cp = .0112;
```

```
C_cp = 649.727;
D_cp = .05107;
low_temp = R(94);
c_temp = R(101);
f_temp = R(12);

% density of outlet water/core area water (kg/m^3)
density_water_13 = A_cp / ( B_cp^(1 + (1 - (R(13) + 273.15)/C_cp)^D_cp));
density_water_92 = A_cp / ( B_cp^(1 + (1 - (R(92) + 273.15)/C_cp)^D_cp));
density_water_94 = A_cp / ( B_cp^(1 + (1 - (R(94) + 273.15)/C_cp)^D_cp));
density_water_102 = A_cp / ( B_cp^(1 + (1 - (R(102) + 273.15)/C_cp)^D_cp));
density_water_103 = A_cp / ( B_cp^(1 + (1 - (R(103) + 273.15)/C_cp)^D_cp));

% density of inlet water, bulk tank (kg/m^3)
density_water_0 =  A_cp / ( B_cp^(1 + (1 - (GV(2) + 273.15)/C_cp)^D_cp));

% Mass of water (kg)
mass_cooling_water_fuel = GV(20) * density_water_13;
mass_cooling_water_graphite_92 = GV(28) * density_water_92;
mass_cooling_water_graphite_94 = GV(28) * density_water_94;
mass_cooling_water_102 = GV(43) * density_water_102;
mass_cooling_water_103 = GV(44) * density_water_103;

% specific heat of inlet water (KJ/kg K)
cp_H2O_KJ_0 = 3.16744e-10 * GV(2)^4 - 1.05772e-7 * GV(2)^3 ...
    + 2.35330e-5 * GV(2)^2 - 1.47670e-3 * GV(2) + 4.20617e0;

% Convert to J/kg
cp_H2O_0 = cp_H2O_KJ_0 * 1000;

% Temperature dependent Specific heat (J/kgK) [steam tables]
cp_H2O_92 = ( 3.16744e-10 * R(92)^4 - 1.05772e-7 * R(92)^3 ...
    + 2.35330e-5 * R(92)^2 - 1.47670e-3 * R(92) + 4.20617e0 ) * 1000;

cp_H2O_13 = ( 3.16744e-10 * R(13)^4 - 1.05772e-7 * R(13)^3 ...
    + 2.35330e-5 * R(13)^2 - 1.47670e-3 * R(13) + 4.20617e0 ) * 1000;

cp_H2O_94 = ( 3.16744e-10 * R(94)^4 - 1.05772e-7 * R(94)^3 ...
    + 2.35330e-5 * R(94)^2 - 1.47670e-3 * R(94) + 4.20617e0 ) * 1000;

cp_H2O_102 = ( 3.16744e-10 * R(102)^4 - 1.05772e-7 * R(102)^3 ...
    + 2.35330e-5 * R(102)^2 - 1.47670e-3 * R(102) + 4.20617e0 ) * 1000;

cp_H2O_103 = ( 3.16744e-10 * R(103)^4 - 1.05772e-7 * R(103)^3 ...
    + 2.35330e-5 * R(103)^2 - 1.47670e-3 * R(103) + 4.20617e0 ) * 1000;

% Use the Plume formulas from Dartmouth Paper/UT LOCA to find current mass flow
% gravity (m/s^2)
gravity = 9.8066;


% Kinetic Viscosity [30C](m^2/s)
kinetic_viscosity_water = .801e-6;

% Dynamic viscosity [30C] (Ns/m^2)
dyn_vis_water = 7.98e-4;

% Expansion Coefficient (1/K)
B_water = .303e-3;

% Thermal conductivity [NIST](W/mK)
k_water_13 = -1.48445 + 4.12292 * ((R(13) + 273.15)/298.15) ...
    - 1.63866 * ((R(13) + 273.15)/298.15)^2;
k_water_92 = -1.48445 + 4.12292 * ((R(92) + 273.15)/298.15) ...
    - 1.63866 * ((R(92) + 273.15)/298.15)^2;
k_water_94 = -1.48445 + 4.12292 * ((R(94) + 273.15)/298.15) ...
    - 1.63866 * ((R(94) + 273.15)/298.15)^2;
k_water_102 = -1.48445 + 4.12292 * ((R(102) + 273.15)/298.15) ...
    - 1.63866 * ((R(102) + 273.15)/298.15)^2;
k_water_103 = -1.48445 + 4.12292 * ((R(103) + 273.15)/298.15) ...
    - 1.63866 * ((R(103) + 273.15)/298.15)^2;
```

```
k_fuel = 17.5730;  % [Simnad]
k_graphite = 112.4;

% Prandtl Number (Pr)
Pr_102 = dyn_vis_water * cp_H2O_102 / k_water_102;
Pr_92 = dyn_vis_water * cp_H2O_92 / k_water_92;
Pr_13 = dyn_vis_water * cp_H2O_13 / k_water_13;
Pr_94 = dyn_vis_water * cp_H2O_94 / k_water_94;
Pr_103 = dyn_vis_water * cp_H2O_103 / k_water_103;

% Thermal diffusivity (m^2/s)
% therm_diff_water = 0.143e-6;
therm_diff_water_13 = k_water_13 / ( density_water_13 * cp_H2O_13 );
therm_diff_water_92 = k_water_92 / ( density_water_92 * cp_H2O_92 );
therm_diff_water_94 = k_water_94 / ( density_water_94 * cp_H2O_94 );

% find this loops transient factor (m(T) * cp(T)) [J/K, J/C]
trans_factor_13 = mass_cooling_water_fuel * cp_H2O_13;
trans_factor_92 = mass_cooling_water_graphite_92 * cp_H2O_92;
trans_factor_94 = mass_cooling_water_graphite_94 * cp_H2O_94;

% find the mass flow rate of inlet (kg/s) rho(T) * A_opening * velocity
% m_dot = R(95) * density_water_13 * area_cooling_pin * number_pins;

%%  Enthalpy (J/kgK)
 % find current specific enthalpy h = cp * (T(t) - T_ref) + h_ref;
enthalpy_ref = 9007; % J/kg @ 0C saturated

% inlet to core from bulk tank
h_0 = cp_H2O_0 * GV(2) + enthalpy_ref;

% out of lower graphite
h_1 = cp_H2O_92 * R(92) + enthalpy_ref;

% out of fuel region
h_2 = cp_H2O_13 * R(13) + enthalpy_ref;

% out of upper graphite
h_3 = cp_H2O_94 * R(94) + enthalpy_ref;

% out of lower fin region
h_102 = cp_H2O_102 * R(102) + enthalpy_ref;

% out of upper fin region
h_103 = cp_H2O_103 * R(103) + enthalpy_ref;

%% Gas and SS expansion coefficients [ UT LOCA]
% Mass (kg)
mass_gas_fuel = .08375 * pi * ( (GV(30) - .000508)^2 - (GV(30) - .000508 - 1.310588235294116e-
04)^2 ) * GV(9);
mass_gas_gr = .08375 * pi * ( (GV(30) - .000508)^2 - (GV(30) - .000508 - 1.310588235294116e-04)^2
) * GV(26);
mass_clad_fuel = 7740 * pi * ( GV(30)^2 - (GV(30) - .000508)^2 ) * GV(9);
mass_clad_gr = 7740 * pi * ( GV(30)^2 - (GV(30) - .000508)^2 ) * GV(26);

% cp (J/kg K)
cp_gas = 14.53e3;
cp_clad = 500;

% dz for conduction (m)
inner_radius = 0.003175;
dz_gas = 1.310588235294116e-04/2;
dz_clad = 0.000508/2;
dz_fuel_unit = ( GV(30) - .000508 - 1.310588235294116e-04 - inner_radius ) /2;

% Gas heat transfer from KSU SAR (W/m^2 K) [Whaley]
h_gas = 2.84e3;

% Thermal conductivity (W/m K)
k_gas = h_gas * 1.310588235294116e-04; % k ~ h/dx
k_clad = 16.2;
```

```
% Area (m^2)
A_gas = pi * ( (GV(30) - .000508)^2 - (GV(30) - .000508 - 1.310588235294116e-04)^2 );
A_clad = pi * ( (GV(30) )^2 - (GV(30) - .000508)^2 );

% Surface areas (m^2)
surface_gas_out_grap = 2 * pi * (GV(30) - .000508) * GV(26);
surface_gas_out_fuel = 2 * pi * (GV(30) - .000508) * GV(9);
surface_gas_in_grap = 2 * pi * (GV(30) - .000508 - 1.310588235294116e-04) * GV(26);
surface_gas_in_fuel = 2 * pi * (GV(30) - .000508 - 1.310588235294116e-04) * GV(9);

%% Momentum balance
% P is a property vector to pass
Pf = [ density_water_13 density_water_92 density_water_94 GV(25) GV(33) ...
     GV(34) therm_diff_water_13 therm_diff_water_92 therm_diff_water_94 ...
     gravity GV(9) GV(26) GV(30) GV(10) GV(24) GV(7) density_water_102 ...
     density_water_103 GV(35) GV(36) GV(37) GV(38) GV(39) GV(40) GV(43) ...
     GV(44) density_water_0 GV(41:59) ];

% Balance function
% m1 - inlet to lower grid
% m2 - lower cone to graphite
% m3 - graphite to fuel
% m4 - fuel to upper graphite
% m5 - upper graphite to upper cone
% m6 - outlet upper grid

% mdot per pin
m_dot_pin = Coolant_properties_1_0( R, Pf );

% mdot
m_dot = m_dot_pin * GV(27);

if ~isreal(m_dot)
    isreal(m_dot)
    m_dot
    return;
end
% Heat transfer coefficient

% lower region

% Fin effects
% Dimensionless numbers
if ( R(104) - R(102)) > 0
    Gr_102_fin = gravity * B_water * GV(35)^3 *  ( R(104) - R(102)) / kinetic_viscosity_water^2;
else
    Gr_102_fin = 0;
end

Ra_102 = Pr_102 * Gr_102_fin;

Nu_102_fin = .59 * Ra_102^.25;

% fin heat transfer coefficient (W/m^2 K)
h_bar_102_fin = Nu_102_fin * k_clad / GV(35);

% efficiency (calculated from mean efficiency effect at 30C)
eff_lower_fin = .2130;

% Heat lost in region 104 from the fin (W)
% q_102_fin = eff_lower_fin * h_bar_102_fin * GV(54) * ( R(104) - R(102) );

% upper region

% Fin effects
% Dimensionless numbers
if ( R(105) - R(103) ) > 0
    Gr_103_fin = gravity * B_water * GV(35)^3 * ( R(105) - R(103) ) / kinetic_viscosity_water^2;
else
    Gr_103_fin = 0;
```

```
end

Ra_103 = Pr_103 * Gr_103_fin;

Nu_103_fin = .59 * Ra_103^.25;

% fin heat transfer coefficient (W/m^2 K)
h_bar_103_fin = Nu_103_fin * k_clad / GV(36);

% efficiency (calculated from mean efficiency effect at 30C)
eff_upper_fin = .1781;

% Cylindrical sections
% cylindrical Nusselt
Nu_102_cyl =  ( .825 + ( .387 * Ra_102^(1/6) ) / ( 1 + ( .492/Pr_102)^(9/16) )^(8/27))^2;
%penn.edu
Nu_103_cyl =  ( .825 + ( .387 * Ra_103^(1/6) ) / ( 1 + ( .492/Pr_103)^(9/16) )^(8/27))^2;
%penn.edu

% Cyl heat transfer coefficient (W/m^2 K)
h_bar_102_cyl = Nu_102_cyl * k_water_102 / GV(48);
h_bar_103_cyl = Nu_103_cyl * k_water_103 / GV(49);

% Conical sections
% Conical section Nusselt [Yaser]
Nu_102_cone = 2.0963 + .669 * Gr_102_fin^.25 * Pr_102^(1/3);
Nu_103_cone = 2.0963 + .669 * Gr_103_fin^.25 * Pr_103^(1/3);

% characteristic length (m)
L_102 = sqrt( GV(39)^2 + GV(30)^2);
L_103 = sqrt( GV(40)^2 + GV(30)^2);

% heat transfer coefficient (W/m^2 K)
h_bar_102_cone = Nu_102_cone * k_water_102 / L_102;
h_bar_103_cone = Nu_103_cone * k_water_103 / L_103;

%% heat transfer coefficient
% Grashof Number [Clarkson.edu]
% Gr_s = reduced_gravity * pin_height^3 / kinetic_viscosity_water^2

% Find the Ra_s [ Kaminski ]
% Ra_s = Gr_s * Pr_water;
if ( R(99) - R(92) ) > 0
    Ra_L_92 =  ( gravity * B_water ) / ( kinetic_viscosity_water * therm_diff_water_92 ) ...
        * ( R(99) - R(92) ) * GV(26)^3;
else
    Ra_L_92 = 0;
end

if ( R(100) - R(13) ) > 0
    Ra_L_13 =  ( gravity * B_water ) / ( kinetic_viscosity_water * therm_diff_water_13 ) ...
        * ( R(100) - R(13) ) * GV(9)^3;
else
    Ra_L_13 = 0;
end

if ( R(101) - R(94) ) > 0
    Ra_L_94 =  ( gravity * B_water ) / ( kinetic_viscosity_water * therm_diff_water_94 ) ...
        * ( R(101) - R(94) ) * GV(26)^3;
else
    Ra_L_94 = 0;
end

% Nusselt number
% external free convection vertical cylinder
Nu_L_92 = ( .825 + ( .387 * Ra_L_92^(1/6) ) / ( 1 + ( .492/Pr_92)^(9/16) )^(8/27))^2; %penn.edu
Nu_L_13 = ( .825 + ( .387 * Ra_L_13^(1/6) ) / ( 1 + ( .492/Pr_13)^(9/16) )^(8/27))^2; %penn.edu
Nu_L_94 = ( .825 + ( .387 * Ra_L_94^(1/6) ) / ( 1 + ( .492/Pr_94)^(9/16) )^(8/27))^2; %penn.edu

% Heat transfer coefficient ( W/ m^2 K )
h_bar_92 = Nu_L_92 * k_water_92 / GV(26);
```

```
h_bar_13 = Nu_L_13 * k_water_13 / GV(9);
h_bar_94 = Nu_L_94 * k_water_94 / GV(26);

%% Delayed Power State Function (W)
% U235 delayed (W)
P_d_235 =  ( P_inst_235 / 200 ) * sum( H_fraction_235 ./ H_lambda_235 );

% U238 delayed (W)
P_d_238 =  ( P_inst_238 / 200 ) * sum( H_fraction_238 ./ H_lambda_238 );

% Pu239 delayed (W)
P_d_Pu_239 = ( P_inst_Pu239 / 200 ) * sum( H_fraction_Pu239 ./ H_lambda_Pu239 );

P_delay = P_d_235 + P_d_238 + P_d_Pu_239;

%% Total power by isotope (W)
% U235
P_i_235 = P_inst_235 + P_d_235;

% U238
P_i_238 = P_inst_238 + P_d_238;

% Pu239
P_i_Pu239 = P_inst_Pu239 + P_d_Pu_239;

P_eff = P_inst - P_delay + sum(R(21:66));

%% Differentials
% Reactor Kinetics
% overall in hour
R_dot(1) = ( R(11) + alpha_fuel_T * ( R(12) - GV(1) ) ...
    + GV(19) * ( R(13) - GV(2) ) - Beff_mix ) / A * R(1) ...
    + lambda_1 * R(2) ...
    + lambda_2 * R(3) ...
    + lambda_3 * R(4) ...
    + lambda_4 * R(5) ...
    + lambda_5 * R(6) ...
    + lambda_6 * R(7) ...
    + AmBe_source ...
    + U238_spontaneous + U235_spontaneous + Pu_239_spontaneuos; % ...
    % - R(1) * velocity_neutron * N_Sm * sig_a_Sm;
    % - R(1) * velocity_neutron * N_Zr * sig_a_Zr;

% DNP groups
R_dot(2) = (B_1_mix / A) * R(1) - lambda_1 * R(2);
R_dot(3) = (B_2_mix / A) * R(1) - lambda_2 * R(3);
R_dot(4) = (B_3_mix / A) * R(1) - lambda_3 * R(4);
R_dot(5) = (B_4_mix / A) * R(1) - lambda_4 * R(5);
R_dot(6) = (B_5_mix / A) * R(1) - lambda_5 * R(6);
R_dot(7) = (B_6_mix / A) * R(1) - lambda_6 * R(7);

% Source strength
R_dot(8) = 0;
R_dot(9) = 0;
R_dot(10) = 0;

% Reactivities
% event reactivity
switch SV(1)
    case 'Pulse'
        R_dot(11) = 0;

    case 'Rod Withdraw'
        if R(11) < GV(3) * Beff_mix
            R_dot(11) = GV(4);

        elseif R(11) >= GV(3) * Beff_mix
            R_dot(11) = 0;

        else
            display (' Error in Reactivity Addition ');
```

```
        end

    otherwise
        R_dot(11) = 0;
end

% Fuel Temperature
R_dot(12) = ( 1 / ( GV(13) * cp_fuel ) ) * ( P_eff ...
    + ( R(91) - R(12) ) / ( GV(22)/k_fuel + GV(29)/k_graphite ) * GV(32) ...
    + ( R(93) - R(12) ) / ( GV(22)/k_fuel + GV(29)/k_graphite ) * GV(32) ...
    + ( R(97) - R(12) ) / ( dz_fuel_unit/k_fuel + dz_gas/k_gas ) *  surface_gas_in_fuel );

% Moderator Temperature
R_dot(13) = (1 / trans_factor_13) * ( h_bar_13 * GV(7) * (R(100) - R(13)) ...
        + m_dot(3) * ( h_1 + gravity * (GV(26) + GV(45)) ) ...
        - m_dot(4) * ( h_2 + gravity * (GV(26) + GV(9) + GV(45)) ) );

% Changes in Beta effective
% [ current model will be 0 ]
R_dot(14) = 0;
R_dot(15) = 0;
R_dot(16) = 0;
R_dot(17) = 0;
R_dot(18) = 0;
R_dot(19) = 0;
R_dot(20) = 0;

%% Decay Heat calculations
% Delayed heat from U235 antecedes
R_dot(21) = H_fraction_235(1) * P_i_235 / 200 - H_lambda_235(1) * R(21);
R_dot(22) = H_fraction_235(2) * P_i_235 / 200 - H_lambda_235(2) * R(22);
R_dot(23) = H_fraction_235(3) * P_i_235 / 200 - H_lambda_235(3) * R(23);
R_dot(24) = H_fraction_235(4) * P_i_235 / 200 - H_lambda_235(4) * R(24);
R_dot(25) = H_fraction_235(5) * P_i_235 / 200 - H_lambda_235(5) * R(25);
R_dot(26) = H_fraction_235(6) * P_i_235 / 200 - H_lambda_235(6) * R(26);
R_dot(27) = H_fraction_235(7) * P_i_235 / 200 - H_lambda_235(7) * R(27);
R_dot(28) = H_fraction_235(8) * P_i_235 / 200 - H_lambda_235(8) * R(28);
R_dot(29) = H_fraction_235(9) * P_i_235 / 200 - H_lambda_235(9) * R(29);
R_dot(30) = H_fraction_235(10) * P_i_235 / 200 - H_lambda_235(10) * R(30);
R_dot(31) = H_fraction_235(11) * P_i_235 / 200 - H_lambda_235(11) * R(31);
R_dot(32) = H_fraction_235(12) * P_i_235 / 200 - H_lambda_235(12) * R(32);
R_dot(33) = H_fraction_235(13) * P_i_235 / 200 - H_lambda_235(13) * R(33);
R_dot(34) = H_fraction_235(14) * P_i_235 / 200 - H_lambda_235(14) * R(34);
R_dot(35) = H_fraction_235(15) * P_i_235 / 200 - H_lambda_235(15) * R(35);
R_dot(36) = H_fraction_235(16) * P_i_235 / 200 - H_lambda_235(16) * R(36);
R_dot(37) = H_fraction_235(17) * P_i_235 / 200 - H_lambda_235(17) * R(37);
R_dot(38) = H_fraction_235(18) * P_i_235 / 200 - H_lambda_235(18) * R(38);
R_dot(39) = H_fraction_235(19) * P_i_235 / 200 - H_lambda_235(19) * R(39);
R_dot(40) = H_fraction_235(20) * P_i_235 / 200 - H_lambda_235(20) * R(40);
R_dot(41) = H_fraction_235(21) * P_i_235 / 200 - H_lambda_235(21) * R(41);
R_dot(42) = H_fraction_235(22) * P_i_235 / 200 - H_lambda_235(22) * R(42);
R_dot(43) = H_fraction_235(23) * P_i_235 / 200 - H_lambda_235(23) * R(43);

% Delayed heat from U238 antecedes
R_dot(44) = H_fraction_238(1) * P_i_238 / 200 - H_lambda_238(1) * R(44);
R_dot(45) = H_fraction_238(2) * P_i_238 / 200 - H_lambda_238(2) * R(45);
R_dot(46) = H_fraction_238(3) * P_i_238 / 200 - H_lambda_238(3) * R(46);
R_dot(47) = H_fraction_238(4) * P_i_238 / 200 - H_lambda_238(4) * R(47);
R_dot(48) = H_fraction_238(5) * P_i_238 / 200 - H_lambda_238(5) * R(48);
R_dot(49) = H_fraction_238(6) * P_i_238 / 200 - H_lambda_238(6) * R(49);
R_dot(50) = H_fraction_238(7) * P_i_238 / 200 - H_lambda_238(7) * R(50);
R_dot(51) = H_fraction_238(8) * P_i_238 / 200 - H_lambda_238(8) * R(51);
R_dot(52) = H_fraction_238(9) * P_i_238 / 200 - H_lambda_238(9) * R(52);
R_dot(53) = H_fraction_238(10) * P_i_238 / 200 - H_lambda_238(10) * R(53);
R_dot(54) = H_fraction_238(11) * P_i_238 / 200 - H_lambda_238(11) * R(54);
R_dot(55) = H_fraction_238(12) * P_i_238 / 200 - H_lambda_238(12) * R(55);
R_dot(56) = H_fraction_238(13) * P_i_238 / 200 - H_lambda_238(13) * R(56);
R_dot(57) = H_fraction_238(14) * P_i_238 / 200 - H_lambda_238(14) * R(57);
R_dot(58) = H_fraction_238(15) * P_i_238 / 200 - H_lambda_238(15) * R(58);
R_dot(59) = H_fraction_238(16) * P_i_238 / 200 - H_lambda_238(16) * R(59);
R_dot(60) = H_fraction_238(17) * P_i_238 / 200 - H_lambda_238(17) * R(60);
```

```
R_dot(61) = H_fraction_238(18) * P_i_238 / 200 - H_lambda_238(18) * R(61);
R_dot(62) = H_fraction_238(19) * P_i_238 / 200 - H_lambda_238(19) * R(62);
R_dot(63) = H_fraction_238(20) * P_i_238 / 200 - H_lambda_238(20) * R(63);
R_dot(64) = H_fraction_238(21) * P_i_238 / 200 - H_lambda_238(21) * R(64);
R_dot(65) = H_fraction_238(22) * P_i_238 / 200 - H_lambda_238(22) * R(65);
R_dot(66) = H_fraction_238(23) * P_i_238 / 200 - H_lambda_238(23) * R(66);

R_dot(68) = H_fraction_Pu239(1) * P_i_Pu239 / 200 - H_lambda_Pu239(1) * R(68);
R_dot(69) = H_fraction_Pu239(2) * P_i_Pu239 / 200 - H_lambda_Pu239(2) * R(69);
R_dot(70) = H_fraction_Pu239(3) * P_i_Pu239 / 200 - H_lambda_Pu239(3) * R(70);
R_dot(71) = H_fraction_Pu239(4) * P_i_Pu239 / 200 - H_lambda_Pu239(4) * R(71);
R_dot(72) = H_fraction_Pu239(5) * P_i_Pu239 / 200 - H_lambda_Pu239(5) * R(72);
R_dot(73) = H_fraction_Pu239(6) * P_i_Pu239 / 200 - H_lambda_Pu239(6) * R(73);
R_dot(74) = H_fraction_Pu239(7) * P_i_Pu239 / 200 - H_lambda_Pu239(7) * R(74);
R_dot(75) = H_fraction_Pu239(8) * P_i_Pu239 / 200 - H_lambda_Pu239(8) * R(75);
R_dot(76) = H_fraction_Pu239(9) * P_i_Pu239 / 200 - H_lambda_Pu239(9) * R(76);
R_dot(77) = H_fraction_Pu239(10) * P_i_Pu239 / 200 - H_lambda_Pu239(10) * R(77);
R_dot(78) = H_fraction_Pu239(11) * P_i_Pu239 / 200 - H_lambda_Pu239(11) * R(78);
R_dot(79) = H_fraction_Pu239(12) * P_i_Pu239 / 200 - H_lambda_Pu239(12) * R(79);
R_dot(80) = H_fraction_Pu239(13) * P_i_Pu239 / 200 - H_lambda_Pu239(13) * R(80);
R_dot(81) = H_fraction_Pu239(14) * P_i_Pu239 / 200 - H_lambda_Pu239(14) * R(81);
R_dot(82) = H_fraction_Pu239(15) * P_i_Pu239 / 200 - H_lambda_Pu239(15) * R(82);
R_dot(83) = H_fraction_Pu239(16) * P_i_Pu239 / 200 - H_lambda_Pu239(16) * R(83);
R_dot(84) = H_fraction_Pu239(17) * P_i_Pu239 / 200 - H_lambda_Pu239(17) * R(85);
R_dot(85) = H_fraction_Pu239(18) * P_i_Pu239 / 200 - H_lambda_Pu239(18) * R(85);
R_dot(86) = H_fraction_Pu239(19) * P_i_Pu239 / 200 - H_lambda_Pu239(19) * R(86);
R_dot(87) = H_fraction_Pu239(20) * P_i_Pu239 / 200 - H_lambda_Pu239(20) * R(87);
R_dot(88) = H_fraction_Pu239(21) * P_i_Pu239 / 200 - H_lambda_Pu239(21) * R(88);
R_dot(89) = H_fraction_Pu239(22) * P_i_Pu239 / 200 - H_lambda_Pu239(22) * R(89);
R_dot(90) = H_fraction_Pu239(23) * P_i_Pu239 / 200 - H_lambda_Pu239(23) * R(90);

%% Input reactivity
switch SV(1)
    case 'Pulse'
        R_dot(67) = 0;

    case 'Rod Withdraw'
        if R(67) < GV(3) * Beff_mix
            R_dot(67) = GV(4);

        elseif R(67) >= GV(3) * Beff_mix
            R_dot(67) = 0;
        else
            display (' Error in Reactivity Addition ');
        end

    otherwise
        R_dot(67) = 0;
end

%% Temperature expansion
% Lower Graphite
R_dot(91) = ( 1 / ( GV(23) * cp_graphite_91 ) ) ...
    * ( ( R(91) - R(12) ) / ( GV(22)/k_fuel + GV(29)/k_graphite ) * GV(32) ...
        + ( R(96) - R(91) ) / ( dz_fuel_unit/k_fuel + dz_gas/k_gas ) * surface_gas_in_grap );

% upper graphite
R_dot(93) = ( 1 / ( GV(23) * cp_graphite_93 ) ) ...
    * ( ( R(93) - R(12) ) / ( GV(22)/k_fuel + GV(29)/k_graphite ) * GV(32) ...
        + ( R(98) - R(93) ) / ( dz_fuel_unit/k_fuel + dz_gas/k_gas ) * surface_gas_in_grap );

% Lower water channel
R_dot(92) = 1/trans_factor_92 * ( h_bar_92 * GV(24) * (R(99) - R(92)) ...
        + m_dot(2) * ( h_0 + gravity * ( GV(45) ) )...
        - m_dot(3) * ( h_1 + gravity * (GV(26) + GV(45)) ) );

% Upper water channel
R_dot(94) = 1/trans_factor_94 * ( h_bar_94 * GV(24) * (R(101) - R(94)) ...
        + m_dot(4) * ( h_2 + gravity * (GV(26) + GV(9) + GV(45)) )...
        - m_dot(5) * ( h_3 + gravity * ( 2 * GV(26) + GV(9) + GV(45)) ) );
```

```
% Velocity
if ( R(13) - R(94) ) > 0
    R_dot(95) = sqrt( therm_diff_water_13 * ( R(13) - R(94) ) * ( GV(22) + GV(29))  );
else
    R_dot(95) = 0;
end

%% Gas/ SS expansion
% Lower gas
R_dot(96) = 1/(mass_gas_gr * cp_gas) * ( ( R(97) - R(96) )* k_gas * A_gas / ( GV(22) + GV(29))
...
        + (  R(91) - R(96) ) / ( dz_fuel_unit/k_graphite + dz_gas/k_gas ) * surface_gas_in_grap
...
        + (  R(99) - R(96) ) / ( dz_clad/k_clad + dz_gas/k_gas ) * surface_gas_out_grap );

% Mid gas
R_dot(97) = 1/(mass_gas_fuel * cp_gas) * ( ( R(96) - R(97) )* k_gas * A_gas / ( GV(22) + GV(29))
...
        + (  R(12) - R(97) ) / ( dz_fuel_unit/k_fuel + dz_gas/k_gas ) * surface_gas_in_fuel ...
        + (  R(100) - R(97) ) / ( dz_clad/k_clad + dz_gas/k_gas ) * surface_gas_out_fuel ...
        + (  R(98) - R(97) ) * k_gas * A_gas / ( GV(22) + GV(29)) );

% Upper gas
R_dot(98) = 1/(mass_gas_gr * cp_gas) * ( ( R(97) - R(98) ) * k_gas * A_gas / ( GV(22) + GV(29))
...
        + (  R(93) - R(98) ) / ( dz_fuel_unit/k_graphite + dz_gas/k_gas ) * surface_gas_in_grap
...
        + (  R(101) - R(98) ) / ( dz_clad/k_clad + dz_gas/k_gas ) * surface_gas_out_grap );

% Lower Clad (SS304)
R_dot(99) = 1/(mass_clad_gr * cp_clad) * ( ( R(100) - R(99) )* k_clad * A_clad / ( GV(22) +
GV(29)) ...
    + (  R(96) - R(99) ) / ( dz_clad/k_clad + dz_gas/k_gas ) * surface_gas_out_grap  ...
    - h_bar_92 * GV(24) * (R(99) - R(92)) );

% Mid Clad (SS304)
R_dot(100) = 1/(mass_clad_fuel * cp_clad) * ( ( R(99) - R(100) )* k_clad * A_clad / ( GV(22) +
GV(29)) ...
    + ( R(101) - R(100) )* k_clad * A_clad / ( GV(22) + GV(29)) ...
    + (  R(97) - R(100) ) / ( dz_clad/k_clad + dz_gas/k_gas ) * GV(7) ...
    - h_bar_13 * GV(7) * (R(100) - R(13)) );

% Upper Clad (SS304)
R_dot(101) = 1/(mass_clad_gr * cp_clad) * ( ( R(100) - R(101) )* k_clad * A_clad / ( GV(22) +
GV(29)) ...
    + (  R(98) - R(101) ) / ( dz_clad/k_clad + dz_gas/k_gas ) * surface_gas_out_grap ...
    - h_bar_94 * GV(24) * (R(101) - R(94)) );

%% Momentum balance expansion
% Coolant area between lower graphite and lower grid plate (inlet)
R_dot(102) = 1 / (mass_cooling_water_102 * cp_H2O_102) * ( ...
    + m_dot(1) * ( h_0 ) - m_dot(2) * ( h_102 + gravity * GV(45) ) ...
    + eff_lower_fin * h_bar_102_fin * GV(54) * (R(104) - R(102)) ...
    + h_bar_102_cyl * GV(56) * (R(104) - R(102)) ...
    + h_bar_102_cone * GV(58) * (R(104) - R(102)) );

% Coolant area above upper and below upper grid plate (outlet)
R_dot(103) = 1 / (mass_cooling_water_103 * cp_H2O_103) * ( ...
    + m_dot(5) * ( h_3 + gravity * ( 2 * GV(26) + GV(9)) ) ...
    - m_dot(6) * ( h_103 + gravity * ( 2 * GV(26) + GV(9) + GV(45))) ...
    + eff_upper_fin * h_bar_103_fin * GV(55) * ( R(105) - R(103)) ...
    + h_bar_103_cyl * GV(57) * (R(105) - R(103)) ...
    + h_bar_103_cone * GV(59) * (R(105) - R(103)) );

% SS region of pin below lower graphite sitting on lower grid plate
R_dot(104) = 1 / (GV(50) * cp_clad) * ( (R(91) - R(104)) / ( GV(52)/k_clad + GV(29)/k_graphite)
...
    - eff_lower_fin * h_bar_102_fin * GV(54) * ( R(104) - R(102)) ...
    - h_bar_102_cyl * GV(56) * (R(104) - R(102)) ...
    - h_bar_102_cone * GV(58) * (R(104) - R(102)) );
```

```
% SS region of pin above upper graphite up to upper grid plate
R_dot(105) = 1 / (GV(51) * cp_clad) * ( (R(93) - R(105)) / ( GV(53)/k_clad + GV(29)/k_graphite)
...
    - eff_upper_fin * h_bar_103_fin * GV(55) * ( R(105) - R(103)) ...
    - h_bar_103_cyl * GV(57) * (R(105) - R(103)) ...
    - h_bar_103_cone * GV(59) * (R(105) - R(103)) );

%% Output
R_dot = R_dot';

if ~isreal(R)
    low_temp
    c_temp
    f_temp
    cp_H2O_94
    cp_H2O_92
    cp_H2O_13
    r92 = R(92)
    r94 = R(94)
    r13 = R(13)
    r99 = R(99)
    r100 = R(100)
    r101 = R(101)
    r102 = R(102)
    r103 = R(103)
    r104 = R(104)
    r105 = R(105)
    m_dot
    h_bar_13
    h_bar_92
    h_bar_94
    return;
end
```

Coolant Flow Development Program

```
function [ m_dot ] = Coolant_properties_1_0( R, P )
%% Coolant property momentum balance
% Author: Greg Kline
% Date: 8 Jul 2016
% Revision 1.0
%
% In order to better quantify the effects of thermal hydraulics, a
% conservation of momentum over conv of mass
% flow is considered driven by the fuel water region to upper graphite
% this gives a state dependent velocity across that border,
% using this, the additional velocities are found using
% pAw^2(in) - pAw^2(out) = F_darcy friction + F_gravity + F_misc
% while prudency may demand using an average or inlet velocity in the
% Darcy factor, the calculation intensity is minimized using the known

%% ODE Variables
% R(1) - neutron density
% R(2) - group 1 concentration
% R(3) - group 2 concentration
% R(4) - group 3 concentration
% R(5) - group 4 concentration
% R(6) - group 5 concentration
% R(7) - group 6 concentration
% R(8) - AmBe source concentration
% R(9) - spontaneous U238 concentration
% R(10) - spontaneous U235 concentration
% R(11) - reactivity at t
% R(12) - temperature of the fuel at t
% R(13) - temperature of the moderator at t
% R(14) - B_eff_mix at t
% R(15) - B_mix_1 at t
% R(16) - B_mix_2 at t
% R(17) - B_mix_3 at t
% R(18) - B_mix_4 at t
```

```
% R(19) - B_mix_5 at t
% R(20) - B_mix_6 at t
% R(21) - H_U2325_group_1 decay heat matrix
% R(22) - H_U2325_group_2
% R(23) - H_U2325_group_3
% R(24) - H_U2325_group_4
% R(25) - H_U2325_group_5
% R(26) - H_U2325_group_6
% R(27) - H_U2325_group_7
% R(28) - H_U2325_group_8
% R(29) - H_U2325_group_9
% R(30) - H_U2325_group_10
% R(31) - H_U2325_group_11
% R(32) - H_U2325_group_12
% R(33) - H_U2325_group_13
% R(34) - H_U2325_group_14
% R(35) - H_U2325_group_15
% R(36) - H_U2325_group_16
% R(37) - H_U2325_group_17
% R(38) - H_U2325_group_18
% R(39) - H_U2325_group_19
% R(40) - H_U2325_group_20
% R(41) - H_U2325_group_21
% R(42) - H_U2325_group_22
% R(43) - H_U2325_group_23
% R(44) - H_U2328_group_1
% R(45) - H_U2328_group_2
% R(46) - H_U2328_group_3
% R(47) - H_U2328_group_4
% R(48) - H_U2328_group_5
% R(49) - H_U2328_group_6
% R(50) - H_U2328_group_7
% R(51) - H_U2328_group_8
% R(52) - H_U2328_group_9
% R(53) - H_U2328_group_10
% R(54) - H_U2328_group_11
% R(55) - H_U2328_group_12
% R(56) - H_U2328_group_13
% R(57) - H_U2328_group_14
% R(58) - H_U2328_group_15
% R(59) - H_U2328_group_16
% R(60) - H_U2328_group_17
% R(61) - H_U2328_group_18
% R(62) - H_U2328_group_19
% R(63) - H_U2328_group_20
% R(64) - H_U2328_group_21
% R(65) - H_U2328_group_22
% R(66) - H_U2328_group_23
% R(67) - control rod reactivity at t
% R(68-90) - Pu239
% R(91) - Lower graphite temp
% R(92) - Lower moderator temp
% R(93) - Upper graphite temp
% R(94) - Upper mod temp
% R(95) - velocity
% R(96) - Lower Gas region
% R(97) - Mid Gas region
% R(98) - Upper Gas region
% R(99) - Lower SS Region
% R(100) - Mid SS region
% R(101) - Upper SS region
% R(102) - Lower pin grid plate coolant region
% R(103) - Upper pin grid plate coolant region
% R(104) - Pin lower fins and region
% R(105) - Pin upper fins and region

%% P = [
%   1  density_water_13
%   2  density_water_92
%   3  density_water_94
%   4  area_cooling_pin
```

```
%    5  flow_outlet_core
%    6  flow_inlet_core
%    7  therm_diff_water_13
%    8  therm_diff_water_92
%    9  therm_diff_water_94
%    10  gravity
%    11  pin_height
%    12  graphite_height
%    13  radius_pin
%    14  inner_hex
%    15  surface_area_graphite
%    16  surface_area_fuel
%    17  density_water_102
%    18  density_water_103
%    19  low_fin_height
%    20  upper_fin_height
%    21  A_flow_outlet_grid
%    22  P_flow_outlet_grid
%    23  lower_cone_height
%    24  upper_cone_height
%    25  volume_cooling_lower_conical
%    26  volume_cooling_upper_conical
%    27  density_water_0
%    28  A_flow_inlet_grid
%    29  P_flow_inlet_grid
%    30  volume_cooling_lower_conical
%    31  volume_cooling_upper_conical ...
%    32  lower_pin_below_gr
%    33  upper_pin_above_gr
%    34  lower_fin_height ...
%    35  lower_cyl_height
%    36  upper_cyl_height
%    37  mass 104 ss region GV(50)
%    38  mass 105 ss region
%    39  dz_lower_ss_cond
%    40  dz_upper_ss_cond
%        ];

%% Designators
% 0 - inlet under or at lower grid plate
% 1 - boundary between lower finned portion and lower edge of graphite
% 2 - boundary between lower graphite and fuel
% 3 - boundary between fuel and upper graphite
% 4 - boundary between upper graphite and upper fuel area
% 5 - outlet or just above upper grid plate

% Darcy Roughness for SS (m) [Eng. toolbox]
e = .01524e-3;

% Kinetic Viscosity (m^2/s)
v = .279e-6;

% gravity (m/s^2)
gravity = 9.8066;

% Find hydraulic diameter (m)
% Wetted perimeter (m)
Pewit = 12 * P(14) / sqrt(3) + 2 * pi * P(13);

% flow area (m^2)
A_cool_1 = P(4);
A_cool_2 = P(4);
A_cool_3 = P(4);
A_cool_4 = P(4);

% Hydraulic diameter (m)
D_H_0 = 4 * P(28) / P(29);
D_H_1 = 4 * A_cool_1 / Pewit;
D_H_2 = 4 * A_cool_2 / Pewit;
D_H_3 = 4 * A_cool_3 / Pewit;
D_H_4 = 4 * A_cool_4 / Pewit;
```

```
D_H_5 = 4 * P(21) / P(22);

% Surface areas of cones
A_cone_lower = pi * P(13) * sqrt( P(23)^2 + P(13)^2 );
A_cone_upper = pi * P(13) * sqrt( P(24)^2 + P(13)^2 );
A_s_102 = 2 * pi * P(13) * P(35);
A_s_103 = 2 * pi * P(13) * P(36);

% w3 is tracked using Boussinesq assumption and the presumption the area
% with the heat flux from fuel drives the overall velocity
% using v3 and a momentum balance, v2 can be found

%%%%% Code to use inlet.  fails at 0 m/s %%%%%%%%%%%%%%%%%%%%%%%%%%%%%%%%
%     function [ y ] = w3_fun ( x )
%         y = P(2) * P(4) * x^2 ...
%             - P(1) * P(4) * R(95)^2 ...
%             - P(2) * gravity * P(4) * P(11) ...
%             - .5 * ( P(11) / D_H_2 ) * P(2) * x^2 * P(16) ...
%             / ( log10( (e/(3.7*D_H_2)) + 5.74/(x*P(11)/v) ) )^2;
%
%     end
%
%     w2 = fzero(@w3_fun,.90*R(95))
%%%%%%%%%%%%%%%%%%%%%%%%%%%%%%%%%%%%%%%%%%%%%%%%%%%%%%%%%%%%%%%%%%%%%%%%%

% Find the Darcy force around fuel (N)
R(95);

%% Fuel section
% fuel area Darcy
F_darcy_13 = .5 * ( P(11) / D_H_2 ) * P(2) * R(95)^2 * P(16) ...
               * ( log10( (e/(3.7*D_H_2)) + 5.74/((R(95)*P(11)/v)^.9) ) )^-2;

% Find the Gravity force around fuel (N)
F_grav_13 = P(1) * gravity * A_cool_2 * P(11);

% find the velocity at 2 (m/s)
if P(1) * A_cool_3 * R(95)^2 - F_darcy_13 - F_grav_13 > 0
    w2 = sqrt( (- F_darcy_13 - F_grav_13 + P(1) * A_cool_3 * R(95)^2) ...
                  / ( P(2) * A_cool_2 ) );
else
    w2 = 0;
end

%% Upper graphite
% Find the Darcy friction of upper graphite (N)
F_darcy_94 = .5 * ( P(12) / D_H_3 ) * P(1) * R(95)^2 * P(15) ...
               * ( log10( (e/(3.7*D_H_3)) + 5.74/((R(95)*P(12)/v)^.9) ) )^-2;

% Find gravity force of upper graphite (N)
F_grav_94 = P(2) * gravity * A_cool_3 * P(12);

% find the velocity at 4 (m/s)
w4 = sqrt( (P(1) * A_cool_3 * R(95)^2 + F_darcy_94 + F_grav_94) ...
              / ( P(2) * A_cool_4 ) );

%% Lower graphite
% Find the Darcy friction of lower graphite region (N)
F_darcy_92 = .5 * ( P(12) / D_H_2 ) * P(17) * w2^2 * P(15) ...
               * ( log10( (e/(3.7*D_H_2)) + 5.74/((w2*P(12)/v)^.9) ) )^-2;

% Gravity force of 92
F_grav_92 = P(3) * gravity * A_cool_1 * P(12);

% find the velocity at 1
if P(2) * A_cool_3 * w2^2 - F_darcy_92 > 0
    w1 = sqrt( (-F_darcy_92 - F_grav_92 + P(2) * A_cool_3 * w2^2) ...
                  / ( P(17) * A_cool_1 ) );
else
    w1 = 0;
end
```

```
%% Lower conical region
% Drag force on the conical region (drag coefficient from rocketry)
F_drag_lower_cone = .5 * P(17) * w1^2 * .2 * A_cone_lower;

% Darcy friction for the small section
F_darcy_102 = .5 * ( P(32) / D_H_1 ) * P(17) * w1^2 * A_s_102 ...
                * ( log10( (e/(3.7*D_H_1)) + 5.74/((w1*P(17)/v)^.9) ) )^-2;

% Gravity force
F_grav_102 = P(17) * gravity * P(25);

% find the velocity at 1
if P(17) * A_cool_3 * w2^2 - F_drag_lower_cone - F_darcy_102 > 0
    w0 = sqrt( (-F_drag_lower_cone - F_darcy_102 - F_grav_102 + P(17) * A_cool_3 * w2^2) ...
                    / ( P(27) * P(28) ) );
else
    w0 = 0;
end

%% Upper conical region
% Drag force on the conical region (drag coefficient from rocketry)
F_drag_upper_cone = .5 * P(18) * w4^2 * .2 * A_cone_upper;

% Darcy friction for the small section
F_darcy_103 = .5 * ( P(33) / D_H_4 ) * P(3) * w4^2 * A_s_103 ...
                * ( log10( (e/(3.7*D_H_4)) + 5.74/((w4*P(3)/v)^.9) ) )^-2;

% Gravity force
F_grav_103 = P(18) * gravity * P(26);

% find the velocity at 1
w5 = sqrt( (P(3) * A_cool_4 * w4^2 + F_drag_upper_cone + F_darcy_103 + F_grav_103) ...
                / ( P(18) * P(21) ) );

%% Build mass flow rate vectors
if R(95) > 0
    m_dot(1) = P(27) * P(28) * w0;
    m_dot(2) = P(17) * A_cool_1 * w1;
    m_dot(3) = P(2) * A_cool_2 * w2;
    m_dot(4) = P(1) * A_cool_3 * R(95);
    m_dot(5) = P(3) * A_cool_4 * w4;
    m_dot(6) = P(18) * P(21) * w5;

else
    m_dot = [ 0 0 0 0 0 0 ];
end

end
```

LOSS OF COOLANT ACCIDENT ANALYSIS FOR THE UNIVERSITY OF TEXAS AT AUSTIN TRIGA REACTOR

1. Introduction

The loss of coolant accident (LOCA) analysis assumes steady state reactor operation at equilibrium (limiting core configuration conditions) followed by a reactor scram with the water cooling simultaneously replaced with air cooling. The analysis models radial heat transfer from the center of the element outward to the air at the axial location/segment of the hot channel fuel element with the maximum specific axial power.

This LOCA analysis includes (1) an overview of physical characteristics of UT TRIGA system, (3) the basis of thermodynamic analysis, (4) development of the UT LOCA model, (5) validation of the model against independent analytical method and against observed data, and (6) summary of the thermodynamic performance following a LOCA.

2. UT TRIGA Characteristics

Physical properties of The University of Texas at Austin (UT) TRIGA reactor fuel are taken from Simnad[1]. The UT reactor fuel contains 8. 5 wt% U enriched to less than 20% ^{235}U in a zirconium-hydride matrix at a ZrH ratio of 1.6. Decay heat as a function of time after shutdown is based on calculations by the CINDER code as reported by George, LaBauve, and England [1980, 1982] and used by Kansas State University University[2]. Decay heat is assumed to have the same spatial distribution as power generation during operation. Core limiting configurations were calculated using neutronic analysis.

2.1. Decay Heat

The decay power fraction remaining from 1 second to 10^6 seconds following an abrupt shutdown is found by equation (1):

$$R(t) = \frac{0.04856 + 0.1189 \cdot \log_{10} t - 0.103 \cdot (\log_{10} t)^2 + 0.000228 \cdot (\log_{10} t)^3}{1 + 2.5481 \cdot \log_{10} t - 0.19632 \cdot (\log_{10} t)^2 + 0.05417 \cdot (\log_{10} t)^3} \quad (1)$$

The fuel element generating the highest power is expected to experience the most severe thermal hydraulic conditions. Calculations with TRACE indicate the maximum power for a fuel element with an acceptable critical heat flux ratio of 2.0 during operation is slightly less than 24kW. Neutronic analysis based on the fuel element divided into 15 equal axial segments shows the maximum power generation within a single segment is 1.2 times the average power in all segments. Therefore the limiting case for thermodynamic response following initiation of a LOCA is based on the maximum specific power and the decay power fraction in the fuel element is calculated from the maximum axial peaking factor for the fuel element in equation (2):

$$q_{gen,i}(t,r) = 1.2 \cdot q_{gen}(r) \cdot R(t) \quad (2)$$

2.2. Fuel Element Geometry

The fuel element model in this analysis is a set of concentric cylinders representing a zirconium rod at the center, the fuel matrix, a gas-gap between the fuel and cladding, and cladding. The

dimensions are taken from the GA drawings and UT Technical Specifications. The Zirconium fill rod radius is 0.003175m. The fuel matrix outer diameter is 1.47 in (0.018771m) diameter. The gas gap is approximately 0.005 in (1.97E-5 m). Cladding is 0.020 in (0.000508m) thick. The total heated length of the fuel (section with Zr-U fuel matrix) is 15 in, segmented for thermal hydraulic analysis into 15 equal lengths leaving a height of 0.0254m.

2.3. Fuel Element Thermodynamic properties

Simnad[1] provides a number of mechanical characteristics and equations for fuel quantities. The thermal conductivity (k) is given, density is calculated from a given equation for a specific Zr:H ratio of 1.6. Density is determined by equation (3):

$$\rho_{Fuel} = \frac{1}{\left(\frac{U_{wt\%}}{\rho_U}\right) + \frac{(1 - U_{wt\%})}{\rho_{Zr}}} \tag{3}$$

Where $U_{tw\%}$ is uranium weight per cent, ρ_U is the density of uranium, and ρ_U is the density of zirconium. Simnad provides the temperature (T) dependent volumetric heat capacity ($c_{p,vol}$) in equation 4(a):

$$c_{p,vol}\left\{\frac{J}{m^3 K}\right\} = 2.04 + 4.17e - 3 \cdot T \tag{4a}$$

Specific heat capacity ($c_{p,fuel}$) is calculated as the ratio of equation (4a) to equation (3) in equation (4b):

$$c_{p,fuel}\left\{\frac{J}{kg * K}\right\} = \frac{\rho_{Fuel}}{c_{p,vol}} \tag{4b}$$

3. Basis of Thermodynamic Analysis

The steady state and transient analyses are developed from a heat balance across a series of finite elements whose energy relation can be built from equation (5a)[3], [4]:

$$\dot{E}_{st} = \dot{E}_{gen} + \dot{E}_{in} - \dot{E}_{out} \tag{5a}$$

Where, $\dot{E}_{st}$ is the stored energy in the structure, $\dot{E}_{gen}$ is energy generated within the structure, $\dot{E}_{in}$ is energy transferred into the structure, and $\dot{E}_{out}$ is the energy transferred out of the structure. This model translates physically into equation (5b):

$$\rho \cdot V \cdot c_p \cdot \frac{dT}{dt} = q_{gen} + q_{cond} + q_{conv} \tag{5b}$$

Stored energy (and the associated temperature change) is a function of material density (ρ), specific heat (c_p), volume (V), and the conduction, convection, and generation terms (q_{gen}, q_{cond}, and q_{conv} respectively).

3.1 Stored Energy ($\rho \cdot V \cdot c_p \cdot T$)

Energy storage is the time dependent material property used in the transient portion of the analysis. It is the dominant factor in peak temperatures as it represents a thermal inertial term[3].

3.2 Energy Generation (q_{gen})

Energy generation in the core is considered a result of fission effects in the fuel only.

3.4 Conduction Heat Transfer (q_{cond})

Heat transfer through conduction within the radius of the fuel element and cladding is modelled with Fourier's law of conduction in radial geometry:

$$q_{cond} = -k \cdot A_s \cdot \frac{dT}{dr} \tag{6}$$

Where k is thermal conductivity, A_s is the surface area through which heat transfer occurs, and $\frac{dT}{dr}$ is the rate of temperature change with respect to radial displacement. As recommended[5], the gas gap is approximated as thermal conductivity, calculated by the gas gap heat transfer coefficient divided by the thickness of the gap.

3.5 Convection Heat Transfer (q_{conv})

Convection heat transfer is modelled using Newton's law of cooling[3], [4]:

$$q_{conv} = h \cdot A_s \cdot (T_s - T_{inf}) \tag{7}$$

Where the outer surface area is A_s, the wall temperature is T_s, and the bulk coolant temperature is T_{inf}, and the heat transfer coefficient is h.

The convection heat transfer coefficient is calculated from dimensionless numbers. For natural convection, the significant dimensionless numbers are the Prandtl (Pr), Grashof (Gr), and modified Rayleigh (Ra) numbers. These values, combined with Nusselt (Nu) correlations, lead to the heat transfer coefficients which are used to find the energy transferred via convection[3], [6].

a. The Prandtl number is a measure of the fluid's viscous diffusion (ν) to kinematic diffusivity (α) of the fluid:

$$Pr = \frac{\nu}{\alpha} \tag{8}$$

Where α is the thermal diffusivity of the fluid, defined as:

$$\alpha = \frac{k}{c_p \cdot \rho} \tag{9}$$ (6)

b. The Grashof number is a dominant number in natural circulation. It is dependent on both surface temperature and channel temperature, fluid expansion coefficient, gravity, dynamic viscosity and channel dimensions. The Grashof number is defined as:

$$Gr_s = \frac{g \cdot \beta \cdot (T_s - T_{inf}) \cdot s^3}{\mu^2} \tag{10}$$

Where g is the acceleration due to gravity, β is the thermal expansion coefficient of the coolant, s is the channel width, and μ is the dynamic viscosity of the coolant.

c. The Rayleigh number is a function of buoyancy effects and momentum vs vicious diffusions and calculated as below[6],:

$$Ra_s = Gr_s Pr = \frac{g\beta\rho^2(T_{wall} - T_{fluid})s^3}{\mu^2} Pr \tag{11}$$

Where s subscript implies channel width is dimension of interest.

d. The Nusselt number relates the conductive and convective heat transfer effects of the fluid. The heat transfer is driven by the temperature difference and is found through the Nusselt number. A correlation for natural circulation in vertical channels for the Nusselt number is[6]:

$$Nu_s = \left\{ \frac{576}{\left[Ra_s\left(\frac{s}{dy}\right)\right]^2} + \frac{2.87}{\left[Ra_s\left(\frac{s}{dy}\right)\right]^{1/2}} \right\}^{-1/2} \tag{12}$$

e. The average heat transfer coefficient, $\bar{h}$, can be found from the average Nusselt number using[3], [7]:

$$\bar{h} = \frac{\overline{Nu}_s . k}{s} \tag{13}$$

4. The UT LOCA Model

The University of Texas Loss of Coolant model is a combination of finite element analysis (FEA) for steady state, and transient fuel conditions, as well as an air channel analysis sub-section to provide effective estimation of air channel heating. This channel sub-model leads to proper parametric variation analysis by giving a real world upper bounding temperature.

4.1 Coolant Air Temperature

In order to find the limiting values of the channel air temperature, a separate, one dimensional vertical model was created independent of the FEA model and geometry used in finding the fuel temperatures. It utilizes an elemental, vertical, constant temperature surface interfacing with buoyant air. See the figure below for details:

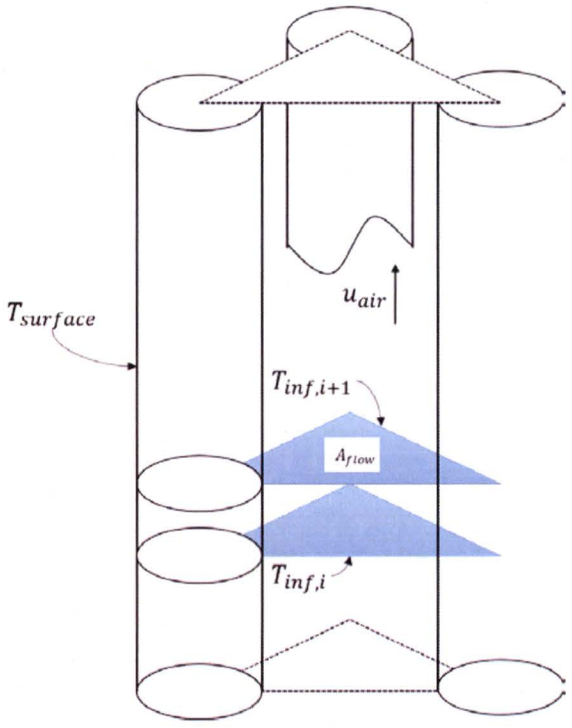

Figure 1. Channel Air Model Geometry

The temperature entering the bottom of the channel surrounding the fuel element is the limiting room air temperature following a loss of coolant. The rise in temperature is found by segmenting the pin vertically. Each iteration has a specific heat flux relative to the temperature difference between the surface and the air, its specific dimensionless parameters, and a constant surface temperature that is user defined. The limiting condition for surface temperature surface is 950°C[8].

The change in air temperature across each segment is a function of the heat generated in the segment and the heat transfer coefficient calculated from local non-dimensional parameters. Heat transfer characteristics in convection depend on intrinsic and extrinsic material properties and fluid temperature, with the heat transfer coefficient calculable though the use of dimensionless numbers. The temperature rise of the fluid entering the region of heat transfer for subsequent segments is the exit temperature for the preceding segment, i.e., the rise in temperature across the previous segment added to the temperature of the coolant entering the previous segment. The channel flow heat up model provided an order of magnitude estimation leading to proper parametric variation.

4.1.1 Fluid flow, and thus the characteristic velocity, is driven by natural convection and is dominated by the buoyancy driven numbers in the Rayleigh number (Ra_s), the product of the Grashof and Prandtl numbers which is driven by temperature difference.

a. The change in coolant temperature from fluid flow across a segment begins by finding the appropriate Rayleigh number (eqn. 11) for the i^{th} segment[6], then the segment's Nusselt number (eqn. 12), then the heat transfer coefficient (eqn. 13). With the heat transfer coefficient now found, the heat flux (q'') is found using:

$$q'' = h_i \cdot (T_s - T_{inf,i}) \tag{15}$$

Where T_s is the cladding surface temperature and $T_{inf,i}$ is the heat sink temperature.

b. Heat flux is used to find the Modified Rayleigh number. For uniform wall heating, the modified Rayleigh (Ra*)[9] is:

$$Ra_s^* = \frac{g \cdot \beta \cdot q'' \cdot \rho^2 \cdot c_p \cdot s^4}{\mu \cdot k^2} \tag{16}$$

Where g is the acceleration due to gravity, β is the thermal expansion coefficient, and μ is dynamic viscosity.

c. The modified Rayleigh number leads to the characteristic channel velocity, U_Z. [8]:

$$U_z = \frac{\alpha}{s}\sqrt{Ra_L^* \cdot Pr} \tag{17}$$

d. T
he change in temperature for fluid flow across a segment of the fuel element along the (axial) direction of flow can be calculated with:

$$\dot{Q}_i = \dot{m} \cdot c_p \cdot \Delta T \tag{18}$$

e. Where the ΔT is calculated as:

$$\Delta T = \frac{q'' \cdot A_{FE,i}}{\rho \cdot A_{flow} \cdot U_Z \cdot c_p} \tag{19a}$$

Where U_Z is calculated from eqn. (17). This ΔT is added to the segment's inlet temperature and becomes the inlet temperature for the next segment. The last segment's channel temperature represents the culmination of all the heating:

$$T_{inf,i} = T_{inf,i-1} + \Delta T_i \tag{19b}$$

4.1.2 As an independent calculation to determine limiting values of air temperature, the temperature rise was found through standard gas laws.

a. The characteristic velocity gives a stay time for the air (heated length divided by characteristic channel velocity). This allows the change in energy to be calculated as follows:

$$dE = q'' \cdot A_s \cdot t_{stay} \tag{20}$$

Where t_{stay} is the time the cooling air is in contact with the cladding surface.

b. By using the density of air and the volume of the channel, the mass of the air in the space at any given time can be found, by neglecting density changes. Using the equation below, the change in temperature can be found:

$$q = mc_v\Delta T \rightarrow$$
$$\Delta T = \frac{q}{mc_v} \Longrightarrow T_f = T_{init} + \Delta T \tag{21}$$

4.1.3 Channel Air Temperature Limiting Values[8]

These two methods routinely agreed across variations in surface temperatures. The geometry in use in reality is far more complex than this simple sub model accounts for, so order of magnitude correlation was acceptable. Especially since the model's purpose was to define reasonable limits for parametric variation. The maximum air temperature in the channel at the exit with 20°C inlet and 950°C fuel element surface temperature is 37°C.

4.2 Finite Element Model Geometry and Basis[10]

The calculation of temperature distribution in the fuel element is accomplished by using the principles of finite element analysis. The fuel element geometry is based on a cylindrical segment. The axial height of the segment is the total heated length (0.381 m) divided by the number of segments (15). Radial dimensions are taken from General Atomics drawings, as specified earlier.

The FEA radii distribution used in computation was selected based on both parameter validation and computational power available. It was essential to adequately capture the temperature effects in the smaller outer geometries and transitions. Thus the, *dr,* value near the outer portion is smaller than in the center fuel meat area. This saved on the size of the solution array, but still allows necessary detail. The limiting geometric parameter of concern is the Biot number, which relates convective and conductive aspects of the element to its volume to surface area ratio, equation (22a):

$$Bi = \frac{h \cdot L_c}{k} \tag{22a}$$

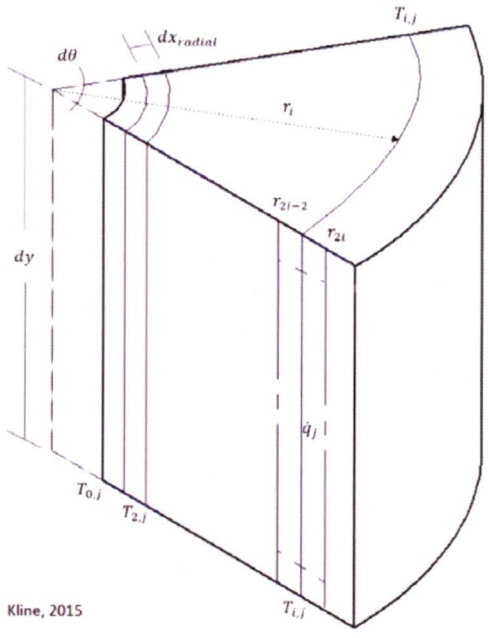

Figure 2. Finite Element Radial Geometry

Where, the characteristic length, L_c, is defined as the volume to surface area ratio:

$$L_c = \frac{V}{A} \tag{22b}$$

Differential radii in the outer portions of the model were chosen to most accurately subdivide the real geometry of the cladding and the gas gap. Internal fuel differential radii were chosen to minimize the Biot number.

In addition to the Biot number, the Fourier number is a transient figure of merit related to the time response and geometry:

$$Fo = \frac{\alpha \cdot t}{L_c} \tag{23}$$

According to Bergman[3], the Biot number must remain below 0.1, and the Fourier number must remain below 0.5 for 1D lumped parameter FEA to be valid. This was the merit to which the differential radii are chosen.

4.3 Steady State Finite Element Analysis

To create a valid transient condition, a valid steady state initial condition must be found, first. To facilitate this, each element is assessed using an energy balance equation across the element. Since the steady state model is not time dependent, the energy balance is reduced in equation (24):

$$\dot{E}_{in} + \dot{E}_{gen} = \dot{E}_{out};\ \dot{E}_{out} = 0 \implies \dot{E}_{in} + \dot{E}_{gen} = 0 \tag{24}$$

In this analysis, all energy flow is considered into the element. Fig. 3 illustrates an element energy balance and temperature definition relationship.

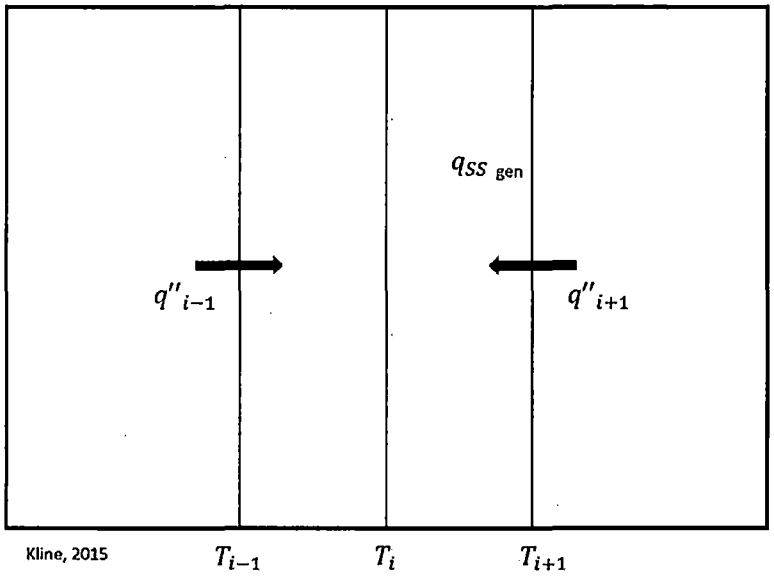

Figure 3. Finite Element Energy Balance

A matrix form of this energy balance is developed to solve for the temperature profile.

$$A\vec{x} = \vec{b} \tag{25}$$

Where, $\vec{x}$ is a vector representing the radial temperature profile, and $\vec{b}$ is a vector representing the energy generation and non-temperature dependent terms. Below is the development of the steady state finite element equations. The cladding end element is the only element containing a convection term, while fuel elements are the only ones containing generation terms. The following relationships are incorporated in the elements of the matrix equations[10]:

Conduction and Convection Terms:

$$q_{gen,SS,r} = q_{max} \cdot q(r) \cdot \pi \cdot dy \cdot ({r_{2i}}^2 - {r_{2i-2}}^2) \tag{26a}$$

$$q_{conv,SS} = h_{water} \cdot \pi \cdot r_{max} \cdot dy \cdot (T_s - T_{inf}) \tag{26b}$$

$$q_{cond,SS} = \frac{2 \cdot \pi \cdot dy \cdot k_{fuel} \cdot (T_{i\pm1} - T_i)}{\ln\left(\frac{r_{larger}}{r_{smaller}}\right)} \tag{26c}$$

Generation and Temperature Independent Terms

$$b_i = -q_{max} \cdot \pi \cdot dy \cdot ({r_{2i}}^2 - {r_{2i-2}}^2); \tag{26d}$$

$$b_{end-1,4} = 0;\ \ (No\ heat\ generation\ in\ cladding/gas) \tag{26e}$$

$$b_{end} = -h_{water} \cdot \pi \cdot r_{end} \cdot dy \cdot T_{inf} \tag{26f}$$

$$\underline{\text{Matrix Elements for } \boldsymbol{A}} = \begin{bmatrix} a_1 \\ a_2 \\ \vdots \\ a_j \\ a_{end} \end{bmatrix}$$

$$a_1 = \left[\frac{2 \cdot \pi \cdot dy \cdot k_{fuel} \cdot (T_{i-1} - T_i)}{\ln\left(\frac{r_2}{r_1}\right)}, \quad \frac{-2 \cdot \pi \cdot dy \cdot k_{fuel} \cdot (T_{i+1} - T_i)}{\ln\left(\frac{r_2}{r_1}\right)} \ldots \right] \tag{24g}$$

(24h)

$$a_i = \left[\ldots, \frac{2 \cdot \pi \cdot dy \cdot k_{fuel(gas,clad)} \cdot (T_{i-1} - T_i)}{\ln\left(\frac{r_{2i-1}}{r_{2i-3}}\right)}, -\left(\frac{2 \cdot \pi \cdot dy \cdot k_{fuel(gas,clad)} \cdot (T_{i-1} - T_i)}{\ln\left(\frac{r_{2i-1}}{r_{2i-3}}\right)} + \frac{2 \cdot \pi \cdot dy \cdot k_{fuel(gas,clad)} \cdot (T_{i+1} - T_i)}{\ln\left(\frac{r_{2i+1}}{r_{2i-1}}\right)} \right), \frac{2 \cdot \pi \cdot dy \cdot k_{fuel(gas,clad)} \cdot (T_{i+1} - T_i)}{\ln\left(\frac{r_{2i+1}}{r_{2i-1}}\right)} \ldots \right]$$

(24i)

$$a_{end} = \left[\ldots, \frac{2 \cdot \pi \cdot dy \cdot k_{clad} \cdot (T_{end-1} - T_{end})}{\ln\left(\frac{r_{end}}{r_{end-1}}\right)}, -\left(\frac{2 \cdot \pi \cdot dy \cdot k_{clad} \cdot (T_{end-1} - T_{end})}{\ln\left(\frac{r_{end}}{r_{end-1}}\right)} + h_{water} \cdot \pi \cdot r_{end} \cdot dy \right) \right]$$

$$\underline{\text{Matrix Formula}}$$

$$\vec{T} = \boldsymbol{A}^{-1} \cdot \vec{\boldsymbol{b}} \tag{24k}$$

The energy generation term in the element is a function of both its axial and radial position. The highest axial peaking factor (1.2) was used to represent the cylindrical segment generating the most power. The radial peaking factor, q(r), is found through a curve fit to the results of neutronic calculations (equation 24):

$$q(r) = C_{axial,peak} q_{max} (247192r^3 - 5377r^2 + 45.882r + .7335) \tag{24l}$$

MATLAB was utilized to build and solve the equation using native commands that maximize the efficiency and accuracy of the matrix inversion method.

4.4 Transient Finite Element Analysis

The transient portion of the model uses the initial steady state temperature profile and systematically walks it forward with time. The basic concept of an energy balance is again used,

with the time dependent components now considered in addition to the other terms. In the UT LOCA model the loss of coolant accident is considered to be instantaneous, and thus the cooling properties switch from water to air at the first iteration.

$$\dot{E}_{st} = \dot{E}_{in} - \dot{E}_{out} + \dot{E}_{gen};\ \dot{E}_{out} = 0 \rightarrow \tag{25a}$$

$$\rho \forall c_p \frac{dT}{dt} = q_{cond} + q_{conv} + q_{gen} \rightarrow \tag{25b}$$

$$\rho \forall c_p \frac{(T_i^{p+1} - T_i^p)}{\Delta t} = q_{cond} + q_{conv} + q_{gen} \tag{25c}$$

This leads to the transient analysis equation set which is related to the steady state equations (equation 26):

$$T_i^{p+1} = \frac{\Delta t}{\rho \forall c_p}[a_i] + T_i^p \tag{26}$$

The differential time element is selected based on the Fourier number (eqn. 23). Additionally, the code calculates a number of output values including a two-dimensional matrix $\vec{B}$ whose horizontal dimension represents the radial temperature distribution and vertical axis as time. This allows three essential model parameters to be extracted. First, the cladding surface temperature versus time is extracted and used to find peak cladding temperature. Second, the temperature profile across the pin at t_i can be found. Third, the maximum temperature both radially and through time can be found[10].

5. Model Validation

A series of validation parameters and tests were run using the model. Steady state fuel temperature profiles developed by the UT code were compared to data from comparable TRACE calculations. Steady state temperatures corresponding to fuel temperature sensor (thermocouple) locations were calculated for a series of operational power levels for comparison to observed fuel temperature measuring channel data. Finally, transient calculations simulating a routine reactor scram (water cooling), and compared to fuel temperature measuring channel data collected on the in-house Integrated Control System recording[11]. Therefore the steady state and transient calculations portions were tested and validated.

5.1 Comparison of TRACE and UT MATLAB Model Steady State Temperature Profile

The core configuration contains 114 fuel elements, with a core radial peaking factor derived from SCALE physics calculation for the core (prior to January 2016) of 1.6, and a maximum axial peaking factor of 1.2. The current normal operating power is 950 kW. The power generated in the maximum segment of the hot channel for comparison using data prior to January 2016 is therefore 12.5 kW.

The steady state solution with water cooling was developed for the maximum power level in a fuel element operating at 12.5 kW and compared to the TRACE calculations (Fig. 4). The TRACE and FEA calculations are in substantial agreement.

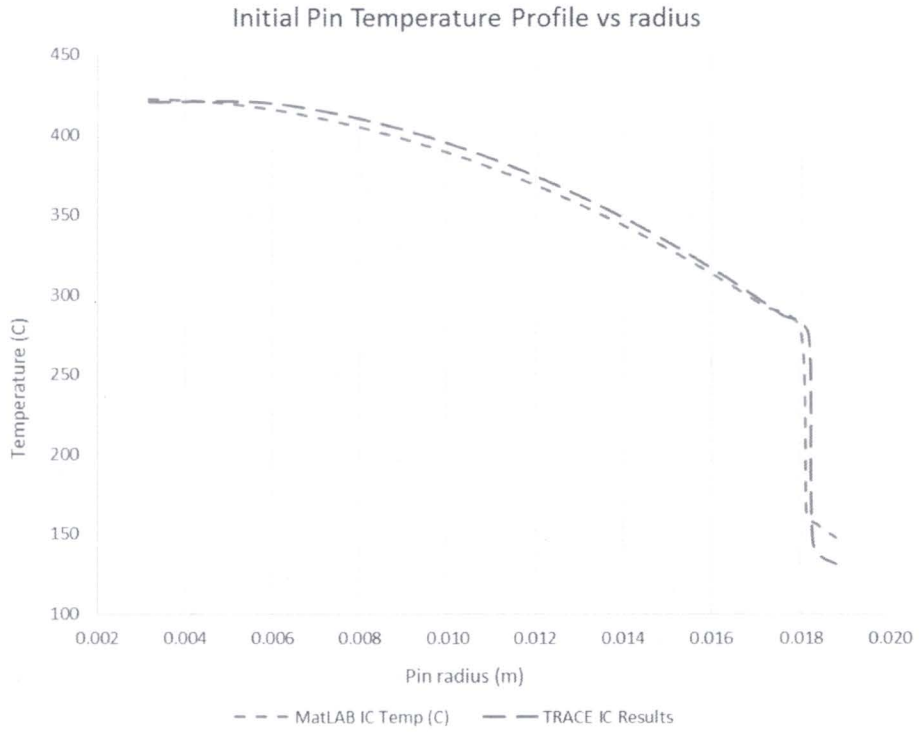

Figure 4. TRACE and UT LOCA model steady state temperature profiles

5.2 Comparison of FT2 Observations and Calculations (TRACE, UT MATLAB Model) Steady State Temperature Response to Power Operation

The MATLAB finite element analysis was applied at power generation in an element from 200 W to the 12.5 kW, and the maximum element temperature compared to the TRACE and FT2 measurements (taken prior to January 2016) across the range.

TRACE and the MATLAB UT LOCA steady state temperature calculations in radial locations associated with thermocouples are essentially the same. There is good agreement between calculated and observed values with some deviation at higher power levels where the heat transfer is presumably affected by the development of bubbles that enhance heat transfer and reduce fuel temperature (Fig. 4).

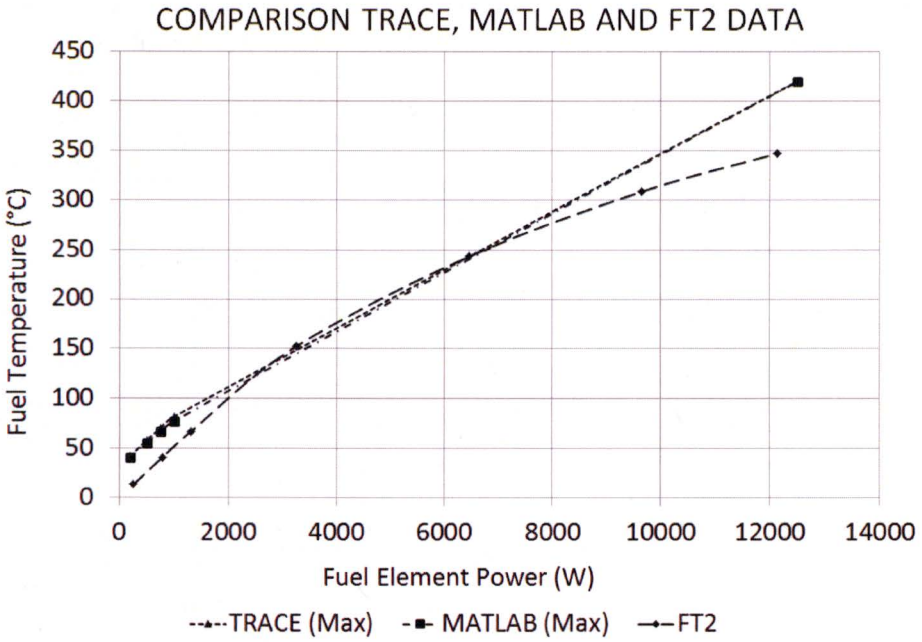

Figure 5. Comparison of Temperatures from Calculations and Observations at Varying Power Levels

5.3 Comparison of FT2 Observations and Calculations (TRACE, UT MATLAB Model) Transient Temperature Response to Shutdown from Normal Operations

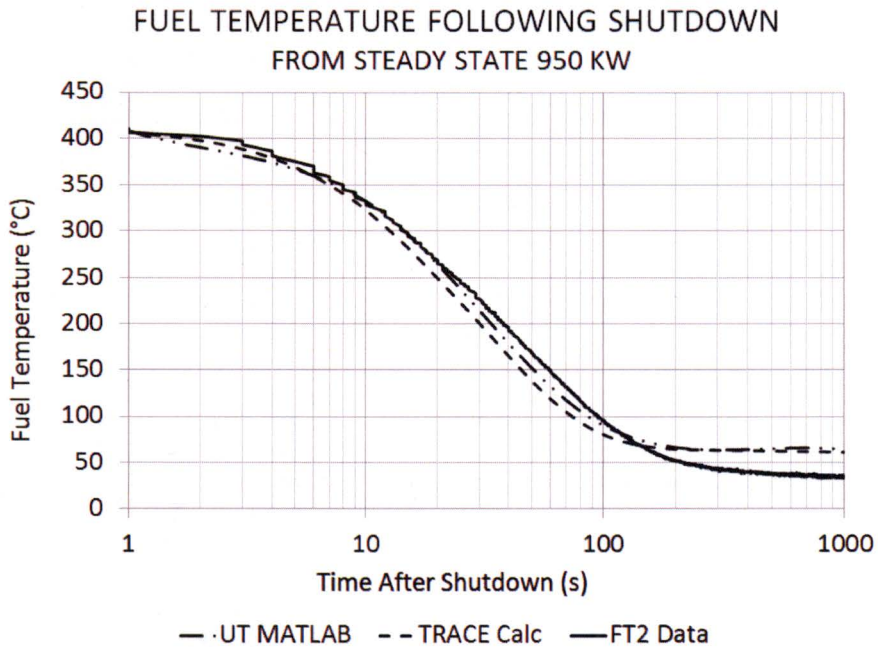

Figure 6. Fuel Temperature, Measuring Channel & Calculations Following Reactor Scram

Transient fuel temperature was recorded with the Integrate Control System log interface following a shutdown from power operations at 950 kW. Calculations were performed to simulate the transient using TRACE and MATLAB UT LOCA model. The temperature data is in good agreement, as shown in Fig. 6.

5.4 Validation Summary

Comparison of fuel temperature measuring channel data to calculated fuel temperatures during steady state and transient conditions is considered to be in good agreement. The agreement between observations and calculations during steady state operations suggests the method is fundamentally correct. The agreement between observations and calculations during transient operations suggests the method will provide reasonably accurate time-dependent calculations.

6. Results and Parametric Variation

The UT MATLAB model calculation was performed for various values of both air channel temperature and pin power. The radial temperature profile of the fuel element segment generating the highest power in the core is provided in Fig. 6 following a shutdown from a limiting operation of 23kW in the element with air cooling at inlet air temperature equal to UT rector bay nominal temperature.

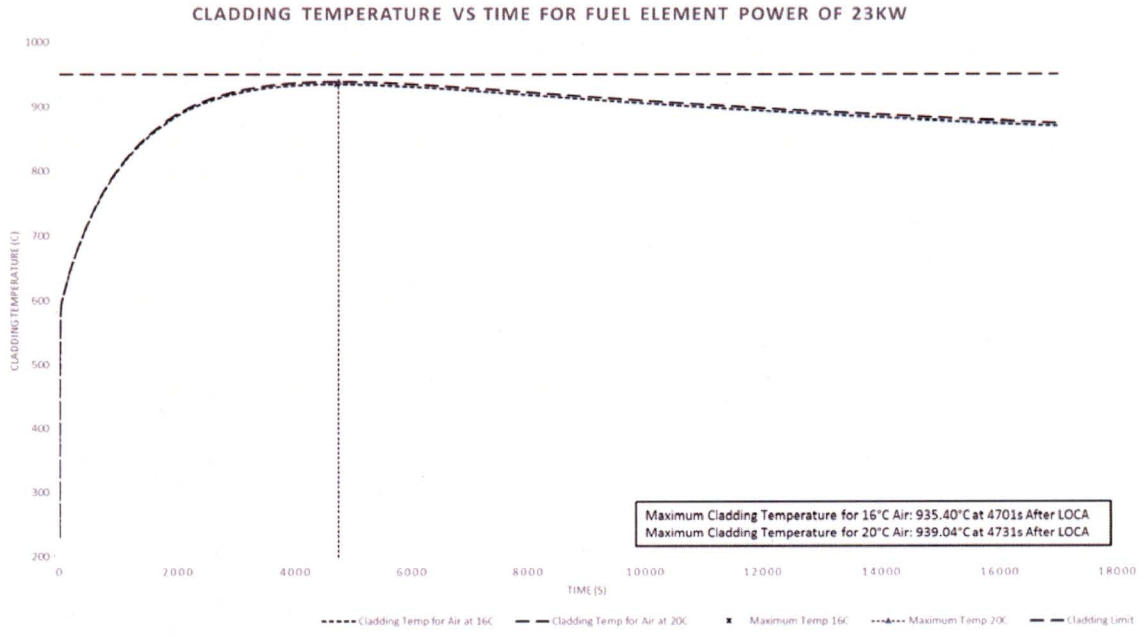

Figure 7. LOCA Cladding Temperature vs Time

Fuel element power level and inlet air temperature were varied to provide an indication to sensitivity to the parameters. Air inlet varied from 16°C to 600°C, while fuel element power varied from 12.5 kW per pin to 27 kW per pin. This ensured all operational areas were covered,

and sufficient data existed to curve fit. The figure below shows the region of interest in this output.

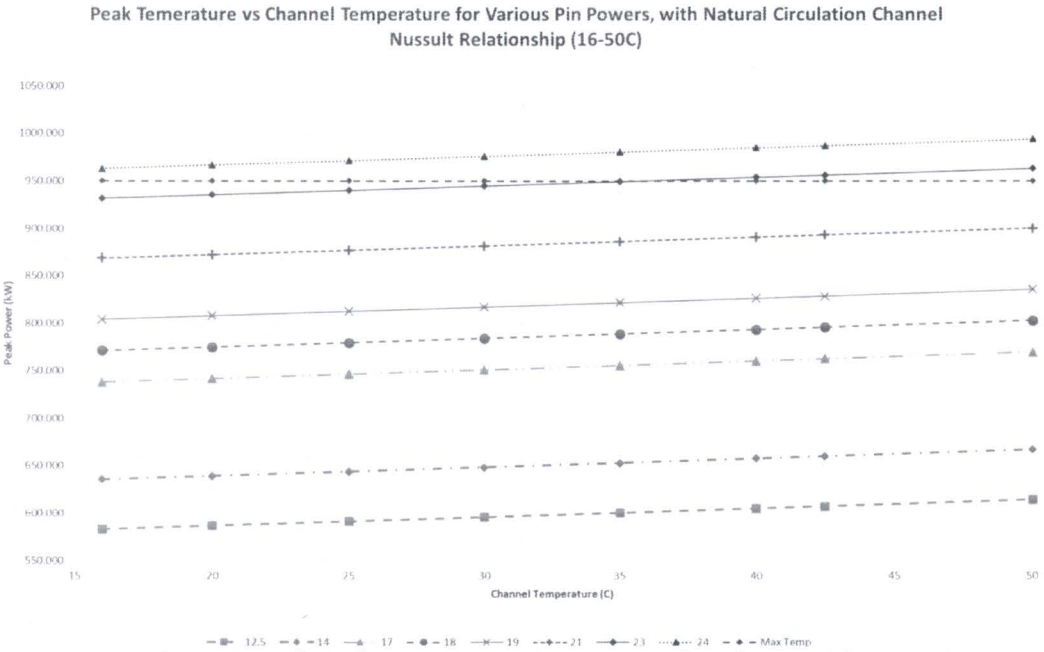

Figure 8. Peak Fuel Temperature during Loss of Coolant Accident

For reactor bay air at 16°C, the maximum fuel element power prior to LOCA initiation that could achieve less than 950°C fuel cladding temperature with air cooling is 23.6 kW in the hot channel. At 23 kW generated in the hot channel fuel element during operation at steady state prior to the LOCA initiation (the maximum power generated in a fuel element in the limiting core configuration), air inlet temperature inlet less than 35°C is calculated not to exceed 950°C fuel cladding temperature. Therefore a LOCA following normal steady operation with a fuel element operating at a maximum of 23 kW will not exceed the fuel temperature safety limit. For nominal UT operations of 12.5 kW in the hot channel, an air inlet temperature of up to 402°C can exist at LOCA initiation and remain below the 950°C cladding temperature.

The UT LOCA model takes place at the point of highest axial power production and assumes only radial heat transfer. Axial conduction in the fuel matrix would tend to reduce the axial temperature profile and reduce peak fuel temperature. Therefore the results for maximum fuel element analysis calculated by the UT LOCA model can be considered conservative.

7. References

[1] M. T. Simnad, "The U-ZrHx Alloy: Its Properties and Use in TRIGA Fuel," *Nucl. Eng. Des.*, vol. 64, pp. 403–422, 1981.

[2] Kansas State, "Kansas State University Safety and Analysis Report '06." KSU, Manhatten, 2006.

[3] T. L. Bergman, A. S. Lavine, F. P. Incropera, and D. P. DeWitt, *Fundamentals of Heat and Mass Transfer*. 2011.

[4] F. P. Incropera, D. P. DeWitt, T. L. Bergman, and A. S. Lavine, *Fundamentals of Heat and*

Mass Transfer, vol. 6th. 2007.
[5] Henri Fenech, *Heat Transfer and Fluid Flow in Nuclear Systems*. Pergamon Press, 1981.
[6] M. J. Deborah Kaminski, *An introduction to Thermal and Fluids Engineering*. Wiley, 2011.
[7] C. O. Popiel and J. Wojtkowiak, "Simple formulas for thermophysical properties of liquid water for heat transfer calculations (from 0 to 150 degrees C) (vol 19, pg 87, 1998)," *Heat Transf. Eng.*, vol. 19, no. 3, pp. 87–101, 1998.
[8] G. Kline, "channel_air_temp_3_0." Greg Kline, Austin, p. 5, 2015.
[9] K. Vafai, C. P. Desai, S. V. Iyer, and M. P. Dyko, "Buoyancy Induced Convection in a Narrow Open-Ended Annulus," *J. Heat Transfer*, vol. 119, p. 483, 1997.
[10] G. Kline, "LOCA_8_5_3_FEM." Greg Kline, Austin, p. 20, 2015.
[11] G. Kline, "PXIe_ICS_Power_Cal_Etc_2015." Greg Kline, Austin, p. 100, 2015.

8. Code

```
%% HEADER
% UT LOCA
% Author: Greg Kline
% Date: 1/21/2015
% Revision 8.5.2
%
% Revision Changes:
% - begin mapping a 1D transient, radial, air cooled naturally circulated
%  fuel pin immediately after shut down with decreasing decay heat
% - 6.0 has liner transient development.
% - 6.1 has radial
% - 6.2 added variable heat transfer coefficient
% - 6.3 added variable specific heat capacity and improved check feature
% - 6.4 worked on adjusted dt and shorter t vector
% - 6.5 added function for channel heat calculation
% Revision 7
% - 7.0 added radial flux distribution
% - 7.1 added titles to graphs that change
% Revision 8
% - 8.0 changed the physical properties of the pin to reflect both the 304SS
%     cladding and the gas gap possibly existent in the pin
% - 8.1 Working to match TRACE
% - 8.2 Cleaned up code and changed n to meet actual cladding thickness and
%     and reduce the gap width to values more realistic
% - 8.3 Updating transient solution to fix it for multiple materials
% - 8.4 Updated the length vector to reduce points between the fuel segments
% - 8.4.1 Changed gas from cp to cv. Since the gas gap volume is considered
%       constant throughout the process
% - 8.4.2 Fixed parenthesis bug
% - 8.5 Made it a function
% - 8.5.1 add natural circulation channel Nusselt number relationship
% - 8.5.2 adjusted for a 30C initial water temperature
% - 8.5.3 Added channel air temperature function to the file for the FEM
%
%
% function [ mT, t_max ] = LOCA_8_5_3_FEM( qtp, Tia)
%
%       qtp - Power in the fuel element (W)
%       Tia - Air temperature at time of LOCA (C)
%       mT - Maximum cladding surface temperature (C)
%       t_max - Time at which the maximum temperature occurs (s)
%
%    FEM Pseudo Code
%       - Constants
%          - Fuel Constants from Simnad, etc.
%             - Fuel geometry
%          - Model Constants
%             - Air and water material properties
%       - Model time parameters
%          - Differential time steps
%          - Time splits
%          - Build time vector
%          - Build decay heat fraction
%          - Find specific power
%       - Heat transfer coefficients
%       - FEA building
%          - number of points (n)
%          - build radial spacing
%          - find the radially fractioned specific energy generation
%          - Find the initial Biot and Fourier values
%       - Steady State Initial Condition
```

```
%           - RHS
%             - Values of generation and temperature independent terms
%           - LHS
%             - Matrix of temperature interactions representing temperature
%               dependent values of energy equation
%               - Build the inner point
%               - cladding points
%               - Gas/fuel interface
%               - inner fuel points
%             - TRACE vector
%             - Solve for the temperature profile in steady state
%       - Transient problem
%           - pre-allocate memory
%           - Transient loop
%               - find the dt for current time space
%               - find the current dimensionless numbers for channel conditions
%               - find the current heat transfer coefficient
%               - find the current temperatures in the profile
%               - find the current model validation values
%               - check to see if it is the maximum so far
%       - Outputs
%           - Build a reduced point matrix to save memory
%           - Find the maximum temperatures
%           - Build output graphs
%
% function [ Tinf ] = channel_air_temp_3_0(T_s, Tinit)
%
%       T_s - Surface temperature (C)
%       Tinit - Initial temperature of the inlet channel air (C)
%       Tinf - Channel outlet temperature (C)
%
%    Channel Air Pseudo Code
%       - Geometry of fuel element
%       - Geometry of air channel
%       - Iterate up the pin vertically
%       - Due back of envelope calculations
%       - Outputs


function [ mT, t_max ]  = LOCA_8_5_3_FEM( qtp, Tia)

tic
display('Initializing LOCA... ');

%% CONSTANTS

% FUEL CONSTANTS
% Initial Temp for model VnV
T_init = 30;

% fuel initial pin power (W)
q_total_pin = qtp;

% Axial Peaking Factor
axial_peaking = 1.2435;

%% FUEL CONSTANTS
% pin height (m)
pin_height = .381;

% Pin radius (m)
radius_pin = 0.018771; % .735in
```

```
inner_radius = 0.003175; %.125in

% clad width (m)
dl_clad = 0.000508;

% vertical sections (#)
vertical_sections = 15;

% enrichment percentage (fraction) [UT SAR]
Rich = .197; % 19.7%

% density (kg/m^3) [Simnad]
density_U = 19070;

% density of ZrH based on ratio (kg/m^3)[Simnad]
density_Zr = 1 / (.1541 + .0145 * 1.6) * 1000;

% Thermal conductivity fuel [Simnad]
% ( cal / s cm C )
k_fuel_cal = .042;

% ( W / m*K )
k_fuel = 17.5730;  % [Simnad]

% Avogadro's number (atoms/mol)
N_A = 6.022e23;

% Molar mass (g/mol) [Burns]
M_U = 238.07;

% weight percent of Uranium in Triga fuel [UT SAR]
U_wt = .085; % 8.5%

% Material Densities (kg/m^3)
density_fuel = 1 / ( U_wt / density_U + (1 - U_wt) / density_Zr ); %[Simnad]
density_gas = .08375; % PNNL
density_304SS = 7740; % makeitfrom.com

% volumetric heat capacity from Simnad (J/ m3 K)
cp_fuel_vol = (2.04 + 4.17e-3 * T_init ) * 1e6;

% Convert to specific heat ( J / kg K )
cp_fuel = cp_fuel_vol / density_fuel;
cp_304SS = 500;
cp_gas = 14.53e3; % PNNL ->
cv_gas = 10.16e3; % Hydrogen

% thermal diffusivity ( m^2 / s)
alpha_fuel = k_fuel / ( cp_fuel * density_fuel);

% pin volume (m^3)
vol_pin = pi * pin_height * ((radius_pin-dl_clad)^2 - inner_radius^2);

% specific pin power (W/m^3)
q_dot_max = q_total_pin / vol_pin;

% This is a slice of a potential 2D model of the pin (m)
dy = pin_height / vertical_sections;

%% MODEL CONSTANTS
% Temperatures (C)
% find the value using sub-model function
```

```
T_inf_air = 1.5 * channel_air_temp_3_0(1150, 16);

% option to set air
% T_inf_air = 20; %Tia;

% Water temperature to build initial condition profile (C)
T_inf_water = 48;

% display temperatures
display(sprintf('T_inf_air is %3.2f C', T_inf_air ));

% Thermal Conductivities (W/mK)
k_air = 0.0257; % engineering toolbox
k_304SS = 16.2; % makeitfrom.com

% Prandtl Number (Pr)
Pr_air = .713;
Pr_water = 1.76;

% Kinetic Viscosity (m^2/s)
kinetic_viscosity_air = 15.11e-6;
kinetic_viscosity_water = .279e-6;

% Expansion Coefficient (1/K)
B_air = 3.43e-3;
B_water = .207e-3;

% Gradient Prandtl (gPr)
gPr_air = (.75 * Pr_air)^.5 / (.609 + 1.221 * Pr_air^.5 + 1.238 * Pr_air)^.25;
gPr_water = (.75 * Pr_water)^.5 / (.609 + 1.221 * Pr_water^.5 + 1.238 * Pr_water)^.25;

% Gravity (m/s^2)
gravity = 9.8066;

%% MODEL TIME PARAMETERS
display(sprintf('Pin power at time 0- is %5.2f W', q_total_pin));

% TIME VECTOR
% Time (s)
dt1 = .00025;
dt2 = .0013;
dt3 = .0015;

% Time to split the dt (s)
t_split1 = 1000;
t_split2 = 2000;

% Time vector for LOCA build (s)
t = [0:dt1:t_split1 t_split1+dt2:dt2:t_split2 t_split2+dt3:dt3:17000];

% Time for decay heat (log(s))
log_t = log10(t);

% Decay power and radial peaking
% Decay Power fraction with time (dimensionless)
Decay_power_fraction = (.04856 + .1189 .* log_t - .0103 .* log_t.^2 + .000228 .* log_t.^3 )./ ...
   (1 + 2.5481 .* log_t - .19632 .* log_t.^2 + .05417 .* log_t.^3);

% Decay power with time ( W )
Decay_power_t = (Decay_power_fraction * q_total_pin)';

% Specific energy generation ( W/m^3 )
```

```
q_dot = axial_peaking  * Decay_power_t / vol_pin; % 1.2 peaking factor

%% HEAT TRANSFER COEFFICIENTS
 % Water heat transfer, found using TRACE analysis
 h_water = 3200;

 % Gas heat transfer from KSU SAR [Whaley]
 h_gas = 2.84e3;

%% FEA BUILDING
% Finite element building
% number of x units to provide adequate spacing for clad and gas geometry(#)
n = 120;

% radius points for determining temperatures (m)
x1 = linspace(inner_radius,radius_pin,n);

% find dx for determination of indices to be used for different materials (m)
dx = x1(2) - x1(1);

% In order to capture clad and gas geometry but not over burden memory usage
% radial spacing near edges is smaller than the spacing in the fuel meat
% Fuel meat spaces (m)
xpt1 = linspace(inner_radius,radius_pin-6*dx,19);

% Cladding gas spacing (m)
xpt2 = linspace(radius_pin-5*dx,radius_pin,5);

% build the vector (m)
x = [ xpt1 xpt2 ];

% clad points (#)
% find the number of x points to accurately represent the clad space (#)
pts_clad = ceil ( dl_clad / dx );

% gas points (#)
% set number of points gas gap occupies (#)
pts_gas = 1; % [Fenech]

% radius vector for determining the volumes for energy generation.  Indexing
% requires the volume around a temperature to be half way between the temperatures
% Fuel radial volume points (m)
rpt1 = linspace(inner_radius,radius_pin-6*dx,2*19-1);

% clad radial points (m)
rpt2 = linspace(radius_pin-5*dx,radius_pin,2 * 5 -1 );

% Build the radial vector m)
r_vol = [ rpt1 radius_pin-5.5*dx rpt2 ];

% Set the radial fraction varied energy production (W/m^3)
q_r = axial_peaking * q_dot_max * (247192.*xpt1.^3 - 5377.*xpt1.^2 + 45.882.*xpt1 + .7335); % initial condition
q_r_t = (247192.*xpt1.^3 - 5377.*xpt1.^2 + 45.882.*xpt1 + .7335); % radial percentage

% Gas thermal conductivity (W/m K)
k_gas = h_gas * dx;

% For transient problems, validity is reached only if:
% Biot # < .1
% Fourier number < .5(1D) .25 (2D)  [Bergman]
L_c_1 = (pi*(r_vol(2)^2 - r_vol(1)^2)*dy) / (dy * 2 * pi * (r_vol(2) + r_vol(1)));
L_c_2 = (pi*(r_vol(end)^2 - r_vol(end-1)^2)*dy) / (dy * 2 * pi * (r_vol(end) + r_vol(end-1)));
```

```
Bi_1 = h_water * L_c_1 / k_fuel;
Bi_2 = h_water * L_c_2 / k_fuel;

Fo_1 = alpha_fuel * dt1 / L_c_1^2;
Fo_2 = alpha_fuel * dt1 / L_c_2^2;

check = Fo_1 * (1+Bi_1); % this must remain <= 1/2

%% STEADY STATE INITIAL CONDITION
% set up the FEA
% At = b => t = A-1b
display('Building initial condition');

% Right Hand Side (RHS)
% The right hand side of the equation represents the energy generation and
% non-temperature dependent values of the energy balance
% pre-allocate vector
b = zeros(length(x),1);

% Most internal fuel point
b(1) = -q_r(1) * pi * dy * (r_vol(2)^2 - r_vol(1)^2);

% Boundary with the fluid
b(end) = - h_water * pi * 2 * r_vol(end) * dy * T_inf_water; % OLD -q_r(end) * pi/6 * dy * (r_vol(end)^2 - r_vol(end-1)^2)

% Gas and Clad gaps
b(end-1) = 0; % No generation in SS or gap
b(end-2) = 0;
b(end-3) = 0;
b(end-4) = 0;

% Gas/Fuel interface
b(end-5) = -q_r(end-2) * dy * pi * (r_vol(end-4)^2 - r_vol(end-5)^2); % gas/fuel interface has half a region of generation

% Left Hand Side (LHS)
% pre-allocate matrix space
A = zeros(length(x));

% Most inner point
A(1,1) = -2 * pi * dy * k_fuel / log(x(2)/x(1));
A(1,2) = 2 * pi * dy * k_fuel / log(x(2)/x(1));

% Cladding Point
A(end,end-1) = 2 * pi * dy * k_304SS / log(x(end)/x(end-1));
A(end,end) = -2 * pi * dy * k_304SS / log(x(end)/x(end-1)) - h_water * pi * 2 * x(end) * dy;

% Stainless gas interface
A(end-1,end-2) = 2 * pi * dy * k_304SS / log(x(end-1)/x(end-2));
A(end-1,end-1) = -2 * pi * dy * k_304SS / log(x(end-1)/x(end-2)) - 2 * pi * dy * k_304SS / log(x(end)/x(end-1));
A(end-1,end) = 2 * pi * dy * k_304SS / log(x(end)/x(end-1));

A(end-2,end-3) = 2 * pi * dy * k_304SS / log(x(end-2)/x(end-3));
A(end-2,end-2) = -2 * pi * dy * k_304SS / log(x(end-1)/x(end-2)) - 2 * pi * dy * k_304SS / log(x(end-2)/x(end-3));
A(end-2,end-1) = 2 * pi * dy * k_304SS / log(x(end-1)/x(end-2));

A(end-3,end-4) = 2 * pi * dy * k_304SS / log(x(end-3)/x(end-4));
A(end-3,end-3) = -2 * pi * dy * k_304SS / log(x(end-3)/x(end-4)) - 2 * pi * dy * k_304SS / log(x(end-2)/x(end-3));
A(end-3,end-2) = 2 * pi * dy * k_304SS / log(x(end-2)/x(end-3));

A(end-4,end-5) = 2 * pi * dy * k_gas / log(x(end-4)/x(end-5));
A(end-4,end-4) = -2 * pi * dy * k_304SS / log(x(end-3)/x(end-4)) - 2 * pi * dy * k_gas / log(x(end-4)/x(end-5));
```

```
A(end-4,end-3) = 2 * pi * dy * k_304SS / log(x(end-3)/x(end-4));

% Gas fuel interface
A(end-5,end-6) = 2 * pi * dy * k_fuel / log(x(end-5)/x(end-6));
A(end-5,end-5) = -2 * pi * dy * k_gas / log(x(end-4)/x(end-5)) - 2 * pi * dy * k_fuel / log(x(end-5)/x(end-6));
A(end-5,end-4) = 2 * pi * dy * k_gas / log(x(end-4)/x(end-5));

% Build the remaining fuel points
for i = 2:length(xpt1)-1
   % RHS
   b(i) = -q_r(i) * pi * dy * (r_vol(2*i)^2 - r_vol(2*i-2)^2);

   % LHS
   A(i,i-1) = 2 * pi * dy * k_fuel / log(x(i)/x(i-1));
   A(i,i) = - (2 * pi * dy * k_fuel / log(x(i)/x(i-1)) + 2 * pi * dy * k_fuel / log(x(i+1)/x(i)));
   A(i,i+1) = 2 * pi * dy * k_fuel / log(x(i+1)/x(i));

end

% Work to compare two different steady state temperature profile
% TRACE Temperatures (C)
T_mike = [ 420.53 420.53   414.33  406.19  397.12  387.41  377.34  366.92  356.28  345.40  334.25  ...
        322.86  311.21  299.33  287.25  274.90  143.51  130.88];

% TRACE x values
xm = [3.18E-03  5.60E-03 7.26E-03 8.60E-03 9.76E-03 0.010801 0.011746 0.012621  0.013439 0.01421 0.014941 0.015638
0.016306 0.016947   0.017564    0.018161    0.018263    0.018771];

% Find the temperature vector using matrix inversion (C)
T = A\b;

%% TRANSIENT PROBLEM
display('Calculating transient matrix');

% pre-allocate a matrix of temperature vs time (C)
T_t = zeros(length(t),length(T));

% Set the initial condition from the steady state value found above (C)
T_t(1,:) = T;

toc
tic

% Set variables to track maximum metric values (dimensionless)
Bi_max = 0;
Fo_max = 0;
Ch_max = 0;

% cp air ( J/kg K )
cp_air = 1.005 * 1000;

% density sir (kg / m^3)
density_air = 1.205;

% cv ( J / kg K )
cv_air = cp_air / 1.4;

% Channel width (m)
width_channel = 0.0061976;

% dynamic viscosity of air (kg / m s )
dyn_vis_air = 1.846e-5;
```

```
% Explicit finite difference method
for j = 2:length(t)
  if t(j) < t_split1
    dt = dt1;
  elseif t(j) >= t_split1 && t(j) < t_split2
    dt = dt2;
  else
    dt = dt3;
  end

  % Update the command line
  if mod(j,500000) == 0
    display(sprintf('Iterating loop %9.0f of %9.0f of transient matrix %3.2f percent complete', ...
      j, length(T_t(:,1)), j/length(T_t(:,1))*100));
  end

  % First find the Rayleigh and Nusselt numbers leading to heat transfer
  % coefficient based on time (j) del_T

  % Find the Ra_s [ Kaminski ]
  Ra_s = ( gravity * B_air * density_air^2 * ( T_t(j-1,end) - T_inf_air ) * width_channel^3 ) ...
    / dyn_vis_air^2;

  % find a denominator value for readability
  RSL = Ra_s * ( width_channel / dy );

  % Nusselt number
  % Nu_s = ( 576/ RSL^2 + 2.87 / RSL^1/2 )^ -1/2
  Nu_s = ( 576 / RSL^2 + 2.87 / RSL^(1/2) )^(-1/2);

  % Heat transfer coefficient ( W/ m^2 K )
  h = Nu_s * k_air / width_channel;

  % Inner most point (C)
  T_t(j,1) = dt / ( density_fuel * ((2.04 + 4.17e-3 * T_t(j-1,i))*1e6/density_fuel) ...
    * pi * dy * (r_vol(2)^2 - r_vol(1)^2)) ...
    * ( 4 * pi * dy * k_fuel / log(x(2)/x(1)) * (T_t(j-1,2)-T_t(j-1,1)) ... %%%
    + q_dot(j) * q_r_t(1) * pi * (r_vol(2)^2 - r_vol(1)^2)*dy ) + T_t(j-1,1);

  % Mid fuel points (C)
  for k = 2:length(T)-6
    T_t(j,k) = dt / ( density_fuel * ((2.04 + 4.17e-3 * T_t(j-1,k))*1e6/density_fuel) ...
      * pi * dy * (r_vol(2*k)^2-r_vol(2*k-2)^2)) ...
      * ( 2 * pi * dy * k_fuel / log(x(k+1)/x(k)) * (T_t(j-1,k+1)-T_t(j-1,k)) ...
      + 2 * pi * dy * k_fuel / log(x(k)/x(k-1)) * (T_t(j-1,k-1)-T_t(j-1,k)) ...
      + q_dot(j) * q_r_t(k) * pi * (r_vol(2*k)^2 - r_vol(2*k-2)^2)*dy ) + T_t(j-1,k);
  end

  % Fuel/gas point (C)
    T_t(j,length(T)-5) = dt / ( density_fuel * ((2.04 + 4.17e-3 * T_t(j-1,length(T)-5))*1e6/density_fuel) * pi ...
      * dy * (r_vol( 2 * (length(T)-5) - 1 )^2 - r_vol( 2 * (length(T)-5) - 2 )^2) ...
      + ( density_gas * cv_gas * pi * dy * (r_vol( 2 * (length(T) -5))^2 - r_vol( 2 * (length(T)-5) -1)^2))) ...
      * ( 2 * pi * k_fuel * dy / log( x(length(T) - 5) / x((length(T) -5) -1)) * ( T_t(j-1,(length(T) -5) -1) ...
      - T_t(j-1,length(T) -5)) + 2 * pi * k_gas * dy / log( x((length(T) -5) +1) / x((length(T) -5)) ) ...
      * ( T_t(j-1,(length(T) -5) +1 ) - T_t( j-1,(length(T) -5)) )  ...
      + q_dot(j) * q_r_t(length(T) -5) * pi * dy * ( (r_vol( 2 * (length(T)-5) - 1))^2 - (r_vol( 2 * (length(T)-5) - 2 ))^2) ) ...
      + T_t(j-1,length(T)-5);

  % Gas/clad point (C)
    T_t(j,length(T)-4) = dt / ( density_304SS * cp_304SS * pi * dy * ((r_vol( 2 * (length(T)-4) ))^2 ...
      - (r_vol( 2 * (length(T) -4) -1))^2) ...
```

```
        + ( density_gas * cv_gas * pi * dy * ((r_vol( 2 * (length(T) -4) -1))^2 - (r_vol( 2 * (length(T) -4) -2))^2) ) ) ...
        * ( 2 * pi * k_gas * dy / log( x(length(T) -4) / x((length(T) -4) -1)) * (T_t(j-1,(length(T) -4) -1) ...
        - T_t(j-1,length(T) -4)) + 2 * pi * k_304SS * dy / log( x((length(T) -4) +1) / x((length(T) -4))) ...
        * ( T_t(j-1,(length(T) -4) +1) - T_t(j-1,(length(T) -4)) ) ) + T_t(j-1,length(T) -4);

    % Mid clad points (C)
    for kc = length(T)-3:length(T)-1
       T_t(j,kc) = dt /( density_304SS * cp_304SS * pi * dy * ((r_vol( 2 * kc))^2 - (r_vol( 2 * kc-2))^2) ) ...
          * ( 2 * pi * k_304SS * dy / log( x(kc) / x(kc-1) ) * ( T_t(j-1,kc-1) - T_t(j-1,kc) ) ...
          + 2 * pi * k_304SS * dy / log( x(kc+1) / x(kc) ) * ( T_t(j-1,kc+1) - T_t(j-1,kc) ) ) ...
          + T_t(j-1,kc);
    end

    % Endpoint (C)
    T_t(j,end) = dt / ( density_304SS * cp_304SS * pi * dy * ( (r_vol(end))^2 - (r_vol(end-1))^2 ) ) ...
       * ( 2 * pi * k_304SS * dy / log( x(end) / x(end-1) ) * ( T_t(j-1,end-1) - T_t(j-1,end) ) ...
       + h * pi * 2 * x(end) * dy * ( T_inf_air - T_t(j-1,end) ) ) ...
       + T_t(j-1,end);

    % Checks on validity
    % current Biot
    Bi_t = h * L_c_1 / k_fuel;

    % current Fourier
    a_t = k_fuel / ((2.04 + 4.17e-3 * T_t(j-1,end)) * density_fuel);
    Fo_t = a_t * dt / L_c_1^2;

    % current check parameter
    check_t  = Fo_t * (1+Bi_t);

    % Track the worst of the numbers
    if Bi_t > Bi_max
       Bi_max = Bi_t;
    end

    if Fo_t > Fo_max
       Fo_max = Fo_t;
       t_max = t(j);
    end

    if check_t > Ch_max
       Ch_max = check_t;
    end

end

toc
tic

%% OUTPUTS
% create a reduced matrix for display
% reduction factor
N_red = 10000;

% Reduced temperature matrix (C)
T_t_reduced = T_t(1:N_red:length(T_t(:,1)),:);

% Reduced time matrix (s)
t_reduced = t(1:N_red:length(T_t(:,1)));

% Max temp (C)
[mT, iT] = max(T_t(:,end));
```

```
% Time of maximum temperature (s)
t_max = t(iT);

% Maximum temperature over entire geometry and time (C)
max_max_temp = max(max(T_t))';

% Surface temp (C)
T_t_surface = T_t(:,end);

display('Building output graphs ');

% Initial condition plot
figure(1)
set(figure(1), 'Position',[200 300 1000 600]);
plot(x,T, 'g', xm, T_mike, 'b')
xlabel( ' Pin Radius (m) ');
ylabel(' Temperature (C) ');
title(sprintf(' Initial pin temperature vs radial point for water at %2.0f C and pin power of %2.1f kW ', ...
   T_inf_water, q_total_pin/1000));
legend(sprintf(' Max Temp(C): %3.2f \n Approx. TC Temp(C): %3.2f \n dT-fuel: %3.2f Wh, %3.2f Gk \n dT-gas: %3.2f Wh,
%3.2f Gk \n dT-Clad: %3.2f Wh, %3.2f Gk \n Ts: %3.2f Wh, %3.2f Gk  ', ...
   max(T), T(9), T_mike(1)-T_mike(end-2), T(1)-T(end-5), T_mike(end-2) - T_mike(end-1), T(end-5) - T(end-4), ...
   T_mike(end-1) - T_mike(end), T(end-4)-T(end), T_mike(end), T(end)),'Location','SouthWest');

% Infiinite pin profile
figure(2)
plot(x,T_t(end,:));
xlabel( ' Pin Radius (m) ');
ylabel(' Temperature (C) ');
title(' Pin Temperature vs Radial Point at t(inf) ');
legend(sprintf(' Max Temp overall(C): %3.2f ',max_max_temp ),'Location','SouthEast');

% Surface temperature vs time
figure(3)
set(figure(3), 'Position',[200 500 1200 800]);
plot(t_reduced,T_t_reduced(:,end));
xlabel( ' Time (s) ');
ylabel(' Temperature (C) ');
title(sprintf(' Pin Surface Temperature vs Time for Air at %2.0f C and Pin Power of %2.1f kW',T_inf_air, q_total_pin/1000));
legend(sprintf(' Max Surface Temp(C): %3.2f at %3.2f s', mT , t(iT)),'Location','SouthEast');

% clear giant matrix
clearvars T_t;

toc

%% Channel Air Temperature
function [ Tinf ] = channel_air_temp_3_0(T_s, Tinit)

% UT LOCA
% Author: Greg Kline
% Date: 12/31/2015
% Revision 3.0
%
% Revision changes:
%    - 2.0
%        - add more accurate correlation for Nu and heat transfer coefficient
%    -3.0
%        - edit out wasted lines to allow integration in FEM code

tic
```

```
display('Initializing Channel Air Temp... ');

% Initial inlet temperature (C)
Tinit = 20; %Tinit;
T_s = 950;

% Geometry
% vertical sections (#)
vertical_sections = 20;

% Pin radius (m)
% outer radius
radius_pin = 0.018669;

% Radius of cooling hexagon (m)
inner_hex = 0.0217678;
outer_hex = 0.025146;

% Total spatial area of cooling hex and pin (m^2)
total_space = sqrt(3)/2 * (2 * inner_hex)^2;

% Area of pin radially (m^2)
Area_pin = pi * radius_pin^2;

% Area of cooling hexagon around pin (m^2)
area_cooling = total_space - Area_pin;

% Area of the flow gap (m^2)
% given the geometry of meeting hexagons the flow area is 6 half hexs plus
% the one around the pin in question
area_flow_gap = 3 * area_cooling;

% pin height (m)
pin_height = .381;

% This is a slice of the pin (m)
dy = pin_height / vertical_sections;

% Thermal conductivity of air ( W/ m K )
k_air = 0.0257;

% Density (kg/m^3)
density_air = 1.205;

% specific heat capacity ( J/kgK )
cp_air = 1.005 * 1000;

% thermal diffusivity (m^2/s)
alpha_air = k_air / ( cp_air * density_air );

% Prandtl Number (Pr)
Pr_air = .713;

% Kinetic Viscosity (m^2/s)
kinetic_viscosity_air = 15.11e-6;

% Expansion Coefficient (1/K)
B_air = 3.43e-3;

% Gradient Prandtl (gPr)
gPr_air = (.75 * Pr_air)^.5 / (.609 + 1.221 * Pr_air^.5 + 1.238 * Pr_air)^.25;
```

```
% Gravity (m/s^2)
gravity = 9.8066;

% Pin Area (m^2)
surface_area_pin = 2 * pi * radius_pin * dy / 12;

% k_gas for air
k_gas_cvcp = 1.4;

% cv
cv_air = cp_air / k_gas_cvcp;

% Channel width (m)
width_channel = ( ( outer_hex + inner_hex/sqrt(3) - radius_pin ) + 2 * ( inner_hex - radius_pin) ) / 2;

% dynamic viscosity of air (kg / m s )
dyn_vis_air = 1.846e-5;

% FIND THE CHANNEL TEMP
% Find characteristic velocity based on entire flow area
% Find the initial Rayleigh
Ra_0 = ( gravity * B_air * density_air^2 * (T_s - Tinit) * (width_channel*12)^3 ) ...
   / (k_air^2 *  dyn_vis_air);

RSL_0 = Ra_0 / ( (width_channel*12) / dy );

% initial Nusselt
Nu_0 = ( 576 / RSL_0^2 + 2.87 / RSL_0^(1/2) )^(-1/2);

% initial h
h_0 = Nu_0 * k_air / dy;

% initial heat flux
q_0 = h_0 * surface_area_pin * (T_s - Tinit);

% initial modified Rayleigh
Ra_0_mod = (gravity * B_air * q_0 * density_air^2 * cp_air * (width_channel*12)^4) ...
   / (k_air^2 *  dyn_vis_air);

% characteristic velocity ( m/s )
velocity_char0 = (alpha_air / (width_channel*12)) * sqrt( Ra_0_mod * Pr_air);

% initial channel temperature
T_inf(1) = Tinit;

% iterate up the pin in a sectionalized region to minimize geometric considerations
for j = 2:vertical_sections + 1

   % First find the Rayleigh and Nusselt numbers leading to heat transfer
   % coefficient for this segment

   % Find the Ra_s [ Fenech ]
   Ra_s(j-1) = ( gravity * B_air * density_air^2 * (T_s - T_inf(j-1)) * width_channel^3 ) ...
      / dyn_vis_air^2 * Pr_air;

   % find a denominator value for readability
   RSL(j-1) = Ra_s(j-1) .* ( width_channel / dy );

   % Nusselt Number
   % Nu_s = ( 576/ RSL^2 + 2.87 / RSL^1/2 )^ -1/2
   Nu_s(j-1) = ( 576 ./ RSL(j-1).^2 + 2.87 ./ RSL(j-1).^(1/2) ).^(-1/2);
```

```
    % heat transfer coefficient ( W/m^2K )
    h(j-1) = Nu_s(j-1) .* k_air ./ dy;

    % sectional heat flux (W/m^2)
    heat_flux(j-1) = h(j-1) * (T_s - T_inf(j-1)); % ( W/m^2)

    % Modified Rayleigh number
    modified_Rayleigh_number(j-1) = (gravity * B_air * heat_flux(j-1) * density_air^2 * cp_air * width_channel^4) ...
    / (k_air^2 *  dyn_vis_air);

    % Velocity in this region ( m/s )
    velocity_char(j-1) = (alpha_air / width_channel) * sqrt( modified_Rayleigh_number(j-1) * Pr_air); % ( m/s)

    % Sectional delta T (C)
    % Q_dot = m_dot * cp * dT
    % m_dot = rho * A * v
    dT(j-1) =  ( heat_flux(j-1) * surface_area_pin ) / ( density_air * area_flow_gap * velocity_char(j-1) * cp_air);

    % Uniform heat flux
    % Nu_x = q_w/dT * x/k [Lienhard]
    % dT = q_w/Nu_x * x/k;
    % dT = Ts - Tinf => Tinf = Ts - q_w/Nu_x * x/k;

    % Find the 'end of section' temperature (C)
    T_inf(j) = T_inf(j-1) + dT(j-1);


end

% Output for the function
Tinf = T_inf(end);

% build output y vector (m)
l_pin = linspace(0,pin_height,length(T_inf));

% Back of envelope calculation
% time in area (s)
t_exposed = pin_height / velocity_char0;

% Energy change in the region (J)
dJ = heat_flux .* surface_area_pin * t_exposed;

% mass of air (kg)
m_air_BOE = density_air * area_cooling/4 * pin_height;

% specific energy (J/kg)
spec_dJ = dJ / m_air_BOE;

% Differential temperature from heat addition (C)
dT_BOE = spec_dJ / cv_air;

% final change
T_inf_BOE_dist = Tinit + dT_BOE;

% max channel value
T_inf_BOE = max(T_inf_BOE_dist);

% OUTPUT
display('Building output graphs ');

figure(4)
```

```
plot(dT)
xlabel( ' Pin axial (m) ');
ylabel(' dT per region (C) ');
title(' Change in temperature vs axial point ');
legend(sprintf(' Max temp(C) %3.2f ', max(T_inf)'),'Location','SouthEast');

figure(5)
plot(l_pin,T_inf)
xlabel( ' Pin axial (m) ');
ylabel(' Channel Temperature (C) ');
title(' Infinite channel temperature vs axial point ');
legend([sprintf(' Max temp calc(C) %3.2f ', max(T_inf)') sprintf(' Max temp BOE(C) %3.2f ',
T_inf_BOE)],'Location','SouthEast');
```

2016

Analysis of Effluent Argon Production, Release, and Exposure for The University of Texas at Austin TRIGA Reactor

G. KLINE, 2016

Table of Contents

List of Figures

List of Tables

Introduction

The main radionuclide of concern in normal operations is Argon-41 produced from the natural argon in the air being exposed to the core. The production and dispersion of Ar-41 is modelled for various core operating parameters and ventilation conditions. These allow for the occupational and general populace exposures to be found.

Background

Argon-41 production comes principally from the soluble argon gas at the core area as well as beam line and rotary specimen rack (RSR) air cavities. There are two ventilation systems responsible for air movement: purge and reactor bay heating and air conditioning (HVAC) system. The HVAC system is a standard building circulation system containing both suction and return fans.[1] The HVAC system draws from the room, contains psychrometric interface, temperature control, and room isolation. The purge system is designed to provide suction from near the point of Ar-41 production in the different facilities. The purge system draws from a number of enclosures (experiment facilities and pool surface) with dilution from the reactor bay air and provides isolation on demand, but provides no return fan.[1] The Argon-41 concentrations and exposure potentials vary with changes in system line ups.

The nuclear engineering teaching laboratory (NETL) is located in a moderately urbanized area. The buildings in the area percentages for the most part are between 2-4 stories and have retail and office occupancy. The prevailing winds come directly from the north in the winter time and directly from the south in the summer time.[2] The NETL building itself is not square, however, the reactor bay size and shape dominates the wake effects and a square-assumption remains valid.[3]–[5] .

The effluent release is modelled using Gaussian plume modelling for the resident prevailing wind speeds and atmospheric conditions.[6]–[9] The ground source estimates are found for effluents trapped in the wake using ground source criteria.[9]–[11] The building has no physical boundary, therefore exposure up to the building walls needs to be considered. Points of interest are found based on occupancy and geographic relationship to NETL. The maximally exposed individual is taken from the maximum of these mappings. Occupational exposure is determined from a person standing in the reactor bay over the core. In either case, a semi-infinite cloud model is used to find dose rate and dose.[12]

Effective stack height, building wake, and atmospheric stability are taken from DOE references.[6] The effects are found for all atmospheric conditions and wind speeds relevant to the Austin, TX area.[2], [6] The most limiting of these conditions for each scenario is used for that scenario's exposure.[3]

Model

List of Variables

Table I: Symbols

V_i	Volume of the i^{th} element (m^3)	$\frac{dN_{4,i}}{dt}$	Change in Argon 41 number density for the i^{th} element $\left(\frac{n^0}{m^3 s}\right)$
A_i	Area of the i^{th}element (m^2)	$N_{a,i}$	Number density of Argon Gas in the i^{th} element $\left(\frac{atoms}{m^3}\right)$
v_i	Velocity of i^{th}element $\left(\frac{m}{s}\right)$	σ_a	Energy averaged cross section of absorption (m^2)
ϕ_i	Core flux in the i^{th} area $\left(\frac{n^0}{m^2 s}\right)$	$\lambda_{j,i}$	j^{th}decay mechanism of the i^{th}area $\left(\frac{1}{s}\right)$
$N_{4,i}$	Number density of Argon 41 in the i^{th} element $\left(\frac{atoms}{m^3}\right)$	$t_{1/2}$	$Half-life$ of Argon (s)
Q_i	Volumetric flow rate of i^{th} item $\left(\frac{m^3}{s}\right)$	N_A	Avagadro's Number $\left(\frac{atoms}{mol}\right)$
P_{air}	Pressure of Air (Pa)	R	Universal Gas Constant $\left(\frac{J}{mol\ K}\right)$
T_{air}	Temperature of Air (K)	$\tilde{C}_{Ar}$	Mol fraction of Argon in air $\left(\frac{mol_{Ar}}{mol_{air}}\right)$
Act_i	Specific activity of concentraiton i $\left(\frac{Bq}{m^3}\right)$	$\dot{D}_\gamma$	Dose rate from semi infinite cloud $\left(\frac{mR}{h}\right)$
k_γ	Conversion factor for cloud model $\left(\frac{Rad}{s}\frac{dis}{MeV}\frac{m^3}{Bq}\right)$	χ_λ	Fraction of Gamma Energy
E_λ	Gamma energy (MeV)	F_T	Generic placeholder for a sum of an effect
Δt	Time duration to be considered after function reaches steady state (s)	t_f	Time function reaches steady state rate of change (s)
t_0	Initialization of ventilation effects (s)	$F(t_f)$	Steady state value for a function rate of change
k_r	Conversion from $\left(\frac{R}{s}\right)$ to $\left(\frac{mR}{h}\right)$	t_{stay}	Stay time (h)

L_r	Radioactive exposure limit (mR)	n_i	Mole density of Argon Gas in the i^{th} element $\left(\frac{atommols}{m^3}\right)$
R_0	Plume exit radius (m)	w	Stack velocity out $\left(\frac{m}{s}\right)$
$\tilde{V}_0, \dot{V}_t$	Plume volume flux, volumetric flow $\left(\frac{m^3}{s}\right)$	$\tilde{F}_i$	Bouyancy flux $\left(\frac{m^4}{s^3}\right)$
$\tilde{M}$	Momentum flux $\left(\frac{m^4}{s^2}\right)$	u	Prevailing wind speed $\left(\frac{m}{s}\right)$
T_e, T_p	Temperature of environment, e, and plume , p (C)	g	Gravity $\left(\frac{m}{s^2}\right)$
ρ_i	Density of i^{th}element $\left(\frac{kg}{m^3}\right)$	s	Atmospheric stability $\left(\frac{1}{s^2}\right)$
z	Atmospheric mixing depth (m)	z_0	Roughness length (m)
u_*	Friction velocity $\left(\frac{m}{s}\right)$	ϵ	Eddy dissipation rate $\left(\frac{m^2}{s^3}\right)$
$\tilde{H}$	Surface bouyancy flux $\left(\frac{m^2}{s^3}\right)$	H, W, L	Building height, width, length (m)
Δh_a	Change in effective height from atmospheric conditions(m)	h_s	Physical stack height from ground(m)
h_a	Stack height with physical height and atmospheric effects(m)	h_d	Downwash corrected stack height(m)
ζ	Smaller of building height (H)or width (W) (m)	ξ	Smaller of building height (H)or width (W) (m)
$\tilde{R}$	Charactoristic length (m)	L_c	Roof cavity distance (m)
H_c	Roof cavity height (m)	Z_{II}, Z_{III}	High turbulance boundary, Roof wake boundary (m)
x_r	Cavity region distance(m)	$\hat{A}, \hat{B}$	Wake cavity constants
h_e	Final effective stack height(m)	C_i	Concentration of the i^{th} region $\left(\frac{kg}{m^3}\right)$
$\dot{m}_i$	Mass flow rate of the i^{th} region $\left(\frac{kg}{s}\right)$	$\sigma_{y,z}$	Standard deviation disspersion coefficients (m)
z'	Bent plume trajectory (m)	$(\sigma_{y,z})_{eff}$	Effectvie standard deviation disspersion coefficients (m)

Argon Production

Argon production at the UT TRIGA is modelled using a first order production decay formula.

$$\frac{dN_{4,i}}{dt} = N_{a,i}\sigma_a\phi_i - \lambda_{j,i}N_{4,i} \quad (1)$$

The production term is found using the area's Argon number density and neutron flux. The removal term has three components including radioactive decay, purge flow, and HVAC flow. The radioactive decay constant is a function of the radionuclide half-life, while ventilation constants are based on flow rate and suction volume.

$$\lambda_{r,i} = \frac{\ln(2)}{t_{1/2}} \quad (2)$$

$$\lambda_{p,i}, \lambda_{H,i} = \frac{Q_i}{V_i} \quad (3)$$

Geometry and Specifications

The reactor bay volume is divided into four main areas including reactor bay, pool area, beam lines, RSR. The reactor bay is the nominal volume of the room, excluding the other three areas. The pool area is the air space above the core, normally enclosed by deck plating.

Beam lines and RSR facilities have production and flow regions. These regions are defined by the suction point of the purge system. The volume between the core interface and the purge suction is the production volume term, while the flow area is the area between the purge suction and the reactor bay.

Volume of the reactor bay is taken from the University of Texas SAR.[1] The pool area volume was taken from measurements of the area, while beam line and RSR volumes come from mechanical blueprints.

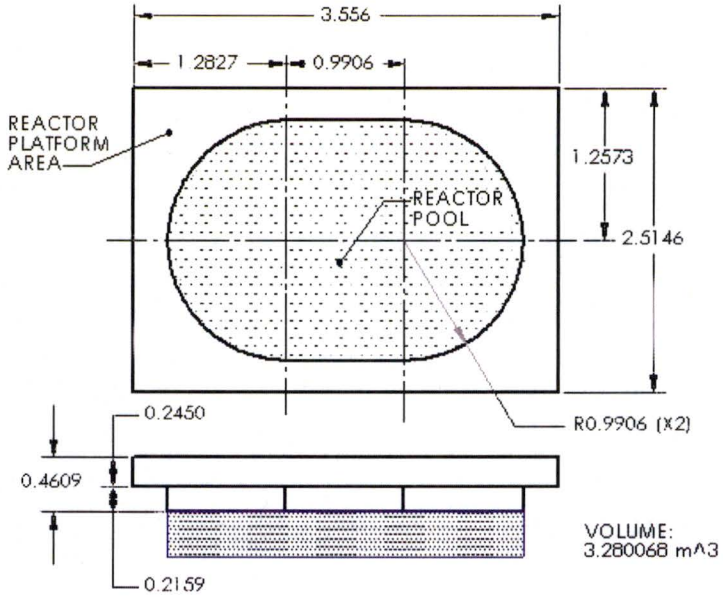

Figure 1. Pool area measurements and volume calculations created in Solidworks. Dimensions are in m.

The pool area volume is taken at the nominal pool depth of 8.100m. Since the solubility of argon at the core depth fluctuates little over the operational depth range, this is considered acceptable.

Table II: Model Volumes

Location	Volume (m^3)
RX Bay	4120
Pool Area (nominal)	3.280
Pool Area (worst case)	2.922
Beam Line Production	1.000
Beam Line Flow	3.000
RSR Production	.0264
RSR Flow	.0066

Flow rates for the various ventilation points are found using the purge and HVAC nominal velocities of 4000fpm and 1700fpm, ($20.32\frac{m}{s}$ and $8.64\frac{m}{s}$), respectively, as well as the area of the item at the point of suction.

$$Q_i = A_i v_i \tag{4}$$

Equation (4) leads to the following flow rates:

Table III: Flow Rates for Ventilation

Location	Velocity $(\frac{m}{s})$	Area (m^2)	Flow $(\frac{m^3}{s})$
HVAC Suction	8.636	1.806	15.60
Purge Pool Suction	20.32	.0324	.6590
Beam Line Suction	20.32	.0014	.0290
RSR Suction	20.32	$2.850e^{-4}$	.0058
RX Bay Purge Suction	20.32	.0324	.6590

The production terms are based on the argon 40 number density and neutron flux of the core at the various locations. The RSR flux is well characterized from gold foil experiments, while the beam line is an overestimate based on the gold foils in the pneumatic tube, near the inside reflector surface. Values from the core are based foil experiments from the central thimble experiment tube (A ring).

Table IV: Flux Values Used in Production

Location	Flux $\left(\frac{n^0}{m^2 s}\right)$
Core	$1e^{17}$
Beam lines	$1e^{15}$
RSR	$2e^{16}$

Historically, gold foil experiments in the past have provided reliable data for flux calculations. Number density for available argon was calculated either from solubility at depth (for activation of water in the pool) or the mole fraction in air (for activation in dry experiment facilities). The Argon-40 absorption cross section was taken from the National Institute of Standards and Technology (NIST) website.[13]

Environment

The reactor bay is maintained at nominal pressure and temperature [NTP], (20°C and 101325 Pa). The beam lines, RSR, and bay are all assumed to be well mixed volumes at NTP.

Gas-liquid phase boundary physics of the pool air-water interface and Argon-air diffusion coefficients were evaluated. These effects are considered negligible, as they add complexity and do not change the steady state concentration of argon in the reactor bay volume, only the rate of approach.[14]–[18]

The number density of argon in air is derived from the natural mole fraction of argon. This density applies to the RSR and the beam lines. The number density of air atoms for nominal temperature and pressure is found by:

$$N_{air} = \frac{N_A P_{air}}{R T_{air}} \tag{5}$$

$$N_{Ar} = \tilde{C}_{Ar} N_{air} \tag{6}$$

The solubility of Argon in water is both temperature and depth dependent. The value used was taken from reference material [19] as 0.941 (mg/L).

Production Calculations

Concentration

To facilitate calculations in the reactor bay, the volumes considered in **Ta**ble II are divided into control volumes. Their relationships and interactions vary based on the physics of the ventilation modes.

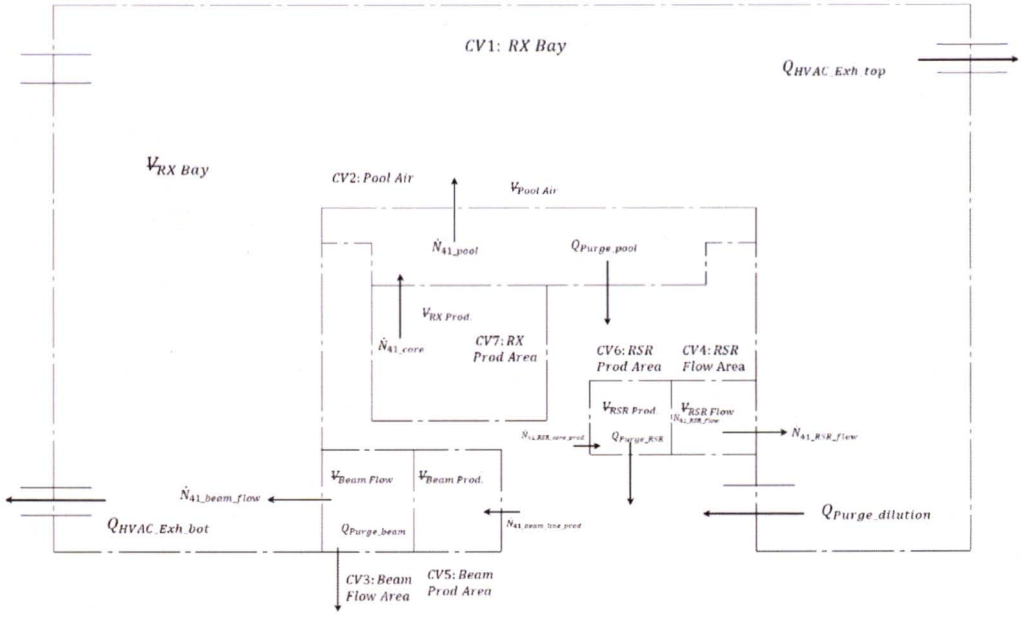

Figure 2. Control Volumes Considered in Effluent Production Analysis

The reactor by and reactor ventilation system operates in four modes, including isolation, HVAC only, purge only, HVAC and purge. All of these modes are evaluated for effects on occupational dose and effluent release. Additionally, three main modes of experiment facility were analyzed based on volumes of Argon-41 is production including (1) core, beam, and RSR; (2) core and beam; and (3) core only. For exposure analysis, the configuration with core, beam, and RSR production (PBR) is considered the worst case scenario.

The effective removal constants of the ventilation modes are provided in Table V. With the exception of the purge draw from the dilution valve, the effects of the removal by the HVAC and purge systems are orders of magnitude greater than reduction from

radioactive decay.

Table V: Effective Decay Constants

Decay Term	Value (1/s)
Radioactive Decay	$1.054e^{-4}$
HVAC	.0038
Beam Purge	.00290
RSR Purge	.2194
Pool Purge	.2009
Dilution Purge	$1.599e^{-4}$

Considering this, in the 'isolation' and 'HVAC only' modes, the control volumes around the pool, beam, and RSR can be neglected with their areas only considered source terms to the reactor bay only. The Argon-41 atoms are drawn into the bay at a rate that exceeds decay. Argon-41 is diluted in the reactor bay and is removed either by decay or removal in the HVAC exhaust. This allows these two removal modes to be considered in first order linear ODEs only. The decay of HVAC in equation (7) only applies in the 'HVAC only' mode. These are solved for the reactor bay concentration of Argon-41.

$$\frac{dN_{4,RX}}{dt} = \frac{\sum N_i \sigma_a \phi_i \cancel{V_i}}{\cancel{V_{total}}} - \lambda_r N_{4,RX} - \{\lambda_H N_{4,RX}\}^* \tag{7}$$

$$N_{4,RX}(SS) = \frac{\sum N_i \sigma_a \phi_i \cancel{V_i}}{\cancel{V_{total}}(\lambda_r + \lambda_H{}^*)} \tag{8}$$

When the purge system is operating, the momentum and draw of the purge valves is significant relative to the diffusion into the bay and radioactive decay. Thus, the system is no longer a single first order ODE; each smaller control volume is its own first order ODE combined into the reactor bay first order ODE. This creates a system of first order ODEs that needs to be solved using ODE solution methods.

$$\frac{dN_{4,RX}}{dt} = \frac{\sum(N_i \sigma_a \phi_i - \lambda_{p,i} N_{4,1})\cancel{V_i}}{\cancel{V_{total}}} - \lambda_r N_{4,RX} - \{\lambda_H N_{4,RX}\}^* - \lambda_{p,dilute} N_{4,RX} \tag{9}$$

In this case, the two scenarios involve first 'purge only' and then 'purge and HVAC.' Only the HVAC decay constant is considered in the 'purge and HVAC' mode. The ODE set is solved in MALAB using ODE45, a variable time step Runge-Kutta 45 method, and extremely tight error tolerances of $1e^8$ % absolute and relative error.[4], [5]

The second order nature of equation (9) leads to a concentration function, which approaches a steady state value on the order of five half-lives of radioactive decay.

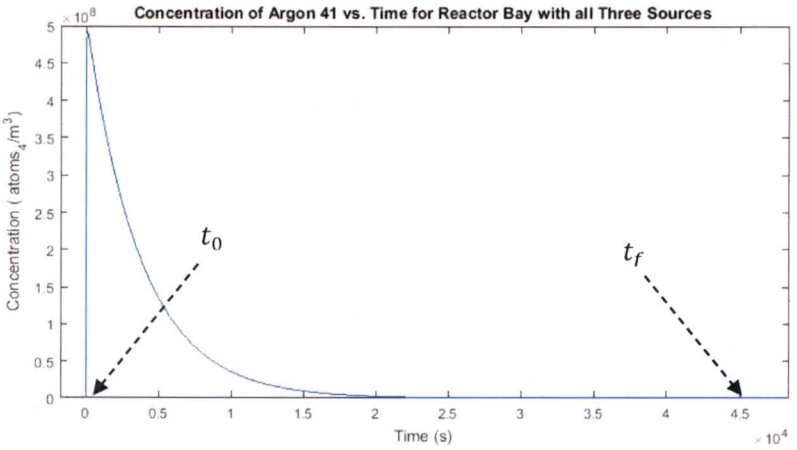

Figure 3. Typical reactor bay concentration trend for purge system operations

To find the total effects of such concentration changes, the integral is used.

$$F_T = \int_{t_0}^{t_f} F(t)dt + F(t_f)\Delta t \tag{10}$$

Table VI. Argon-41 Concentrations in Source Locations with HVAC and Purge Running

Location	Concentration (µCi/mL)
Reactor Bay	$1.168e^{-6}$
Pool Area (nominal)	.0013
Pool Area (worst)	.0012
Stack (nominal)	$5.457e^{-5}$
Stack (worst)	$4.907e^{-5}$
RSR	.0043
Beam Lines	.0016

Based on the above calculations, the pool volume considered to be the worst case scenario leads to lower concentrations. The rest of the analysis uses the higher concentration.

Activity and Dose

Semi-infinite cloud exposure calculations require the specific activity from concentration and the radioactive decay constant.

$$Act_i = N_i\lambda_r \tag{11}$$

The semi-infinite cloud model uses the specific activity, gamma energy, and constants to convert the activity from equation (10) into an effective dose rate.[12]

$$\dot{D}_\gamma = k_r k_\gamma Act_i \sum \chi_\lambda E_\lambda \tag{12}$$

Argon-41 is a gamma emitter and with a quality factor of 1, making the Rad to REM conversion factor 1. This equation is used to find the reactor bay dose rate.

Argon Dispersion

With potential concentrations calculated, area dispersion is considered. A local meteorologist was consulted for environmental conditions.[20] DOE/TIC—11223 provides equations for effective stack height, Gaussian plume,[6], [7], [11], [21] and ground sources.[6], [9], [22] Points of interest around the building include the maximum individual, ground exposure, multiple commercial facilities nearby, and the closest operational laboratory.

Effective Stack Height

The effective stack height is a pseudo-physical stack height created from the stack's physical height in combination with different physical process factors such as atmospheric stability, stagnation velocity, prevailing wind velocity, and building and surrounding wake effects.

Building and Stack Geometry

NETL is a building formed from three main cubical sections. The reactor bay stands in the middle, is significantly taller than the other two sections, and is much longer. For the sake of the model, building length is in the north-south direction, width is east to west and height is vertical. The entire building sits atop a built up berm, adding about 2 m of height. The blueprints have the reactor bay walls at 18.288 m wide by 15.698 m high, giving a north-south cross sectional area of 287 m^2.

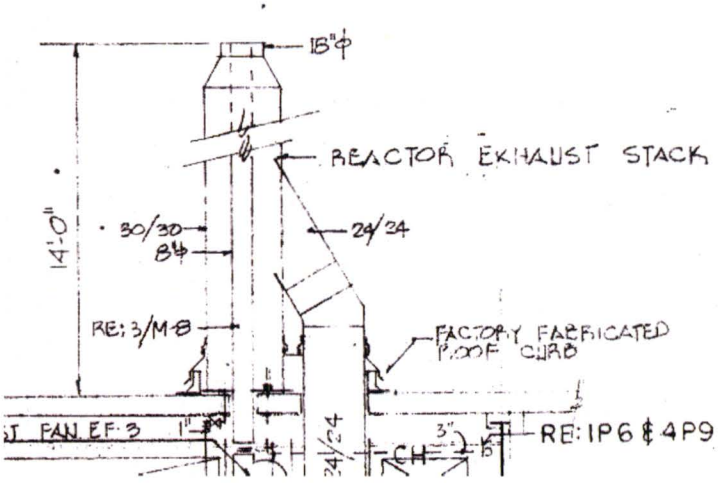

Figure 4. NETL Stack Layout

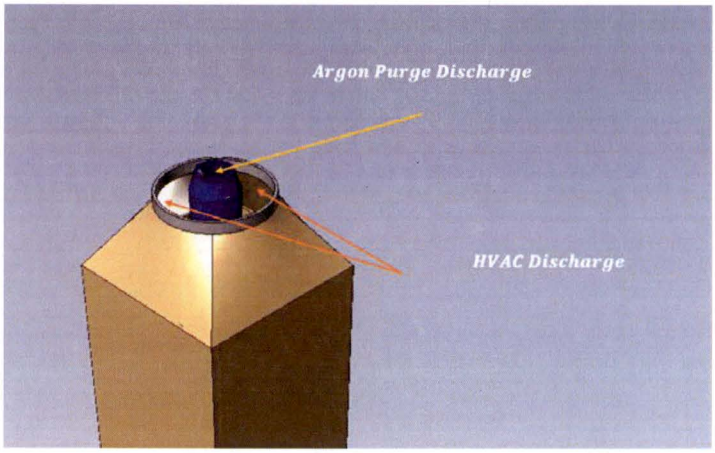

Figure 5. NETL Stack Concentric Configuration

The ventilation stack sits atop the reactor bay roof. The ventilation stack consists of concentric discharge lines, with the argon purge system being the inner portion.

The concentric stacks sit ~4.26m off the roof surface and have nozzle features that increase the exit velocities. System velocities are measured up stream at the fan interfaces, and are adjusted for assuming conversation of volumetric flow.

Table VII: NETL Stack Parameters

System	Discharge Area (m^2)	Exit Velocity (m/s)	Volumetric Flow (m^3/s)
HVAC	.1317	35.94	4.734
Purge	.0182	36.12	1.353

The exit velocities of the two effluent streams are similar, allowing a mixture to dilute with little momentum loss. The purge suction lines draw at a point of higher concentration but the purge stream is initially diluted through a reactor bay air suction line. Then, the purge stream is entrained in the HVAC reactor bay suction line. The HVAC volumetric flow is higher, creating an entrained, diluted mixture.

$$n_{mix} = \frac{\sum n_i \dot{V}_i}{\dot{V}_{Total}} \tag{13}$$

Environment

The Austin area NETL is in has two sets of prevailing winds.[2], [20] The wind direction changes based on the season, with the wind coming from the north in winter and from the south in summer.

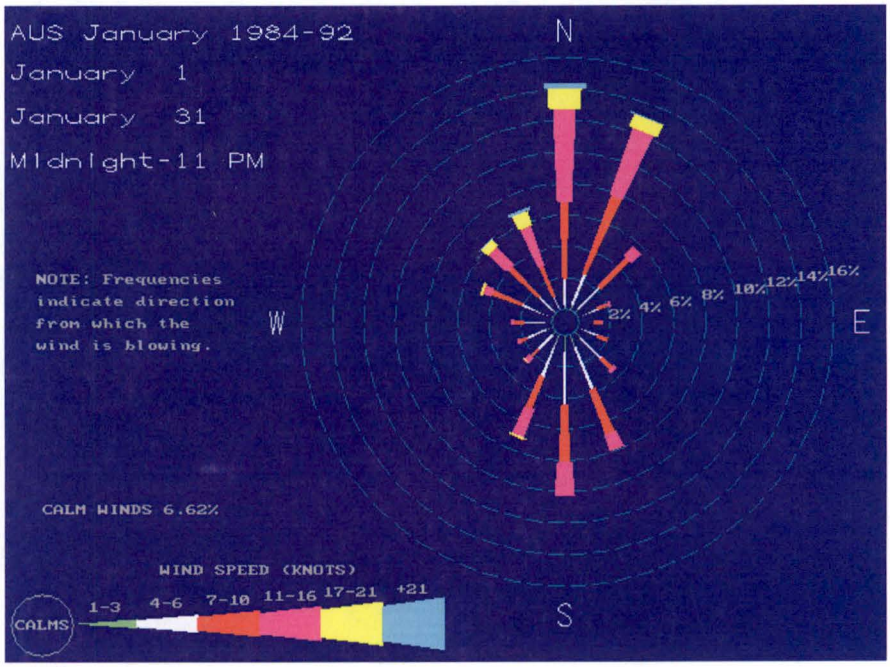

Figure 6. Winter wind rose

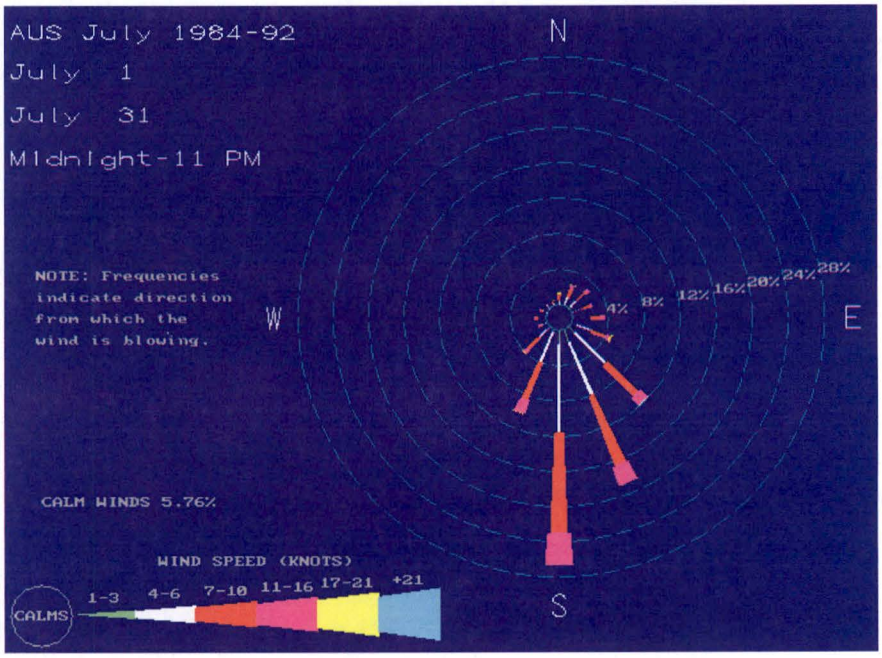

Figure 7. Summer wind rose

A wind speed velocity vector is developed from 0 to 21knots, as to represent the range of wind conditions. The temperature ranges of Texas vary considerably, while the plume temperature tends to be steady. For these calculations a plume temperature of 25°C, and environment of 20°C was chosen. These temperatures are used to find the buoyancy and momentum fluxes. With the environment at a higher temperature than the stack, the fluxes are negative, and the plume is caught in the wake. For the times of

the year when the plume is warmer, these temperatures are nominally offset by the range used.

To find the effects on stack height based on atmospheric conditions, the stability, wind speed, plume speed and fluxes all come into play. The velocity flux (a.k.a. volumetric flow) is found first.

$$\tilde{V}_0 = w_0 {R_0}^2 (vertical);\ \tilde{V}_0 = u{R_0}^2 (bent\ over) \tag{14}$$

From the velocity flux and the densities found from temperatures, the buoyancy and momentum fluxes can be found.

$$\tilde{F}_0 = \frac{g}{T_{p0}}(T_{p0} - T_{e0})\tilde{V}_0 \tag{15}$$

$$\tilde{M} = \frac{\rho_{p0}}{\rho_{e0}} w_0 \tilde{V}_0 \tag{16}$$

In addition to these parameters, the atmospheric stability needs to be found. For the short heights involved with the NETL plume, the change in environmental temperature with height is ignored.

$$s = \frac{g}{T_e}\left(\frac{\partial T_e}{\partial z} + .0098\right) \tag{17}$$

A multitude of atmospheric stack height changes exists based on plume shape and surroundings. These include: rise limited by atmospheric stability; nearly neutral conditions; and convective conditions. To maintain a conservative approach to stack height change, each change in height was found for each wind speed in the vector. Then, the minimum height for each prevailing wind speed was used. This ensures credit is given for plume rise, but worst case scenarios are considered.

Three conditions are considered: rise limited by ambient stability, ambient turbulence neutral conditions and ambient turbulence in convective conditions. For buoyant bent over plumes, the need arises for a friction velocity. This involves a mixing depth and roughness length relative to the building height.

$$z_0 = \frac{H}{10} \tag{18}$$

$$u_* = \frac{.4u}{\ln\left(\frac{z}{z_0}\right)} \tag{19}$$

For the convective conditions, the eddy dissipation rate leads to a surface buoyancy flux needed to find this condition's change in height.

$$\epsilon = \frac{{u_*}^3}{.4z} \tag{20}$$

$$\epsilon = .25\tilde{H} \tag{21}$$

Below are the four methods. Each method is applied to every wind speed, and the lowest height change for each wind speed is used.

$$\Delta \boldsymbol{h_a} = 2.6\left(\frac{F_0}{\boldsymbol{us}}\right)^{1/3} (ambient\ stability, bent\ over\ plume) \tag{22}$$

$$\Delta \boldsymbol{h_a} = 1.54\left(\frac{F_0}{\boldsymbol{u}{u_*}^2}\right)^{2/3} {h_s}^{1/3}\ (nearly\ neutral\ bouyant\ bent\ over\ plume) \tag{23}$$

$$\Delta \boldsymbol{h_a} = 3(2R_0)\left(\frac{w_0}{\boldsymbol{u}} - 1\right)\ (nearly\ neutral\ vertical\ jet) \tag{24}$$

$$\Delta \boldsymbol{h_a} = 3\left(\frac{F_0}{\boldsymbol{u}}\right)^{3/5} \tilde{H}^{-2/5}\ (convective\ conditions) \tag{25}$$

At this point the effective stack height incorporates the physical height and the atmospheric effects.

$$h_a(i) = h_s + min_j\langle \Delta \boldsymbol{h_{a,i}} \rangle \tag{26}$$

Building Wake Effects and Downwash

The first effect to consider is downwash around the stack. This occurs when the stack velocity to prevailing wind speed ratio is less than 1.5.[6]

$$\Delta h_d = 2\left(\frac{w_0}{u} - 1.5\right)(2R_0) \tag{27}$$

$$h_d = h_a + \Delta h_d \tag{28}$$

While the building is not perfectly cubical, the features are cubical enough to allow the building wake to be found using DOE/TIC.[6] Features to be considered include roof separation region, cavity zone, wake boundary and turbulent zone boundary.

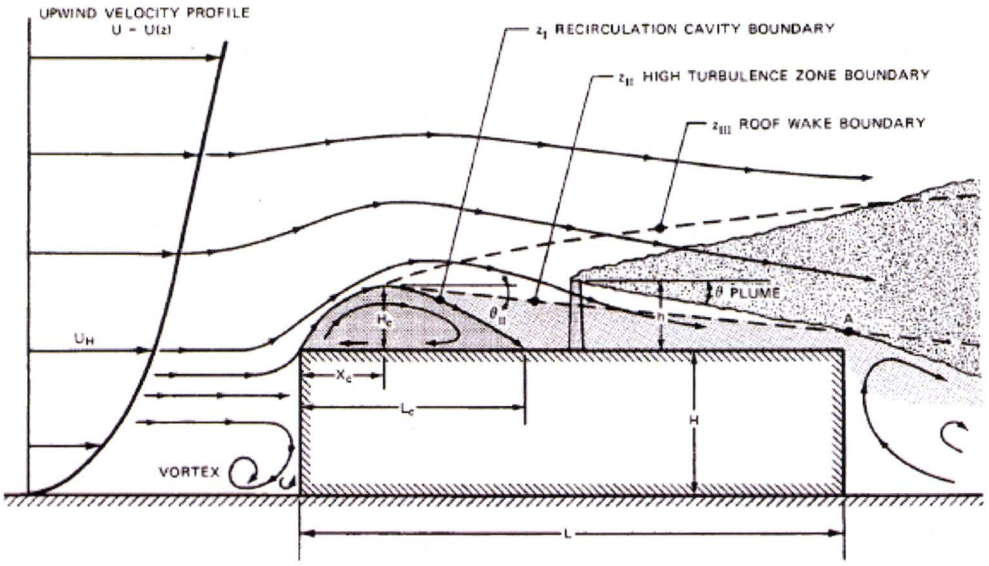

Figure 8. Building wake development[6]

First, calculations must be made to see if the plume is trapped in a developed roof wake. This begins with finding a characteristic length based off of building criteria, then develop equations for the boundary layers.

$$\tilde{R} = \zeta^{2/3}\xi^{1/3} \tag{29}$$

$$L_c \approx .9\tilde{R} \tag{30}$$

$$H_c \approx .22\tilde{R} \tag{31}$$

$$x_c \approx \frac{\tilde{R}}{2} \tag{32}$$

$$\frac{Z_{II}}{\tilde{R}} \approx .27 - .1\frac{x}{\tilde{R}} \tag{33}$$

$$\frac{Z_{III}}{\tilde{R}} \approx .28\left(\frac{x}{\tilde{R}}\right)^{1/3} \tag{34}$$

For NETL, the recirculation height is ~3.3m while the stack is 4.2m. The plume clears the roof wake effects in all conditions but those where it is trapped in the cavity.

For plumes caught in the cavity region, it is necessary to find the geometry of this region. The distance from the building is found based on the building length to height ratio. NETL's building to height ratio is >1.6, making $\hat{A}$=1.75, $\hat{B}$=.25

$$\frac{x_r}{H} = \frac{\hat{A}\left(\frac{W}{H}\right)}{1 + \hat{B}\left(\frac{W}{H}\right)} \tag{35}$$

For NETL, this distance is 24.8m. Plumes trapped in the building wake still need to be considered for their dose, however, because the walls of NETL are accessible from non rad worker personnel such as grounds keepers and maintenance.

Final effective stack height is found by taking into account the effect the building has on the downwash corrected, atmospheric corrected plume. The effects are relative to plume height and building properties.

$$h_e = h_d \ \{ h_d > H + 1.5\zeta \} \tag{36}$$

$$h_e = 2h_d - (H + 1.5\zeta) \ \{ h_d < H + 1.5\zeta \ \& \ h_d > H \} \tag{37}$$

$$h_e = h_d - 1.5\zeta \ \{ h_d < H \ \& \ h_d > .5\zeta \} \tag{38}$$

$$h_e = 0 \ \{ h_d < .5\zeta, Ground\ Source \} \tag{39}$$

For the ground source portion, the plume is considered to have zero height and be trapped in the building wake. For wind speeds less than 1m/s, the plume is near vertical and the effective height is found using buoyancy flux.[6]

$$h_e = h_d + \frac{4\tilde{F}_0^{.25}}{s^{.375}} \tag{40}$$

The effective stack heights at NETL are the vectorized relative to wind speed.

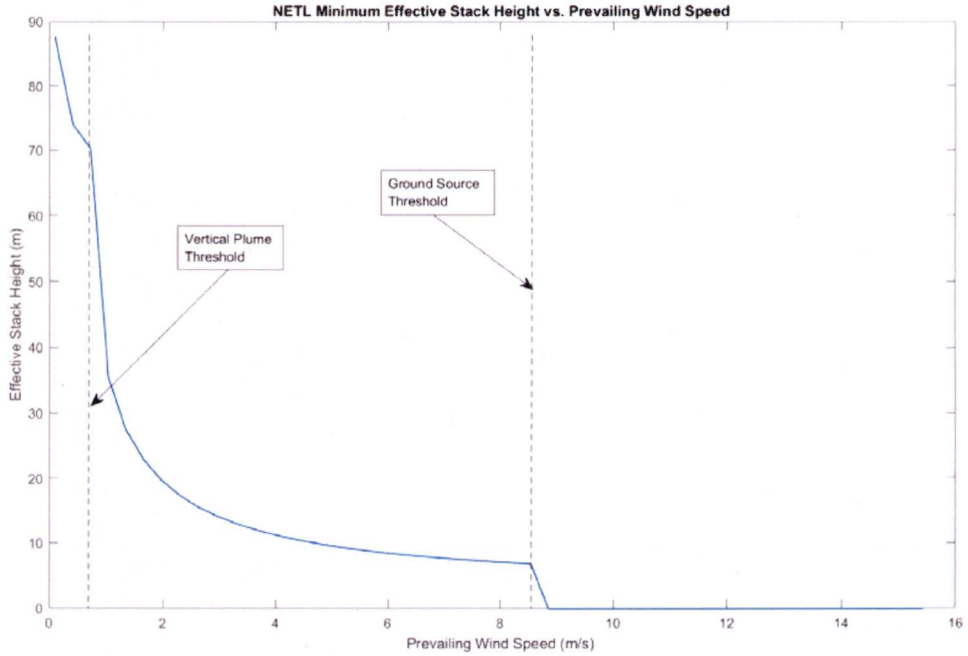

Figure 9. Effective Stack Height at NETL

Plume Development and Dispersion

Plume dispersion is separated into two main outcomes: ground source capture (or building wake effects), and Gaussian plume.

Ground Source

Ground source plumes are trapped in the building wake area, act as a ground sources, and create a concentration based on equation (41).

$$C_{ground} = \frac{\dot{m}_{plume}}{(\pi\sigma_y\sigma_z + cWH)u} \tag{41}$$

The concentration trapped in the building wake (C_{ground}) ranges between .5 and 2. The highest concentration is 0.5, used as the more conservative value. The dispersion coefficients used were the worst case, atmospherically and taken for the 100m point.

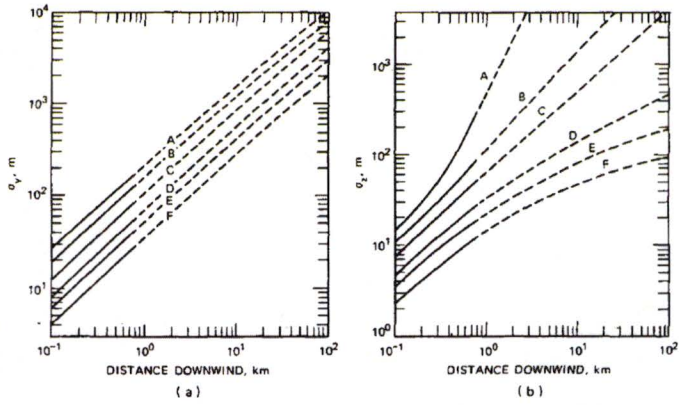

Fig. 4.4 Curves of σ_y and σ_z for turbulence types based on those reported by Pasquill (1961). [From F. A. Gifford, Turbulent Diffusion-Typing Schemes: A Review, *Nucl. Saf.*, 17(1): 71 (1976).]

Figure 10. Dispersion coefficients used in ground source calculations.

Gaussian Plume

The steady state Gaussian plume model gives concentrations at points downwind from the point of continuous release. For this release, the origin is set at the effective stack height for each of the atmospheric and prevailing wind speed conditions. The x-direction is taken in the north-south direction away from NETL. The y-direction is the east-west, while z-direction is height.

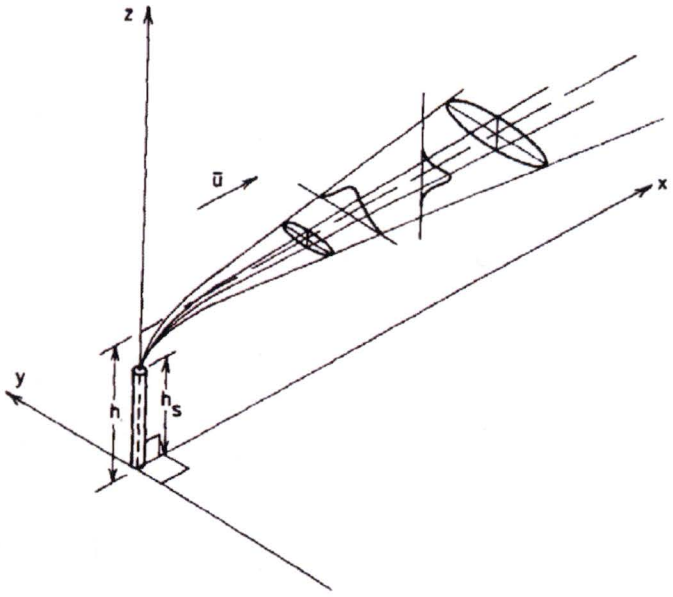

Figure 11. Plume orientation from NETL

This model takes the time average exposure in an area and assumes Gaussian distributed concentrations radially and orthogonal to wind direction vector. The wind is assumed to be constant as well as the concentration out of the stack. While the puff

model may be more representative to the true operational conditions, these puff concentrations would be lower than that of a constant plume, based on the time it takes for the plume to become steady state in the normal operation modes.[23], [24]

The area is mapped in 1m by 1m horizontal grids and the concentration is found at the desired height using (42). Here, a is the atmospheric condition, w is the wind speed; the equation is separated into the effective portions for ease of reading.

$$C(a,w,x,y) = \left(\frac{\dot{m}_{plume}}{u(w)}\right)\left(\frac{1}{2\pi\sigma_y(a,w,x)\sigma_z(a,w,x)}\right) * \left(e^{\frac{-y^2}{2\sigma_y^2(a,w,x)}}\right)\left[e^{\frac{-(z-h_e)^2}{2\sigma_z^2(a,w,x)}} + e^{\frac{-(z+h_e)^2}{2\sigma_z^2(a,w,x)}}\right] \quad (42)$$

For the dispersion constants, their values relative to x are found based on atmospheric conditions. NETL is situated in an urban area, thus the bottom set are used.

Table 4.5 Formulas Recommended by Briggs (1973) for $\sigma_y(x)$ and $\sigma_z(x)$ ($10^2 < x < 10^4$ m)

Pasquill type	σ_y, m	σ_z, m
	Open-Country Conditions	
A	$0.22x(1 + 0.0001x)^{-1/2}$	$0.20x$
B	$0.16x(1 + 0.0001x)^{-1/2}$	$0.12x$
C	$0.11x(1 + 0.0001x)^{-1/2}$	$0.08x(1 + 0.0002x)^{-1/2}$
D	$0.08x(1 + 0.0001x)^{-1/2}$	$0.06x(1 + 0.0015x)^{-1/2}$
E	$0.06x(1 + 0.0001x)^{-1/2}$	$0.03x(1 + 0.0003x)^{-1}$
F	$0.04x(1 + 0.0001x)^{-1/2}$	$0.016x(1 + 0.0003x)^{-1}$
	Urban Conditions	
A–B	$0.32x(1 + 0.0004x)^{-1/2}$	$0.24x(1 + 0.001x)^{1/2}$
C	$0.22x(1 + 0.0004x)^{-1/2}$	$0.20x$
D	$0.16x(1 + 0.0004x)^{-1/2}$	$0.14x(1 + 0.0003x)^{-1/2}$
E–F	$0.11x(1 + 0.0004x)^{-1/2}$	$0.08x(1 + 0.00015x)^{-1/2}$

Figure 12. Dispersion coefficients for atmospheric conditions.

For values of x close to the building, the dispersion coefficients do not fully represent the entrainment of atmospheric air and the development of the plume in the "bent-over" region. To account for this an effective dispersion coefficient is found using the calculated trajectory.[21], [24]

First the plume trajectory in the bent portion is found.

$$z'(x) = \frac{1.6\sqrt[3]{F_0 x^2}}{u} \quad (43)$$

The effective dispersion coefficients in this range are then found.

$$(\sigma_i^2)_{eff} = \left(\frac{z'}{3.5}\right)^2 + \sigma_i^2 \tag{44}$$

The dispersion patterns of interest exist at 1.5m, 8m, and 20m. The plume patterns are found below.

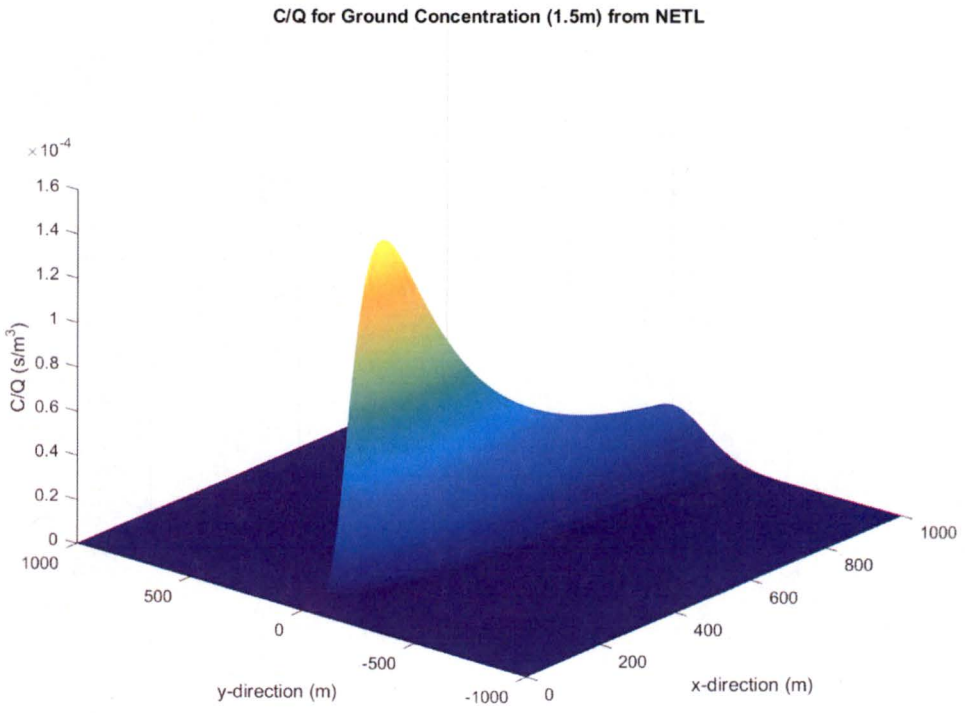

Figure 13. Ground pattern[3]

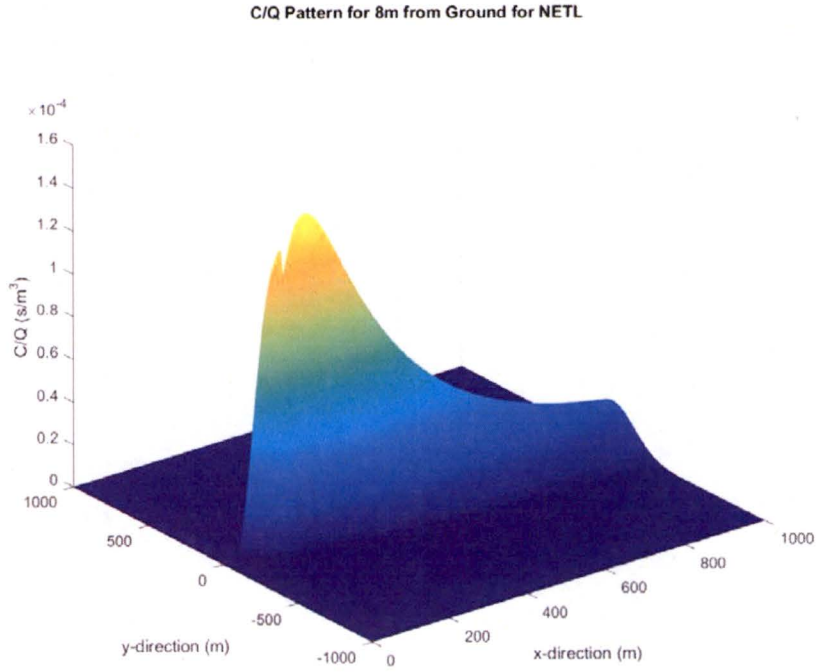

Figure 14. 8m Pattern[3]

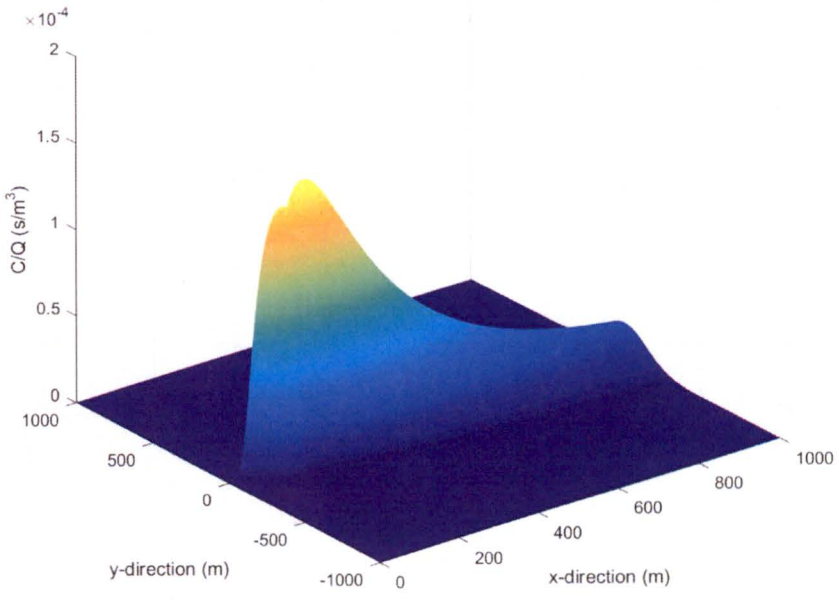

Figure 15. 20m Pattern[3]

These patterns can be used to find the maximum dose rate and location relative to NETL. It can also be used to find the exposure at various points of interest.

Area Points of Interest

There are four main points of interest at NETL, including the maximum exposed individual, IBM north, Macy's north and ARL south. The maximum individual is necessary for NETL's public exposure limit calculation. The maximum exposed individual is located 214 m due north of the stack in the parking lot of IBM. While highly unlikely, there is no constraint to prevent a person to stand there all year; therefore no occupancy times are used.

IBM is located ~240m due north of the stack and is the closest facility in the plume. There are no external access areas such as balconies, so the ventilation suctions are taken as the height and location of interest. This gives the maximum public exposure to the employees inside. Macy's and ARL have the same situation, except that Macy's is taller and ARL is south.

Table VIII. Points of Interest in NETL plume exposure.

Location	North/South (m)	East/West (m)	Height (m)
Maximum Individual	214.0	0.000	1.500
IBM	240.0	104.6	7.836
Macy's	174.8	480.2	19.97
ARL	751.0	71.59	7.836

Results

Occupational Dose and Stay Time

Equations (10), (11) and (12) provide the dose rates in the reactor bay and lead to occupational dose for a given exposure time. Focus is put on stay time, or how long a worker can be in the reactor bay before exceeding a specified limit. For this, the limit comes from 10 CFR 20 as 5000mR/yr. Since the entire analysis is taken over the course of one year, the limit is 5000mR.

$$t_{stay} = \frac{L_r}{\dot{D}_\gamma} \tag{45}$$

In the case of the purge modes calculations, equation (13) is slightly modified to account for the distribution function. The integrated dose from initiation of the ventilation lineup to steady state dose rate development is subtracted from the 10 CFR 20 limit. The remaining available dose is divided by the steady state dose rate and added to the transient time to find the total stay time.

$$t_{stay} = \frac{\left[L_r - \int_{t_0}^{t_f} \dot{D}_\gamma(t)dt\right]}{\dot{D}_\gamma} + (t_f - t_0) \tag{46}$$

It can easily be seen that the large decay constants of ventilation have significant effects on the stay time and dose rates in the bay. For the transient analyses, the steady state dose rate and peak are shown.

Table IX: Dose Rates and Stay Times in the Reactor Bay for Various Ventilation Lineups with All Three Sources (Pool, Beam, RSR)

Lineup	Concentration (μCi/mL)	Dose Rate (mR/h)	Stay Time (h)
Isolation	$2.125e^{-3}$	2260	2.21
HVAC only	$5.757e^{-5}$	61.38	81.5
Purge only	$1.400e^{-6}$(pk.), $2.524e^{-12}$(SS)	1.493(pk.), $2.691e^{-6}$(SS)	$1.86e^{9}$
HVAC and Purge	$1.168e^{-6}$(pk.), $1.372e^{-23}$(SS)	1.246(pk.), $4.184e^{-18}$(SS)	$1.20e^{21}$
10 CFR 20 Limit (Ar^{41})	$3e^{-6}$		

The effectiveness of the purge system can clearly be seen; however, it is also valid to show that under worst case conditions (all sources and isolation), plenty of time is available for personnel to evacuate the reactor bay. In a worst case situation, a worker can evacuate the reactor bay in ~3 min, receiving an estimated dose of ~113mR. This would involve a situation where the primary floor's exit is blocked, forcing a move to another floor. In a nominal situation, the exit time is ~30s, receiving a dose of ~19mR.

Under normal operation, the reactor is operated with both ventilations systems running and averaging 30 hours of operational time per week, with varying powers. The analysis above assumed 168 hours of full power operations per week, thus the stay time for normal operations is even longer than in Table IX. However, using equation (10), the dose received from a staff worker in the reactor bay for 8760 hours of continuous full power operation and full experimental facilities is 86.13mR. This is less than $1/10^{th}$ of the local NETL exposure limit. The NETL limit is set with ALARA in mind, and meeting this limit with such a margin shows the effectiveness of the system to meet ALARA standards.

Effluent Dose to Environment and Maximum Exposed Individual

Ground Source

The ground source dose rate varies with the oncoming wind speed. The worst case scenario is the sudden release of Argon-41 after steady state operations with the ventilation system isolated.

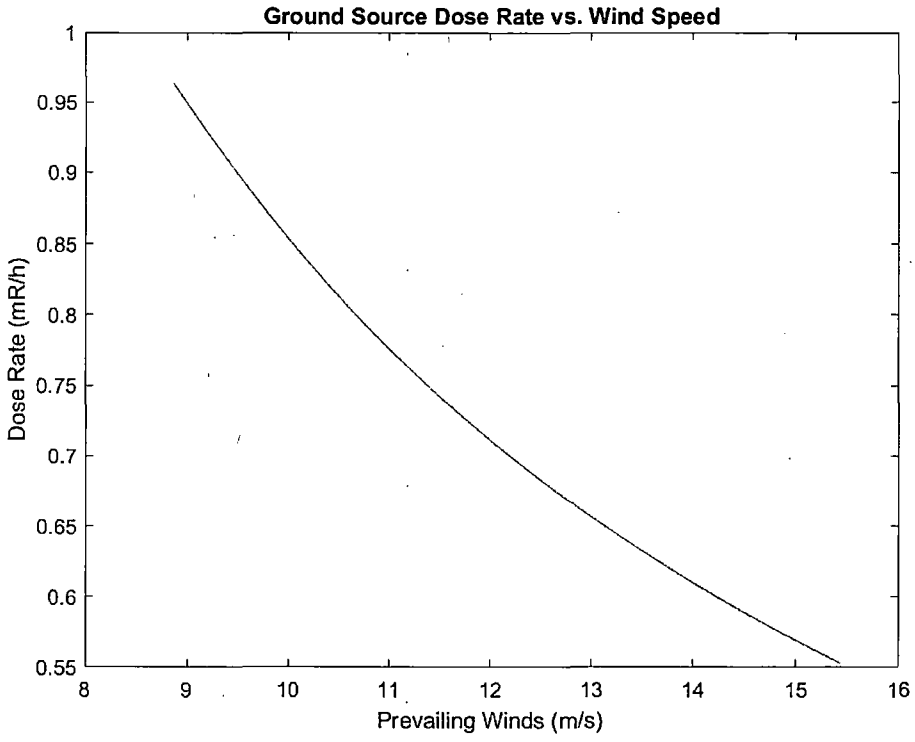

Figure 16. Ground source dose rates for prevailing winds for isolation release.

For the worst case wind in this situation, the dose rate, when evacuating from an isolation condition, is .96mR/h, meeting the 10 CFR 20 limit of 2mR/h.

Under normal operating conditions with both systems running, the ground source reduces to 24.7μR/h (.0247mR/h). This is well below 10 CFR 20 limits.

Gaussian Plume

Using the Gaussian plume distribution and the points of interest, the following dose rates and exposure for one year are found.

Table X. Exposures and Dose Rates at Points of Interest

Location	Isolation			Normal Operations		
	Dose Rate (mR/h)	Dose (mR)	Concentration (μCi/mL)	Dose Rate (mR/h)	Dose (mR)	Concentration (μCi/mL)
Maximum Individual	.1718	1504.9	$5.971e^{-104}$	.0088	77.298	$3.066e^{-105}$
IBM	$3.306e^{-59}$	$2.896e^{-55}$	$7.410e^{-76}$	$1.697e^{-60}$	$1.487e^{-56}$	$3.805e^{-77}$
Macy's	$3.204e^{-33}$	$2.807e^{-29}$	$7.183e^{-50}$	$1.645e^{-34}$	$1.441e^{-30}$	$3.689e^{-51}$
ARL	$4.112e^{-15}$	$3.602e^{-11}$	$9.217e^{-32}$	$2.111e^{-16}$	$1.850e^{-12}$	$4.733e^{-33}$
Ground Source	.9600	8409.6	$2.085e^{-17}$	.0247	2163.7	$1.071e^{-18}$

Conclusion

This analysis provides extremely conservative estimates for the exposures. The production terms involve worst case flux considerations, concentrations, and a state of reactor equilibrium far beyond what would be achieved within a normal working week.

The building wake effects are worst case by considering the most conservative atmospheric conditions and considering that the yearly status. In reality, the weather and climate of Texas are extremely dynamic.

The maximum exposed individual falls below 10 CFR 20 dose limits for 8760 hours of continuous normal operations. All area exposures fall below public dose rate limits as well. The isolation condition is an extreme situation that, if it occurred, the argon-41 would be allowed to decay in place in the reactor bay prior to release, making these numbers far above the realm of possibility.

References

[1] M.Krause, "The University of Texas at Austin TRIGA Safety and Analysis Report," Austin, TX, 1991.

[2] TCEQ, "Texas Commission on Environmental Quality," 2015. [Online]. Available: https://www.tceq.texas.gov/airquality/monops/windroses.html. [Accessed: 01-Jan-2016].

[3] G. Kline, "Plume_Model_2016." 2016.

[4] G. Kline, "Argon_Concentration_script." 2016.

[5] G. Kline, "Argon_Concentration_script_ODE." 2016.

[6] J. P. Lodge, *Handbook on atmospheric diffusion*, vol. 17, no. 3. 1983.

[7] D. T. Allen and C. J. Durrenberger, "Gaussian Plume Modeling." 2014.

[8] D. Coast, "Plumes and Thermals," pp. 163–180.

[9] A. G. Robins, "Plume dispersion from ground level sources in simulated atmospheric boundary layers," *Atmos. Environ.*, vol. 12, no. 5, pp. 1033–1044, 1978.

[10] S. etman M. Embaby, A.B. Mayhoub, K.S. M. Essa, "Worst case ground concentration.pdf," *Atmosfera*, vol. 15, pp. 185–191, 2002.

[11] K. S. M. Essa and M. Embaby, "Worst Air Concentration From Non-Gaussian Plume Model," no. 2007, pp. 11–15, 2009.

[12] J. J. Bevelacqua, *Contemporary Health Physics*, 1st ed. Weinheim: WILEY-VCH, 2004.

[13] NIST, "NIST Cross sections," 2016. [Online]. Available: https://www.ncnr.nist.gov/resources/n-lengths/elements/ar.html. [Accessed: 01-Jan-2016].

[14] "Kinetic Transport Interactions in Gas-Liquid-Solid systems.pdf." .

[15] A. J. Wagner and C. M. Pooley, "Interface width and bulk stability: Requirements for the simulation of deeply quenched liquid-gas systems," *Phys. Rev. E - Stat. Nonlinear, Soft Matter Phys.*, vol. 76, no. 4, pp. 1–5, 2007.

[16] W. Whitman, "The two film theory of gas absorption," *Int. J. Heat Mass Transf.*, vol. 5, no. May, pp. 429–433, 1962.

[17] M. Y. Christi, "Gas-Liquid Mass Transfer Fundamentals," *Airlift bioreactors*. pp. 12–32, 1989.

[18] T. R. Marrero and E. A. Mason, "Gaseous Diffusion Coefficients," *Journal of Physical and Chemical Reference Data*, vol. 1, no. 1. pp. 3–118, 1972.

[19] C. John, *Dissolved Gas Concentration in Water*, 2nd ed. Elsevier, 2012.

[20] T. Kimmel, "Consultation." Austin, TX, 2016.

[21] U. of Washington, "Gaussian Plumes from ' Point ' Sources." Seattle, pp. 1–27.

[22] S. E. M. Embaby, A.B. Mayhoub, K.S. Essa, "Worst case ground concentration.pdf," *Atmosfera*, vol. 15, pp. 185–191, 2002.

[23] B. T. O. Formulation, "Plume / Puff Spread and Mean Concentration Module Specifications," no. December, pp. 1–26, 2012.

[24] J. Bluett, N. Gimson, G. Fisher, C. Heydenrych, T. Freeman, and J. Godfrey, *Good practice guide for atmospheric dispersion modelling*. 2004.

Code

Argon Production

```
% Script to easily compute concentrations etc
% Author: Greg Kline
% Date: 11/10/2016
% Revision: 3.0
%
% Core Model Parameters
% gradient model additions
beam_length = 2; %m
beam_purge_x = .25;
RSR_length = 8;
RSR_purge_x = .25;
pool_l = .5;
pool_purge_x = .1;

% flux
% Core flux (n0/cm^2/s)
% Flux_cm2_core = 2e12; % G-ring
Flux_cm2_core = 1e13; % Central thimble
Flux_cm2_RSR = 2e12; % RSR flux
Flux_cm2_Beam_line = 1e11; %Beam port average flux

% Core flux (n0/m^2/s)
Flux_m2_core = Flux_cm2_core * 10000;
Flux_m2_RSR = Flux_cm2_RSR * 10000; % RSR flux
Flux_m2_Beam_line = Flux_cm2_Beam_line * 10000; %Beam port average flux

% core mid height depth (m)
core_vol_depth = 7.1;

% Argon Values
% Half-life of Ar-41 (s)
half_life_Ar_41 = 6.5766e3;

% Density of air (kg/m^3)
```

```
density_air = 1.204;

% mol fraction of Ar-40 in air ( mol / mol )
mol_frac = .00934;

% molar weight of air (kg/mol)
M_air = 28.966 / 1000;

% molar density of air ( mol / m^3)
num_air = 2.69e25;

% mol Argon in air ( mol /m^3 )
Number_density_Ar_air_m3 = mol_frac * num_air;

% Molar mass Argon 41 (kg/mol)
M_Ar = 41e-3;

% Avogadro's number (atoms/mol)
N_A = 6.022e23;

% Cross section of absorption Ar-40 (m^2)
xs_absorp_Ar_40 = 6.6e-29;

% Bulk pool temperature (K) [20C]
bulk_pool_temp = 293.15;

% Bulk bay air temperature (K) [20C]
bulk_bay_temp = 293.15;

% Boltzman's constant (J/K)
k_Boltz = 1.38064852e-23;

% mass of one Ar atom (kg)
mass_one_Ar = M_Ar / N_A;

% Velocity of Argon in the Bay (m/s)
velocity_gas =  sqrt( 3 * k_Boltz * bulk_bay_temp / mass_one_Ar) *.1;

% soluabiltiy @ 7m
soluability_at_core_mgL = .941;

% kg/m^3
soluability_at_core_kgm3 = soluability_at_core_mgL / 1e3;

% (mol / m^3)
Number_density_Ar_at_core_mol = soluability_at_core_kgm3 / M_Ar;

% (atoms/m^3)
Number_density_Ar_at_core_atomm3_1 = Number_density_Ar_at_core_mol * N_A;

soluability_at_surface_mgL = .5562; % (mg/L)
soluability_at_surface_kgm3 = soluability_at_surface_mgL / 1000; % (kg/m^3)

% Dimensionless Henry's coefficient (c_aq/c_gas)
H_cc = 3.425e-2;

%% Flows, Areas and Volumes

% Area (m^2)
area_purge_pool = 0.03242927866;
area_return_duct = .762 * 1.0668;
area_HVAC_pipe = (0.4572/2)^2 * pi; % per unit, 2 exh, 11 supply
area_HVAC_supply_top = area_HVAC_pipe * 5;
area_HVAC_supply_bot = area_HVAC_pipe * 6;
area_HVAC_supply = area_HVAC_supply_top + area_HVAC_supply_bot;
area_HVAC_exh = area_HVAC_supply; % mass balance

% Velocity of purge [4000 fpm] (m/s)
velocity_purge = 20.319999999957;

% Velocity of HVAC [1700 fpm] (m/s)
```

```
velocity_HVAC = 8.6359999999819;

% Volume (m^3)
volume_pool_area = 3.280068;
volume_pool_grates = .04 * 2.5146 * 3.556;
volume_pool_area_worst = volume_pool_area - volume_pool_grates;

% Make a thing here to make it easier to run numbers
% volume_pool_area = volume_pool_area_worst;

volume_RX_bay = 4120; % TechSpec volume of the bay
volume_BP1_5 = 2;
volume_BP_2 = .5;
volume_BP_3 = .5;
volume_BP_4 = 1;
volume_BP_total = volume_BP1_5 + volume_BP_2 + volume_BP_3 + volume_BP_4;
volume_beam_flow = .75 * volume_BP_total;
volume_beam_prod = volume_BP_total - volume_beam_flow;
volume_RSR = .0330;
volume_RSR_prod = .8 * volume_RSR;
volume_RSR_flow = volume_RSR - volume_RSR_prod;
volume_total = volume_RX_bay + volume_BP_total + volume_RSR ...
    + volume_pool_area;

% Flow in and out [Q_dot] (m^3/s)
% Flow of the dilution valve in the first bay is the same as the pool purge
% flow rate, however, suction comes from the RC and thus the concentration
% of AR-41 can be considered nonexistent (m^3/s )
flow_rate_purge_pool = area_purge_pool * velocity_purge;
flow_rate_HVAC_exh = area_HVAC_exh * velocity_HVAC;
flow_rate_HVAC_supply = area_HVAC_supply * velocity_HVAC;
flow_rate_beam_purge_single = pi * 0.009525^2 * velocity_purge;
flow_rate_RSR_purge = flow_rate_beam_purge_single;
flow_dilution_valve = flow_rate_purge_pool;

%% Argon diffusion [Lienhard 11.4]
% Dab = (1.8583e-7)T^3/2/(p*rho^2 * Omega_D)* sqrt(1/MA + 1/MB)
% constants
LJ_p_air = 1; %atm
LJ_rho_Ar = 3.542; %Angstrom
LJ_rho_air = 3.711;

e_kb_Ar = 93.3; %K
e_kb_air = 78.6;

LJ_MA_Ar = 39.95; % kg/kmol
LJ_MA_air = 28.96;

% find Dab
LJ_rho_AB = .5 * (LJ_rho_Ar + LJ_rho_air);
e_kb_AB = sqrt(e_kb_Ar * e_kb_air);
LJ_T = 293.15;

k_bT_eAB = LJ_T / e_kb_AB; %3.4232

Omega_D = .9186; % for kbT/eAB of 3.4

% diffusion constant of argon in air ( m^2/s )
D_AB = (1.8583e-7 * LJ_T^(3/2))/(LJ_p_air * LJ_rho_AB^2 * Omega_D) ...
    * sqrt( 1/LJ_MA_Ar + 1/LJ_MA_air); %

%% Concentrations for Various conditions ( atoms / m^3 )

% Decay constants (1/s)
    % flow rate decay constants are a ratio of flow to volume drawn from
    lambda_Ar_41 = log(2) / half_life_Ar_41;
    lambda_HVAC = flow_rate_HVAC_exh / volume_RX_bay;
    lambda_purge_pool = flow_rate_purge_pool / volume_pool_area;
    lambda_purge_pool_worst = flow_rate_purge_pool / volume_pool_area_worst;

    % lambda_purge_pool = lambda_purge_pool_worst;
```

```
    lambda_purge_RSR = flow_rate_RSR_purge / volume_RSR_prod;
    lambda_purge_beam = 5 * flow_rate_beam_purge_single / volume_beam_prod;
    lambda_purge_RX = flow_dilution_valve / volume_RX_bay;

% Sources ( n / ( s ) )
    % Pool area
    source_pool = Number_density_Ar_at_core_atomm3_1 * xs_absorp_Ar_40 ...
        * Flux_m2_core * volume_pool_area;

    % Beam
    source_beam = Number_density_Ar_air_m3 * xs_absorp_Ar_40 ...
        * Flux_m2_Beam_line * volume_beam_prod;

    % RSR
    source_RSR = Number_density_Ar_air_m3 * xs_absorp_Ar_40 ...
        * Flux_m2_RSR * volume_RSR_prod;

% Isolation ( n / m^3 )
    % Pool, Beams, and RSR
    C_Iso_PBR = ( source_pool + source_beam + source_RSR ) ...
        / ( volume_total * lambda_Ar_41 );

    % Pool and Beams
    C_Iso_PB = ( source_pool + source_beam ) ...
        / ( volume_total * lambda_Ar_41 );

    % Pool
    C_Iso_P = ( source_pool ) ...
        / ( volume_total * lambda_Ar_41 );

% HVAC Only ( n / m^3 )
    % Pool, Beams, and RSR
    C_HVAC_PBR = ( source_pool + source_beam + source_RSR ) ...
        / ( volume_total * ( lambda_Ar_41 + lambda_HVAC ) );

    % Pool and Beams
    C_HVAC_PB = ( source_pool + source_beam ) ...
        / ( volume_total * ( lambda_Ar_41 + lambda_HVAC ) );

    % Pool
    C_HVAC_P = ( source_pool ) ...
        / ( volume_total * ( lambda_Ar_41 + lambda_HVAC ) );

% Purge and Both Purge and HVAC ODE ( n / m^3 )
% Define an array of variables to pass to the ODE solver to remove need for
% global variables and speed process up
NV = [ Number_density_Ar_at_core_atomm3_1
       Number_density_Ar_air_m3
       lambda_Ar_41
       lambda_HVAC
       lambda_purge_pool
       lambda_purge_RSR
       lambda_purge_beam
       lambda_purge_RX
       Flux_m2_core
       volume_pool_area
       Flux_m2_Beam_line
       volume_beam_prod
       Flux_m2_RSR
       volume_RSR_prod
       volume_total
       volume_RX_bay
       xs_absorp_Ar_40
       lambda_purge_pool_worst ];

% ODE Initial Conditions  ( number density )
% IC = [ Rx_bay_purge_PBR  Rx_bay_purge_PB  Rx_bay_purge_P  pool_purge
%          beam_purge  RSR_purge  Rx_bay_purge_HVAC_PBR  Rx_bay_purge_HVAC_PB
%          Rx_bay_purge_HVAC_P  pool_purge_HVAC  beam_purge  RSR_purge_HVAC ];
IC = [ 0 0 0 0 0 0 0 0 0 0 0 0 0 ];
```

```
% ODE option vector
option = odeset('RelTol', 1e-8,'AbsTol',1e-8);

% Solve the ODE ( n / m^3 )
t_0 = 0; % Initial time (s)
t_f = 50000; % Final time (s)

[ Model_time, Con_loop ] = ode45(@(t,y)Argon_Concentration_script_ODE_3_0( t, y, NV ) ...
    ,[ t_0 t_f],IC,option);

% switch conditions from columns to rows ( n / m^3 )
Con_loop = Con_loop';

%% Specific Activities ( Bq / ( m^3 s ))
% Iso
A_Iso_PBR = C_Iso_PBR * lambda_Ar_41;
A_Iso_PB = C_Iso_PB * lambda_Ar_41;
A_Iso_P = C_Iso_P * lambda_Ar_41;

% HVAC Only
A_HVAC_PBR = C_HVAC_PBR * lambda_Ar_41;
A_HVAC_PB = C_HVAC_PB * lambda_Ar_41;
A_HVAC_P = C_HVAC_P * lambda_Ar_41;

% Purge
for a = 1:9
    Act_purge(a,:) = Con_loop(a,:) * lambda_Ar_41;
end

%% Dose and Dose Rate Calculations
% Convert activity to Dose in mR
% Semi-infinite cloud model [Bevelacqua 2004] (R/s)
%
% Dose constant
k_1 = (1/100) * 1.6e-6 * (1/1293) * .5;

% Gamma energy and fraction ( fraction * NRG in MeV)
gamma_Energy = [.9995*1.2936 .0005*1.6772];

% Isolation
% Dose rate Iso (R/s)
Dose_rate_Iso_PBR_mRh  = k_1 * A_Iso_PBR * sum(gamma_Energy) * 1000 * 3600;
Dose_rate_Iso_PB_mRh  = k_1 * A_Iso_P * sum(gamma_Energy) * 1000 * 3600;
Dose_rate_Iso_P_mRh  = k_1 * A_Iso_P * sum(gamma_Energy) * 1000 * 3600;

% Dose Iso in one year (mR)
Dose_Iso_PBR_mRh = Dose_rate_Iso_PBR_mRh * 8736;
Dose_Iso_PB_mRh = Dose_rate_Iso_PB_mRh * 8736;
Dose_Iso_P_mRh = Dose_rate_Iso_P_mRh * 8736;

% HVAC Only
% Dose rate HVAC (R/s)
Dose_rate_HVAC_PBR_mRh = k_1 * A_HVAC_PBR * sum(gamma_Energy) * 1000 * 3600;
Dose_rate_HVAC_PB_mRh = k_1 * A_HVAC_PB * sum(gamma_Energy) * 1000 * 3600;
Dose_rate_HVAC_P_mRh = k_1 * A_HVAC_P * sum(gamma_Energy) * 1000 * 3600;

% Dose Iso in one year (mR)
Dose_HVAC_PBR_mRh = Dose_rate_HVAC_PBR_mRh * 8736;
Dose_HVAC_PB_mRh = Dose_rate_HVAC_PB_mRh * 8736;
Dose_HVAC_P_mRh = Dose_rate_HVAC_P_mRh * 8736;

% Dose rate for purge items (mR/h)
for dr = 1:9
    Dose_rate_purge(dr,:) = k_1 * Act_purge(dr,:) * sum(gamma_Energy) * 1000 * 3600;
end

% Purge
Dose_rate_purge_PBR_mRh = Dose_rate_purge(1,:);
Dose_rate_purge_PB_mRh = Dose_rate_purge(2,:);
Dose_rate_purge_P_mRh = Dose_rate_purge(3,:);
```

```
% Purge and HVAC
Dose_rate_purge_HVAC_PBR_mRh = Dose_rate_purge(7,:);
Dose_rate_purge_HVAC_PB_mRh = Dose_rate_purge(8,:);
Dose_rate_purge_HVAC_P_mRh = Dose_rate_purge(9,:);

% Steady state dose rate (mR/h)
Dose_rate_SS = Dose_rate_purge(:,end);

% the combo lineup converges very fast and fluctuates near 0 so efforts to find a good
% steady state value need to be performed.
for pf = 1:length(Dose_rate_SS)
    temp_find = Dose_rate_purge(pf,:);
    pf_find = find(temp_find > 0 );
    Dose_rate_SS(pf) = Dose_rate_purge(pf, max(pf_find) );
end

% Dose for purge items (mR)
% convert to mR/s for integration
Dose_rate_purge_mRs = Dose_rate_purge ./ 3600;

for d = 1:9
    Dose_purge(d) = trapz(Model_time,Dose_rate_purge_mRs(d,:));
end

% Dose from a worker for a full year both systems
% Transient dose + remaining time * SS Dose rate
Dose_both_staff_year = Dose_purge(1) ...
    + ( 8736 * 3600 - Model_time(end) ) * Dose_rate_SS(1);

%% Reactor Bay Stay times ( h )
% Based on 10 CFR 20 Limits of 5R/yr
% Limit
limit_mR = 5000;

% Stay times Isolation (h)
Stay_time_Iso_PBR = limit_mR / Dose_rate_Iso_PBR_mRh;
Stay_time_Iso_PB = limit_mR / Dose_rate_Iso_PB_mRh;
Stay_time_Iso_P = limit_mR / Dose_rate_Iso_P_mRh;

% Stay times HVAC Only (h)
Stay_time_HVAC_PBR = limit_mR / Dose_rate_HVAC_PBR_mRh;
Stay_time_HVAC_PB = limit_mR / Dose_rate_HVAC_PB_mRh;
Stay_time_HVAC_P = limit_mR / Dose_rate_HVAC_P_mRh;

% Stay times Purge (h)
Stay_time_purge_PBR = ( limit_mR - Dose_purge(1) ) / Dose_rate_SS(1) + ( t_f - t_0 )/3600;
Stay_time_purge_PB = ( limit_mR - Dose_purge(2) ) / Dose_rate_SS(2) + ( t_f - t_0 )/3600;
Stay_time_purge_P = ( limit_mR - Dose_purge(3) ) / Dose_rate_SS(3) + ( t_f - t_0 )/3600;

% Stay times purge and HVAC (h)
Stay_time_purge_HVAC_PBR = ( limit_mR - Dose_purge(7) ) / Dose_rate_SS(7) + ( t_f - t_0
)/3600;
Stay_time_purge_HVAC_PB = ( limit_mR - Dose_purge(8) ) / Dose_rate_SS(8) + ( t_f - t_0
)/3600;
Stay_time_purge_HVAC_P = ( limit_mR - Dose_purge(9) ) / Dose_rate_SS(9) + ( t_f - t_0 )/3600;

%% Convert to kg/m^3 for plume
% Isolation
    % Pool, Beams, and RSR
    C_Iso_PBR_kgm3 = C_Iso_PBR * M_Ar / N_A;
    % Pool and Beams
    C_Iso_PB_kgm3 = C_Iso_PB * M_Ar / N_A;
    % Pool
    C_Iso_P_kgm3 = C_Iso_P * M_Ar / N_A;

% HVAC Only ( n / m^3 )
    % Pool, Beams, and RSR
    C_HVAC_PBR_kgm3 = C_HVAC_PBR * M_Ar / N_A;
    % Pool and Beams
    C_HVAC_PB_kgm3 = C_HVAC_PB * M_Ar / N_A;
```

```
    % Pool
    C_HVAC_P_kgm3 = C_HVAC_P * M_Ar / N_A;

% Purge
% Use molar balance to do mixing ratios for teh purge and purge HVAC

% Purge only
% All three experiment facilities draw plus reactor bay
total_purge_flow = flow_rate_purge_pool + flow_dilution_valve ...
    + flow_rate_beam_purge_single * 5 + flow_rate_RSR_purge;

% Concentration of purge exit (n/m^3)
Con_Purge_mix = ( Con_loop(1,:) .* flow_dilution_valve + Con_loop(4,:) .*
flow_rate_purge_pool ...
    + Con_loop(5,:) .* flow_rate_beam_purge_single .* 5 ...
    + Con_loop(6,:) .* flow_rate_RSR_purge ) ./ total_purge_flow;

% Convert to (kg/m^3) for plume
Con_purge_mix_kgm3 = Con_Purge_mix * M_Ar / N_A;

% Concentration of HVAC and purge
% Find new purge mix
Con_Purge_mix_H = ( Con_loop(7,:) .* flow_dilution_valve + Con_loop(4,:) .*
flow_rate_purge_pool ...
    + Con_loop(5,:) .* flow_rate_beam_purge_single .* 5 ...
    + Con_loop(6,:) .* flow_rate_RSR_purge ) ./ total_purge_flow;

% Mixture at stack (n/m^3)
Con_HVAC_purge = ( Con_Purge_mix_H .* total_purge_flow ...
    + Con_loop(7) .* flow_rate_HVAC_exh ) ./ ( total_purge_flow + flow_rate_HVAC_exh);

% Convert to kg/m^3
Con_HVAC_purge_kgm3 = Con_HVAC_purge * M_Ar / N_A;
```

Argon Production ODE

```
function [ R_dot ] = Argon_Concentration_script_ODE( t, R, NV )
% Differential equation solver for purge related things

% Sources
% Pool area only purge
R_dot(4) = NV(1) * NV(17) * NV(9) - NV(5) * R(4);

% Beam lines only purge
R_dot(5) = NV(2) * NV(17) * NV(11) - NV(7) * R(5);

% RSR only purge
R_dot(6) = NV(2) * NV(17) * NV(13) - NV(6) * R(6);

% Reactor bay
% Rx Bay with only purge PBR
R_dot(1) = ( R_dot(4) * NV(10) + R_dot(5) * NV(12) + R_dot(6) * NV(14) ) / NV(16) ...
    - R(1) *  ( NV(3) + NV(8) ) ;

% Rx Bay with only purge PB
R_dot(2) = ( R_dot(4) * NV(10) + R_dot(5) * NV(12) ) / NV(16) ...
    - R(2) *  ( NV(3) + NV(8) ) ;

% Rx Bay with only purge P
R_dot(3) = ( R_dot(4) * NV(10) ) / NV(16) ...
    - R(3) *  ( NV(3) + NV(8) ) ;

% Rx Bay HVAC and Purge PBR
R_dot(7) = ( R_dot(4) * NV(10) + R_dot(5) * NV(12) + R_dot(6) * NV(14) ) / NV(16) ...
```

```
    - R(7) *  ( NV(3) + NV(8) + NV(4) ) ;

% Rx Bay HVAC and Purge PB
R_dot(8) = ( R_dot(4) * NV(10) + R_dot(5) * NV(12) ) / NV(16) ...
    - R(8) *  ( NV(3) + NV(8) + NV(4) ) ;

% Rx Bay HVAC and Purge P
R_dot(9) = ( R_dot(4) * NV(10) ) / NV(16) ...
    - R(9) *  ( NV(3) + NV(8) + NV(4) ) ;

% Copies for now.  If the method changes these will be used
% Pool area HVAC purge
R_dot(10) = NV(1) * NV(17) * NV(9) - NV(5) * R(4);

% Beam line HVAC and purge
R_dot(11) = NV(2) * NV(17) * NV(11) - NV(7) * R(5);

% RSR HVAC and purge
R_dot(12) = NV(2) * NV(17) * NV(13) - NV(6) * R(6);

R_dot = R_dot';
end
```

Plume Modelling

```
% function [ Dose ] = Plume_Model_2016( A, u )
% Plume Model 2016
% Author: Greg Kline
% Date: 10/25/2016
% Revision 2.0
%
% The first revision was lost in the cloud due to a data leak.  This model calculates the
% dose and equivalent dispersion of Ar-41 from the stack at NETL. It uses calculations
% from facility features and the work of DOE/TIC--11223 Handbook on atmospheric diffusion.
% The facility features are taken from the blue prints and calculations based on
%% operational parameters
tic
% Wind speed (m/s)
u = linspace(.1,15.4333,50);

% Concentration from stack (kg/m^3)
% These values are calculated from the Argon production scenarios in RAIs
% C_0_Iso
 C_0 = 5.0796e-14;

% C_0_HVAC
% C_0 = 1.3760e-15;

% C_0_Purge_SS
% C_0 = 1.6351e-14;

% C_0_Purge_HVAC_SS
% C_0 = 1.3042e-15;

% Concentration from stack (kg/m^3)
% All normal facilities operating, 1e13 at core, concertation volume is
% the RX bay.  This is the plausible, isolated, worse case scenario
% C_0 = 1.5090e-10;

% Concentration from stack (kg/m^3)
% All normal facilities operating, 2.5e13 at core, concertation volume is
% the RX bay.  This is the plausible, isolated, worse case scenario
% C_0 = 3.6183e-10;

% Concentration from stack (kg/m^3)
% All normal facilities make Ar_41 and this is concentrated in pool area
```

```
% C_0 = 4.5449e-7;

% All possible air in the reactor bay makes it through the central thimble,
% hits equilibrium, and is then concentrated into the pool area with pool
% suction only (kg/m^3)
% C_0 = 5.6944e-4;

% All possible air in the reactor bay makes it through the central thimble,
% hits equilibrium, and is then concentrated into the RSR facility, the
% smallest suction-able volume (kg/m^3)
% C_0 = .0576;

%% Building Constants
% NETL dimensions
% The building has 3 main parts: n0 gen room, rx bay, offices which are Nn, Nrx, No
% respectively.  dimensions are taken from an overhead view with (+) being in the north
% and east directions. Length is northward, width is eastward
% Building dimensions (m)
% Neutron generator room (m)
Nn_width = 12.192;
Nn_length = 12.192;
Nn_height = 7.214;

% Reactor bay (m)
Nrx_width = 18.288;
Nrx_length = 25.908;
Nrx_height = 13.564;

% Office space (m)
No_width = 30.48;
No_length = 12.192;
No_height = 9.550;

% Building designations
% Berm height (m)
N_berm = 2.134;

% NETL Argon Stack
% Height from roof (m)
N_stack_roof = 4.2672;

% Purge pipe radius (m)
N_purge_stack_radius_in = .1016;

% Nozzle radius (m)
N_purge_stack_radius_out = .0762;

% HVAC radius (m)
N_HVAC_radius_out = 0.2286;

% Stack distance from building end (m)
N_stack_north_edge = 21.31;

% Purge nozzle Velocity in (m/s)
N_purge_stack_velocity_in = 20.32;

% HVAC system
N_HVAC_stack_velocity_in = 8.6360;

% Pressure of air (Pa)
p = 101325;

% specific gas constant for air ( J / kg K )
R_air = 287.058;

% specific gas constant for Argon ( J / kg K )
R_argon = 208;

% Volume of the reactor bay ( m^3 )
V_rx = 4120;
```

```
% changes in building geometry analysis are easier to do here
N_L = Nrx_length;
N_W = Nrx_width;
N_H = Nrx_height + N_berm;

% Radius changes with HVAC and purge
N_stack_radius_out = N_purge_stack_radius_out;
% N_stack_radius_out = N_HVAC_radius_out;

%% Average wind direction calculations
% majority headings are directly north or directly south.  This section is
% a vector additive calculation.  For plume modelling, both directions will
% be considered.
%
% % wind directions in rad ( 0rad == east, CCW )
% heading = 0:pi/8:2*pi-pi/8;
%
% % occupation percentage (%/100)
% occ_per = [ .035 .035 .06 .08 .08 .04 .04 .03 .025 .02 .03 .07 ...
%         .17 .14 .10 .045 ];
%
% % x component
% Vx = sum(occ_per.*cos(heading));
%
% % y component
% Vy = sum(occ_per.*sin(heading));
%
% % probability adjusted angle (deg)
% wind_dir = atan( Vx/Vy );
%
% % Adjust building width to compensate for wind direction (m)
% % if wind is EW in direction, the length and width values need swapped
% if abs(wind_dir) <= 45
%     [ N_L, N_W ] = deal(N_W,N_L);
% end
%
% % Adjust width for angle (m)
% N_W = N_W / cos(wind_dir);

%% Model Constants
% northerly ground distance from stack (m)
Z_x = linspace(N_stack_north_edge-N_L,1000,10000);

% Gravity ( m/s^2)
g = 9.8066;

% Avogadro's number ( atoms/mol )
N_A = 6.022e23;

% Molecular mass (kg/mol)
M_Ar = 41 / 1000;
M_air = 28.9 / 1000;

% Half-life of Ar-41 (s)
half_life_Ar_41 = 6.5766e3;

% Decay constant Ar-41 (1/s)
lambda_Ar_41 = log(2) / half_life_Ar_41;

%% Building Calculations
% Stack distance from south edge (m)
N_stack_south_edge = Nrx_length - N_stack_north_edge;

% Stack area in (m^2)
A_purge_stack_in = pi * N_purge_stack_radius_in^2;
A_HVAC_stack_in = 0.762^2 - A_purge_stack_in; % 30in x 30in - area purge

% Stack area out (m^2)
% Purge system
A_purge_stack_out = pi * N_purge_stack_radius_out^2;
```

```
% HVAC system ( annulus )
% Nozzle sits slightly above the HVAC release so larger radius is
% subtracted from HVAC
A_HVAC_stack_out = pi * ( N_HVAC_radius_out^2 - N_purge_stack_radius_in^2 );

% Velocity of Argon out of stack (m/s)
% Purge system with nozzle
N_purge_stack_velocity_out = N_purge_stack_velocity_in ...
    * A_purge_stack_in / A_purge_stack_out;

% HVAC system with nozzle
N_HVAC_stack_velocity_out = N_HVAC_stack_velocity_in ...
    * A_HVAC_stack_in / A_HVAC_stack_out;

% Initial stack height (m)
N_stack_height_0 = N_H + N_stack_roof;

% Section 3 designations (m)
N_zeta = min( Nrx_height, N_W );
N_xi = max( Nrx_height, N_W );

% Characteristic length (m)
N_R = N_zeta^(2/3) * N_xi^(1/3);

% Roof cavity (m)
N_Lc = .9 * N_R;

% cavity height (m)
N_Hc = .22 * N_R;

% cavity distance (m)
N_xc = N_R / 2;

% Shear layer boundary (m)
N_Z_II = N_R * ( .27 - .1 * (Z_x/N_R) );

% Roof wake boundary (m)
N_Z_III = N_R * .28 * (Z_x/N_R).^(1/3);

% Cavity zone
% Cavity constants
if N_L / N_H <= 1
    A = -2.0 + 3.7 * (N_L/N_H)^(-1/3);
    B = -.15 + .305 * (N_L/N_H)^(-1/3);

elseif N_L / N_H > 1
    A = 1.75;
    B = .25;
else
    display(' Cavity Error ');
end

% Cavity length (m)
N_xr = N_H * ( ( A * N_W / N_H ) / (1 + B * N_W / N_H) );

% Mass of argon in Rx bay (kg)
m_argon_inside = C_0 * M_Ar / N_A;

% Initial mass flow of purge (kg/s)
Q_purge = C_0 * A_purge_stack_out * N_purge_stack_velocity_out;

% Initial mass flow of HVAC (kg/s)
Q_HVAC = C_0 * A_HVAC_stack_out * N_HVAC_stack_velocity_out;

% total mass flow (kg/s)
% Purge only
 Q = Q_purge;

% % HVAC only
% Q = Q_HVAC;
%
```

```
% % Purge and HVAC
% Q = Q_purge + Q_purge;

%% Point of Interest Constants
% Distances to points of interest (m) % Direction from stack
R_netl_to_fence = 64.71; % N
R_netl_to_IBM = 277.97; % N
R_netl_to_ARL = 699.40; % S
R_netl_to_wells_fargo = 207.41; % SSE
R_netl_to_macys = 535.25; % SE

%% Top hat model equations
display(' Beginning top hat calculations ... ');
% Initial volume flux (m^4/2)
Initial_volume_flux = N_purge_stack_velocity_out * pi * N_stack_radius_out^2; %V0

% Plume temperature correction ( C / g/mol)
% Temepratures (C)
T_plume = 25;
T_enviro = 20;

% Corrected temperatures ( C / kg/mol )
T_p0 = T_plume;
T_e0 = T_enviro;

% Initial buoyancy flux ( m^5 / s^3 )
Initial_bouyancy_flux = g / T_p0 * ( T_p0 - T_e0 ) * Initial_volume_flux; %F0

% Density of air ( kg/m^3 )
density_air_outside = p / ( R_air * ( T_enviro + 273.15) );
density_air_inside = p / ( R_air * ( T_plume + 273.15) );

% Mass of air in the reactor bay ( kg )
m_air_inside = density_air_inside * V_rx;

% Reactor mixutre gas constant ( J / kg K )
R_mix = ( R_argon * m_argon_inside + R_air * m_air_inside ) ...
    / ( m_argon_inside + m_air_inside );

% Density of mixture ( kg/m^3 )
density_mix_inside = p / ( R_mix * T_plume );

% Initial momentum flux ( m^5 / s^2 )
Initial_momentum_flux = density_mix_inside / density_air_outside ...
    * N_purge_stack_velocity_out * Initial_bouyancy_flux;

% Atmospheric stability (s^-2)
s = g/T_enviro * ( .0098);

%% Atmospheric conditional stack height changes
% Many conditions exist that change the effective height based on stability and the
% ambient wind speed.  Each condition is calculated and the minimum stack height is used
% as the change in stack height to ensure worst case scenario per wind speed

display(' Calculating atmospheric effects on stack height ...');

% Rise limited by ambient stability
% Atmospheric final rise of a buoyant plume
stack_dH(1,:) = 2.6 * ( Initial_bouyancy_flux ./ ( u .* s ) ).^(1/3);

% Nearly neutral conditions
% Mixing depth (m)
z = 1500;

% Roughness length (m)
z0 = N_H / 10;

% Friction velocity (m/s)
u_star = .4 .* u ./ log ( z/z0);

% Nearly neutral conditions delta height (m)
```

```
% buoyant bent over plume (m)
stack_dH(2,:) = 1.54 * ( Initial_bouyancy_flux ./ ( u .* u_star )).^(2/3) ...
    .* N_stack_height_0^(1/3);

% Jet (m)
stack_dH(3,:) = 3 .* ( N_purge_stack_radius_out * 2 ) * ( N_purge_stack_velocity_out ./ ...
    u - 1);

% Convective conditions (m)
% Eddy dissipation rate
eddy_rate = u_star.^3 / (.4 * z);

% Surface buoyancy flux
surface_bouyancy_flux = eddy_rate / .25;

stack_dH(4,:) = 3 * ( Initial_bouyancy_flux ./ u ).^(3/5) ...
    .* surface_bouyancy_flux.^(-2/5);

% Correct for inf and nan situations
stack_dH(~isfinite(stack_dH)) = 0;

% Create effective stack height adjustment (m)
stack_h_atmos = N_stack_height_0 + min(stack_dH);

%% Downwash Calculations
display(' Calculating downwash and ground source ... ');

% Downwash height (m)
stack_Hd = 2 * ( N_purge_stack_velocity_out ./ u - 1.5) * ( N_purge_stack_radius_out * 2 );

% Ratios greater than 1.5 do not have downwash, thus  a positive value has no meaning
stack_Hd(stack_Hd > 0) = 0;

% Adjust effective stack height for downwash (m)
stack_h_prime = stack_h_atmos + stack_Hd;

% Building effects corrected effective stack height (m)
%Conditions
cond1 = stack_h_prime > Nrx_height + 1.5*N_zeta;
cond2 = stack_h_prime <= Nrx_height + 1.5*N_zeta & stack_h_prime >= Nrx_height;
cond3 = stack_h_prime < Nrx_height;

% Apply the formulas
stack_He(cond1) = stack_h_prime(cond1);
stack_He(cond2) = 2 .* stack_h_prime(cond2) - ( N_H + 1.5 * N_zeta);
stack_He(cond3) = stack_h_prime(cond3) - 1.5 * N_zeta;

% Look for trapped plumes
% the 0 m/s wind condition would be grabbed by this, but that is a vertical
% plume
ground_source = find( stack_He < .5 * N_zeta & u ~= 0);
stack_He(ground_source) = 0;

% Find vertical plumes ( DOE suggests for wind speeds < 1 m/s )
vert_plume = find( u < 1);
stack_He(vert_plume) = stack_h_prime(vert_plume) + 4 * Initial_bouyancy_flux^.25 / s^.375;

%% Gaussian Plume
display(' Performing Gaussian plume calculations ...');

% point density (#)
points = 1000;

% Develop an x direction vector, 0 is at the stack and positive is
% northbound
x = linspace(0,1000,points);

% Develop a y direction vector, 0 is at the stack and west is positive IAW
% fig 4.1
y = linspace(-1000,1000,2*points);
```

```
% % Develop a z vector,  0 is at stack height, so z is a 2D matrix, the rows
% % are the z values, while the columns are the wind speeds
% z = zeros(points, length(u));
%
% for l = 1:length(u)
%     a = -u(l); % stack height (m)
%     b = 1000-u(l); % 1km ceiling minus stack height
%     % Build a 2D array
%     z(:,l) = linspace(a,b,points);
% end

% Standard deviation constants are considered using the Urban Conditions of
% table 4.5, as NETL sits in an urban area as of 2016, here, the A-B
% conditions use the same equation, as well as the E-F conditions, creating
% a 4 x wind sp x length(x) array of values
% sig y (m)
sig_y(1,:) = .32 .* x .* ( 1 + .004 .* x ).^(-1/2);
sig_y(2,:) = .22 .* x .* ( 1 + .004 .* x ).^(-1/2);
sig_y(3,:) = .16 .* x .* ( 1 + .004 .* x ).^(-1/2);
sig_y(4,:) = .11 .* x .* ( 1 + .004 .* x ).^(-1/2);

% sig z (m)
sig_z(1,:) = .24 .* x .* ( 1 + .001 .* x).^(1/2);
sig_z(2,:) = .20 .* x;
sig_z(3,:) = .14 .* x .* ( 1 + .0003 .* x).^(-1/2);
sig_z(4,:) = .08 .* x .* ( 1 + .00015 .* x).^(-1/2);

% find the values of u that are not trapped in the plume
u_plume = u(stack_He >= .5 * N_zeta );

% % Gaussian equation blows up for u < 1;
% u_plume(u_plume<1)=1;

% near the stack ( x < 100m ) the sigma diffusion equations blow up, it is
% necessary to consider the buoyancy of the plume being developed here
% and the dispersion of the net-over plume

% z_prime units for x <150m
z_prime_x = x(x <=150);

% z prime ( wind sp rows dist column)
for zs = 1:length(u_plume)
    z_prime(zs,:) = 1.6 .* ( Initial_bouyancy_flux .* z_prime_x.^2 ).^(1/3) ./ u_plume(zs);
end

% update the sigmas to represent the plume conditions
for d = 1:length(u_plume)
    sig_y_eff(d,:) = sqrt( sig_y(1,1:length(z_prime_x)).^2 + ( z_prime(d,:) / 3.5 ).^2 );
    sig_z_eff(d,:) = sqrt( sig_z(1,1:length(z_prime_x)).^2 + ( z_prime(d,:) / 3.5 ).^2 );
end

% make a 3D matrix to account for plume trap by source
% sig( atmos, dist, wind )
sig_y = repmat(sig_y,1,1,length(u_plume));
sig_z = repmat(sig_z,1,1,length(u_plume));

% Find the 1.5m off the ground concentration per atmospheric conditions and
% wind speeds the 2D map is relative to y and x direction
C_1_5m = zeros(length(sig_y(:,1)),length(u_plume),length(x),length(y));

% set the height for personal ground exposure (m)
z15 = 1.5;

% Build an array of 2D maps for height of 1.5m for varying wind and
% atmospheres for plumes not trapped.  C(atmos,wind sp, x, y) [kg/m3]
% atmos = [ A-B C D E-F]
for atmos = 1:length(sig_y(:,1,1))
    for wind_sp = 1:length(u_plume)
        for i = 1:length(x)
            for j = 1:length(y)
                C_1_5m(atmos, wind_sp, i, j) = ( Q ./ u(wind_sp) ) ...
```

```
                    .* ( 1 ./ ( 2 .* pi .* sig_y(atmos,i,wind_sp) .* sig_z(atmos,i,wind_sp) )
) ...
                    .* ( exp( -y(j)^2 ./ (2 .* sig_y(atmos,i,wind_sp).^2) ) ) ...
                    .* ( exp( -( z15 - stack_He(wind_sp) )^2 ./ (2 .*
sig_z(atmos,i,wind_sp).^2) ) ...
                    + exp( -( z15 + stack_He(wind_sp) )^2 ./ (2 .* sig_z(atmos,i,wind_sp).^2)
) );
            end
        end
    end
end

% The 1.5m point blows up using the effective sigma functions.
% update the values for the effective ones
for as = 1:length(sig_z(:,1,1))
    sig_y(as,1:length(z_prime_x),:) = sig_y_eff';
    sig_z(as,1:length(z_prime_x),:) = sig_z_eff';
end

% ~8m off the ground represents the intake height of the IBM building accross
% the street and the 2nd story balcony height of the apartments behind it
% as well as the air intakes of buildings to the south (m)
z8 = 7.836;

% Pre-allocate array space
C_8m = C_1_5m .* 0;

% Build an array of 2D maps for height of 1.5m for varying wind and
% atmospheres for plumes not trapped.  C(atmos,wind sp, x, y)
% atmos = [ A-B C D E-F]
for atmos = 1:length(sig_y(:,1,1))
    for wind_sp = 1:length(u_plume)
        for i = 1:length(x)
            for j = 1:length(y)
                C_8m(atmos, wind_sp, i, j) = ( Q ./ u(wind_sp) ) ...
                    .* ( 1 ./ ( 2 .* pi .* sig_y(atmos,i,wind_sp) .* sig_z(atmos,i,wind_sp) )
) ...
                    .* ( exp( -y(j)^2 ./ (2 .* sig_y(atmos,i,wind_sp).^2) ) ) ...
                    .* ( exp( -( z8 - stack_He(wind_sp) )^2 ./ (2 .*
sig_z(atmos,i,wind_sp).^2) ) ...
                    + exp( -( z8 + stack_He(wind_sp) )^2 ./ (2 .* sig_z(atmos,i,wind_sp).^2)
) );
            end
        end
    end
end

% Macy's air intake happens to be close to the height of the stack
z20 = 19.9652;

% Pre-allocate array space
C_20m = C_1_5m .* 0;

% Build an array of 2D maps for height of 1.5m for varying wind and
% atmospheres for plumes not trapped.  C(atmos,wind sp, x, y)
% atmos = [ A-B C D E-F]
for atmos = 1:length(sig_y(:,1,1))
    for wind_sp = 1:length(u_plume)
        for i = 1:length(x)
            for j = 1:length(y)
                C_20m(atmos, wind_sp, i, j) = ( Q ./ u(wind_sp) ) ...
                    .* ( 1 ./ ( 2 .* pi .* sig_y(atmos,i,wind_sp) .* sig_z(atmos,i,wind_sp) )
) ...
                    .* ( exp( -y(j)^2 ./ (2 .* sig_y(atmos,i,wind_sp).^2) ) ) ...
                    .* ( exp( -( z20 - stack_He(wind_sp) )^2 ./ (2 .*
sig_z(atmos,i,wind_sp).^2) ) ...
                    + exp( -( z20 + stack_He(wind_sp) )^2 ./ (2 .* sig_z(atmos,i,wind_sp).^2)
) );
            end
        end
    end
```

```
end

%% Infinite Cloud constants
display(' Performing infinite cloud dose calculations ... ');
% Dose rate RX bay (mR)
% Semi-infinite cloud model [Bevelacqua 2004] (R/s)
%
% Dose constant
k_1 = (1/100) * 1.6e-6 * (1/1293) * .5;

% Gamma energy and fraction ( fraction * NRG in MeV)
gamma_Energy = [.9995*1.2936 .0005*1.6772];

%% Plume Dose Rate Items
% 1.5m off the ground
% specific activity 1.5m off the ground activity (Bq/m^3)
Act_1_5m = C_1_5m .* ( N_A / M_Ar ) .* lambda_Ar_41;

% Dose rate 1.5m off the ground (mR/h)
Dose_Rate_1_5m_mRh = k_1 * Act_1_5m * sum(gamma_Energy) * 1000 * 3600;

% 8m off the ground
% specific activity 8m off the ground activity (Bq/m^3)
Act_8m = C_8m .* ( N_A / M_Ar ) .* lambda_Ar_41;

% Dose rate 8m off the ground (mR/h)
Dose_Rate_8m_mRh = k_1 * Act_8m * sum(gamma_Energy) * 1000 * 3600;

% 20m off the ground
% specific activity 20m off the ground activity (Bq/m^3)
Act_20m = C_20m .* ( N_A / M_Ar ) .* lambda_Ar_41;

% Dose rate 20m off the ground (mR/h)
Dose_Rate_20m_mRh = k_1 * Act_20m * sum(gamma_Energy) * 1000 * 3600;

%% Ground source dose rate items
% Standard deviation constants at 0M from the building (m)
sig_y_GND = 4;
sig_z_GND = 2.5;

% Gifford's constant (DOE/TIC -- 11223) [unit-less]
% suggest .5 to 2, .5 is more conservative
Giff_c = .5;

% Ground concentration (kg/m^3)
C_GND = Q ./ ( ( pi * sig_y_GND * sig_z_GND + Giff_c * N_W * N_H ) ...
    .* u(ground_source) );

% Ground Activity Concentration ( Bq/m^3 )
Act_GND = C_GND * ( N_A / M_Ar ) * lambda_Ar_41;

% Dose rate ground source (mR/h)
Dose_rate_GND_mRh = k_1 * Act_GND * sum(gamma_Energy) * 1000 * 3600;

%% Total Received Dose in 1yr
% Total dose (mR)
% Ground source
total_dose_year_mR_GND(ground_source) = Dose_rate_GND_mRh * 8760;

% 1.5m exposure (mR)
total_dose_year_1_5m = Dose_Rate_1_5m_mRh * 8760;

% 8m exposure (mR)
total_dose_year_8m = Dose_Rate_8m_mRh * 8760;

% 20m exposure (mR)
total_dose_year_20m = Dose_Rate_20m_mRh * 8760;

%% Mapping points
display(' Finding points of interest and exposure ... ');
```

```
% Physical distances (m)
% NETL to IBM (m)
NETL_to_IBM_N = 240.04;
NETL_to_IBM_W = 104.64;

% NETL to Wells Fargo (m)
NETL_to_WF_N = 129.30;
NETL_to_WF_W = 146.04;

% NETL to Macys (m)
NETL_to_Macys_N = 174.83;
NETL_to_Macys_W = 480.16;

% NETL to ARL (m)
NETL_to_ARL_S = 751.02;
NETL_to_ARL_E = 71.59;

%NETL building maximum (m)
NETL_side_N = N_stack_south_edge;
NETL_side_W = 0;

% Index points (index)
% NETL to IBM (m)
[ it, NETL_to_IBM_N_pt ] = min(abs(x-NETL_to_IBM_N)); %#ok<*ASGLU>
[ it, NETL_to_IBM_W_pt ] = min(abs(x-NETL_to_IBM_W));

% NETL to Wells Fargo (m)
[ it, NETL_to_WF_N_pt ] = min(abs(x-NETL_to_WF_N));
[ it, NETL_to_WF_W_pt ] = min(abs(x-NETL_to_WF_W));

% NETL to Macys (m)
[ it, NETL_to_Macys_N_pt ] = min(abs(x-NETL_to_Macys_N));
[ it, NETL_to_Macys_W_pt ] = min(abs(x-NETL_to_Macys_W));

% NETL to ARL (m)
[ it, NETL_to_ARL_S_pt ] = min(abs(x-NETL_to_ARL_S));
[ it, NETL_to_ARL_E_pt ] = min(abs(x-NETL_to_ARL_E));

% NETL side (m)
[ it, NETL_side_N_pt ] = min(abs(x-NETL_side_N));
[ it, NETL_side_W_pt ] = min(abs(x-NETL_side_W));

%% Maps of dose rates and exposure for locations
% Dose rate (mR/h)
% Dose rate at IBM air intake vents (mR/h)
Dose_Rate_IBM_air_intake_mRh = squeeze(
Dose_Rate_8m_mRh(:,:,NETL_to_IBM_N_pt,NETL_to_IBM_W_pt) );

% Dose rate at IBM air intake vents (mR/h)
Dose_Rate_WF_air_intake_mRh = squeeze(
Dose_Rate_1_5m_mRh(:,:,NETL_to_WF_N_pt,NETL_to_WF_W_pt) );

% Dose rate at IBM air intake vents (mR/h)
Dose_Rate_Macys_air_intake_mRh = squeeze(
Dose_Rate_20m_mRh(:,:,NETL_to_Macys_N_pt,NETL_to_Macys_W_pt) );

% Dose rate at IBM air intake vents (mR/h)
Dose_Rate_ARL_air_intake_mRh = squeeze(
Dose_Rate_8m_mRh(:,:,NETL_to_ARL_S_pt,NETL_to_ARL_E_pt) );

% Dose rate at NETL side (mR/h)
Dose_Rate_building_side_mRh = squeeze( Dose_Rate_1_5m_mRh(:,:,NETL_side_N_pt,NETL_side_W_pt)
);

% Total dose for one year (mR)
% Dose at IBM air intake vents (mR)
Dose_IBM_air_intake_mR = squeeze( Dose_Rate_8m_mRh(:,:,NETL_to_IBM_N_pt,NETL_to_IBM_W_pt) ) *
8760;

% Dose at IBM air intake vents (mR)
```

```
Dose_WF_air_intake_mR = squeeze( Dose_Rate_1_5m_mRh(:,:,NETL_to_WF_N_pt,NETL_to_WF_W_pt) ) *
8760;

% Dose at IBM air intake vents (mR)
Dose_Macys_air_intake_mR = squeeze(
Dose_Rate_20m_mRh(:,:,NETL_to_Macys_N_pt,NETL_to_Macys_W_pt) ) * 8760;

% Dose at IBM air intake vents (mR)
Dose_ARL_air_intake_mR = squeeze( Dose_Rate_8m_mRh(:,:,NETL_to_ARL_S_pt,NETL_to_ARL_E_pt) ) *
8760;

% Dose at NETL side (mR)
Dose_building_side_mR = squeeze( Dose_Rate_1_5m_mRh(:,:,NETL_side_N_pt,NETL_side_W_pt) ) *
8760;

%% Output
display(' Creating output patterns ... ');

% Diffusion concentration patterns (kg/m^3)
pattern_1_5m = squeeze(C_1_5m(1,2,:,:));
pattern_8m = squeeze(C_8m(1,2,:,:));
pattern_20m = squeeze(C_20m(1,2,:,:));

% Finddose for 1yr exposure (mR)
[ D20, D20_rate ] = Con2Dose(pattern_20m);

% impossible speed, model blows up
pattern_20m_i = squeeze(C_20m(1,1,:,:));

% Find dose for 1yr exposure (mR)
[ D20_i, D20_rate_i ] = Con2Dose(pattern_20m_i);

% Find dose rate for IBM exposure side(mR)
[ D8, D8_rate ] = Con2Dose(pattern_8m);

% Find dose rate for 1yr exposure side(mR)
[ D1, D1_rate ] = Con2Dose(pattern_1_5m);

toc
% end
```

Table of Contents

1. DEFINITIONS

The following frequently used terms are defined to aid in the uniform interpretation of these specifications. Capitalization is used in the body of the Technical Specifications to identify defined terms.

ACTION (REQUIRED ACTION)

REQUIRED ACTION(s) are steps to be accomplished within COMPLETION TIME specified if a required SPECIFICATION is not met, as described or stated in the CONDITION column of the "Actions" section. The following guidance applies:

- If a CONDITION exists, the REQUIRED ACTION consists of completing all required steps within the specified COMPLETION TIME unless:

  1. The CONDITION is corrected prior to completion of the steps (in which case no further action is required),

  OR

  2. The reactor is placed in mode where the SPECIFICATION applicable (in which case no further action is required).

- COMPLETION TIME for the REQUIRED ACTION starts at discovery of the CONDITION

- When IMMEDIATELY is used as a COMPLETION TIME:

  (1) The REQUIRED ACTION SHALL be pursued without delay and in a controlled manner

  (2) REQUIRED ACTION SHALL be completed within one hour

  (3) The one-hour limit for completion does not authorize or permit deferring or postponing action, or imply that such deferral or postponement is acceptable

- "AND" in REQUIRED ACTION means all linked steps need to be performed to complete the action;

- "OR" in REQUIRED ACTION indicates options or alternatives; only one of the linked actions is required to complete the associated action.

- If there is more than one CONDITION for an LCO SPECIFICATION each CONDITION is linked to the failure to meet the SPECIFICATION by the letter associated with the SPECIFICATION and numbers unique to the conditions.

ANNUAL	12 months, not to exceed 15 months.
BIENNIAL	Every two years, not to exceed a 30-month interval.
CHANNEL	A channel is the combination of sensor, line, amplifier, and output devices that are connected for the purpose of measuring the value of a parameter.
CHANNEL CALIBRATION	A channel calibration is an adjustment of the channel so that its output responds, with acceptable range and accuracy, to known values of the parameter that the channel measures. Calibration shall encompass the entre channel, including equipment actuation, alarm, or trip, and shall be deemed to include a channel test.
CHANNEL CHECK	A channel check is a qualitative verification of acceptable performance by observation of channel behavior. This verification shall include comparison of the channel with expected values, other independent channels, or other methods of measuring the same variable where possible.
CHANNEL TEST	A channel test is the introduction of an input signal into a channel to verify that it is operable. *NOTE:* *A functional test of operability is a channel test.*
CONFINEMENT	The enclosure which controls the movement of air into and out of the reactor bay through an engineered controlled path.
CONFINEMENT ISOLATION	Alignment of the reactor bay ventilation system in which: (1) dampers controlling confinement ventilation are closed, and (2) confinement ventilation fans are secured (3) the reactor bay fume/sort hood fans are secured (4) the reactor bay fume/sort hood dampers are closed The purge system may be operated in manual override
CONTROL ROD (STANDARD)	A standard control rod (stainless steel clad, borated graphite, B4C powder, or boron and its compounds in solid form with a fuel follower) is one having an electric induction or stepper motor drive coupled to the control rod by an electromagnet, with scram capability.
CONTROL ROD (TRANSIENT)	A transient control rod (aluminum clad, borated graphite, B4C powder, or boron and its compounds in solid form followed by air

	or aluminum) is one that is pneumatically coupled to the control rod drive, is capable of initiating a power pulse, is operated by a motor drive, and/or air pressure operated and has scram capability.
DAILY	Prior to initial operation each calendar day (when the reactor is operated), or before an operation extending more than 1 calendar day
ENSURE	Verify existence of specified condition or (if condition does not meet criteria) take action necessary to establish the condition
EXCESS REACTIVITY	That amount of reactivity above the critical condition which would exist if all the control rods were moved to the maximum positive reactivity condition
	NOTE: *Limiting values for EXCESS REACTIVITY are based on REFERENCE CORE CONDITIONS*
EXPERIMENT	An EXPERIMENT is (1) any apparatus, device, or material placed in the reactor core region (in an EXPERIMENTAL FACILITY associated with the reactor, or in line with a beam of radiation emanating from the reactor) or (2) any in-core operation designed to measure reactor characteristics.
EXPERIMENTAL FACILITY	Experimental facilities are the beamports, pneumatic transfer systems, central thimble, rotary specimen rack, and displacement of fuel element positions used for EXPERIMENTS (single-element positions and the multiple element positions fabricated in the upper grid plate displacing 3, 6 or 7 elements).
IMMEDIATE	Without delay, and not exceeding a one hour.
INITIAL STARTUP	A reactor startup and approach to power following: (1) Modifications to reactor safety or control rod drive systems, (2) Fuel element or control rod relocations or installations (i.e., to different grid positions) within the reactor core region, (3) Relocation or installation of any experiment in the core region with a reactivity worth of greater than one dollar, or (4) Recovery from an unscheduled (a) shutdown or (b) significant

power reductions.

INTSTRUMENTED FUEL ELEMENT	An instrumented fuel element (IFE) is a stainless steel clad fuel element containing thermocouples embedded in the fuel element.
LIMITING CONDITION FOR OPERATION (LCO)	The lowest functional capability or performance levels of equipment required for safe operation of the facility.
LIMITING SAFETY SYSTEM SETTING (LSSS)	Settings for automatic protective devices related to those variables having significant safety functions. A limiting safety system setting is specified for a variable on which a SAFETY LIMIT placed, the setting shall be chosen so that the automatic protective action will correct the abnormal situation before a SAFETY LIMIT is exceeded.
MEASURED VALUE	The measured value of a parameter is the value as indicated at the output of a MEASURING CHANNEL.
MONTHLY	30 days, not to exceed 6 weeks.
MOVABLE EXPERIMENT	A MOVABLE EXPERIMENT is one where the EXPERIMENT may be moved into, out-of or near the reactor while the reactor is OPERATING.
OPERABLE	A system or component is OPERABLE when it is capable of performing its intended function in a normal manner
OPERATING	A system or component is OPERATING when it is performing its intended function.
PULSE MODE	The reactor is in the PULSE MODE when the key switch is in the "on" position, the back-lit "pulse" reactor mode switch is actuated and the reactor display indicates the associated mode ("pulse-ready mode") *NOTE:* *In the PULSE MODE, reactor power may be increased on a period of much less than I second by motion of the transient control rod.*
QUARTERLY	3 months, not to exceed 4 months
REACTOR SAFETY SYSTEM	The REACTOR SAFETY SYSTEM is that combination of MEASURING CHANNELS and associated circuitry that is designed to initiate a

reactor scram or that provides information that requires manual protective action to be initiated.

REACTOR SECURED MODE

The reactor is secured when the conditions of either item (1) or item (2) are satisfied:

(1) There is insufficient moderator or insufficient fissile material in the reactor to attain criticality under optimum available conditions of moderation and reflection

(2) All of the following:

a. At least three control rods are fully inserted

b. The console key is it the OFF position and the key is removed from the lock

c. No work is in progress involving core fuel, core structure, installed control rods, or control rod drives (unless the drive is physically decoupled from the control rod)

d. No experiments are being moved or serviced that have, on movement, a reactivity worth greater than $1.00

REACTOR SHUTDOWN

The reactor is shutdown if it is subcritical by at least the minimum required amount of reactivity (SHUTDOWN MARGIN) in the REFERENCE CORE CONDITION with the reactivity worth of all experiments included.

REFERENCE CORE CONDITION

The condition of the core when it is at ambient temperature (cold) and the reactivity worth of xenon is negligible (<$0.30)

SAFETY CHANNEL

A safety channel is a MEASURING CHANNEL in the REACTOR SAFETY SYSTEM.

SAFETY LIMITS

Limits on important process variables which are found to be necessary to protect reasonably the integrity of the principal barriers (i.e., fuel element cladding) which guard against the uncontrolled release of radioactivity. The principal barrier is the fuel element cladding.

SECURED EXPERIMENT	A secured EXPERIMENT is an EXPERIMENT held firmly in place by a mechanical device or by gravity providing that the weight of the EXPERIMENT is such that it cannot be moved by forces (1) normal to the operating environment of the experiment or (2) that might result from credible failures.
SHALL (SHALL NOT)	Indicates specified action is required to be performed/ (or required not to be performed)
SEMIANNUAL	Every six months, with intervals not greater than 7 ½ months
SHUTDOWN MARGIN	The shutdown margin is the minimum shutdown reactivity necessary to provide confidence that the reactor: (1) can be made subcritical by means of the control and safety systems, (a) starting from any permissible operating condition (the highest worth MOVEABLE EXPERIMENT in its most positive reactive state, each SECURED EXPERIMENT in its most reactive state), (b) with the most reactive rod in the most reactive position, and that the reactor; and (2) will remain subcritical without further operator action.
STANDARD FUEL ELEMENT	A standard fuel element is a single TRIGA element of standard type, U-ZrH clad in stainless steel with nominal hydrogen to zirconium ratio of 1.6.
STEADY-STATE MODE	The reactor is in the steady-state mode when the key switch is in the "on" position, the reactor mode selector backlit pushbutton switch for the "manual," "automatic," or "square wave" function has been actuated, and the reactor display indicates steady-state ('manual" or "square wave" selected) or automatic (automatic selected).

TECHNICAL SPECIFICATION VIOLATION	(1) A violation of a SAFETY LIMIT occurs when the SAFETY LIMIT value is exceeded. (2) A violation of a Limiting Safety System Setting or Limiting Condition for Operation) occurs when a CONDITION exists which does not meet a SPECIFICATION and the corresponding REQUIRED ACTION has not been met within the required COMPLETION TIME. (3) A violation of a Limiting Safety System Setting or Limiting Condition for Operation has not occurred if (within COMPLETION TIME): (a) the REQUIRED ACTION statement of an LSSS or LCO has been completed, (b) the SPECIFICATION is restored, - or - (c) the reactor is placed in a mode where the SPECIFICATION is not applicable
WEEKLY	7 days, not to exceed 10 days

2. SAFETY LIMITS AND LIMITING SAFETY SYSTEM SETTINGS

2.1 Fuel Element Temperature SAFETY LIMIT

2.1.1 Applicability

Specification A and B apply with the reactor in STEADY STATE MODE, REACTOR SHUTDOWN condition, REACTOR SECURED MODE, and the PULSE MODE; specification B applies in STEADY STATE MODE.

2.1.2 Objective

This SAFETY LIMIT ensures the integrity of the stainless steel cladding.

2.1.3 Specification

A	Fuel Temperature SHALL NOT exceed 1150°C in STEADY STATE MODE during transient operation
B	Steady state fuel temperature shall not exceed 750°C in STEADY STATE MODE during steady state operations.
C	Fuel Temperature SHALL NOT exceed 830°C in PULSED MODE operation

2.1.4 Actions

CONDITION	REQUIRED ACTION	COMPLETION TIME
A. Stainless steel clad, high-hydride fuel element temperature exceeds 1150°C in transient operations.	A. ENSURE SHUTDOWN condition AND Report per Section 6.8	A. IMMEDIATE
B. Stainless steel clad, high-hydride fuel element temperature exceeds 750°C in steady state operations	B. ENSURE SHUTDOWN condition AND Report per Section 6.8	B. IMMEDIATE

C. Stainless steel clad, high-hydride fuel element temperature exceeds 830°C	C. ENSURE SHUTDOWN condition AND Report per Section 6.8	C. IMMEDIATE

2.1.5 Basis

Safety Analysis Report Chapter 4 (4.2.1 B) identifies design and operating constraints for TRIGA fuel that will ensure cladding integrity is not challenged. The important process variable for a TRIGA reactor is the fuel element temperature. This parameter is well suited as a single specification, and it is readily measured. During operation, fission product gases and dissociation of the hydrogen and zirconium builds up gas inventory in internal components and spaces of the fuel elements. Fuel temperature acting on these gases controls fuel element internal pressure. Limiting the maximum temperature prevents excessive internal pressures that could be generated by heating these gases.

NUREG 1282 identifies the SAFETY LIMIT for the high-hydride ($ZrH_{1.6}$) fuel elements with stainless steel cladding based on the stress in the cladding (resulting from the hydrogen pressure from the dissociation of the zirconium hydride). This applied stress will remain below the yield strength of the stainless steel cladding with fuel temperatures below 1150°C. A change in yield strength occurs for stainless steel cladding temperatures of 500°C, but there is no scenario for fuel cladding to achieve 500°C while submerged or in air[1,2]; consequently the fuel temperature SAFETY LIMIT for all operations in STEADY STATE MODE is 1150°C.

Fuel growth and deformation can occur during normal operations, as described in Chapter 4 (4.2.1 Z). Damage mechanisms include fission recoils and fission gases, strongly influenced by thermal gradients. Limiting steady state operating fuel temperature to less than 750°C in STEADY STATE MODE for long term, steady state operations limits potential fuel growth, and the SAFETY LIMIT for transient operation in STEADY STATE MODE is 750°C.

In 2008 a study by Argonne National Laboratory (TRD 070.01006.05 REV A, Pulsing Temperature Limit for TRIGA LEU Fuel) recommended reducing a maximum pulsing fuel temperature limit of 830°C. Therefore, the SAFETY LIMIT for PULSED MODE operations is 830°C.

---

[1] Reference A (*LOSS OF COOLANT ACCIDENT ANALYSIS FOR THE UNIVERSITY OF TEXAS AT AUSTIN TRIGA REACTOR* G. Kline, 2016) pg. 33-36

[2] Reference B (MODELLING A STEP INSERTION AND CONTINUOUS ROD WITHDRAW EVENTS IN A TRIGA G. Kline, 2016) , pg. 45

2.2 Limiting Safety System Settings (LSSS)

2.2.1 Applicability

This specification applies when the reactor in STEADY STATE MODE

2.2.2 Objective

The objective of this specification is to ensure the SAFETY LIMIT is not exceeded.

2.2.3 Specifications

A	Power level SHALL NOT exceed 1100 kW (th) in STEADY STATE MODE of operation
B	Instrumented elements in the B or C ring SHALL indicate less than 550°C

2.2.4 Actions

CONDITION	REQUIRED ACTION	COMPLETION TIME
A. Steady state power level exceeds 1100 kW (th)	A. Reduce power to less than 1100 kW (th)	A. IMMEDIATE
B. An INTSTRUMENTED FUEL ELEMENT in the B or C ring indicates greater than 550°C	B. ENSURE REACTOR SHUTDOWN condition AND EVALUATE whether Safety Limit was exceeded	B. IMMEDIATE

2.2.5 Basis

Analysis demonstrates that if operating thermal (th) power is 1100 kW, the maximum steady state fuel temperature is less than the SAFETY LIMIT for steady state operations by a large margin.[3] Therefore, steady state operations at a maximum of 1100 kW meet requirements for safe operation with respect to maximum fuel temperature and thermal hydraulics by a wide margin. Steady state operation of 1100 kW was assumed in analyzing the loss of cooling and maximum hypothetical accidents. The analysis assumptions are protected by assuring that the maximum steady state operating power level is 1100 kW. The actual safety system setting will be chosen to ensure that a scram will occur at a level that does not exceed 1100 kW.

Instrumented fuel element temperatures less than 550°C ensure the SAFETY LIMITs on fuel temperature are met.

[3] Reference A (Loss of Coolant Accident Analysis for The University of Texas at Austin TRIGA Reactor, G. Kline, 2016) , pg. 30

3. LIMITING CONDITIONS FOR OPERATION (LCO)

3.1 Core Reactivity Limitations

3.1.1 Applicability

These specifications are required prior to entering STEADY-STATE MODE or PULSING MODE in OPERATING conditions; reactivity limits on PULSED MODE OPERATIONS are specified in Section 3.2; reactivity limits on experiments are specified in Section 3.8.

3.1.2 Objective

This LCO ensures the reactivity control system is OPERABLE, and that an accidental or inadvertent reactivity transient does not result in exceeding the SAFETY LIMIT.

3.1.3 Specification

A	The maximum available core reactivity (EXCESS REACTIVITY) with all control rods fully withdrawn does not exceed 4.9% Δk/k ($7.00) when: 1. REFERENCE CORE CONDITIONS exists 2. No MOVEABLE EXPERIMENTS with net-negative reactivity worth are in place
B	SHUTDOWN MARGIN in REFERENCE CORE CONDITIONS is more than 0.2% Δk/k ($0.29)

3.1.4 Actions

CONDITION	REQUIRED ACTION	COMPLETION TIME
A. Reactivity with all control rods fully withdrawn exceeds 4.9% Δk/k ($7.00)	A.1 ENSURE REACTOR SHUTDOWN AND A.2 Configure reactor to meet LCO	A.1 IMMEDIATE A.2 Prior to continued operations

B. The reactor is not subcritical by more than 0.2% Δk/k ($0.29) under specified conditions	B.1 ENSURE operable control rods are fully inserted AND Secure electrical power to the control rod circuits (magnet or motor power) AND Secure all work on in-core experiments or installed control rod drives AND B.2 Configure reactor to meet LCO	B.1 IMMEDIATE B.2 Prior to continued operations

3.1.5 Basis

Fuel temperatures resulting from specific reactivity insertion (assuming limiting pool water temperature and zero power) demonstrate that insertion of the maximum excess reactivity value of $7.00 will result in a maximum fuel temperature of 1125°C, less than the STEADY STATE MODE limit for transient operations, and insertion of the maximum excess reactivity value of any CONTROL ROD will not exceed the maximum SAFETY LIMIT for PULSED MODE operation.[4]

The limiting SHUTDOWN MARGIN is necessary so that the reactor can be shut down from any operating condition, and will remain shutdown after cool down and xenon decay, even if the most reactive control rod remains in the fully withdrawn position. Analysis in Chapter 4 (4.5.1) demonstrates the capability of the control rods to meet this requirement.

[4] Reference B op cit

3.2 PULSED MODE Operations

3.2.1 Applicability

These specifications apply to operation of the reactor in the PULSE MODE.

3.2.2 Objective

This Limiting Condition for Operation prevents fuel temperature SAFETY LIMIT from being exceeded during PULSE MODE operation.

3.2.3 Specification

A	The transient rod drive is positioned for reactivity insertion (upon withdrawal) less than or equal to 2.8% δk ($4.00)

3.2.4 Actions

CONDITION	REQUIRED ACTION	COMPLETION TIME
A. With all stainless steel clad fuel elements, the worth of the pulse rod in the transient rod drive position is greater than $4.00 in the PULSE MODE	A. Position the transient rod drive for pulse rod worth less than or equal to $4.00 OR Place reactor in STEADY STATE MODE	A. Prior to commencement of pulsing operation

3.2.5 Basis

The maximum calculated fuel temperature resulting from $4.00 reactivity insertion with limiting pool water temperature at zero power is 580°C. This is well within the SAFETY LIMIT for PULSED MODE operations.[5]

[5] Reference B op cit

3.3 MEASURING CHANNELS

3.3.1 Applicability

This specification applies to the reactor MEASURING CHANNELS during STEADY STATE MODE and PULSE MODE operations.

3.3.2 Objective

The objective is to require that sufficient information is available to the operator to ensure safe operation of the reactor

3.3.3 Specifications

A	The neutron count rate on the startup channel is greater 2 mW
B-H	The MEASURING CHANNELS specified in TABLE 1 SHALL be OPERATING

TABLE 1: MINIMUM MEASURING CHANNEL COMPLEMENT

MEASURING CHANNEL		Minimum Number Operable	
		STEADY STATE MODE	PULSE MODE
B	Reactor power level[1]	2	1
C	Pool Water Temperature	1	1
D	Fuel Temperature	1	1
E	Pool area radiation monitor[2]	1	1
F	Lower or middle level area monitor[2]	1	1
G	Argon 41 effluent monitor[3]	1	1
H	Particulate air continuous air monitor	1	1

NOTE [1]: One "Startup Channel" required to have range that indicates <10 W
NOTE [2]: High-level alarms audible in the control room may be used
NOTE [3]: When the auxiliary purge system is operating

3.3.4 Actions

CONDITION	REQUIRED ACTION	COMPLETION TIME
A. The neutron count rate on the startup channel is not greater than $2x10^{-7}$ %	A.1 Do not perform a reactor startup OR A.2 Perform a neutron-source check on the startup channel	A.1 IMMEDIATE A.2 Prior to startup

CONDITION	REQUIRED ACTION	COMPLETION TIME
B. Required reactor power channels not OPERATING OR Communications between DAC and control console interrupted > 10 s OR High voltage to reactor safety channel (power level) detector less than 80% of required operating value	B.1 ENSURE REACTOR SHUTDOWN B.2 Restore channel to operation	B.1 IMMEDIATE B.2 Prior to startup
C. Pool water temperature CHANNEL not operable	C. Restore channel to operation OR Monitor pool water temperature at least once per hour	C. IMMEDIATE
D. Fuel temperature CHANNEL not operable	D.1 ENSURE REACTOR SHUTDOWN D.2 Restore channel to operation	D.1 IMMEDIATE D.2 Prior to startup

CONDITION	REQUIRED ACTION	COMPLETION TIME
E. Pool Area Radiation Monitor is not OPERATING	E.1 Restore MEASURING CHANNEL OR E.2 ENSURE personnel are not on the upper level OR ENSURE personnel on upper level are using portable survey meters to monitor dose rates	E.1 Prior to startup E.2 IMMEDIATE
F. Required number of lower or middle level area monitors are not OPERATING	F.1 Restore MEASURING CHANNEL OR ENSURE personnel are not in the reactor bay OR ENSURE personnel entering reactor bay are using portable survey meters to monitor dose rates	F.1 IMMEDIATE
G. Argon monitor is not OPERATING	G.1 Restore MEASURING CHANNEL OR ENSURE continuous air radiation monitor is OPERATING G.2 Restore MEASURING CHANNEL within 30 working days	G.1 IMMEDIATE G.2 Within 30 working days

CONDITION	REQUIRED ACTION	COMPLETION TIME
H. Continuous particulate air radiation monitor is not OPERATING	H.1 Restore MEASURING CHANNEL OR ENSURE Argon 41 monitor radiation monitor is OPERATING	H.1 IMMEDIATE
	H.2 Restore MEASURING CHANNEL	H.2 Within 30 working days

3.3.5 Basis

Experience has shown that subcritical multiplication with the neutron source used in the reactor does not provide enough neutron flux to correspond to an indicated power level of $2x10^{-7}$ %. Therefore, an indicated power of $2x10^{-7}$ % (or 2 mW) or more indicates operating in a potential critical condition, and at least one neutron channel is required with sensitivity at a neutron flux level corresponding to reactor power levels less than $2x10^{-7}$ % ("Startup Channel"). If the indicated neutron level is less than the minimum sensitivity for the channel, a neutron source will be used to determine that the channel is responding to neutrons, and therefore assure that the channel is functioning prior to startup.

Maximum steady state power level is 1100 kW; neutron detectors measure reactor power level. Chapter 4 and 13 discuss normal and accident heat removal capabilities. Chapter 7 discusses radiation detection and monitoring systems, and neutron and power level detection systems.

Communications between the digital acquisition system and the control console computer is monitored by a periodic 'watchdog' signal. If the periodic signal stops, the control system initiates a SCRAM.

General Atomics recommends detector voltages at least 80% of nominal operating value for reliable, accurate nuclear instrumentation. Therefore, if operating voltage falls below the minimum value the power level channel is considered inoperable.

Pool water temperature indication is required to assure water temperature limits are met, protecting primary cleanup resin integrity. Analysis in Chapter 4 and 13 assume a maximum fuel temperature based on protection of resin integrity. Fuel temperature indication provides a means of observing that the SAFETY LIMITS are met.

The upper and lower level area radiation monitors provide information about radiation hazards in the reactor bay. A loss of reactor pool water (Chapter 13), changes in shielding effectiveness (Chapter 11), and releases of radioactive material to the restricted area (Chapter 11) that could cause changes in radiation levels within the reactor bay detectable by these monitors. Portable survey instruments will detect changes in radiation levels.

The air monitors (continuous particulate air- and argon radiation-monitor) provide indication of airborne contaminants in the reactor bay. These channels provide evidence of fuel element failure on independent channels; the particulate air monitor gas has maximum sensitivity to radioiodine and particulate activity, while the argon channel detects radioactive noble gas.

Permitting operation using a single channel of airborne contamination monitoring will reduce unnecessary shutdowns while maintaining the ability to detect abnormal conditions as they develop. Relative indications ensure discharges are routine; abnormal indications trigger investigation or action to prevent the release of radioactive material to the surrounding environment. Ensuring the alternate airborne contamination monitor is functioning during outages of one system provides the contamination monitoring required for detecting abnormal conditions. Limiting the outage for a single unit to a maximum of 30 days ensures radioactive atmospheric contaminants are monitored while permitting maintenance and repair outages on the other system.

SAR Chapter 13 discusses inventories and releases of radioactive material from fuel element failure into the reactor bay, and to the environment. Particulate and noble gas channels monitor more routine discharges. SAR Chapter 11 discusses routine discharges of radioactive gasses generated from normal operations into the reactor bay and into the environment. SAR Chapters 3 and 9 identifies design basis for the confinement and ventilation system. SAR Chapter 7 discusses air-monitoring systems. The 30-day interval is selected as adequate to accomplish complex repairs, and limited enough that with one system functional there is no significant chance that the system will fail during a period that requires detection of airborne radioactivity.

3.4 Safety Channel and Control Rod Operability

3.4.1 Applicability

This specification applies to the reactor MEASURING Channels during STEADY STATE MODE and PULSE MODE operations.

3.4.2 Objective

The objectives are to require the minimum number of REACTOR SAFETY SYSTEM channels that must be OPERABLE in order to ensure that the fuel temperature SAFETY LIMIT is not exceeded, and to ensure prompt shutdown in the event of a scram signal.

3.4.3 Specifications

A	The SAFETY SYSTEM CHANNELS specified in TABLE 2 are OPERABLE
B	CONTROL RODS (STANDARD) are capable of full insertion from the fully withdrawn position in less than 1 sec.

TABLE 2: REQUIRED SAFETY SYSTEM CHANNELS

Safety System Channel or Interlock	Minimum Number Operable	Function	Required OPERATING Mode	
			STEADY STATE MODE	PULSE MODE
Reactor power level	2	Scram	YES	NA
Manual scram bar	1	Scram	YES	YES
Fuel Temperature	1	Scram	YES	YES
Pool water level	1	Scram	YES	YES
CONTROL ROD (STANDARD) position interlock	1	Prevent withdrawal of standard rods in the PULSE MODE	NA	YES
Pulse rod interlock[1]	1	Prevent inadvertent pulsing while in STEADY STATE MODE	YES	NA

NOTE [1]: The pulse rod interlock prevents air from being applied to the pulse rod unless the transient rod is fully inserted except during pulse mode or square wave operations.

3.4.4 Actions

CONDITION	REQUIRED ACTION	COMPLETION TIME
A. Any required SAFETY SYSTEM CHANNEL or interlock function is not OPERABLE during operation	A. Restore channel or interlock to operation	A. IMMEDIATE
B.1 Any CONTROL ROD is not OPERABLE during operation	B.1 Restore to OPERABLE	B.1 IMMEDIATE
B.2 Any CONTROL ROD or SAFETY SYSTEM CHANNEL is not OPERABLE while shutdown	B.2 Restore to OPERABLE AND Limit operations to maintenance and testing	B.2 Prior to continued normal operations

3.4.5 Basis

The power level scram is provided to ensure that reactor operation stays within the steady state licensed power, therefore preventing exceeding fuel temperature limits. The power level scram is not credited in analysis, but provides defense in depth to assure that the reactor is not operated in conditions beyond the assumptions used in analysis (Chapter 4 and 13).

The manual scram allows the operator to shut down the system if an unsafe or abnormal condition occurs.

Fuel temperature scram assures the LSSS is met.

The pool water level scram secures operation on a loss of pool water level.

The CONTROL ROD (STANDARD) interlock function is to prevent withdrawing control rods (other than the pulse rod) when the reactor is in the PULSE MODE. This will ensure the reactivity addition rate during a pulse is limited to the reactivity added by the pulse rod only.

The pulse rod interlock function prevents air from being applied to the transient rod drive when it is withdrawn while disconnected from the control rod to prevent inadvertent pulses during STEADY STATE MODE operations. The control rod interlock

prevents inadvertent pulses which would be likely to exceed the maximum range of the power level instruments configured for steady state operations.

3.5 Gaseous Effluent Control

3.5.1 Applicability

This specification applies to gaseous effluent in STEADY STATE MODE and PULSE MODE.

3.5.2 Objective

The objective is to ensure that exposures to the public resulting from gaseous effluents released during normal operations and accident conditions are within limits and ALARA.

3.5.3 Specification

A	The reactor bay HVAC confinement system SHALL provide ventilation to the reactor bay when particulate continuous air monitor indicates less than 10,000 cpm
B	The reactor bay confinement system will initiate CONFINEMENT ISOLATION if the particulate continuous air monitor is in-service and indicates greater than 10,000 cpm
C	Argon purge system SHALL exhaust from reactor bay pool area and in-use experiment areas

3.5.4 Actions

CONDITION	REQUIRED ACTION	COMPLETION TIME
A. The reactor bay HVAC confinement ventilation system is not OPERABLE	A. ENSURE argon purge system is OPERATING	A. IMMEDIATE
B The particulate continuous air monitor is in service and indicates greater than 10,000 cpm with reactor bay confinement system not in CONFINEMENT ISOLATION	B. SECURE reactor bay ventilation, and argon purge AND SECURE the fume/sorting hood	B. IMMEDIATE

CONDITION	REQUIRED ACTION	COMPLETION TIME
C. The auxiliary purge system is not OPERABLE	C. ENSURE reactor bay HVAC confinement ventilation system is OPERATING OR (1) Secure EXPERIMENT operations for EXPERIMENT with failure modes that could result in the release of radioactive gases or aerosols AND (2) ENSURE no irradiated fuel handling	C. IMMEDIATE

3.5.5 Basis

The confinement and ventilation system is described in Chapter 9. Routine operations produce radioactive gas, principally Argon 41, in the reactor bay. If the confinement system is not functioning and the purge system is not operating, radioactive gasses will buildup in the reactor bay. During this interval, experiment activities that might cause airborne radionuclide levels to be elevated are prohibited.

Chapter 13 addresses the maximum hypothetical fission product inventory release. Using unrealistically conservative assumptions, concentrations for a few nuclides of iodine would be in excess of occupational derived air concentrations for a matter of hours or days. ^{90}Sr activity available for release from fuel rods previously used at other facilities is estimated to be at most about 4 times the ALI. In either case (radio-iodine or -Sr), there is no credible scenario for accidental inhalation or ingestion of the undiluted nuclides that might be released from a damaged fuel element. Finally, fuel element failure during a fuel handling accident is likely to be observed and mitigated immediately.

3.6 Limitations on Experiments

3.6.1 Applicability

This specification applies to operations in STEADY STATE MODE and PULSE MODE.

3.6.2 Objectives

The objective is to prevent reactivity excursions that might cause the fuel temperature to exceed the SAFETY LIMIT (with possible resultant damage to the reactor), and the excessive release of radioactive materials in the event of an EXPERIMENT failure

3.6.3 Specifications

A	The reactivity worth of any individual MOVEABLE EXPERIMENT SHALL NOT exceed \$1.00 (0.007 Δk/k)
B	The reactivity worth of any individual SECURED EXPERIMENT SHALL NOT exceed \$2.50 (0.0175 Δk/k)
C	The total reactivity worth of all EXPERIMENTS shall not exceed \$3.00 (0.021 Δk/k)

3.6.4 Actions

CONDITION	REQUIRED ACTION	COMPLETION TIME
A. MOVEABLE EXPERIMENT worth is greater than \$1.00	A.1 ENSURE the reactor is SHUTDOWN AND A.2 Remove the experiment	A.1 IMMEDIATE A.2 Prior to continued operations
B. SECURED EXPERIMENT worth is greater than \$2.50	B.1 ENSURE the reactor is SHUTDOWN AND B.2 Remove the experiment	B.1 IMMEDIATE B.2 Prior to continued operations

C. Total EXPERIMENT worth is greater than $3.00	C.1 ENSURE the reactor is SHUTDOWN AND C.2 Configure experiments to meet requirements	C.1 IMMEDIATE C.2 Prior to continued operations

3.6.5 Basis

Chapter 13 demonstrates that pulsed reactivity worth less than 2.8% Δk/k ($4.00) will not challenge fuel integrity. These limits provide assurance that experiments do not exceed the reactivity analyzed. Experiment limits are established lower than analysis limits assuring a margin for experimental error.

3.7 Fuel Integrity

3.7.1 Applicability

This specification applies to operations in STEADY STATE MODE and PULSE MODE.

3.7.2 Objective

The objective is to prevent the use of damaged fuel in the UT TRIGA reactor.

3.7.3 Specifications

A	Fuel elements in the reactor core SHALL NOT be (1) elongated more than 1/10 in. over manufactured length OR (2) laterally bent more than 1/16 in.
B	Fuel elements SHALL NOT have visual indications of cladding integrity failure.
C	During normal operations, fuel elements in the core SHALL NOT release fission products.

3.7.4 Actions

CONDITION	REQUIRED ACTION	COMPLETION TIME
A. Any fuel element is elongated greater than 1/10 in. over manufactured length, or bent laterally greater than 1/16 in.	A. Do not re-insert the fuel element into the upper core grid plate.	A. IMMEDIATE
B. Fuel elements have visual indication of cladding integrity failure	B.1 Do not insert or re-insert the fuel element into the upper core grid plate. B.2 Discharge failed element(s) from the core	B.1 IMMEDIATE B.2 Prior to continued operations

C. Fission products are determined to be leaking from fuel elements in the core	C.1 SECURE PULSE MODE operations AND Operate in STEADY STATE MODE only to identify the failed element AND C.2 Remove the failed element from service	C.1 IMMEDIATE C.2 Prior to resuming normal operations

3.7.5 Basis

The above limits on the allowable distortion of a fuel element have been shown to correspond to strains that are considerably lower than the strain expected to cause rupture of a fuel element and have been successfully applied at TRIGA installations. Fuel cladding integrity is important since it represents the only process barrier for fission product release from the TRIGA reactor.

Lateral bend less than 1/16 in. in adjacent fuel elements assures that there is adequate clearance to prevent element contact during operation.

A release of fission products indicates cladding challenge. Limiting the use of fuel elements where cladding has been challenged as specified limits release of fission products to the minimum required for assessing fuel elements.

3.8 Reactor Pool Water

3.8.1 Applicability

This specification applies to operations in STEADY STATE MODE, PULSE MODE, and SECURED MODE.

3.8.2 Objective

The objective is to set acceptable limits on the water quality, temperature, conductivity, and level in the reactor pool.

3.8.3 Specifications

A	Water temperature at the exit of the reactor pool SHALL NOT exceed 110°F (48.9°C)
B	Water conductivity SHALL be less than or equal to 5 µmho/cm averaged over 1 month
C	Water level above the core SHALL be at least 6.5 m from bottom of the pool
D	The pressure difference between chilled water outlet from the pool heat exchanger and pool water inlet SHALL NOT be less than 7 kPa (1 psig)

3.8.4 Actions

CONDITION	REQUIRED ACTION	COMPLETION TIME
A. Water temperature at the exit of the reactor pool exceeds 110°F (48.9°C)	A Secure flow through the demineralizer AND Initiate action to reduce water temperature to less than 110°F	A IMMEDIATE

CONDITION	REQUIRED ACTION	COMPLETION TIME
B. Water conductivity is greater than 5 µmho/cm	B.1 Restore conductivity to less than 5 µmho/cm B.2 Verify 30-day average of conductivity remained less than 5 µmho/cm OR Submit a plan for verification of fuel integrity to the USNRC	B.1 Within 1 month B.2 Prior to continued operations
C. Water level above the core SHALL be at least 6.5 m from the bottom of the pool for all operating conditions	C. Restore water level	C. IMMEDIATE
D. The pressure difference between chilled water outlet from the pool heat exchanger and pool water inlet is less than 7 kPa (1 psig)	D Verify pressure differential is greater than 7 kPa (1 psig) OR RESTORE pressure difference to greater than 7 kPa (1 psig) OR Isolate chill water	D. IMMEDIATE

3.8.5 Basis

The resin used in the mixed bed deionizer limits the water temperature of the reactor pool. Resin in use (as described in Section 5.4) maintains mechanical and chemical integrity at temperatures below 110°F (48.9°C). Therefore, thermal hydraulic analysis was conducted to a maximum pool temperature of 48.9°C, and limiting pool temperature ensures analysis conditions are met.

Maintaining low water conductivity over a prolonged period prevents possible corrosion, deionizer degradation, or slow leakage of fission products from degraded cladding. Although fuel degradation does not occur over short time intervals, long-term integrity of the fuel is important, and a 4-week interval was selected as an appropriate maximum time for averaging conductivity values.

For normal pool temperature, calculations in Chapter 4 assuming 8.1 and 6.5 m above the bottom of the pool demonstrate that the heat flux of the hottest area of the fuel rod generating the highest power level in the core during operations is less than the critical heat flux by a large margin up to the maximum permitted cooling temperatures; margin remains even at temperatures approaching bulk boiling for atmospheric conditions. Therefore, pool levels greater than 6.5 m above the pool floor meet requirements for safe operation with respect to maximum fuel temperature and thermal hydraulics by a wide margin.

The principle contributor to radiation dose rates at the pool surface is Nitrogen 16 generated in the reactor core and dispersed in the pool. Pool surface radiation dose rates from Nitrogen 16 with 6.5 m of water above the core are acceptable; therefore, a minimum pool level of 6.5 feet above the core is adequate to support the core cooling and provide shielding.

The specified pressure difference assures that any postulated heat exchanger leakage will not release potentially contaminated water outside the operations boundary.

3.9 Retest Requirements

3.9.1 Applicability

This specification applies to operations in STEADY STATE MODE and PULSE MODE.

3.9.2 Objective

The objective is to ensure Technical Specification requirements are met following maintenance or operational activities that occur within surveillance test intervals.

3.9.3 Specifications

Maintenance or operational activities SHALL NOT change, defeat or alter equipment or systems in a way that prevents the systems or equipment from being OPERABLE (when required) or otherwise prevent the systems or equipment from fulfilling the safety basis

3.9.4 Actions

CONDITION	REQUIRED ACTION	COMPLETION TIME
Maintenance or an operational activity is performed that has the potential to change a setpoint, calibration, flow rate, or other parameter that is measured or verified in meeting a surveillance or operability requirement	Perform surveillance OR Operate only to perform retest	Prior to continued, normal operation in STEADY STATE MODE or PULSE MODE

3.9.5 Basis

Operation of the UT TRIGA reactor will comply with the requirements of Technical Specifications. This specification ensures that if maintenance or operations might challenge a Technical Specifications requirement, the requirement is verified prior to resumption of normal operations.

4. Surveillance Requirements

Surveillance activities (except those specifically required for safety when the reactor is shutdown), may be deferred during reactor shutdown, however, they must be completed prior to reactor startup unless reactor operation is necessary for performance of the activity. If reactor operation is necessary for performance of the activity, reactor operations will be limited to support for surveillance activity. If a surveillance schedule cannot be met because the reactor is operating while performance requires the reactor not be operating, performance may be deferred until the reactor is shutdown.

4.1 Core Reactivity

4.1.1 Objective

This surveillance ensures that the minimum SHUTDOWN MARGIN requirements and maximum excess reactivity limits of section 3.1 are met.

4.1.2 Specification

SURVEILLANCE REQUIREMENTS

SURVEILLANCE	FREQUENCY
SHUTDOWN MARGIN Determination	ANNUAL
EXCESS REACTIVITY Determination	ANNUAL
	Following Insertion of experiments with measurable positive reactivity
Control Rod Reactivity Worth determination	BIENNIAL

4.1.3 Basis

Experience has shown verification of the minimum allowed SHUTDOWN MARGIN at the specified frequency is adequate to assure that the limiting safety system setting is met

When core reactivity parameters are affected by operations or maintenance, additional activity is required to ensure changes are incorporated in reactivity evaluations.

Reactivity limits are verified by comparing critical control rod positions to reference values. The reference values change with burnup and core configuration. Biennial

evaluation of control rod position is adequate, although other activities may result in control rod worth determination through retest requirements.

4.2 PULSE MODE

4.2.1 Objectives

The verification that the pulse rod position does not exceed a reactivity value corresponding to $4.00 assures that the limiting condition for operation is met.

4.2.2 Specification

SURVEILLANCE REQUIREMENTS

SURVEILLANCE	FREQUENCY
ENSURE Transient Pulse Rod position corresponds to reactivity not greater than $4.00	Prior to pulsing operations

4.2.3 Basis

Verifying pulse rod position corresponds to less than or equal to $4.00 ensures that the maximum pulsed reactivity meets the limiting condition for operation.

4.3 MEASURING CHANNELS

4.3.1 Objectives

Surveillances on MEASURING CHANNELS at specified frequencies ensure instrument problems are identified and corrected before they can affect operations.

4.3.2 Specification

SURVEILLANCE REQUIREMENTS

SURVEILLANCE	FREQUENCY
Reactor power level CHANNEL	
CHANNEL TEST	DAILY when operating
Calorimetric calibration	ANNUAL
CHANNEL CHECK loss of high voltage to required power level instruments	DAILY when operating
CALIBRATION high voltage to required power level instruments	ANNUAL
Primary pool water temperature CHANNEL	
CHANNEL TEST	DAILY when operating
CHANNEL CALIBRATION	ANNUAL
Fuel temperature CHANNEL	
CHANNEL TEST	DAILY when operating
CHANNEL CALIBRATION	ANNUAL
Upper level Area radiation monitor	
CHANNEL CHECK	WEEKLY
CHANNEL CALIBRATION	ANNUAL
Lower or middle level Area Radiation Monitor	
CHANNEL CHECK	WEEKLY
CHANNEL CALIBRATION	ANNUAL
(Particulate) Continuous Air Radiation Monitor	
CHANNEL CHECK	DAILY when operating
CHANNEL CALIBRATION	ANNUAL
Argon Monitor	
CHANNEL CHECK	DAILY when operating

SURVEILLANCE REQUIREMENTS

SURVEILLANCE	FREQUENCY
CHANNEL CALIBRATION (Electronic)	BIENNIAL
Startup Count Rate	DAILY when operating

4.3.3 Basis

The DAILY CHANNEL CHECKS will ensure that the SAFETY SYSTEM and MEASURING CHANNELS are operable. The required periodic calibrations and verifications will permit any long-term drift of the channels to be corrected.

4.4 Safety Channel and Control Rod Operability

4.4.1 Objective

The objectives of these surveillance requirements are to ensure the REACTOR SAFETY SYSTEM will function as required. Surveillances related to safety system MEASURING CHANNELS ensure appropriate signals are reliably transmitted to the shutdown system; the surveillances in this section ensure the control rod system is capable of providing the necessary actions to respond to these signals.

4.4.2 Specifications

SURVEILLANCE REQUIREMENTS

SURVEILLANCE	FREQUENCY
Pool level scram SHALL be functionally tested	MONTHLY
CONTROL ROD (STANDARD) drop times SHALL be measured to have a drop time from the fully withdrawn position of less than 1 sec.	ANNUAL
The control rods SHALL be visually inspected for corrosion and mechanical damage at intervals	BIENNIAL
CONTROL ROD (STANDARD) position interlock functional test	SEMIANNUAL
Pulse rod interlock functional test	SEMIANNUAL
The CONTROL ROD (TRANSIENT) rod drive cylinder and the associated air supply system SHALL be inspected, cleaned, and lubricated, as necessary.	ANNUAL

4.4.3 Basis

Manual and automatic scrams are not credited in accident analysis, although the systems function to assure long-term safe shutdown conditions. The manual scram and control rod drop timing surveillance s are intended to monitor for potential degradation that might interfere with the operation of the control rod systems. The functional test of pool level trip channel assures that the channel will function on demand.

The control rod inspections (visual inspections and transient drive system inspections) are similarly intended to identify potential degradation that lead to control rod degradation or inoperability.

A test of the interlock that prevents the pulse rod from coupling to the drive in the state mode unless the drive is fully down or square wave mode is being used assures that pulses will not unintentionally occur. In particular, instrumentation alignment for the

pulsing mode causes safety channels to be capable of monitoring pulse power; if pulsing occurs while the instruments are set to normal, steady state operations, they will not be capable of monitoring peak power.

A test of the interlock that prevents standard control rod motion while in the pulse mode assures that the interlock will function as required.

The functional checks of the control rod drive system assure the control rod drive system operates as intended for any pulsing operations. The inspection of the pulse rod mechanism will assure degradation of the pulse rod drive will be detected prior to malfunctions.

4.5 Gaseous Effluent Control

4.5.1 Objectives

These surveillances ensure that routine releases are normal, and (in conjunction with MEASURING CHANNEL surveillance) that instruments will alert the facility if conditions indicate abnormal releases.

4.5.2 Specification

SURVEILLANCE REQUIREMENTS

SURVEILLANCE	FREQUENCY
ENSURE confinement HVAC operable	DAILY when operating
ENSURE adequate auxiliary air purge system valve alignment	Prior to entering an operating mode with an EXPERIMENTAL FACILITY in use
CONFINEMENT ISOLATION functional test	MONTHLY
CONFINEMENT ISOLATION damper inspection	ANNUALLY

4.5.3 Basis

Verification that the confinement HVAC system is operable daily is adequate to assure the HVAC function.

Since the experimental facilities in use may vary between operations, the auxiliary purge system valve line up may require multiple manipulations on a given day of operations. If the EXPERIMENTAL FACILITES used in an operation do not change, a review of operating logs and records may be adequate to verify proper valve alignment.

Confinement isolation functional test frequency is adequate to ensure potential failures are detected prior to system demand.

The annual test is adequate to detect degradation of sealing surfaces.

4.6 Limitations on Experiments

4.6.1 Objectives

This surveillance ensures that experiments do not have significant negative impact on safety of the public, personnel or the facility.

4.6.2 Specification

SURVEILLANCE REQUIREMENTS

SURVEILLANCE	FREQUENCY
Experiments SHALL be evaluated and approved prior to implementation.	Prior to inserting a new experiment for purposes other than determination of reactivity worth
Measure and record experiment worth of the EXPERIMENT (where the absolute value of the estimated worth is greater than $0.50).	Initial insertion of a new experiment where absolute value of the estimated worth is greater than $0.50

4.6.3 Basis

These surveillances support determination that the limits of 3.6 are met.

Experiments with an absolute value of the estimated significant reactivity worth (greater than $0.50) will be measured to assure that maximum experiment reactivity worths are met. If an absolute value of the estimate indicates less than $0.50 reactivity worth, any error less than 100% will result in actual reactivity less than the assumptions used in analysis for inadvertent pulsing at low power operations in the Safety Analysis Report (13.2.3, Case I).

4.7 Fuel Integrity

4.7.1 Objective

The objective is to ensure fuel element integrity.

4.7.3 Specification

SURVEILLANCE REQUIREMENTS

SURVEILLANCE	FREQUENCY
The STANDARD FUEL ELEMENTS SHALL be visually inspected for corrosion and mechanical damage, and measured for length and bend	500 pulses of magnitude equal to or greater than a pulse insertion of $3.00 AND Following the exceeding of a limited safety system set point with potential for causing degradation
Approximately 1/4 of the core SHALL be visually inspected annually for corrosion and mechanical damage	BIENNIAL
Complete full core inspection	4, not to exceed 5, years

4.7.4 Basis

The most severe stresses induced in the fuel elements result from pulse operation of the reactor, when temperature causes increased gas pressure and fuel-to-cladding differential expansion. The magnitude of $3.00 pulses warrants inspection following a sufficient number of cycles.

Visual inspection of fuel elements at the specified intervals combined with measurements at intervals determined by pulsing as described is considered adequate to identify potential degradation of fuel prior to catastrophic fuel element failure.

Monitoring required by Gaseous Effluent Controls (Technical Specifications 3.5) provides continuous monitoring of potential fission product release during operation; therefore, no separate surveillance requirements are necessary to assure that fission products are not released from fuel during operations.

4.8 Reactor Pool Water

This specification applies to the water contained in the UT TRIGA reactor pool.

4.8.1 Objective

The objective is to provide surveillance of reactor primary coolant water quality, pool level, temperature and (in conjunction with MEASURING CHANNEL surveillances), and conductivity.

4.8.2 Specification

SURVEILLANCE REQUIREMENTS

SURVEILLANCE	FREQUENCY
Verify reactor pool water level above the inlet line vacuum breaker	DAILY when operating
Verify reactor pool water temperature channel operable	DAILY when operating
Measure reactor pool water conductivity	WEEKLY
	At least every 30 days
CALIBRATE pool water conductivity channel	ANNUALLY
CALIBRATE heat exchanger differential pressure channel	ANNUALLY
CHANNEL CHECK heat exchanger differential pressure channel with loss of differential pressure	DAILY when operating

4.9.3 Basis

Surveillance of the reactor pool will ensure that the water level is adequate before reactor operation. Evaporation occurs over longer periods of time, and daily checks are adequate to identify the need for water replacement. Pool water level status (not high, not low) is indicated on the control console.

Pool water temperature must be monitored to ensure that the temperature limit related to resin will not be exceeded, and that the conditions for analysis are maintained. A daily check on the pool temperature instrument prior to reactor operation is adequate to ensure the instrument is operable when it will be needed.

Water conductivity must be checked to ensure that the pool cleanup system is performing properly and to detect any increase in water impurities. A weekly check is adequate to verify water quality is appropriate and also to provide data useful in trend analysis. If the reactor is not operated for long periods of time, the requirement for

checks at least every 30 days ensures water quality is maintained in a manner that does not permit fuel degradation.

Annual calibration of the conductivity channel is adequate to assure the channel functions as required.

Annual calibration of the heat exchanger differential pressure channel has proven adequate to assure the required specification is met.

A daily functional test using loss of differential pressure is adequate to ensure the channel functions as required.

4.9 Retest Requirements

4.9.1 Objective

The objective is to ensure that a system is OPERABLE within specified limits before being used after maintenance or operational activities has been performed.

4.9.2 Specification

SURVEILLANCE REQUIREMENTS

SURVEILLANCE	FREQUENCY
Evaluate potential for maintenance or operational activities to affect operability and function of equipment required by Technical Specifications; for standard procedures, this evaluation is incorporated in instructions.	Following maintenance or operational activities for systems of equipment required by Technical Specifications
Perform surveillance to assure affected function meets requirements	Prior to resumption of normal operations

4.9.3 Basis

This specification ensures that work on systems or components has been properly carried out and that the system or component has been properly reinstalled or reconnected before reliance for safety is placed on it.

5. Design Features

5.1 Reactor Fuel

5.1.1 Applicability

This specification applies to the fuel elements used in the reactor core.

5.1.2 Objective

The objective is to ensure that the fuel elements are of such a design and fabricated in such a manner as to permit their use with a high degree of reliability with respect to their mechanical integrity.

5.1.3 Specification

(l) The high-hydride fuel element shall contain uranium-zirconium hydride, clad in nominal 0.020 in. of 304 stainless steel. It shall contain nominally 8.5%$_{wt}$ uranium which has a maximum nominal enrichment of 20%. There shall be nominally 1.6 hydrogen atoms to 1.0 zirconium atoms.

(2) For the fuel loading process, elements shall be loaded in an array except for experimental facilities or for single positions occupied by control rods and a neutron startup source.

5.1.4 Basis

These types of fuel elements have a long history of successful use in TRIGA reactors.

5.2 Reactor Fuel and Fueled Devices in Storage

5.2.1 Applicability

This specification applies to reactor fuel elements in storage

5.2.2 Objective

The objective is to ensure fuel elements or fueled devices in storage are maintained Subcritical in a safe condition.

5.2.3 Specification

(1) All fuel elements or fueled devices shall be in a safe, stable geometry;

(2) The k_{eff} of all fuel elements or fueled devices in storage is less than 0.9;

(3) The k_{eff} of fuel elements or fueled devices in an approved shipping container will meet the applicable Certificate of Compliance specifications for k_{eff};

(4) Irradiated fuel elements or fueled devices will be stored in an array which will permit sufficient natural convection cooling by air or water such that the fuel element or fueled device will not exceed design values.

5.2.4 Basis

This specification is based on American Nuclear Society standard 15.1, section 5.4.

5.3 REACTOR BUILDING

5.3.1 Applicability

This specification applies to the building that houses the TRIGA reactor facility.

5.3.2 Objective

The objective is to ensure that provisions are made to restrict the amount of release of radioactivity into the environment.

5.3.3 Specification

(l) The reactor shall be housed in a closed room designed to restrict leakage when the reactor is in operation, with HVAC system designed to maintain negative differential pressure with respect to adjacent spaces and the environment.

(2) The minimum free volume of the reactor room shall be at least approximately 4120 m^3.

(3) The reactor bay HVAC confinement ventilation system and the auxiliary purge system is capable of exhausting air or other gases from the reactor room at a minimum of 60 ft. above ground level.

(4) Reactor bay HVAC confinement ventilation system operation is designed to provide a minimum of 2 changes of reactor bay air per hour.

5.3.4 Basis

To control the escape of gaseous effluent, the reactor room contains no windows that can be opened. The room air is exhausted through an independent exhaust system, and discharged above the roof to provide dilution.

5.4 EXPERIMENTS

5.4.1 Applicability

This specification applies to the design of experiments.

5.4.2 Objective

The objective is to ensure that experiments are designed to meet criteria.

5.4.3 Specifications

(1) EXPERIMENTS with design reactivity worth greater than $1.00 SHALL be securely fastened (as defined in Section I, Secured Experiment).

(2) Design shall ensure that failure of an EXPERIMENT SHALL NOT lead to a direct failure of a fuel element or of other experiments that could result in a measurable increase in reactivity or a measurable release of radioactivity due to the associated failure.

(3) EXPERIMENTS SHALL be designed so that they do not cause bulk boiling of core water

(4) EXPERIMENT design SHALL ensure no interference with control rods or significant shadowing of reactor control instrumentation.

(5) EXPERIMENT design SHALL minimize the potential for industrial hazards, such as fire or the release of hazardous and toxic materials.

(6) Where the possibility exists that the failure of an EXPERIMENT (except fueled EXPERIMENTS) could release radioactive gases or aerosols to the reactor bay or atmosphere, the quantity and type of material shall be limited such that

the airborne concentration of radioactivity is less than 1,000 times the Derived Air Concentration.

For in-core samples a decay time of five minutes following irradiation may be used in radioactive inventory calculations to account for processing prior to potential exposure.

(7) Each fueled experiment shall be limited such that the total inventory of (1) radioactive iodine isotopes 131 through 135 in the experiment is not greater than 9.32E5 μCi, and (2) radioactive strontium is not greater than 9.35E4 μCi.

Alternate calculations may be accomplished to demonstrate equivalent times for protective actions based on DAC limits for specific experiments, if desired.

These limits do not apply to TRIGA fuel elements used in experiments as maximum hypothetical accident analysis applies. For in-core samples a decay time of five minutes following irradiation to account may be used in calculations.

(8) The following assumptions shall be used in experiment design:

a. If effluents from an experimental facility exhaust through a hold-up tank which closes automatically at a high radiation level, at least 10% of the gaseous activity or aerosols produced will escape.

b. If effluents from an experimental facility exhaust through a filter installation designed for greater than 99% efficiency for 0.3 micron particles, at least 10% of the aerosols produced will escape.

c. For materials whose boiling point is above 130ºF and where vapors formed by boiling this material could escape only through an undisturbed column of water above the core, at least 10% of these vapors will escape.

(9) Use of explosive solid or liquid material with a National Fire Protection Association Reactivity (Stability) index of 2, 3, or 4 in the reactor pool or biological shielding SHALL NOT exceed the equivalent of 25 milligrams of TNT without prior NRC approval.

5.4.4 Basis

Designing the experiment to reactivity and thermal-hydraulic conditions ensures that the experiment is not capable of breaching fission product barriers or interfering with the control systems (interferences from other - than reactivity - effects with the control and safety systems are also prohibited). Design constraints on industrial hazards

ensure personnel safety and continuity of operations. Design constraints limiting the release of radioactive gasses prevent unacceptable personnel exposure during off-normal experiment conditions.

A Derived Air Concentration assumes a 2000 hour per year exposure; if exposure is controlled to a specific time limit, such as time required for recognizing the situation and evacuating, limiting values for an experiment can be higher than a DAC.

Limits on radioiodine and radioactive strontium in fueled experiments permits a 1-hour evacuation time for releases of radioiodine and a 2-hour evacuation time for releases of radioactive strontium based on a TRIGA fuel distribution of the radioisotopes from fission of ^{235}U.

6. Administrative Controls

6.1 Organization and Responsibilities of Personnel

This chapter describes and discusses the Conduct of Operations at The University of Texas TRIGA. The Conduct of Operations involves the administrative aspects of facility operations, the facility emergency plan, the security plan, the Reactor Operator selection and requalification plan, and environmental reports. License is used in Chapter 12 in reference to reactor operators and senior reactors subject to 10CFR50.55 requirements.

6.1.1 Structure

University Administration:

Fig. 1 illustrates the organizational structure that is applied to the management and operation of the University of Texas and the reactor facility. Responsibility for the safe operation of the reactor facility is a function of the management structure of Fig. 1[6]. These responsibilities include safeguarding the public and staff from undue radiation exposures and adherence to license or other operation constraints. Functional organization separates the responsibilities of academic functions and business functions. The office of the President administers these activities and other activities through several vice presidents.

NETL Facility Administration:

The facility administrative structure is shown in Fig. 2. Facility operation staff consists of a director and at least four full time equivalent persons. This staff of four provides for basic operation requirements. Four typical staff positions consist of an associate director, a reactor supervisor, a reactor operator, and a health physicist. One or more of the listed positions may also include duties typical of a research scientist. The reactor supervisor, health physicist, and one other position are to be full time. One full-time equivalent position may consist of several part-time persons such as assistants, technicians and secretaries. Faculty, students, and researchers supplement the organization. Titles for staff positions are descriptive and may vary from actual designations. Descriptions of key components of the organization follow.

[6] "Standard for Administrative Controls" ANSI/ANS - 15.18 1979

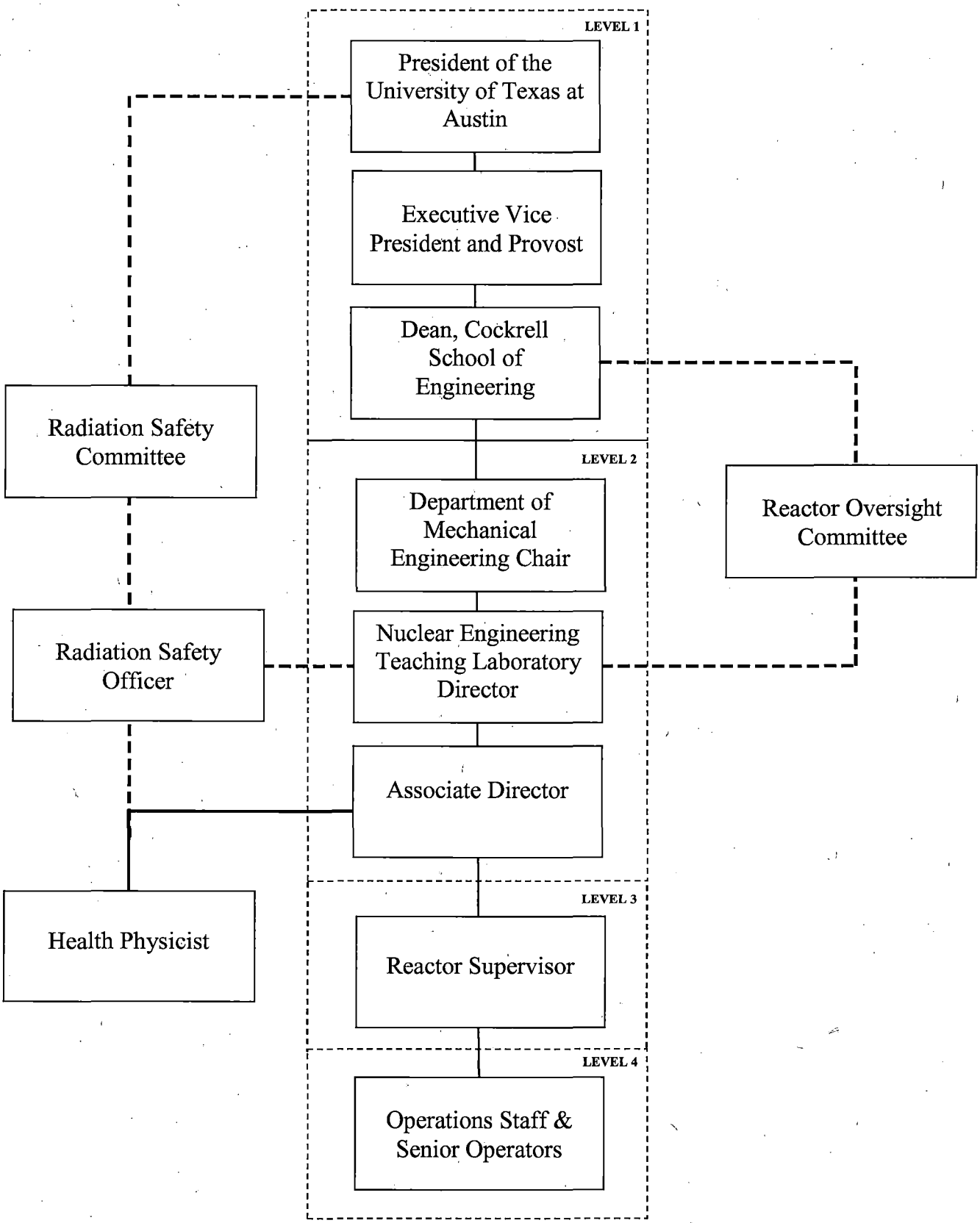

Figure 1: University of Texas Line Management for the UT TRIGA

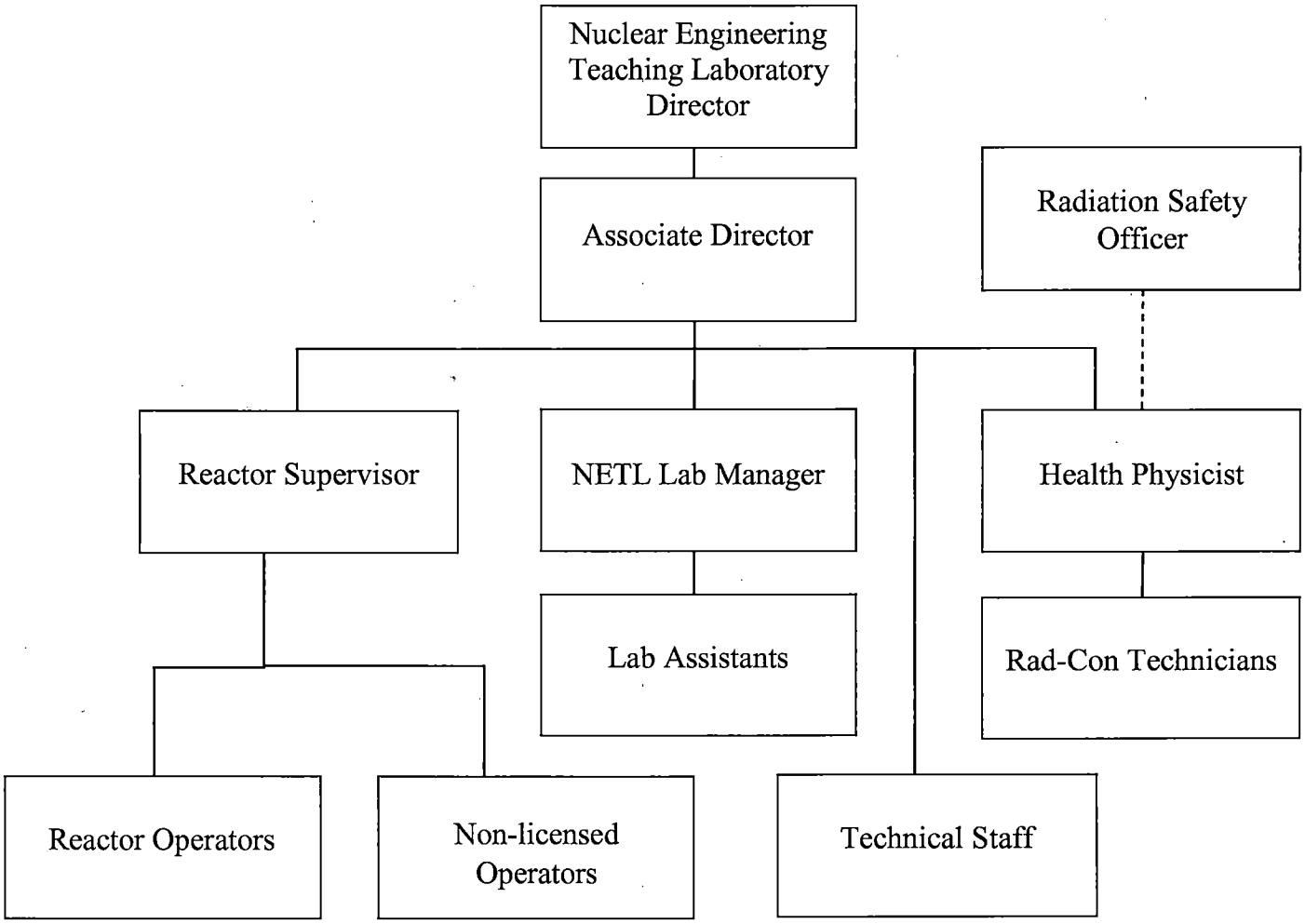

Figure 2: Facility Organization

6.1.2 Functional Responsibility

President of the University of Texas at Austin	Responsibility for all aspects of the University is vested in the President.
Vice President and Provost	Research and academic educational programs are administered through the Office of the Executive Vice President and Provost. Separate officers assist with the administration of research activities and academic affairs with functions delegated to the Dean of the College of Engineering and Chair of the Mechanical Engineering Department.
Executive Vice President and Chief Financial Officer Provost	Financial and Administrative Services are administered through the Office of the Senior Vice President and Provost. This office is responsible for management of financial, business, information technology (IT), safety and security, physical infrastructure, and operational service units.

Dean, Cockrell School of Engineering	Management of the Cockrell School of Engineering Academic programs is provided by the Dean.
Chair, Department of Mechanical Engineering	The Nuclear Engineering Teaching Laboratory supports the Nuclear and Radiation Engineering area of study in the Department of Mechanical Engineering, with the Department managed by the Chair.
Director, Nuclear Engineering Teaching Laboratory	Nuclear Engineering Teaching Laboratory programs are directed by a senior classified staff member or faculty member. The Director oversees strategic guidance of the Nuclear Engineering Teaching Laboratory including aspects of facility operations, research, and service work. The Director must interact with senior University of Texas at Austin management regarding issues related to the Nuclear Engineering Teaching Laboratory.
Associate Director, Nuclear Engineering Teaching Laboratory	The Associate Director performs the day-to-day duties of directing the activities of the facility. The Associate Director is knowledgeable of regulatory requirements, license conditions, and standard operating practices. The associate director will also be involved in soliciting and carrying out research utilizing the reactor and other specialized equipment at the Nuclear Engineering Teaching Laboratory.
Reactor Oversight Committee	The Reactor Oversight Committee is established through the Office of the Dean of the College of Engineering of The University of Texas at Austin. Broad responsibilities of the committee include the evaluation, review, and approval of facility standards for safe operation. The Dean shall appoint at least three members to the Committee that represent a broad spectrum of expertise appropriate to reactor technology. The committee will meet at least twice each calendar year or more frequently as circumstances warrant. The Reactor Oversight Committee shall be consulted by the Nuclear Engineering Teaching Laboratory concerning unusual or exceptional actions that affect administration of the reactor program.
Radiation Safety Officer	A Radiation Safety Officer acts as the delegated authority of the Radiation Safety Committee in the daily implementation of policies and practices regarding the safe use of radioisotopes and sources of radiation as determined by the Radiation Safety Committee. The Radiation Safety Program is administered through the University Environmental Health and Safety division. The responsibilities of the Radiation Safety Officer are outlined in The University of Texas at Austin Manual of Radiation Safety.

Radiation Safety Committee

The Radiation Safety Committee is established through the Office of the President of The University of Texas at Austin. Responsibilities of the committee are broad and include all policies and practices regarding the license, purchase, shipment, use, monitoring, disposal, and transfer of radioisotopes or sources of ionizing radiation at The University of Texas at Austin.

The President shall appoint at least four members to the Committee and appoint one as Chairperson. The Committee will meet at least once each year on a called basis or as required to approve formally applications to use radioactive materials. The Radiation Safety Committee shall be consulted by the University Safety Office concerning any unusual or exceptional action that affects the administration of the Radiation Safety Program.

Reactor Supervisor

The Reactor Supervisor shall be qualified as a senior operator, and is to be knowledgeable of regulatory requirements, license conditions, and standard operating practices. The Reactor Supervisor is responsible for directing or performing reactor operations. Activities of reactor operators with USNRC licenses will be subject to the direction of a person with a USNRC senior operator license.

The reactor supervisor shall assess facility conditions and select appropriate response procedures during normal, abnormal and emergency situations.

(1) Prior to operations, the Reactor Supervisor shall ensure conditions and limitations of the license, Technical Specifications, and experiment approvals (as applicable) are met.

(2) Reactor Supervisor shall directly supervise all INITIAL STARTUPs.

(3) The Reactor Supervisor will provide direction for, or respond to, situations requiring activation of the Emergency Plan.

(4) In an emergency, the Reactor Supervisor is authorized to direct or perform a reasonable course of action that departs from a license condition or a Technical Specification when this action is immediately needed to protect the public health and safety, and no action consistent with license conditions and technical specifications that can provide adequate or equivalent protection is immediately apparent[7].

Health Physicist

Radiological safety of the Nuclear Engineering Teaching Laboratory is monitored by a health physicist, who will be knowledgeable of the facility

[7] 10CFR50.54(x)

radiological hazards. Responsibilities of the health physicist will include calibration of radiation detection instruments, measurements of radiation levels, control of radioactive contamination, maintenance of radiation records, and assistance with other facility monitoring activities.

Activities of the health physicist will depend on two conditions. One condition will be the normal operation responsibilities determined by the director of the facility. A second condition will be communications specified by the radiation safety officer. This combination of responsibility and communication provides for safety program implementation by the director, but establishes independent review. The health physicist's activities will meet the requirements of the director and the policies of an independent university safety organization.

Laboratory Manager	Laboratory operations and research support is provided by a designated Laboratory Manager. The function is typically combined with the Health Physicist position.
Reactor Operators	Reactor operators (and senior reactor operators) are licensed by the USNRC to operate the UT TRIGA II nuclear research reactor. University staff and/or students may be employed as reactor operators.
Non-licensed Operators	Auxiliary positions and operators in training
Technical Staff	Staff positions supporting various aspects of facility operations are assigned as required.
Radiological Controls Technicians	Radiological Controls Technicians are supervised by the Health Physicist to perform radiological controls and monitoring functions. Radiological Controls Technicians are generally supported as Undergraduate Research Assistant positions.
Laboratory Assistants	Laboratory Assistants are supervised by the Laboratory Manager to perform laboratory operations and analysis. Laboratory Assistants are generally supported as Undergraduate Research Assistant positions.

6.1.3 Staffing

Operation of the reactor and activities associated with the reactor, control system, instrument system, radiation monitoring system, and engineered safety features will be the function of staff personnel with the appropriate training and certification[8].

[8] "Selection and Training of Personnel for Research Reactors", ANSI/ANS -15.4 - 1970 (N380)

Whenever the reactor is not secured, the reactor shall be (1) under the direction of or (2) directly operated by a (USNRC licensed) Senior Operator, designated as Reactor Supervisor. The Supervisor may be on call if cognizant of reactor operations and capable of arriving at the facility within thirty minutes.

Whenever the reactor is not secured, a (USNRC licensed) Reactor Operator (or Senior Reactor Operator) who meets requirements of the Operator Requalification Program shall be at the reactor control console, and directly responsible for control manipulations; as indicated above, the Reactor Supervisor may be the Reactor Operator at the controls.

Only the Reactor Operator at the controls or personnel authorized by, and under direct supervision of, the Reactor Operator at the controls shall manipulate the controls. Whenever the reactor is not secured, operation of equipment that has the potential to affect reactivity or power level shall be manipulated only with the knowledge and consent of the Reactor Operator at the controls. The Reactor Operator at the controls may authorize persons to manipulate reactivity controls who are training either as (1) a student enrolled in academic or industry course making use of the reactor, (2) to qualify for an operator license, or (3) in accordance the approved Reactor Operator requalification program.

Whenever the reactor is not secured, a second person (i.e., in addition to the reactor operator at the control console) capable of initiating the Reactor Emergency Plan will be present in the NETL building. Unexpected absence of this second person for greater than two hours will be acceptable if immediate action is taken to obtain a replacement. If the reactor supervisor is in the NETL building and not acting as the Reactor operator at the controls, the Reactor Supervisor may act as the second person.

Staffing required for performing experiments with the reactor will be determined by a classification system specified for the experiments. Requirements will range from the presence of a certified operator for some routine experiments to the presence of a senior operator and the experimenter for other less routine experiments.

6.2 Review and Audit

The review and audit process is the responsibility of the Reactor Oversight Committee (ROC).

6.2.1 Composition and Qualifications

The ROC shall consist of at least three (3) members appointed by the Dean of the College of Engineering that are knowledgeable in fields which relate to nuclear safety. The university radiological safety officer shall be a member or an ex-officio member. The committee will perform the functions of review and audit or designate a knowledgeable person for audit functions.

6.2.2 Charter and Rules

The operations of the ROC shall be in accordance with an established charter, including provisions for:

a. Meeting frequency (at least twice each year, with approximately 4-8-month frequency).
b. Quorums (not less than one-half the membership where the operating staff does not contribute a majority).
c. Dissemination, review, and approval of minutes.
d. Use of subgroups.

6.2.3 Review Function

The responsibilities of the Reactor Oversight Committee to shall include but are not limited to review of the following:

a. All new procedures (and major revisions of procedures) with safety significance
b. Proposed changes or modifications to reactor facility equipment, or systems having safety significance
c. Proposed new (or revised) experiments, or classes of experiments, that could affect reactivity or result in the release of radioactivity
d. Determination of whether items a) through c) involve unreviewed safety questions, changes in the facility as designed, or changes in Technical Specifications.
e. Violations of Technical Specifications or the facility operating licensee
f. Violations of internal procedures or instruction having safety significance
g. Reportable occurrences
h. Audit reports

Minor changes to procedures and experiments that do not change the intent and do not significantly increase the potential consequences may be accomplished following review and approval by a senior reactor operator and independently by one of the Reactor Supervisor, Associate Director or Director. These changes should be reviewed at the next scheduled meeting of the Reactor Oversight Committee.

6.2.4 Audit Function

The audit function shall be a selected examination of operating records, logs, or other documents. Audits will be by a Reactor Oversight Committee member or by an individual appointed by the committee to perform the audit. The audit should be by any individual not directly responsible for the records and may include discussions with cognizant personnel or observation of operations. The following items shall be audited and a report made within 3 months to the Director and Reactor Committee:

a. Conformance of facility operations with license and technical specifications at least once each calendar year.

b. Results of actions to correct deficiencies that may occur in reactor facility equipment, structures, systems, or methods of operation that affect safety at least once per calendar year.

c. Function of the retraining and requalification program for reactor operators at least once every other calendar year.

d. The reactor facility emergency plan and physical security plan, and implementing procedures at least once every other year.

6.3 Procedures

Written procedures shall govern many of the activities associated with reactor operation. Activities subject to written procedures will include:

a. Startup, operation, and shutdown of the reactor
b. Fuel loading, unloading, and movement within the reactor.
c. Control rod removal or replacement.
d. Routine maintenance, testing, and calibration of control rod drives and other systems that could have an effect on reactor safety.
e. Administrative controls for operations, maintenance, conduct of experiments, and conduct of tours of the Reactor Facility.
f. Implementing procedures for the Emergency Plan or Physical Security Plan.

Written procedures shall also govern:

a. Personnel radiation protection, in accordance with the Radiation Protection Program as indicated in the Safety Analysis Report, Chapter 11
b. Administrative controls for operations and maintenance
c. Administrative controls for the conduct of irradiations and experiments that could affect core safety or reactivity

A master Procedure Control procedure specifies the process for creating, changing, editing, and distributing procedures. Preparation of the procedures and minor modifications of the procedures will be by certified operators. Substantive changes or major modifications to procedures, and new prepared procedures will be submitted to the Reactor Oversight Committee for review and approval. Temporary deviations from the procedures may be made by the reactor supervisor or designated senior operator provided changes of substance are reported for review and approval.

Proposed experiments will be submitted to the reactor oversight committee for review and approval of the experiment and its safety analysis[9], as indicated in Chapter 10. Substantive changes to approved experiments will require re-approval while insignificant changes that do not alter experiment safety may be approved by a senior operator and independently one of the following, Reactor Supervisor, Associate Director, or Director. Experiments will be approved first as proposed experiments for one-time application, and subsequently, as approved experiments for repeated applications following a review of the results and experience of the initial experiment implementation.

6.4 Review of Proposals for Experiments

a) All proposals for new experiments involving the reactor shall be reviewed with respect to safety in accordance with the procedures in (b) below and on the basis of criteria in (c) below.

b) Procedures:

1. Proposed reactor operations by an experimenter are reviewed by the Reactor Supervisor, who may determine that the operation is described by a previously approved EXPERIMENT or procedure. If the Reactor Supervisor determines that the proposed operation has not been approved by the Reactor Oversight Committee, the experimenter shall describe the proposed EXPERIMENT in written form in sufficient detail for consideration of safety aspects. If potentially hazardous operations are involved, proposed procedures and safety measures including protective and monitoring equipment shall be described.

2. The scope of the EXPERIMENT and the procedures and safety measures as described in the approved proposal, including any amendments or conditions added by those reviewing and approving it, shall be binding on the experimenter and the OPERATING personnel. Minor deviations shall be allowed only in the manner described in Section 6 above. Recorded affirmative votes on proposed new or revised experiments or procedures

[9] ANSI/ANS 15.6, op. cit.

indicate that the Committee determines that the proposed actions do not involve changes in the facility as designed, changes in Technical Specifications, changes that under the guidance of 10 CFR 50.59 require prior approval of the NRC, and could be taken without endangering the health and safety of workers or the public or constituting a significant hazard to the integrity of the reactor core.

3. Transmission to the Reactor Supervisor for scheduling.

c) Criteria that shall be met before approval can be granted shall include:

1. The EXPERIMENT must meet the applicable Limiting Conditions for Operation and Design Description specifications.

2. It must not involve violation of any condition of the facility license or of Federal, State, University, or Facility regulations and procedures.

3. The conduct of tests or experiments not described in the safety analysis report (as updated) must be evaluated in accordance with 10 CFR 50.59 to determine if the test or experiment can be accomplished without obtaining prior NRC approval via license amendment pursuant to 10 CFR Sec. 50.90.

4. In the safety review the basic criterion is that there shall be no hazard to the reactor, personnel or public. The review SHALL determine that there is reasonable assurance that the experiment can be performed with no significant risk to the safety of the reactor, personnel or the public.

6.5 Operator Requalification

An NRC approved UT TRIGA Requalification Plan is in place to maintain training and qualification of reactor operators and senior reactor operators. License qualification by written and operating test, and license issuance or removal, are the responsibility of the U.S. Nuclear Regulatory Commission. No rights of the license may be assigned or otherwise transferred and the licensee is subject to and shall observe all rules, regulations and orders of the Commission. Requalification training maintains the skills and knowledge of operators and senior operators during the period of the license. Training also provides for the initial license qualification.

6.6 Emergency Plan and Procedures

An NRC approved Emergency Plan following the general guidance set forth in ANSI/ ANS15.16, Emergency Planning for Research Reactors is in place. The plan specifies two action levels, the first level being a locally defined Non-Reactor Specific Event, and the second level being the lowest level FEMA classification, a Notification of Unusual Event.

Procedures reviewed and approved by the Reactor Oversight Committee are established to manage implementation of emergency response.

6.7 Physical Security Plan

An NRC approved Security Plan is in place. The plan incorporates compensatory measures implemented following security posture changes initiated post 9/11. The Plan and portions of the procedures are classified as Oversight Information. Security procedures implementing the plan, approved by the Reactor Oversight Committee, are established.

6.8 Action To Be Taken In The Event A SAFETY LIMIT Is Exceeded

In the event that a SAFETY LIMIT is not met,

a. The reactor shall be shutdown and secured.
b. The Reactor Supervisor, Associate Director, and Director shall be notified
c. The SAFETY LIMIT violation shall be reported to the Nuclear Regulatory Commission within 24 hours by telephone, confirmed via written statement by email, fax or telegraph
d. A SAFETY LIMIT violation report shall be prepared within 14 days of the event to describe:
    1. Applicable circumstances leading to the violation including (where known) cause and contributing factors
    2. Effect of the violation on reactor facility components, systems, and structures
    3. Effect of the violation on the health and safety of the personnel and the public
    4. Corrective action taken to prevent recurrence
e. The Reactor Oversight Committee shall review the report and any follow-up reports
f. The report and any follow-up reports shall be submitted to the Nuclear Regulatory Commission.
g. Operations shall not resume until the USNRC approves resumption.

6.9 Action To Be Taken In The Event Of A Reportable Occurrence

a) A reportable occurrence is any of the following conditions:

1. Any actual safety system setting less conservative than specified in Section 2.2, Limiting Safety System Settings;

2. VIOLATION OF SL, LSSS OR LCO;

NOTES

Violation of an LSSS or LCO occurs through failure to comply with an "Action" statement when "Specification" is not met; failure to comply with the "Specification" is not by itself a violation.

Surveillance Requirements must be met for all equipment/components/conditions to be considered operable.

Failure to perform surveillance within the required time interval or failure of a surveillance test shall result in the equipment /component/condition being inoperable

3. Incidents or conditions that prevented or could have prevented the performance of the intended safety functions of an engineered safety feature or the REACTOR SAFETY SYSTEM;

4. Release of fission products from the fuel that cause airborne contamination levels in the reactor bay to exceed 10CFR20 limits for releases to unrestricted areas;

5. An uncontrolled or unanticipated change in reactivity greater than $1.00;

6. An observed inadequacy in the implementation of either administrative or procedural controls, such that the inadequacy has caused the existence or development of an unsafe condition in connection with the operation of the reactor.

b) In the event of a reportable occurrence, as defined in the Technical Specifications, and in addition to the reporting requirements,

1. The Reactor Supervisor, the Associate Director and the Director shall be notified
2. If a reactor shutdown is required, resumption of normal operations shall be authorized by the Associate Director or Director
3. The event shall be reviewed by the Reactor Oversight Committee during a normally scheduled meeting

6.10 Plant Operating Records

Records of the following activities shall be maintained and retained for the periods specified below[10]. The records may be in the form of logs, data sheets, electronic files,

[10] "Records and Reports for Research Reactors", ANSI/ANS - 15.3-1974 (N399).

or other suitable forms. The required information may be contained in single or multiple records, or a combination thereof.

Lifetime Records

Lifetime records are records to be retained for the lifetime of the reactor facility. (Note: Applicable annual reports, if they contain all of the required information, may be used as records in this section.)

a. Gaseous and liquid radioactive effluents released to the environs.

b. Offsite environmental monitoring surveys required by Technical Specifications.

c. Events that impact or effect decommissioning of the facility.

d. Radiation exposure for all personnel monitored.

e. Updated drawings of the reactor facility.

Five Year Period

Records to be retained for a period of at least five years or for the life of the component involved whichever is shorter.

a. Normal reactor facility operation (supporting documents such as checklists, log sheets, etc. shall be maintained for a period of at least one year).

b. Principal maintenance operations.

c. Reportable occurrences.

d. Surveillance activities required by technical specifications.

e. Reactor facility radiation and contamination surveys where required by applicable regulations.

f. Experiments performed with the reactor.

g. Fuel inventories, receipts, and shipments.

h. Approved changes in operating procedures.

i. Records of meeting and audit reports of the review and audit group.

One Training Cycle

Training records to be retained for at least one license cycle are the requalification records of licensed operations personnel. Records of the most recent complete cycle shall be maintained at all times the individual is employed.

6.11 Reporting Requirements

This section describes the reports required to NRC, including report content, timing of reports, and report format. Refer to section 12.4 above for the reporting requirements for SAFETY LIMIT violations, radioactivity releases above allowable limits, and reportable occurrences. All written reports shall be sent within prescribed intervals to the United States Nuclear Regulatory Commission, Washington, D.C., 20555, Attn: Document Control Desk.

Operating Reports

Routine annual reports covering the activities of the reactor facility during the previous calendar year shall be submitted to licensing authorities within three months following the end of each prescribed year. Each annual operating report shall include the following information:

a. A narrative summary of reactor operating experience including the energy produced by the reactor or the hours the reactor was critical, or both.

b. The unscheduled shutdowns including, where applicable, corrective action taken to preclude recurrence.

c. Tabulation of major preventive and corrective maintenance operations having safety significance.

d. Tabulation of major changes in the reactor facility and procedures, and tabulation of new tests or experiments, or both, that are significantly different from those performed previously, including conclusions that no new or unanalyzed safety questions were identified.

e. A summary of the nature and amount of radioactive effluents released or discharged to the environs beyond the effective control of the owner-operator as determined at or before the point of such release or discharge. The summary shall include, to the extent practicable, an estimate of individual radionuclides present in the effluent. If the estimated average release after dilution or diffusion is less than 25% of the concentration allowed or recommended, a

statement to this effect is sufficient.

f. A summarized result of environmental surveys performed outside the facility.

g. A summary of exposures received by facility personnel and visitors where such exposures are greater than 25% of that allowed or recommended.

Other or Special Reports

There shall be a report not later than the following working day by telephone and confirmed in writing by facsimile or similar conveyance of any reportable occurrence identified in 6.9.

There shall be a written report describing the circumstances of any reportable occurrence identified in 6.9 within 14 days of occurrence.

There shall be a written report within 30 days of:

a. Permanent changes in the facility organization involving Director or Supervisor.

b. Significant changes in the transient or accident analysis as described in the Safety Analysis Report.